# ADVANCES IN
# SUPRAMOLECULAR CHEMISTRY

## Editor: GEORGE W. GOKEL

### Volume 4    1997

ADVANCES IN
SUPRAMOLECULAR CHEMISTRY


*Volume 4* • 1997

This Page Intentionally Left Blank

# ADVANCES IN SUPRAMOLECULAR CHEMISTRY

*Editor:* GEORGE W. GOKEL

*Department of Molecular Biology and Pharmacology*

*Washington University School of Medicine*

*St. Louis, Missouri*

VOLUME 4 • 1997

# CONTENTS

# LIST OF CONTRIBUTORS

*Andrei Andrievsky*

Department of Chemistry and Biochemistry
University of Texas at Austin
Austin, Texas

*Jun-ichi Anzai*

Pharmaceutical Institute
Tohoku University
Sendai, Japan

*Jerry L. Atwood*

Department of Chemistry
University of Missouri
Columbia, Missouri

*Philippe Bühlmann*

Department of Chemistry
The University of Tokyo
Tokyo, Japan

*A. Prasanna de Silva*

School of Chemistry
Queen's University
Belfast, Northern Ireland

*John W. Genge*

Department of Chemistry and Biochemistry
University of Texas at Austin
Austin, Texas

*H. Q. Nimal Gunaratne*

School of Chemistry
Queen's University
Belfast, Northern Ireland

*Thorfinnur Gunnlaugsson*

School of Chemistry
Queen's University
Belfast, Northern Ireland

*K. Travis Holman*

Department of Chemistry
University of Missouri
Columbia, Missouri

*Allen J. M. Huxley*                     School of Chemistry
                                         Queen's University
                                         Belfast, Northern Ireland

*Yoshihisa Inoue*                        Department of Molecular Engineering
                                         Osaka University
                                         Osaka, Japan

*Yoshiaki Kobuke*                        Department of Materials Science
                                         Shizuoka University
                                         Hamamatsu, Japan

*Kenji Koga*                             Faculty of Pharmaceutical Sciences
                                         The University of Tokyo
                                         Tokyo, Japan

*Colin P. McCoy*                         School of Chemistry
                                         Queen's University
                                         Belfast, Northern Ireland

*Kazunori Odashima*                      Faculty of Pharmaceutical Sciences
                                         The University of Tokyo
                                         Tokyo, Japan

*Tetsuo Osa*                             Pharmaceutical Institute
                                         Tohoku University
                                         Sendai, Japan

*Jude T. Rademacher*                     School of Chemistry
                                         Queen's University
                                         Belfast, Northern Ireland

*Terence E. Rice*                        School of Chemistry
                                         Queen's University
                                         Belfast, Northern Ireland

*Jonathan L. Sessler*                    Department of Chemistry and Biochemistry
                                         University of Texas at Austin
                                         Austin, Texas

*Jonathan W. Steed*                      Department of Chemistry
                                         King's College London
                                         London, England

*Masao Sugawara*                    Department of Chemistry
                                    The University of Tokyo
                                    Tokyo, Japan

*Koji Tohda*                        Department of Chemistry
                                    The University of Tokyo
                                    Tokyo, Japan

*Yoshio Umezawa*                    Department of Chemistry
                                    The University of Tokyo
                                    Tokyo, Japan

*Takehiko Wada*                     Department of Molecular Chemistry
                                    Osaka University
                                    Osaka, Japan

This Page Intentionally Left Blank

# PREFACE

The goal in Volume 4 of *Advances in Supramolecular Chemistry* remains the same as for previous volumes: to present a broad range of supramolecular science recorded by an international panel of distinguished researchers. Contributions in this volume span the scientific range from electronic device development to novel synthetic receptor molecules to biomimetic ion channels.

The true breadth of the supramolecular chemistry field is sometimes overlooked. By their very nature, focused monographs cannot span the range of efforts that include analytical, inorganic, organic, physical, and biochemistry. Even considering the wide range of studies underway, there is some polarization between the biological side of supramolecular science and materials development. It is hoped that the quality of the presentations in this volume will demonstrate that there is original, fascinating, and excellent science on both sides and throughout the field of supramolecular chemistry.

George W. Gokel
*Editor*

This Page Intentionally Left Blank

# SUPRAMOLECULAR PHOTOIONIC DEVICES:

## PHOTOINDUCED ELECTRON TRANSFER (PET) SYSTEMS WITH SWITCHABLE LUMINESCENCE OUTPUT

A. Prasanna de Silva, H. Q. Nimal Gunaratne,

Thorfinnur Gunnlaugsson, Allen J. M. Huxley,

Colin P. McCoy, Jude T. Rademacher, and

Terence E. Rice

# 1.  INTRODUCTION

In this review we aim to demonstrate that supramolecular devices which operate via the interconversion of ionic and photonic signals can be useful for the gathering and processing of chemically relevant information. We will restrict ourselves to discussing those systems which involve the competing processes of luminescence emission and PET (photoinduced electron transfer). The emphasis will be placed on the recent literature.

# 2.  WHY PHOTOIONIC DEVICES?

The usefulness of supramolecular systems[1-4] which operate with ionic inputs and luminescence output stems from many features.

Ions were present at the creation of supramolecular chemistry. It is remarkable that all three inventors of the field commenced their research by designing and constructing receptors for ions of the s-block in the periodic table.[5-7] Therefore researchers into photoionic devices have the rare benefit of drawing on the entire resources of a research area right from its inception.

Ions are available in a myriad of shapes, sizes, and charges due to the combinations arising from the elements in the periodic table in their various oxidation states.[8] These involve many selectivity patterns with regard to potential receptors.[9] As opposed to electrons, the different natures of ions give rise to qualitative distinguishability. Their local concentration gives quantitation of the input signal. Interesting ramifications arise. For instance, molecular-scale systems[10] with multiple receptors can select different ionic inputs into the different receptors without additional guidance, i.e. the inputs are wireless. Practical distinguishability of ionic signals by molecular-scale devices without "wiring" is unparalleled in conventional electronics at any level of integration and has considerable potential for exploitation by chemically minded scientists.

Ions are the prime movers of life. Some of them are the signal carriers in the nervous systems controlling intelligence and motion in the higher life forms.[11] Even in the simplest cases, ions carry the intracellular signals which are essential for survival of the cell.[12] This involvement of ions in intelligence naturally draws designers of photoionic devices into the area of signal processing. On the other hand, spying on these ions will provide a window on some of the inner workings of life. Hence, many photoionic devices have been targeted for ion sensing in biological environments. Of course, there are beautiful examples of related devices in nature operating in the photon in–ion out mode, which is the reverse of the type discussed here, e.g. rhodopsin in retinal rods of the human eye[11,13] and bacteriorhodopsin in membranes of purple bacteria.[14]

Ions can easily serve as the "finger" on the molecular-scale light switch.[15] Due to their intrinsic charge, ions can be marshalled and directed by electric fields. Therefore, electrochemical control of local ion concentrations is feasible, especially with ultramicroelectrodes.[16] At a more subtle level, membrane potentials are capable of large modulations of local ion concentrations in microenvironments.[17] However it must be noted that both these approaches are currently limited to a scale somewhat larger than the single molecule. Nevertheless, with the advent of scanning electrochemical microscopy[18] there is hope for the future because scanning microscope probe tips routinely handle single molecules.[19] Molecule-based approaches are also available in the form of photoswitchable ion receptors,[20–26] some of which can provide ion pulses within ns timescales. Photoreleasable caged ions are irreversible versions.[27–32] A potentially powerful combination would be the excitation of these ion complexes via the probe tip of a near-field scanning optical microscope.

Photon emitting, i.e. luminescent molecules, are detectable with extreme sensitivity at the single molecule level.[33] Thus luminescence is a natural approach to the operation of devices at the molecular level. It is also notable that luminescent molecules can yield information with <nm spatial resolution (though not visualization) even without special microtechniques.[34] Luminescence output signals can be received in the human domain in various colors, i.e. multiplexing is naturally feasible. The intensity of the various colors permits quantitation of the output signals. Luminescent molecules interface smoothly with confocal microscopes[35] for 2D or 3D imaging at µm resolution and photon-scanning tunnelling[3]/near-field scanning optical[37] microscopes for 3D imaging at nm resolution. Most luminescent devices have the personal touch since they are easily tested/demonstrated at the ensemble level by visual observation. The luminescence lifetime (which can vary from ~ns to ~ms) should, in principle, allow rapid information handling, though the associated ion interactions will usually be rate-limiting. Transactions with protons over minimum distances in aqueous media will result in maximum rates, though protonic transactions in other media are also of interest.[38]

Molecular photoionic devices with switchable response,[39] at the ensemble level, display nonlinear in/out characteristics which can be operated either as analogue or digital devices by proper control of the ion concentration input variable.[40] When

employed in smaller numbers, they should show "on/off" action, reminiscent of single-channel events in electrophysiology.[41]

## 3.  WHY PHOTOINDUCED ELECTRON TRANSFER?

Since PET lies at the heart of natural photosynthesis,[42] there is a wealth of information available to device designers. Some of this data has arisen from exploratory photochemistry,[43,44] while some have their origins in artificial photosynthesis research.[45–47]

Since electrons are of rather low mass, PET rates can be extremely fast with transit times in the ps–ns range. Molecular switches where the only "moving part" is an electron are likely to be much faster than those involving nuclear motion.[48,49] Since they require ion movement, photoionic devices based on PET will operate at slower rates. However these are fast enough compared to the human timescales.

Electron transfer rates are naturally subject to molecular-scale electric fields. Therefore, ion binding to a molecule is an effective way of controlling PET within it. Since PET is an excited state deactivation pathway, the competing radiative route, i.e. luminescence, also becomes exposed to ionic manipulation. Under favorable conditions, PET rates can be much faster ($10^{12}$ $s^{-1}$)[50] than luminescence ($10^3$–$10^{10}$ $s^{-1}$). At the other extreme, conditions can be arranged under which PET is effectively non-existent. Therefore, luminescence can be ionically switched between "off" and "on" states representing digital action.[40]

The transfer of an electron requires a donor and an acceptor, i.e. a multicomponent system is necessary if the process is to occur within a single molecular entity. Molecular-scale devices employing PET are therefore necessarily supramolecular. The integrity of the individual components or subunits will be best maintained if they are held together by weak associations. Nevertheless the same outcome can be largely achieved, especially for photochemical purposes, by connecting the components together with covalent σ bonds. While these can allow some degree of inter-component interaction,[51–53] this approach has been adopted by most device designers in the field mainly because robust systems result. PET-type processes are also found in mechanically interlocked systems such as rotaxanes and catenanes, especially those which rely on charge transfer (CT) interactions for their assembly.[54] It will only be a matter of time before ionically switchable luminescent devices are developed from this approach as well.[55] Overall, PET systems will continue to play a major part in the growth of supramolecular photochemistry.

## 4.  LUMOPHORE–SPACER–RECEPTOR SYSTEMS (NORMAL LOGIC)

A large fraction of the research in ionically switchable luminescent devices is in this category. Several reviews of the early work are available.[15,39,40,56–65] Figure 1
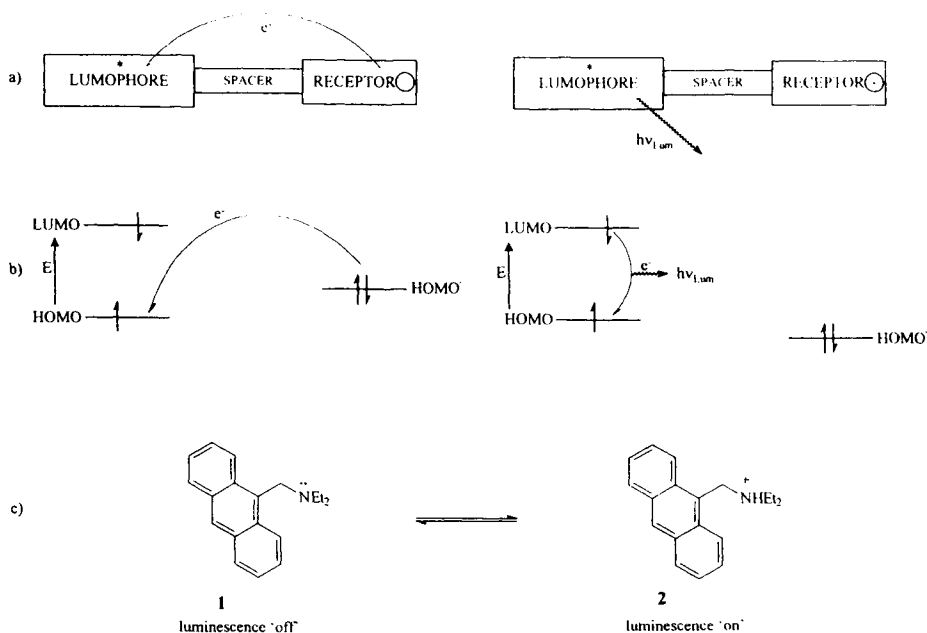
***Figure 1.*** (a) Schematic representation of the three-module format of an ionically switchable photoactive dyad (normal logic). Receptors are shown throughout with a hole even though a cavity is not a prerequisite for binding a guest ion. Note that the excitation (∗) in the lumophore drives the intramolecular, intermodular electron transfer which quenches the luminescence. The electron transfer may transfer along the bonds in the spacer or through space even though the latter has been chosen for reasons of clarity in all figures. The direction of the electron transfer is such that the presence of a cationic guest on/in the receptor would discourage the process (arguing at the simplest electrostatic level). Now luminescence wins the competition. (b) Frontier molecular orbital energy diagrams corresponding to part (a). Note that ground state nomenclature is used throughout this article even though the electron occupancy corresponds to the excited state of the lumophore. The intermodular electron transfer is exergonic only in the cation-free case where the HOMO′ of the receptor is higher than that of the HOMO of the lumophore. The HOMO′ of the receptor is stabilized upon binding the cation. Electron transfer is relatively fast (c.f. luminescence) at moderate exergonicities. (c) An example illustrating the principles of parts (a) and (b) from the aminomethyl aromatic family. The luminescence is switched "off" when the amine unit is unprotonated. At sufficiently high proton concentrations (pH < p$K_a$) the amine becomes protonated and the luminescence is switched "on".

summarizes the key principles of these lumophore–spacer–receptor systems along with a representative example (**1**)[39] from the aminoalkyl aromatic family. System **3**[66] is a recent example of this type where the relatively long intrinsic fluorescence lifetime of the discoidal pyrene fluorophore is used to develop a lifetime sensor for pH. Lifetime sensing[67] has an advantage over intensity sensing since no complications arise from environmental variables such as optical path length or local concentration of the sensor or quenchers. Of course, the fluorescence intensity of **3** is smoothly pH-dependent as well.

The switching efficiency of lumophore–spacer–receptor systems can be improved by using multiple receptor modules. The PET rate is increased in the device when free of guest ions since more than one site can provide the transiting electron. The simplest cases, such as **4**,[57,68] are those where the receptor units are well separated to prevent interdependent ion binding with an interposed lumophore to minimize the lumophore–receptor spacing for maximum PET rates. Besides this statistical effect, receptors may also cooperatively participate in PET.[69] This may be the case in **5**[70] and **6**.[71]

Systems with neighboring receptors tend to show multiple steps in the fluorescence intensity–pH profile since (1) the $pK_a$ values of the neighboring receptors tend to differ considerably, and (2) receptors at different distances from the lumophore have different PET rates when they are free of guest ions. However these cases are usually designed to exploit their chelating ability towards metal ions with pH studies being of secondary interest. Systems **5**,[70] **7**,[72] and **8**[73] were aimed at $Zn^{2+}$, and **9**[74] raises interesting possibilities for binding a variety of inorganic and organic guests. In some of these situations, the cyclophane nature of **9** would suggest the involvement of the benzene fluorophore in a receptor role as well.

Lumophores other than hydrocarbons have been incorporated into the aminoalkyl aromatic family of ionically switchable luminescent devices. For instance, metalloporphyrin systems such as **10**[75] have been used to good advantage. These cases absorb and emit at wavelengths as long as 596 and 650 nm, respectively. Such red-shifted systems are particularly attractive for monitoring ion movements in
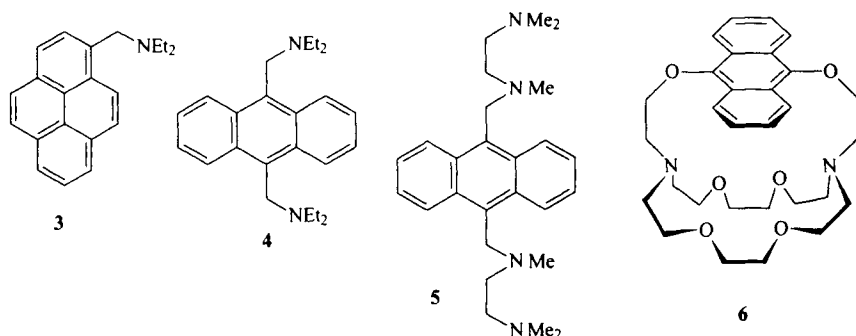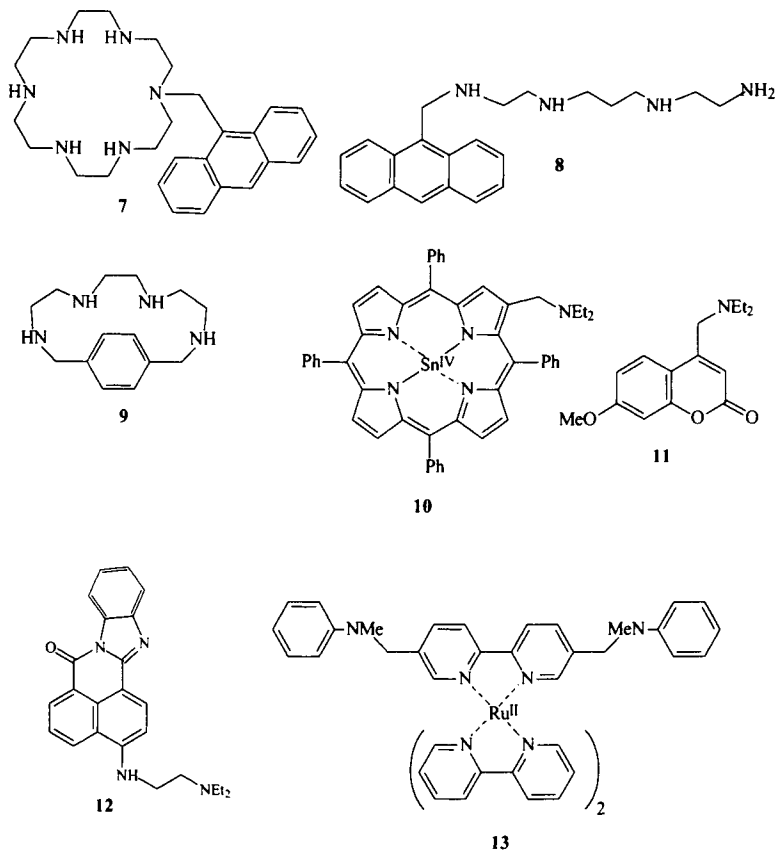
intrinsically colored biomatrices. A large addition can be made to the aminoalkyl aromatic family if we look towards heteroaromatic compounds as lumophores. This can be particularly profitable and interesting in the following way.

The PET systems of the aminoalkyl aromatic type discussed so far display a very simple behavior in that luminescence intensity (or quantum yield) is the only variable. Such systems are very user-friendly as a result and tolerate a wide variety of communication wavelengths. However these simple systems could be adapted to include an additional absorptiometric sensing channel which can confirm the results of ion density (pH say) obtained via luminescence. Of course, such increased user-confidence is only attained with a proportionate reduction in simplicity. Now excitation needs to be done at the isosbestic wavelength. These systems, e.g. 11 and 12, use a push–pull fluorophore with electron donor and acceptor substituents which give rise to internal charge transfer (ICT) excited states.[76] In contrast, the simple PET systems employed aromatic hydrocarbon fluorophores with essentially pure $\pi\pi^*$ excited states.[68] The charge separation in ICT states can cause electrostatic

interactions across the spacer with the ion-bound receptor. Thus, the absorption spectrum undergoes pH-dependent shifts. The observed emission spectrum shows much smaller shifts (if any) because only the ion-bound system is emissive in most cases. Systems **11** and **12** are important because they are dual-channel sensors using both emission and absorption. Closely related examples arise from inorganic chemistry since charge transfer is common during the excitation of metal complexes. For instance, tris(2,2'bipyridyl)Ru(II) displays an emissive excited state with metal-to-ligand charge transfer (MLCT) character. This has been built into the proton switchable system **13**.[77] However, the exploitation of heteroaromatic lumophores with ICT or MLCT excited states has to be approached carefully since they can introduce interesting kinetic effects, as the following case demonstrates.

While the thermodynamic basis for the design of ionically switchable luminescent PET devices is now well established,[39,40] the switching action is eventually controlled by the competition between the *rates* of luminescence and electron transfer. The connection between the rates and the thermodynamics is of intense current interest.[50] In the regioisomeric pairs **14** and **15**, PET sensor action is found to be sensitively controlled by kinetic factors.[78] System **14** displays strong fluorescence switching "off–on" action with protons, whereas **15** is essentially unaffected. This can be understood as being due to the dipole created in the ICT excited state attracting or repelling the transiting electron in **14** or **15**, respectively, even though the thermodynamic driving force is essentially the same. The present phenomenon is important for two additional reasons:

1. This is the first demonstration of self-regulated PET, i.e. the PET process is controlled by the characteristics of the lumophore within the working device. Self-regulation is an important aspect of self-organized molecular processes.[1]
2. PET within the photosynthetic reaction center occurs along preferentially along one of two nearly identical branches.[42] It may interest students of this modern enigma that a similar path selectivity has now been demonstrated within the much smaller supramolecular systems **14** and **15**.



14

15

16
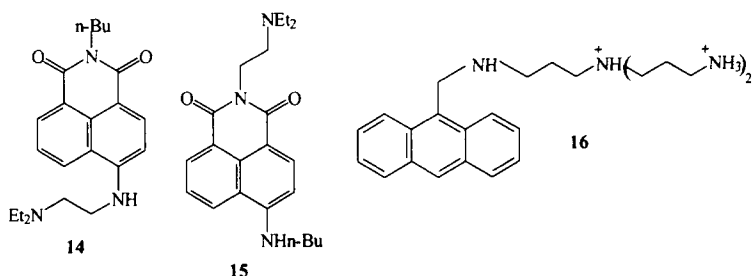
Lumophore–spacer–receptor systems are not by any means limited to the aminoalkyl aromatic family even if we focus on the receptor unit. Still, the latter family is likely to remain a major provider of ionically switchable luminescent devices. Aminoalkyl aromatics also serve as the platform for the development of luminescent PET sensors for a whole class of nonionic saccharides.[79] While aliphatic amines, either singly or in arrays, can serve as receptors for a variety of cationic (e.g. $Zn^{2+}$ as in **8**[73]) and anionic (e.g. $HPO_4^{2-}$ as in **16**[80,81]) guests, their intrinsically high basicity causes a strong sensitivity towards protons. This has led to the use of aromatic amine derivatives or even entirely nitrogen-free moieties[82] as receptors. Before these are discussed, it is worth pointing out that amines are not the only choice even for proton receptors in this field. Carboxylates, pyridines, and phenolates have been incorporated into lumophore–spacer–receptor systems **17**[83], **18**,[84] and **19**[85] in this regard. Though these examples are still very small in number, these three receptor classes have interesting contrasts with the conventional amine-based systems. For instance, phenolates become more hydrophobic upon protonation, whereas the opposite is true for amines. Such hydrophobicity alterations can be important during the positioning of luminescent devices in microheterogeneous environments (see Sections 9 and 10). Aromatic carboxylates and pyridines become electron acceptors following protonation, whereas amines lose their electron-donating ability. These will be detailed in Section 5.

The development of receptors for various ionic species with selectivity against protons has been driven by, among other things, the need for sensors targeting physiological situations. Several excellent examples of such receptors have been integrated into fluorescent sensors (see Section 8). However, they can also be developed into off–on switchable fluorescent systems of the PET type. For instance, London's **20** is known to bind $Mg^{2+}$ selectively under physiological conditions[86] and has been used in $^{19}F$ NMR probes[86] and ratiometric fluorescent sensors based on wavelength shifts.[87] System **20** could be rationally incorporated into a lumo-



**18**



Calix[4]arene

**19**
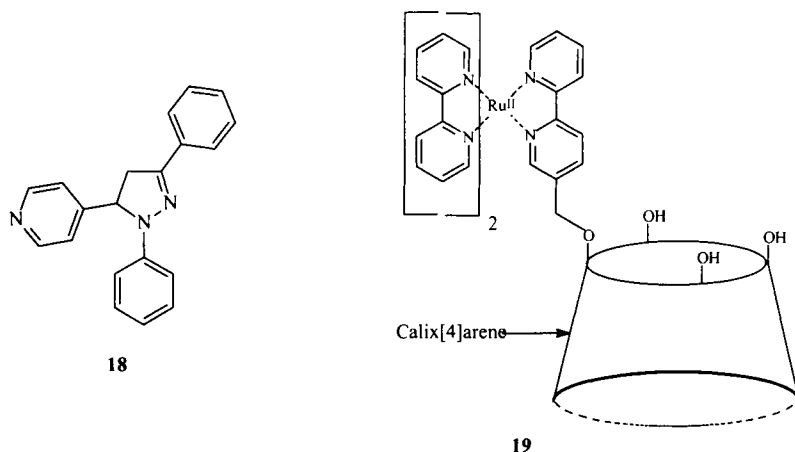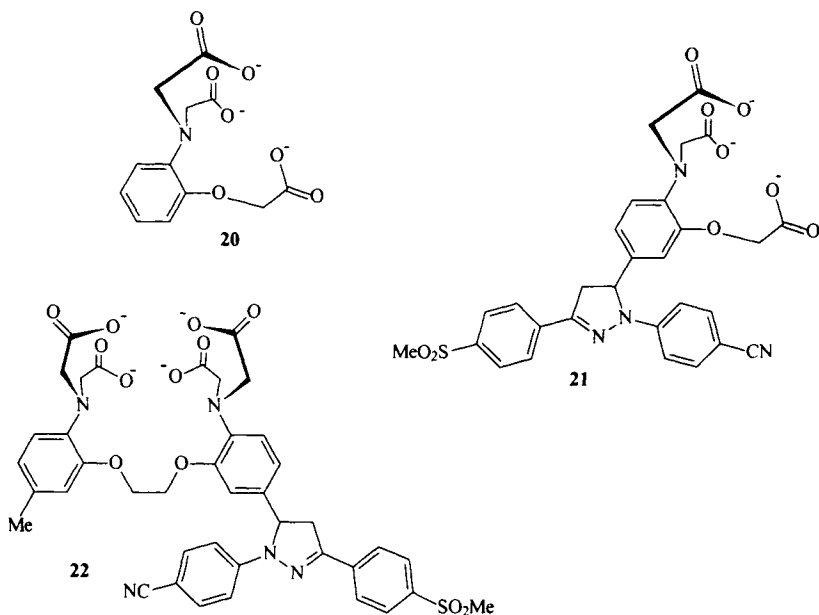
phore–spacer–receptor system. For example, **21** shows a $Mg^{2+}$-induced fluorescence enhancement of 67.[88] Such off–on action without significant changes in emission band position or shape allows powerful visual demonstration of $Mg^{2+}$ in neutral water and can also permit sensitive monitoring of pMg status in cell populations. In spite of the lack of ratiometric capability, the availability of strong off–on action in **21** can potentially allow pMg imaging in single cells at least semiquantitatively. The design of **21** according to the lumophore–spacer–receptor format also means that their optical and ion sequestration properties are nearly quantitatively inherited from the parent lumophore and receptor units.

System **22**[89] is an earlier example which incorporates Tsien's selective calcium receptor **23**.[90] System **23** has also been employed for the construction of ratiometric fluorescent sensors involving wavelength shifts.[90,91] System **22** and other related PET sensors provide some of the most visually dramatic fluorescence off–on switching induced by biologically relevant levels of calcium ions in addition to their consistent predictability of most sensor parameters.

The construction of **22** employs the 5-methine group of the pyrazoline ring as the spacer module. Amide groups can also serve in a segregatory capacity in spite of its formally conjugated nature. Gust and Moore have used amides in this way to isolate π-electron systems during their elegant studies on triads and higher versions as analogues of the photosynthetic reaction center.[92] System **24** is an example of an off–on switchable fluorescent system which accommodates this feature.[93] The
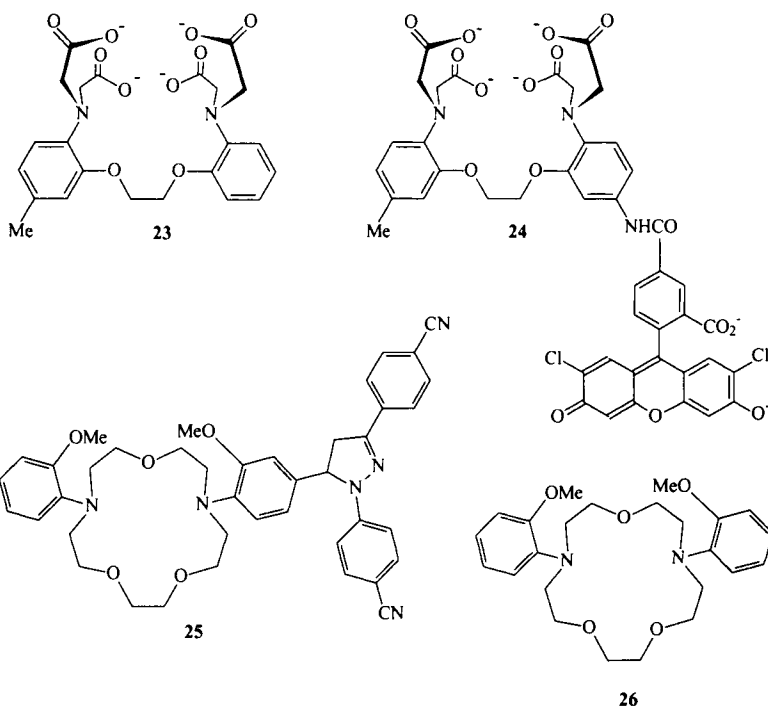
coupling of lumophores with receptors via amide spacers is particularly attractive regarding synthesis.

Macrocyclic 25[94] has been constructed with pseudocryptand 26 which can be discerned within Tsien's ratiometric fluorescent sensors[95] as the $Na^+$ receptor unit. Conformational changes by 26 upon ion binding allows strong off–on PET sensing action due to the ion-induced increase of its oxidation potential. X-ray structural evidence for the $Na^+$-induced conformational changes in 26 shows decreased conjugation with a 40° twist about the C–N bond of the 2-anisidine unit. X-ray evidence is also available[96] for similar conformational changes in the non-macro-cyclic $Ca^{2+}$ receptor 23. A related analysis has been made for a $Ag^+$–phenyl-azacrown ether interaction which involves a soft–soft component.[97]

The switching efficiency of lumophore–spacer–receptor systems can also be improved by using multiple lumophore modules to obtain the statistical advantage as mentioned earlier with regard to multiple receptors. For instance, the fluorescent enhancement factor of 92 induced by $Ca^{2+}$ in 22[89] could be increased even further to 116 in the case of the bifluorophoric derivative 27.[98] In suitable cases such as 27, lumophore–lumophore interactions can be induced remote from the $Ca^{2+}$ binding site, i.e allosteric effects of biology can be imported into luminescent PET sensor designs. Indeed, this represents a new approach to the modulation of the $Ca^{2+}$ binding constant and subsequently the sensing range of the supramolecular device.

**27**
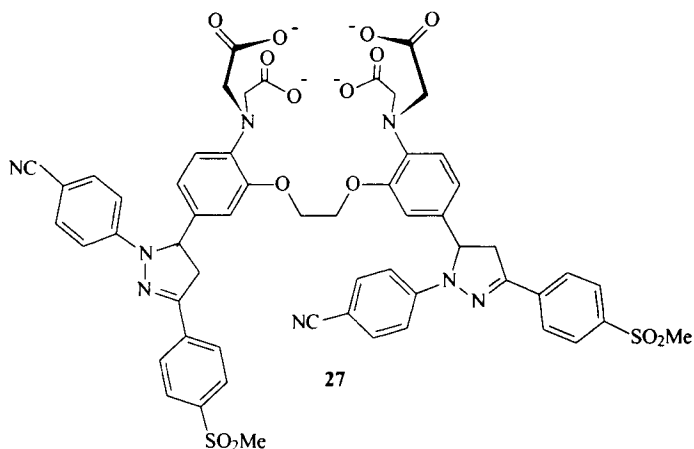
Metcalfe[99] has recently used substituents near the $Ca^{2+}$ binding site in **28** to modulate the sensing range of ratiometric sensors.

Excimer formation, an obvious lumophore–lumophore interaction, was not seen in this case. In the related case **29**,[93] nonradiative inter-lumophore interactions are sterically allowed only in the absence of $Ca^{2+}$. This is therefore an additional enhancement mechanism for the $Ca^{2+}$-induced switching "on" of luminescence. System **30**, based on multiple receptors and lumophores, shows off–on fluorescence switching with $H^+$ but not with $\alpha,\omega$-diammonium ions in spite of the demonstrable binding of the latter.[100] This is understandable since the relative disposition of the nitrogen atoms in the diazacrown components cannot simultaneously allow binding of all four nitrogen lone electron pairs necessary for the switching "on" of fluorescence. This problem does not arise in **31** which has only monoazacrown components and strong off–on switching is seen.[101] In addition, **30** shows no excimers in spite of its quasi-parallel pair of lumophores. Off–on switching behavior is not observed in **32**[102] upon binding $Rb^+$ or $\alpha,\omega$-diammonium ions. The reason is possibly because PET is less likely with the relatively poor acceptor property of 9,10 dialkoxyanthracene across the dimethylene spacers. Instead, monomer–excimer switching is found. However, there are old (**33**[103,104]) and new (**34**[105,106]) examples where PET processes and excimer formation are concurrent. The monomer and excimer bands are differently influenced by the concentration of the guest ion $Zn^{2+}$. The ratio of these two band intensities is controlled only by the guest ion concentration and not by the physical variables of the microenvironment (see Sections 8 and 13).

Ionically switchable lumophore–spacer–receptor systems can also be outfitted with an additional PET inactive receptor to enhance guest binding, especially when larger organic structures are involved. For instance, GABA is one of the most important neurotransmitters with the GABA receptor being one of the most studied

**28**



**29**



**30**



**31**
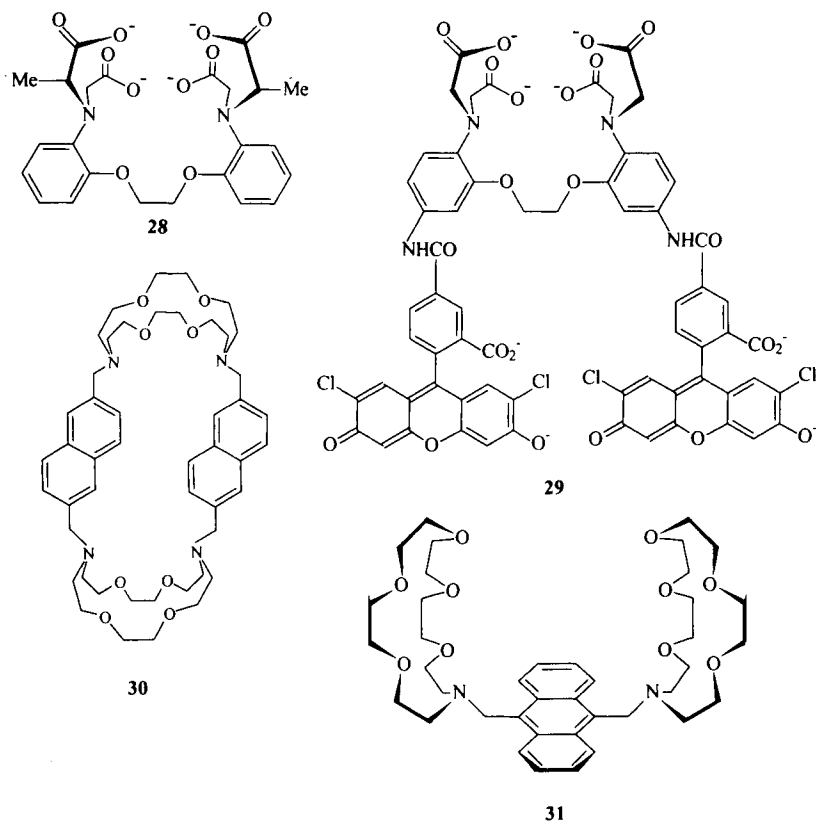
systems of its kind,[107] especially regarding this decade of the brain. Such studies could be greatly assisted by the availability of a molecular fluorescent sensor for GABA. System **35** is a step in this direction[108]—it has been designed according to fluorescent PET sensor principles and responds to GABA in mixed aqueous methanolic solution at pH 9.5. The sensor embodies a guanidinium unit for binding the carboxylate terminus of GABA and an aza-18-crown-6 ether moiety for binding the ammonium terminus with an anthracene unit serving both as the signaling fluorophore and the rigid backbone which defines the length of the guest being recognized. It should be noted that **35** owes a conceptual debt to **31** which responded to α,ω-diammonium ions such as putrescinium in nonaqueous medium.[101] The availability of more effective receptors for amino acids including GABA[109] should allow the construction of fluorescent PET sensors for GABA and relatives operating in neutral aqueous solution.

Occasionally, the spacer module can fulfill extra functions. System **36**[73] has a potential PET donor in the *N,N*- dimethylaniline unit but its large distance from the lumophore prevents any real contribution. The dominant PET donors are the two

32

33
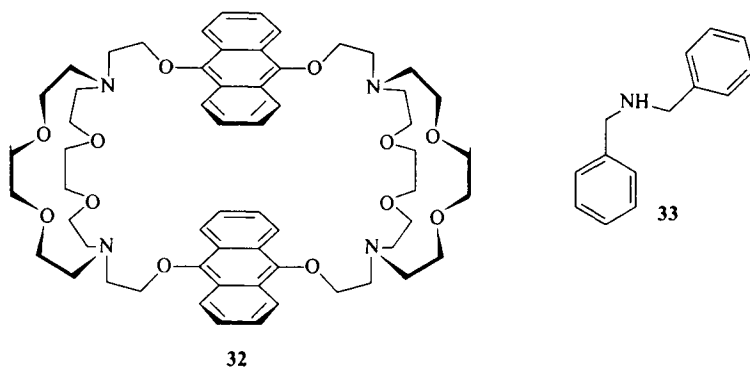
aliphatic amine units closest to the lumophore. These PET donors can be blocked by coordination to $Zn^{2+}$. However, fluorescence remains quenched because the dimethylaniline unit is brought into the neighborhood of the lumophore by $Zn^{2+}$-induced folding of the tetraamine chain. Thus the tetraamine chain in **36** can be considered an "active" spacer between the anthracene lumophore and the dimethylaniline. The spacer displays ion-coordination activity besides its own PET donation. A similar example which employs a ferrocene moiety instead of dimethylaniline[109] brings in electron energy transfer (EET)[110] as a quenching channel in addition to PET. Such guest-induced folding of coordinatively active spacers or even guest-induced deaggregation of subunits in order to bring photoactive termini closer or further are known from electron energy transfer studies by Valeur[111] and Tsien,[112]

34

35

NH NH NH NH

**36**

NMe₂

CF₃

O O O O O O O NH O O

**37**
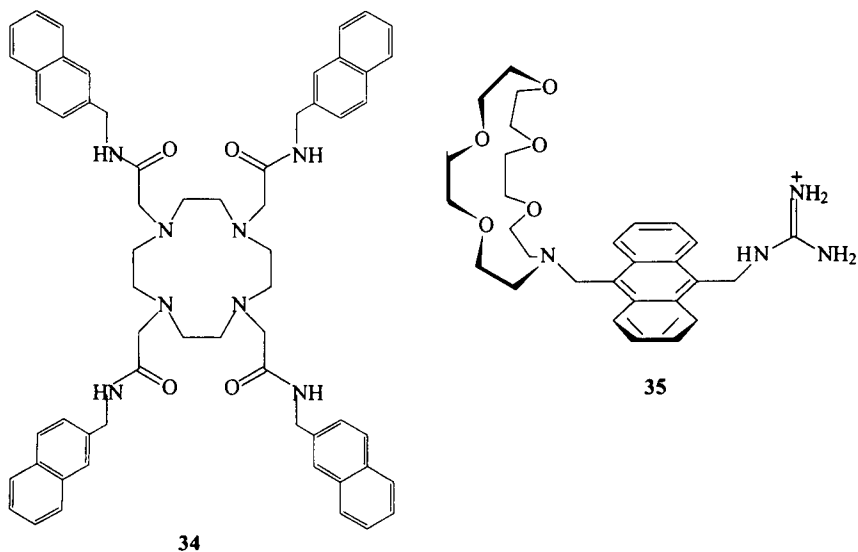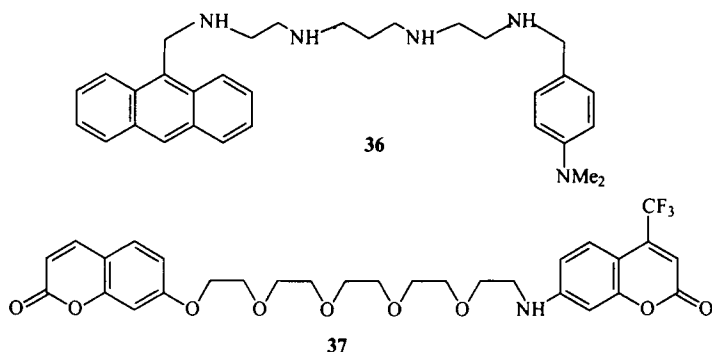
respectively. Tsien's example is based on c-AMP (cyclic adenosine monophosphate) interacting with a protein kinase, whereas Valeur's case **37** is Pb²⁺-controllable.

Shinkai's **38**[113] is also a PET system whose fluorescence is controlled by Na⁺ binding to a coordinatively active spacer which is a calix[4]arene tetraester in this case. However, the through-space distance between the photoactive termini is expanded by Na⁺ complexation, thus reducing the PET efficiency. Kuhn's **39**[93] is not dissimilar in that a PET-type quencher (a nitroaromatic unit) is held away from the lumophore by Ca²⁺ binding. However a conventional lumophore–spacer–receptor is also contained within **39** as found in **24**. At this point it would not be out of place to mention several important studies on the control of PET/EET by ion binding to a coordinatively active spacer between photoactive terminii.[114-117] System **36** is structurally related to Verhoewen's **40**[118] since they both contain an aromatic lumophore and an aromatic amine with one or more interposed aliphatic amines. System **40** also displays the functional similarities that PET processes were

O₂N

CO₂Et

CO₂Et

O O O O O O

O O

Calix[4]arene

**38**

**39**

**40**

**41**
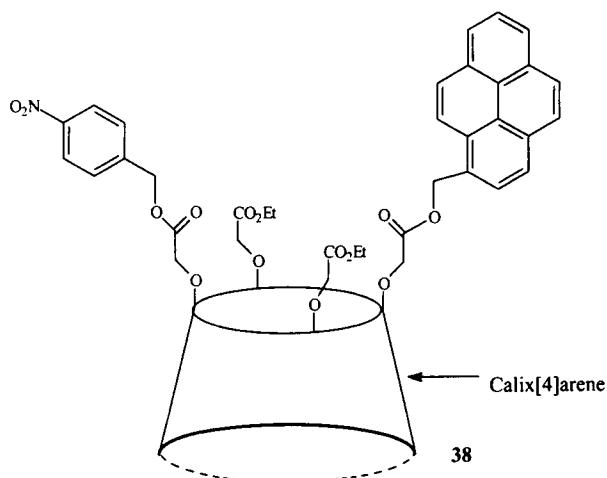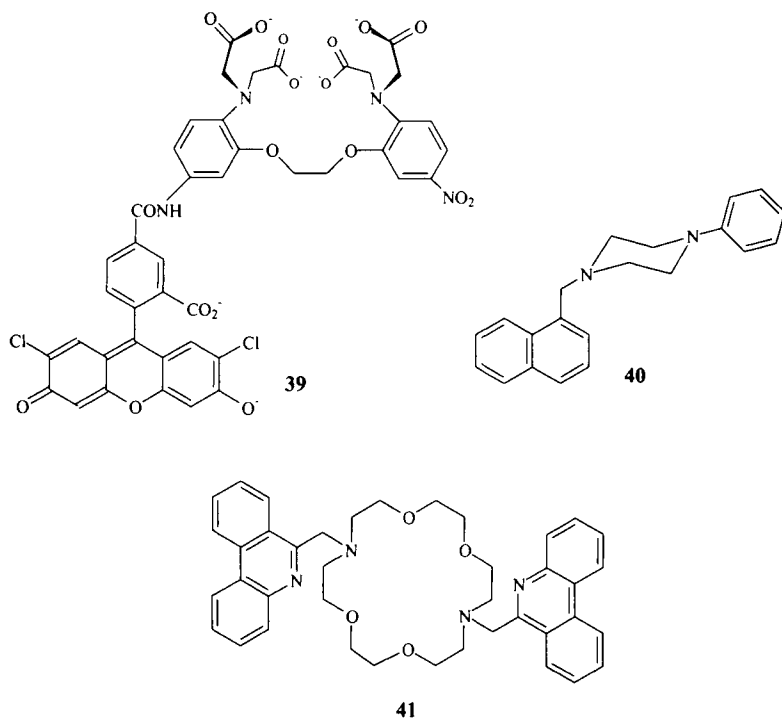
involved and that the central amine could be ion-bound selectively. The similarities end there, however, with the semirigid bridge in **40** permitting a long-range charge transfer interaction between the termini.

Zinic's **41**[119] is the latest addition to the small group of lumophore–spacer–receptor systems where the lumophore also acts the role of receptor.[120] The uniqueness of **41** is that it offers X-ray crystallographic evidence for the dual role of the lumophore. Both phenanthridinyl nitrogen atoms form part of the first coordination sphere of the guest $K^+$. The favorable stacking interaction appears to drive the *syn* arrangement of the two lumophores, whereas **26** showed an *anti* arrangement of the two capping groups. Nevertheless, alkali cations are ineffective at switching fluorescence, unlike other lumophore-appended crown ethers.[121] However, off–on switching is found with $Sr^{2+}$ in spite of the quenching nature of the nitrate counteranion.

Before closing this section, we note that Ueno's elegantly derivatized cyclodextrins[122,123] can also be viewed as lumophore–spacer–receptor systems. However, these show many differences from the cases described here. These do not generally involve PET, though specific examples containing twisted internal charge transfer (TICT) phenomena have emerged.[124] Their general mechanism of action requires an intrinsically environmentally sensitive lumophore and some degree of self-com-

plexation or inclusion/association of the lumophore by the cyclodextrin receptor. The sensing action arises from the reversal of this self-complexation by the entry of hydrophobic guests (which may carry ionic groups). The displaced location of the lumophore leads to an altered emission signal. A recent example uses natural aromatic amino acids as lumophores in a similar design.[125]

## 5. LUMOPHORE–SPACER–RECEPTOR SYSTEMS (REVERSE LOGIC)

As the title suggests, the subject of this section is closely connected to what has gone before. Figure 2 also emphasizes this close and opposite connection when it is compared to Figure 1. Nevertheless, lumophore–spacer–receptor systems which show guest ion-induced on–off switching of luminescence are severely underrepresented in the literature compared to their off–on cousins. There may be several reasons for this paucity, but the most important of these appears to have its origin in analytical chemistry. It is well appreciated that a fluorescent reagent will have a lower limit of detection for a given analyte if the analyte causes fluorescent enhancement rather than quenching.[126] It appears that designers of luminescent devices have been inhibited from researching on–off switchable systems due to this influence. However this inhibition is unfounded since the conditions of application of single-use analytical reagents tend to be very different from those reversibly switchable devices or sensors. The latter need to respond continuously to analyte concentrations which can deviate positively or negatively from the normal. In many instances, this normal value of analyte concentration can be moderately high since it is determined by the biologically relevant range. This is well above the limit of detection of the analyte by fluorescence methods. Furthermore, the analyte concentration range to which the switchable luminescent device is sensitive would be controlled by the binding constant and this would usually not be limited by the luminescent properties.

Another reason why device designers have shied away from luminescent systems which are switched "off" by guest ions is the fear of nonspecific quenching. Again, this fear is more apparent than real in many situations. When such nonspecific quenching paths are dynamic in nature, their efficiency is limited by Stern–Volmer kinetics. On the other hand, designed on–off systems will produce very efficient static quenching. If the receptor module can be chosen to be very selective for the guest ion, extraneous static quenching paths can be avoided.

Given the success of PET switches and sensors of the off–on type (Section 5), there is no fundamental reason why "on–off" systems cannot grow to be similarly useful. However there is little doubt that off–on systems are more visually appealing. Besides this aesthetic factor, off–on systems and especially the aminoalkyl aromatic family tend to be synthetically more accessible since amine synthons are available in great variety.
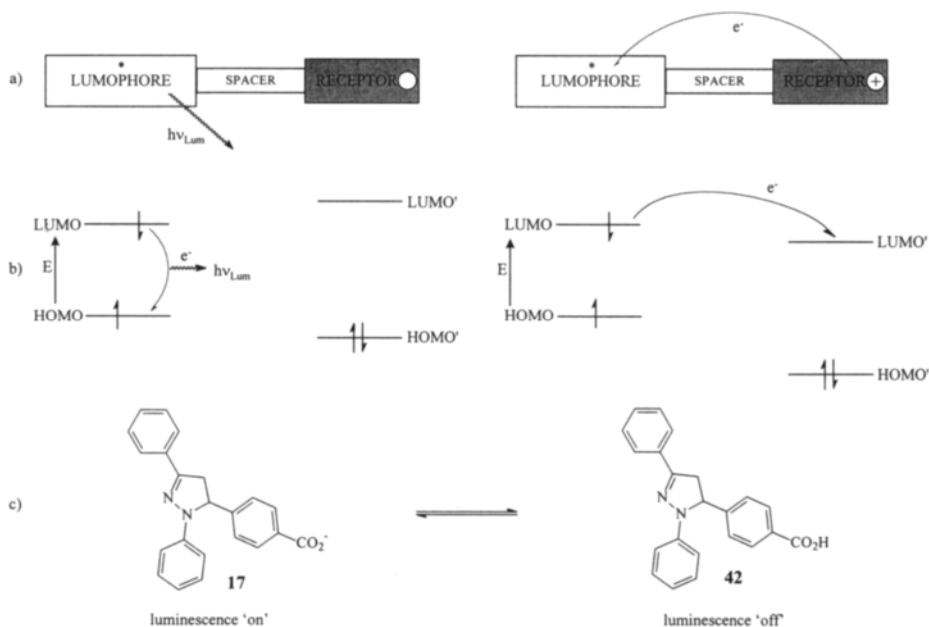
**Figure 2.** (a) Schematic representation of the three-module format of an ionically switchable photoactive dyad (reverse logic). For a given lumophore, the receptors required here are more electron deficient than those used in Figure 1. We have tried to symbolize this with grey shading in the present case. In contrast to Figure 1, the direction of the electron transfer is such that the process is encouraged only when the cationic guest is bound to the receptor. Now luminescence loses the competition when cationic guests are present on/in the receptor. (b) Frontier molecular orbital diagrams corresponding to part (a). The intermolecular electron transfer is exergonic only in the cation-bound case when the LUMO' of the receptor is lower in energy than the LUMO of the lumophore. Note that the LUMO' and the HOMO' of the receptor are stabilized upon cation binding. Of course, as implied in part (a), the frontier orbital energies of the receptor are lower than in the corresponding situation of Figure 1. (c) An example illustrating the principles of parts (a) and (b) from the 1,3 diarylpyrazolin-5-yl benzoate family. The luminescence is switched "on" when the carboxylate group is unpro-tonated. At sufficiently high proton concentrations the carboxylate group is protonated and the luminescence is switched "off".

Nevertheless, the example **17** has been available since 1989.[83] This was the first case where all the optical and ion-binding parameters of a functioning device were quantitatively predictable from model compounds within experimental error. The only exception was the emission quantum yield of the switched-"on" state which deviated negatively by 30%. Part of this deviation was caused by the different solvent conditions which were necessary for examining the model lumophore. This was an illustration of rather exact molecular engineering since the specifications at

the design stage were accurately transferred to the working device. The remarkable predictability of the device characteristics has to be attributed to the success of isolating the lumophore from the carboxylate moiety (which is the heart of the receptor) by the methine group and also by the adjacent benzene ring. The success of the PET process in the "off" state of **17** at low pH values (**42** in Figure 2) in spite of this isolation must be due to the one-atom separation between the two π-electron systems.

The same lumophore appears in **18** which shows similar on–off switching with protons.[84] However **18** is quite distinct in several respects. Its pyridine receptor is particularly suitable for incorporation into PET schemes since electrochemical data are available for both the unprotonated and protonated forms.[127] The powerful electron-accepting capability of pyridinium moieties has previously led to intramolecular fluorescence quenching in anthracene and other derivatives.[128–130] The strength of this capability permits proton-induced on–off switching with several pyrazoline derivatives including **18** which leads to a wide range of absorption and emission colors. The charge on the pyridinium unit succeeds in perturbing the ICT excited state of the lumophore across the methine spacer which is reflected in the pH-dependent absorption spectra of **18**, as seen before in **11** and **12**.

## 6. LUMOPHORE–SPACER–RECEPTOR SYSTEMS WITH REDOX ACTIVE GUESTS

As Figure 3 illustrates, redox active guests introduce PET processes almost by definition and luminescent on–off switching is the norm. However, the inhibitions outlined in Section 5 have not prevented the designers of switchable luminescent devices from exploring systems which bind redox active guests. The combined forces of inorganic coordination chemistry and supramolecular science have proved to be too attractive in many of these instances. It is to be hoped that some of this effort will filter across to the examination of more on–off systems like **17** and **18**.

System **43** is a clever modification of the aminomethyl aromatic motif.[131] The polyamine serves as a receptor for $Zn^{2+}$ (as in **5** and **7**), which in turn serves as a receptor for the 4-nitrobenzoate ion. The successful on–off switching seen here due to the electron-accepting property of the guest anion is also matched by the 4-dimethylaminobenzoate ion which acts as an electron donor for the PET process. Such second-sphere coordination[132] can also be identified in the free base form of **16** which requires the sequential attachment of protons and monohydrogenphosphate, though it is of the off–on type. A more closely related example is **45** where the luminescence is switched "off" only when $SCN^-$ is bound by $Ba^{2+}$ which is the guest of the crown ether receptor.[133] Related $I^-$-induced quenching of luminescence is also known for lumophores integrated into crown ethers such as **46**[134] (see Section 8), especially at high concentrations of the iodide salt. The high atomic number of $I^-$ also may have a role in the luminescence quenching since cases of rather remote
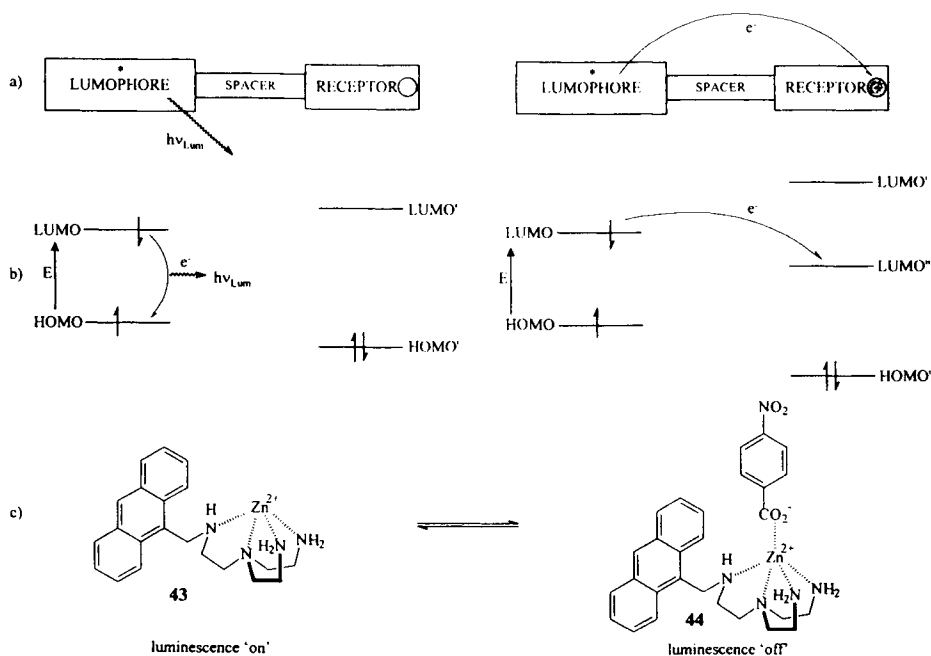
**Figure 3.** (a) Schematic representation of the three-module format of an ionically switchable photoactive dyad where the guest ion is redox active. In contrast to Figures 1 and 2, the charge sign of the guest ion is only of secondary importance. Note that the receptor is not directly involved in the electron transfer, again in contrast to Figures 1 and 2. In general, the nature of the redox activity will determine the direction of the electron transfer, i.e. either direction can be encouraged depending on the guest. Luminescence has no competition until the redox active guest is bound by the receptor. (b) Frontier molecular orbital energy diagrams corresponding to part (a). The electron transfer from the excited lumophore to the guest ion must be exergonic, i.e. the LUMO" of the guest must be lower in energy than the LUMO of the lumophore. The opposite situation (not shown) relating the energy of the HOMO" of the guest ion to that of the HOMO of the lumophore is equally valid. A third situation, which is not shown either, can combine the previous two. This leads to electronic energy transfer from the lumophore to the guest ion by electron exchange, thus quenching the luminescence of the lumophore. Luminescence originating from the guest may be observed in certain cases. (c) An example illustrating the principles of parts (a) and (b) from the work of Fabbrizi and colleagues. The luminescence is switched "off" only when 4-nitrobenzoate is present in large enough concentration to bind to the $Zn^{2+}$ center.

**45**
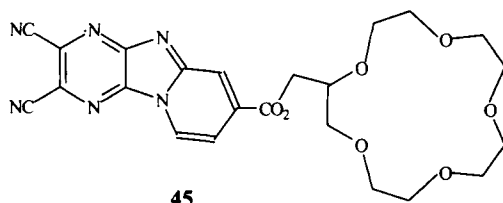
"heavy-atom" quenching are known.[135] Other halides[136,137] and nucleotide deriva-
tives[138,139] also show luminescence quenchings of this general type.

The general scheme in Figure 3 can apply to cations with equal validity. For
instance, **47**[140] binds **48**[54] with CT interactions and shows on–off switching of
luminescence. The fact that the guest ion in this case is macrocyclic takes nothing
away from the principle. However, metallic guest ions have been the most popular.
d-Block metal ions have long been known as luminescent quenchers when directly
bound to lumophores.[141] Lumophore–spacer–receptor systems which act in a
similar fashion are of much more recent vintage. Hg(II) switches "off" the emission
from protonated **7**[72] and Ni(II) has the same effect on **49**.[142] While PET activity is
the probable mechanism for posttransition metal ions such as Hg(II), the jury is still
out in cases involving transition metal ions in general. These metal ions possess



**46**



**47**



**48**



**49**
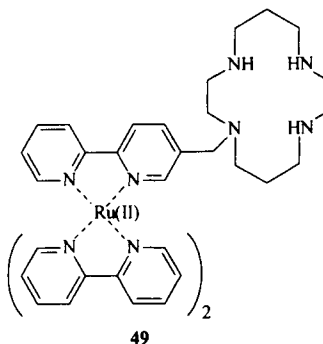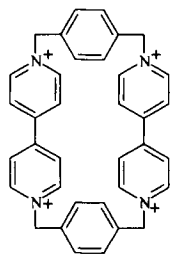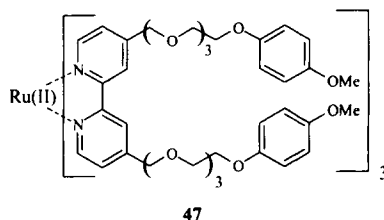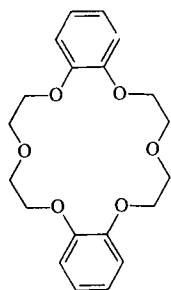
rather low-lying but nonemissive excited states of their own. Thus they can cause luminescence quenching by electronic energy transfer (EET) from the lumophore to the guest metal ion.[110] The PET–EET debate can be resolved in certain instances by measurements in low temperature glasses since PET would be hindered if it involves a charge separation (but less so if it was a charge shift), whereas EET remains undisturbed.[143] Additional evidence suggesting possible EET would be the observation of low energy absorption bands connected to the metal ion, which is the case for Cu(II) and doubly deprotonated **50**.[144] The same mechanistic dilemma applies to **51**[145] and **52**,[146] though these are distinguished by their near-specificity for Fe(III) inherited from their siderophore receptors. Since **52** has three pyrene lumophores of rather long intrinsic excited-state lifetime, it naturally shows an excimer–monomer equilibrium. As in the cases such as **34**,[105,106] this equilibrium can be modulated when nonquenching ions such as Ga(III) are able to bind with the siderophore moiety even though no PET processes are involved.

Cu(II) is one of the best examples of a redox active guest, but apparently not when it is imprisoned in a cryptand such as **53**.[147] In this case, the Cu(II) is silent over a wide potential range during cyclic voltammetry. System **53** is designed as a lumophore–spacer–receptor system such as **28–30** and **33–34** in Section 1 with multiple lumophores. It also shows similar luminescence off-on switching with $H^+$ and even with Cu(II). The possibility of Cu(II) induced production of $H^+$ from moisture appears to have been ruled out. The absence of EET is a mystery which can only be dispelled by further studies on this interesting system.

The quenching of luminescence by d-block ions is not universal; **53** is an unusual illustration. Even in more common situations, different oxidation states of the same metal can act very differently. Some cases are clear. Cu(II) quenches the lumines-



**50**

**51**

**52**

**53**

**54**
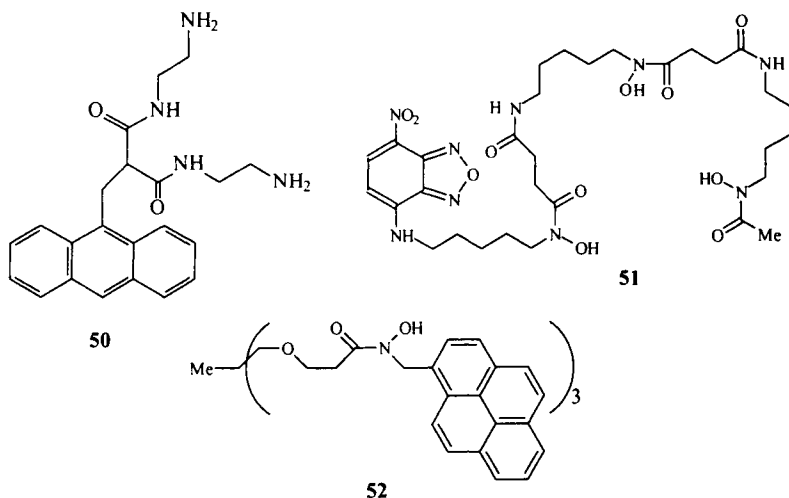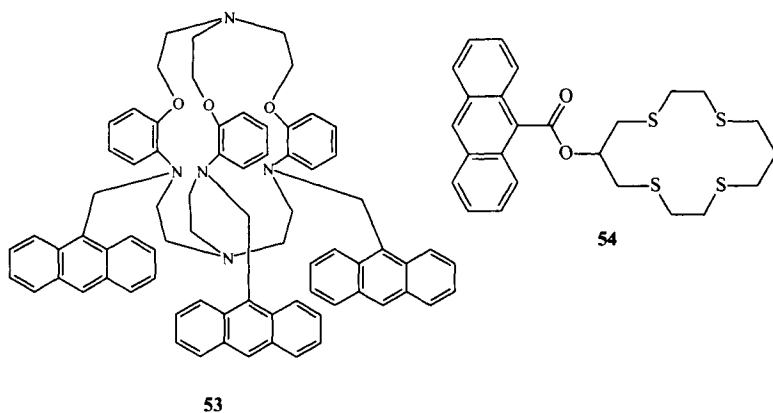
cence of **54** and Cu(I) does not because the latter has a $d^{10}$ configuration.[148] Luminescence studies in a 77K glass prove the PET nature of the luminescence quenching by Cu(II) since PET is prevented under such conditions. Consideration of PET thermodynamics suggests PET from the lumophore to the Cu(II) center. Similar considerations show that PET is much less likely in the Cu(I) state. The thiacrown ether receptor in **54** plays a critical role in stabilizing the Cu center in oxidation state 1. In general, this means that the luminescence of some of these systems can be switched by altering the metal oxidation state under electrochemical or chemical redox control. In the present instance the Cu complex of **54** can be electrochemically switched between the Cu(I) and Cu(II) states by setting the potential on either side of 0.6 V (versus SCE). This gives rise to voltage-responsive luminescence which has obvious implications for electrochromic applications in displays. It is to be noted in passing that the voltage sensitive fluorescent dyes of membrane physiology are quite different in their mode of operation.[149]

While many metal centers can be reversibly cycled between two (or more) oxidation states, few organic moieties can match such reversibility especially in protic media. Nevertheless, the first supramolecular example of an electroswitchable luminescent device involved the benzoquinone–hydroquinone couple. The luminescence of **55**[150] is switched "off" due to PET in the benzoquinone state of the redox couple. Electrochemical or chemical reduction of the benzoquinone under protic conditions to hydroquinone recovers the luminescence of the tris(2,2'-bipyridyl) Ru(II) unit. It is noted that the luminescence of tris(2,2'-bipyridyl) Ru(II) itself is electroswitchable. Indeed tris(2,2'–bipyridyl) Ru(II) came to fame as a solar energy material[151] from more humble beginnings as a luminescent redox indicator.[152] However **55** achieves the same switching at a lower magnitude of reduction potential. Here lies the advantage of the supramolecular design. Like tris(2,2'–bipyridyl) Ru(II), many lumophores show electroswitchable luminescence. An

**55**

**56**
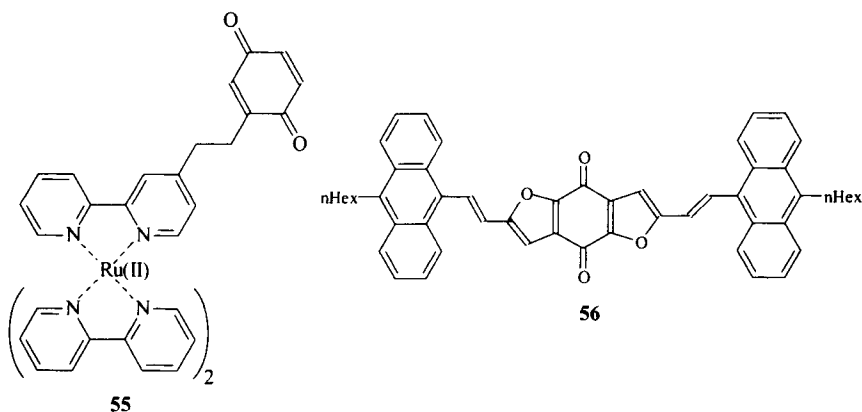
all-organic example would be anthracene whose bright blue emission would be lost upon generation of the radical anion in aprotic medium.[153] All-organic supra-molecular systems with electroswitchable luminescence are also available, e.g. Daub's **56**.[154] Overall, it appears that lumophore–spacer–receptor systems with redox active guests have many treats in store for chemists of widely differing backgrounds.

## 7. ORTHOGONAL LUMOPHORE–RECEPTOR SYSTEMS

Another important strategy that has been introduced into luminescent PET devices is the idea of virtual spacers in lumophore–spacer–receptor systems. Here an orthogonality is maintained between the lumophore and receptor modules by steric interactions. System **57** is an example of such a twisted lumophore–receptor system (Figure 4) which when first synthesized (on an empirical design basis) by Tsien showed a $Ca^{2+}$-induced emission enhancement of only 3.[155] It has been synthesized by a different route and shows a very respectable enhancement of 25—a visually clear off–on action.[98] Kuhn at Molecular Probes Inc. has also prepared samples of **57** with high emission enhancements.[156] Related examples were collected in a 1993 review.[40] It is interesting that one of the earliest examples of luminescence off–on switching with a redox active guest was the orthogonal lumophore–receptor system **59** with Ag(I).[97] The understanding of the behavior of **59** appears less problematic than that of **53** discussed earlier. In the Ag(I) complex of **59**, EET complications are absent and PET processes between the Ag(I) center and the acridinium lumo-phore can be estimated to be difficult in either direction. On the other hand, the PET-type process from the $N$-phenyl azacrown receptor to the acridinium lumo-phore in Ag(I)-free **59** is strongly allowed. The tables are turned upon entry of Ag(I) owing to the strong Ag(I)–N interaction. More generally, the scope of luminescent PET sensors/switches can be significantly increased by including orthogonal
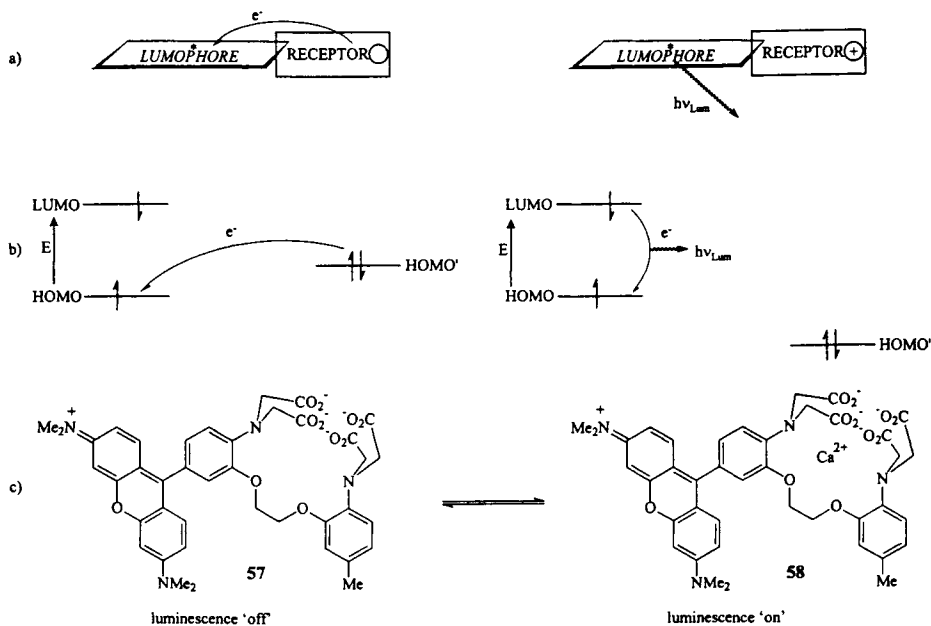
**Figure 4.** (a) Schematic representation of the orthogonal two-module format of an ionically switchable photoactive dyad. The simple picture presented here in terms of an electron transfer driven by excitation localized in the lumophore is convenient and sufficient for our purposes. A more sophisticated picture acknowledges the importance of twisted internal charge transfer (TICT) excited states in the photophysics of these systems, even those these states are rarely emissive in ionically switchable cases. Given this simplification, the arguments parallel those in Figure 1. (b) Frontier molecular orbital energy diagrams corresponding to the simple picture in part (a). (c) An example illustrating the principles of parts (a) and (b) from the work of Tsien and colleagues. The luminescence is switched "on" only when $Ca^{2+}$ binds to the amino-carboxylate receptor.

lumophore–receptor systems. At a fundamental level, this allows a meeting of two major principles of modern photochemistry—PET[42-47] and twisted intramolecular charge transfer (TICT).[157,158] The latter principle encompasses lumophore–receptor systems which can pass into an orthogonal arrangement in the excited state. System **57** and relatives are sterically preorganized for such an evolution. On the other hand there are a number of cases with no such preorganization such as **60** whose behavior can nevertheless be rationalized according to TICT ideas. The reader is referred to the extensive work by Lapouyade and Rettig[159,160] for detailed discussions of these very interesting systems.

**59**

**60**
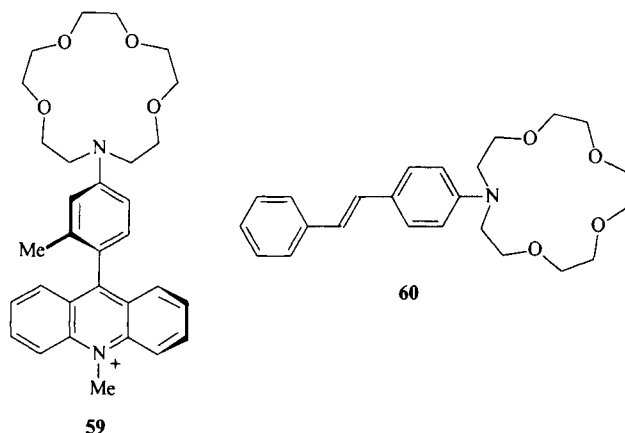
# 8.  INTEGRATED LUMOPHORE–RECEPTOR SYSTEMS

These systems are outside the scope of the present review for several reasons. Since the lumophore and the receptor merge almost seamlessly, they cannot be classed as supramolecular systems in a structural and compartmental sense. In fact, the only supramolecular feature is in the binding of guest ions. Mechanistically these systems cannot involve PET processes since the components needed for electron transfer are not clearly distinguishable (however, see Section 7 where the components can emerge in the excited state). Even from a behavioral viewpoint, integrated lumophore–receptor systems do not fit with the rest of this review since they do not display ion-induced off–on switching or a simple variant thereof. In spite of all these arguments, the sheer quantity and quality (in terms of utility) of these systems demands at least a brief discussion to see the bulk of this review in perspective.

Figure 5 outlines a relevant representation of integrated lumophore–receptor systems. System **61**,[161] for example, switches from a red emission to yellow when protonated, and would be typical in that the excited state has internal charge transfer (ICT) character. Such excited states were encountered as an important adjunct to lumophore–spacer–receptor systems in Section 4. In contrast, ICT excited states are the very heart of integrated lumophore–receptor systems. It is the excited state dipole which interacts with the ionic guest to give rise to the spectral shift observed. However the same interaction can lead to guest ejection from the receptor. Unfortunately for sensing applications, many of the cases available to date develop the positive terminal of the excited state dipole adjacent to the cation receptor. Elegant studies by Valeur[24,25] and Lapouyade[23] have detailed the disengagement process for metal ions, the precedent being set for protons by Gutman and Huppert.[22] Only a handful of examples escape the consequences of this action, i.e. the erasure of ion-induced shift in the emission spectrum. System **61** is one of these atypical examples for proton guests, whereas **63** is a similar rarity for $Ca^{2+}$ guests[91] (see
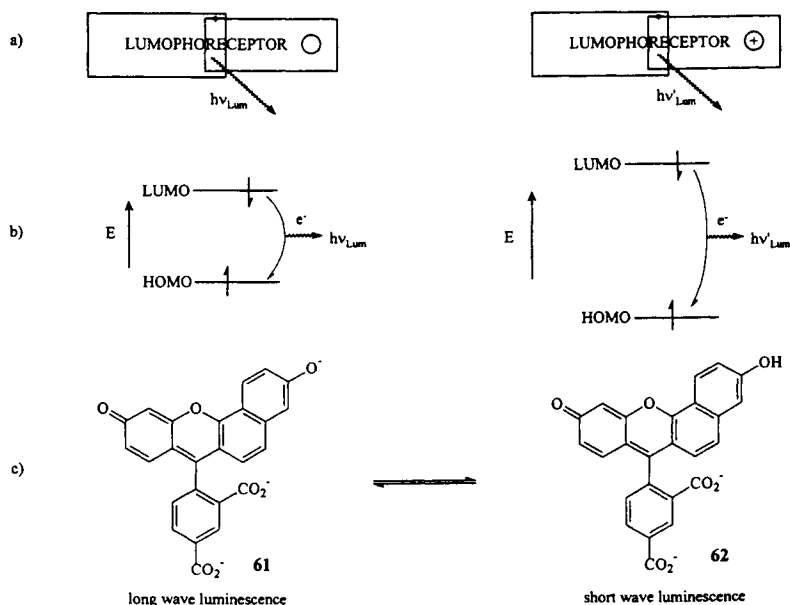
**Figure 5.** (a) Schematic representation of the integral format of an ionically switchable photoactive system. Note that the lumophore and the receptor overlap considerably, preventing their separate identification with any confidence. The excitation (∗) is delocalized over most, if not all, of the molecular π-electron system. The sole supramolecular aspect of these cases emerges only in terms of binding the guest ion. Furthermore the luminescence of these systems are not generally switchable in an "off–on" or "on–off" sense even though many show intensity variations. Rather, the switching is from one wavelength range to another. Even here, complications emerge and practical cases are uncommon. The common cases, of which there are many, show ion-controlled switching from one wavelength to another in the luminescence excitation spectrum but not in emission. (b) Frontier molecular orbital energy diagrams corresponding to part (a). An example illustrating the principles of parts (a) and (b) from work at Molecular Probes Inc. The luminescence shifts from red to yellow when the system is protonated.

Section 13) and **64** is successful for $Na^+$.[162] All this notwithstanding, several integrated lumophore–receptor systems, e.g. **65**,[91] have been persuaded to act as cation sensors in physiology with respect to their excitation spectra. The influence of these sensors have been immense and Tsien has been a pioneer in this general area.[90,12,163]

There have also been some recent developments which promise interesting offshoots. $Ca^{2+}$-sensitive **66**[99] has the tried-and-tested features of **65** along with a new twist. The $Ca^{2+}$-induced conformational change alters the lumophore structure from resembling a rhodamine to a fluorescein lookalike. Not only does **66** maintain
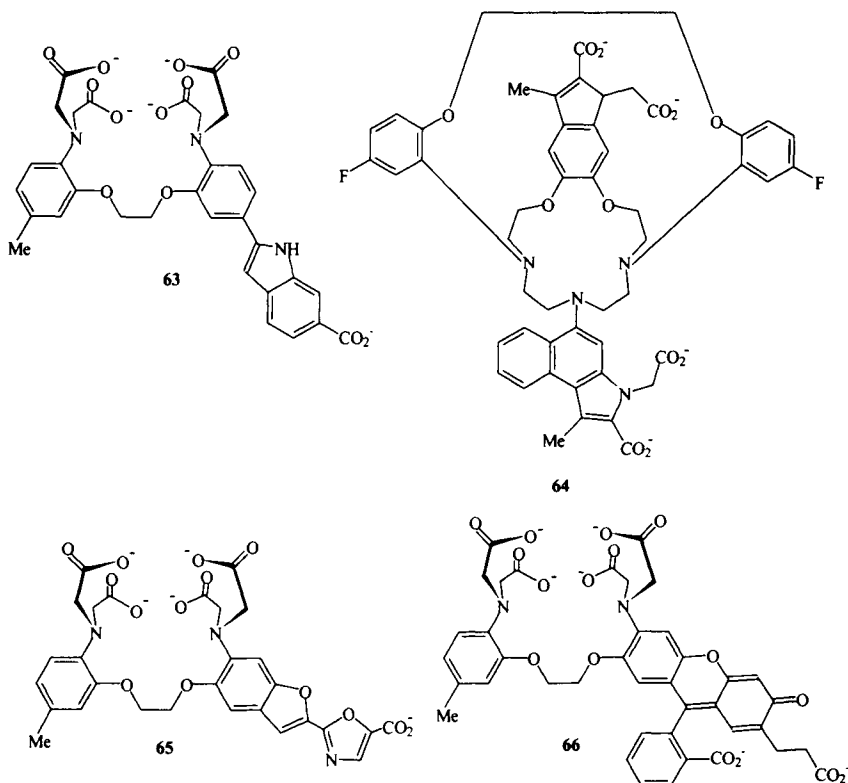
the ratiometric advantage for sensing purposes (Section 13), but it also switches between two lumophores beloved to biochemists. Furthermore, the ratiometry is successful in the emission mode. Some formally integrated lumophore–receptor systems can also include segregatory features. The heart of the proton receptor in **67**[164] is not only remote from the Ru(II) terpyridyl lumophore, but its lone electron pairs are separated from the π-electron system at least to a first approximation.[165] Also, a biaryl link[166] is interposed between the two regions. This example shows a remarkable proton-induced lengthening of the typically short emission lifetime of the Ru(II) terpyridyl center as well as a red shifted emission expected for an integrated lumophore–receptor system of this general type. A relative stabilization of the MLCT excited state relative to the nonemissive metal-centered excited state is one of the causes of this remarkable behavior.

The positive electrostatic charge of Ru(II) polypyridyl complexes has been combined with hydrogen-bond donating primary carboxamide groups in Beer's **68**[167] to yield anion-sensitive luminescent systems. Structural variations have allowed strong biasing of $Cl^-/H_2PO_4^-$ selectivity in either direction. Macrocyclic **69** also raises interesting questions about PET/EET processes (Section 13) across

**67**

**68**

**69**

**70**
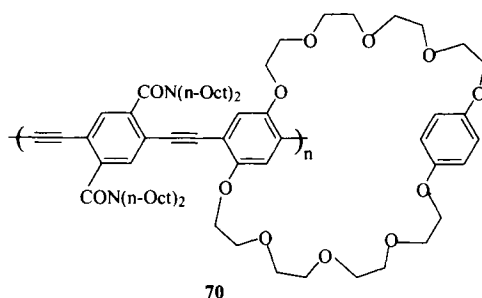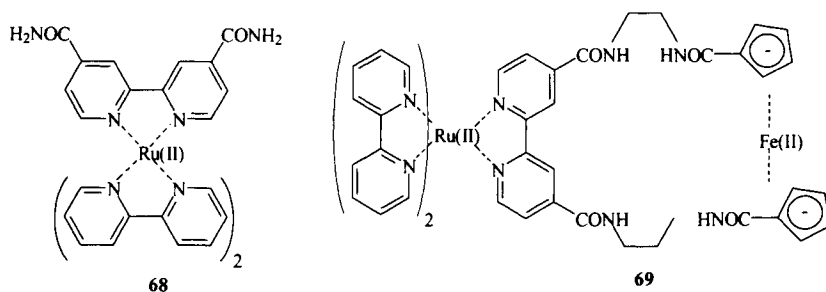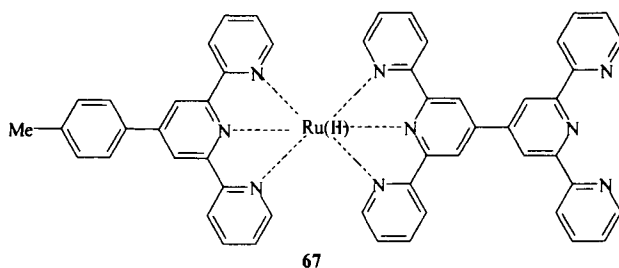
mediating guests. However there is no question about the success of anion-induced luminescent switching action in these cases.

The final call on this whistle-stop tour concerns an extension of integrated lumophore–receptor systems, in both a conceptual and a literal sense, with polymeric lumophores. Swager's **70**[168] employs a poly(phenyleneethynylene) lumophore, where the excitation can be widely delocalized, with an inbuilt benzocrown ether receptor. Upon entry of $N,N'$-dimethyl-4,4'-bipyridyl guest ion,[54] the emission is quenched by a PET-type CT interaction. The on–off switching is particularly efficient because the exciton can be ambushed over a long section of the polylumophore corresponding to the exciton diffusion length. Further adaptations of polylumophores for switching/sensing applications are eagerly awaited.

The vibrancy of integrated systems, as illustrated by these diverse examples, serves as a counterpoint to the more overtly supramolecular systems under discussion in this review.

## 9.  SHIELDED LUMOPHORE–SPACER–RECEPTOR SYSTEMS

The modular construction of lumophore–spacer–receptor systems allows the use of intrinsically delicate lumophores since they can be selectively shielded from the ravages of the environment while leaving the receptor exposed for the necessary interaction with guest ions. Of course, the shield module must be transparent to the incoming and outgoing photons as they interact with the lumophore. Such regioselective self-assembly of the luminescent system with the shield module can be arranged in aqueous solution by ensuring that the lumophore unit is more hydrophobic than the receptor component. Usually, the shield presents an externally hydrophilic face while possessing a hydrophobic interior. While several macrocyclic hosts fit the bill, β-cyclodextrin has been the most successful in the current context. Figure 6 details the mode of operation of such a shielded system. Before proceeding any further, it is important to discuss why shielded systems can be particularly useful. Several classes of lumophore need protection from the very environment in which they must operate. When protection is provided, these lumophores display their true colors which can be rather unique. The case of lanthanide ions will be taken up in Section 11. Our spotlight here is on organic phosphors. These are notoriously sensitive to emission quenching in fluid solution, partly because of their intrinsically long excited-state lifetime.[169] However, such long lifetimes in the millisecond range can be put to good use since the output signal from a phosphorescent device would outlive any competing signals arising from matrix autofluorescence or scattering. Pulse excitation and delayed observation can thus cut through environmentally generated noise. System **71** is such a case where the bromonaphthalene component displays phosphorescence off–on switching when protons bind to the amine receptor.[170] As discussed in the Figure 6 legend, PET processes can occur either before or after the lowest triplet excited state is reached following the population of the lowest excited singlet. It is gratifying that **71** is experimentally well-behaved in spite of this mechanistic dilemma. "Message in a bottle" systems such as **71** are bound to multiply since they combine attractive

*Figure 6.* (a) Schematic representation of the four-module format of an ionically switchable photoactive dyad. This requires a shield module owing to the exceptional sensitivity of its emissive state towards collisional quenching. However, this emission can be put to good use, as discussed in the text. In many respects however, the situation in Figure 1 is applicable here. Note that the relative position of the dyad with respect to the shield can depend on whether the receptor is ion-bound or not.  (continued)
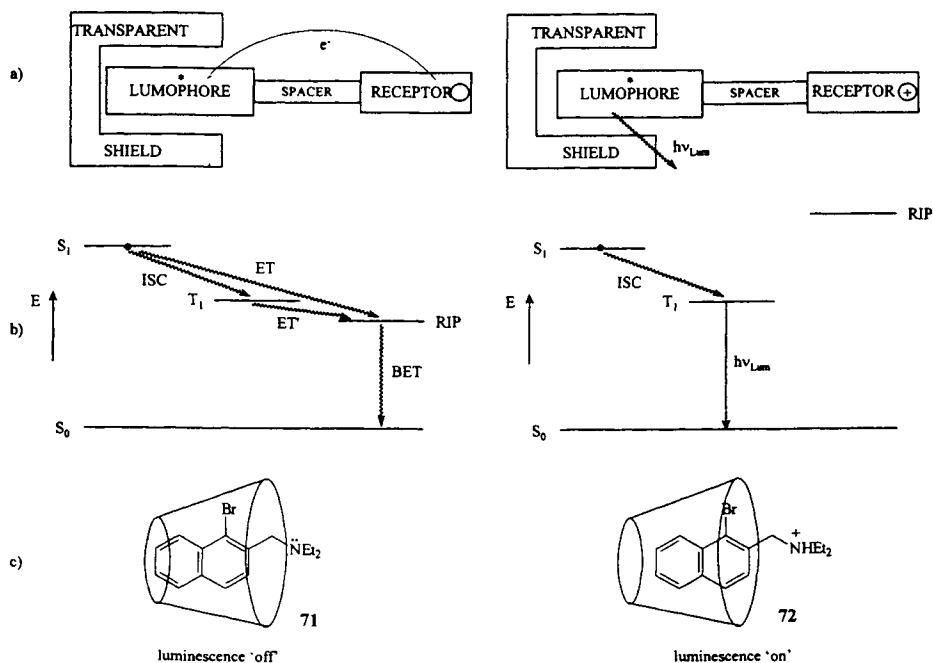
**Figure 6.** (continued) (b) State energy diagrams corresponding to part (a). Note that many of these higher generation systems in this and the following figures are developed without frontier molecular orbital energy diagrams since they are either easily obtained as combinations of earlier figures or because, as in the present case, state energy diagrams are more appropriate. In the present case, ground ($S_0$), first excited singlet ($S_1$) and triplet states ($T_1$) of the lumophore are involved along with the electron transferred radical ion pair state (RIP). All nonradiative processes are understood to be adiabatic in spite of the simpler representation which is used for clarity. Two electron transfer processes are possible when the receptor is free of ionic guests. One (ET) occurs from $S_1$ in competition with the rather rapid intersystem crossing (ISC) which usually overpowers any emission (fluorescence) from $S_1$ in well-designed instances. This electron transfer pathway is rather exergonic. The other electron transfer route (ET') occurs from $T_1$ in competition with the rather slow luminescence (phosphorescence). ET' is fast enough to win this competition even if it is substantially endergonic (though a slightly exergonic case is shown). The RIP state undergoes fast back electron transfer (BET) to recover the ground state. This is common to all the cases discussed in this chapter. The electron transfer processes come to a virtual standstill when the receptor is bound to a guest ion. Now the RIP state is at inaccessibly high energies and luminescence emerges from $T_1$ unopposed (except for unavoidable $T_1$–$S_0$ nonradiative processes intrinsic to the lumophore). (c) An example illustrating the principles of parts (a) and (b) from the cyclodextrin-complexed aminomethyl bromoaromatic family. The luminescence is switched "off" when the amine unit is unprotonated. The switching "on" takes place upon protonation.

self-assembly schemes with very useful switchable luminescence. Shielded phosphors have also been cleverly exploited by Nocera where they trap a third component such as an alcohol to unleash phosphorescence.[171] The facts that near-zero backgrounds and aerated solutions are involved add to the attraction. Variations with ionic guests are likely to be on their way.

# 10.  TARGETED LUMOPHORE–SPACER–RECEPTOR SYSTEMS

It is possible to develop the potential of molecular luminescent devices for mapping of ion densities at molecular-scale distances. The basic lumophore–spacer–receptor dyad can be expanded by adding targeting and anchoring modules (Figure 7) so that the receptor can be positioned to observe guest ions in microheterogeneous fields. A large family of fluorescent PET sensors, e.g. **73**,[34] which act as molecular submarines located near the membrane–water interface at various depths are now available. Thus the effective local pH can be easily obtained as a function of position of the molecular submarine periscope. Large variations of the local pH over 2–3 units are seen as the molecular periscope is brought very close to the membrane. Such results support the theories of bioenergetics highlighted by Mitchell and by Williams[17c] where membrane-bounded proton gradients fuel the generation of ATP, the universal energy provider in biology. System **73** and its relatives can provide molecular tools for researchers in this area.

The targeting modules in **73** enable it to find its own way to a particular location with respect to the membrane which is a self-assembled polymer. While the self-organizing aspect of **73** is highlighted in this application, the location of the sensory supermolecule can be fixed by covalent attachment to a conventional (covalently constructed) polymer. The mysteries of polymer tertiary structure will, of course, remain. Nevertheless, such polymer-bound luminescent devices are of considerable interest. In the case of soluble polymers, especially those which are ionic, many principles can be carried over from membrane science. One of these is that the polyion will concentrate counterions near its surface. Thus the appended sensory supermolecule will show an increased sensitivity. This general point can be illustrated from the work of Shirai et al.[172] with **75**, even though some related studies with unattached lumophores have been available from Kimura and Smid since 1981.[173] This idea can be extended by employing strongly switchable PET-based luminescent systems. For example, **76a**,[174] which is a polymer-attached version of the 10-year-old **77**,[175] shows a significant luminescence enhancement factor of 2.5 upon addition of K$^+$. The free acid form **76b** can only respond with a small decrease of emission due to the ion exchange of the receptor-bound protons. It will only be a matter of time before cross-linked, and insoluble, versions are examined for use at the tips of fiber-optic macrodevices.
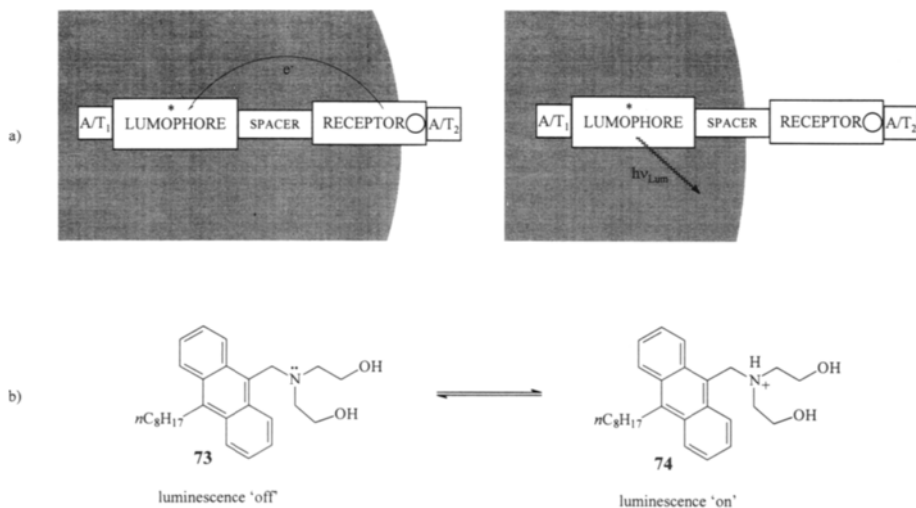
**Figure 7.** (a) Schematic representation of the five-module format of an ionically switchable photoactive dyad which can be targeted to a microlocation. This requires two anchoring/targeting molecules (A/T$_1$ and A/T$_2$) at the terminals. The one near the receptor controls fine positioning since the receptor is responsible for sampling the guest ion density, i.e. the concentration information pertains to the exact location of the receptor. A/T$_1$ serves a gross anchoring role once it has driven the system to the approximate location in the microheterogeneous field. The electron transfer characteristics and their control by the guest ion are similar to that given in Figure 1. Note that the relative position of the dyad with respect to the pseudo-phase boundary can depend on whether the receptor is ion-bound or not. This means that the guest ion concentration information comes from an averaged position of the receptor. (b) An example illustrating the principles of part (a) from the aminomethyl aromatic family. The luminescence is switched "off" unless the receptor is in a region of high enough proton density.

Organic polymers are attractive as matrices for the attachment of switchable luminescent devices at least partly because of their synthetic versatility. At the same time, inorganic polymers possess the attraction of robustness. This is one of the driving forces for the development of silica-attached luminescent switches. Aminopropyl silica particles, commercially available as a chromatography phase, can be synthetically elaborated into a lumophore–spacer–receptor system **78**.[176] Naturally, its emission intensity–pH profile is displaced relative to silica-free model compounds but the proton-induced off–on switching is preserved. Low coverages regarding the lumophore and the capping of the unreacted aminopropyl groups are conducive to good proton-induced switching behavior. System **78** is currently

**75**

**76a; R=Li**
**76b; R=H**

**77**

**78**
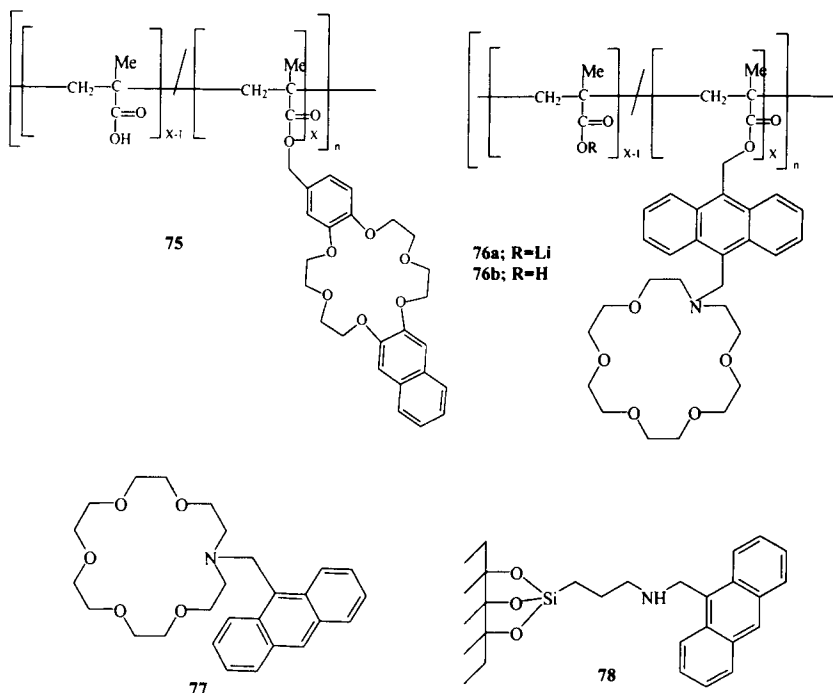
employed as a suspension which can be filtered off and reused. Furthermore, the potential exists for integration into fiber-optic systems. A precedent has been set by the attachment of a single-controlled pore glass (CPG) bead to a single fiber where the pH-sensitive lumophore fluorescein was covalently bound to the aminopropyl groups on the CPG surface.[177] So it seems reasonable to conclude that the cases discussed here have only scratched the surface of what is possible with targeted and anchored lumophore–spacer–receptor systems.

## 11. LUMOPHORE–RECEPTOR₁–SPACER–RECEPTOR₂ SYSTEMS

Almost all the examples discussed so far use covalent bonds to hold the receptor at a reasonable distance from the lumophore. However, alternative strategies are available. For instance, receptor$_2$ selective for the guest ion of interest may be covalently linked to another receptor$_1$ which is chosen for its ability to selectively bind a lumophore. This approach has the reward of versatility. Once synthesized, the receptor$_1$–spacer–receptor$_2$ system may be combined with any one of several different lumophores with a range of optical properties. Any enthusiasm this may generate must be tempered because this approach can also have its dangers due to

insufficient selectivities. This notwithstanding, progress is possible on several fronts.

For example, the success of ionically switchable PET-based lumophore–spacer–receptor systems[39,40] can be transplanted into the field of lanthanide delayed luminescence.[178] This idea has been buoyed up by the continuing success of delayed luminescence immunoassay in providing an alternative to radioimmunoassay as a medical diagnostic tool.[179] Therefore delayed luminescent PET sensors/switches would carry over the advantages of time-resolved observation into general ion monitoring by entirely avoiding interference from matrix autofluorescence and light scattering. The design is best illustrated by comparing it (Figure 8) to the parent system (Figure 1). The receptor₁ serves to bind the lanthanide ion strongly and to protect it from water. The latter function is important for maximizing the luminescence quantum yield by suppressing energy loss via O–H vibrators,[180] though proximal N–H and C–H vibrators remain.[7] Receptor₁ also serves as a photon antenna since lanthanide ions are intrinsically poor photon absorbers. It is clear that the PET process has two possible paths terminating at either the antenna or at the lanthanide center. Shinkai has independently examined lanthanide delayed luminescence of **81** in the context of switchable PET processes even though his emphasis was on uncovering the source of the antenna effect.[182]

Excitation at the longest wavelength possible is a practical consideration in biological and medical investigations since competitive light absorption by the matrix can be reduced. In the field of lanthanide sensitizers, the excitation wavelength limit is still at the blue edge of the visible spectrum. The terpyridyl-based luminescent label developed by Toner[183] absorbs at 340 nm and its Eu(III) complex provides excellent detection limits in immunoassay procedures.[184] This label has now been modified so that it would carry a receptor selective for $H^+$ (against $Ln^{3+}$)—in this case a tertiary amine proved to be adequate. The delayed luminescence of **79** shows clear off–on switching as the pH of the medium is swept across the $pK_a$ value of the amine side chain towards more acidic values.[185] Acid and base



calix[4]arene

**81**
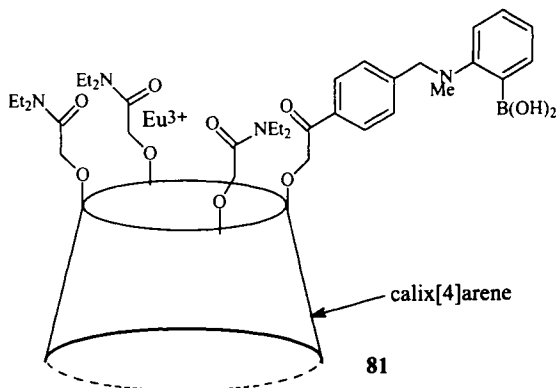
hydrolysis of lanthanide complexes can also lead to pH-dependent luminescence,[186] but such collapse of complexes is not meant for continuous sensing. System **80** and its relatives have rather long emission lifetimes of ~0.6 ms and high luminescence quantum yields (~0.5) in the "on" state. The long emission lifetime is of special interest to industrialists since sensors based on lifetime (rather than on emission intensity) can be constructed with low-cost, modulated light-emitting diodes (LEDs). Lifetime sensing of ions, so far only available for fluorescence[66,67] where LED modulation is not feasible, carries an internal reference for self-calibration (unlike simple intensity sensing) which makes them immune to microenvironmental variations in optical path, sensor incorporation, and quencher concentration.

Lanthanide ion lumophores have also been included in receptor$_1$–spacer–receptor$_2$ systems outside of the PET design principle. Nocera has targeted ionic or nonionic aromatic guests.[187–189] The aromatic character of the guest is critical since receptor$_2$ (as well as receptor$_1$) is chosen to be optically transparent in this scheme. Since the guest serves to receive photonic excitation for subsequent EET to the lanthanide lumophore, the guest switches the luminescence "on."

Organic lumophores can also be used in conjunction with receptor$_1$–spacer–receptor$_2$ systems. Aminoalkyl cyclodextrins are particularly suitable in this regard since amines and cyclodextrins show almost mutually exclusive receptor properties.

---

*Figure 8.* (a) Schematic representation of the four-module format of an ionically switchable photoactive dyad. Several points in Figure 6 are seen here. However the lumophore (L) in the present case is an atomic species, usually a trivalent lanthanide ion. The receptor$_1$ module not only holds L but it also serves to receive photonic excitation which is then transferred as electronic energy (EET) to L which is otherwise a poor photon absorber. Receptor$_1$ also shields L from excessive hydration and luminescence quenching arising therefrom. The EET symbol is reserved for this key sensitization process from the receptor$_1$ to L, even though there are other electronic energy transfer processes occurring between, e.g. S$_1$ and T$_1$ which is labeled an ISC. Note that receptor$_1$ selectively binds L, whereas receptor$_2$ chooses the ionic guest when it is available in sufficient concentration. This system can have two electron transfer routes from the receptor$_2$ module (when it is free of guest ion). The first of these has the receptor$_1$ module as the final destination, the lumophore metal only becoming directly involved in the case of any luminescence emission. The other electron transfer process terminates at L either directly or with involvement of receptor$_1$. In the latter instance superexchange or a discrete intermediate is possible. The latter situation has some similarity with the first electron transfer route. (b) and (c) State energy diagrams corresponding to the two electron transfer routes in part (a). Only the essential processes are shown for clarity. Further, only the more common situation of T$_1$ sensitization of the metal centered excited state (MC) of the lumophore is shown. Part (b) is nearly identical to the situation in Figure 6(b) except that EET to the MC intercepts the T$_1$ state of receptor$_1$ thus preventing any phosphorescence emission.
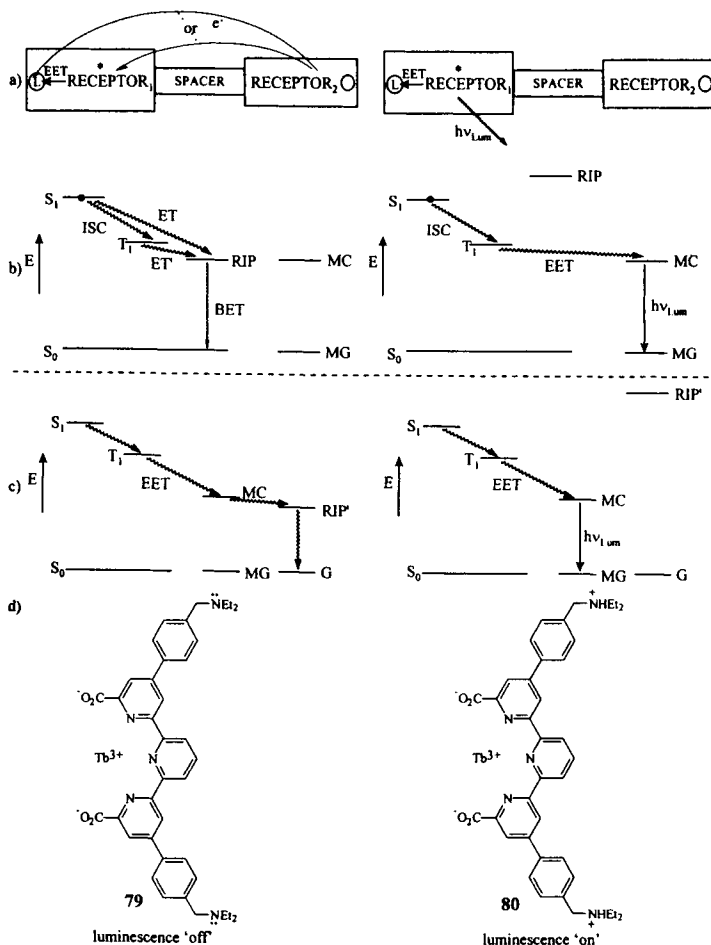
**Figure 8.** (Continued) This applies when the receptor₂ is bound to the guest ion. The lumophore MC state emits luminescence and returns to the ground state of the lanthanide metal ion (MG). When receptor₂ is free of guest ions, the MC state is not significantly populated due to the rapid diversion of $T_1$ energy via the electron transfer ET'. Part (c) has some significant differences from part (b). Now the electron transfer process (ET) is powered by the MC state and involves oxidation state changes in the lanthanide. The electron-transferred radical ion-pair state (RIP') is so described to maintain consistency with Figure 6 even though a lanthanide ion oxidation state and a receptor₂ radical ion are the relevant partners. In particular, the RIP' state has contributions from both the organic and inorganic electron systems. The back electron transfer (BET) from RIP' returns both these systems to their respective electronic ground states, collectively labeled G. (d) An example illustrating the principles of parts (a) and (b) but not (c) from a family of aminomethyl terpyridyl complexes with terbium (III). The luminescence is switched "on" only when both the amine units are protonated.

Yoshida et al.[190] used anilinonaphthalene sulfonate derivatives as lumophores. These have a history of emission switching "on" when included in cyclodextrin and other hydrophobic cavities away from aqueous solution.[191,192] Such cases usually show pH-independent emission. However, the derivatization of the cyclodextrin with aminoalkyl units leads to marked pH-dependent emission from the same lumophores as guests. PET processes do not appear to be involved. Instead, the different abilities of aminoalkyl sidechains to act as caps in their different protonation states control the extent of binding of the anionic lumophore. We find that suitable combinations of aminoalkyl cyclodextrins and aromatic lumophores can yield proton-induced switching behavior reminiscent of PET schemes, though with reduced efficiency.[193] Taken together, these examples suggest an interesting future for switchable luminescent devices which sacrifice some key covalent bonds in order to make new connections.

## 12. LUMOPHORE–SPACER$_1$–RECEPTOR$_1$– SPACER$_2$–RECEPTOR$_2$ SYSTEMS

After establishing the concept of switchable luminescent PET systems, it is possible to design and build advanced versions which begin to display features previously seen only in electronic devices of various types. For example, consider the photoionic AND logic gate **82** (Figure 9). Molecules which are inherently capable of logic functions are important, especially so since their two switchable states are so easily observed visually to be "on" or "off" via the "high" or "low" level of fluorescence. These systems begin to mimic the action of solid-state electronic logic gates[200] which triggered the electronic computer revolution. The fluorescence output of **82** switches "on" only if H$^+$ and Na$^+$ are both simultaneously present at high concentrations, i.e. if [H$^+$] > 10$^{-4}$ M and [Na$^+$] > 10$^{-2}$ M. The corresponding truth table is shown in Figure 10. Such a system with the lumophore–spacer$_1$–receptor$_1$–spacer$_2$–receptor$_2$ format would then have a fluorescence quenching PET channel even if a single-receptor module was unoccupied by its corresponding cation (Figure 9). **82**[194] could be confidently designed on the foundations laid by its first-generation precursors **1**[39,68] for H$^+$ and **84**[82] for Na$^+$.

The predictive power of the luminescent PET sensor principle is again apparent here. Further, the benzocrown ether and the amine receptors would selectively bind Na$^+$ and H$^+$, respectively. A remarkable feature here is that no molecular "wiring" is needed to allow the human operation of this two-input molecular device. The device self-selects its own ion inputs into the appropriate signal channels by means of the chemoselective receptor modules. Since the output signal is fluorescence, even a single molecule can interface with detectors in the human domain, including the dark-adapted eye. Tanaka's **45**[133] is another example where fluorescence quenching is achieved only when Ba$^{2+}$ and SCN$^-$ are present. This was mentioned in Section 6. Similarly, several sensor systems—**1, 17,** and **21**—could be employed
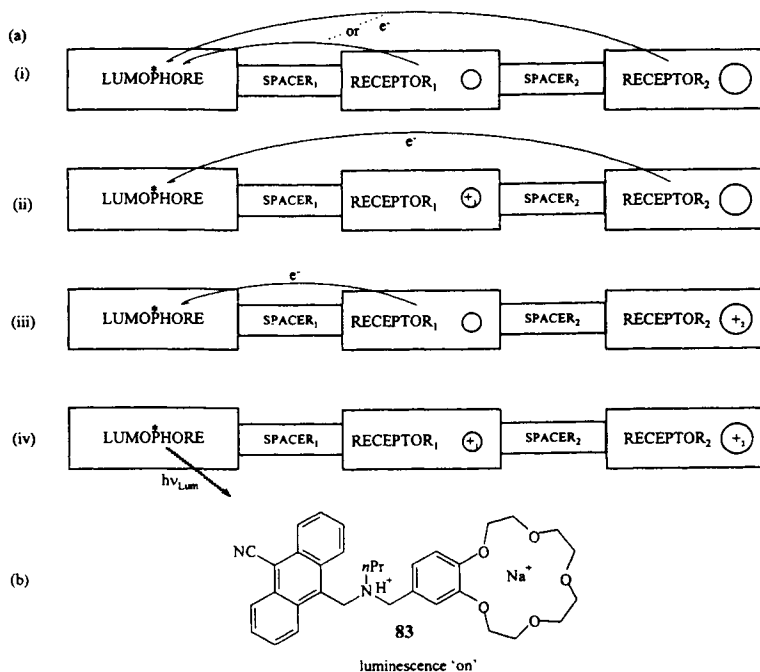
**Figure 9.** (a) Schematic representation of the five-module format of a photoactive triad which is switchable only by the simultaneous presence of a pair of ions. This design involves the multiple application of the ideas in Figure 1. The four distinct situations are shown. Note that the presence of each guest ion in its selective receptor only suppresses that particular electron transfer path. The mutually exclusive selectivity of each receptor is symbolized by the different hole sizes. All electron transfer activity ceases when both guest ions have been received by the appropriate receptors. The case is an AND logic gate at the molecular scale. While this uses only two ionic inputs, the principle established here should be extensible to accommodate three inputs or more. (b) An example illustrating the principles of part (a) from an extension of the aminomethyl aromatic family. The case shown applies to the situation (iv) in part (a) where both receptors are occupied. It is only then that luminescence is switched "on". Protons and sodium ions are the relevant ionic inputs.

as pass (YES), NOT, and OR logic devices, respectively. Figure 10 summarizes these along with their truth tables. System 1, discussed in Figure 1, is the archetypal fluorescent PET system whose fluorescence is switched "off" due to a designed PET process if $H^+$ levels are low, but its fluorescence flares up to the "on" state when $H^+$ levels are high enough to bind with the receptor. The threshold level of $H^+$ can be set by choosing $H^+$ receptors of different strengths or $pK_a$ values. The NOT device uses a PET process which springs into action only when the chosen
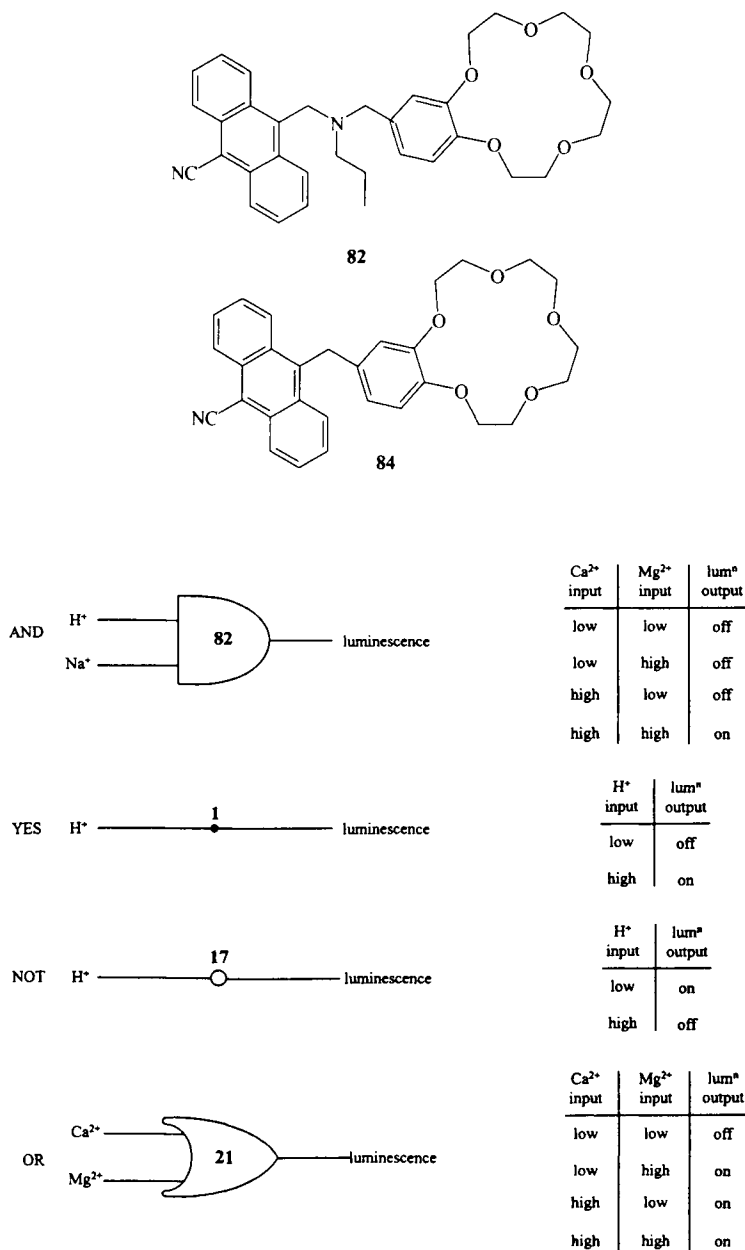
82

84



**Figure 10.** Schematic representation of four common types of ion input–photon output in terms of the symbols commonly encountered in electronics. Their corresponding truth tables are also given in terms of chemically/physically measurable quantities.

ion lodges in the receptor, thereby quenching the fluorescence. Thus **17**, discussed in Figure 2, shows strong fluorescence when $H^+$ is at a low level. When the $H^+$ input is high, the fluorescence output collapses. OR photoionic devices take advantage of poor chemoselectivity of an ion receptor. In fact, the ideal photoionic OR gate should have a completely unselective receptor. System **21** illustrates the approach by achieving a nearly constant quantum yield of fluorescence in the "on" state when high levels of either $Mg^{2+}$ or $Ca^{2+}$ are supplied. As discussed in Section 4, **21** is a very selective luminescent sensor for $Mg^{2+}$ over $Ca^{2+}$ under simulated physiological conditions. Nevertheless, it also provides almost perfectly unselective switching of luminescence intensity if both ions are used at high enough concentrations.[88] It is remarkable that one molecule can cater to these different requirements of physiological monitoring and information processing. The reason for the unselective switching of luminescence quantum yield is that both $Mg^{2+}$ and $Ca^{2+}$ induce the same conformational change in the receptor module of **21**, i.e. the extent of PET suppression is virtually the same and guest charge density effects are negligible. Bharadwaj's **53** is a more recent example[147] whose interesting features were discussed in Section 6.

These cases represent the beginnings of a family of molecular logic operations which is unique when elegant developments elsewhere are considered: Potember's photonic logic operations require a macroscopic gel-derived glass matrix;[195] Wasielewski's molecular system is promising but logic functions are yet to be demonstrated;[196] and Wild's logic operations rely on physical image superposition rather than on molecular characteristics.[197] It is important to notice that the chosen logic function is pre-programmed into molecules **82, 1, 17, 21, 45**, and **53** at the synthesis stage.

System **82** is also useful from the vantage point of molecular sensors for biological use. The simultaneous presence of two ions could be optically signaled by a second generation PET device employing two separately selective receptors. In addition, **82** is a valuable prototype for the fluorescent sensing of synergistic situations. Of course, biology abounds with examples of synergy which can now be rationally targeted by device designers.

Lumophore–spacer$_1$–receptor$_1$–spacer$_2$–receptor$_2$ systems can also be exploited in other ways. For instance, we can choose the two receptors for the same ionic guest, though with different affinities, to have opposite PET characteristics; i.e. one of them will combine with the lumophore to produce guest-ion-induced off–on behavior, whereas the other receptor will give rise to on–off action at the lumophore. The integration of these two opposite switching functions within a single supermolecule produces "off–on–off" behavior (Figure 11). This means that luminescence is seen only over a narrow range of ion concentrations. Such sensors are sophisticated enough to directly indicate the occurrence of a concentration window with no signal processing. This means that when a large visual field is examined, regions which satisfy the concentration window criterion will announce themselves with a bright luminescence. Concentration windows for chemical species are
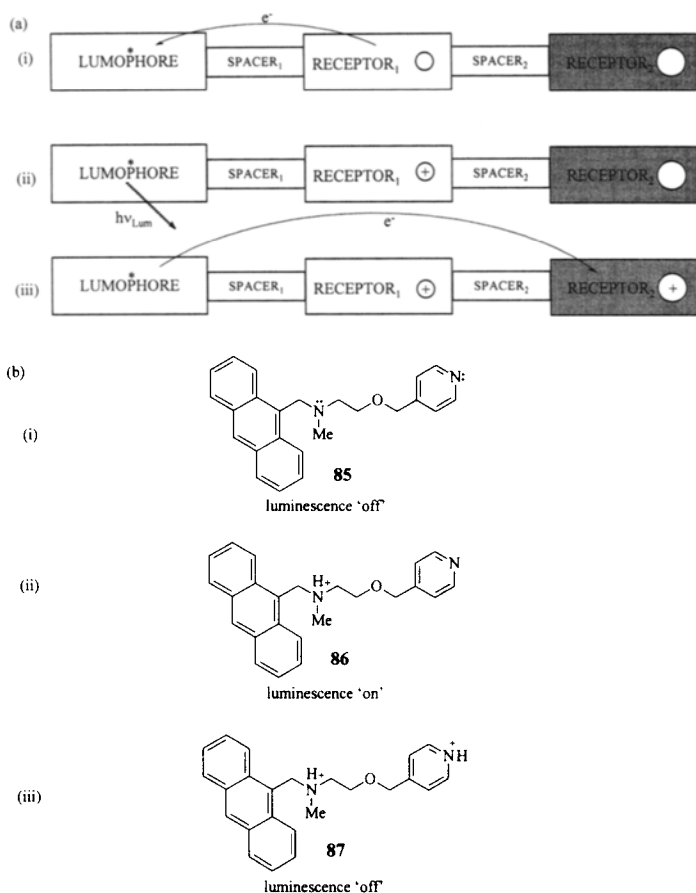
**Figure 11.** (a) Schematic representation of the five-module format of a photoactive triad which is ionically switchable in an "off–on–off" manner. These systems are switched "on" only within a concentration window of the guest ion. This design combines features of the Figures 1 and 2. Note that both receptors select the same guest ion (though at different concentrations thresholds). We have tried to symbolize this by showing both receptors with identical hole sizes. However the two receptors have opposite electron transfer properties. Receptor1 supports electron transfer only when it is free of the guest ion and then it serves as an electron donor. Receptor2 supports electron transfer only when it is bound to the guest ion and then it serves as an electron acceptor. This difference is symbolized by the different shading of the receptor components. Increasing concentrations of the guest ion lead to the three situations (i–iii) shown. Receptor1 traps the guest ion at lower concentrations than receptor2 does. (b) An example illustrating the principles of part (a) from an extension of the aminomethyl aromatic family. The three protonation states (i–iii) corresponding to the three situations in part (a) are shown. In order that the luminescence is switched "on", the amine unit should be protonated and the pyridine unit should not, i.e. the pH should be such that $pK_{a,R2} < pH < pK_{a,R1}$.

common, indeed essential, in living systems. For instance, the blood pH in humans is held close to 7.2 within very narrow limits.[198] So, off–on–off sensors are useful for the rapid screening of (micro)environments for their suitability to sustain biological[198] and some chemical processes. Schiff-base hydrolysis[199] is an example of the latter category. Quite separately, off–on–off switches have interesting similarities with the current–voltage characteristics of tunnel diodes in electronics.[200] Tunnel diodes are remarkable since they achieve negative resistance over a certain voltage range. Since molecular emulation of electronic devices is an important chemical endeavor,[10] **86** is a contribution to this field. Figure 11 outlines the design of such an off–on–off switchable system for pH. Protons are the prototype guest ion for the design of such hybrid systems since efficient off–on and on–off cases are available.

System **86** is a molecular example which uses an aminoalkyl aromatic assembly for the off–on segment of the switching, whereas a pyridylalkyl aromatic can be discerned within **86** as the source of the on–off segment. In practice, **86** behaves almost according to plan. The only slight deviation is caused by the incomplete on–off switching due to the rather large separation between the anthracene lumophore and the lumophore and the pyridyl receptor$_2$. Nevertheless, the on–off switching behavior is large enough to be useful.

An additional feature of interest is that the direction of PET is reversed on moving between acidic and basic media. PET occurs from the lumophore under acidic conditions, whereas it occurs to the lumophore at basic pH. While maxima in luminescence intensity–pH profiles have been seen before on many occasions,[201] the designed off–on–off switching of luminescence by external (but intramolecular) receptors is novel. The designed PET approach allows (1) the tuning of the off–on and on–off steps along the pH axis, i.e. the width of the "bell" can be tailored to order, (2) control over the extent of switching, i.e. LE values, and (3) rational extension to other guest ions other than protons. The pH-dependent emission behavior of **67**[164] also shows a component which displays off–on–off action of the Ru(II) terpyridyl moiety due to protonation at the remote terpyridine unit. Other interesting systems with similar formats are available though these have been designed for different purposes. Fabbrizzi's **36**[73] and Verhoewen's **40**[118] are two of these.

## 13. LUMOPHORE₁–SPACER₁–RECEPTOR–SPACER₂–LUMOPHORE₂ SYSTEMS

The growing success of fluorescent sensors in the biomedical sciences is at least partly due to the ability to cancel out microenvironmental fluctuations such as local optical paths, quenching agents, and degrees of sensor incorporation by using ratioing of two optical channels.[12] Most commonly, this means that two excitation wavelengths are used separately, one of which yields ion-sensitive fluorescence and

the other which is largely independent of ion density. Faster sensing is possible if two emission wavelengths can be used instead but practical examples are uncommon. For instance, indo-1 (**63**) is the only calcium sensor which can be currently operated in this mode[12] and only emerged after many structural variations.[202] It is therefore useful to design and build lumophore$_1$–spacer$_1$–receptor–spacer$_2$–lumophore$_2$ systems (responsive to pH in the first instance) with one emission band which is much more pH-sensitive than the other (Figure 12).The emission of the PET inactive lumophore therefore acts as an internal reference channel which allows the calibration of the emission of the PET active lumophore against local environmental fluctuations. This makes available a rational and predictive basis for the design of luminescent switchable devices with the feature of self-calibration.

In the case of **88**,[203] lumophore$_1$(anthracene) is designed to be PET active with the receptor (an aliphatic amine), whereas lumophore$_2$(aminonaphthalimide) is designed to be PET inactive. As predicted, when the anthracene module of these cases is excited they showed strongly pH-dependent anthracene emission, whereas the aminonaphthalimide emission arising via electronic energy transfer (EET) was much less affected by pH. This means that the latter emission serves as an internal reference. Ratioing of these two emissions yields a smooth sigmoidal function versus pH which is immune to microenvironmental variations. Current sensors[12] achieve self-calibration by using one population of sensor molecules (say ion-bound) as the internal reference for the other population of ion-free sensor molecules. Systems such as **88** are distinguished by the fact that internal referencing is
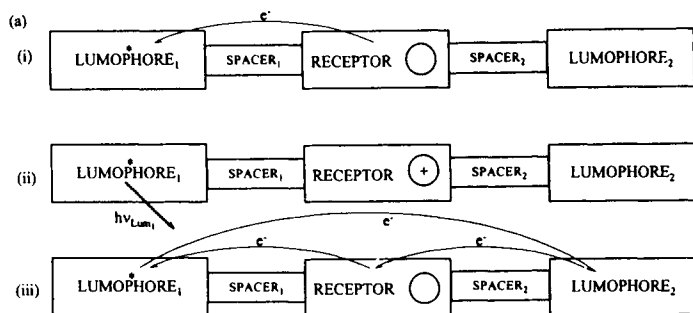


*Figure 12.* (a) Schematic representation of the five-module format of an ion switchable photoactive triad with internal referencing. The two simple situations are shown (i and ii). Situation (iii) is an outgrowth of (i) and represents an electronic energy transfer of the electron exchange type facilitated by the receptor. Direct electronic electron transfer from lumophore₁ to lumophore₂ is not shown even though it occurs in situation (ii) and, with reduced efficiency, in situation (i). These energy transfer paths lead to luminescence emission from lumophore₂. (continued)
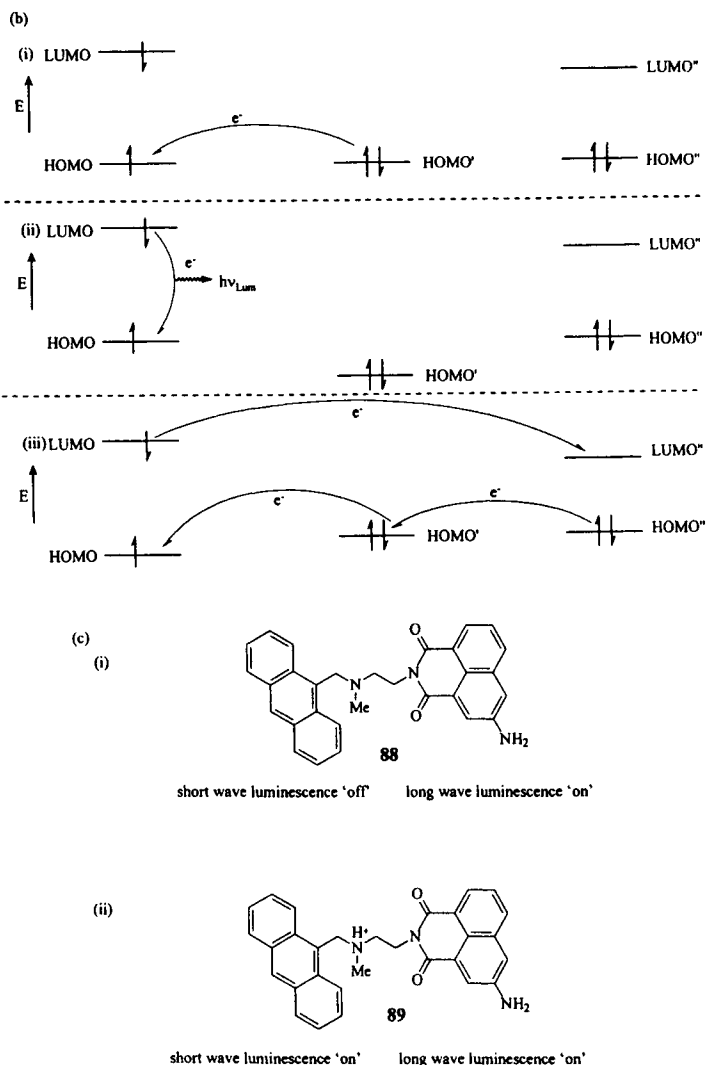
(b)

(i) LUMO

E

HOMO — e⁻ → HOMO'  HOMO"  LUMO"

(ii) LUMO

E

e⁻ → hv_Lum

HOMO  HOMO'  HOMO"  LUMO"

(iii) LUMO

E

e⁻  e⁻  e⁻

HOMO  HOMO'  HOMO"  LUMO"

(c)
(i)

**88**

short wave luminescence 'off'    long wave luminescence 'on'

(ii)

**89**

short wave luminescence 'on'    long wave luminescence 'on'

***Figure 12.*** (continued) (**b**) Frontier molecular orbital energy diagrams corresponding to part (**a**). Note that in situation (i) the energies of HOMO, HOMO', and HOMO" are similar, whereas LUMO" lies lower in energy than LUMO. Situation (ii) may involve electron transfer from HOMO" to HOMO or from LUMO to LUMO" which can quench some of the luminescence from lumophore₁. However such processes are limited by the relatively large distance separating the lumophores. Situation (iii) clarifies the facilitated electronic energy transfer. This process leaves lumophore₁ in its ground state, allowing emission from lumophore₂. (**c**) An example illustrating the principles of situations (i and iii) of parts (**a**) and (**b**) from an extension of the aminomethyl aromatic family. Lumophore₁ with short wave emission is switched "on" only when the receptor unit is protonated. Lumophore₂ maintains its long wave emission in the "on" state whether the amine receptor unit is protonated or not.

45

achieved at the level of the single molecule rather than a large population. This will have ramifications for molecular information handling in the future.[10] Another appealing feature of **88** is as follows. Since the two fluorescence bands are well-separated and since the band shapes and wavelength positions are pH-independent, the sensory and reference channels can accommodate very wide wavelength bands to allow higher light throughput and easier detection. The closest relation in the literature is a polydisperse polymer doubly labeled with the pH-sensitive fluorophore fluorescein and pH-insensitive rhodamine.[204] This is neither a well-characterized small molecule nor is it based on PET designs. Besides its utility for biomonitoring, **88** also shows how the competition between PET and EET is influenced by pH. In particular, **88** acts as a triad system. Some triads have received much attention as solar energy converters.[92] EET in **88** occurs across an intervening electron pair via a "stepping stone" mechanism. Interestingly, this stepping stone can be ionically switched in or out of the EET path. Such experiments will be useful to workers interested in the mechanisms of EET and PET in the photosynthetic reaction center.[42] As mentioned in Section 4, multi-lumophore versions of lumophore–spacer–receptor systems can also produce a pair of spectral observables (monomer and excimer emission) which can be employed for purposes of internally referenced sensing/switching. Therefore it appears that the supramolecular approach to internally referenced luminescent switching devices has only begun.

## 14.  CONCLUSION

The foregoing pages attempted to outline the diverse formats according to which lumophores and receptors can be brought together within a supramolecular structure to result in useful information handling. Each format appears to possess its own niche in terms of mechanistic issues and application areas. The fact that a given format is generic and not limited to structural classes is a driving force for growth. We are left with the inescapable impression that switchable supramolecular photoionic devices are set to shine for a long time to come.

## ACKNOWLEDGMENTS

## REFERENCES AND NOTES

1. Lehn, J.-M. *Supramolecular Chemistry*; VCH: Weinheim, 1995.
2. Lehn, J.-M. *Angew. Chem. Int. Ed. Engl.* **1990**, *29*, 1304.

3. (a) *Supramolecular Photochemistry*; Balzani V., Ed.; Reidel: Dordrecht, 1987; (b) Balzani, V. *Tetrahedron* **1992**, *48*, 10443; (c) Balzani, V.; Credi, A.; Scandola, F. In *Transition Metals in Supramolecular Chemistry*; Fabbrizzi, L.; Poggi, A., Eds.; Kluwer: Dordrecht, 1994.

4. Balzani, V.; Scandola, F. *Supramolecular Photochemistry*; Ellis-Horwood: Chichester, 1991.

5. Pedersen, C. J. *Angew. Chem. Int. Ed. Engl.* **1988**, *27*, 1021.

6. Lehn, J.-M. *Angew. Chem. Int. Ed. Engl.* **1988**, *27*, 89.

7. Cram, D. J. *Angew. Chem. Int. Ed. Engl.* **1988**, *27*, 1009.

8. Cotton, F. A.; Wilkinson, G. *Advanced Inorganic Chemistry*; 2nd ed.; Interscience: New York, 1966.

9. Izatt, R. M.; Bradshaw, J. S.; Nielsen, S. A.; Lamb, J. D.; Christensen, J. J.; Sen, D. *Chem. Rev.* **1985**, *85*, 271; Izatt, R. M.; Pawlak, K.; Bradshaw J. S.; Bruening, R. L. *Chem. Rev.* **1991**, *91*, 1721.

10. (a) *Molecular Electronic Devices*; Carter, F. L.; Siatkowski, R. E.; Wohltjen, H., Eds.; Elsevier: Amsterdam, 1988; (b) Bryce, M.; Underhill, A. E.; Stoddart, J. F.; Bradley, D. D. C.; Findlay, J.; Barker, J. *Chem. Brit.* **1991**, *27*, 707; (c) de Silva, A. P.; McCoy, C. P. *Chem. Ind.* **1994**, 992.

11. *Principles of Neural Science*, 3rd ed.; Kandel, E. R.; Schwartz, J. H.; Jessell, T. M., Eds.; Elsevier: New York, 1991.

12. Tsien, R. Y. *Chem. Eng. News* **1994**, July 18, 34.

13. Schoenlein, R. W.; Peteanu, L. A.; Mathies, R. A.; Shank, C. V. *Science* **1991**, *254*, 412; Mathies, R. A.; Lin, S. W.; Ames, J. B.; Pollard, W. T. *Ann. Rev. Biophys. Biophys. Chem.* **1991**, *20*, 491.

14. El-Sayed, M. A. *Acc. Chem. Res.* **1992**, *25*, 279.

15. Fabbrizzi, L.; Poggi, A. *Chem. Soc. Rev.* **1995**, *24*, 197.

16. Collinson, M. M.; Wightman, R. M. *Science* **1995**, *268*, 1883; see also Tsang, S. C.; Davis, J. J.; Green, M. L. H.; Hill, H. A. O.; Leung, Y. C.; Sadler, P. J. *J. Chem. Soc., Chem. Commun.* **1995**, 2579.

17. (a) Fendler, E. J.; Fendler, J. H. *Catalysis in Micellar and Macromolecular Systems*; Academic: New York, 1975; (b) Fendler, J. H. *Membrane Mimetic Chemistry*; Wiley: New York, 1982; (c) Harold, F. M. *The Vital Force; A study of Bioenergetics*; Freeman: New York, 1986.

18. Mirkin, M. V. *Anal. Chem.* **1996**, *68*, A177.

19. Frommer, J. *Angew. Chem. Int. Ed. Engl.* **1992**, *31*, 1298.

20. Adams, S. R.; Kao, J. P. Y.; Tsien, R. Y. *J. Am. Chem. Soc.* **1989**, *111*, 7957.

21. Shinkai, S.; Manabe, O. *Top. Curr. Chem.* **1984**, *121*, 67.

22. (a) Gutman, M.; Huppert, D.; Pines, E. *J. Am. Chem. Soc.* **1981**, *103*, 3709; (b) Pines, E.; Huppert, D.; Gutman, M.; Nachliel, M. *J. Phys. Chem.* **1986**, *90*, 6366.

23. (a) Dumon, P.; Jonusauskas, G.; Dupuy, F.; Pee, P.; Rulliere, C.; Letard, J.-F.; Lapouyade, R. *J. Phys. Chem.* **1994**, *98*, 10391; (b) Mathevet, R.; Jonusauskas, G.; Rulliere, C.; Letard, J.-F.; Lapouyade, R. *J. Phys. Chem.* **1995**, *99*, 15709.

24. Martin, M. M.; Plaza, P.; Dai Hung, N.; Meyer, Y. H.; Bourson, J.; Valeur, B. *Chem. Phys. Lett.* **1993**, *202*, 425; Martin, M. M.; Plaza, P.; Meyer, Y. H.; Begin, L.; Bourson, J.; Valeur, B. *J. Fluoresc.* **1994**, *4*, 271.

25. Martin, M. M.; Plaza, P.; Meyer, Y. H.; Badaoui, F.; Bourson, J.; Valeur, B. *J. Phys. Chem.* **1996**, *100*, 6879.

26. Takeshita, M.; Uchida, K.; Irie, M. *Chem. Commun.* **1996**, 1807; a related case for nonionic saccharides.

27. *Bioorganic Photochemistry; Biological Applications of Photochemical Switches*; Morrison, H., Ed.; Wiley: New York, 1993.

28. Givens, R. S.; Kueper, L. W. *Chem. Rev.* **1993**, *93*, 55.

29. Grell, E.; Warmuth, R. *Pure Appl. Chem.* **1993**, *65*, 373.

30. (a) Adams, S. R.; Kao, J. P. Y.; Grynkiewicz, G.; Minta, A.; Tsien, R. Y. *J. Am. Chem. Soc.* **1988**, *110*, 3212; (b) Adams, S. R.; Kao, J. P. Y.; Tsien, R. Y. *J. Am. Chem. Soc.* **1989**, *111*, 7959.

31. Ellis-Davies, G. C. R.; Kaplan, J. H. *Proc. Nat. Acad. Sci. USA*, **1994**, *91*, 187.

32. Valeur, B.; Bardez, E. *Chem. Brit.* **1995**, *31*, 216.
33. (a) Dovichi, N. J.; Martin, J. C.; Jett, J. H.; Trukla, M.; Keller, R. A. *Anal. Chem.* **1984**, *56*, 348; (b) Orrit, M.; Bernard, J. *Phys. Rev. Lett.* **1990**, *65*. 2716.
34. Bissell, R. A.; Bryan, A. J.; de Silva, A. P.; McCoy, C. P. *J. Chem. Soc., Chem. Commun.* **1994**, 405.
35. Dixon, A. J.; Benham, G. S. *Int. Lab.* **1988**, *4*, 38.
36. Sharp, S. L.; Warmack, R. J.; Goudonnet, J. P.; Lee, I.; Ferrell, T. L. *Acc. Chem. Res.* **1993**, *26*, 377.
37. Lewis, A.; Lieberman, K. *Anal. Chem.* **1991**, *63*, 625A.
38. Eichen, Y.; Lehn, J.-M.; Scheri, M.; Haarer, D.; Casalegno, R.; Corval, A.; Kuldova, K.; Trommsdorff, H. P. *J. Chem. Soc., Chem. Commun.* **1995**, 713.
39. Bissell, R. A.; de Silva, A. P.; Gunaratne, H. Q. N.; Lynch, P. L. M.; Maguire, G. E. M.; Sandanayake, K. R. A. S. *Chem. Soc. Rev.* **1992**, *21*, 187.
40. Bissell, R. A.; de Silva, A. P.; Gunaratne, H. Q. N.; Lynch, P. L. M.; Maguire, G. E. M.; McCoy, C. P.; Sandanayake, K. R. A. S. *Top. Curr. Chem.* **1993**, *168*, 223.
41. Luckhoff, A.; Clapham, D. E. *Nature* **1992**, *355*, 356.
42. (a) *The Photosynthetic Reaction Center;* Diesenhofer, J.; Norris, J. R., Eds.; Academic Press: San Diego, 1993, Vols. I and II; (b) Huber, R. *Angew. Chem. Int. Ed. Engl.* **1989**, *28*, 848; Diesenhofer, J.; Michel, H. *Angew. Chem. Int. Ed. Engl.* **1989**, *28*, 829.
43. (a) Weller, A. *Pure Appl. Chem.* **1968**, *16*, 115; (b) Rehm, D.; Weller, A. *Isr. J. Chem.* **1970**, *8*, 259.
44. (a) Birks, J. B. *Photophysics of Aromatic Molecules;* Wiley: London, 1970; (b) Turro, N.J. *Modern Molecular Photochemistry;* University Science Books: Mill Valley, CA, 1991.
45. *Photoinduced Electron Transfer;* Fox, M. A.; Chanon, M., Eds.; Elsevier: Amsterdam, 1988, Parts A–D.
46. *Photoinduced Electron Transfer;* Parts I–V. Mattay, J., Ed.; *Top. Curr. Chem.,* 1990, **156**, **158**; 1991, **159**; 1992, **163**; 1993, **168**; *Electron transfer. Part I* (Mattay, J., ed.), *Top. Curr. Chem.,* 1994, **169**.
47. Wasielewski, M. R. *Chem. Rev.* **1992**, *92*, 435.
48. O'Neil, M. P.; Niemczyk, M. P.; Svec, W. A.; Gosztola, D.; Gaines, G. L.; Wasielewski, M. R. *Science* **1992**, *257*, 63.
49. Nagamura, T. *Pure Appl. Chem.* **1996**, *68*, 1449.
50. Marcus, R. A. *Angew. Chem. Int. Ed. Engl.* **1993**, *32*, 1111.
51. Paddon-Row, M. N. *Acc. Chem. Res.* **1994**, *27*, 18.
52. Closs, G. L.; Miller, J. R. *Science* **1988**, *240*, 440.
53. Verhoewen, J. W. *Pure Appl. Chem.* **1990**, *62*, 1585.
54. Amabilino, D. B.; Stoddart, J. F. *Chem. Rev.* **1995**, *95*, 2725.
55. Ballardini, R.; Balzani, V.; Credi, A.; Gandolfi, M. T.; Langford, S. J.; Menzer, S.; Prodi, L.; Stoddart, J. F.; Venturi, M.; Williams, D. J. *Angew. Chem. Int. Ed. Engl.* **1996**, *35*, 978.
56. Bryan, A. J.; de Silva, A. P.; de Silva, S. A.; Rupasinghe, R. A. D. D.; Sandanayake, K. R. A. S. *Biosensors* **1989**, *4*, 169.
57. Bissell, R. A.; Calle, E.; de Silva, A. P.; de Silva, S. A.; Gunaratne, H. Q. N.; Habib-Jiwan, J.-L.; Peiris, S. L. A.; Rupasinghe, R. A. D. D.; Samarasinghe, T. K. S. D.; Soumillion, J.-P. *J. Chem. Soc., Perkin Trans. 2* **1992**, 1559.
58. Bissell, R. A.; de Silva, A. P.; Gunaratne, H. Q. N.; Lynch, P. L. M.; Maguire, G. E. M.; McCoy, C. P.; Sandanayake, K. R. A. S. *ACS Symp. Ser.* **1993**, *538*, 45.
59. Czarnik, A. W. *Acc. Chem. Res.* **1994**, *27*, 302.
60. Czarnik, A. W. *Adv. Supramol. Chem.* **1993**, *3*, 131.
61. Czarnik, A. W. In *Topics in Fluorescence Spectroscopy. Probe Design and Chemical Sensing;* Lakowicz, J. R., Ed.; Plenum: New York, 1994, Vol. 4, p. 49.
62. Czarnik, A. W. *ACS Symp. Ser.* **1993**, *538*, 104.

63. *Fluorescent Chemosensors for Ion and Molecule Recognition*; Czarnik, A. W. Ed.; *ACS Symp. Ser.* 1993, **538**: has articles by Czarnik, Masilamani, Bouas-Laurent, Tsien, Kuhn, Sousa, and ourselves concerning PET systems.

64. (a) Valeur, B. In *Molecular Luminescence Spectroscopy*, Part 3; Schulman, S.G., Ed.; Wiley: New York, 1993, p. 25; (b) Valeur, B. In *Topics in Fluorescence Spectroscopy. Probe Design and Chemical Sensing*; Lakowicz, J. R., Ed.; Plenum: New York, 1994, Vol. 4, p. 21.

65. de Silva, A. P.; Gunaratne, H. Q. N.; Gunnlaugsson, T.; McCoy, C. P.; Maxwell, P. R. S.; Rademacher, J. T.; Rice, T. E. *Pure Appl. Chem.* **1996**, *68*, 1443.

66. Draxler, S.; Lippitsch, M. E. *Sensors Actuators B. Chem.* **1995**, *29*, 199.

67. (a) Pardo, A., Poyato, J. M. L.; Martin, E.; Camacho, J. J.; Reyman, D. *J. Lumin.* **1990**, *46*, 381; (b) Szmacinski, H.; Lakowicz, J. R.; *Anal. Chem.* **1993**, *65*, 1668; (c) Van den Bergh, V., Boens, N.; de Schryver, F. C.; Gallay, J.; Vincent, M. *Photochem. Photobiol.* **1995**, *61*, 442.

68. de Silva, A. P.; Rupasinghe, R. A. D. D. *J. Chem. Soc., Chem. Commun.* **1985**, 1669.

69. (a) Davidson, R. S.; Whelan, T. D. *J. Chem. Soc., Chem. Commun.* **1978**, 911; *J. Chem. Soc., Perkin Trans. 2*, **1983**, 241; (b) Hub, W.; Dorr, F.; Oxman, J. D.; Lewis, F. D. *J. Am. Chem. Soc.* **1984**, *106*, 701.

70. Huston, M. E.; Haider, K. W.; Czarnik, A. W. *J. Am. Chem. Soc.* **1988**, *110*, 4460.

71. Fages, F.; Desvergne, J.-P.; Bouas-Laurent, H.; Marsau, P.; Lehn, J.-M.; Kotzyba-Hibert, F.; Albrecht-Gary, A. M.; Al Joubbeh, M. *J. Am. Chem. Soc.* **1989**, *111*, 8672.

72. Akkaya, E. U.; Huston, M. E.; Czarnik, A.W. *J. Am. Chem. Soc.* **1990**, *112*, 3590.

73. Fabbrizzi, L.; Licchelli, M.; Pallavicini, P.; Taglietti, A. *Inorg. Chem.* **1996**, *35*, 1733.

74. Bernardo, M. A.; Parola, A. J.; Pina, F.; Garcia-Espana, E.; Marcelino, V.; Luis, S. V.; Miravet, J. F. *J. Chem. Soc., Dalton Trans.* **1995**, 993.

75. Grigg, R.; Norbert, W. D. J. A. *J. Chem. Soc., Chem. Commun.* **1992**, 1298.

76. de Silva, A. P.; Gunaratne, H. Q. N.; Lynch, P. L. M.; Patty, A. J.; Spence, G. L. *J. Chem. Soc., Perkin Trans. 2* **1993**, 1611.

77. Grigg, R.; Norbert, W. D. J. A. *J. Chem. Soc., Chem. Commun.* **1992**, 1300.

78. de Silva, A. P.; Gunaratne, H. Q. N.; Habib-Jiwan, J.-L.; McCoy, C. P.; Rice, T. E.; Soumillion, J.-P. *Angew. Chem. Int. Ed. Engl.* **1995**, *34*, 1728.

79. James, T. D.; Linnane, P.; Shinkai, S. *J. Chem. Soc., Chem. Commun.* **1996**, 281.

80. Huston, M. E.; Akkaya, E. U.; Czarnik, A. W. *J. Am. Chem. Soc.* **1989**, *111*, 8735.

81. (a) Vance, D. H.; Czarnik, A. W. *J. Am. Chem. Soc.* **1994**, *116*, 9397. (b) Czarnik, A.W. *ACS Symp. Ser.* **1994**, *561*, 314.

82. de Silva, A. P.; Sandanayake, K. R. A. S. *J. Chem. Soc., Chem. Commun.* **1989**, 1183.

83. de Silva, A. P.; de Silva, S. A.; Dissanayake, A. S.; Sandanayake, K. R. A. S. *J. Chem. Soc., Chem. Commun.* **1989**, 1054.

84. de Silva, A. P.; Gunaratne, H. Q. N.; Lynch, P. L. M. *J. Chem. Soc., Perkin Trans. 2* **1995**, 685.

85. Grigg, R.; Holmes, J. M.; Jones, S. K.; Norbert, W. D. J. A. *J. Chem. Soc., Chem. Commun.* **1994**, 185.

86. Levy, L. A.; Murphy, E.; Raju, B.; London, R. E. *Biochemistry* **1988**, *27*, 4041.

87. Raju, B.; Murphy, E.; Levy, L. A.; Hall, R. D.; London, R. E. *Am. J. Physiol.* **1989**, *256*, C540; London, R. E. *Ann. Rev. Physiol.* **1991**, *53*, 241.

88. de Silva, A. P.; Gunaratne, H. Q. N.; Maguire, G. E. M. *J. Chem. Soc., Chem. Commun.* **1994**, 1213.

89. de Silva, A. P.; Gunaratne, H. Q. N. *J. Chem. Soc., Chem. Commun.* **1990**, 186.

90. Tsien, R. Y. *Biochemistry* **1980**, *19*, 2396.

91. Grynkiewicz, G.; Poenie, M.; Tsien, R. Y. *J. Biol. Chem.* **1985**, *260*, 3440.

92. (a) Gust, D.; Moore T. A. *Top. Curr. Chem.* **1991**, *159*, 103; (b) Gust, G.; Moore, T.A.; Moore, A. L. *Acc. Chem. Res.* **1993**, *26*, 198.

93. Kuhn, M. *ACS Symp. Ser.* **1993**, *538*, 147.

94. de Silva, A. P.; Gunaratne, H. Q. N.; Gunnlaugsson, T. *Chem. Commun.* **1996**, 1967.

95. Minta, A.; Tsien, R. Y. *J. Biol. Chem.* **1989**, *264*, 19449.

96. Gerig, J. T.; Singh, P.; Levy, L. A.; London, R. E. *J. Inorg. Biochem.* **1987**, *31*, 113.

97. (a) Jonker, S. A.; Ariese, F.; Verhoewen, J. W. *Rec. Trav. Chem. Pays Bas* **1989**, *108*, 109; (b) Jonker, S. A.; Verhoewen, J. W.; Reiss, C. A.; Goubitz, K.; Heijdenrijk, D. *Rec. Trav. Chem. Pays Bas* **1990**, *109*, 154; (c) Jonker, S. A.; Van Dijk, S. A.; Goubitz, K.; Reiss, C. A.; Schuddeboom, W.; Verhoewen, J. W. *Mol. Cryst. Liq. Cryst.* **1990**, *183*, 273.

98. de Silva, A. P.; Gunaratne, H. Q. N.; Kane, A. T. M.; Maguire, G. E. M. *Chem. Lett.* **1995**, 125.

99. Clarke, S. D.; Metcalfe, J. C.; Smith, G. A. *J. Chem. Soc., Perkin Trans. 2* **1993**, 1187; 1195.

100. Ballardini, R.; Balzani, V.; Credi, A.; Gandolfi, M. T.; Kotzyba-Hibert, F.; Lehn, J.-M.; Prodi, L. *J. Am. Chem. Soc.* **1994**, *116*, 5741.

101. de Silva, A. P.; Sandanayake, K. R. A. S. *Angew. Chem. Int. Ed. Engl.* **1990**, *29*, 1173.

102. (a) Fages, F.; Desvergnes, J.-P.; Kampke, K.; Bouas-Laurent, H.; Lehn, J.-M.; Konopelski, J.-P.; Marsau. P.; Barrans, Y. *J. Chem. Soc., Chem. Commun.* **1990**, 655; (b) Fages, F.; Desvergnes, J.-P.; Kampke, K.; Bouas-Laurent, H.; Lehn, J.-M.; Meyer, M.; Albrecht-Gary, A.-M. *J. Am. Chem. Soc.* **1993**, *115*, 3658.

103. Wang, Y. C.; Morawetz, H. *J. Am. Chem. Soc.* **1976**, *98*, 3611.

104. Goldenberg, M.; Emert, J.; Morawetz, H. *J. Am. Chem. Soc.* **1978**, *100*, 7171.

105. Parker, D.; Williams, J. A. G. *J. Chem. Soc., Perkin Trans. 2* **1995**, 1305.

106. Beeby, A.; Parker, D.; Williams, J. A. G. *J. Chem. Soc., Perkin Trans. 2* **1996**, 1565.

107. Feigenspan, A.; Wassle, H.; Bormann, J. *Nature* **1993**, *361*, 159.

108. de Silva, A. P.; Gunaratne, H. Q. N.; McVeigh, C.; Maguire, G. E. M.; Maxwell, P. R. S.; O'Hanlon, E. *Chem. Commun.* **1996**, 2191.

109. Askew, B. C. *Tetrahedron Lett.* **1990**, *31*, 4245.

110. Sauvage, J. P.; Collin, J. P.; Chambron, J. C.; Guillerez, S.; Coudret, C.; Balzani, V.; Barigelletti, F.; de Cola, L.; Flamigni, L. *Chem. Rev.* **1994**, *94*, 993.

111. (a) Valeur, B.; Bourson, J.; Pouget, J.; Kaschke, M.; Ernsting, N. P. *J. Phys. Chem.* **1992**, *96*, 6545; (b) Valeur, B.; Bourson, J.; Pouget, J. *J. Lumin.* **1992**, *52*, 345.

112. Adams, S. R.; Harootunian, A.; Buechler, Y. J.; Taylor, S. S.; Tsien, R. Y. *Nature* **1991**, *349*, 694.

113. Aoki, I.; Sakaki, T.; Shinkai, S. *J. Chem. Soc., Chem. Commun.* **1992**, 730.

114. Iyoda, T.; Morimoto, M.; Kawasaki, N.; Shimidzu, T. *J. Chem. Soc., Chem. Commun.* **1991**, 1480.

115. (a) Brun, A. M.; Atherton, S. J.; Harriman, A.; Heitz, V.; Sauvage, J.-P. *J. Am. Chem. Soc.* **1992**, *114*, 4632; (b) Harriman, A.; Sauvage, J.-P. *Chem. Soc. Rev.* **1996**, *25*, 41; see also; Harriman, A.; Ziessel, R. *J. Chem. Soc., Chem. Commun.* **1996**, 1707.

116. Yoon, D. I.; Bergbrennan, C. A.; Lu, H.; Hupp, J. T. *Inorg. Chem.* **1992**, *31*, 3192.

117. Martensson, J.; Sandros, K.; Wennerstrom, O. *J. Phys. Org. Chem.* **1994**, *7*, 534.

118. Mes, G. F.; Van Ramesdonk, H. J.; Verhoewen, J. W. *J. Am. Chem. Soc.* **1984**, *106*, 1335.

119. Alihodzic, S.; Zinic, M.; Klaic, B.; Kiralj, R.; Kojic-Prodic, B.; Herceg, M.; Cimerman, Z. *Tetrahedron Lett.* **1993**, *34*, 8345.

120. (a) Wallach. D. F. H.; Steck, D. L. *Anal. Chem.* **1963**, *35*, 1035; (b) Nishida, H.; Katayama, Y.; Katsuki, H.; Nakamura, H.; Tagaki, M.; Ueno, K. *Chem. Lett.* **1982**, 1853; (c) Bourson, J.; Borrel, M. N.; Valeur, B. *Anal. Chim. Acta* **1992**, *257*, 189; (d) Bourson, J.; Pouget, J.; Valeur, B. *J. Phys. Chem.* **1993**, *97*, 4552.

121. de Silva, A. P.; de Silva, S. A. *J. Chem. Soc., Chem. Commun.* **1986**, 1709.

122. Ueno, A. *Adv. Mater.* **1993**, *5*, 132.

123. Ueno, A. *ACS Symp. Ser.* **1993**, *538*, 74.

124. (a) Hamasaki, K.; Ueno, A.; Toda, F. *J. Chem. Soc., Chem. Commun.* **1993**, 331; (b) Hamasaki, K.; Ikeda, H.; Nakamura, A.; Ueno, A.; Toda, F.; Suzuki, I.; Osa, T. *J. Am. Chem. Soc.* **1993**, *115*, 5035.

125. Eddaoudi, M.; Parrot-Lopez, H.; de Lamotte, S. F.; Fichieux, D.; Prognon, P.; Coleman, A. W. *J. Chem. Soc., Perkin Trans. 2* **1996**, 1711.

126. Guilbault, G. G. *Practical Fluorescence. Theory, Methods and Techniques*; Plenum: New York, 1973.
127. Siegerman, H. In *Technique of Electroorganic Synthesis*. Part II; Weinberg, N.L., Ed.; Wiley: New York, 1975, p. 667.
128. Saeva, F. D. *J. Photochem. Photobiol. A: Chem.* **1994**, *78*, 201.
129. Ashton, P. R.; Ballardini, R.; Balzani, V.; Credi, A.; Gandolfi, M. T.; Menzer, S.; PerezGarcia, L.; Prodi, L.; Stoddart, J. F.; Venturi, M.; Williams, D. J. *J. Am. Chem. Soc.* **1995**, *117*, 11171.
130. Ashton, P. R.; Ballardini, R.; Balzani, V.; Belohradsky, M.; Gandolfi, M. T.; Philp, D.; Prodi, L.; Raymo, F. M.; Reddington, M. V.; Spencer, N.; Stoddart, J. F.; Venturi, M.; Williams, D. J. *J. Am. Chem. Soc.* **1996**, *118*, 4931.
131. De Santis, G.; Fabbrizzi, L.; Licchelli, M.; Poggi, A.; Taglietti, A. *Angew. Chem. Int. Ed. Engl.* **1996**, *35*, 202.
132. Colquhoun, H. M.; Stoddart, J. F.; Williams, D. J. *Angew. Chem. Int. Ed. Engl.* **1986**, *25*, 487; Stoddart, J. F.; Zarzycki, R. *Rec. Trav. Chim. Pays Bas* **1988**, *107*, 515.
133. Iwata, S.; Tanaka, K. *J. Chem. Soc., Chem. Commun.* **1995**, 1491.
134. Wolfbeis, O. S.; Offenbacher, H. *Monatsh. Chem.* **1984**, *115*, 647.
135. Turro, N. J.; Kavarnos, G. J.; Fung, F.; Lyons, A. L.; Cole, T. *J. Am. Chem. Soc.* **1972**, *94*, 1392; Davidson, R. S.; Goodwin, J. W.; Kemp, G. *Tetrahedron Lett.* **1980**, 2911.
136. Wolfbeis, O. S.; Urbano, E. *Fresenius Z. Anal. Chem.* **1983**, *314*, 577.
137. Biwersi, J.; Verkman, A. S. *Biochemistry* **1991**, *30*, 7779.
138. Hosseini, M. W.; Blacker, A. J.; Lehn, J.-M. *J. Am. Chem. Soc.* **1990**, *112*, 3896.
139. Dhaenens, M.; Lehn, J.-M.; Vigneron, J.-P. *J. Chem. Soc., Perkin Trans. 2* **1993**, 1379.
140. Seiler, M.; Durr, H.; Willner, I.; Joselevich, E.; Doron, A.; Stoddart, J. F. *J. Am. Chem. Soc.* **1994**, *116*, 3399.
141. Gouterman, M. In *The Porphyrins*; Dolphin, D., Ed.; Academic: New York, 1978, Vol. 3, p. 1.
142. Rawle, S. C.; Moore, P. *J. Chem. Soc., Chem. Commun.* **1992**, 684; see also; Kimura, E.; Wada, S.; Shionoya, M.; Takahashi, T.; Iitaka, Y. *J. Chem. Soc., Chem. Commun.* **1990**, 397; Fujita, E.; Milder, S. J.; Brunschwig, B.S. *Inorg. Chem.* **1992**, *31*, 2079.
143. Fabbrizzi, L.; Licchelli, M.; Pallavicini, P.; Perotti, A.; Taglietti, A.; Sacchi, D. *Chem. Eur. J.* **1996**, *2*, 75.
144. Fabbrizzi, L.; Licchelli, M.; Pallavicini, P.; Perotti, A.; Sacchi, D. *Angew. Chem. Int. Ed. Engl.* **1994**, *33*, 1975.
145. Lytton, S. D.; Cabantchik, Z. I.; Libman, J.; Shanzer, A. *Molec. Pharmacol.* **1991**, *40*, 584; Lytton, S. D.; Mester, B.; Libman, J.; Shanzer, A.; Cabantchik, Z. I. *Anal. Biochem.* **1992**, *205*, 326.
146. Fages, F.; Bodenant, B.; Weil, T. *J. Org. Chem.* **1996**, *61*, 3956.
147. Ghosh, P.; Bharadwaj, P. K.; Mandal, S.; Ghosh, S. *J. Am. Chem. Soc.* **1996**, *118*, 1553.
148. De Santis, G.; Fabrizzi, L.; Licchelli, M.; Mangano, C.; Sacchi, D. *Inorg. Chem.* **1995**, *34*, 3581.
149. Hassner, A.; Birnbaum, D.; Loew, L. M. *J. Org. Chem.* **1984**, *49*, 2546; Loew, L. M. *Pure Appl. Chem.* **1996**, *68*, 1405.
150. Goulle, V.; Harriman, A.; Lehn, J.-M. *J. Chem. Soc., Chem. Commun.* **1993**, 1034.
151. Watts, R. J. *J. Chem. Educ.* **1983**, *60*, 834; Balzani, V. *New Scientist* **1994**, *144*, (1951), 31.
152. Kratochvil, B.; Zatko, D. A. *Anal. Chem.* **1964**, *36*, 527.
153. Fox, M. A. *Chem. Rev.* **1979**, *79*, 253.
154. Daub, J.; Beck, M.; Knorr, A.; Spreitzer, H. *Pure Appl. Chem.* **1996**, *68*, 1399.
155. Minta, A.; Kao, J. P. Y.; Tsien, R. Y. *J. Biol. Chem.* **1989**, *264*, 8171.
156. Kuhn, M. *Bioprobes* **1993**, *16*, 5.
157. Rettig, W. *Angew. Chem. Int. Ed. Engl.* **1986**, *25*, 971; Rettig, W. *Top. Curr. Chem.* **1994**, *169*, 253.
158. Bounacic-Koutecky, V.; Koutecky, J.; Michl, J. *Angew. Chem. Int. Ed. Engl.* **1987**, *26*, 170.
159. Letard, J.-F.; Lapouyade, R.; Rettig, W. *Mol. Cryst. Liq. Cryst.* **1993**, *36*, 41.
160. Rettig, W.; Majenz, W.; Herter, R.; Letard, J.-F.; Lapouyade, R. *Pure Appl. Chem.* **1993**, *65*, 1699; Letard, J.-F.; Lapouyade, R.; Rettig, W. *Pure Appl. Chem.* **1993**, *65*, 1705.

161. Whitaker, J. E.; Haugland, R. P.; Prendergast, F. G. *Anal. Biochem.* **1991**, *194*, 330.
162. Smith, G. A.; Hesketh, T. R.; Metcalfe, J. C. *Biochem. J.* **1988**, *250*, 227.
163. Tsien, R. Y. *Am. J. Physiol.* **1992**, *263*, C723.
164. Barigelletti, F.; Flamigni, L.; Guardigli, M.; Sauvage, J.-P.; Collin, J.-P.; Sour, A. *Chem. Commun.* **1996**, 1329.
165. Heilbronner, E.; Bock, H. *The HMO Model;* Wiley: New York, Vol. 1, 1968.
166. Jaffe, H. H.; Orchin, M. *Theory and Applications of Ultraviolet Spectroscopy,* Wiley: New York, 1962.
167. Beer, P. D. *J. Chem. Soc., Chem. Commun.* **1996**, 689.
168. Zhou, Q.; Swager, T. M. *J. Am. Chem. Soc.* **1995**, *117*, 7017.
169. Turro, N. J.; Bolt, J. D.; Kuroda, Y.; Tabushi, I. *Photochem. Photobiol.* **1982**, *35*, 69.
170. Bissell, R. A.; de Silva, A. P. *J. Chem. Soc., Chem. Commun.* **1991**, 1148.
171. Ponce, A.; Wong, P. A.; Way, J. J.; Nocera, D. G. *J. Phys. Chem.* **1993**, *97*, 11137.
172. Shirai, M.; Ishimaru, S.; Tsunooka, M. *J. Fluoresc.* **1993**, *3*, 51.
173. Kimura, K.; Smid, J. *Makromol. Chem. Rapid Commun.* **1981**, *2*, 235.
174. Klok, H.-A.; Moller, M. *Makromol. Chem. Phys.* **1996**, *197*, 1395.
175. de Silva, A. P.; de Silva, S. A. *J. Chem. Soc., Chem. Commun.* **1986**, 1709.
176. Ayadim, M.; Habib-Jiwan, J.-L.; de Silva, A. P.; Soumillion, J.-P. *Tetrahedron Lett.* **1996**, *37*, 7039.
177. Fuh, M. R. S.; Burgess, L. W.; Hirschfeld, T.; Christian, G. D.; Wang, F. *Analyst* **1987**, *112*, 1159.
178. Sabbatini, N.; Guardigli, M.; Lehn, J.-M. *Coord. Chem. Rev.* **1993**, *123*, 201; Frey, S.T.; Gong, M. L.; Horrocks, W.deW. *Inorg. Chem.* **1994**, *33*, 3229.
179. Mayer, A.; Neuenhofer, S. *Angew. Chem. Int. Ed. Engl.* **1994**, *33*, 1044.
180. Horrocks, W. DeW.; Sudnick, D. R. *Acc. Chem. Res.* **1981**, *14*, 384.
181. Hemmila, I.; Mukkala, V.-M.; Takalo, H. *J. Fluoresc.* **1995**, *5*, 159; Dickins, R.S.; Parker, D.; de Sousa, A. S.; Williams, J. A. G. *Chem. Commun.* **1996**, 697.
182. Matsumoto, H.; Ori, A.; Inokuchi, F.; Shinkai, S. *Chem. Lett.* **1996**, 301.
183. Toner, J. L. *USP* **1989**, 4837169.
184. Saha, A. K.; Kross, K.; Kloszewski, E. D.; Upson, D. A.; Toner, J. L.; Snow, R.A.; Black, C.D.V.; Desai, V. D. *J. Am. Chem. Soc.* **1993**, *115*, 11032.
185. de Silva, A. P.; Gunaratne, H. Q. N.; Rice, T. E. *Angew. Chem. Int. Ed. Engl.* 1996, **35**, 2116.
186. Sammes, P. G.; Yahioglu, G.; Yearwood, G. D. *J. Chem. Soc., Chem. Commun.* **1992**, 1282.
187. Mortellaro, M. A.; Nocera, D. G. *Chemtech.* **1996**, *26*, 17.
188. Mortellaro, M. A.; Nocera, D. G. *J. Am. Chem. Soc.* **1996**, *118*, 7414.
189. Pikramenou, Z.; Nocera, D. G. *Inorg. Chem.* **1992**, *31*, 532.
190. Ito, N.; Yoshida, N.; Ichikawa, K. *J. Chem. Soc., Perkin Trans. 2* **1996**, 965.
191. Kosower, E. M.; Huppert, D. *Ann. Rev. Phys. Chem.* **1986**, *37*, 127.
192. Aoyama, Y.; Nagai, Y.; Otsuki, J.; Kabayashi, K.; Toi, H. *Angew. Chem. Int. Ed. Engl.* **1992**, *31*, 745.
193. de Silva, A. P.; Gunaratne, H. Q. N., unpublished studies.
194. de Silva, A. P.; Gunaratne, H. Q. N.; McCoy, C. P. *Nature* **1993**, *364*, 42.
195. Potember, R. S.; Hoffman, R. C.; Hu, S. W., ref. 10a, p. 663.
196. Wasielewski, M. R.; O'Neil, M. P.; Gosztola, D.; Niemczyk, M. P.; Svec, W. A. *Pure Appl. Chem.* **1992**, *64*, 1319.
197. Wild, U. P.; Bernat, S.; Kohler, B.; Renn, A. *Pure Appl. Chem.* **1992**, *64*, 1335.
198. Stryer, L. *Biochemistry,* 3rd ed.; Freeman: New York, 1988.
199. Isaacs, N. S. *Physical Organic Chemistry;* Longman: Burnt mill, 1987.
200. Ryder, J. D. *Engineering Electronics,* 2nd ed.; McGraw-Hill: New York, 1967.
201. *Biochemical Fluorescence: Concepts,* Chen, R. F.; Edelhoch, H., Eds.; Dekker: New York, 1976, Vol. 2; Schulman, S. G.; Threatte, R.; Capomacchia, A.; Paul, W. *J. Pharm. Sci.* **1974**, *63*, 876.
202. Tsien, R. Y. *Ann. Rev. Biophys. Bioeng.* **1983**, *12*, 91.

203. de Silva, A. P.; Gunaratne, H. Q. N.; Gunnlaugsson, T.; Lynch, P. L.M. *New J. Chem.* **1996**, *20*, 871.
204. Cain, C. C.; Murphy, R. F. *J. Cell. Biol.* **1988**, *106*, 269.

This Page Intentionally Left Blank

# MOLECULAR RECOGNITION IN
# CHEMISTRY AND BIOLOGY AS
# VIEWED FROM ENTHALPY–ENTROPY
# COMPENSATION EFFECT:

## GLOBAL UNDERSTANDING OF

## SUPRAMOLECULAR INTERACTIONS

Yoshihisa Inoue and Takehiko Wada

# 1. INTRODUCTION

Historically, chemistry has developed as a science of molecular transformations in which strong interatomic forces, producing covalent and ionic bonds, play the major roles in controlling chemical reactions. By contrast, molecular recognition systems in nature, such as enzymes and DNA, are controlled in very precise and efficient manners, not by using strong forces but through cooperative weak interactions such as hydrogen bonding, van der Waals forces, ion–dipole, and other interactions. Each force involved is usually well below 5 kcal/mol, but the directed cooperation of several weak interactions defines the precise molecular recognition in biological systems.[1–7]

Molecular recognition phenomena are not restricted, however, to sophisticated biological systems and widely adapted to simpler synthetic host–guest systems. They represent a crucial key concept that covers a wide area of chemistry and biology called host–guest chemistry, supramolecular chemistry, biomimetic chemistry, or "lock-and-key" interactions where several weak interactions work cooperatively.[1–18] Much effort has already been devoted to investigations of cation binding by ionophores, inclusion complexation by molecular hosts, enzymatic reaction, antigen–antibody interaction, DNA duplex formation, and other chemical and biological self-assembling or self-organizing (supra)molecular systems.

Representative chemical and biological hosts are illustrated in Figures 1–7. Despite the analogous weak interactions involved, molecular recognition phenom-
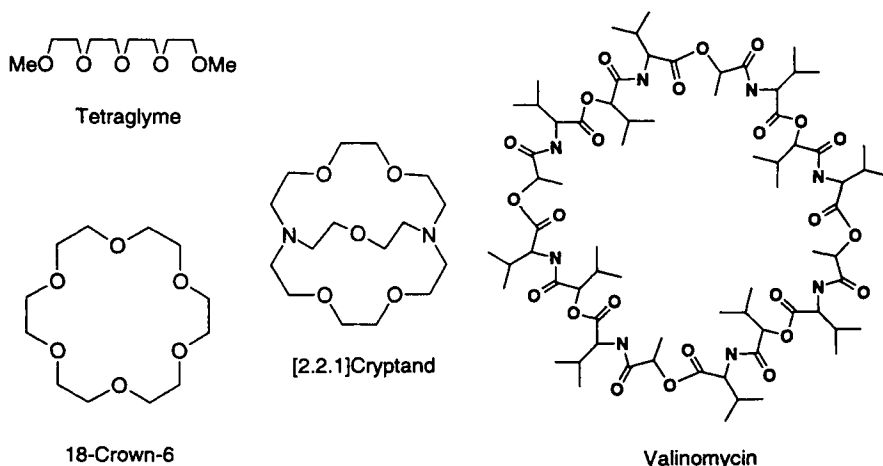


**Figure 1.** Glyme, crown, cryptand, and ionophore antibiotic.
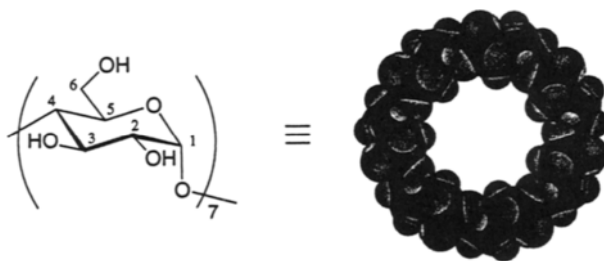
**Figure 2.** β-Cyclodextrin: glucopyranose unit (*left*) and space-filling model viewed from primary hydroxyl side (*right*).
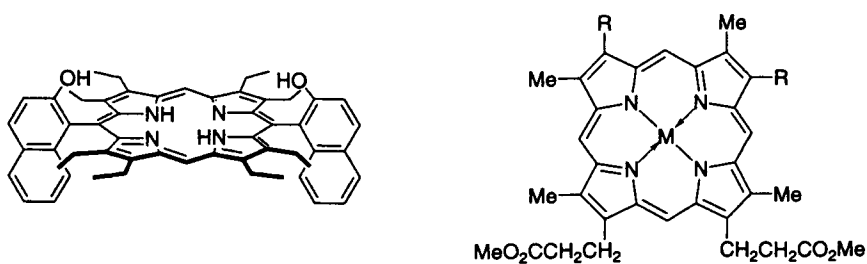


**Figure 3.** Quinone-receptor porphyrin (*left*) and metalloporphyrin (*right*).
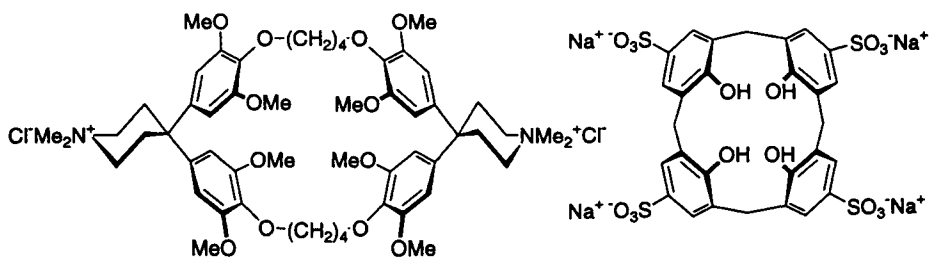


**Figure 4.** Cyclophane (*left*) and calixarene (*right*).

Antigen        Antibody

Antigen-antibody complex
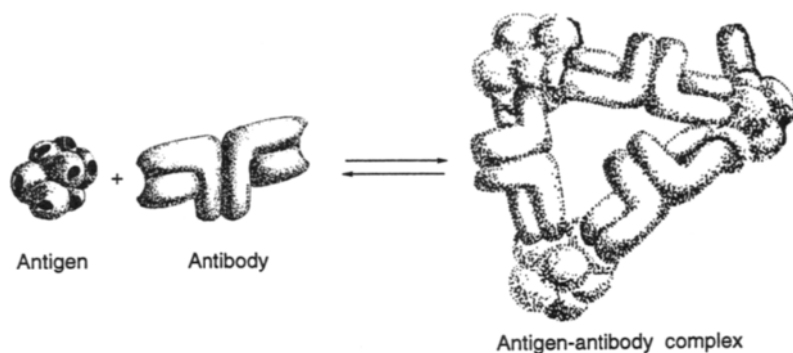
**Figure 5.** Antigen–antibody reaction.

ena in chemistry and biology have been discussed individually in most cases or merely compared as mimics in a symbolic or qualitative way, but have never been analyzed globally and quantitatively under a common concept that is applicable to both systems. For a deeper and more comprehensive understanding of the mechanism and factors controlling the supramolecular interactions in chemistry and biology, complexation thermodynamics have intensively been investigated with various combinations of host and guest ions and molecules, and a tremendous amount of



Intercalating agent

**Figure 6.** B-Type double-stranded DNA (*left*) and intercalated DNA (*right*).
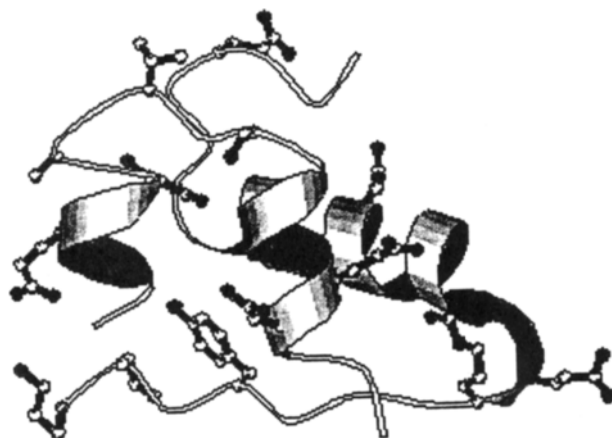
***Figure 7.*** Structure of insulin.

thermodynamic quantities have hitherto been compiled.[17,19] Nonetheless, the thermodynamic data obtained have been analyzed rather individually in each system or discipline and do not necessarily appear to be discussed or correlated with each other from a more global point of view.

Recently, we have demonstrated that the compensatory enthalpy–entropy relationship, affording a linear $\Delta H$–$T\Delta S$ plot, is observed in cation binding by acyclic and macro(bi)cyclic ligands such as glyme, crown ether, and cryptand.[19,20] Interestingly, these ligands possessing divergent topologies give distinctly different slopes and intercepts which can be used respectively as quantitative measures of the conformational change and the extent of desolvation upon host–guest complexation.[19–24] More recently, we have shown that this interpretation of the extrathermodynamic relationship between $\Delta H$ and $T\Delta S$ is applicable also to the inclusion complexation by molecular hosts such as cyclodextrin, porphyrin, and cyclophane.[25,26]

In this review, we first overview the compensatory enthalpy–entropy relationship observed for the chemical molecular recognition systems involving various cation and molecule binders. Then, we introduce an empirical theory that interprets and utilizes this extrathermodynamic relationship as a potential tool to analyze globally the molecular recognition phenomena as a chemistry of weak interactions. We further expand the scope of this extrathermodynamic relationship and its interpretation to the biological supramolecular systems, and discuss its general validity and significance as a universal tool for understanding various types of supramolecular interactions in chemistry and biology.

## 2.  HOSTS AND GUESTS

Discussing the chemical and biological molecular recognition phenomena from a global and unified point of view means inevitably to deal in a systematic way with a very wide variety of host–guest combinations from rather simple cation–ionophore pairs to much more sophisticated antigen–antibody and complementary DNA pairs, as exemplified in Figures 1–7. Hence, it seems indispensable not to insist on the detailed structural and mechanistic differences among the hosts but to extract the essential common features from the illusive diversity and complexity in host structure, working force, and recognition mechanism involved in supramolecular interactions.

A wide variety of known synthetic and natural hosts may be classified tentatively into three categories according to the size or complexity of guests as shown in Table 1. This classification by guest size coincides with that by the principal weak forces involved in the host–guest interactions, irrespective of the substantial diversity in host design. Thus, the number of weak forces working cooperatively increases as a guest's structure becomes more complex. Each host category may further be classified into several subcategories that correspond to the conventional host families, according to the host's topology or dimensionality. It should be emphasized, however, that this type of classification is tentative and just for convenience purposes, but is still useful in examining the relationship between a host's topology and the thermodynamic quantities obtained for each host category. As can be recognized gradually in the sections that follow, a deeper and broader understanding of molecular recognition phenomena is achieved not by merely analyzing the data

***Table 1.***  Classification of Host Molecules According to Guest's Size or Complexity and Representative Interactions Involved

| Guest | Host | Interaction |
|---|---|---|
| ion | glyme | ion–dipole |
| | crown ether | dipole–dipole |
| | cryptand | |
| | ionophore antibiotic | |
| molecule | cyclodextrin | van der Waals |
| | porphyrin | hydrogen bonding |
| | cyclophane/calixarene | hydrophobic |
| biomolecule | enzyme | electrostatic |
| | antibody | van der Waals |
| | DNA/RNA | hydrogen bonding |
| | | hydrophobic |
| | | $\pi$–$\pi$ stacking |

for an individual host–guest combination but by correlating globally the thermo-dynamic data with the profiles of dynamic changes in both conformation and solvation upon host–guest complexation beyond the apparent differences in host, guest, solvent, and interaction involved.

## 3. WEAK INTERACTIONS AND COOPERATIVE EFFECT

As mentioned above, all types of molecular recognition in chemistry and biology involve only noncovalent interactions such as electrostatic (ion–ion, ion–dipole, dipole–dipole, dipole-induced dipole), van der Waals, hydrophobic, hydrogen-bonding, $\pi$-$\pi$ stacking, and charge-transfer. It is more important however to recognize that the precise control of the supramolecular systems, simple or sophisticated, is made possible not by a single strong force or many weak forces working independently but through the directed cooperation of several and somewhat weak interactions, each of which is not strong enough to associate two molecules. Thus the chemical and biological molecular recognition phenomena may be unified as the chemistry of cooperative weak interactions.

In molecular recognition processes, the cooperative effect plays a crucial role in controlling structure and function of host–guest complexes. One of the major reasons why the combination of weak forces is frequently employed in chemical and, in particular, biological supramolecular systems is that only the cooperative weak interactions can materialize the threshold that enables the "on/off" switching of (supra)molecular functions. For instance, the numerous highly ordered hydrogen bonds in a DNA duplex are made or broken not independently but synchronously in a seemingly single step, enabling the "all-or-none" association–dissociation control in a very narrow range of temperature.

To understand the origin of cooperative effect,[27,8] let us consider an idealized situation in which two functional groups, X and Y, located in a single or separate molecule(s) bind to the corresponding complementary binding sites in a receptor, as shown in Figure 8. In case (a), two ligands, each possessing X or Y, interact independently with the corresponding receptor sites, while in case (b) a ligand carrying both X and Y is bound to the same receptor without any severe conformational changes upon complexation.



( a )　　　　　( b )
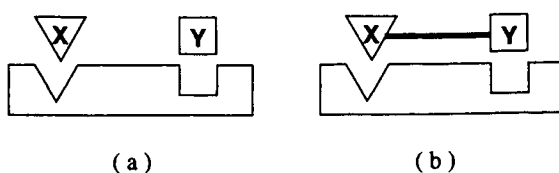
*Figure 8.* Schematic drawing of cooperative effect:
(**a**) independent binding; (**b**) cooperative binding.

In case (a), the overall free energy change ($\Delta G^\circ_{X+Y}$) upon ligation of X and Y to the receptor is simply equal to the sum of $\Delta G^\circ_X$ and $\Delta G^\circ_Y$ obtained separately and is expressed by the enthalpy and entropy changes of independent sole ligations by X and Y, i.e. $\Delta H^\circ_X$, $\Delta H^\circ_Y$, $\Delta S^\circ_X$, and $\Delta S^\circ_Y$:

$$\Delta G^\circ_{X+Y} = \Delta G^\circ_X + \Delta G^\circ_Y$$

$$= \Delta H^\circ_X + \Delta H^\circ_Y - T(\Delta S^\circ_X + \Delta S^\circ_Y) \tag{1}$$

On the other hand, when both X and Y are incorporated in a single molecule and are bound cooperatively to the receptor sites as in case (b), the free energy change ($\Delta G^\circ_{XY}$) upon ligation of X–Y is more negative than $\Delta G^\circ_{X+Y}$. This extra stabilization originates from the entropic factor, called chelate or preorganization effect, and also from the enthalpic contribution from mutual enhancement of the binding energies for X and Y, owing to the occurrence in the same molecule.

The chelate effect is entropic in origin in the first place. In case (a), both ligands X and Y lose substantial degrees of translational and rotational freedom, which leads to a large loss of entropy associated with the complex formation. By contrast, the loss of freedom upon complexation is much decreased in case (b), since the ligands X and Y are initially bound to each other and therefore the entropic loss is much smaller than in case (a). Hence, even if the enthalpic gain upon complexation is the same in cases (a) and (b), the complexation is more favorable for the linked ligand X–Y than for the separated ligand pair X and Y:

$$\Delta S^\circ_{XY} > \Delta S^\circ_X + \Delta S^\circ_Y \tag{2}$$

$$\Delta G^\circ_{XY} = \Delta H^\circ_X + \Delta H^\circ_Y - T\Delta S^\circ_{XY}$$

$$< \Delta G^\circ_{X+Y} = \Delta H^\circ_X + \Delta H^\circ_Y - T(\Delta S^\circ_X + \Delta S^\circ_Y) \tag{3}$$

The enthalpic enhancement of ligation also occurs by incorporating X and Y in a single ligand. In case (b) where the independent movement of X and Y is restricted, once either X or Y is bound to a receptor site, subsequent ligation of the rest in the same molecule is much enhanced and both bindings are reinforced each other. Under such circumstances, the binding enthalpy for X becomes more negative by the preceding ligation of Y than the original value and vice versa; $\Delta H^\circ_X{}' < \Delta H^\circ_X$ and $\Delta H^\circ_Y{}' < \Delta H^\circ_Y$. Then, the overall enthalpy change obtained for the linked ligand X–Y is much more negative than the sum of the values for the separated ligand pair X and Y:

$$\Delta H^\circ_{XY}{}' = \Delta H^\circ_X{}' + \Delta H^\circ_Y{}'$$

$$< \Delta H^\circ_{XY} = \Delta H^\circ_X + \Delta H^\circ_Y \tag{4}$$

In the classical chelate effect, the enthalpic changes are supposed not to be altered by linking X and Y as shown in Eq. 3, but the enthalpic factor also contributes to the enhanced ligation, giving much increased complex stabilities in the case of linked ligand X–Y:

$$\Delta G°_{XY}{}' = \Delta H°_X{}' + \Delta H°_Y{}' - T\Delta S°_{XY}$$

$$\ll \Delta G°_{X+Y} = \Delta H°_X + \Delta H°_Y - T(\Delta S°_X + \Delta S°_Y) \tag{5}$$

Thus, the cooperative effect is attributable to both enthalpic and entropic contributions and is one of the most important and essential factors governing and characterizing the molecular recognition phenomena based on weak interactions. It is also emphasized that the host molecules, though possessing well-organized original structures, frequently undergo considerable conformational changes upon complexation so as to optimize the effect of cooperative weak interactions which are much more sensitive to the host–guest distance but less sensitive to the working direction as compared with the strong interactions.

# 4. THERMODYNAMICS

In discussing quantitatively the molecular recognition phenomena in supramolecular chemistry, it is indispensable to determine the thermodynamic parameters for each (supra)molecular interaction of interest. In principle, these parameters should be determined by means of calorimetry. However, in spite of its long history as an established methodology,[29,30] the calorimetry does not appear to be the first choice to determine the thermodynamic quantities for various supramolecular systems. This is probably because a relatively large sample amount, sophisticated equipment, and some experience are required in the precise calorimetric measurement.[29,30]

Instead, a wide variety of spectroscopic and electrochemical titration methods are often employed to determine the equilibrium constants for a molecular recognition process at several different temperatures, which are then analyzed by the van't Hoff equation to give the thermodynamic parameters for the process. However, there is a critical tradeoff between the accuracy of the value obtained and the convenience of the measurement since the thermodynamic parameters, evaluated through the van't Hoff treatment, do not take into account the possible temperature dependence of the enthalpy change, i.e. heat capacity, and are less accurate in principle. In fact, it has been demonstrated with some supramolecular systems that the van't Hoff treatment leads to a curved plot and therefore the thermodynamic parameters deviated considerably from those determined by calorimetry.[31,32] Hence one should be cautious in handling thermodynamic parameters determined by spectroscopic titration and particularly in comparing the values for distinct systems determined by different methods.

In a typical stoichiometric host–guest interaction shown in Eq. 6, the association constant ($K$) is expressed by Eq. 7. The Gibbs free energy change ($\Delta G°$) for this equilibrium reaction is given by Eq. 8 and is related to the enthalpy change ($\Delta H°$) and entropy change ($\Delta S°$) through the Gibbs–Helmholtz relationship (Eq. 9):

$$H + G \xrightleftharpoons{K} H·G \tag{6}$$

$$K = \frac{[H·G]}{[H][G]} \tag{7}$$

$$\Delta G° = -RT \ln K \tag{8}$$

$$\Delta G° = \Delta H° - T\Delta S° \tag{9}$$

Combination of Eqs. 8 and 9 gives the van't Hoff equation:

$$\ln K = -\frac{\Delta H°}{RT} + \frac{\Delta S°}{R} \tag{10}$$

According to Eq. 10, the natural logarithm of the equilibrium constants at several temperatures are plotted as a function of reciprocal temperature to give a straight line in most cases. From its slope and intercept, one may calculate the enthalpy change ($\Delta H°$) and entropy change ($\Delta S°$), respectively. In this treatment, we assume that both $\Delta H°$ and $\Delta S°$ do not vary within the temperature range employed. However, this assumption, overlooking the temperature dependence of $\Delta H°$ and $\Delta S°$, is not always true and may lead to a curved van't Hoff plot if there is a considerable difference in heat capacity between the right and left sides of the equilibrium (Eq. 6).[31,32]

In titration calorimetry, minute heat change or flow is measured as a function of the concentrations of equilibrating species, affording a thermogram. Computer simulation of the thermogram gives the enthalpy change ($\Delta H°$) and the equilibrium constant ($K$) simultaneously.[29,30] Since the measurements are run at constant temperature, the ambiguities in the van't Hoff analysis do not exist in principle and the thermodynamic parameters determined are more accurate. Therefore, in the following sections we mostly employ the thermodynamic parameters determined by calorimetry except for some biological supramolecular systems in which the low sample availability makes the calorimetric measurement difficult.

## 5. ENTHALPY–ENTROPY COMPENSATION EFFECT AS EXTRATHERMODYNAMIC RELATIONSHIP

First of all, we should emphasize that the compensatory enthalpy–entropy relationship cannot be derived directly from the fundamental thermodynamic equations but

is just an empirical rule that was proposed originally by Leffler.[33,34] This rule has hitherto been exemplified amply with the activation and thermodynamic parameters obtained for a wide variety of reactions and equilibria.

In chemical reactions and equilibria, both rate constant ($k$) and equilibrium constant ($K$) are critical functions of the reaction condition employed. Thus, the enthalpy and entropy changes ($\Delta H^\circ$ and $\Delta S^\circ$) as well as the activation enthalpy and entropy ($\Delta H^\ddagger$ and $\Delta S^\ddagger$) are affected by internal and external perturbing factors such as substituents introduced and solvent employed. It is widely observed also that, when a reaction or equilibrium system is perturbed by changing substituent, solvent, or any other factors, the induced change in $k$ or $K$ ($\Delta\Delta G^\ddagger$ or $\Delta\Delta G^\circ$) is more or less smaller in general than that expected solely from the enthalpic change ($\Delta\Delta H^\ddagger$ or $\Delta\Delta H^\circ$), as the corresponding entropy term ($\Delta\Delta S^\ddagger$ or $\Delta\Delta S^\circ$) always deviates in the direction that cancels part of the enthalpic change induced.

For instance, in a reaction proceeding through a transition state that is more polarized than the reactant, the use of a more polar solvent reduces the free energy of activation ($\Delta\Delta G^\ddagger$) through enthalpic stabilization of the transition state by enhanced solvation. However, the situation is not so simple. The enthalpic gain ($\Delta\Delta H^\ddagger < 0$) is not fully reflected to the reaction rate or $\Delta G^\ddagger$ but is canceled at least in part by the entropic loss ($\Delta\Delta S^\ddagger < 0$) arising from the reduced freedom in the transition state caused also by the increased solvation. Consequently, the enthalpy and entropy terms show inherent tendency to compensate each other, affording a linear relationship illustrated in Figure 9. Hence, the compensatory enthalpy–entropy relationship has widely been observed in the activation and thermodynamic parameters for numerous reactions and equilibria.

Extensive theoretical analyses of the compensatory enthalpy–entropy relationship were first carried out by Leffler[33] and later by Leffler and Grunwald,[34] Exner,[35] and Li.[36] The empirical linear relationship between the thermodynamic or activation parameters ($\Delta H$ and $\Delta S$) directly leads to Eq. 11, where the proportional coefficient $\beta$, or the slope of the straight line in Figure 9, has a dimension of temperature.[33] Merging Eq. 11 into the differential form of the Gibbs–Helmholtz Eq. 12 gives Eq. 13:

$$\Delta\Delta H = \beta\Delta\Delta S \qquad (11)$$

$$\Delta\Delta G = \Delta\Delta H - T\Delta\Delta S \qquad (12)$$

$$\Delta\Delta G = (1 - T/\beta)\Delta\Delta H \qquad (13)$$

From Eq. 13 one can immediately recognize that, when the temperature is equal to $\beta$, any changes in $\Delta H$ never affect the reaction rate or equilibrium and the original $\Delta G$ value is conserved under any reaction conditions as far as no change in mechanism occurs. The critical temperature $\beta$, which gives the same rate or equilibrium constant irrespective of the reaction conditions, is called the isokinetic
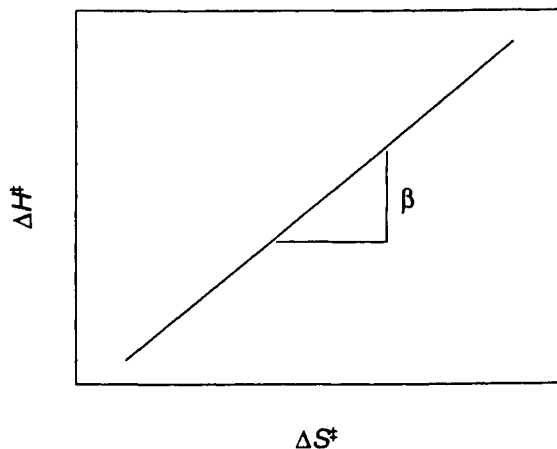
**Figure 9.** Compensatory entropy–enthalpy relationship.

or isoequilibrium temperature.[33] Such phenomena have abundantly been observed within the experimental temperature range employed. Of course, the compensation effect is observed only when the perturbation applied does not alter the mechanism, stoichiometry, or species involved in the reaction or equilibrium. Interestingly, the strong correlation between $\Delta H$ and $\Delta S$ may be taken as indirect evidence for consistent mechanism or species involved.

It would be somewhat surprising that the enthalpy–entropy compensation, though never derived from the fundamental thermodynamic relationships, is found so abundantly in various reactions and equilibria and that the reaction rate and equilibrium are independent of any perturbing factors at the specific temperature.[33] However, it seems natural at the same time that chemical events are not controlled exclusively by a single factor but are rather governed by multiple factors correlating each other.

In examining earlier discussion on the enthalpy–entropy compensation effect,[33–36] we have realized that the emphasis is placed mostly on the reliability of the linear $\Delta H$–$\Delta S$ plot, and merely the slope of the plot is used to calculate the isokinetic or isoequilibrium temperature, while the intercept has been discussed neither qualitatively nor quantitatively. In the next section, we will discuss the physical meanings of both slope and intercept of the compensation plot obtained with a wide variety of supramolecular systems, and attempt to understand globally the molecular recognition phenomena in chemistry and biology.

# 6. A THERMODYNAMIC VIEW FOR GLOBAL UNDERSTANDING OF MOLECULAR RECOGNITION[19-26,28,37-39]

With a variety of chemical and biological molecular recognition systems, the thermodynamic quantities have already been compiled, analyzed, and discussed in order to extract some insights into the mechanistic profile of molecular recognition. However, most of these specific discussion and conclusions, though certainly self-consistent within the specific and closely related systems, unfortunately seem *ad hoc* in many cases and are not always applicable to the other molecular recognition systems composed of different categories of host–guest combinations. Typically, the ideas and conclusions obtained for cation binding do not appear in general to contribute to further understanding of the molecular inclusion, for example, by cyclodextrin.

An attempt to treat globally the thermodynamic data is a classification by the major and minor factors contributing to the complex stability, using the signs of enthalpy and entropy changes ($\Delta H^\circ$ and $\Delta S^\circ$).[40,41] Thus, all host–guest interactions fall into the following four categories, the first term being the major contributor:

1. $\Delta H^\circ < 0$, $\Delta S^\circ > 0$
2. $\Delta H^\circ < 0$, $\Delta S^\circ < 0$
3. $\Delta S^\circ > 0$, $\Delta H^\circ < 0$
4. $\Delta S^\circ > 0$, $\Delta H^\circ > 0$

In the first two categories, the host–guest complexes are stabilized primarily by the favorable enthalpy change ($\Delta H^\circ < 0$), which is either assisted by the positive entropy change ($\Delta S^\circ > 0$) or canceled in part by the negative entropy change ($\Delta S^\circ < 0$), respectively. On the other hand, in the last two categories the major driving factor to form complex is the positive entropy change ($\Delta S^\circ > 0$) accompanied by minor stabilizing ($\Delta H^\circ < 0$) or destabilizing enthalpic contribution ($\Delta H^\circ > 0$). However, the classification itself does not particularly lead to deeper understanding of the molecular recognition phenomena.

Apart from the classification, the thermodynamic terms have occasionally been correlated with each other in several chemical and biological molecular recognition systems.[42-66] For instance, Izatt et al.,[42] Michaux and Reisse,[43] and Ouchi et al.[44] demonstrated in the studies on cation binding by crown ethers that $\Delta H$ and $\Delta S$ compensate each other with $\Delta H$ being the dominant quantity in determining the complex stability. Similar compensatory $\Delta H$–$\Delta S$ relationships have also been observed by several researchers in various biological molecular recognition, but analyzed merely within the individual cases.[31,46,50,53-55,57,59,62,64] The general va-

lidity and physical meanings of this compensation effect have not been discussed from a more global point of view until recently.[16,19,28,38,39]

In this chapter, we first analyze the compensation effect observed for the most simple molecular recognition system, i.e. cation binding by ionophores of different basic designs. The analyses lead us to a theory that is compatible with the physical image of cation-binding behavior and applicable to the other more complicated cation-binding systems. In this theory, we assign the slope and intercept of the compensation plot respectively to the conformational change and the degree of desolvation induced by the host–guest association. Then, we extend the scope of this theory to the inclusion complexation by molecular hosts like cyclodextrin, cyclophane, and porphyrin. Following the successful applications in the cation- and molecule-binding systems, we will demonstrate that the basic idea of this correlation analysis and interpretation of the thermodynamic data is further applicable to a variety of biological systems, promoting the global and unified understanding of the supramolecular interactions in both chemistry and biology beyond their apparent diversities in structure and behavior.

## 6.1.  Ionophores: Cation Binding[19–25]

We first discuss the thermodynamics of cation binding by ionophores where only a couple of weak interactions are mainly involved and the binding behavior seems relatively simple to analyze.

A wide variety of ionophores synthesized so far may be classified into three categories, according to the ligand's topology or dimensionality that defines their structural rigidity. As shown in Figure 1, glymes are composed of several oxyethylene units or their aza or thia analogues. Possessing the donor atoms at the appropriate positions in a straight chain, these acyclic ligands inherently suffer considerable conformational changes upon cation binding. In contrast, crown ethers, originally possessing *preorganized* cyclic structures, do not have to alter significantly the conformation upon complexation. In the bicyclic ligands, called cryptands, the donor atoms are both *preorganized* in space and *preoriented* in direction to maximize the cation-binding ability, and therefore the structural changes upon complexation must be minimal.

The guest cations hitherto examined cover broadly uni- to trivalent and inorganic to organic ions that include alkali, alkaline earth, heavy and transition metal ions, as well as (ar)alkyl ammonium and diazonium ions. As to the complex stoichiometry between cation and ligand, both 1:1 stoichiometric and 1:2 sandwich complexes are analyzed. The solvent systems employed also vary widely from protic and aprotic homogeneous phase to binary-phase solvent extraction.

Although the thermodynamic data obtained with different types of host–guest combinations had not been either related to each other or discussed globally, the compensatory enthalpy–entropy relationship was found to be held first in the cation

binding by acyclic and macro(bi)cyclic ligands such as glyme, crown ether, and cryptand, affording linear $\Delta H$–$T\Delta S$ plots.

### Linear $\Delta H$–$T\Delta S$ Plot: Glyme, Crown Ether, and Cryptand

A considerable amount of thermodynamic parameters have been reported for the complexations of uni- and bivalent cations with various glymes mostly in protic solvents like water and methanol.[17,19,20] As has already been demonstrated,[19,20] the plot of the entropy change ($T\Delta S$) as a function of the enthalpy change ($\Delta H$) gives a good straight line as shown in Figure 10. The slope ($\alpha$) and the intercept ($T\Delta S_0$) of the regression line are calculated as 0.89 and 2.0, respectively. Much more abundant thermodynamic data are available for the correlation analysis of the complexation by crown ethers of uni- to trivalent organic and inorganic cations in various solvents. As can be seen from Figure 11, the $\Delta H$–$T\Delta S$ compensation plot using more than 600 data points also exhibits strong positive correlation, affording a regression line of somewhat different slope ($\alpha$ 0.77) and intercept ($T\Delta S_0$ 2.9). In the case of cryptands shown in Figure 12, the $\Delta H$–$T\Delta S$ plot, though more scattered, shows moderate positive correlation between $T\Delta S$ and $\Delta H$, giving a much smaller slope ($\alpha$ 0.42) and larger intercept ($T\Delta S_0$ 4.0) than those for the former two ligands.

The compensatory $\Delta H$–$\Delta S$ relationship itself is not specific to the cation–ligand complexation thermodynamics but have amply been exemplified in a variety of
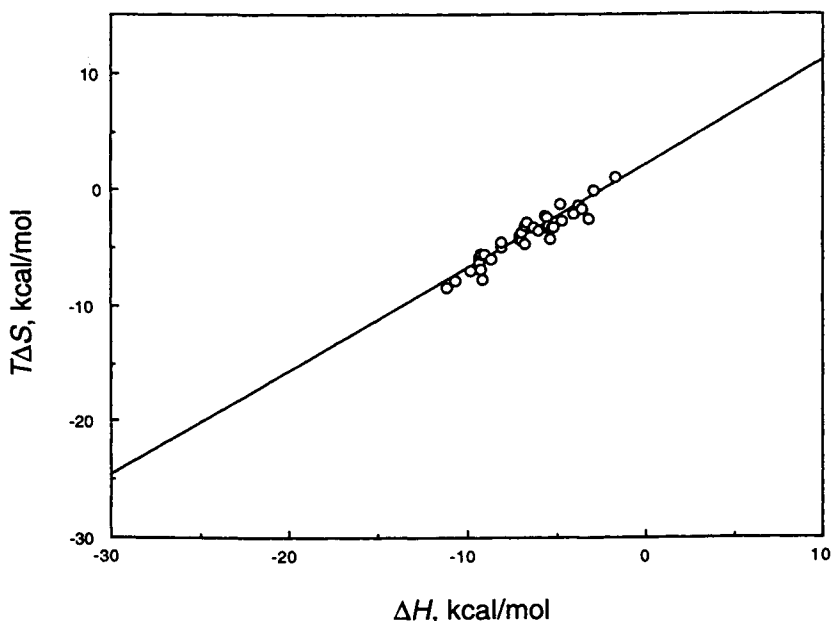


**Figure 10.** $\Delta H$–$T\Delta S$ plot for cation binding by glymes.
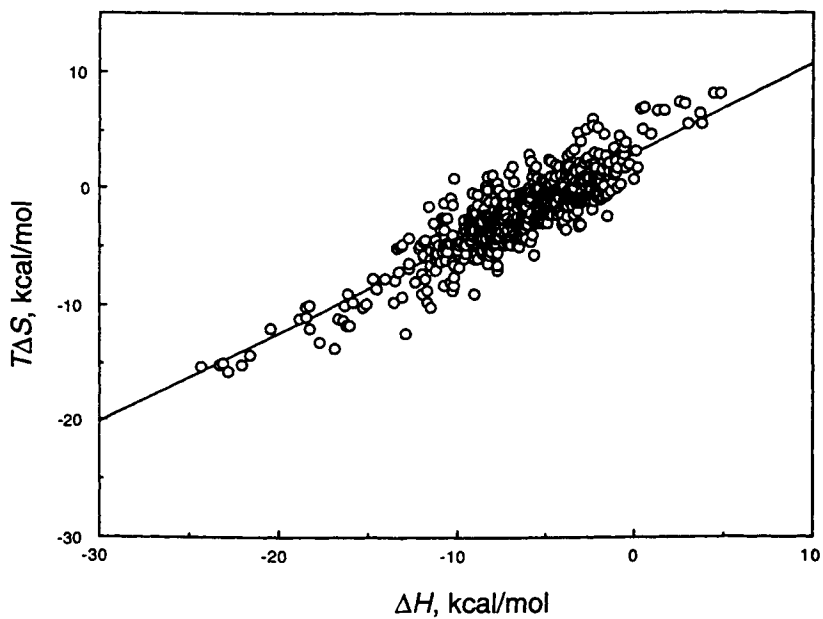
**Figure 11.** $\Delta H - T\Delta S$ plot for cation binding by crown ethers.
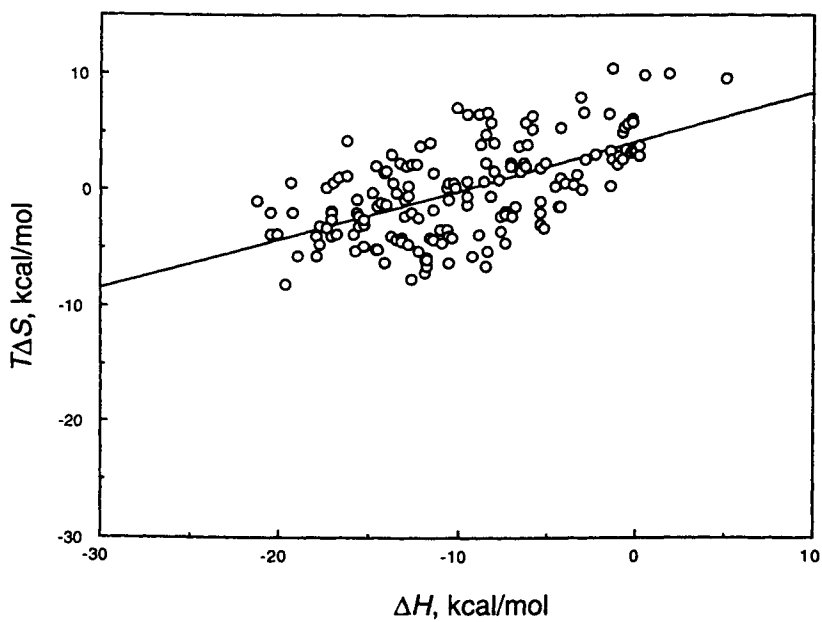


**Figure 12.** $\Delta H - T\Delta S$ plot for cation binding by cryptands.
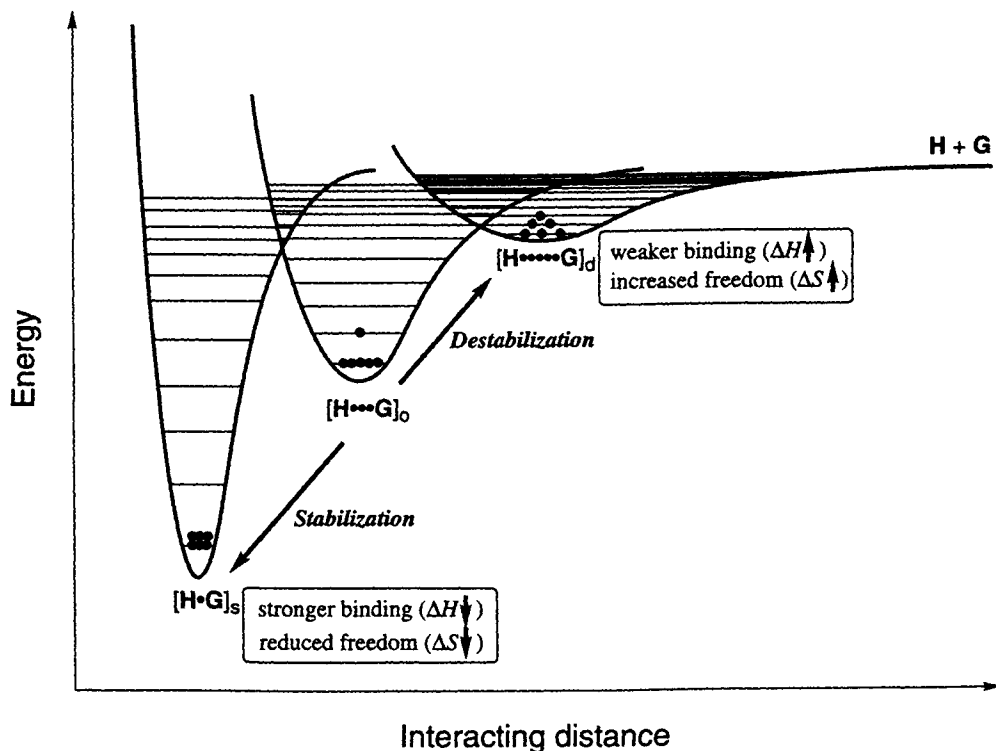
**Figure 13.** Consequences of perturbations to a host–guest complex [H•••G]$_0$; stabilizing perturbations lead to a deeper, narrower potential well and more spaced vibrational levels which mean stronger binding and reduced freedom in the resulting complex [H•G]$_s$, while destabilizing perturbations lead to a more shallow, broader well, and congested vibrational levels which correspond to weaker binding and increased freedom in the destabilized complex [H••••••G]$_d$.

reactions and equilibria.[34-36] The origin of the extrathermodynamic compensation effect found here may be illustrated schematically in Figure 13. We suppose a moderately stable host–guest complex [H•••G]$_0$ shown in the middle of Figure 13. The stability of this original complex [H•••G]$_0$ is affected by changing the host, guest, solvent, or any other perturbing factors to afford a stabilized complex [H•G]$_s$ (lower left) or a destabilized complex [H•••••G]$_d$ (upper right). The increased stability, arising from stronger binding (more negative $\Delta H$), inevitably accompanies reduced freedoms (more negative or less positive $\Delta S$) of the complex formed and vice versa.

As illustrated in Figure 13 (lower left), the stabilization of the complex makes both components closer in distance, the potential well deeper, and the vibrational levels more spaced in energy. As a consequence, only the lowest vibrational level is populated and the ranges of stretching and rotational vibrations are quite limited in the extreme case shown here; in other words, the freedom of the stabilized complex $[H \cdot G]_s$ is much reduced, although the binding is greatly reinforced. On the contrary, destabilization of the original complex $[H \cdot \cdot \cdot G]_o$ leads to the less-stable, looser complex $[H \cdot \cdot \cdot \cdot \cdot G]_d$ with shallow, broadened potential curve shown in Figure 13 (upper right). The shallow well, though indicating weaker binding or less negative $\Delta H$, simultaneously brings less-spaced vibrational levels of broader vibrating ranges. This enables the destabilized complex $[H \cdot \cdot \cdot \cdot \cdot G]_d$ of looser binding to populate to the upper levels and also to stretch over wider ranges than the original complex even at the same temperature, which is synonymous to much increased freedom or less negative or more positive $\Delta S$, as schematically illustrated in Figure 13 (upper right).

In summary, the enthalpy and entropy terms do not vary independently but compensate each other in nature as far as the weak interactions are concerned, while the extent of $\Delta H$–$\Delta S$ compensation appears to depend significantly on the host's topology.

### Slope: Measure of Conformational Change

As experimentally demonstrated above, in the complexation thermodynamics involving cationic species as guests and ionophores as hosts, the entropic change $T\Delta\Delta S$, induced by altering cation, ligand, or solvent, is proportional to the enthalpic change $\Delta\Delta H$. This correlation immediately leads to an empirical Eq. 14 with a proportional coefficient $\alpha$, integration of which affords an extrathermodynamic relationship between $T\Delta S$ and $\Delta H$. Thus, Eq. 15 is the quantitative expression of the observed compensation effect:

$$T\Delta\Delta S = \alpha\Delta\Delta H \qquad (14)$$

$$T\Delta S = \alpha\Delta H + T\Delta S_0 \qquad (15)$$

Combining Eq. 14 with the differential form of the Gibbs–Helmholtz equation (Eq. 12), we obtain Eq. 16:

$$\Delta\Delta G = (1 - \alpha)\Delta\Delta H \qquad (16)$$

Equation 16 indicates that, even if one changes the cation, ligand, solvent, or any other perturbing factor(s) in order to stabilize a cation–ligand complex, the enthalpic gain thus obtained ($\Delta\Delta H$) is not fully reflected to the complex stability but is canceled in part $(1 - \alpha)$ by the entropic loss ($\Delta\Delta S$). Hence, the slope of $\Delta H$–$T\Delta S$ plot is taken as a quantitative measure of the entropic loss upon complex formation.

The three categories of ionophores, shown in Figure 14, originally possess different topologies or dimensionalities, and the ligand structure is altered upon complexation to the extent that depends on the structural differences before and after complexation. Then, it is reasonable to assume tentatively that the tendency of $\alpha$ is related to the degree of the induced structural changes.

As can be seen from Figure 14, the donor atoms (D) in acyclic glymes, which possess extended original structures, have to encircle the guest cation, suffering most comprehensive conformational changes and structural fixation. This entropic disadvantage makes these acyclic ionophores relatively poor cation binders. By contrast, cation binding by cyclic crown ethers with preorganized donor atoms causes no serious structural changes and is entropically more advantageous. Bicyclic cryptands, whose donor atoms are preorganized and preoriented, suffer minimal conformational changes upon complexation and are entropically most favored.

Interestingly, the slope $\alpha$ of $\Delta H - T\Delta S$ plot decreases dramatically from 0.89 for acyclic glyme to 0.42 for bicyclic cryptand as the degree of conformational change upon complexation decreases. According to Eq. 16, these $\alpha$ values indicate that as high as 89% of the enthalpic gain ($\Delta\Delta H$) is canceled by the entropic loss in the case of glyme, while only 42% of $\Delta\Delta H$ is canceled entropically in the cryptand case. Taking into account the tendency of the $\alpha$ values obtained for each ligand type and the fact that the $\alpha$ value represents how much enthalpic gain acquired upon ligation is canceled by the entropic loss from the accompanying conformational fixation, it
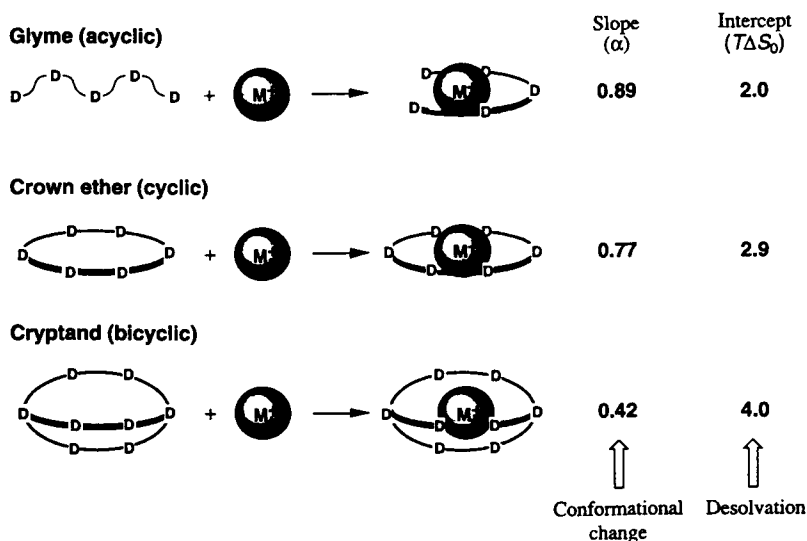


**Figure 14.** Schematic drawings of conformational changes upon cation binding by glymes, crown ethers, and cryptands (D denotes donor atom); also shown are the slopes ($\alpha$) and intercepts $T\Delta S_0$ of $\Delta H - T\Delta S$ plots as measures of conformational change and desolvation.

is natural to adopt the $\alpha$ value as a quantitative scale to measure the conformational changes caused upon complexation. In this context, it would be somewhat unexpected that even the most rigid three-dimensional ligand cryptand loses nearly half the enthalpic gain by the entropic canceling effect. However, this seems reasonable since cation binding inherently involves a molecular association process, which inevitably needs to pay the entropic cost. Yet, it may be emphasized that no other supramolecular system affords such a low $\alpha$ value and cryptand as a three-dimensional ligand is one of the entropically most optimized hosts.

## Intercept: Measure of Desolvation

In this section, we discuss the physical meaning of the intercept $T\Delta S_0$ of $\Delta H - T\Delta S$ plot. Similar to the slope $\alpha$, the intercept $T\Delta S_0$ is specific to the ligand topology, but its changing profile is inverse as the $T\Delta S_0$ value increases from 2.0 for glyme to 2.9 for crown ether and further to 4.0 for cryptand with increasing ligand's dimensionality. Another distinct feature is that the intercept never goes negative for all ligand types. The positive $T\Delta S_0$ value means that, even if no heat production is obtained upon complexation ($\Delta H = 0$ and therefore $\Delta G = -T\Delta S$), the entropy change $T\Delta S$ can be a positive value that is equal to the intercept $T\Delta S_0$, according to Eq. 15. Then, even in the case of endothermic association, the complexation is assisted by the intrinsic entropic contribution of $-T\Delta S_0$ to afford a negative free energy change. As can be seen from Figures 11 and 12, such an entropy-driven complex formation, affording positive $T\Delta S$ and zero to positive $\Delta H$, does occur indeed in several cases. In such an endothermic system, the only source of the positive entropy change is the increased freedom arising from the complexation-induced desolvation of guest cation and/or host ionophore. The complexation causes desolvation mainly from cation in aprotic polar solvents but from both cation and ionophore in protic solvents.
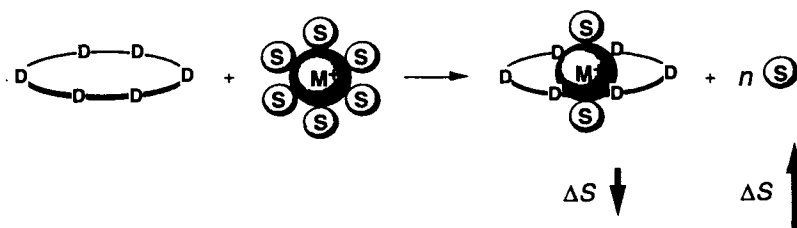


**Figure 15.** Schematic drawing of complexation-induced desolvation from cation and ligand (solvation to the latter is not shown): the complex formation itself reduces the entropy of the system to some extent but the accompanying desolvation leads to much larger increase in entropy ascribed to the liberation of solvent molecules.

Consequently, we employ the slope $T\Delta S_0$ as a quantitative measure of the extent of desolvation caused by host–guest association. The complexation-induced desolvation process is schematically illustrated for cation binding by crown ether in Figure 15. It is evident that a considerable part of the solvent molecules surrounding cation ($M^+$) and ligand have to be released upon complexation. The molecular association process itself accompanies inherently negative $\Delta S$, while the extensive desolvation from cation and ligand gives rise to a much larger positive $\Delta S$. However, the number of solvent molecules removed from the solvation shell around the cation depends significantly upon the ligand topology. As can be seen from Figure 14, both acyclic glyme and cyclic crown ether wrap around the cation (quasi)circularly to liberate most or all solvent molecules that are originally placed in the coordination plane, leaving the axial solvation intact. Hence, these two ligands, though original structures differ substantially, are expected to resemble each other in the desolvation behavior. In contrast, the desolvation induced by complexation with bicyclic cryptands is much more thorough and extensive, liberating most solvent molecules originally surrounding the cation and the host. These schematic views of the induced desolvation nicely coincide with the tendency of the intercept $T\Delta S_0$, experimentally confirming the assignment of the $T\Delta S_0$ value to the extent of desolvation.

### Sophisticated Ionophores: Long Glyme, Lariat Ether, Bis(crown ethers), and Ionophore Antibiotic[20]

We now proceed to more complicated ionophores in order to testify the validity of this extrathermodynamic relationship and its hypothetical interpretation as an attempt to understand the nature of supramolecular interactions more generally and deeply. The thermodynamic parameters[20] are plotted in Figures 16–19 for long glymes, (pseudo)cyclic ionophore antibiotics, lariat ethers with donating side-arm(s), and bis(crown ethers), whose structural changes upon complexation are schematically illustrated in Figure 20.

All of the $\Delta H$–$T\Delta S$ plots gave good to excellent straight lines of different slopes and intercepts, again depending upon the topology of individual ligand. Both the slopes and intercepts for these ligands, listed in Table 2, are particularly large: $\alpha =$ 0.89–1.03 and $T\Delta S_0 = 4.2$–5.4. The large $\alpha$ values close to unity indicate that the conformational changes are more extensive than the simple glyme case shown in Figures 10 and 14, and further mean that all efforts to enhance cation-binding ability will not be rewarding due to the large entropic losses. Then, the extent of induced conformational changes is deduced to increase in the order: cryptand (0.42) < crown ether (0.77) < glyme (0.89) = lariat ether (0.89) < ionophore antibiotic (0.93) < bis(crown ethers) $\cong$ (1.03) long glyme (1.03). This analysis, according to the proposed theory that the slope $\alpha$ is a quantitative measure of the conformational changes upon complexation, is well compatible with the binding behavior of long glyme, ionophore antibiotic, bis(crown ethers), and lariat ether since these ligands
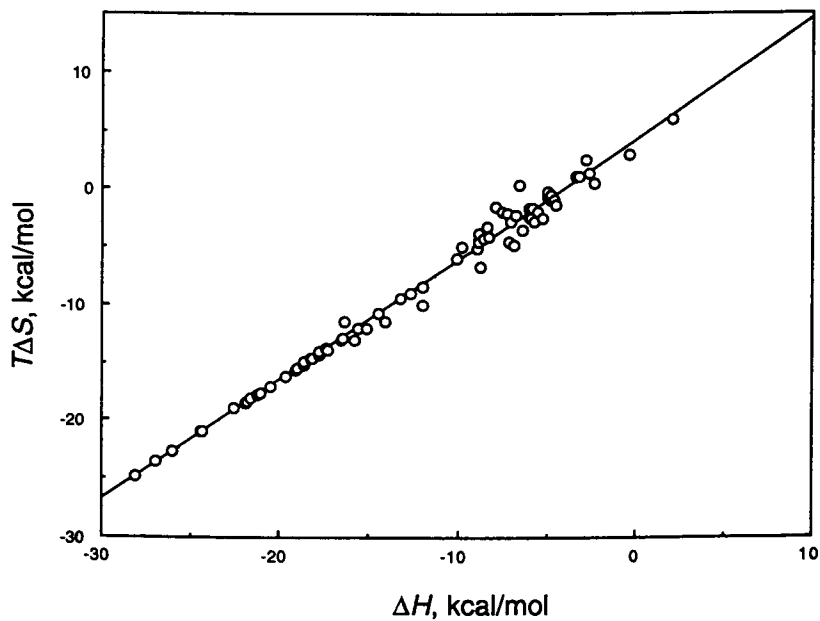
**Figure 16.** ΔH–TΔS plot for cation binding by long glymes.
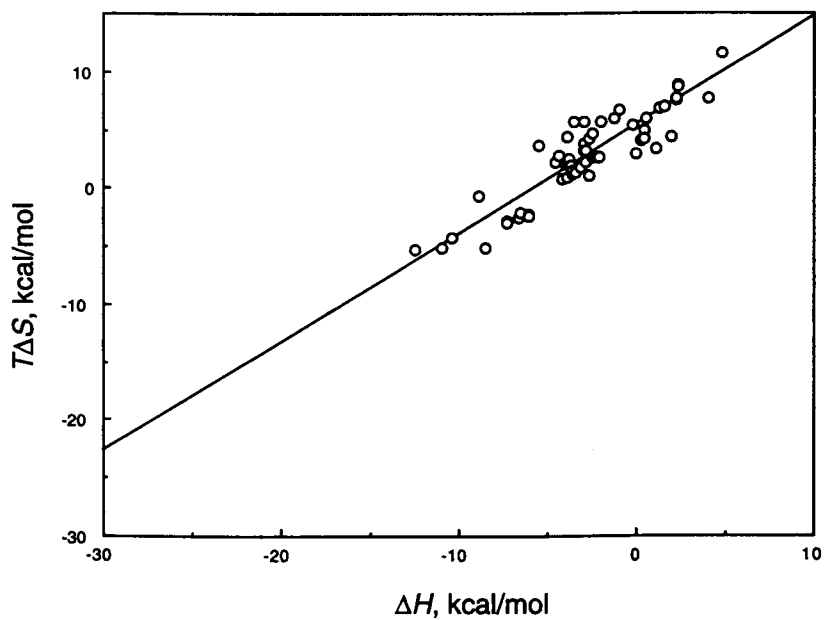


**Figure 17.** ΔH–TΔS plot for cation binding by (pseudo)cyclic antibiotics.
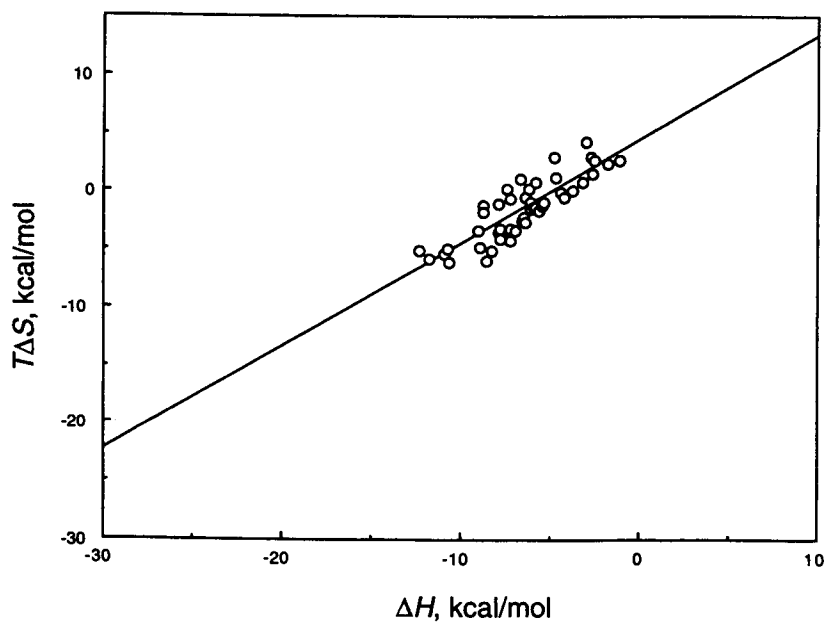
**Figure 18.** ΔH–TΔS plot for cation binding by lariat ethers.
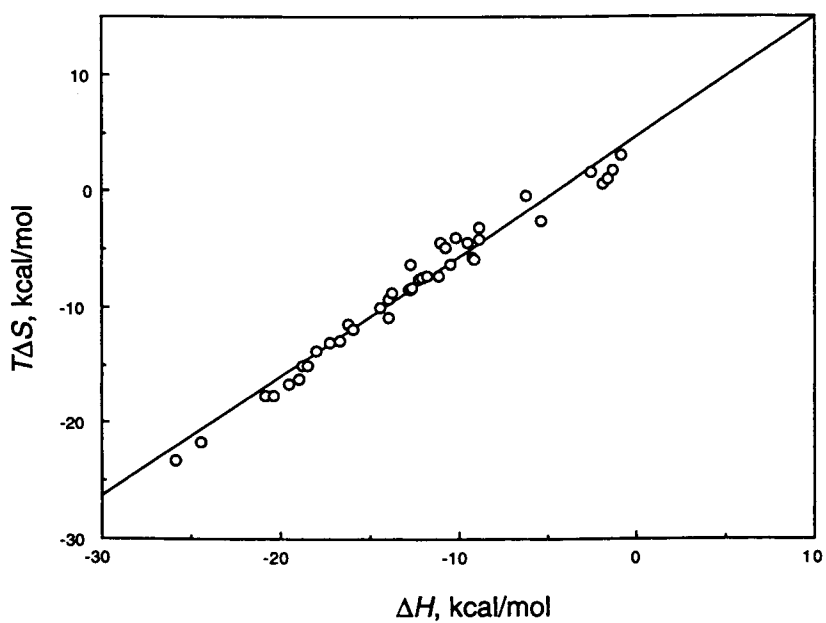


**Figure 19.** ΔH–TΔS plot for cation binding by bis(crown ethers).

78

|  | Slope ($\alpha$) | Intercept ($T\Delta S_0$) |
|---|---|---|
| **Long glyme** | 1.03 | 4.2 |
| **Antibiotic** | 0.93 | 5.4 |
| **Lariat ether** | 0.89 | 4.3 |

**Bis (crown ethers)**



1.03    4.6

**Sandwich complex**



0.94    3.2

Conformational    Desolvation
change
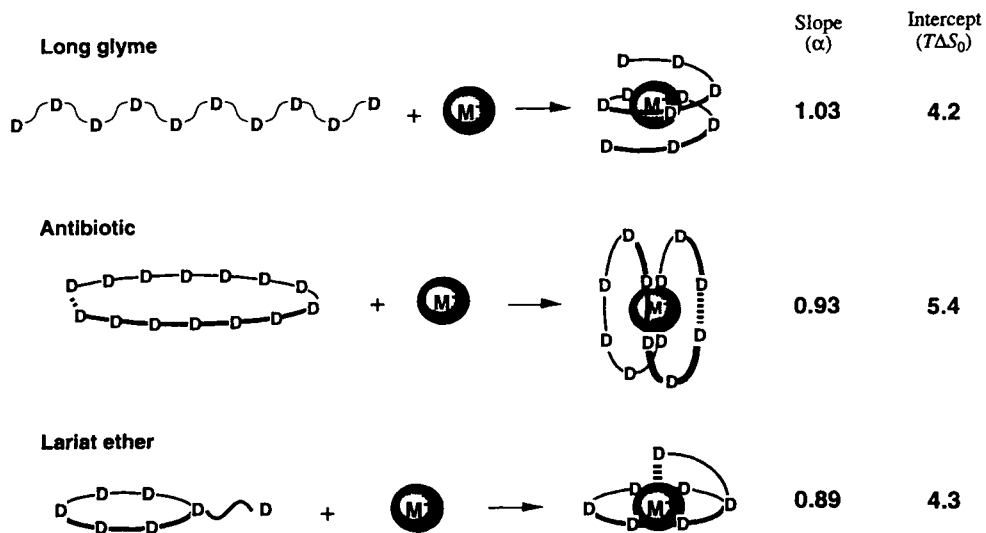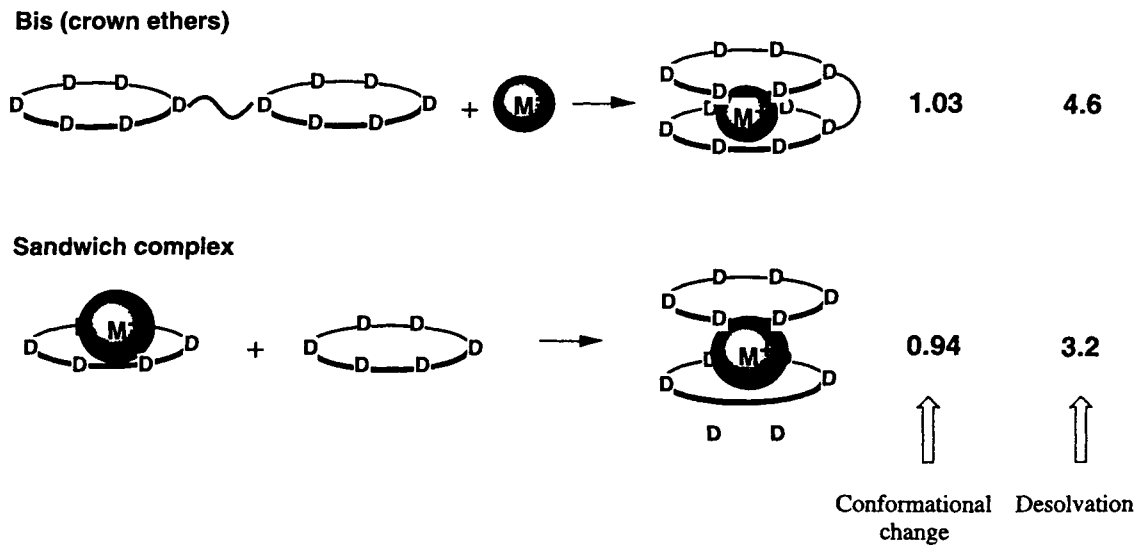
*Figure 20.* Schematic drawings of conformational changes upon cation binding by some sophisticated ligands and the slopes ($\alpha$) and intercepts ($T\Delta S_0$) of $\Delta H$–$T\Delta S$ plots as measures of conformational change and desolvation.

**Table 2.** Slope ($\alpha$) and Intercept ($T\Delta S_0$) of the $\Delta H$–$T\Delta S$ Plots for Supramolecular Interactions of Natural and Synthetic Hosts with a Variety of Ionic, Molecular, and Biomolecular Guests in Homogeneous and Heterogeneous Solutions

| Host | Guest | Solvent | $\alpha$ | $T\Delta S_0$ |
|---|---|---|---|---|
| glyme | ion | aqueous | 0.89 | 2.0 |
| crown ether | ion | aqueous | 0.77 | 2.9 |
| crown ether | ion | solvent extraction | 0.73 | 2.6 |
| crown ether (sandwich complex) | ion | aqueous | 0.94 | 3.2 |
| cryptand | ion | aqueous | 0.42 | 4.0 |
| long glyme | ion | aqueous | 1.03 | 4.2 |
| ionophore antibiotic | ion | aqueous | 0.93 | 5.4 |
| lariat ether | ion | aqueous | 0.89 | 4.3 |
| bis(crown ethers) | ion | aqueous | 1.03 | 4.6 |
| cyclodextrin | organic molecule | aqueous | 0.93 | 3.3 |
| quinone-receptor porphyrin | quinone | organic | 0.60 | 0.0 |
| metalloporphyrin | pyridine | organic | 0.61 | 1.6 |
| cyclophane/calixarene | organic molecule | aqueous | 0.78 | 3.4 |
| enzyme | coenzyme/substrate/inhibitor | aqueous | 1.11 | 7.0 |
| antibody | antigen | aqueous | 0.88 | 8.7 |
| DNA/RNA | DNA/RNA/intercalator | aqueous | 1.03 | 8.5 |

suffer considerable but different degrees of structural alterations in the process to wrap around a cation.

On the other hand, the $T\Delta S_0$ values, which are comparable or even larger than that for cryptand, indicate fairly extensive desolvation, according to the present theory. This is totally agreeable since the wrapping complexation by these types of ligands should replace most of the solvent molecules that is originally occupying the cation's coordination sites with the ligand's donor atoms. The order of the desolvation ability is: glyme (2.0) < crown ether (2.9) < cryptand (4.0) ≤ long glyme (4.2) ≤ lariat ether (4.3) < bis(crown ethers) (4.6) < ionophore antibiotic (5.3), as listed in Table 2.

## Sandwich Complexation[20]

Although the ligands incorporated are the same, the sandwich complexation of a cation with two molecules of crown ethers should be discussed separately. The sandwich complexes are formed in two successive processes consisting of usual stoichiometric 1:1 complexation followed by further ligation by another molecule
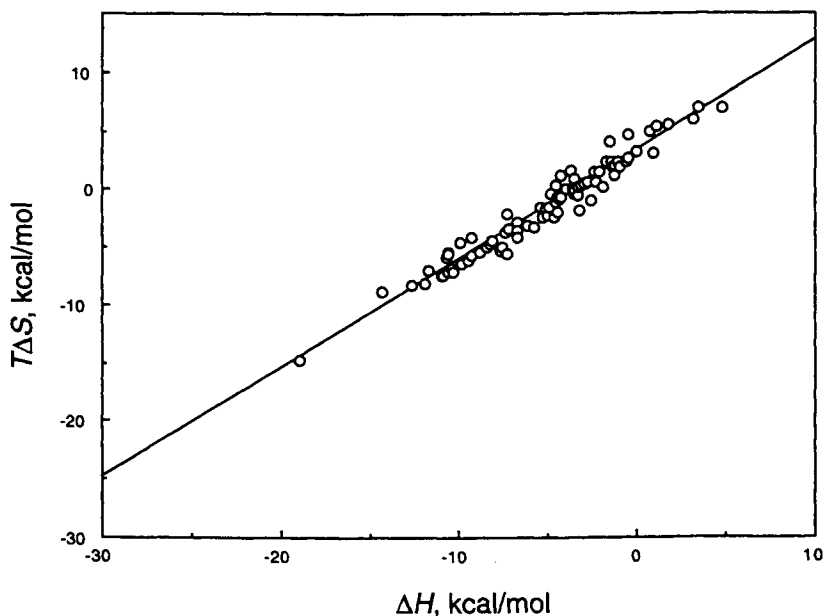
***Figure 21.*** $\Delta H - T\Delta S$ plot for sandwich complexation of cations with crown ethers.

of the ligand, as illustrated in Figure 20. Here we discuss the thermodynamic view of the second step.

The $\Delta H - T\Delta S$ plot for the sandwich complexation[20] afforded an excellent straight line as shown in Figure 21. The slope $\alpha$ and the intercept $T\Delta S_0$ obtained for the sandwich complexation with crown ethers are 0.94 and 3.2, respectively. Interestingly, these values are much larger than those for the first step ($\alpha$ 0.77 and $T\Delta S_0$ 2.9). These values indicate that the further ligation of the second crown ether to the original 1:1 complex induces substantial conformational changes not only to the second crown ether but also to the originally ligating crown ether, and that the desolvation caused by the second ligation is more extensive than the first step.

## Solvent Extraction

We have hitherto dealt with the complexation thermodynamics in the homogeneous solutions. However, the above interpretation based on the linear enthalpy–entropy relationship may be extended to the complexation behavior in the solvent extraction of aqueous metal salts with ionophores in organic solvent.

Although the thermodynamic data reported for the solvent extraction equilibria are limited,[20] we obtained a well-correlated $\Delta H - T\Delta S$ compensation plot (Figure 22) for the solvent extraction of aqueous metal picrates with crown ethers in organic solvents. Quite interestingly, the slope ($\alpha$ 0.73) and the intercept ($T\Delta S_0$ 2.6) are very
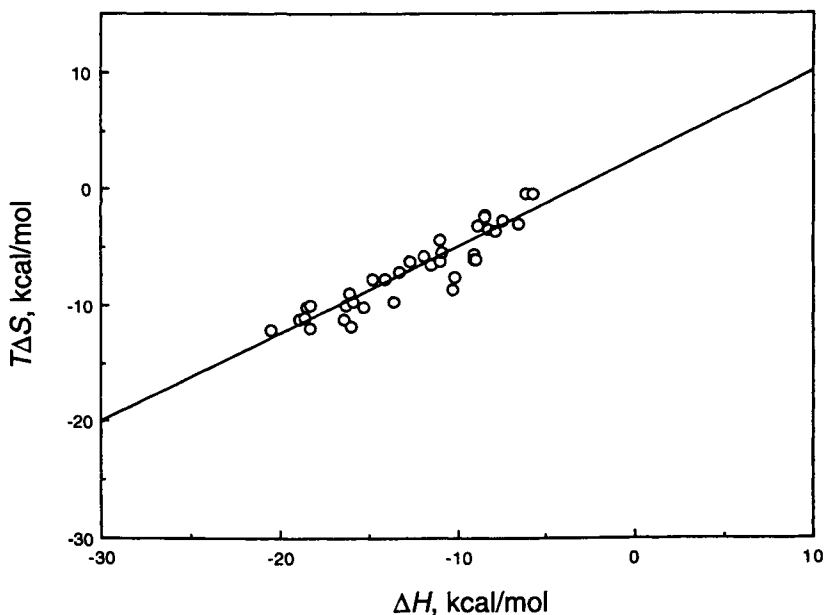
**Figure 22.** ΔH–TΔS plot for solvent extraction with crown ethers.

similar to the corresponding values ($\alpha$ 0.77 and $T\Delta S_0$ 2.9) observed in the homogeneous-phase complexation. It is deduced therefore that, as far as the same ligand is concerned, the degrees of conformational changes and desolvation are essentially the same, irrespective of the solvent system employed.

In view of the compensatory enthalpy–entropy relationship observed for a wide variety of ionophore types, we may conclude that the cation-binding behavior, where the weak ion–dipole and dipole–dipole interaction is the major driving force for complexation, can be quantitatively analyzed and characterized by the slope and intercept of the $\Delta H$–$T\Delta S$ plot without any exception. In this context, it is stimulating to extend the scope of this theory to the inclusion complexation of organic guests with molecular hosts.

## 6.2. Molecular Hosts: Inclusion Complexation

There are several types of natural and synthetic molecular hosts, such as cyclodextrin and cyclophane, that are shaped to accommodate neutral and charged organic molecules in the three-dimensional cavity. The inclusion complexation by molecular hosts is driven by various weak forces like van der Waals, hydrophobic, hydrogen bonding, ion–dipole, and dipole–dipole interactions, and therefore the molecular recognition process seems much more complicated. In expanding the scope of the present theory, it is intriguing and inevitable to perform the extrather-

modynamic analysis of the inclusion complexation by molecular hosts such as cyclodextrin, porphyrin, cyclophane, and calixarene.

## Cyclodextrin[25,26]

α-, β- and γ-Cyclodextrins are a series of cyclic oligosaccharides composed of six, seven, and eight glucopyranose units forming a truncated cone structure.[11,67] Possessing a hydrophobic cavity, these natural cyclic hosts are known to include a variety of size-matched organic molecules in the cavity and are often employed as model systems that mimic some enzymatic functions.[9,11,67] The secondary hydroxyl groups at C2 and C3 of the glucose units are successively hydrogen-bonded to the hydroxyl groups of the adjacent glucose to form a tightly knit hydrogen-bond network circling the wider opening of cyclodextrin molecule, while the primary hydroxyls at C6 located at the narrow end contribute to the solubility into aqueous solution. It is well documented that cyclodextrins in aqueous solution hold several "high energy" water molecules in the cavity,[11,67] which are released upon guest inclusion enhancing the complexation entropically.

A considerable amount of thermodynamic data have already been collected for the inclusion complexation of simple organic molecules and more sophisticated drugs with α- to γ-cyclodextrins in aqueous solutions.[25,26] Using these thermodynamic parameters, we plotted the entropy change against the enthalpy change in Figure 23. The data for α-, β-, and γ-cyclodextrins, marked individually in Figure 23, show no appreciably different tendencies in the plot, affording practically the same regression line of large slope (α 0.93) and moderate intercept ($T\Delta S_0$ 3.3).

The large slope as high as 0.93 indicates that only 7% of the enthalpic gain or loss ($\Delta\Delta H$) induced by any alterations in host, guest, or solvent is reflected to the overall complex stability ($\Delta\Delta G$), owing to the accompanying entropic canceling effect ($\Delta\Delta S$). This would seem curious in view of the apparently rigid structure of cyclodextrin. However, the rearrangement of the peripheral hydrogen bond network and the accompanying minor skeletal conformational changes[11,67] are considered to be responsible for the large α value.

On the other hand, the intercept obtained for cyclodextrin cannot directly be compared with those for ionophores since the species and weak interactions involved are obviously different in these two host categories. Nonetheless, the $T\Delta S_0$ value of 3.3 is not small but comparable to those for crown ether (2.9) and cryptand (4.0). Thus, the entropic gain, arising from desolvation upon guest inclusion, is undoubtedly significant. Both the release of "high energy" water molecules included originally in the cavity and the induced dehydration from the peripheral hydroxyl groups of cyclodextrin must be responsible for the large intrinsic entropic gain ($T\Delta S_0$).

It is thus demonstrated that the inclusion behavior of cyclodextrins is similarly analyzed and interpreted in terms of the enthalpy–entropy compensation effect, although the major weak forces involved are quite different from those working in
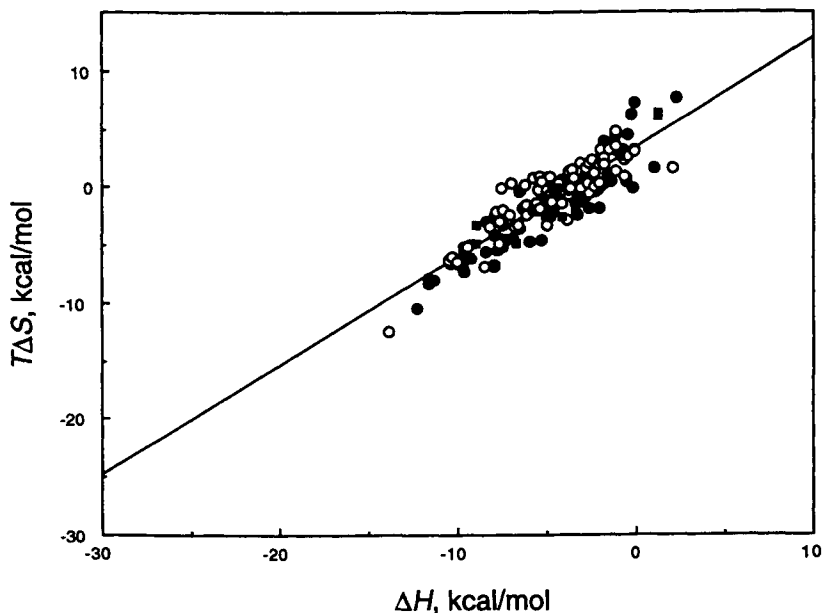
**Figure 23.** $\Delta H - T\Delta S$ plot for inclusion complexation of organic guests by α-(●), β-(○), and γ-cyclodextrins (⊞).

the cation binding process. These results prompted us to further extensions of this theory to other molecular recognition systems.

### Porphyrin[26,37]

Recently, Aoyama et al.[37] synthesized a quinone-receptor porphyrin that possesses two 2-naphthol moieties at the transannular positions of porphyrin (Figure 3). Positioned at the exact distance and directed properly, these two naphthol units bind various p-quinone derivatives by forming two hydrogen bonds. This molecular recognition system has some characteristic features differing from the above-mentioned cation- or molecule-binding systems: (1) the host molecule with a very rigid skeleton suffers quite limited conformational changes upon complexation only at the peripheral naphthol moieties; (2) the associated weak forces are limited in number and clearly defined, i.e. the hydrogen bonding and the charge-transfer π–π interaction between porphyrin and quinone; and (3) the solvent used is not protic but the less-polar aprotic organic solvent, chloroform.

The thermodynamic parameters[37] reported for the complexation of various quinone derivatives with this porphyrin derivative are plotted to give an excellent straight line, as shown in Figure 24 (closed circle). The small slope obtained (α 0.60) is immediately related to the rigid skeleton and the restricted motion of the
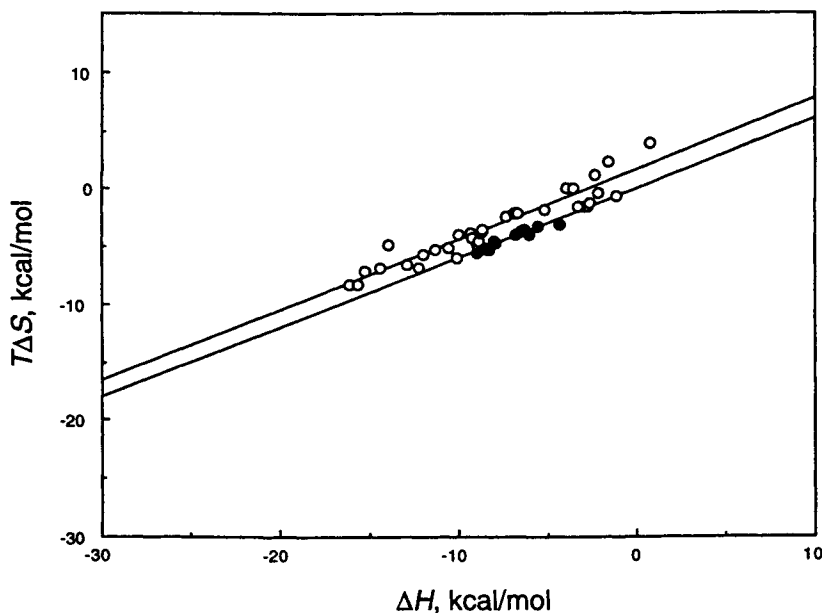
**Figure 24.** $\Delta H$–$T\Delta S$ plot for complexation by quinone-receptor porphyrins (●) and ligation to metalloporphyrins (○).

naphthol moieties upon quinone binding, and indicates that any enthalpic efforts to enhance the binding ability is rewarded at a fairly high return up to 40%. Importantly, the intercept ($T\Delta S_0$) observed for this quinone-receptor porphyrin is literally zero, clearly indicating that no entropic assist is gained from the release of solvent molecules upon complexation. Since practically no complexation-induced desolvation is expected to occur in view of the nonsolvating nature of the solvent used, this result is quite reasonable and strongly supports the theory that the intercept of the $\Delta H$–$T\Delta S$ plot serves as a quantitative measure of the extent of desolvation.

The ligation thermodynamics of various metalloporphyrins[26] (Figure 3) are also analyzed successfully by this theory. The $\Delta H$–$T\Delta S$ plot obtained for the ligation of pyridine derivatives to metalloporphyrins, also shown in Figure 24 (open circle), gives practically the same slope ($\alpha$ 0.61), indicating again that the rigid porphyrin skeleton suffers little significant conformational changes upon ligation of pyridines. Furthermore, the intercept is also very small ($T\Delta S_0$ 1.6), indicating trivial desolvation caused by ligation.

## Cyclophane and Calixarene[26]

Cyclophanes and calixarenes[9,13,14] are aromatic hosts that share the same grand design and common structural and functional features as exemplified in Figure 4:

(1) two or more aromatic rings, placed circularly in space, are connected to each other with methylene or oxyethylene chains to construct a hydrophobic cavity of appropriate size surrounded by several aromatic rings; and (2) some hydrophilic groups are appended at the peripheral positions in order to make them water-soluble.

Thermodynamic data reported for the inclusion complexation of organic molecules with these aromatic hosts[26] are treated as above to give a linear $\Delta H$–$T\Delta S$ plot shown in Figure 25. The slope obtained ($\alpha$ 0.78) is comparable with that for crown ether ($\alpha$ 0.77). This reveals that these hosts composed of several aromatic rings connected with methylene or oxyethylene chains suffer considerable conformational changes upon inclusion, probably due to the structural flexibility which is comparable to crown ether. The relatively large intercept obtained ($T\Delta S_0$ 3.4) is indicative of moderate desolvation from both host and guest upon inclusion complexation. Beyond all the differences in host structure, guest type, and weak forces involved, the cation binding by crown ethers and the molecular inclusion by cyclophanes and calixarenes share the same strategy to create a apparently different but essentially resembling two-dimensional arrangement of interacting sites that optimizes the cooperative weak interactions between host and guest.

It has thus been demonstrated that the complexation behavior of various synthetic hosts, including ionophores and molecular hosts, can be interpreted quantitatively and systematically in terms of the slope ($\alpha$ as a measure of complexation-induced
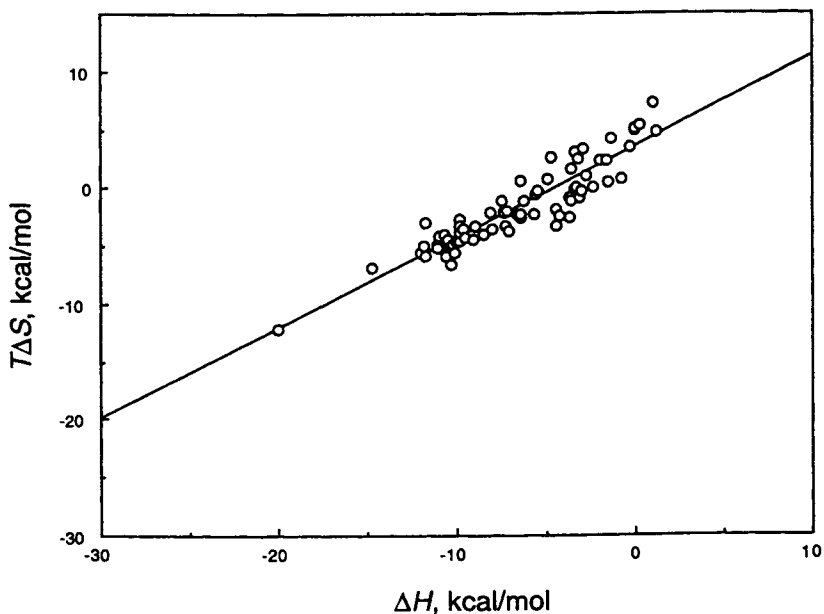


**Figure 25.** $\Delta H$–$T\Delta S$ plot for inclusion complexation by cyclophanes and calixarenes.

conformational changes) and the intercept ($TAS_0$ as a measure of desolvation upon complexation) of the $\Delta H$–$TAS$ plot, in spite of the vast diversity in host design, guest type, complex stoichiometry, solvent property, and particularly weak interaction involved.

## 6.3. Biological Hosts: Supramolecular Complexation

Since the present theory has been shown to be useful in analyzing molecular recognition of relatively simple guests with most synthetic hosts, we now proceed to the supramolecular interactions in more sophisticated biological systems where relatively abundant thermodynamic data are available in the literature.

We will discuss the interaction of enzyme with coenzyme, substrate, and inhibitor; the antigen–antibody reaction; and the duplex formation and intercalation of DNA and RNA. In these biological supramolecular systems, molecular recognition takes place in a hydrophobic pocket or environment surrounded by water. Most of the weak forces discussed above are involved more or less in the biological supramolecular interactions, constituting most sophisticated molecular recognition systems that appear difficult to analyze in the same manner. It should be emphasized however that the precise biological molecular recognition is also materialized by the cooperation of several weak interactions, as is the case with the synthetic host–guest systems. We therefore believe that these apparently complicated biological systems should also be discussed by using the same theory proposed for the chemical molecular recognition systems. Otherwise, this theory does not have a general validity and should perish.

### Enzyme[38,39]

Enzymes, composed of various amino acids, constitute hydrophobic interior and hydrophilic exterior by arranging in space the appropriate amino acid residues. The hydrophobic receptor site is usually located inside and the hydrophilic amino acid residues located on the surface of enzyme are heavily solvated by water molecules in aqueous solution. Then, the supramolecular interactions with specific coenzymes, substrates, and inhibitors inevitably accompany extensive dehydration and conformational change of both enzyme and ligand.

Relatively ample thermodynamic data are available for the interaction of enzyme with coenzyme, substrate, and inhibitor in aqueous solution.[68–71] The enzymes investigated are aldolase,[68,69] ATPase,[54,69] chymotripsin,[69] dehydrogenase,[69–71] lipase,[69] lysozyme,[69] phosphofructokinase,[71] ribonuclease A,[69] tRNA synthetase,[69] and trypsin.[70] The thermodynamic parameters obtained for the enzyme–coenzyme, enzyme–substrate, and enzyme–inhibitor combinations are plotted separately in Figure 26. Although the data for each combination tend to flock together, essentially all the data points fall on the same regression line whose slope ($\alpha$) and intercept ($TAS_0$) are 1.11 and 7.0, respectively. The large slope, slightly exceeding unity, means that the enthalpic gain from the supramolecular association of enzymes is
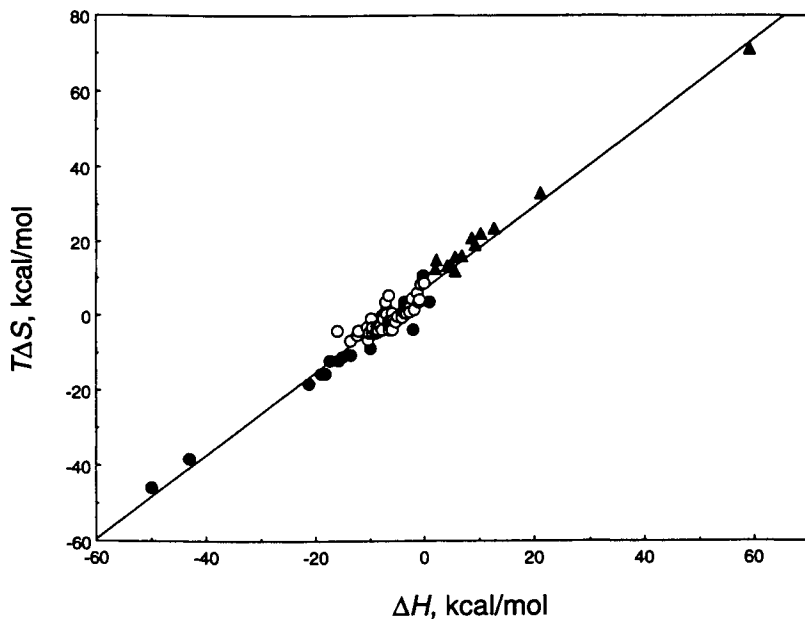
**Figure 26.** $\Delta H$–$T\Delta S$ plot for supramolecular interaction of enzyme with substrates (●), coenzymes (○), and inhibitors (▲).

completely canceled out by the entropic loss arising from the conformational changes upon enzymatic interaction. On the other hand, the very large intercept as high as 7.0 indicates that the enzymatic reactions in aqueous solutions are driven exclusively by the far-reaching desolvation from enzyme itself and also from coenzyme, substrate, and inhibitor to be bound.

### Antibody[38,39]

The antigen-specific supramolecular interaction of antibody is also made possible through cooperative weak interactions and is therefore worth pursuing the extrathermodynamic analysis. Composed of the same components, i.e. amino acids, antibody behaves like enzyme upon interaction with its specific antigen. Thus, the binding of antigen to the concave hydrophobic pocket of antibody in aqueous solution induces considerable structural changes especially in antibody and extensive dehydration of both components around the receptor site. Unfortunately, only a limited number of thermodynamic data are available for antigen–antibody reaction.[53,69] The antigens examined are di- or trinitrophenyl (DNP or TNP) derivatives of amino acids such as lysine and glycine, menadione, and ribo- and lumiflavins, with which anti-DNP or -TNP antibody,[69] mouse plasmacytoma protein,[69] and aporiboflavin binding protein[53] interact specifically to produce the corresponding antigen–antibody complexes.
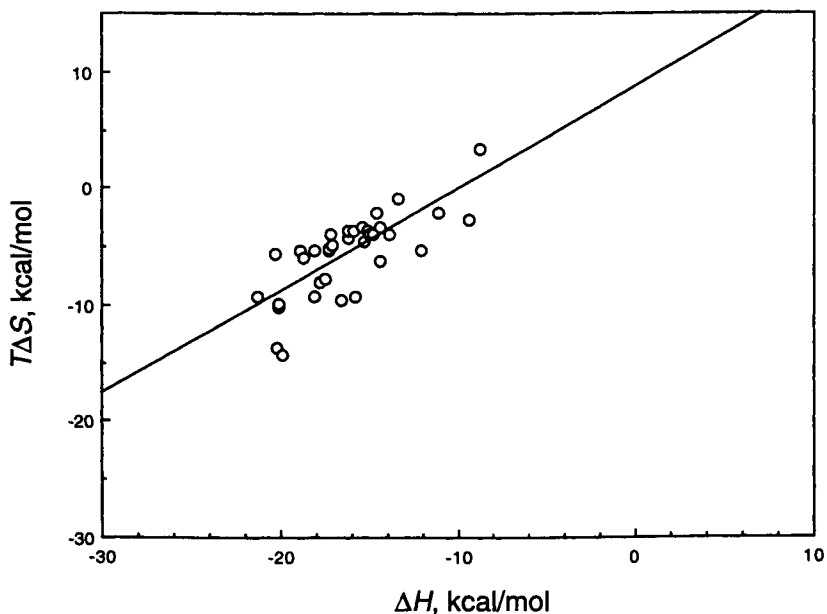
**Figure 27.** ΔH–TΔS plot for supramolecular interaction of antibodies.

Although the ΔH–TΔS plot shown in Figure 27 is moderately scattered, the slope (α) and intercept ($T\Delta S_0$) are calculated as 088 and 8.7, respectively. Again, both values are very large, indicating significant conformational changes and very extensive dehydration occurring upon antigen–antibody binding interaction.

## DNA and RNA[38,39]

One of the most intriguing biological supramolecular systems that should be examined by the enthalpy–entropy compensation theory is the duplex formation and intercalation of DNA and RNA.

DNA, RNA, and polynucleotides constitute the most sophisticated supramolecular systems that play the crucial, essential roles in living organisms. DNA possesses several functions of transmission, transcription, and duplication of genetic information, and protein synthesis, all of which involve the equilibrium between single- and double-stranded DNA. Hydrophobic domains of nucleic acid bases in single-stranded DNA are known to associate together in aqueous solutions, while the hydrophilic phosphates and the carbonyl and amino groups of nucleic acid bases are exposed to aqueous solvent and therefore heavily hydrated. Hence, the duplex formation of DNA inevitably requires the initial dissociation of single-strand aggregation followed by the bimolecular association, which undoubtedly accompany drastic conformational changes and extensive dehydration. In double-stranded

DNA, functional groups of nucleic acid bases are completely dehydrated and located inside the hydrophobic domain of duplex, forming efficient interhelix hydrogen bonds as shown in Figure 6.

Another type of supramolecular interaction of DNA is the intercalation of fused aromatic compounds into the stacked base pairs in double-stranded DNA (see Figure 6). Intercalation induces not only dehydration from the polar groups in intercalator but also concomitant unwinding, lengthening, dehydration, and stiff-ening of the DNA double helix.

In the thermodynamic study of duplex formation, a variety of complementary pairs of relatively simple, well-defined oligonucleotides are employed,[73-77] while the intercalation thermodynamics was examined with more complex or natural DNA duplexes.[57,59,69,78-89] Typical intercalating agents examined are acridine orange,[78] acriflabine,[78] actinomycin,[79] daunomycin,[57,59,79-81] ethidium bro-mide,[59,69,78,82,83] and netropsin.[59,74,79,84,85]

As can be seen from Figure 28, the $\Delta H$–$T\Delta S$ plots for intercalation and duplex formation give practically the same regression line of large slope ($\alpha$ 1.04) and intercept ($T\Delta S_0$ 8.5), although the data for duplex formation are spread more widely than those for intercalation. Hence, both the conformational changes and the extent of dehydration are deduced to be tremendous not only in the duplex formation but also in the intercalation of rather simple molecules. It is interesting to note that, in
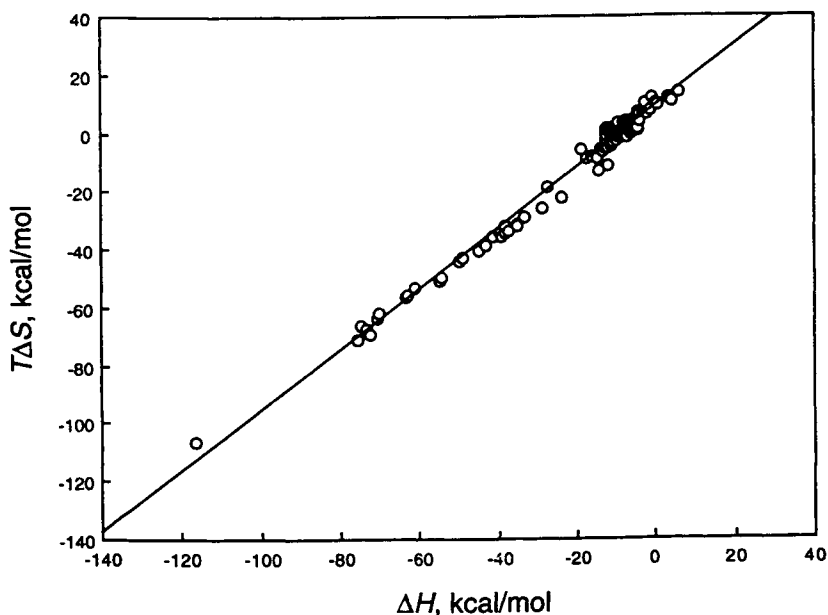


**Figure 28.** $\Delta H$–$T\Delta S$ plot for duplex formation (○) and intercalation (●) of DNA/RNA.

spite of the apparent differences in mechanism and weak forces involved, the duplex formation and the intercalation of DNA and RNA can be analyzed and discussed globally.

# 7. SCOPE AND LIMITATIONS[20]

As demonstrated broadly for chemical and biological molecular recognition systems, the compensatory enthalpy–entropy relationship is hold in general and the interpretations using the slope $\alpha$ and intercept $T\Delta S_0$ of linear $\Delta H$–$T\Delta S$ plots serve as a versatile tool for analyzing the degree of conformational changes and the extent of desolvation upon supramolecular association based on the cooperative weak interactions. It is, however, intriguing and inevitable to explore the limitations of this extrathermodynamic analyses.

As representative cases in which stronger interactions are involved upon complexation, we chose coordination reactions of soft, heavy, and transition metal ions with chelating agents that carry soft nitrogen and/or sulfur donors. Unlike alkali and alkaline earth metal ions that form complexes with ionophores such as glymes and crown ethers through weak interactions, heavy and transition metal ions constitute clearly defined and directed coordination sites around the ion. The chelate ligation of these soft metal ions by soft ligands leads to the formation of highly covalent bonds between the soft ion and soft donor atoms. Essentially different behavior has been observed for the complexation thermodynamics of these soft cation–soft ligand combinations.[20]

A typical result was obtained with the coordination reaction of heavy and transition metal ions with acyclic chelating agents carrying two or more soft donors like nitrogen and sulfur atoms. Using the thermodynamic parameters reported for these soft glymes, the entropy changes are plotted against the enthalpy changes to give a completely different, very flat plot of poor correlation, as shown in Figure 29. It is noted that, although the $\Delta H$ values spread over a wide range of –30 to 0 kcal/mol, the $T\Delta S$ values stay in a relatively narrow range around zero.

These results clearly indicate that the chelate ligation is driven primarily by the enthalpic factor and the entropy plays merely a trivial role in determining the complex stability. This is quite reasonable since the structures of these chelate complexes are strictly defined by the number and direction of the coordination sites of given heavy/transition metal ions, and therefore there is little room for the entropic term to adjust flexibly the complex structure and stability. On the contrary, alkali and alkaline earth metal ions also have the formal coordination numbers, but the actual number and direction of ligand coordination are highly flexible in the weak interaction-driven ligation by hard donors like glyme and crown ether.

It is advised therefore that the extrathermodynamic analysis based on the enthalpy–entropy compensation effect should be restricted to the (supra)molecular recognition phenomena governed by cooperative weak interactions.
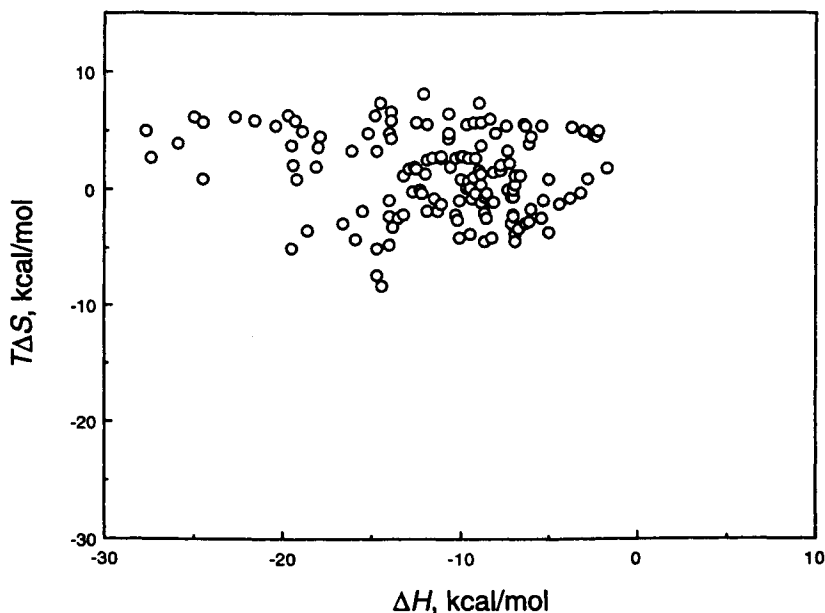
**Figure 29.** $\Delta H$–$T\Delta S$ plot for chelation of heavy and transition metal ions by soft glymes (containing more than two nitrogen and/or sulfur atoms).

## 8. CONCLUSION: THERMODYNAMIC VIEW OF SUPRAMOLECULAR INTERACTIONS

We have described a theory, based on the compensatory enthalpy–entropy relationship, to understand globally the chemical and biological molecular recognition systems governed by cooperative weak interactions. The slope $\alpha$ and intercept $T\Delta S_0$ of the linear $\Delta H$–$T\Delta S$ plot, which are distinctly different for each host category (see Table 2), are employed respectively as quantitative measures of the conformational changes and the extent of desolvation caused by host–guest complexation. This thermodynamic way of understanding molecular recognition phenomena, proposed originally for the cation binding by ionophores,[19,20] can be extended not only to the inclusion complexation by natural and synthetic molecular hosts like cyclodextrin, porphyrin, and cyclophane but also to the biological supramolecular interaction of enzyme, antibody, and DNA. Hence, this empirical theory can be used as a versatile tool to analyze quantitatively a wide variety of molecular recognition behavior in chemistry and biology from a global and unified point of view.

In Figure 30, all types of molecular recognition systems discussed above are mapped graphically as a function of the complexation-induced conformational change ($\alpha$) and desolvation ($T\Delta S_0$). As can be seen from Figure 30, both parameters, $\alpha$ and $T\Delta S_0$, do not appear to correlate each other, and the molecular recognition
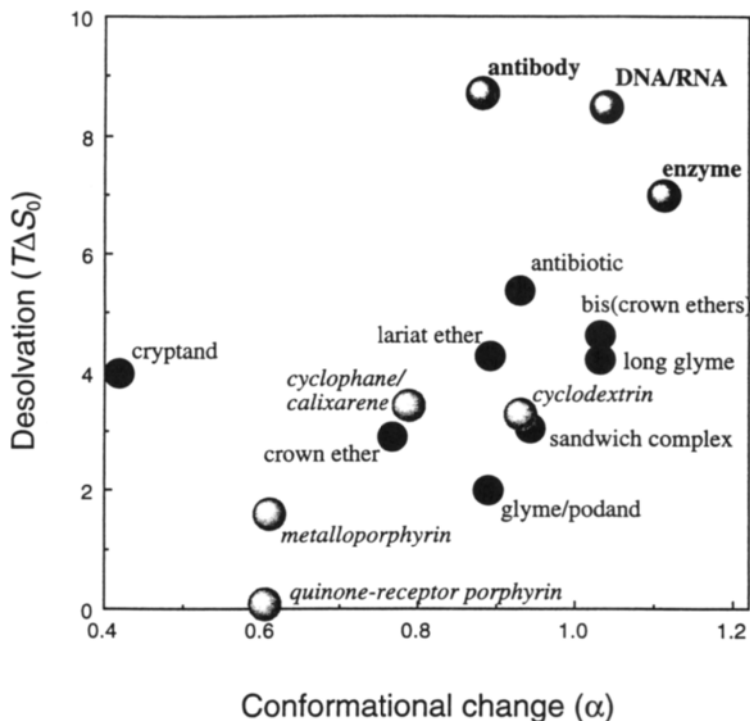
**Figure 30.** Slopes ($\alpha$) and intercepts ($T\Delta S_0$) obtained for a variety of cation binding (*closed circle*), molecular inclusion (*lightly shadowed; in italic*), and biological supramolecular interaction (*shadowed; in bold*).

behavior can be discussed from the structural rigidity of the host molecule and the solvent property. Thus, the rigid hosts with fixed two- or three-dimensional frameworks do not suffer appreciable conformational changes upon complexation and therefore give very small slopes ($\alpha$) of 0.4–0.6, while more flexible hosts, particularly biological supramolecules, suffer serious conformational changes, affording large slopes up to unity. Apart from the quinone-receptor porphyrin in chloroform,[37] the complexation of the other natural and synthetic hosts is more or less enhanced by desolvation from both host and guest molecules. Particularly in the biological supramolecular systems, the unfavorable canceling effect due to the extensive conformational changes is overcome by the great entropic contribution from desolvation. From these analyses, we may conclude that the biological systems that employ flexible natural macromolecules as receptors conquer the intrinsic entropic disadvantage arising from the inevitable conformational changes upon molecular association by means of the extensive dehydration in aqueous solution, realizing an ultimate entropy-governed molecular recognition system after a billion years of chemical and biological evolution on Earth.

Some practical guidelines for designing efficient and selective host molecules may also be extracted from this compensation theory. There are two entirely different or even opposite routes to excellent hosts. The first one is to construct a very rigid two- or three-dimensional cavity surrounded by conformationally fixed binding sites that interact with the included guest through multiple cooperative weak interactions. Good examples are cryptand and quinone-receptor porphyrin derivatives. However, the entropic assist through desolvation is not expected to be very large in these cases. In this strategy, the (enthalpic) effort to enhance binding ability by molecular engineering should be concentrated on the system that gives a small slope ($\alpha$), in which an appreciable part ($1 - \alpha$) of the enthalpic gain will be reflected to the complex stability.

The second strategy to optimize both binding ability and selectivity is the way that nature employs. In the biological molecular recognition in aqueous solution, macromolecular hosts carrying numerous mutually interacting functional groups suffer significant conformational changes upon supramolecular interaction, leading to the total cancellation of the enthalpic gain from binding. However, since the biological recognition process usually occurs in aqueous media and both host and guest are fully hydrated, the complexation inevitably induces very extensive dehydration, resulting in large entropic gains that cannot be realized only by the enthalpic gain.

Finally, we wish to emphasize that, to the best of our knowledge, only the present theory can consistently explain the whole molecular recognition systems and present a global and unified view to understand the sophisticated supramolecular interactions in chemistry and biology. It is also said that the molecular recognition phenomenon through cooperative weak interactions is synonymous to *entropy-governed chemistry*.

# REFERENCES AND NOTES

1. Shanzer, A.; Libman, J.; Weizman, H.; Mester, B.; Hadar, Y.; Chen, Y.; Jurkevitch, E.; Ardon, O. *Pure Appl. Chem.* **1996**, *68*, 757.
2. Wallace, A. C.; Laskowski, R. A.; Singh, J.; Thornton, J. M. *Biochem. Soc. Trans.* **1996**, *24*, 280.
3. Sowdhamini, R.; Srinivasan, N.; Guruprasad, K.; Rufino, S.; Dhanaraj, V.; Wood, S. P.; Emsley, J.; White, H. E.; Blundell, T. *Pharm. Acta Helv.* **1995**, *69*, 185.
4. Lehn, J.-M. *Pharm. Acta Helv.* **1995**, *69*, 205.
5. Lilley, D. M. *J. Mol.Recognit.* **1994**, *7*, 71.
6. Whitesides, G. M.; Simanek, E. E.; Mathias, J. P. *Acc. Chem. Res.* **1995**, *28*, 37.
7. *Molecular Recognition: Chemical and Biological Problems II*; Roberts, S. M., Ed.; Royal Soc. Chem.: Cambridge, 1992.
8. Lehn, J. M. *Supramolecular Chemistry*; VCH: Weinheim, 1995.
9. *Inclusion Compounds*; Atwood, J. L.; Davies, J. E. D.; MacNicol, D. D., Eds.; Academic: London, 1984, Vols. 1–3.
10. *Host-Guest Complex Chemistry*; Vögtle, F., Ed.; Springer-Verlag: Berlin, 1981, 1982, 1984, Vols. 1–3.
11. *Cyclodextrin*; Ueno, A., Ed.; Sangyo Tosho: Tokyo, 1995 (in Japanese).

12. *Frontiers in Supramolecular Organic Chemistry and Photochemistry*; Schneider, H.-J.; Dürr, H., Eds.; VCH: Weinheim, 1991.
13. Diederich, F. *Cyclophane*; Royal Soc. Chem.: Cambridge, 1991.
14. Gutsche, C. D. *Calixarene*; Royal Soc. Chem.: Cambridge, 1989.
15. Gokel, G. W. *Crown Ethers and Cryptands*; Royal Soc. Chem.: Cambridge, 1991.
16. *Cation Binding by Macrocycles*; Inoue, Y.; Gokel, G. W., Eds.; Marcel Dekker: New York, 1990.
17. Christensen, J. J.; Izatt, R. M. *Handbook of Metal Ligand Heats and Related Thermodynamic Quantities*; Marcel Dekker: New York, 1983.
18. De Jong, F.; Reinhoudt, D. N. *Stability and Reactivity of Crown-ether Complexes*; Academic: London, 1981.
19. Inoue, Y.; Hakushi, T. *J. Chem. Soc., Perkin Trans. 2* **1985**, 935.
20. Inoue, Y.; Hakushi, T.; Liu, Y. In *Cation Binding by Macrocycles*; Y. Inoue and G. W. Gokel, Eds.; Marcel Dekker: New York, 1990, Chapter 1.
21. Inoue, Y.; Hakushi, T.; Liu, Y.; Tong, L.-H.; Hu, J.; Zhao, G.-D.; Huang, S.; Tian, B.-Z. *J. Phys. Chem.* **1988**, 92, 2371.
22. Inoue, Y.; Amano, F.; Okada, N.; Inada, H.; Ouchi, M.; Tai, A.; Hakushi, T.; Liu, Y.; Tong, L.-H. *J. Chem. Soc., Perkin Trans. 2* **1990**, 1239.
23. Liu, Y.; Tong, L.-H.; Inoue, Y.; Hakushi, T. *J. Chem. Soc., Perkin Trans. 2* **1990**, 1247.
24. Liu, Y.; Tong, L.-H.; Huang, S.; Tian, B.-Z.; Inoue, Y.; Hakushi, T. *J. Phys. Chem.* **1990**, 94, 2666.
25. Inoue, Y.; Hakushi, T.; Liu, Y.; Tong, L.-H.; Shen, B.-J.; Jin, D.-S. *J. Am. Chem. Soc.* **1993**, 115, 475.
26. Inoue, Y.; Liu, Y.; Tong, L.-H.; Shen, B.-J.; Jin, D.-S. *J. Am. Chem. Soc.* **1993**, 115, 10637.
27. Searle, M. S.; Westwell, M. S.; Williams, D. H. *J. Chem. Soc., Perkin Trans. 2* **1995**, 141.
28. Inoue, Y.; Wada, T. In *Molecular Recognition Chemistry*; H. Tsukube, Ed.; Sankyo: Shuppan, 1996; Chapter 2 (in Japanese).
29. Grime, J. K. *Analytical Solution Calorimetry*; Wiley: New York, 1985.
30. Inoue, Y.; Liu, Y. In *Comprehensive Supramolecular Chemistry*; Pergamon: Oxford, 1996, Vol. 8, Chapter 1, Section 4.1.
31. Smithrud, D. B.; Wyman, T. B.; Diederich, F. *J. Am. Chem. Soc.* **1991**, 113, 5420.
32. Naghibi, H.; Tamura, A.; Sturtevant, J. M. *Proc. Natl. Acad. Sci. USA* **1995**, 92, 5597.
33. Leffler, J. E. *J. Org. Chem.* **1955**, 20, 1202.
34. Leffler, J. E.; Grunwald, E. *Rates and Equilibria of Organic Reactions*; Wiley: New York, 1963; reprinted version from Dover: New York, 1989.
35. Exner, O. *Correlation Analysis of Chemical Data*; Plenum: New York, 1988.
36. Chen, R. T. *Correlation Analysis in Coordination Chemistry*; Anhui Educational Publishing: Hefei, 1995 (in Chinese).
37. Aoyama, Y.; Asakawa, M.; Matsui, Y.; Ogoshi, H. *J. Am. Chem. Soc.* **1991**, 113, 6233.
38. Inoue, Y. In *6th Int'l Sem. Incl. Compd.*; Istanbul, 1995, p. 27.
39. Inoue, Y.; Wada, T.; Yamashoji, Y. In *70th Ann. Meeting Chem. Soc. Jpn.*; Tokyo, 1996, p. 1035 (1G537-539).
40. Kauffmann, E.; Lehn, J.-M.; Sauvage, J.-P. *Helv. Chim. Acta* **1976**, 59, 1099.
41. Vögtle, F.; Weber, E. *The Chemistry of Ethers, Crown Ethers, Hydroxy Groups, and their Sulfur Analogues*; Wiley: New York, 1980.
42. Izatt, R. M.; Terry, R. E.; Haymore, B. L.; Hansen, L. D.; Dalley, N. K.; Avondet, A. G.; Christensen, J. J. *J. Am. Chem. Soc.* **1976**, 98, 7620.
43. Michaux, G.; Reisse, J. *J. Am. Chem. Soc.* **1982**, 104, 6895.
44. Ouchi, M.; Inoue, Y.; Kanzaki, T.; Hakushi, T. *J. Org. Chem.* **1984**, 49, 1408.
45. Cole, S. J.; Curthoys, G. C.; Magnusson, E. A. *J. Am. Chem. Soc.* **1970**, 92, 2991.
46. Lumry, R.; Rajender, S. *J. Phy. Chem.* **1971**, 75, 1387.
47. Lewis, E. A.; Hansen, L. D. *J. Chem. Soc., Perkin Trans. 2* **1973**, 2081.
48. Krug, R. R.; Hunter, W. G.; Grieger, R. A. *J. Phys. Chem.* **1976**, 80, 2335.

49. Krug, R. R.; Hunter, W. G.; Grieger, R. A. *J. Phys. Chem.* **1976**, *80*, 2341.
50. Szewczuk, M. R.; Mukkur, T. K. S. *Immunology* **1977**, *32*, 111.
51. Komiyama, M.; Bender, M. L. *J. Am. Chem. Soc.* **1978**, *100*, 4576.
52. Harata, K. *Bioorg. Chem.* **1981**, *10*, 255.
53. Becvar, J.; Palmer, G. *J. Biol. Chem.* **1982**, *257*, 5607.
54. Dittrich, F. *Acta. Biol. Med. Germ.* **1982**, *41*, 873.
55. Eftink, M. R.; Anusiem, A. C.; Biltonen, R. L. *Biochemistry* **1983**, *22*, 3884.
56. Takagi, S.; Kimura, T.; Maeda, M. *Thermochimica Acta* **1985**, *88*, 247.
57. Chaires, J. B. *Biopolymers* **1985**, *24*, 403.
58. Eastman, M. P.; Freiha, B.; Hsu, C. C.; Lum, K. C.; Chang, C. A. *J. Phys. Chem.* **1987**, *91*, 1953.
59. Breslauer, K. J.; Remeta, D. P.; Chou, W.-Y.; Ferrante, R.; Curry, J.; Zaunczkowski, D.; Snyder, J. G.; Marky, L. A. *Proc. Natl. Acad. Sci. USA* **1987**, *84*, 8922.
60. Harata, K.; Tsuda, K.; Uekama, K.; Otagiri, M.; Hirayama, F. *J. Inclusion Phenom.* **1988**, *6*, 135.
61. Eftink, M. R.; Andy, M. L.; Bystrom, K.; Perlmutter, H. D.; Kristol, D. S. *J. Am. Chem. Soc.* **1989**, *111*, 6765.
62. Chakraborty, S.; Nandi, R.; Maiti, M. *Biochem. Pharm.* **1990**, *39*, 1181.
63. Aoyama, Y.; Asakawa, M.; Matsui, Y.; Ogoshi, H. *J. Am. Chem. Soc.* **1991**, *113*, 6233.
64. Kuroki, R.; Nitta, K.; Yutani, K. *J. Biol. Chem.* **1992**, *267*, 24297.
65. Rekharsky, M. V.; Goldberg, R. N.; Schwarz, F. P.; Tewari, Y. B.; Ross, P. D.; Yamashoji, Y.; Inoue, Y. *J. Am. Chem. Soc.* **1995**, *117*, 8830.
66. Rekharsky, M. V.; Mayhew, M. P.; Goldberg, R. N.; Ross, P. D.; Yamashoji, Y.; Inoue, Y. *J. Phys. Chem.* **1997**, *101*, 87.
67. Bender, M. L.; Komiyama, M. *Cyclodextrin Chemistry*; Springer: New York, 1978.
68. Grazi, E.; Trombetta, G. *Biochim. Biophys. Acta* **1974**, 120.
69. Biltonen, R. L.; Langerman, N. *Method Enzym.* **1979**, *61*, 287.
70. Hinz, H.-J. *Ann. Rev. Biophys. Bioeng.* **1983**, *12*, 285.
71. Reinhart, G. D.; Hartleip, S. B.; Symcox, M. M. *Proc. Natl. Acad. Sci. USA* **1989**, *86*, 4032.
72. Genderen, M. H. P. van; Koole, L. H.; Buck, H. M. *Prok. K. Ned. Akad. Wet., Ser. B: Palaeontol., Geol., Phys., Chem. Anxhropol.* **1988**, *91*, 179.
73. Nelson, J. W.; Martin, F. H.; Tinoco, Jr., I. *Biopolymers* **1981**, *20*, 2509.
74. Rentzeperis, D.; Ho, J.; Marky, L. A. *Biochemistry* **1993**, *32*, 2564.
75. Rentzeperis, D.; Kupke, D. W.; Marky, L. A. *Biochemistry* **1994**, *33*, 9588.
76. Durand, M.; Peloille, S.; Thuong, N. T.; Maurizot, J. C. *Biochemistry* **1992**, *31*, 9197.
77. Rentzeperis, D.; Alessi, K.; Marky, L. A. *Nucleic Acids Res.* **1993**, *21*, 2683.
78. Wille, H.; Pauluhn, J.; Zimmermann, H. W. *Z. Naturforsch., C. Biosci.* **1982**, *37*, 413.
79. Marky, L. A.; Snyder, J. G.; Remeta, D. P.; Breslauer, K. J. *J. Biomol. Struct. Dynam.* **1983**, *1*, 487.
80. Chaires, J. B. *Biophysics* **1990**, *35*, 191.
81. Remata, D. P.; Mudd, C. P.; Berger, R. L.; Breslauer, K. J. *Biochemistry* **1993**, *32*, 5064.
82. Hopkins, H. P., Jr.; Fumero, J.; Wilson, W. D. *Biopolymers* **1990**, *29*, 449.
83. Hopkins, H. P., Jr.; Wilson, W. D. *Biopolymers* **1987**, *26*, 1347.
84. Marky, L. A.; Kupke, D. W. *Biochemistry* **1989**, *28*, 9982.
85. Dabrowiak, J. C.; Goodisman, J.; Kissinger, K. *Biochemistry* **1990**, *29*, 6139.
86. Hopkins, H. P., Jr.; Ming, Y.; Wilson, W. D.; Boykin, D. W. *Biopolymers* **1991**, *31*, 1105.
87. Kanoh, K.; Baba, Y.; Kagemoto, A. *Polymer J.* **1988**, *20*, 1135.
88. Hopkins, H. P., Jr.; Stevenson, K. A.; Wilson, W. D. *J. Solution Chem.* **1986**, *15*, 563.
89. Baba, Y.; Kunihiro, A.; Kagemoto, A. *Themochim. Acta* **1992**, *202*, 241.

# ANION BINDING BY SAPPHYRINS

Jonathan L. Sessler, Andrei Andrievsky, and

John W. Genge

# 1.  INTRODUCTION

The *porphyrins* (e.g., **1**) and their tetrapyrrolic analogues been studied extensively since the turn of the century. These molecules play critical roles in a large number of biological processes,[1] and are widely recognized for their diverse coordination chemical properties.[1a,2] The porphyrins also show promise for use in applications as far ranging as magnetic resonance imaging (MRI)[3] and photodynamic therapy (PDT),[4] and have proved useful in the construction of molecular devices[5] and light-harvesting arrays.[6]

In recent years, increasing attention has begun to be devoted to the sub-branch of porphyrin chemistry that involves the synthesis and study of so-called *expanded porphyrins*.[7] In general terms, expanded porphyrins may be defined as being systems (aromatic and nonaromatic) that contain at least one pyrrole or other five-atom heterocycle constrained within a macrocycle possessing an internal ring core of at least 17 atoms (one more than the number of atoms present in the inner core of porphyrin). Expanded porphyrins, by virtue of containing a greater number of π-electrons, a greater number of donating heteroatoms, and a larger central core possess properties that differ significantly from those of the porphyrins. These differences include, but are not limited to, chemical reactivity, photophysical characteristics, and metal coordination capability. Taken together, these features have made certain expanded porphyrins, notably the so-called texaphyrins, attractive as MRI contrast agents,[8a] radiation sensitizers,[8b] and photodynamic-therapy[9] sensitizers. One further feature also distinguishes many of the expanded porphyrins from their simple tetrapyrrolic "parents". This is an ability to chelate anions and polyanions.[10] This unique ability, which derives from the enhanced basicity many expanded porphyrins display relative to the porphyrins, has made this class of molecules attractive candidates for use in anion-recognition-based applications, including several medical and analytical ones such as drug delivery, antisense-like oligonucleotide modification, and chromatography.
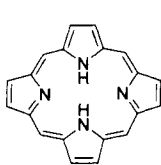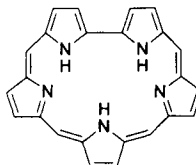


1                2

In this review, written in a personal, account-like style, we have chosen to illustrate the anion binding potential of the expanded porphyrins in general by showing how a prototypic system, *sapphyrin* (e.g., **2**), is able to function in this regard. We will thus start this review by presenting evidence that supports the conclusion that monomeric sapphyrins can indeed bind anions both in solution and in the solid state. Next, we will detail the solution-phase anion-recognition properties of sapphyrin conjugates and sapphyrin oligomers. Following this, the DNA-chelation chemistry of water-soluble sapphyrins will be summarized. Finally, the results of HPLC analyses made using sapphyrin-derived stationary phases will be described. Taken together, these various summaries should suffice to provide a fairly complete picture of the known anion binding properties of the sapphyrins and should allow for an inference of what may be possible using other expanded porphyrin systems. Still, to limit the size of this review, we will not discuss heterosapphyrins (sapphyrin analogues in which nitrogens are partially replaced by oxygen or sulfur atoms), and other expanded porphyrins. Some of the latter, particularly the rubyrins,[11] rosarins,[12] anthraphyrins,[13] and turcasarins,[14] show promise as anion binding agents but have yet to be studied extensively in this regard.

Sapphyrin (e.g., **2**) is the most venerable of the many expanded porphyrins now known. It was first discovered serendipitously in the Woodward group more than 30 years ago during the course of studies directed toward the synthesis of vitamin $B_{12}$.[15a-c] Recently improved syntheses of sapphyrin have been developed by the authors.[15d,e] This has made it possible to study this molecule in detail and, as described below, allowed for the discovery that sapphyrin can act as a *bona fide* anion binding agent.

Unlike simple porphyrins, sapphyrins contain five pyrroles and four *meso* carbons. They also possess an aromatic 22 $\pi$-electron framework, rather than the 18 $\pi$-electron periphery found in porphyrins. Monomeric sapphyrins display intense red-shifted Soret-like absorption at ca. 450 nm, and Q-like bands in the 600–710 nm region of the visible spectrum. As a result, the sapphyrins are not porphyrin-like purple in color, but rather blue-green in the solid state and dark-green in solution (hence the name sapphyrin). The free-base form of sapphyrin has three protonated pyrroles and two $sp^2$-hybridized nitrogen atoms. These latter nitrogen atoms are relatively basic with $pK_a$ values of ca. 4.8 and 8.8 being recorded for the corresponding conjugate acids.[16] This basicity has important consequences. It means sapphyrins are monoprotonated under neutral conditions and effectively diprotonated at pH values below ca. 3.5. Typical unsubstituted porphyrins, on the other hand, are but weakly basic. Indeed, they remain unprotonated at neutral pH and become monoprotonated only at very low pH values. The sapphyrins, possessing an inner cavity of ca. 2.5 Å radius, are also substantially larger than the porphyrins (for which radii of ca. 2.0 Å are routinely recorded). This fact, which surely accounts for their increased relative basicity, helps make the sapphyrins anion chelating agents *par excellence.*

## 2. ANION COMPLEXES OF SAPPHYRINS IN THE SOLID STATE
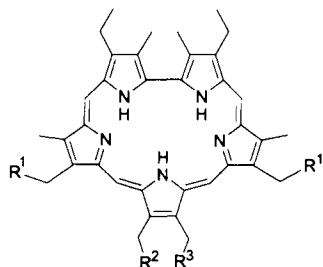


3   $R^1 = R^2 = R^3 = CH_3$
4   $R^1 = CH_2CH_2OH$; $R^2 = R^3 = CH_3$
5   $R^1 = CH_2CO_2H$; $R^2 = R^3 = CH_3$
6   $R^1 = CH_3$; $R^2 = CH_2CO_2H$; $R^3 = H$

### 2.1. Halide Anion Complexes

The first anion complex of sapphyrin was obtained fortuitously. It resulted form an attempt to obtain X-ray quality crystals of the bis-HPF$_6$ salt of decaalkyl sapphyrin 3. Instead of the expected structure, an X-ray crystal diffraction analysis of what was thought to be this bis-HPF$_6$ salt revealed the presence of only one $PF_6^-$ counteranion per sapphyrin. This same analysis, however, also indicated the presence of unexpected electron density at the center of the sapphyrin core that, on the basis of fitting procedures and independent synthesis, was ascribed to an F$^-$ anion.[17] This bound fluoride anion, presumably extracted from $PF_6^-$, was found to be held in place by a combination of Coulombic effects involving the protonated nitrogens and the negatively charged fluoride anion, and hydrogen-bonding interactions. The five N–H···F bonds were found to be nearly linear and ca. 2.7 Å in length (Figure 1). Subsequent solution studies confirmed this binding motif and indicated a high degree of selectivity for fluoride over the other halide anions (*vide infra*).[17,18] Therefore, looking back, the authors view these initial structural results as being seminal; they provided the critical "hint", now fully realized, that sapphyrins, unlike simple porphyrins, can serve as generalized anion binding agents.

Following the discovery of the above solid-state fluoride anion complex, the authors succeeded in crystallizing the bishydrochloride salt of this same system, 3.[10a,17b] The X-ray structure of this derivative revealed the presence of two chloride counterions bound via hydrogen bonds to the diprotonated macrocycle (Figure 2). In contrast to what was seen in the case of the fluoride anion structure, in this instance neither of the counteranions is located in the plane of the sapphyrin macrocycle. Rather, they are found in near symmetric fashion ca. 1.8 Å above and below the mean N$_5$ plane. This out-of-plane binding reflects, presumably, the fact
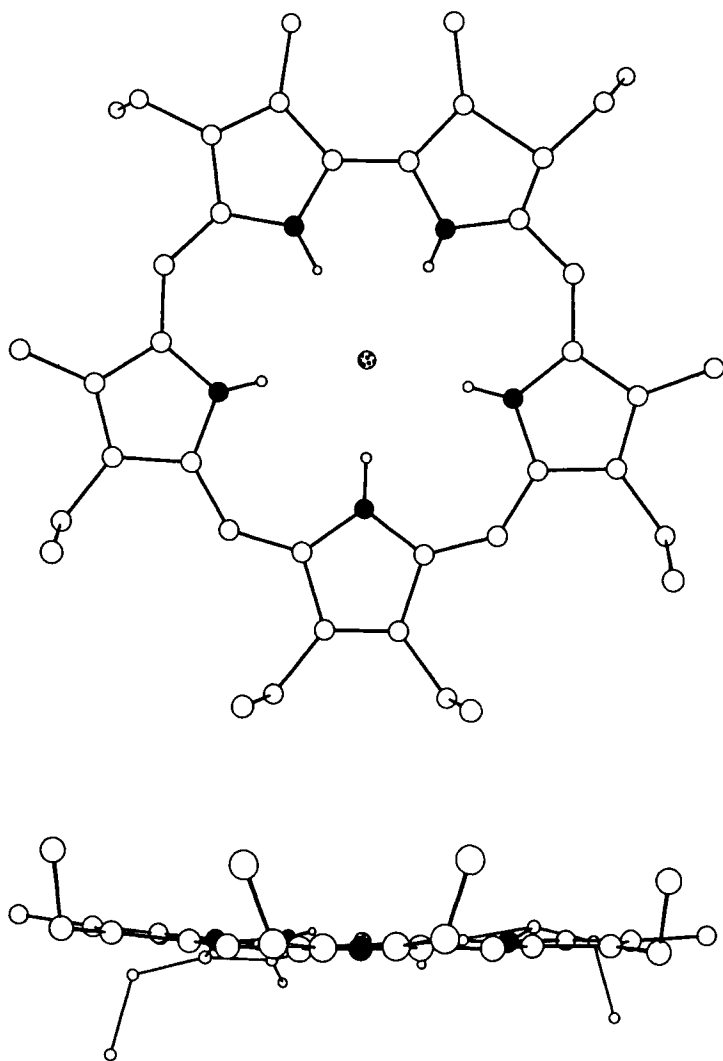
***Figure 1.*** Single crystal X-ray structure of the mixed HF-HPF$_6$ salt of sapphyrin **3**. This figure was generated using information down-loaded from the Cambridge Crystallographic Data Centre and corresponds to a structure originally reported in ref. 17. Atom labeling scheme: carbon: ○; nitrogen: ●; fluorine: ⊕; hydrogen: ○. Selected hydrogen atoms have been omitted for clarity.
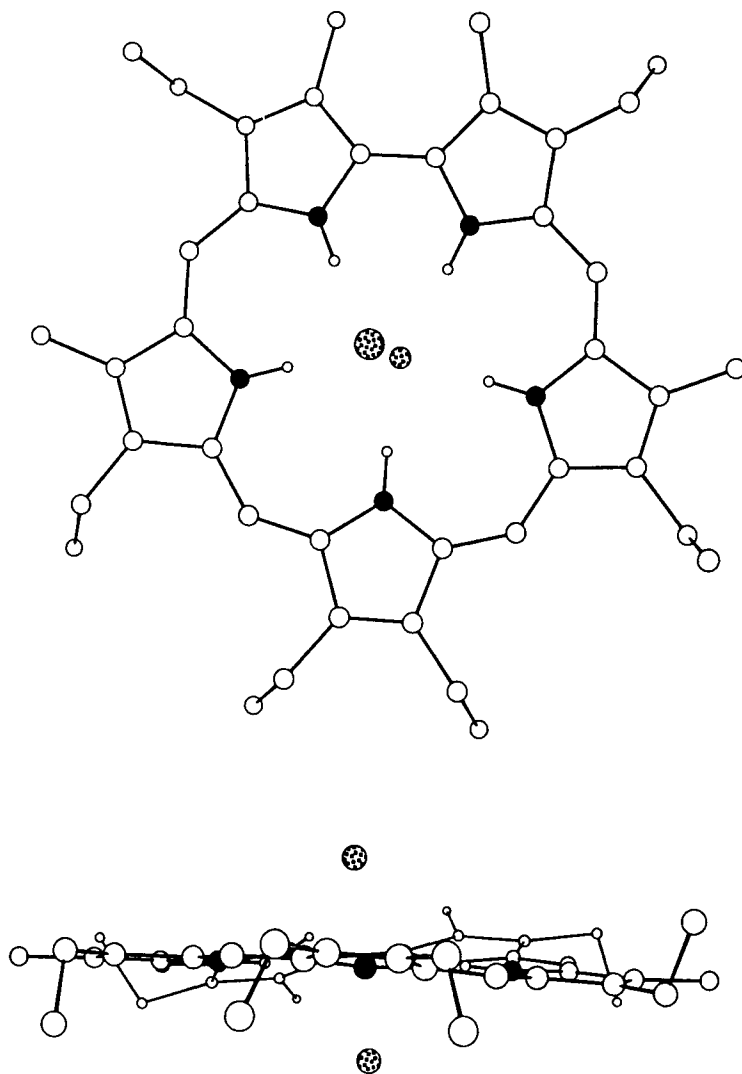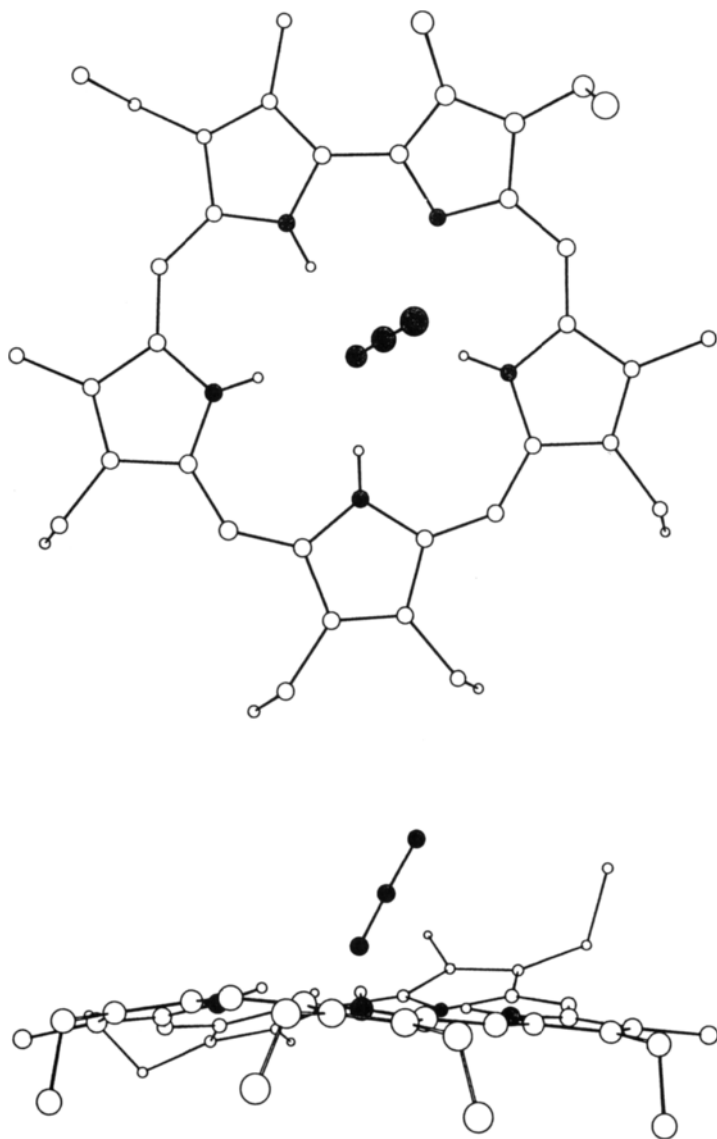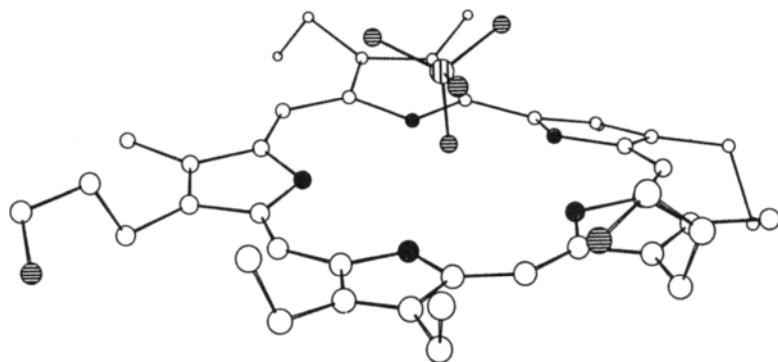
**Figure 2.** Single crystal X-ray structure of the bis-HCl salt of sapphyrin **3**. This figure was generated using information down-loaded from the Cambridge Crystallographic Data Centre and corresponds to a structure originally reported in ref. 17b. Atom labeling scheme: carbon: ◌; nitrogen: ●; chlorine ⬤; hydrogen o. Selected hydrogen atoms have been omitted for clarity.

that anionic chloride is significantly larger than anionic fluoride (atomic radii = 1.67 and 1.19 Å, respectively[19]), and that the shape of the doubly protonated sapphyrin cavity is rather invariant.

The above results were later complemented by the observation that the monoprotonated form of sapphyrin is also capable of chelating chloride anion in the solid state.[10a] Here, in analogy to what was seen in the case of the bishydrochloride salt, the single chloride counteranion was found to lie ca. 1.72 Å above the macrocycle plane, being held there by four hydrogen bonds (Figure 3).

Currently, the only other monoprotonated sapphyrin–monoanion complex to be solved by X-ray diffraction analysis is that of $3 \cdot HN_3$.[10a] As expected, in this complex the azide counteranion is bound above the sapphyrin plane by a combination of anisotropic electrostatic interactions and oriented hydrogen bonds (Figure 4). As such, this structure supports the conclusion, reached in the case of $3 \cdot HCl$, that a single positive charge on the sapphyrin is enough to effect anion recognition of anionic substrates, at least in the solid state.

## 2.2. Phosphate Complexes

As a part of our program to develop new adjuvants for the into-cell delivery of phosphorylated nucleotide-type antiviral agents (see Section 3 of this chapter), we became interested in developing a sapphyrin-based approach to phosphate anion chelation. As proved true for halide anion recognition, important initial support for the idea that sapphyrins could function as phosphate anion receptors came from single crystal X-ray diffraction studies. In fact, to date, five X-ray structures of sapphyrin–phosphate complexes have been obtained.[10,16]

The structures of a 1:1 inner-sphere, cationic complex of formally monobasic phosphoric acid with diprotonated sapphyrin **4**, and the analogous neutral 1:1 complex formed between dibasic phosphoric acid and diprotonated sapphyrin **4** are shown in Figures 5 and 6, respectively. The first of these complexes is characterized by a single bound dihydrogen phosphate counteranion tethered via five hydrogen bonds to a diprotonated phosphate receptor. This results in an umbrella-like arrangement with the other three oxygen atoms of the bound $H_2PO_4^-$ anion being splayed out like spokes on a wheel. The bound oxygen atom is located 1.22 Å above the sapphyrin plane. While not relevant to the details of the sapphyrin–phosphate interaction, this structure is further complicated by phosphate aggregation in the crystal lattice. Indeed, in the solid state, six phosphate groups are found to be linked in an hydrogen-bonded array. This array is terminated by a sapphyrin at each end and contains the second needed counteranion bound to a phosphate, as opposed to a sapphyrin. This latter counteranion thus plays no appreciable role in defining the details of the sapphyrin-to-phosphate chelation. The actual protons, however, were not localized in this structure. Thus, the assignment of this structure as being a cationic complex between diprotonated sapphyrin **4** and monobasic phosphoric acid holds true only in a formal sense; alternatively, it could also be described as
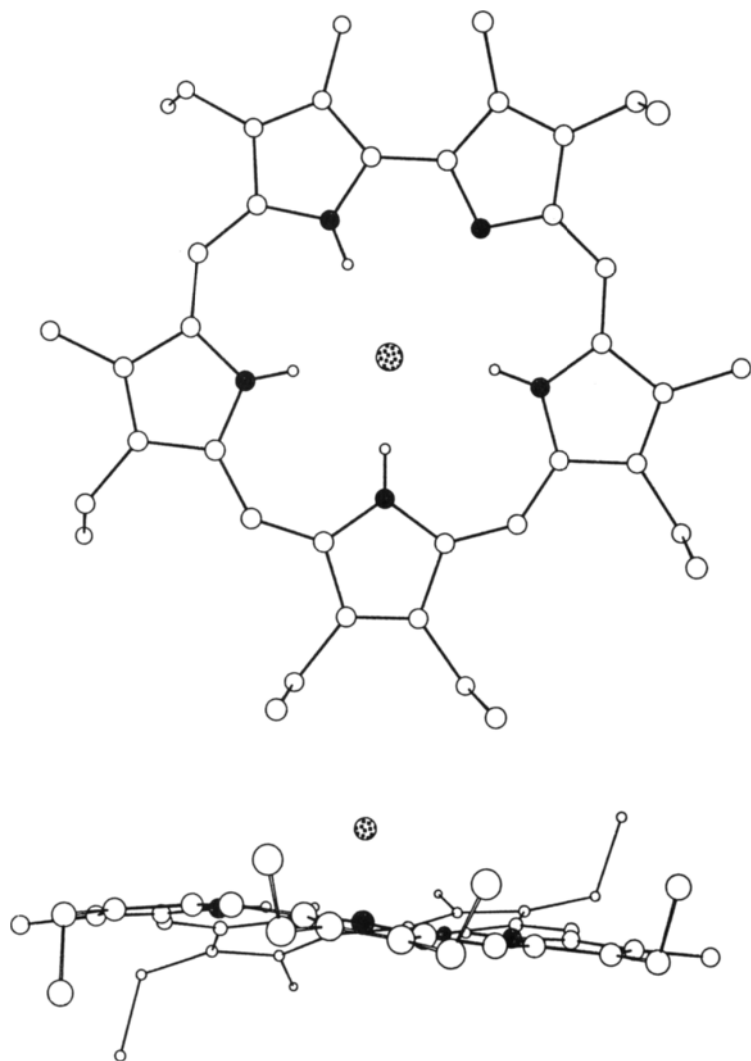
**Figure 3.** Single crystal X-ray structure of the mono-HCl salt of sapphyrin **3**. This X-ray structural figure was generated using unpublished data provided by Sessler et al., but corresponds to a structure originally reported in ref. 10a. Atom labeling scheme: carbon: ○; nitrogen: ◉; chlorine ⊕; hydrogen ○. Selected hydrogen atoms have been omitted for clarity.

**Figure 4.** Single crystal X-ray structure of the mono-HN$_3$ salt of sapphyrin **3**. This X-ray structural figure was generated using data provided by Sessler et al., but corresponds to a structure originally reported in ref. 10. Atom labeling scheme: carbon: ○; nitrogen: ●; hydrogen ○. Selected hydrogen atoms have been omitted for clarity.

**Figure 5.** View of the 1:1 cationic inner-sphere complex formed between sapphyrin **4** and monobasic phosphoric acid. This X-ray structural figure was generated using information down-loaded from the Cambridge Crystallographic Data Centre and corresponds to a structure originally reported in ref. 16a. Atom labeling scheme: carbon: ◯; nitrogen: ◉; oxygen ⊜; phosphorous ⦿; hydrogen ○. Selected hydrogen atoms have been omitted for clarity.

being a neutral complex between monoprotonated sapphyrin and phosphoric acid. Arguing against this latter interpretation, however, is the finding that the analogous 1:1 complex between the dibasic phosphoric acid and diprotonated sapphyrin **4** (Figure 6) shows a second interaction, namely one involving a protonated nitrogen-
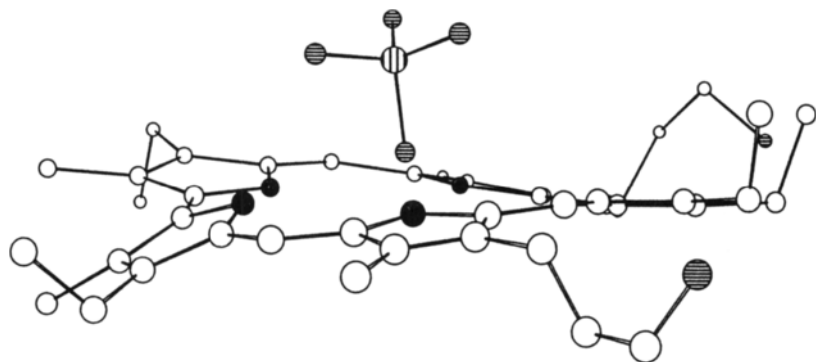


**Figure 6.** View of the 1:1 neutral complex formed between diprotonated sapphyrin **4** and dibasic phosphoric acid. This X-ray structural figure was generated using information down-loaded from the Cambridge Crystallographic Data Centre and corresponds to a structure originally reported in ref. 16a. Atom labeling scheme: carbon: ◯; nitrogen: ●; oxygen ⊜; phosphorous ⦿; hydrogen ○. Selected hydrogen atoms have been omitted for clarity.
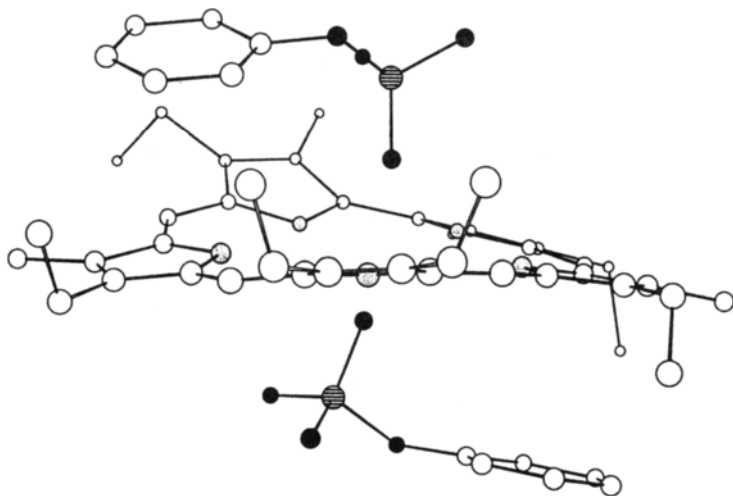
**Figure 7.** View of the 1:2 complex formed between diprotonated sapphyrin **3** and monobasic phenylphosphate. This X-ray structural figure was generated using information down-loaded from the Cambridge Crystallographic Data Centre and corresponds to a structure originally reported in ref. 16a. Atom labeling scheme: carbon: ○; nitrogen: ◉; oxygen ●; phosphorous ◉; hydrogen ○. Selected hydrogen atoms have been omitted for clarity.

to-phosphorus oxygen hydrogen bond. Interestingly, in this case, no excess phosphoric acid is found in the complex.

Two of the other phosphate structures solved, namely the 2:1 inner sphere complex of monobasic phenylphosphate with diprotonated sapphyrin **3** (Figure 7), and the 2:1 complex of the diphenyl phosphate with diprotonated sapphyrin **4** (Figure 8) bear a significant resemblance to the structure of the sapphyrin–dichloride complex described earlier (Figure 2). For instance, the key ligated oxygen atoms are held both above and below the sapphyrin plane by three and two hydrogen bonds to the NH groups. However, it is of interest that in both cases the chelated oxygen atoms are found to lie much closer to the sapphyrin plane than do the chloride anions in the analogous sapphyrin–bishydrochloride structure of Figure 2. For example, the "chelated" oxygen atoms of monobasic phenylphosphate are bound 1.22 and 1.60 Å, respectively, above and below the mean sapphyrin plane. In addition, the phenyl portions of the phenylphosphate molecular anion are found to reside over a portion of the aromatic sapphyrin skeleton at distances similar to those expected for van der Waals contact. By contrast, the phenyl substituents in the analogous diphenylphosphate–sapphyrin complex do not adopt an orientation parallel to the sapphyrin macrocycle.

The fifth sapphyrin–phosphate structure to be solved is of the mixed chloride/monobasic cyclic AMP salt of diprotonated sapphyrin **4** (Figure 9). While the general features of binding are similar to the other phosphate ester structures
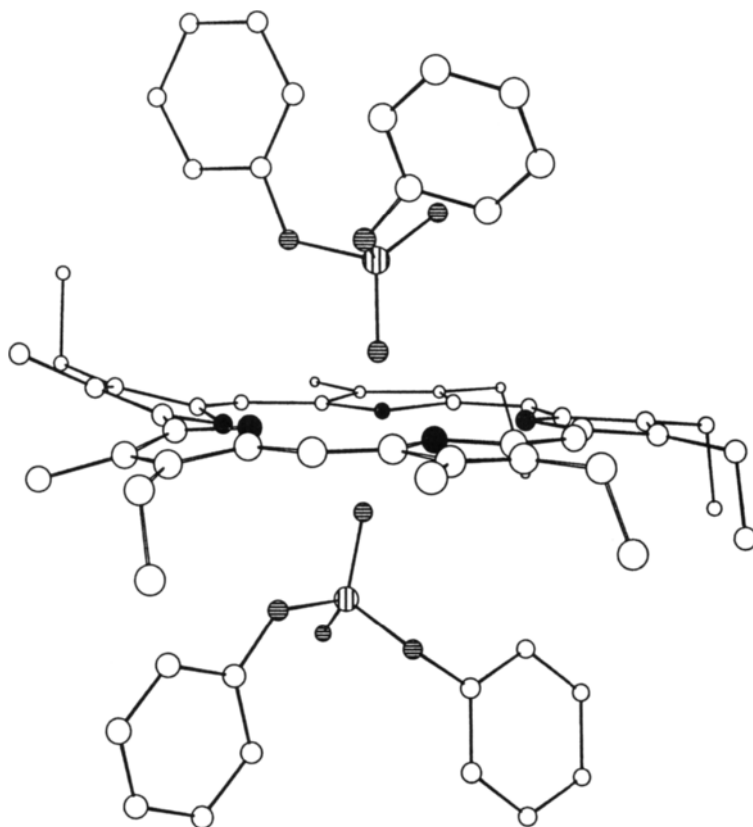
**Figure 8.** View of the 1:2 complex formed between diprotonated sapphyrin **4** and diphenyl phosphate. This X-ray structural figure was generated using information down-loaded from the Cambridge Crystallographic Data Centre and corresponds to a structure originally reported in ref. 16a. Atom labeling scheme: carbon: ○; nitrogen: ●; oxygen ◉; phosphorous ◐; hydrogen ○. Selected hydrogen atoms have been omitted for clarity.

described above, this particular complex was considered particularly interesting. It provided *prima facie* evidence that biologically important phosphorylated nucleotides could be bound by protonated sapphyrins, at least in the solid state.[16b]

## 2.3. Carboxylate Complexes

In addition to phosphate and halide anion binding, carboxylate chelation by sapphyrin macrocycles has been the subject of recent investigation. To date, two crystal structures have been solved.[20,21] A 2:1 complex formed between diprotonated sapphyrin **3** and trifluoroacetic acid shows that the oxyanions are chelated above and below the sapphyrin plane (Figure 10).[20] Greater complexity of organi-
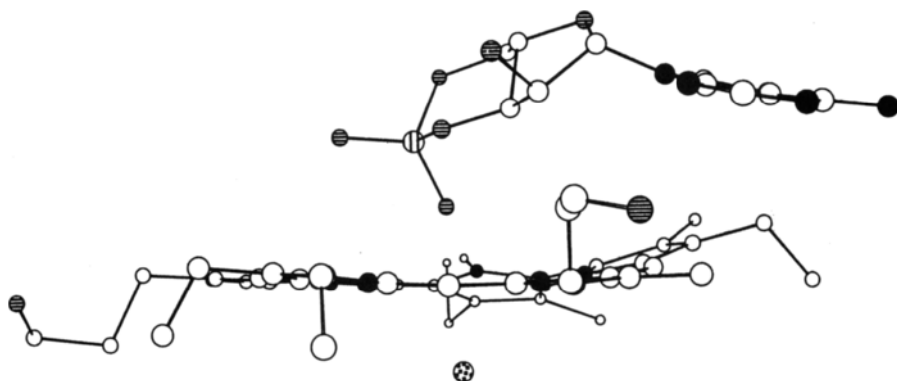
**Figure 9.** Single crystal X-ray structure of the mixed salt formed between sapphyrin **4**, HCl, and the acid form of *c*-AMP. This figure was generated using information down-loaded from the Cambridge Crystallographic Data Centre and corresponds to a structure originally reported in ref. 16b. Atom labeling scheme: carbon: ○; nitrogen: ●; oxygen ⊜; chlorine ⊕; phosphorous ⬤; hydrogen ○. Selected hydrogen atoms have been omitted for clarity.
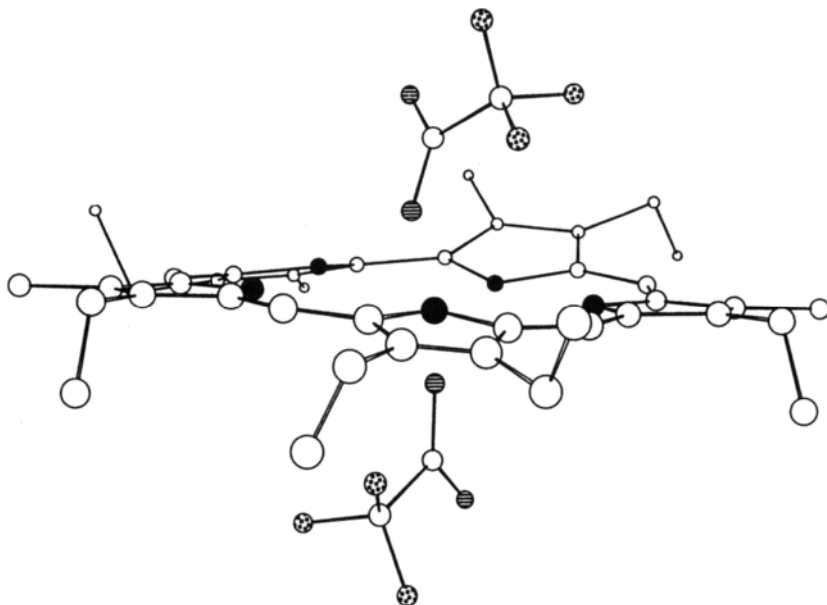


**Figure 10.** Single crystal X-ray structure of the bis-TFA salt of sapphyrin **3**. This X-ray structural figure was generated using unpublished data provided by Sessler et al. Atom labeling scheme: carbon: ○; nitrogen: ●; oxygen ⊜; fluorine ⊕; phosphorous ⬤; hydrogen ○. Selected hydrogen atoms have been omitted for clarity.
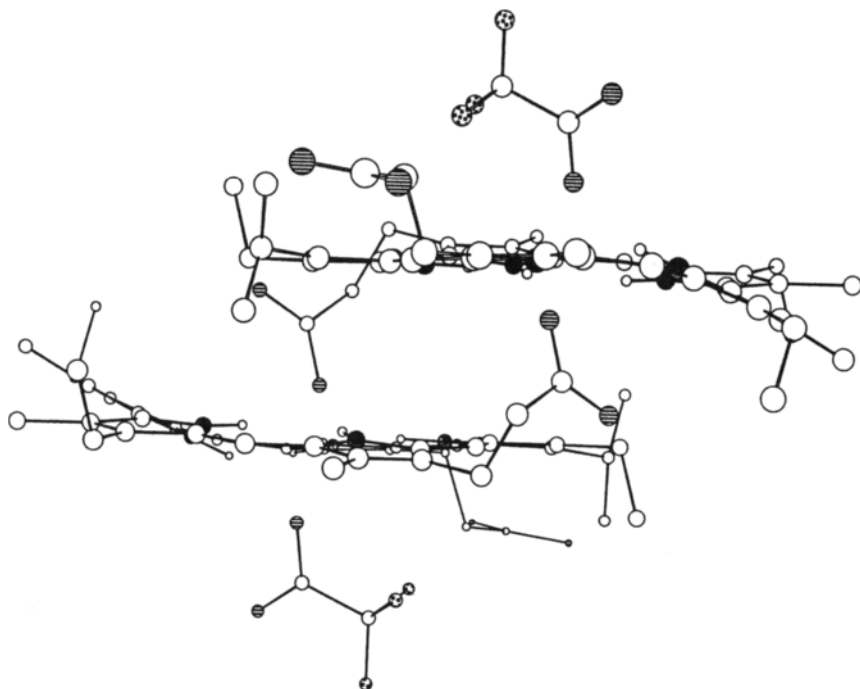
***Figure 11.*** View of the self-assembled dimer formed from sapphyrin 5 in the presence of trifluoroacetic acid. This X-ray structural figure was generated information down-loaded from the Cambridge Crystallographic Data Centre and corresponds to a structure originally reported in ref. 21. Atom labeling scheme: carbon: ◌; nitrogen: ⬤; oxygen: ⬗; fluorine ⊙; phosphorous ⬤; hydrogen ○. Selected hydrogen atoms have been omitted for clarity.

zation was revealed in the solid-state structure of the sapphyrin carboxylate **5** complex with trifluoroacetic acid.[21] This species is zwitterionic, containing both a carboxylate anion, and a protonated sapphyrin macrocycle. These two self-comple-mentary subunits are linked by short ethylene spacers. The short length of these spacers prevent internal sapphyrin-to-carboxylate "tail-biting" interactions. As a result, compound **5** crystallizes so as to form a supramolecular dimer in the solid state (Figure 11). In this dimer, a carboxylate "hook" from one molecule of **5** is chelated to the pyrrolic core of a second. This second macrocycle, in turn, shares its carboxylate "tail" with the first sapphyrin subunit. A trifluoroacetate ion is coordinated to each of unchelated faces in the dimer and prevents these sites from being involved in further binding. Perhaps as a result of this, the second carboxylic acid is not bound to a sapphyrin core, but is coordinated to a methanol molecule. The planes of the two constituent sapphyrins of this supramolecular dimer lie

parallel to each other in an offset fashion at a typical van der Waals distance of 3.39 Å. It is thus possible that these latter interactions play an important role in defining the details of the structure in the solid state.

The all-important finding that carboxylate-appended sapphyrins can self-assemble was confirmed in the case of the sapphyrin monocarboxylate **6**.[20] For both compounds the self-assembly phenomena were shown to take place not only in the solid state, but also in solution and in the gas phase (see Section 3.3). This meant that the carboxylate-binding properties of the sapphyrins could be used as the key molecular recognition basis for engendering the spontaneous self-assembly of appropriately designed supramolecular ensembles.

## 3. ANION CHELATION BY SAPPHYRINS IN SOLUTION
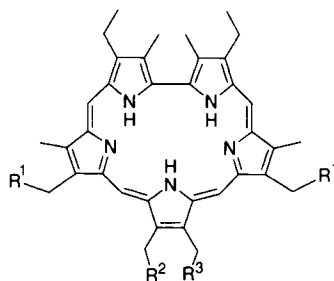


**3** $R^1 = R^2 = R^3 = CH_3$
**4** $R^1 = CH_2CH_2OH; R^2 = R^3 = CH_3$
**5** $R^1 = CH_2CO_2H; R^2 = R^3 = CH_3$
**6** $R^1 = CH_3; R^2 = CH_2CO_2H; R^3 = H$
**7** $R^1 = CH_2CON(CH_2CH_2OH)_2; R^2 = R^3 = CH_3$

The solid-state evidence for anion chelation described in the previous section provided an important "augury" that the sapphyrins could also function as anion binding agents in solution and in the gas phase. Subsequent studies by the authors established that this was in fact the case. What makes anion recognition in solution especially timely (and important) is the fact that many anions, particularly phosphates, chloride, and carboxylates, are ubiquitous in biology.[1c] Their roles are various and sundry and vary from information storage and processing to energy transduction.[22a–c] These negatively charged species are also involved in metabolic processes and in protein conformation regulation.[22d–f] Finally, certain phosphorylated nucleotide analogues are known to exhibit antiviral properties.[23] For these reasons it is nearly a truism that finding ways to chelate and transport anions is one of the most important challenges facing supramolecular chemists today.

In the case of the sapphyrins, initial documentation of their anion binding ability under nonsolid state conditions was made using fast atom bombardment mass spectrometric (FAB MS) analysis. These studies, which were often carried out in a "screening" sense, involve taking mixtures of the chosen sapphyrin receptor and the putative anionic substrates in an appropriate solvent and subjecting them to low- and high-resolution FAB MS analyses. In most cases, a clear correlation between binding under the matrix desorption/gas phase conditions of the MS experiments and chelation in solution was observed. In fact, without exception, if a peak corresponding to the sapphyrin–anion complex could be detected in the mass spectrum, binding in solution was later confirmed. Thus, in the authors' hands, these simple FAB MS screening studies define an important tool that can be used easily to check for the viability of any given receptor–substrate combination.

More detailed analyses of sapphyrin anion chelation in solution were made using a full range of "tricks" borrowed from the supramolecular field. Thus both spectroscopic techniques (e.g., NMR, UV-vis, fluorescence spectroscopy)[24] and transport studies (carried out in a model Pressman type U-tube membrane system[25]) were employed. From these analyses, it became clear that sapphyrin does in fact bind various negatively charged substrates in solution, but does so both with variable affinity and oft-times remarkable selectivity. These findings/conclusions are detailed further in the paragraphs below.

## 3.1. Halide Binding

The desire to study the halide binding properties of sapphyrin in solution was largely inspired by the solid state sapphyrin–fluoride and sapphyrin–chloride structures described above (Figures 1, 2, and 3). It was also inspired in part, however, by a very important public health problem, namely cystic fibrosis.[26] Cystic fibrosis is the most common lethal genetic disease in Caucasians, affecting one out of 2500 infants in the U.S.[26d] This disease is characterized by an inability to produce properly functioning chloride anion channels.[26c] The dysfunctional ion channels are believed unable to effect sufficient chloride and fluid excretion from, among others, pulmonary epithelia cells.[26b,c] This, in turn, leads to a thick build up of mucous deposits in the lungs and to a higher than normal susceptibility for fatal pulmonary infections. It is these infections, often of the *Pseudomonas aeruginosa* type,[26b] that are generally the causative agents of cystic fibrosis death. While some recent progress towards treating this disease has been made of late, cystic fibrosis remains a serious medical concern.[27]

In view of the above, it is not surprising that significant efforts have been dedicated to the problem of generating synthetic chloride receptors. Indeed, a number of such systems are known.[28,29,30] Unfortunately, many of them are hydrophilic polycations and, accordingly, suffer from low solubility in organic media.[29a–m] Others are metal- or metalloid-derived systems. The clinical utility of these is clouded by metal toxicity.[29o–x] The sapphyrins, being both wholly organic and

hydrophobic, were considered likely to be free from these kinds of "prior art" problems. It was thus this hope that helped fuel a desire on the part of the authors to determine whether or not the protonated sapphyrins would function as halide anions in solution.

After completing initial mass spectrometric studies, it was quickly found, much to the authors delight, that sapphyrin 3, when protonated, acts as an efficient receptor and carrier for chloride and fluoride anions (as judged from the U-tube model membrane studies); *vide infra*.[17,18] Further, using visible absorption and fluorescence spectroscopic analyses, it proved possible to derive a binding constant ($K_a$) of ca. $9.6 \times 10^4$ $M^{-1}$ for fluoride anion in methanol. For comparison, chloride anion was found to be bound with much lower affinity in this same solvent ($K_a \approx 10^2$ $M^{-1}$), whereas bromide anion hardly formed a complex at all ($K_a \leq 10^2$ $M^{-1}$).

The extremely high fluoride-to-chloride/bromide selectivity (more than 1000-fold!) was attributed to the fact that fluoride anion, unlike chloride and bromide, could be encapsulated fully within the mean sapphyrin plane. This contention was further supported by visible, fluorescent, and NMR spectroscopic studies carried out in dichloromethane. Here, the choice of solvent was actually considered critical to the studies. First, the use of this less polar solvent was expected to promote stronger interaction between the protonated sapphyrin receptor and halide substrates. Second, by using this solvent, the problem of sapphyrin aggregation could be avoided.[31] The results obtained (i.e., higher affinities; reduced aggregation) led to the suggestion that both the hydrochloride and hydrobromide salts of sapphyrin exist as out-of-plane-chelated tight ion pairs in dichloromethane solution, whereas the fluoride anion sits in the sapphyrin core. Thus under these solution-phase conditions, the anion binding modes were considered to reflect those seen in the solid state.

Complementing the $K_a$ determination studies were the through-model-membrane transport experiments alluded to above.[18] These revealed, interestingly, that it was chloride anion (i.e., the species that is less well bound) that is transported at the greatest rate. This finding, although initially surprising, was interpreted as meaning that it is the off-rate for fluoride anion release from the sapphyrin–fluoride complex that plays a significant, perhaps rate-limiting, role in mediating the actual transport process. In any event, it was found that the transport could be effected not only via simple synport, but also via antiport, in which a particular target anion is transported through a membrane at the expense of back-transmission of some other negatively charged species. These critical findings clearly bode well for the eventual use of sapphyrin-based halide anion transport systems in clinical situations.

## 3.2. Binding of Phosphates

Subsequent to the work with halide anions, efforts were made to quantify the extent to which phosphate anions are bound by protonated sapphyrin.[10,16] As for chloride and fluoride, the rationale for this work was both chemical and biological.

Chemically, it is a challenge to design phosphate receptors.[28,32] Also, it is of interest to see if the solid-state sapphyrin phosphate structures reflect events in solution. On the biological side, phosphate anions play critical roles in numerous metabolic and energy transduction processes.[1c,22a] Also, phosphate entities are present in the active forms of many antiviral agents.[23]

In terms of actual experiment, a range of spectroscopic techniques were used to determine the nature of the different phosphate anion-to-protonated sapphyrin interactions and to probe the extent of binding. Proton and $^{31}$P NMR spectroscopic analyses were used, for instance, to obtain direct evidence of phosphate anion binding. Here, changes in the chemical shifts of either the sapphyrin proton or phosphorous $^{31}$P signals were monitored as a function of various receptor-to-substrate ratios. From these changes, which were often substantial (up to 16 ppm! in the case of $^{31}$P NMR spectroscopic analyses), standard curve-fitting procedures were used (in well behaved cases) to derive the relevant binding constants.[24] While intellectually straightforward, these analyses were often made complicated by multiple equilibria involving sapphyrin protonation, anion binding, and/or anion exchange.[16a] To avoid technical complications associated with these multiple equilibria, it often proved advantageous to define the protonation state of sapphyrin and the nature of the counteranion bound (if any) by separate extraction experiments at different (but known) pH values. Also complicating these studies, especially in more polar media and at higher sapphyrin concentrations, were dimerization and aggregation processes involving sapphyrin itself. Similar processes involving the phosphate substrates also had to be considered.[16a,17b] Fortunately, by carefully choosing the solvent system, the concentration of species under investigation, and the sapphyrin receptor itself, clean binding isotherms for the formation of either 1:1 or 2:1 phosphate-to-protonated sapphyrin complexes could often be obtained. Depending on the nature of receptor and the substrate, protonation stage of the sapphyrin, the nature of counterion, if any, and the solvent system, binding constants of up to a $1.8 \times 10^4$ M$^{-1}$ were observed. This puts phosphate anions second, as a class, only to fluoride anion in terms of the avidity with which it is bound by sapphyrin.

To support the above conclusion, phosphate anion displacement (i.e., competitive binding) studies were carried out. From these studies, the following affinity series was deduced for anion binding in methanol: F$^-$ > H$_2$PO$_4^-$ > C$_6$H$_5$CO$_2^-$ > ClO$_4^-$ > NO$_3^-$ > AcO$^-$ > Cl$^-$. These results thus reinforce the notion that sapphyrin, when protonated, functions as a highly effective phosphate anion receptor in organic solution. Further, they also support, but certainly don't establish definitively, the idea that the binding interactions in solution as well as in the solid state involve a combination of (1) electrostatic attractions between the positively charged sapphyrin core and the negatively charged phosphate oxyanion, and (2) multiple hydrogen-bonding interactions between this same phosphate oxyanion and the pyrrolic hydrogens of the protonated sapphyrin core.

## 3.3. Carboxylate Chelation and Self-Assembly

The last small anion class to be studied in detail were the carboxylates. While it was appreciated that these anions would be bound more weakly than fluoride or phosphate (*vide supra*), it was also recognized that anionic carboxylate groups play a critical role in Nature.[1c] Indeed, amino acids, enzymes, antibodies, and other natural products contain carboxylate functionality that often plays a critical role in shaping the relevant biochemistry. In terms of molecular recognition, carboxylates are important because they are capable of acting as chelates for a range of positively charged substrates, including protonated amines and metal cations. Not surprisingly, therefore, considerable effort has been devoted to the problem of preparing carboxylate-binding receptors and a number of such systems are now known.[32g,s,33]

In the case of sapphyrin-based carboxylate receptors, the relative binding affinities were found to depend on the nature of the substrate. In particular, aromatic carboxylates were found to be bound with higher affinity to protonated sapphyrins than aliphatic ones. Indeed, in the case of the decaalkyl sapphyrin **3**, affinity constants measured in dichloromethane, were found to be ca. $10^3 \text{ M}^{-1}$ for aromatic substrates but less than $10^2 \text{ M}^{-1}$ for aliphatic ones.

This finding that sapphyrins bind carboxylate anions in dichloromethane solution led us to consider exploiting this interaction to design a new kind of supramolecular energy transfer ensemble. The specific system proposed is shown in Figure 12 and is based on the binding of a carboxylate-appended, free-base porphyrin photodonor by a monoprotonated sapphyrin acceptor.[34] Upon irradiation at 573 nm, singlet–singlet energy transfer from the porphyrin to the sapphyrin subunits takes place readily with energy transfer dynamics consistent with a Föster-type mechanism. This system, which is still in the process of being studied further, thus appears to be a first example of what could be an important new class of photosynthetic model system that is based on the use of anion chelation.

Also investigated in solution were the self-assembly processes "hinted at" by the X-ray structure of **5** (Figure 11). Solution state self-assembly of complementary fragments occurs throughout Nature and plays an essential role in the construction of such biologically critical "superstructures" as nucleic acids, multicomponent enzymes, cell membranes, and viral capsids.[1c] In these instances, the structural information required for self-assembly is "preprogrammed" into the topography and functionalization of the various "building block" surfaces. Reversible assembly of the building blocks then serves to generate the final supramolecular ensemble as the result of multiple weak noncovalent interactions. This minimalistic yet effective approach to molecular architecture has challenged supramolecular chemists to design artificial systems capable of self-assembly. While a number of such systems are now known,[35–37] few are based strictly on anion chelation.[38]

It occurred to us that the anion binding properties of sapphyrins could be employed for the self-assembly of these species. In particular, we speculated, that the zwitterionic sapphyrins **5** and **6** should self-assemble. These species contain
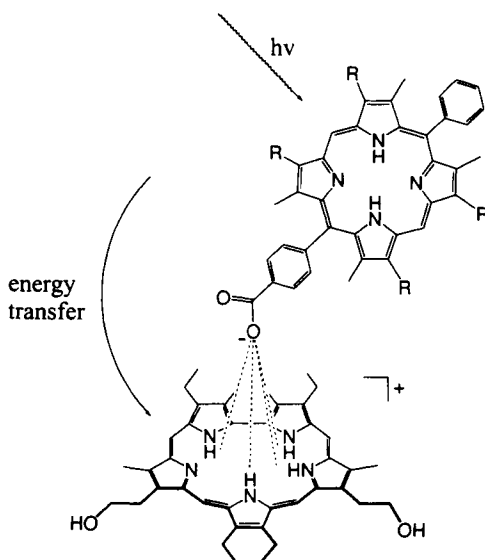
**Figure 12.** Proposed noncovalent ensemble for energy transfer.

anionic carboxylate groups attached to a protonated sapphyrin core, but are prevented from "biting their own tails" due to the length of the carboxylate–sapphyrin spacer. In contrast to the previously reported anionic systems capable of self-assembly,[38] the sapphyrin-based carboxylate building blocks are self-complementary and would not require the presence of extra components for the desired self-association to take place. To our delight, the anion chelation-driven dimerization of carboxylate-appended sapphyrin 5 was observed in the solid state (see Section 2.3).[21]

In the specific case of the "tailed" sapphyrin carboxylates 5 and 6, for which evidence of self-assembly was noted in the solid state (*vide supra*), $^1$H NMR spectroscopic studies carried out in $d_4$-methanol, $d$-chloroform, and mixtures of the two solvents showed strong line broadening, and upfield shifts of the methylene "tail" peaks. Such findings are, of course, fully consistent with the proposed dimerization. Further, dilution experiments performed over a concentration range of 50 to 5 mM in these solvents showed little change in the spectra, indicating that the dimeric form prevails under these conditions, even in highly polar solvents. In the case of 6, the actual dimeric stoichiometry was confirmed by vapor pressure osmometry (VPO) measurements carried out in 1,2-dichloroethane.

To test further the self-assembly process, experiments were carried out in the presence of fluoride anion. As noted above, protonated sapphyrins have a significantly higher affinity for fluoride anion as compared to other anions.[17b] It was thus expected that adding fluoride anion to a solution of 6 would serve to inhibit the

2 [sapphyrin monomer] ⇌ [sapphyrin dimer] ⇌ [sapphyrin carboxylate-fluoride complex]

fluoride

sapphyrin          sapphyrin          sapphyrin carboxylate-
carboxylate, 6     dimer, 6 • 6       fluoride complex, 6 • F⁻
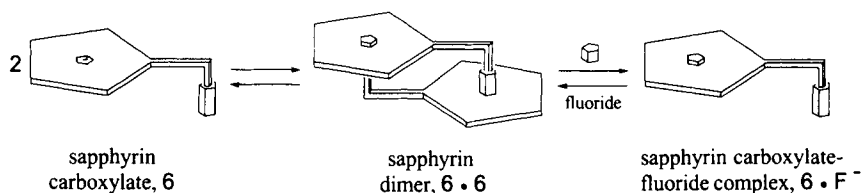
**Figure 13.** Schematic representation showing both the dimerization of sapphyrin, **6**, that occurs spontaneously in solution, and the inhibition of this dimerization process that can be effected by adding fluoride anion.

dimerization process. As confirmed by detailed ¹H NMR analyses, this indeed proved to be the case. Specifically, adding F⁻ breaks the dimers and reestablishes the "normal" lower-field chemical shift for the methylene signals that is seen in sapphyrin monomers (Figure 13).

# 4. SAPPHYRIN CONJUGATES

The processes Nature uses for chelation of substrates, now increasingly well understood, continue to provide an inspiration for chemists to design effective receptors for complex *multidentate* guests (i.e. those containing multiple functional groups). Here it has been come to be appreciated over the years that multidentate receptors, containing recognition sites that complement those found on their targeted substrates, offer an advantage in terms of achieving effective binding. However, the design and synthesis of multidentate receptors is not easy. First, and foremost, one needs to bring together building blocks that are known to be capable of binding at least one of the functional groups present in the prospective substrates. Second, these building blocks need to be connected to each other in such a way that the number of host–guest interactions is maximized. Third, the actual tethering process should be one that not only establishes an appropriate overall receptor topography but also helps achieve a desirable level of solubility. In addition, in those cases where stereoselective substrate binding is desired, chiral receptors, featuring at least three-point interactions with the substrate,[39] are required. In this section, we describe the sapphyrin-based approaches to generating functionalized multidentate receptors capable of binding such important biological substrates as nucleotide monophosphates and amino acids.

## 4.1. Sapphyrin–Nucleobase Conjugates

Nucleotide monophosphates based on purine and pyrimidine-derived systems play critical roles in various biological processes such as signal processing, feedback inhibition, energy transduction, gene replication, and enzymatic regula-

tion.[1c,22a] Also, as noted previously in this chapter, some phosphorylated nucleotide analogs exhibit antiviral activity in vitro.[23] Many of these latter compounds, however, fail to cross the lipophylic cell membrane in their charged form. They are thus inactive in vivo.[40] Indeed, in the normal course of clinical practice, these substances are administered in their uncharged, nucleoside form. Upon gaining entry to the cytoplasm, enzyme-mediated phosphorylation gives the corresponding active, ionic species. However, the efficiency of this phosphorylation process is often low, or does not occur at all.[41] Given the above, it is not surprising that intensive efforts have been made to solve the problem of phosphate recognition and transport.[28,32]

Our approach to nucleotide analogue transport derives from an appreciation that these compounds are divergent in structure: they contain both an ionic phosphate and a potentially hydrogen-bonding nucleic acid base linked together by a spacer. We, therefore, sought to design a *ditopic* receptor, having recognition sites for both the charged phosphate and the nucleobase moiety. These, we thought, could be used to bind, neutralize, and transport nucleotide phosphates through a membrane.

In accord with these thoughts, a first generation prototypical conjugate **8**, designed to bind and transport guanosine 5'-monophosphate (GMP), was synthesized in the authors' laboratories. It is comprised of two parts: a sapphyrin macrocycle and a tethered cytosine nucleobase.[42a,b,43a] In preparing this system, the expectation was that the nucleobase portion of **8** would bind the guanine part of the GMP via hydrogen bonds, while the protonated sapphyrin would serve to neutralize the phosphate part of this same multifunctional substrate. To our delight, this conjugated receptor (**8**) was found to be an effective carrier for GMP, effecting through-membrane transport in a model U-tube system under neutral conditions.

One of the interesting aspects of the above finding is that effective transport was observed even though (1) the sapphyrin portion of the carrier is monoprotonated at neutral pH while (2) the GMP substrate is mostly dianionic[43b] (roughly 66%) under these conditions. This means that either the second $pK_a$ of GMP (6.66) is changed when this species is bound to **8**, or, as implied by Figure 14, receptor **8** binds and transports the minor, monoanionic form of GMP so effectively that over the course of the transport experiment, the amount of GMP is depleted as the result of (1) a fast GMP $^{2-}$ to GMP$^-$ interconversion followed by (2) an effective through-membrane transport of GMP$^-$. In any event, the transport process is both viable and selective; carrier **8** shows a high preference for GMP over the other nucleotide monophosphates.[42a,b] This, presumably, is due to the fidelity of the guanine–cytosine base-pairing interactions. In the best cases, the relative rate enhancements for GMP transport over CMP and AMP are 100:1 and 11:1, respectively.[42a,b] To achieve this selectivity and to provide a high overall flux, a strongly basic receiving phase had to be used in a model membrane. Presumably, this latter observation just reflects the fact that deprotonation of the sapphyrin is necessary for rapid substrate release.

8                                    8 • GMP
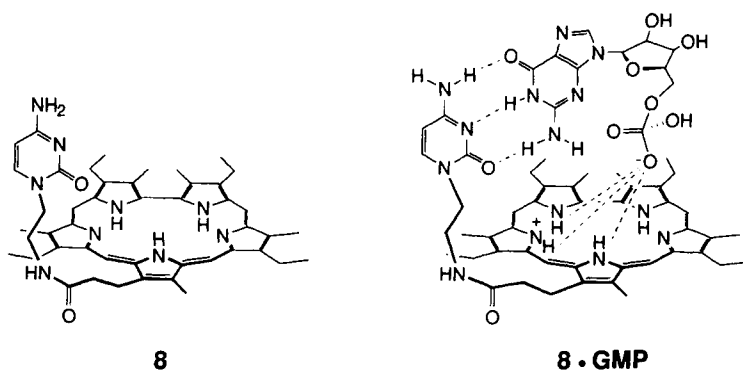
**Figure 14.** Proposed supramolecular complex formed between conjugate **8** and monobasic GMP.

Subsequent to the preparation of **8**, a number of other sapphyrin–nucleobase conjugated carriers were synthesized in the authors' laboratories.[42c] These include compound **9** that has two cytosine moieties appended to the sapphyrin macrocycle, as well as two guanine-bearing sapphyrins, **10** and **11**. Here, as expected, the ditopic sapphyrin–guanine receptor **10** served to enhance the transport of cytosine-5'-monophosphate (but not GMP or AMP). By contrast, the two tritopic receptors, namely **9** and **11**, were designed with the intention of allowing for the formation of the complexation-derived "triple-helix-like" C-G-C and G-C-G motifs in addition to phosphate chelation by sapphyrin. In other words, it was expected that a centrally



9



10                                    11
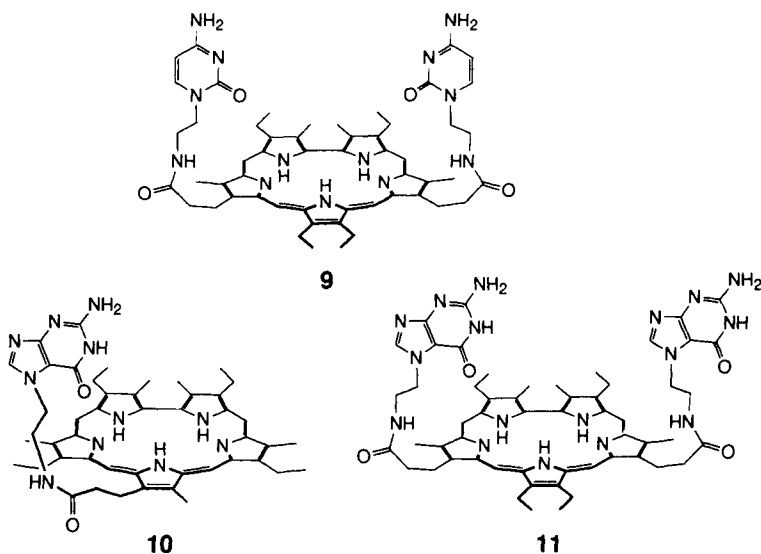
bound nucleobase subunit would participate in two different kinds of hydrogen-bonding interactions, involving both Watson–Crick and Hoogsteen recognition patterns. To the extent such hypothetical thinking proved valid, it was anticipated that these extra interactions would lead to an enhanced stability for the critical nucleotide phosphate–receptor complex and, accordingly, an augmentation of the through-membrane transport rate. It was also expected that a higher level of substrate selectivity might be observed. In spite of such predicative thoughts, it was found that the doubly functionalized cytosine derivative 9 was both less effective and less selective than its monofunctionalized analog, 8, perhaps as a result of internal cytosine-to-cytosine interactions or an inability of one of the cytosine subunits to bind under the transport conditions (as would be required for Hoogsteen binding). On the other hand, highly selective transport was observed using the bis-guanosine sapphyrin 11, leading to the conclusion that the double base-pairing design considerations are not necessarily devoid of merit. Accordingly, current work is focused on the design of more sophisticated (but similar), receptor systems as well as on the in vitro testing of the sapphyrin–nucleotide conjugates prepared to date.

## 4.2. Sapphyrin–Lasalocid Conjugate

In another development, the authors have used the carboxylate binding properties of sapphyrin for the construction of a receptor for zwitterionic aromatic amino acids. Binding and transport of amino acids constitutes an important problem in supramolecular chemistry from both the analytical and biomimetic points of view.[44] Presently, some information is available about the regulation and dynamics of amino acid transport in nature, but a detailed mechanistic and structural under-standing remains lacking.[45] This relative lack of information is providing an incentive to develop synthetic systems that are capable of carrying out amino acid transport.[46] Unfortunately, the normal zwitterionic nature of α-amino acids tends to make both the carboxylate and protonated amino portions of the molecule difficult to bind concurrently. This makes the design of receptors for zwitterionic amino acids extremely challenging. Further, in water, the best solvent for these doubly ionic species, the strengths of normally-used supramolecular binding inter-actions (e.g. hydrogen bonds, Coulombic attractions) are weakened substan-tially.[46b] On the other hand, the low solubility of amino acids in organic solvents imposes a costly energetic burden on their recognition in non-aqueous solutions. Thus, in order to bind an amino acid in its zwitterionic form effectively, bidentate receptors must contain recognition sites for both the carboxylate anion and the protonated amino group. In addition, in order to effect enantioselective recognition, specific interactions involving the amino acid side chain must be established and exploited.[39,47] This adds yet an additional challenge to this already very tough problem in molecular recognition.
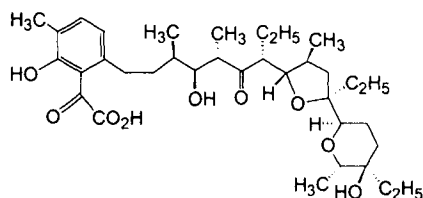
**12**

We have shown previously that sapphyrins, unlike their simple porphyrin congeners, when mono-, or diprotonated act as excellent receptors for a variety of anions including *carboxylates* (see paragraphs 2.3 and 3.3). We reasoned that an appropriate protonated amine receptor, when attached to sapphyrin, would make an effective amino acid receptor. It occurred to us that *lasalocid* (c.f., parent structure **12**)[48–50] might function well as the requisite "attachable amine receptor." Lasalocid is a naturally occurring polyether antibiotic[48] that is composed of a conformationally constrained acyclic polyether chain terminated by a carboxylate anion at one end and an hydroxyl group at the other. These structural features allow lasalocid to (1) form intramolecular head-to-tail hydrogen bonds, (2) establish a pseudo-cyclic cavity, and (3) accommodate, in a stereo-differentiating way, a range of cationic substrates, including protonated amines.[49,50] Thus, it was thought that a covalently connected sapphyrin–lasalocid conjugate (e.g., **13**) would function as such a sought-after binding agent for zwitterionic amino acids.[51] Such a putative receptor would be of further interest in that it should both feature non self-complementary binding sites (precluding it from internal collapse) and contain 10 asymmetric centers making it of potential utility as an enantioselective receptor.

As expected, system **13** did in fact bind and transport zwitterionic α-amino acids through a model membrane barrier with good selectivity under conditions where the porphyrin-derived control system (**14**), lacking the carboxylate anion chelation ability inherent in **13**, would not. Specifically, it was found that at neutral pH compound **13** acts as a very efficient carrier for the through model membrane[25] ($H_2O$–$CH_2Cl_2$–$H_2O$) transport of phenylalanine and tryptophan. Further, in direct competition experiments, L-phenylalanine was found to be transported four times faster than L-tryptophan and 1000 times faster than L-tyrosine. As implied above, little or no transport was observed when a porphyrin control (**14**) was used. Nor was significant transport observed when a mixture of sapphyrin and lasalocid was used.

Further support for the contention that conjugate **13** can act as an amino acid binding agent came from quantitative visible spectroscopic titrations carried out in dichloromethane. It was determined that compound **13** forms 1:1 complexes with both phenylalanine and tryptophan with relatively high association constants ($K_a$ = $4.86 \times 10^5$ $M^{-1}$ (L-Phe), $5.35 \times 10^5$ $M^{-1}$ (D-Phe), $0.83 \times 10^5$ $M^{-1}$ (L-Trp), and $0.94 \times 10^5$ $M^{-1}$ (D-Trp)).

13                                        14
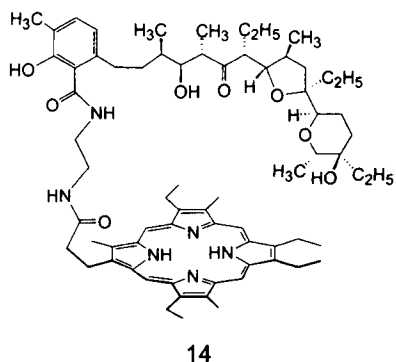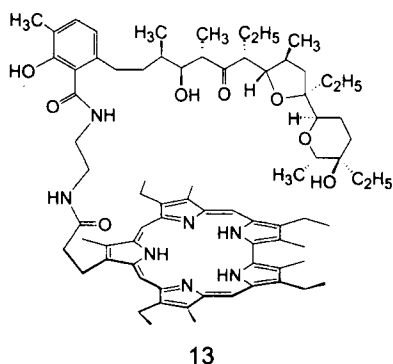
# 5.  SAPPHYRIN OLIGOMERS

Unlike *conjugated* receptors, which are constructed from covalently linked, but intrinsically different building blocks, *oligomeric* receptors are comprised of several identical sapphyrin-type binding units tied together by various tethering groups. Such systems, which serve to define sapphyrin-based "supermolecules" offer several fascinating opportunities from a molecular recognition perspective. First, they can provide for the multiple interactions a polydentate substrate may need in order to be chelated effectively; this could allow for the full electrostatic neutralization of a polyanionic species thereby allowing for its efficient through-membrane transport. Second, the use of oligosapphyrin receptors provides a platform that allows a range of host–guest interactions, involving differing parts of the sapphyrin receptor and the substrate, to be explored. In this way, the macroscopic and binding properties of a multidentate receptor could, in principle, be "fine tuned" by changing the number of sapphyrin "parts" and/or by varying the tethering "spacers" that link them. In view of these considerations, it was considered worthwhile to prepare a series of sapphyrin-based oligomers and to study them as possible polyanion binding receptors. The results of these studies are summarized below.

## 5.1.  A Covalently Linked Sapphyrin Dimer

· Our first generation sapphyrin–sapphyrin dimer is represented by structure **15**. In this system, two covalently connected anion binding sites are contained within the same overall recognition framework. It was thus expected that system **15** would act as an effective receptor for dicarboxylate anions under conditions where the corresponding monomeric systems (e.g. **3**) would not.[52] Indeed, this proved to be the case (*vide infra*).

Our desire to generate a receptor for dicarboxylate anions came from an appreciation that di- and tricarboxylates play critical roles in numerous metabolic processes including, for instance, those associated with the citric acid and glyoxylate cycles.[1c] They also play important roles in the generation of high-energy
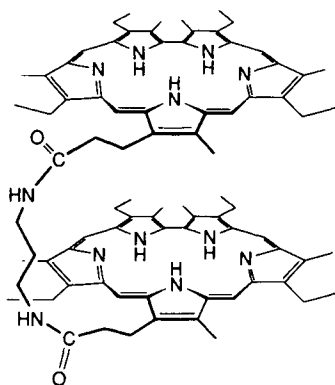
**15**

phosphate bonds and in the biosynthesis of important intermediates. Given this importance, it is not surprising that numerous groups have targeted the problem of dicarboxylate anion binding.[53] In our sapphyrin-based approach (i.e., **15**), two protonated sapphyrin subunits serve as the key carboxylate-binding "building blocks," while a flexible diaminopropane "tether" serves as the all-important macrocycle-to-macrocycle linking chain. This system, as it transpired, binds dicarboxylate anions in polar solvents (e.g., methanol) as well as the best current systems while, at the same time, displaying a unique substrate selectivity.

Part of what makes dimer **15** so interesting is that, apart its substrate recognition properties, it displays some quite characteristic spectral features. Indeed, visible spectral analyses of the dimer revealed the presence of two conformations in organic solution: a closed *endo*-like conformation ($\lambda_{max}$ = 426 nm in dichloromethane) and an open *exo*-like conformation ($\lambda_{max}$ = 450 nm in dichloromethane). Addition of trifluoroacetic acid afforded complete conversion to the open *exo* form. While such a conformational change could indicate specific anion binding (as desired), it could also simply reflect generalized protonation effects. Since only the former phenomenon would be of interest in a molecular recognition sense, efforts were made to distinguish between these two limiting possibilities.

Mass spectrometric studies were carried out as a first qualitative means of checking for dicarboxylate anion binding (see also Section 3). Here, mixtures of sapphyrin dimer **15** and several representative dicarboxylate anions, such as oxalate, 4-nitrophthalate, 5-nitroisophthalate and nitroterephthalate in methanol, were subjected to high resolution FAB mass spectrometric (HR FAB MS) analysis using FAB positive NBA matrix. In general, peaks for the putative complexes were seen, lending credence to the hypothesis that the dicarboxylate substrates in question were, in fact, being bound by **15** under the matrix desorption/gas phase conditions used to effect these mass spectrometric analyses.

More definitive proof of binding came from transport experiments. Here, in analogy to earlier work involving phosphate anion transport,[42,43] a standard Pressman-type, Aq. I–$CH_2Cl_2$–Aq. II, model membrane system[25] was used. Under standard conditions, it was found that dimer 15 acts as an efficient carrier for a range of dicarboxylate anions including various isomeric ones derived from nitrobenzene (e.g., 4-nitrophthalate, 5-nitroisophthalate and nitroterephthalate dianions). Interestingly, in direct competition experiments, nitroterephthalate dianion was found to be transported three times more quickly than 4-nitrophthalate dianion by dimer 15. By contrast, the use of the monomeric control sapphyrin 3 resulted in a minimal transport of all the isomeric nitrophthalate anions tested.

Quantitative assessments of dicarboxylate binding efficacy in methanol were made using standard $^1$H NMR titration techniques. Here, in order to avoid problems associated with proton transfer, the mono- and diprotonated forms of sapphyrins 3 and 15 (as their hydrochloride salts) and the bis(trimethylammonium) salts of the various dicarboxylic acids substrates were used. In general, chemical shifts of the aromatic protons of the carboxyl-containing substrate were monitored as a function of increased receptor concentration.[24] In some instances, well-resolved shifts could not be observed in the appropriate $^1$H NMR spectra. Here, either visible spectroscopic titration procedures were used or deuterated substrates were employed such that the binding process could be followed by $^2$H NMR. The results of these binding studies confirm what was concluded from the transport studies, namely that system 15 is both an excellent and inherently selective receptor for dicarboxylate-type substrates. System 15, for instance, shows little affinity for monocarboxylate-derived substrates ($K_a \leq 20$ M$^{-1}$ for trifluoroacetate) while showing affinities for certain dicarboxylates (e.g., $K_a = 9.1 \times 10^3$ M$^{-1}$ for nitroterephthalate dianion) that rival those of the very best receptor systems known.[53] Further, within the class of derivatives of dicarboxylic substrates, system 15 displays a preference for linear over bent substrates and aromatic over aliphatic substrates, this is remarkable given the flexible nature of this receptor. It is also consistent with the binding mechanism proposed, namely that the sapphyrin dimer 15 forms a well-defined "sandwich"-like complex with the various dicarboxylate anions it binds.[52]

## 5.2. Sapphyrin Trimers and Tetramers

It has been emphasized in the previous paragraphs that effecting the through-membrane transport of artificial antiviral nucleotide analogs would be beneficial in that it might allow the direct into-cytoplasm entry of species that would be otherwise inactive in vivo (due to an inability to cross hydrophobic cell membranes).[40,41] Within the overall scope of this problem, finding ways to effect the into-cell transport of nucleotide di- and triphosphates is deemed particularly important. This is because it is often these forms that are the most potent.

In spite of the importance of the above problem, few receptors are known at present that are capable of binding and transporting di- and triphosphates or

oligonucleotides, even under laboratory conditions.[54] The reason for this is that near or full electrostatic neutralization is generally required for the transport of these highly charged species and this, in turn, imposes much tougher requirements on the design of multidentate receptors.

Based on our recent discovery that several expanded porphyrins, including sapphyrins, can function as specific receptors and carriers for phosphates and phosphonates,[16] we considered it likely that oligosapphyrins would function as specific receptors and carriers for biologically important phosphorylated species such as mono-, di-, and triphosphates. To test this hypothesis, compounds **15** and **16–18**, prepared from the sapphyrin monoacid **6** and corresponding amines, were constructed. These systems contain sapphyrin "monomers" connected by flexible "linkers".[55] As such, it was thought that the various sapphyrin subunits would provide the basic phosphate chelation needed for binding, while the flexible linking chains would allow for the kind of generalized conformational mobility required to accommodate a range of substrates. It was also appreciated that the spacers might allow for additional stabilizing interactions, including hydrogen bonds (involving the amides) and, in the case of **16** and **18**, Coulombic attractions (as the result of the protonated amines in the tethers).

Visible spectroscopic analyses of the tetramer **18** and trimers **16** and **17** gave results that were analogous to those obtained with compound **15**. However, as might



17



16

18
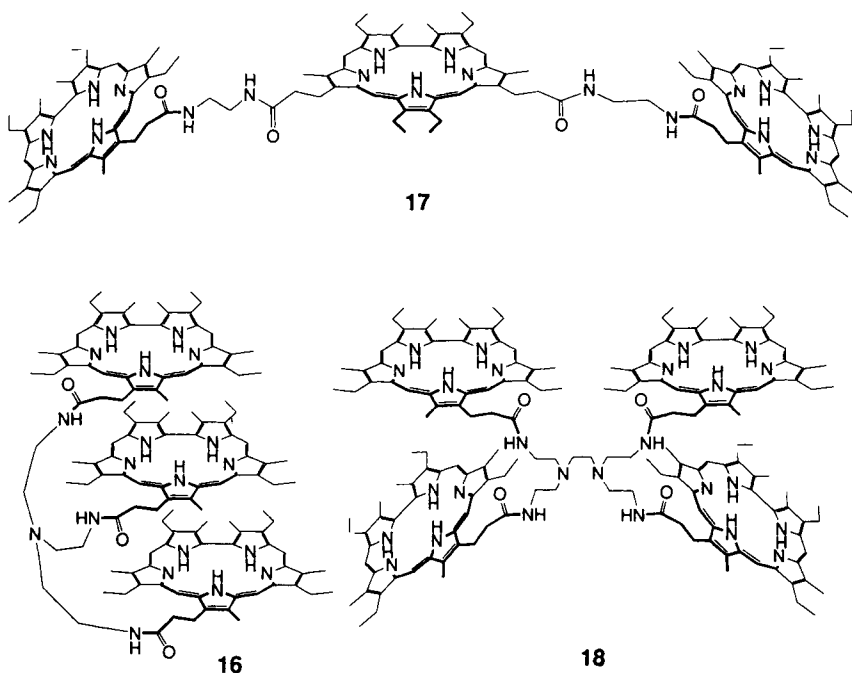
be expected intuitively, there is a clear tendency towards higher aggregation as the number of sapphyrin units in the molecule is increased. Addition of anionic species, in particular phosphates, to solutions of these oligosapphyrins in methanol causes the Soret-like band with the higher wavelength maximum to increase in intensity at the expense of the one at lower wavelength. This kind of behavior, which is seen throughout the series **15** and **16–18**, is attributed to deaggregation of an "internally stacked", or "folded over", macrocyclic species as the result of anion chelation. By following the decrease in relative absorbance, it also proved possible to determine association constants $(K_a)$, accurate at least in a relative sense, for the formation of 1:1 complexes between receptors **16–18** and ADP or ATP.[24] The relevant association constants $(K_a)$ were found to be on the order of $1.9 \times 10^3 \, M^{-1} - 6.8 \times 10^3 \, M^{-1}$.

As detailed above, simple monomeric sapphyrins and nucleobase-substituted sapphyrin conjugates can function as viable carriers for the transport of nucleotide monophosphates across bulk liquid membranes.[42,43a] However, the efficiency of these systems is strongly pH-dependent. In the case of an unmodified sapphyrin **3**, for instance, the upper pH limit for detectable transport is 5.5.[43a] Even after a complementary nucleobase recognition subunit is attached (to give, for instance, **8**), the effective transport rates were found to drop off dramatically as neutral pH is approached. On the other hand, even at neutral pH, the oligosapphyrins **16–18** function as effective carriers for nucleotide-type species (as judged from standard U-tube type model membrane experiments[25]). Interestingly, the sapphyrin trimers **16** and **17** were found to be very efficient carriers for nucleotide diphosphates at neutral pH. These same species, however, proved ineffectual as carriers for nucleotide triphosphates. By contrast, the tetrameric species **18** was found to be a highly effective carrier for all studied phosphorylated species (i.e., mono-, di-, and triphosphates). Interestingly, with this carrier (as with **15–17**), adenosine-derived nucleotides (i.e., AXP; X = M, D, T) were always found to be transported with greater efficiency than UXP, CXP, or GXP. This selectivity, although not yet fully understood, has been observed previously by others.[56]

For the linear species **15** and **17**, further insight into the mode of binding was obtained from $^{31}$P NMR experiments. In the case of receptor **15** we found that the phosphate oxyanions of *both* AMP and ADP are all complexed by (or at least located in the vicinity of) the sapphyrin subunits of dimer **15**, as judged by the upfield shifts of the relevant $^{31}$P signals. In the case of receptor **17**, however, the situation was found to be more complex. Specifically, it was found that the $^{31}\beta$ signal migrates to higher field, whereas the $^{31}P\alpha$ and $\gamma$ signals are shifted to lower field upon binding. These results, although not analyzed in detail, were interpreted as meaning that $P_\beta$ is located near the edge of the sapphyrin macrocycle, as opposed to being chelated in a "regular" fashion above the plane.

# 6. INTERACTION OF SAPPHYRIN AND ITS CONJUGATES WITH OLIGONUCLEOTIDES AND DNA

Oligonucleotides and nucleic acids are essential for numerous biological processes.[1c,22a] As a result, Nature has developed highly selective methods for manipulating these phosphorylated materials.[57] This, in turn, has inspired synthetic chemists to try their hand at generating small molecules that might be capable of effecting the specific recognition and transport of these all-important anionic entities.[28,32]

## 6.1. Studies Involving Monomeric Sapphyrins

The finding that sapphyrin interacts well with simple phosphate anions both in solution and in the solid state[10,16,42,43a] inspired us to examine how sapphyrin might interact with oligonucleotides such as DNA. While there are three modes of binding that small molecules generally exhibit when binding to DNA—referred to as intercalation, groove binding, and simple electrostatic attraction[58]—it was found, interestingly, that sapphyrin interacts via none of these. Rather, as detailed further in the ensuing paragraphs, monoprotonated sapphyrin, often as a non-covalent dimer, binds to both single-stranded (ssDNA) and double-stranded (dsDNA) DNA in an unique way that can best be referred to as "phosphate chelation".[10,16b,59] At higher sapphyrin-to-phosphate ratios, a second mode of binding, involving the aggregation of highly ordered sapphyrin domains along the surface of the DNA, becomes relevant. Finally, under certain conditions, hydrophobic attractions, involving interaction between the large aromatic surfaces of the pentapyrrolic sapphyrin and the purine or pyrimidine-containing nucleic acid residues,[16b] serves to complement the basic phosphate chelation mode of binding.

Initial evidence for the proposed phosphate chelation mode of binding came from studies involving the water-soluble sapphyrin **7**.[16b,59] Here, it was first found that simply mixing an excess (on a per phosphate basis) of this sapphyrin with dsDNA at neutral pH leads to immediate precipitation of the dsDNA in the form of green

**4**   $R^1 = CH_2CH_2OH$;   $R^2 = R^3 = CH_3$

**7**   $R^1 = CH_2CON(CH_2CH_2OH)_2$;
     $R^2 = R^3 = CH_3$

**19**   $R^1 = CH_2CONH(CH_2)_2NH(CH_2)_2NH_2$;
      $R^2 = R^3 = CH_3$

**20**   $R^1 = CH_2CONH(CH_2)_2O(CH_2)_2O(CH_2)_2NH_2$;
      $R^2 = R^3 = CH_3$

**21**   $R^1 = CH_2CONH(CH_2)_2N(CH_2CH_2NH_2)_2$;
      $R^2 = R^3 = CH_3$
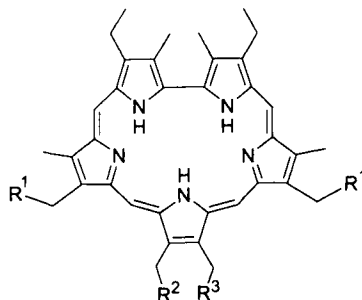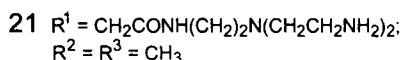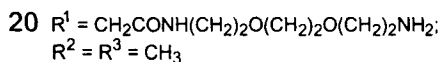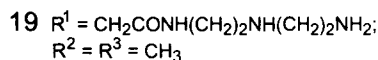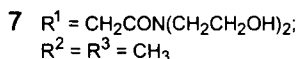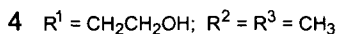
fibers. Since sapphyrin is green, it was assumed that this meant that the monoprotonated form of sapphyrin was binding to, and neutralizing the charge on, the DNA (i.e., rendering it insoluble in aqueous media).

The above precipitate, once isolated, was studied using solid-state $^{31}$P NMR spectroscopy. Such analyses revealed that the $^{31}$P signal of the sapphyrin-bound DNA was shifted upfield by 3.6 ppm, a value that was found to compare favorably with the 3.8 ppm upfield shift observed for the $^{31}$P signal of a "control" sapphyrin– phosphoric acid complex. This was taken as meaning that the same type of binding interaction, namely the "phosphate chelation" binding of Figure 5, is responsible for the sapphyrin-to-phosphate binding process in the case of both DNA and the simpler phosphates studied by X-ray diffraction methods.

UV-vis spectroscopy was also used to probe the nature of the presumed sapphyrin–DNA complex. Before such studies could be made, however, it proved necessary to map out the spectroscopic properties of sapphyrin itself when constrained to an aqueous medium. As the result of these latter predicative analyses, it was determined that sapphyrin can exist in three spectroscopically distinct states in aqueous media. The first spectroscopically distinct state, characterized by a Soretlike absorbance at $\lambda_{max}$ = 450 nm, is ascribed to a monomeric form. The second, assigned to dimerized forms of sapphyrin, is readily identified by its characteristic Soret-like band at $\lambda_{max}$ = 420 nm. The third state, identified on the basis of its signature 400-nm Soret-like absorption maximum, corresponds to the highly aggregated form of sapphyrin; it is this form that is generally dominant in simple aqueous media.

When either dsDNA or ssDNA is added to the otherwise dominant aggregated form of sapphyrin, spectroscopic changes occurred that were best interpreted in terms of the level of aggregation being lowered (i.e., sapphyrin aggregated → DNA-bound sapphyrin dimer; $\lambda_{max}$ = 420 nm). Such a reduction in aggregation is expected since the proposed "phosphate chelation" binding to DNA would necessarily serve to "dilute" the sapphyrin and compete energetically with a tendency towards aggregation. To the extent such interpretations are correct, the spectral changes can be used quantitatively; doing so allowed an estimated binding constant of ca. $10^4$ M$^{-1}$ to be derived for sapphyrin 7 chelating to dsDNA at low sapphyrinto-DNA ratios.

A critical consequence of the above studies is that they allowed groove binding to be ruled out as a dominant sapphyrin–DNA recognition mode. This is because in the presence of sapphyrin 7, (1) the same spectral features were seen for both ss- and dsDNA, yet (2) only the latter contains a well-defined set of major and minor grooves.

Ruling out intercalation as a critical recognition mode proved harder on a spectroscopic basis. Thus resort was made to a biochemical Topoisomerase I assay. This assay, which sapphyrin passed in a negative sense, can be used to detect the unwinding that is considered diagnostic of intercalation.[60c]

Currently, efforts are underway to augment our understanding of the seemingly unique way whereby sapphyrin recognizes and binds to DNA. Towards this end, a number of new sapphyrin derivatives, including the more water soluble systems **19–21** are being studied. These new systems contain amines that should be protonated at neutral pH and which are expected to augment the affinity for the interaction of sapphyrin with DNA. Another way the interactions between sapphyrin and DNA are being probed is through the construction of sapphyrin–oligonucleotide conjugates and functionalized sapphyrin derivatives. Initial work along these latter lines is described in the ensuing subsections.

## 6.2. Sapphyrin–Oligonucleotide Conjugate

The appreciation that sapphyrin is a viable singlet oxygen generating photosensitizer[31] led us to test whether DNA photocleavage could be effected using this unique chromophore. Towards this end, a general pBR322 plasmid DNA assay[60a,b] was employed; using it, the authors determined that sapphyrin **7** would indeed cleave supercoiled DNA successfully with a 17% photo-efficiency when irradiated at wavelengths above 700 nm.[61]

Obviously the above results were considered highly encouraging. They showed that sapphyrin could indeed be used as a DNA-modifying photosensitizer. Further, because wavelengths in the far-red portion of the visible spectrum were used (i.e., $\lambda \geq 700$ nm), these results led the authors to speculate that this basic sapphyrin-based approach to DNA photomodification could have real merit if and when it came time to apply it in vivo. This is because it is light of these wavelengths that is best transmitted through bodily tissues.[60d] Accordingly, it was predicted that this photosensitizer might prove better on a per-photon basis than other light-based DNA approaches currently being pursued (*vide infra*).

While the above promise continues to invigorate our efforts in the area, it was also appreciated that for the DNA photomodifying properties of sapphyrin to be applied most effectively they would have to be site-directed. This would allow targeting DNA sequences at sites that would mediate the greatest biological effect (e.g., at a susceptible site of, say, an oncogene). Towards this end, efforts have been made to attach sapphyrin covalently to different oligonucleotides; so far these efforts have given rise to the preparation of the prototypic system **22** whose properties are discussed below.[62]

It has long been known that oligonucleotides of sufficient length will bind to complementary sequences and that these same oligonucleotides can be functionalized so as to either enhance their binding affinity or convey specific DNA-modifying properties via the attachment of specialized functional groups.[63,64] Not surprisingly, therefore, the use of such modified oligonucleotides as a means of regulating gene expression is receiving considerable current attention. One approach, germane to the authors' work with sapphyrin-moidified oligonucleotides, involves using photo-activatable groups as the DNA-modifying antisense "reactive

22
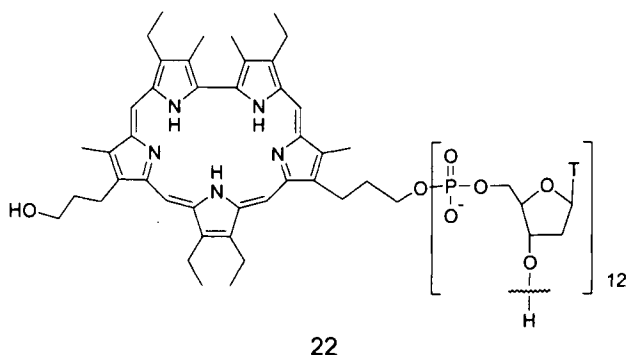
sites".[64] The advantage of this strategy is that it gives an agent with an "on–off" switch that may be activated via irradiation with a particular wavelength of light. Unfortunately, most of the agents currently being tested in this context require the use of the wavelengths below 700 nm. Since this is the spectral region where absorption of bodily tissues is high, these systems are necessarily less efficient than those, like sapphyrin, that can be activated by longer (i.e., more-red) wavelengths of light.

The prototypic sapphyrin conjugate **22** was made using the H-phosphonate method and involved attaching the sapphyrin nucleus to a thymidine 12-mer precursor site isolated on controlled pore glass.[62] After deprotection, oxidation, and cleavage from the solid support, the resulting sapphyrin-modified thymidine 12-mer was characterized by UV-vis and MALDI-MS methods. Melting temperature studies were also carried out to determine what effect, if any, sapphyrin had on oligonucleotide binding. Using complementary oligodeoxyribonucleotide targets, a substantial melting temperature difference (2.7 °C) between the sapphyrin derivatized oligonucleotide and a nonderivatized thymidine 12-mer was observed; this indicates that the presence of the sapphyrin on the thymidine backbone facilitates binding to complementary oligonucleotides. Interestingly, however, this enhanced binding was ascribed to hydrophobic effects rather than phosphate chelation.[62]

When tested as a light-activatable, site-specific DNA-modifying agent, conjugate **22** proved quite effective, with, as expected, good cleavage being observed at proximate G sites following photoirradiation at > 620 nm and subsequent piperidine treatment. Controls demonstrated that the combination of light, attached sapphyrin, and hybridization were all required to effect observed site-directed cleavage and led to the conclusion that the mechanism of photomodification involves, most likely, both electron transfer and singlet oxygen-mediated processes.

### 6.3. Sapphyrin–EDTA Conjugate

While many sapphyrin-derived conjugates can be conceived that would allow one to study more extensively the interactions of this fascinating chromophore/anion binding agent with DNA, most of these remain as yet unprepared at present.
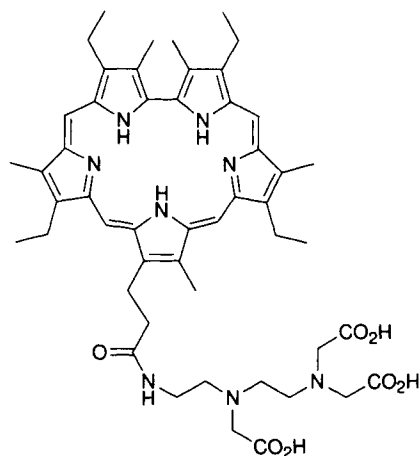
**23**

One critical exception is the sapphyrin–ethylenediaminetetraacetic (EDTA) conjugate (**23**).[65] Previous studies of small molecule-EDTA conjugates have shown that these species, in the presence of iron(II), $O_2$, and a suitable reducing agent, can effect the cleavage of the DNA backbone.[66] In turn, so-called "affinity cleavage" can be used to elucidate the specificity of the small molecule–DNA interactions. It was thus considered worth making **23**.[65]

Once synthesized, a supercoiled plasmid DNA assay[60a,b] was employed to test whether conjugate **23** would or would not work as an effective DNA-binding and cleavage reagent. To do this, the iron chelate of **23** was prepared in situ by adding ferrous ammonium sulfate. In the presence of $O_2$ and the reducing agent dithiothreitol (DTT) this iron chelate was then found to effect cleavage of the supercoiled plasmid pBR322 very efficiently (i.e., at concentrations roughly 20-fold lower than those needed for cleavage using Fe·EDTA alone). These results are important not only because they show that Fe·**23** is indeed an efficacious reagent for the cleavage of DNA, but also because they provide an extra bit of proof that sapphyrin *per se* has a high affinity for DNA.

# 7.  ANION SEPARATION BY SOLID SUPPORT BOUND SAPPHYRINS

Purification and analysis of biologically important anions and zwitterions represents an ongoing challenge for analytical chemists. To date, the primary focus has been on the resolution of amino acids[67] and nucleotides[68]. In this context, a variety of chromatographic methods have been employed including ion-exchange chromatography,[69] dynamic ion-exchange chromatography,[70] ion-pair chromatography,[71]

and affinity chromatography.[72] Often anion binding plays a role in these separa-
tions[73] and is also an important analytical problem in its own right. In this context,
the use of ion-pair chromatography, to effect separations of anionic species such as
nucleotides[74] and amino acids[75] needs to be mentioned, as should be more recent
approaches based on the use of polymer-, and silica-bound azacrown ethers[76] and
metalloporphyrins.[77]

Our entry into the anion separations field was inspired by the findings, described
above, that the protonated forms of sapphyrin will bind a wide range of anionic
species, including phosphate- and carboxylate-type anions. This led us to consider
whether sapphyrin, as an anion-recognizing group, could be used to generate solid
supports that would allow for the separation of these and other anionic substrates.
To test this possibility, a sapphyrin-substituted silica gel was synthesized (shown
schematically in Figure 15).[78] This derivatized silica gel, when used in the HPLC
chromatographic columns, was found to allow the separation of many phosphory-
lated entities, including simple phosphates, mononucleotides, and oligonucleotides
under standard, isochratic conditions at neutral pH. As expected, the retention times
correlated quantitatively with the total phosphate number. Thus, these sapphyrin-
modified silica gel columns provide a new, nonelectophoretic, HPLC method for
achieving separations of phosphate-containing anionic entities that also comple-
ments the kinds of separations that may be achieved by using more standard
diethylaminoethyl (DEAE)-based approaches.[79]

The sapphyrin-modified silica gels also proved effective for HPLC separation of
various anions other than phosphates, but not neutral or cationic species. For
instance, various monoanionic species such as diphenyl phosphate, benzene sul-
fonic acid, phenyl arsenate, phenyl phosphate, and benzoate could all be separated
from each other. Nucleotide mono-, di-, and triphosphates such as AMP, ADP, and
ATP were also retained on these columns and were found to be readily separable
from one another under isochratic HPLC conditions.[78] Likewise, in what is still
unpublished work, it has been found that these columns can be used to separate
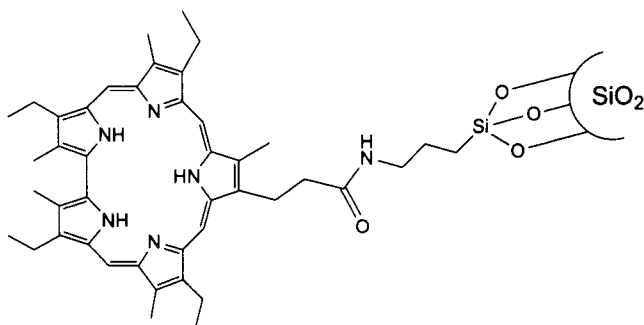


*Figure 15.* Sapphyrin-substituted silica gel.

nitrate-, sulfate-, and halide-type anions. Based on an integrated view of these findings, it is now believed that the key anion binding motif involves a specific interaction between the relevant oxyanion (or halide anion) portion of the substrate and the positively charged sapphyrin core, as observed in solution and in the solid state (*vide supra*).

Unfortunately, the first-generation sapphyrin-modified HPLC columns built using the silica gels of Figure 15 were found to be limited in some respects. For instance, these columns proved ineffectual at separating mixtures of CMP, GMP, AMP, and GDP, even though as mentioned above they would work to separate the relevant monophosphates (XMP) from the corresponding diphosphates (XDP). In order to circumvent this limitation, it was considered prudent to attach a nucleic acid base to the sapphyrin core prior to attaching the latter to the silica gel solid support; such an approach proved successful in the case of the U-tube type transport experiments described in Section 4.1 above.[42]

To test the above hypothesis, a silica gel was prepared that was modified with a cytosine-appended sapphyrin (c.f. Figure 16 for a schematic representation).[80] When incorporated into an HPLC column, this new material allowed for excellent separations of AMP, CMP, GMP, UMP, ADP, UDP, GDP, ATP, UTP, and GTP under neutral isochratic conditions. Thus, it did in fact prove to be far superior as a solid support than the corresponding unmodified sapphyrin system shown in Figure 15. In spite of its superior characteristics, it is important to note that this new material was inefficacious at separating AD(T)P from UD(T)P. However, this result is not entirely unexpected in view of the fact that neither adenosine nor uridine will normally interact with cytosine-derived receptors; it merely leads the authors to suggest that analogous columns, derived from sapphyrins bearing other nucleic acid bases, would need to be used if the separation of these di- or triphosphates is being targeted.
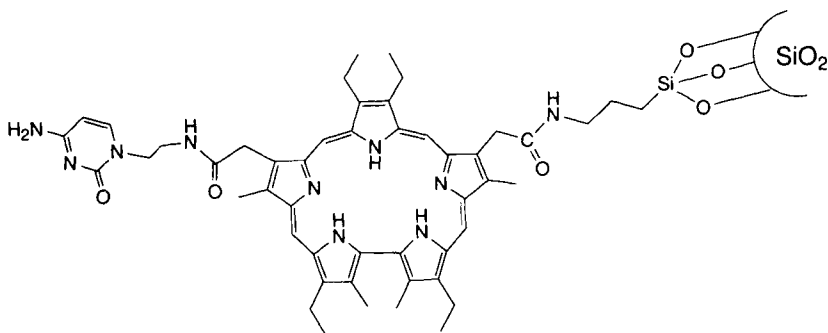


**Figure 16.** Cytosine-sapphyrin conjugate attached to silica gel.

## 8. CONCLUSION

In this review, the authors have tried to show some of the range and power protonated sapphyrins possess when considered as anion binding agents. Not only do they form stable complexes with a wide range of anions in the solid state, they also act to bind and transport some of the most physiologically relevant anionic entities under typical solution-phase and model-membrane transport conditions. These anionic entities are not limited to such all-important small molecules as chloride anion and mononucleotides; they also include, as shown by the HPLC-related work and DNA-targeted studies, higher order entities such as oligonucleotides. This diversity of action and scope of utility makes the protonated sapphyrins quite unique as anion chelating agents. It also serves to raise the intriguing question of whether other expanded porphyrins containing other heteroatom cores or larger macrocyclic geometries might not only show a diversity equal to sapphyrin but a selectivity that is markedly different. This would allow the present approach to anion recognition to move into quite a number of new directions.

## ACKNOWLEDGMENTS

## REFERENCES AND NOTES

1. (a) *The Porphyrins*; Dolphin, D., Ed.; Academic Press: New York, 1978; (b) de Matteis, F.; Aldrige, W. N. *Heme and Hemoproteins*; Springer: Berlin, 1978; (c) Voet, D.; Voet, J. G. *Biochemistry*, 2nd ed.; Wiley: New York, 1995.
2. *Porphyrins and Metalloporphyrins*; Smith, K. M., Ed.; Elsevier: Amsterdam, 1975.
3. (a) Edelman, R.; Warach, S. *New England J. Med.* **1993**, *328*, 708; (b) Lauffer, R. B. *Chem. Rev.* **1987**, *87*, 901; (c) Tweedle, M. F.; Brittain, H. G.; Eckelman, W. C.; Gaughan, G. T.; Hagan, J. J.; Wedeking, P. W.; Runge, V. M. In *Magnetic Resonance Imaging*, 2nd ed., Partain, C. L., Ed.; Philadelphia, 1988, Vol. 1, p. 793; (d) Moonen, C. T.; van Zijil, P. C.; Franck, J. A.; Le-Bihan, D.; Becker, E. D. *Science* **1990**, *250*, 53; (e) Young, C. W. *Magnetic Resonance Imaging: Basic Principles*, Raven Press: New York, 1988; (f) Lauffer, R. B. *Chem. Rev.* **1987**, *87*, 901; (g) Mann, J. S.; Brasch, R. C. In Handbook of Metal-Ligand Interactions in Biological Fluids: Bioinorg. Med., Berthon, G., Ed.; Dekker: New York, 1995, Vol. 2, p. 1358; (h) Morris, P. G. *Nuclear Magnetic Resonance Imaging in Medicine and Biology*, Claredon Press: Oxford, 1986; (i) Øksendal, A. N.; Hals, F.-A. *J. Magn. Res. Imag.* **1993**, *3*, 157; (j) Fossheim, S.; Johansson, C.; Fahlvik, A. K.; Grace, D.; Klaveness, J. *Magn. Res. Med.* **1996**, *35*, 201.
4. (a) Dougherty, T. J. *Photochem. Photobiol.* **1993**, *58*, 895; (b) Kessel, D. *The Spectrum* **1990**, *3*, 13; (c) Gomer, C. J. *Sem. Hematol.* **1989**, *26*, 27; (d) Moan, J.; Berg, K. *Photochem. Photobiol.* **1992**, *55*, 931; (e) Dougherty, T. J. *Photochem. Photobiol.* **1987**, *45*, 879; (f) Kessel, D. *Photochem. Photobiol.* **1984**, *39*, 851; (g) Kreimer-Birnbaum, M. *Sem. Hematol.* **1989**, *26*, 157; (h) Buskard, N. A.; Wilson, B. C. *Sem. Oncol.* **1994**, *21(6)S15*, 1; (i) Manyak, M. J.; Russo, A.; Smith, P. D.;

Glatstein, E. *J. Clin. Oncol.* **1988**, *6*, 380; (j) Brown, S. B.; Truscott, T. G. *Chem. in Brit.* **1993**, 955; (k) Pass, H. I. *J. Natl. Cancer Inst.* **1993**, *85*, 443; (l) Henderson, B. W.; Dougherty, T. J. *Photochem. Photobiol.* **1992**, *55*, 145; (m) Dougherty, T. J. *Adv. Photochem.* **1992**, *17*, 275; (n) Parker, S. L.; Tong, T.; Bolden, S.; Wingo, P. A. *CA Cancer J. Clin.* **1996**, *46*, 5; (o) Ben-Hur, E.; Horowitz, B. *Photochem. Photobiol.* **1995**, *62*, 383; (p) Ben-Hur, E.; Geacintov, N. E.; Studamire, B.; Kenney, M. E.; Horowitz, B. *Photochem. Photobiol.* **1995**, *61*, 190; (q) Hua, Z.; Gibson, S. L.; Foster, T. H.; Hilf, R. *Cancer Res.* **1995**, *55*, 1723; (r) Marcus, S. L.; Sobel, R. S.; Golub, A. L.; Carroll, R. L.; Lundahl, S.; Shulman, D. G. *Proc. SPIE Int. Opt. Eng.* **1996**, *2675*, 32; (s) Razum, N. J.; Snyder, A. B.; Doiron, D. R. *Proc. SPIE Int. Opt. Eng.* **1996**, *2675*, 43; (t) Cincotta, L.; Szeto, D.; Lampros, E.; Hasan, T.; Cincotta, A. H. *Photochem. Photobiol.* **1996**, *63*, 229; (u) Zuk, M. M; Rihter, B. D.; Kenney, M. E.; Rodgers, M. A. *Photochem. Photobiol.* **1996**, *63*, 132; (v) Biolo, R.; Jori, G.; Soncin, M.; Rihter, B.; Kenney, M. E.; Rodgers, M. A. J. *Photochem. Photobiol.* **1996**, *63*, 224; (w) Hahn K. A.; Panjehpour, M.; Lu, X. *Photochem. Photobiol.* **1996**, *63*, 117; (x) Xie, L. Y.; Boyle, R. W.; Dolphin, D. *J. Am. Chem. Soc.* **1996**, *118*, 4853; (y) Boyer, R. W.; Dolphin, D. *Photochem. Photobiol.* **1996**, *64*, 469.

5.  (a) *Frontiers in Supramolecular Organic Chemistry and Photochemistry*; Schneider, H. J.; Dürr, H., Eds.; VCH: Weinheim, 1991; (b) Balzani, V.; Scandola, F. *Supramolecular Photochemistry*, Ellis Horwood: Chichester, 1991; see also Balzani, V.; Scandola, F. in ref. 28j, vol. *10*, 687, and references therein.

6.  See ref. 5, and (a) *Photochemical Energy Conversion*; Norris, Jr., J. R.; Meisel, D., Eds.; Elsevier: Amsterdam, 1989; (b) Gilbert, A.; Baggot, J. *Essentials of Molecular Photochemistry*; Blackwell: London, 1991; (c) *Photochemical Conversion and Storage of Solar Energy*; Connolly, J. S., Ed.; Academic Press: New York, 1981.

7.  For reviews, see: (a) Sessler, J. L.; Burrell, A. K. *Top. Curr. Chem.* **1991**, *161*, 177; (b) Sessler, J. L.; Burrell, A. K.; Furuta, H.; Hemmi, G. W.; Iverson, B. L.; Král, V.; Magda, D. J.; Mody, T. D.; Shreder, K.; Smith, D.; Weghorn, S. J. In *Transition Metals in Supramolecular Chemistry*, NATO ASI Series, Fabbrizzi, L.; Poggi, A., Eds.; Kluwer: Amsterdam, 1994; (c) Sessler, J. L.; Weghorn, S. J. *Expanded, Contracted, and Isomeric Porphyrins*; Elsevier: London, 1997, in press.

8.  (a) Sessler, J. L.; Mody, T. D.; Hemmi, G. W.; Lynch, V.; Young, S. W.; Miller, R. A. *J. Am. Chem. Soc.* **1993**, *115*, 10368; (b) Young, S. W.; Qing, F.; Harriman, A.; Sessler, J. L.; Dow, W. C.; Mody, T. D.; Hemmi, G.; Hao, Y.; Miller, R. A. *Proc. Natl. Acad. Sci. USA* **1996**, *93*, 6610.

9.  (a) Sessler, J. L.; Hemmi, G. W.; Mody, T. D.; Murai, T.; Burrell, A.; Young, S. W. *Acc. Chem. Res.* **1994**, *27*, 43; (b) Young, S. W.; Woodburn, K. W.; Wright, M.; Mody, T. D.; Fan, Q.; Sessler, J. L.; Dow, W. C.; Miller, R. A. *Photochem. Photobiol.* **1996**, *63*, 892.

10. For short reviews by the authors, see: (a) Sessler, J. L.; Cyr, M.; Furuta, H.; Král, V.; Mody, T.; Morishima, T.; Shionoya, M.; Weghorn, S. *Pure Appl. Chem.* **1993**, *65*, 393; (b) Iverson, B. L.; Shreder, K.; Král, V.; Smith, D. A.; Smith, J.; Sessler, J. L. *Pure Appl. Chem.* **1994**, *66*, 845.

11. Furuta, H.; Morishima, T.; Král, V.; Sessler, J. L. *Supramol. Chem.* **1993**, *3*, 5.

12. Sessler, J. L.; Weghorn, S. J.; Morishima, T.; Rosingana, M.; Lynch, V.; Lee, V. *J. Am. Chem. Soc.* **1992**, *114*, 8306.

13. Sessler, J. L.; Mody, T. D.; Ford, D. A.; Lynch, V. *Angew. Chem. Int. Ed. Engl.* **1992**, *31*, 452.

14. Sessler, J. L.; Weghorn, S. J.; Lynch, V.; Johnson, M. R. *Angew. Chem. Int. Ed. Engl.* **1994**, *33*, 1509.

15. (a) First reported by R. B. Woodward at the aromaticity conference, Sheffield, UK, 1966; (b) King, M. M. Ph.D. Dissertation, Harvard University, Cambridge, MA, 1970; (c) Bauer, V. J.; Clive, D. L. J.; Dolphin, D.; Paine III, J. B.; Harris, F. L.; King, M. M.; Loder, J.; Wang, S-W. C.; Woodward, R. B. *J. Am. Chem. Soc.* **1983**, *105*, 6429; (d) For syntheses of various functionalyzed sapphyrins, see refs. 16, 17, 34b, 42, 51, 52, 55, 62, 65, and Sessler, J. L.; Cyr, M. J.; Burrell, A. K. *Tetrahedron* **1992**, *48*, 9661; (e) Sessler, J. L.; Lisowski, J.; Boudreaux, K. A.; Lynch, V.; Barry, J.; Kodadek, T. J. *J. Org. Chem.* **1995**, *60*, 5975; (f) Chmielewski, P. J.; Latos-Grazynski, L.; Rachlewicz, K. *Chem. Eur. J.* **1995**, *1*, 68.

16. (a) Král, V.; Furuta, H.; Shreder, K.; Lynch, V.; Sessler, J. L. *J. Am. Chem. Soc.* **1996**, *118*, 1595; (b) Iverson, B. L.; Shreder, K.; Král, V.; Sansom, P.; Lynch, V.; Sessler, J. L. *J. Am. Chem. Soc.* **1996**, *118*, 1608.

17. (a) Sessler, J. L.; Cyr, M. J.; Lynch, V.; McGhee, E.; Ibers, J. A. *J. Am. Chem. Soc.* **1990**, *112*, 2810; (b) Shionoya, M.; Furuta, H.; Lynch, V.; Harriman, A.; Sessler, J. L. *J. Am. Chem. Soc.* **1992**, *114*, 5714.

18. Sessler, J. L.; Ford, D. A.; Cyr, M. J.; Furuta, H. *J. Chem. Soc., Chem. Commun.* **1991**, 1733.

19. *CRC Handbook of Chemistry and Physics*, 59th ed.; Weast, R. C.; Astle, M. J., Eds.; CRC Press: West Palm Beach, 1979.

20. Sessler, J. L.; Andrievsky, A.; Lynch, V., unpublished results.

21. Sessler, J. L.; Andrievsky, A.; Gale, P. A.; Lynch, V. *Angew. Chem. Int. Ed. Engl.* **1996**, *35*, 2782.

22. (a) *The Biochemistry of Nucleic Acids*, 10th ed.; Adams, R. L. P.; Knowler, J. T.; Leader, D. P., Eds.; Chapman and Hall: New York, 1986; (b) Kirk, K. L. *Biochemistry of the Elemental Halogens and Inorganic Halides*, Plenum Press, New York, 1991; (c) *Chloride Transport Coupling in Biological Membranes and Epithelia*; Gerenscser, G., Ed.; Elsevier: Amsterdam, 1984; (d) Perutz, M. F.; Shih, D. T.; Williamson, D. *J. Mol. Biol.* **1994**, *239*, 555; (e) Bhat, M. K.; Pickersgill, R. W.; Perry, B. N.; Brown, R. A.; Jones, S. T.; Mueller-Harvey, I.; Sumner, I. G.; Goodenough, P. W. *Biochemistry* **1993**, *32*, 12203; (f) Ranganathan, D.; Vaish, N. K.; Shah, K. *J. Am. Chem. Soc.* **1994**, *116*, 6545, and references therein.

23. *Nucleotide Analogs as Antiviral Agents*; Martin, J. C., Ed.; ACS Symposium Series 401, American Chemical Society, Washington, DC, 1989.

24. Connors, K. A. *Binding Constants*, Wiley: New York, 1987.

25. Araki, T.; Tsukube, H. *Liquid Membranes: Chemical Applications*; CRC Press: Boca Raton, FL, 1990.

26. For an introduction to cystic fibrosis, see: (a) Boat, T. F.; Welsh, M. J.; Beaudet A. L. In *The Metabolic Basis of Inherited Disease*, 6th ed.; Scriver, C. R.; Beaudet, A. L.; Sly, W. S.; Valle, D., Eds.; McGraw-Hill: New York, 1989; (b) Davis, P. B. *N. Engl. J. Med.* **1991**, *325*, 575; (c) Quinton, P. M. *FASEB* **1990**, *4*, 2709; (d) Weiss, R. *Science News* **1991**, *139*, 132; for a conference proceedings book describing the discovery of the CFTR gene and its implications, see: (e) *The Identification of The CF (Cystic Fibrosis) Gene, Recent Progress and New Research Strategies*; Tsui, L.-C.; Romeo, G.; Greger, R.; Gorini, S., Eds.; Plenum: New York, 1991.

27. (a) Knowles, M. R.; Clarke, L. L.; Boucher, R. C. *N. Engl. J. Med.* **1991**, *325*, 533; (b) Information concerning Pulmozyme (Genentech) can be found on the web site http://pharminfo.com/pubs/msb/dnase.htm/

28. (a) A first book, entirely dedicated to the problem of molecular recognition of anions, is due to appear soon: *The Supramolecular Chemistry of Anions*; Bianchi, A.; Bowman-James, K.; Garcia-España, Eds.; VCH: 1997, in press; (b) Dietrich, B. *Pure. Appl. Chem.* **1993**, 65, 1457; (c) Kimura, E. *Top. Curr. Chem.* **1985**, *128*, 113; (d) Lehn, J.-M. *Science* **1985**, *227*, 849; (e) Schmidtchen, F. P.; Gleich, A.; Schummer, A. *Pure. Appl. Chem.* **1989**, 61, 1535; (f) Kaufmann, D. E.; Otten, A. *Angew. Chem. Int. Ed. Engl.* **1994**, *33*, 1832; (g) Beer, P. D. *Chem. Commun.* **1996**, 689; (h) Atwood, J. L.; Holman, K. T.; Steed, J. W. *Chem. Commun.* **1996**, 1401; (i) Izatt, R. M.; Pawlak, K.; Bradshaw, J. S.; Bruening, R. L. *Chem. Rev.* **1995**, *95*, 2529; (j) For an excellent collection of reviews on molecular recognition, see: *Comprehensive Supramolecular Chemistry*; Atwood, J. L.; Davies, J. E. D.; Macnicol, D. D.; Vögtle, F., Eds.; Elsevier: Exeter, 1996; see also ref. 36a.

29. (a) Park, C. H.; Simmons, H. E. *J. Am. Chem. Soc.* **1968**, *90*, 2431; (b) Graf, E.; Lehn, J.-M. *J. Am. Chem. Soc.* **1976**, *98*, 6403; (c) Kintzinger, J.-P.; Lehn, J.-M.; Kauffmann, E.; Dye, J. L.; Popov, A. I. *J. Am. Chem. Soc.* **1983**, *105*, 7549; (d) Hosseini, M. W.; Kintzinger, J.-P.; Lehn, J.-M.; Zahidi, A. *Helv. Chim. Acta* **1989**, 72, 1078; (e) Metz, B.; Rosalky, M. J.; Weiss, R. *J. Chem. Soc., Chem. Commun.* **1976**, 533; (f) Dietrich, B.; Lehn, J.-M.; Guilhem, J.; Pascard, C. *Tetrahedron Lett.* **1989**, *30*, 4125; (g) Cullinane, J.; Gelb, R. I.; Margulis, T. N.; Zompa, L. J. *J. Am. Chem. Soc.* **1982**, *104*, 3048; (h) Gelb, R. I.; Lee, B. T.; Zompa, L. J. *J. Am. Chem. Soc.* **1985**, *107*, 909; (i)

Dietrich, B.; Fyles, T. M.; Hosseini, M. W.; Lehn, J.-M.; Kaye, K. C. *J. Chem. Soc., Chem. Commun.* **1988**, 691; (j) Cramer, R. E.; Fermin, V.; Kuwabara, E.; Kirkup, R.; Selman, M.; Aoki, K.; Adeyemo, A.; Yamazaki, H. *J. Am. Chem. Soc.* **1991**, *113*, 7033; (k) Stang, P. J.; Zhdankin, V. V. *J. Am. Chem. Soc.* **1993**, *115*, 9808; (l) Stang, P. J.; Cao, D. H.; Saito, S.; Arif, A. M. *J. Am. Chem. Soc.* **1995**, *117*, 6273; (m) Beer, P. D.; Hesek, D.; Hodacova, J.; Stokes, S. E. *J. Chem. Soc., Chem. Commun.* **1992**, 270; (n) Scheerder, J.; Fochi, M.; Engbersen, J. F. J.; Reinhoudt, D. N. *J. Org. Chem.* **1994**, *59*, 7815; (o) Beauchamp, A. L.; Olievier, M. J.; Wuest, J. D.; Zacharie, B. *J. Am. Chem. Soc.* **1986**, *108*, 73; (p) Blanda, M. T.; Newcomb, M. *Tetrahedron Lett.* **1989**, *27*, 3501; (q) Jurkschat, K.; Kuivila, H. G.; Liu, S.; Zubieta, J. A. *Organometallics* **1989**, *8*, 2755; (r) Jung, M. E.; Xia, H. *Tetrahedron Lett.* **1988**, *29*, 297; (s) Aoyagi, S.; Ogawa, K.; Tanaka, K.; Takeuchi, Y. *J. Chem. Soc. Perkin Trans. 2* **1995**, 355; (t) Jacobson, S.; Pizer, R. *J. Am. Chem. Soc.* **1993**, *115*, 11216; (u) Katz, H. E. *J. Am. Chem. Soc.* **1986**, *108*, 7640; (v) Katz, H. E. *Organometallics* **1987**, *6*, 1134; (w) Yang, X.; Knobler, C. B.; Hawthorne, M. F. *Angew. Chem. Intl. Ed. Engl.* **1991**, *30*, 1507; (x) Zinn, A. A.; Zheng, Z.; Knobler, C. B.; Hawthorne, M. F. *J. Am. Chem. Soc.* **1996**, *118*, 70; (y) Worm, K.; Schmidtchen, F. P.; Schier, A.; Schafer, A.; Hesse, M. *Angew. Chem. Int. Ed. Engl.* **1994**, *33*, 327; (z) Worm, K.; Schmidtchen, F. P. *Angew. Chem. Int. Ed. Engl.* **1995**, *34*, 65; (aa) Scheerder, J.; van Duynhoven, J. P. M.; Engbersen, J. F. J.; Reinhoudt, D. N. *Angew. Chem. Int. Ed. Engl.* **1996**, *35*, 1090; (ab) Davis, A. P.; Gilmer, J. F.; Perry, J. J. *Angew. Chem. Int. Ed. Engl.* **1996**, *35*, 1312; (ac) Beer, P. D.; Szemes, F. *J. Chem. Soc., Chem. Commun.* **1995**, 2245.

30. For examples of expanded porphyrin-derived chloride receptors (other than sapphyrin), see: Sessler, J. L.; Morishima, T.; Lynch, V. *Angew. Chem. Int. Ed. Engl.* **1991**, *30*, 977, and refs. 12–14.

31. (a) Maiya, B. G.; Cyr, M.; Harriman, A.; Sessler, J. L. *J. Phys. Chem.* **1990**, *94*, 3597; (b) Judy, M. M.; Matthews, J. L.; Newman, J. T.; Skiles, H. L.; Boriack, R. L.; Sessler, J. L.; Cyr, M.; Mayia, B. G.; Nichol, S. T. *Photochem. Photobiol.* **1991**, *53*, 101.

32. (a) Tabushi, I.; Kobuke, Y.; Imuta, J. *J. Am. Chem. Soc.* **1981**, *103*, 6152; (b) Li, T.; Krasne, S. J.; Persson, B.; Kaback, H. R.; Diederich, F. *J. Org. Chem.* **1993**, *58*, 380; (c) Li, T.; Diederich, F. *J. Org. Chem.* **1992**, *57*, 3449; (d) Mertes, M. P.; Mertes, K. B. *Acc. Chem. Res.* **1990**, *23*, 413; (e) Hosseini, M. W.; Lehn, J.-M. *J. Chem. Soc., Chem. Commun.* **1991**, 451; (f) Hosseini, M. W.; Lehn, J.-M.; Jones, K. C.; Plute, K. E.; Mertes, K. B.; Mertes, M. P. *J. Am. Chem. Soc.* **1989**, *111*, 6330; (g) Kimura, E.; Kuramoto, Y.; Koike, T.; Fujioka, H.; Kodama, M. *J. Org. Chem.* **1990**, *55*, 42; (h) See ref. 28c, and references therein; (i) Schmidtchen, F. P. *Top. Curr. Chem.* **1986**, *132*, 101 and ref. therein; (j) Marecek, J. F.; Fischer, P. A.; Burrows, C. J. *Tetrahedron Lett.* **1988**, *29*, 6231; (k) Claude, S.; Lehn, J.-M.; Schmidt, F.; Vigneron, J.-P. *J. Chem. Soc., Chem. Commun.* **1991**, 1182; (l) van Arman, S. A.; Czarnik, A. W. *Supramol. Chem.* **1993**, *1*, 99; (m) Vance, D. H.; Czarnik, A. W. *J. Am. Chem. Soc.* **1994**, *116*, 9397; (n) Schneider, H.-J.; Blatter, T.; Palm, B.; Pfingstag, U.; Rüdiger, V.; Theis, I. *J. Am. Chem. Soc.* **1992**, *114*, 7704; (o) Andrés, A.; Burguete, M. I.; García-España, E.; Luis, S. V.; Miravet, J. F.; Soriano, C. *J. Chem. Soc. Perkin Trans. 2* **1993**, 749; (p) Aoyama, Y.; Nonaka, S.; Motomura, T.; Toi, H.; Ogoshi, H. *Chem. Lett.* **1991**, 1241; (q) Kuroda, Y.; Hatakeyama, H.; Seshimo, H.; Ogoshi, H. *Supramol. Chem.* **1994**, *3*, 267; (r) Dietrich, B.; Fyles, D. L.; Fyles, T. M.; Lehn, J.-M. *Helv. Chim. Acta* **1979**, *62*, 2763; (s) Schmidtchen, F. P. *Tetrahedron Lett.* **1989**, *30*, 4493; (t) Schiessel, P.; Schmidtchen, F. P. *J. Org. Chem.* **1994**, *59*, 509; (u) Galán, A.; Pueyo, E.; Salmerón, A.; de Mendoza, J. *Tetrahedron Lett.* **1991**, *32*, 1827; (v) Galán, A.; de Mendoza, J.; Toiron, C.; Bruix, M.; Deslongchamps, G.; Rebek, J., Jr. *J. Am. Chem. Soc.* **1991**, *113*, 9424; (w) Deslongchamps, G.; Galán, A.; de Mendoza, J.; Rebek, J., Jr. *Angew. Chem. Int. Ed. Engl.* **1992**, *31*, 61; (x) Andreu, C.; Galán, A.; Kobiro, K.; de Mendoza, J.; Park, T. K.; Rebek, J., Jr.; Salmerón, A.; Usman, N. *J. Am. Chem. Soc.* **1994**, *116*, 5501; (y) Ariga, K.; Anslyn, E. V. *J. Org. Chem.* **1992**, *57*, 417; (z) Flatt, L. S.; Lynch, V.; Anslyn, E. V. *Tetrahedron Lett.* **1992**, *33*, 2785; (aa) Kneeland, D. M.; Ariga, K.; Lynch, V. M.; Huang, C.-Y.; Anslyn, E. V. *J. Am. Chem. Soc.* **1993**, *115*, 10042; (ab) Chu, F.; Flatt, L. S.; Anslyn, E. V. *J. Am. Chem. Soc.* **1994**, *116*, 4194; (ac) Dixon, R. P.; Geib, S. J.; Hamilton, A. D. *J. Am. Chem. Soc.* **1992**, *114*, 365; (ad) Hirst, S. C.; Tecilla, P.; Geib, S. J.; Fan, E.; Hamilton, A. D. *Israel J. Chem.* **1992**, *32*, 105;

(ae) Jubian, V.; Veronese, A.; Dixon, R. P.; Hamilton, A. D. *Angew. Chem. Int. Ed. Engl.* **1995**, *34*, 1237; (af) Geib, S. J.; Hirst, S. C.; Vicent, C.; Hamilton, A. D. *J. Chem. Soc., Chem. Commun.* **1991** 1283; (ag) Sasaki, D. Y.; Kurihara, K.; Kunitake, T. *J. Am. Chem. Soc.* **1991**, *113*, 9685; (ah) Rudkevich, D. M.; Stauthamer, W. P. R. V.; Verboom, W.; Engbersen, J. F. J.; Harkema, S.; Reinhoudt, D. N. *J. Am. Chem. Soc.* **1992**, *114*, 9671; (ai) Visser, H. C.; Rudkevich, D. M.; Verboom, W.; de Jong, F.; Reinhoudt, D. N. *J. Am. Chem. Soc.* **1994**, *116*, 11554; (aj) Rudkevich, D.M.; Verboom, W.; Brzozka, Z.; Palys, M. J.; Stauthamer, W. P. R. V.; van Hummel, G. J.; Franken, S. M.; Harkema, S.; Engbersen, J. F. J.; Reinhoudt, D. N. *J. Am. Chem. Soc.* **1994**, *116*, 4341; (ak) Rudkevich, D. M; Verboom, W.; Reinhoudt, D. N. *J. Org. Chem.* **1994**, *59*, 3683; (al) Rudkevich, D. M.; Brzozka, Z.; Palys, M.; Visser, H. C.; Verboom, W.; Reinhoudt, D. N. *Angew. Chem. Int. Ed. Engl.* **1994**, *33*, 467; (am) Valiyaveettil, S.; Engbersen, J. F. J.; Verboom, W.; Reinhoudt, D. N. *Angew. Chem. Int. Ed. Engl.* **1993**, *32*, 900; (an) Beer, P. D.; Gale, P. A.; Hesek, D. *Tetrahedron Lett.* **1995**, *36*, 767; (ao) Eliseev, A. V.; Schneider, H.-J. *Angew. Chem. Int. Ed. Engl.* **1993**, *32*, 1331; (ap) Beer, P. D.; Chen, Z.; Goulden, A. J.; Graydon, A.; Stokes, S. E.; Wear, T. *J. Chem. Soc., Chem. Commun.* **1993**, 1834; (aq) Manabe, K.; Okamura, K.; Date, T.; Koga, K. *J. Am. Chem. Soc.* **1992**, *114*, 6940; (ar) Menger, F. M.; Catlin, K. K. *Angew. Chem. Int. Ed. Engl.* **1995**, *34*, 2147; (as) Aguilar, J. A.; Garcia-España, E.; Guerrero, J. A.; Luis, S. V.; Llinares, J. M.; Miravet, J. F.; Ramirez, J. A.; Soriano, C. *J. Chem. Soc., Chem. Commun.* **1995**, 2237; (at) Cudic, P.; Zinic, M.; Tomisic, V.; Simeon, V.; Vigneron, J.-P.; Lehn, J.-M. *J. Chem. Soc., Chem. Commun.* **1995**, 1073; (au) Nishizawa, S.; Bühlmann, P.; Iwao, M.; Umezawa, Y. *Tetrahedron Lett.* **1995**, *36*, 6483.

33. (a) Hosseini, M. W.; Lehn, J.-M. *Helv. Chim. Acta* **1988**, *71*, 749; (b) Heyer, D.; Lehn, J.-M. *Tetrahedron Lett.* **1986**, *27*, 5869; (c) Dietrich, B.; Hosseini, M. W.; Lehn, J.-M. *J. Am. Chem. Soc.* **1981**, *103*, 1282; (d) Dietrich, B.; Hosseini, M. W.; Lehn, J.-M. *Helv. Chim. Acta* **1983**, *66*, 1262; (e) Hosseini, M. W.; Lehn, J.-M. *Helv. Chim. Acta* **1986**, *69*, 587; (f) Dietrich, B.; Guilhem, J.; Lehn, J.-M.; Pascard, C.; Sonveaux, E. *Helv. Chim. Acta* **1984**, *67*, 91; (g) Jazwinski, J.; Lehn, J.-M.; Lilienbaum, D.; Ziessel, R.; Guilhem, J.; Pascard, C. *J. Chem. Soc., Chem. Commun.* **1987**, 1691; (h) Lehn, J.-M.; Méric, R.; Vigneron, J.-P.; Bkouche-Waksman, I.; Pascard, C. *J. Chem. Soc., Chem. Commun.* **1991**, 62; (i) Hosseini, M. W.; Lehn, J.-M. *J. Am. Chem. Soc.* **1982**, *104*, 3525; (j) Kimura, E.; Sakonaka, A.; Yatsunami, T.; Kodama, M. *J. Am. Chem. Soc.* **1981**, *103*, 3041; (k) Kimura, E. *Pure Appl. Chem.* **1989**, *61*, 823, and references therein; (l) Kataoka, M.; Naganawa, R.; Odashima, K.; Umezawa, Y.; Kimura, E.; Koike, T. *Anal. Lett.* **1989**, *22*, 1089; (m) Bencini, A.; Bianchi, A.; Burguete, M. I.; Dapporto, P.; Domenech, A.; Garcia-España, E.; Luis, S. V.; Paoli, P.; Ramirez, J. A. *J. Chem. Soc., Perkin Trans. 2* **1994**, 569. For a review of guanidinium-based anion receptors, see: (n) Hannon, C. L.; Anslyn, E. V. In *Bioorganic Chemistry Frontiers*; Springer-Verlag: Berlin, 1993. See also: (o) Müller, G.; Riede, J.; Schmidtchen, F. P. *Angew. Chem. Int. Ed. Engl.* **1988**, *27*, 1516; (p) Echavarren, A.; Galan, A.; de Mendoza, J.; Salmeron, A.; Lehn, J.-M. *Helv. Chim. Acta* **1988**, *71*, 685; (q) Kurzmeier, H.; Schmidtchen, F. P. *J. Org. Chem.* **1990**, *55*, 3749; (r) Gleich, A.; Schmidtchen, F. P. *Chem. Ber.* **1990**, *123*, 907; (r) Echavarren, A.; Galan, A.; Lehn, J.-M.; de Mendoza, J. *J. Am. Chem. Soc.* **1989**, *111*, 4994; (s) Gleich, A.; Schmidtchen, F. P.; Mikulcik, P.; Müller, G. *J. Chem. Soc., Chem. Commun.* **1990**, 55; (t) Schiessel, P.; Schmidtchen, F. P. *Tetrahedron Lett.* **1993**, *34*, 2449. For synthesis of more rigid dibenzoguanidine receptor for oxyanion recognition, see: (u) Chicharro, J.-L.; Prados, P.; de Mendoza, J. *J. Chem. Soc., Chem. Commun.* **1994**, 1193. For other receptors, see: (v) Beer, P. D.; Drew, M. G. B.; Hazlewood, C.; Hesek, D.; Hodacova, J.; Stokes, S. E. *J. Chem. Soc., Chem. Commun.* **1993**, 229; (w) Lacy, S. M.; Rudkevich, D. M.; Verboom, W.; Reinhoudt, D. N. *J. Chem. Soc. Perkin Trans. 2* **1995**, 135; (x) Konishi, K.; Yahara, K.; Toshishige, H.; Aida, T.; Inoue, S. *J. Am. Chem. Soc.* **1994**, *116*, 1337; (y) Inokuma, S.; Sakai, S.; Yamamoto, T.; Nishimura, J. *J. Membrane Sci.* **1994**, *97*, 175; (z) Geib, S. J.; Vicent, C.; Fan, E.; Hamilton, A. D. *Angew. Chem. Int. Ed. Engl.* **1993**, *32*, 119; (aa) Fan, E.; van Arman, S. A.; Kincaid, S.; Hamilton, A. D. *J. Am. Chem. Soc.* **1993**, *115*, 369; (ab) Garcia-Tellado, F.; Goswami, S.; Chang, S.-K.; Geib, S. J.; Hamilton, A. D. *J. Am. Chem. Soc.* **1990**, *112*, 7393; (ac) Hamilton, A. D.; Fan, E.; Van Arman,

S. A.; Vicent, C.; Garcia-Tellado, F.; Geib, S. J. *Supramol. Chem.* **1993**, *1*, 247; (ad) Ballester, P.; Costa, A.; Deyà, P. M.; Gonzáles, J. F.; Rotger, M. C. *Tetrahedron Lett.* **1994**, *35*, 3813; (ae) Crego, M.; Raposo, C.; Caballero, M. C.; Garcia, E.; Saez, J. G.; Morán, J. R. *Tetrahedron Lett.* **1992**, *33*, 7437; (af) Raposo, C.; Crego, M.; Mussons, M. L.; Caballero, M. C.; Morán, J. R. *Tetrahedron Lett.* **1994**, *35*, 3409; (ag) Tanaka, Y.; Kato, Y.; Aoyama, Y. *J. Am. Chem. Soc.* **1990**, *112*, 2807; (ah) Albert, J. S.; Hamilton, A. D. *Tetrahedron Lett.* **1993**, *34*, 7363. For receptor systems that possess chirality, see: (ai) Garcia-Tellado, F.; Albert, J.; Hamilton, A. D.; *J. Chem. Soc., Chem. Commun.* **1991**, 1761; (aj) Alcazar, V.; Tomlinson, L.; Houk, K. N.; Diederich, F. *Tetrahedron Lett.* **1991**, *32*, 5309; (ak) Alcazar, V.; Diederich, F. *Angew. Chem. Int. Ed. Engl.* **1992**, *31*, 1521; (al) Alcazar, V.; Morán, J. R.; Diederich, F. *Isr. J. Chem.* **1992**, *32*, 69; (am) Owens, L.; Thilgen, C.; Diederich, F.; Knobler, C. B. *Helv. Chim. Acta* **1993**, *76*, 2757; (an) Goodman, M. S.; Weiss, J.; Hamilton, A. D. *Tetrahedron Lett.* **1994**, *35*, 8943; (ao) Goodman, M. S.; Jubian, V.; Hamilton, A. D. *Tetrahedron Lett.* **1995**, *36*, 2551; (ap) Goodman, M. S.; Hamilton, A. D.; Weiss, J. *J. Am. Chem. Soc.* **1995**, *117*, 8447; (aq) De Santis, G.; Fabbrizzi, L.; Licchelli, M.; Poggi, A.; Taglietti, A. *Angew. Chem. Int. Ed. Engl.* **1996**, *35*, 202; (ar) Prévot-Halter, I.; Smith, T. J.; Weiss, J. *Tetrahedron Lett.* **1996**, *37*, 1201. For other receptors, see: (as) Tsukube, H.; Shiba, H.; Uenishi, J. *J. Chem. Soc., Dalton Trans.* **1995**, 181; (at) Jeong, K.-S.; Park, J. W.; Cho, Y. L. *Tetrahedron Lett.* **1996**, *37*, 2795; (au) Kimura, E.; Ikeda, T.; Shionoya, M.; Shiro, M. *Angew. Chem. Int. Ed. Engl.* **1995**, *34*, 663. For a recent review, see ref. 46a.

34. (a) Král, V.; Springs, S. L.; Sessler, J. L. *J. Am. Chem. Soc.* **1995**, *117*, 8881. For an early work involving covalently linked sapphyrin-porphyrin dimer, see: (b) Sessler, J. L.; Brucker, E.; Král, V.; Harriman, A. *Supramol. Chem.* **1994**, *4*, 35.

35. For examples of self-assembly in biological systems, see: (a) Branden, C.; Tooze, J. *Introduction to Protein Structure*; Garland: New York, 1991; (b) Fersht, A. *Enzyme Structure and Mechanism*, 2nd ed.: Freeman: New York, 1985. See also ref. 1c.

36. For reviews, see: (a) Lehn, J.-M. *Supramolecular Chemistry*; VCH: Weinheim, 1995; (b) Lawrence, D. S.; Jiang, T.; Levett, M. *Chem. Rev.* **1995**, *95*, 2229; (c) Vögtle, F.; *Supramolecular Chemistry*; Wiley: Chichester, 1991; (d) Whitesides, G. M.; Simanek, E. E.; Mathias, J. P.; Seto, C. T.; Chin, D. N.; Mammen, M.; Gordon, D. M. *Acc. Chem. Res.* **1995**, *28*, 37; (e) Lindsey, J. S. *New J. Chem.* **1991**, *15*, 153; (f) Rebek, J., Jr. *Angew. Chem. Int. Ed. Engl.* **1990**, *29*, 245; (g) Hunter, C. A. *Angew. Chem. Int. Ed. Engl.* **1995**, *34*, 1079; (h) Philp, D.; Stoddart, J. F. *Angew. Chem. Int. Ed. Engl.* **1996**, *35*, 1154. See also ref. 28j (vols. *4, 6, 7, 9*).

37. (a) Amabilino, D. A.; Stoddart, J. F. *Chem. Rev.* **1995**, *95*, 2725; (b) Chambron, J.-C.; Dietrich-Buchecker, C. O.; Sauvage, J.-P. *Top. Curr. Chem.* **1993**, *165*, 131; (c) Vögtle, F.; Dunnwald, T.; Schmidt, T. *Acc. Chem. Res.* **1996**, *29*, 451; (d) Meissner, R. S.; Rebek J., Jr.; de Mendoza, J. *Science* **1995**, *270*, 1485; (e) Branda, N.; Grotzfeld, R. M.; Valdés, C.; Rebek, J., Jr. *J. Am. Chem. Soc.* **1995**, *117*, 85, and references therein; (f) Shimizu, K. D.; Rebek, J., Jr. *Proc. Natl. Acad. Sci. USA* **1995**, *92*, 12403; (g) Cram, D. J.; Cram, J. M. *Container Molecules and their Guests*; Graham: Cambridge, 1994; (h) Hunter, C. A.; Sarson, L. D. *Angew. Chem. Int. Ed. Engl.* **1994**, *33*, 2313; (i) Goodman, M. S.; Hamilton, A. D.; Weiss, J. *J. Am. Chem. Soc.* **1995**, *117*, 8447; (j) Wintner, E. A.; Tsao, B.; Rebek, J., Jr. *J. Org. Chem.* **1995**, *60*, 7997, and references therein; (k) Sievers, D.; von Kiedrowski, G. *Nature* **1994**, *369*, 221, and references therein; (l) Zimmerman, S. C.; Zeng, F.; Reichert, D. E. C.; Kolotuchin, S. V. *Science* **1996**, *271*, 1095–1098; (m) Hartgerink, J. D.; Granja, J. R.; Milligan, R. A.; Ghadiri, M. R. *J. Am. Chem. Soc.* **1996**, *118*, 43; (n) Ghadiri, M. R.; Granja, J. R.; Buehler, L. K. *Nature* **1994**, *369*, 301; (o) Bisson, A. P.; Carver, F. J.; Hunter, C. A.; Waltho, J. P. *J. Am. Chem. Soc.* **1994**, *116*, 10292; (p) Ulman, A. *An Introduction to Ultrathin Organic Films: From Langmuir-Blodgett to Self-Assembly*; Academic Press: San Diego, 1991; (q) Lahiri, J.; Fate, G. D.; Ungashe, S. B.; Groves, J. T. *J. Am. Chem. Soc.* **1996**, *118*, 2347; (r) MacDonald, J. C.; Whitesides, G. M. *Chem. Rev.* **1994**, *94*, 2383; (s) Aakeröy, C. B.; Seddon, K. R. *Chem. Soc. Rev.* **1993**, *22*, 397; (t) Molecular Engineering and Structure Design, *Isr. J. Chem.* **1985**, *25*, special issue.

38. For examples of self-assembly involving anion chelation, see: (a) Sánchez-Quesada, J.; Seel, C.; Prados, P.; de Mendoza, J.; Dalcol, I.; Giralt, E. *J. Am. Chem. Soc.* **1996**, *118*, 277; (b) Ohata, N.; Masuda, H.; Yamauchi, O. *Angew. Chem. Int. Ed. Engl.* **1996**, *35*, 531; (c) Geib, S. J.; Hirst, S. C.; Vicent, C.; Hamilton, A. D. *J. Chem. Soc., Chem. Commun.* **1991**, 1283. (d) Hosseini, M. W.; Ruppert, R.; Schaeffer, P.; De Cian, A.; Kyritsakas, N.; Fischer, J. *J. Chem. Soc., Chem. Commun.* **1994**, 2135.

39. For a review see: Webb, T. H.; Wilcox, C. S. *Chem. Soc. Rev.* **1993**, 383.

40. Farrow, S. N.; Jones, A. S.; Kumar, A.; Walker, R. T.; Balzarini, J.; de Clerq, E. *J. Med. Chem.* **1990**, *33*, 1400.

41. *Approaches to Antiviral Agents*; Harden, M. R., Ed.; VCH Publishers: Deerfield Beach, Florida, 1985.

42. (a) Král, V.; Sessler, J. L.; Furuta, H. *J. Am. Chem. Soc.* **1992**, *114*, 8704; (b) Sessler, J. L.; Furuta, H.; Král, V. *Supramol. Chem.* **1993**, *1*, 209; (c) Král, V.; Sessler, J. L. *Tetrahedron*, **1995**, *51*, 539.

43. (a) For the early nucleotide monophosphate transport results using simple sapphyrin as a carrier, see: Furuta, H.; Cyr, M. J.; Sessler, J. L. *J. Am. Chem. Soc.* **1991**, *113*, 6677; (b) Phillips, R.; Eisenberg, P.; George, P.; Rutman, R. J. *J. Biol. Chem.* **1965**, *240*, 4393.

44. For general biochemical implications of amino acid transport, see ref. 1c. For problems relevant to amino acid analytical chemistry, see: *Amino Acid Analysis*; Rattenbury, J. M., Ed.; Ellis Horwood, Chichester, 1981.

45. For reviews of biological amino acid transport systems, see: (a) *Mammalian Amino Acid Transport. Mechanisms and Control*; Kilberg, M. S.; Häussinger, D., Eds.; Plenum Press: New York, 1992; (b) Kilberg, M. S.; Stevens, B. R.; Novak, D. A. *Annu. Rev. Nutr.* **1993**, *13*, 137; (c) Ring, K. *Angew. Chem. Int. Ed. Engl.* **1970**, *9*, 345.

46. For a recent review see: (a) Seel, C.; Galán, A.; de Mendoza, J. *Top. Curr. Chem.* **1995**, *175*, 101, and references therein. For zwitterionic α-amino acid recognition, see: (b) Rebek, J., Jr.; Askew, B.; Nemeth, D.; Parris, K. *J. Am. Chem. Soc.* **1987**, *109*, 2432; (c) Galán, A.; Andreu, D.; Echavarren, A. M.; Prados, P.; de Mendoza, J. *J. Am. Chem. Soc.* **1992**, *114*, 1511; (d) Tabushi, I.; Kuroda, Y.; Mizutani, T. *J. Am. Chem. Soc.* **1986**, *108*, 4514; (e) Aoyama, Y.; Asakawa, M.; Yamagishi, A.; Toi, H.; Ogoshi, H. *J. Am. Chem. Soc.* **1990**, *112*, 3145; (f) Sunamoto, J.; Iwamoto, K.; Mohri, Y.; Kominato, T. *J. Am. Chem. Soc.* **1982**, *104*, 5502; (g) Marx-Tibbon, S.; Willner, I. *J. Chem. Soc., Chem. Commun.* **1994**, 1261; (h) Bonomo, R. P.; Cucinotta, V.; D'Allessandro, F.; Impellizzeri, G.; Maccarrone, G.; Rizzarelli, E.; Vecchio, G. *J. Incl. Phenomena* **1993**, *15*, 167; (i) Corradini, R.; Dossena, A.; Impellizzeri, G.; Maccarrone, G.; Marchelli, R.; Rizzarelli, E.; Sartor, G.; Vecchio, G. *J. Am. Chem. Soc.* **1994**, *116*, 10267; (j) Scrimin, P.; Tecilla, P.; Tonellato, U. *Tetrahedron* **1995**, *51*, 217; (k) Mohler, L. K.; Czarnik, A. W. *J. Am. Chem. Soc.* **1993**, *115*, 7037; (l) Reetz, M. T.; Huff, J.; Rudolph, J.; Töllner, K.; Deege, A.; Goddard, R. *J. Am. Chem. Soc.* **1994**, *116*, 11588; (m) Chen, H. C.; Ogo, S.; Fish, R. H. *J. Am. Chem. Soc.* **1996**, *118*, 4993; (n) Tsukube, H.; Uenishi, J.; Kanatani, T.; Itoh, H.; Yonemitsu, O. *Chem. Commun.* **1996**, 477; (o) Higashi, N.; Saitou, M.; Mihara, T.; Niwa, M. *J. Chem. Soc., Chem. Commun.* **1995**, 2119.

47. Multiple-point interactions involving amino acid side chains are thought to provide the basis for the recognition events described in refs. 46b, c, d, h, i, j, o.

48. Dobler, M. *Ionophores and Their Structures*; Wiley: New York, 1981.

49. For examples of metal cations complexation by lasalocid, see ref. 48 and (a) Lyazghi, R.; Pointud, Y.; Dauphin, G.; Juillard, J. *J. Chem. Soc., Perkin Trans. 2* **1993**, 1681, and references therein; (b) Tsukube, H.; Takagi, K.; Higashiyama, T.; Iwachido, T.; Hayama, N. *Inorg. Chem.* **1994**, *33*, 2984, and references therein. For examples of adducts of lasalocid with metal complexes, see: (c) Chia, P. S. K.; Lindoy, L. F.; Walker, G. W.; Everett, G. W. *Pure Appl. Chem.* **1993**, *65*, 521, and references therein; (d) Ballardini, R.; Gandolfi, M. T.; Moya, M. L.; Prodi, L.; Balzani, V. *Isr. J. Chem.* **1992**, *32*, 47.

50. For examples of amine cation complexation effected by lasalocid and its derivatives, see: (a) Westley, J. W.; Evans, R. H., Jr.; Blount, J. F. *J. Am. Chem. Soc.* **1977**, *99*, 6057; (b) Tsukube, H.;

Sohmiya, H. *J. Org. Chem.* **1991**, *56*, 875; (c) Tsukube, H.; Sohmiya, H. *Supramol. Chem.* **1993**, *1*, 297, and references therein; (d) Gueco, R. C. R.; Everett, G. W. *Tetrahedron* **1985**, *41*, 4437; (e) Kinsel, J. F.; Melnik, E. I.; Lindenbaum, S.; Sternson, L. A.; Ovchinnikov, Yu. A. *Biochim. Biophys. Acta* **1982**, *684*, 233; (f) Kinsel, J. F.; Melnik, E. I.; Sternson, L. A.; Lindenbaum, S.; Ovchinnikov, Yu. A. *Biochim. Biophys. Acta* **1982**, *692*, 377; (g) Shen, C.; Patel, D. J. *Proc. Natl. Acad. Sci. USA* **1977**, *74*, 4734.

51. Sessler, J. L.; Andrievsky, A. *Chem. Commun.* **1996**, 1119.

52. Král, V.; Andrievsky, A.; Sessler, J. L. *J. Am. Chem. Soc.* **1995**, *117*, 2953.

53. For leading references, see: 32r, and 33i, l, t, v, y, z, aa, af, am, an, ao, ap, ar, at, au.

54. For leading references, see: 32a, b, h, m, n, s, ag, ao, and 28.

55. Král, V.; Andrievsky, A.; Sessler, J. L. *J. Chem. Soc., Chem. Commun.* **1995**, 2349.

56. Kuroda, Y.; Hatakeyama, H.; Seshimo, J.; Ogoshi, H. *Supramol. Chem.* **1994**, *3*, 267. See also refs. 32n, ao.

57. See, for example: Luecke, H.; Quiocho, F. A. *Nature* **1990**, *347*, 402.

58. (a) Long, E. C.; Barton, J. K. *Acc. Chem. Res.* **1990**, *23*, 271, and references therein; (b) Bailly, C.; Henichart. J.-P. *Bioconjugate Chem.* **1991**, *2*, 379, and references therein; (c) Schneider, H.-J.; Blatter, T. *Angew. Chem. Int. Ed. Engl.* **1992**, *31*, 1207; (d) For a review of porphyrin-DNA interactions, see: Fiel, R. J. *J. Biomol. Struct. Dyn.* **1989**, *6*, 1259.

59. Iverson, B. L.; Shreder, K.; Král, V.; Sessler, J. L. *J. Am. Chem. Soc.* **1993**, *115*, 11022.

60. (a) Praseuth, D.; Gaudemer, A.; Verlhac, J.-B.; Kraljic, I.; Sissoëff, I.; Guillé, E. *Photochem. Photobiol.* **1986**, *44*, 717; (b) Croke, D. T.; Perrouault, L.; Sari, M. A.; Battioni, J.-P.; Mansuy, D.; Hélène, C.; Le Doan, T. *J. Photochem. Photobiol. B: Biol.* **1993**, *18*, 41; (c) Fisher, L. M.; Kuroda, R.; Sakai, T. T. *Biochemistry* **1985**, *24*, 3199; (d) Wan, S.; Parrish, J. A.; Anderson, R. R.; Madden, M. *Photochem. Photobiol.* **1981**, *34*, 679.

61. Magda, D.; Wright, M.; Miller, R. A.; Sessler, J. L.; Sansom, P. I. *J. Am. Chem. Soc.* **1995**, *117*, 3629.

62. Sessler, J. L.; Sansom, P. I.; Král, V.; O'Connor, D.; Iverson, B. L. *J. Am. Chem Soc.* **1996**, *118*, 12323.

63. (a) De Mesmaeker, A.; Häner, R.; Martin, P.; Moser, H. E. *Acc. Chem. Res.* **1995**, *28*, 366; (b) *Antisense Research and Applications*; Crooke, S. T.; Lebleu, B., Eds.; CRC Press, Boca Raton, Florida, 1993; (c) Uhlmann, E.; Peyman, A. *Chem. Rev.* **1990**, *90*, 543; (d) Hélène, C.; Toulmé, J.-J. *Biochim. Biophys. Acta* **1990**, *1049*, 99; (e) *Prospects for Antisense Nucleic Acid Therapy of Cancer and AIDS*; Wickstrom, E., Ed.; Wiley-Liss: New York, 1991.

64. (a) Mastruzzo, L.; Woisard, A.; Ma, D. D. F.; Rizzarelli, E.; Favre, A.; Le Doan, T. *Photochem. Photobiol.* **1994**, *60*, 316; (b) Fedorova, O. S.; Savitskii, A. P.; Shoikhet, K. G.; Ponomarev, G. V. *FEBS Lett.* **1990**, *259*, 335; (c) Vlassov, V. V.; Deeva, E. A.; Ivanova, E. M.; Knorre, D. G.; Maltseva, T. V.; Frolova, E. I. *Nucleosides & Nucleotides* **1991**, *10*, 641; (d) Le Doan, T.; Praseuth, D.; Perrouault, L.; Chassignol, M.; Thuong, N. T.; Hélène, C. *Bioconjugate Chem.* **1990**, *1*, 108; (e) Le Doan, T. ; Perrouault, L.; Praseuth, D.; Habhoub, N.; Decout, J.-L.; Thuong, N. T.; Lhomme, J.; Hélène, C. *Nucleic Acids Res.* **1987**, *15*, 7749; (f) Levina, A. S.; Berezovskii, M. V.; Venjaminova, A. G.; Dobrikov, M. I.; Repkova, M. N.; Zarytova, V. F. *Biochimie* **1993**, *75*, 25; (g) Praseuth, D.; Perrouault, L.; Le Doan, T.; Chassignol, M.; Thuong, N.; Hélène, C. *Proc. Natl. Acad. Sci. USA* **1988**, *85*, 1349; (h) Perrouault, L.; Asseline, U.; Rivalle, C.; Thuong, N. T.; Bisagni, E.; Giovannangeli, C.; Le Doan, T.; Hélène, C. *Nature* **1990**, *344*, 358; (i) Bhan, P.; Miller, P. S. *Bioconjugate Chem.* **1990**, *1*, 82; (j) Teare, J.; Wollenzien, P. *Nucleic Acids Res.* **1989**, *17*, 3359; (k) Pieles, U.; Englisch, U. *Nucleic Acids Res.* **1989**, *17*, 285; (l) Takasugi, M.; Guendouz, A.; Chassignol, M.; Decout, J. L.; Lhomme, J.; Thuong, N. T.; Hélène, C. *Proc. Natl. Acad. Sci. USA* **1991**, *88*, 5602; (m) Praseuth, D.; Le Doan, T.; Chassignol, M.; Decout, J.-L.; Habhoub, N.; Lhomme, J.; Thuong, N. T.; Hélène, C. *Biochemistry* **1988**, *27*, 3031; (n) Boutorine, A. S.; Tokuyama, H.; Takasugi, M.; Isobe, H.; Nakamura, E.; Hélène, C. *Angew. Chem. Int. Ed. Engl.* **1994**, *33*, 2462.

65. Iverson, B. L.; Shreder, K.; Morishima, T.; Rosingana, M.; Sessler, J. L. *J. Org. Chem.* **1995,** *60,* 6616.

66. (a) Dervan, P. B. *Science* **1986,** *283,* 464; (b) Moser, H. E.; Dervan, P. B. *Science* **1987,** *238,* 645; (c) Sluka, J. P.; Horvath, S. J.; Bruist, M. F.; Simon, M. I.; Dervan, P. B. *Science* **1987,** *238,* 1129.

67. Wilce, M. C. J.; Aguilar, M. I.; Heran, M. T. W. *J. Chromatography* **1993,** *632,* 11, and references therein.

68. (a) Pearson, J. D.; Regnier, F. E. *J. Chromatography* **1983,** *255,* 137; (b) Ramos, D. R.; Schoffstall, A. M. *J. Chromatography* **1983,** *261,* 83; (c) Bergot, B. J.; Egan, W. *J. Chromatography* **1992,** *599,* 35; (d) Polverelli, M.; Berger, M.; Odin, F.; Cadet, J. *J. Chromatography* **1993,** *613,* 257.

69. *Advances in Chromatography;* Giddings, J. C.; Keller, R. A., Eds.; Marcel Decker: New York, 1965.

70. Sorel, R. H. A.; Hulshoff, A. *Advances in Chromatography;* Marcel Decker: New York, 1983, Vol. 21.

71. Hearn, M. T. W. *Advances in Chromatography;* Marcel Decker: New York, 1980, Vol. 18.

72. Fassina, G.; Chaiken, I. M. *Advances in Chromatography;* Marcel Decker: New York, 1987, Vol. 27.

73. Snyder, L. R.; Glajch, J. L.; Kirkland, J. J. *Practical HPLC Method Development;* Wiley: New York, 1988.

74. Deleenheer, A. P.; Cosyns-Duyck, M. C.; Van Vaerenberg, P. M. *J. Pharm. Sci.* **1977,** *66,* 1190.

75. Hearn, M. T. W.; Hancock, W. S. *Trends in Biochemica* **1978,** *4,* 58.

76. (a) Ziníc, M.; Frkanec, L.; Skaríc, V.; Trafton, J.; Gokel, G. *J. Chem. Soc., Chem. Commun.* **1990,** 1726; (b) Takagi, M.; Nakamura, H. *J. Coord. Chem.* **1986,** *15,* 53; (c) Izatt, R. M.; Bruening, R. L.; Tarbet, B. J.; Griffin, D. L.; Bruening, M. L.; Krakowiak, K. E.; Bradshaw, J. S. *Pure Appl. Chem.* **1990,** *62,* 1115; (d) Konisi, M; Okuno, K.; Hashimoto, H. *Chromatographia* **1994,** *38,* 381.

77. (a) Kibbey, C. E.; Meyerhoff, M. E. *Anal. Chem.* **1993,** *65,* 2189; (b) Kliza, D. M.; Meyerhoff, M. E. *Electroanalysis* **1992,** *4,* 841; (c) Kokufuta, E.; Watanabe, H.; Saito, K.; Nakamura, I. *Appl. Polym. Sci.* **1981,** *26,* 2601; (d) Xiao, J.; Savina, R.; Martin, G. B.; Francis, A. H.; Meyerhoff, M. E. *J. Am. Chem. Soc.* **1994,** *116,* 9341.

78. Iverson, B. L.; Thomas, R. E.; Král, V.; Sessler, J. L. *J. Am. Chem. Soc.* **1994,** *116,* 2663.

79. Pearson, J. D.; Regnier, F. E. *J. Chromatography* **1983,** *255,* 137.

80. Sessler, J. L.; Genge, J. W.; Král, V.; Iverson, B. L. *Supramol.Chem.* **1996,** *8,* 45.

# AVIDIN–BIOTIN SUPRAMOLECULAR COMPLEXATION FOR BIOSENSOR APPLICATIONS

Jun-ichi Anzai and Tetsuo Osa

# 1.  INTRODUCTION

The functions of living organisms rely not only on single molecular performance but on those of the molecular assemblies or supramolecular systems. Typical examples can be found in the structure and functions of cell–membrane, in which proteins and other active molecules are embedded in a self-organized lipid bilayer to form a supramolecular system. The interactions of enzyme–substrate, antibody–antigen, and receptor–hormone or drug are representative constituents of the biological supramolecular systems. The structure and function of the biological systems have long been mimicked by organic chemists for constructing synthetic counterparts of the supramolecular systems, including host–guest compounds, molecular monolayer and ordered multilayers, self-assembled aggregates, etc.[1–4] On the other hand, little has been reported on the development of artificial supramolecular systems using protein as a building block. It is reasonable to assume that protein molecules are considered to be intrinsic supramolecules which are made up of three-dimensionally well-arranged amino acid residues to form binding or catalytic sites of the protein. Such protein-based artificial supramolecules would find many potential applications due to the highly functionalized nature of protein itself. The function of the protein-based supramolecules should be more than the sum of the function of each component protein. This chapter describes preparation of an avidin-based enzyme monolayer and ordered multilayers and their use in biosensor fabrications.

# 2.  AVIDIN–BIOTIN SYSTEM

Avidin is a glycoprotein (molecular mass: 68,000 Da) found in egg white, and usually isolated as a tetramer of identical 128-residue polypeptide chains.[5] The most characteristic feature of avidin is that each subunit contains a binding site to biotin and forms a highly stable complex with biotin noncovalently, the binding constant being reported to be $10^{15}$ $M^{-1}$ (Figure 1). Thus, a single avidin molecule can accommodate up to four biotin residues simultaneously. The high-affinity avidin and its homologous protein streptavidin, isolated from *Streptomyces avidinii*,[5] have been studied as prototypes for understanding high-affinity protein–ligand interactions. At the same time, this strong and specific binding has led to widespread use of the system in diagnostic and biochemical assays in which the formation of practically irreversible and specific complexes between macromolecules is required.[6] This is due to the fact that avidin binds not only biotin itself but chemically derivatized forms of biotin whose carboxyl side chain is modified covalently with proteins, lipids, nucleic acids, etc. For this purpose, many kinds of activated biotins for labeling and even biotin- or avidin-labeled reagents have been developed and are now commercially available.

Although many applications of avidin–biotin systems have been developed so far the nature and mechanism of the tight binding are not yet fully understood. It
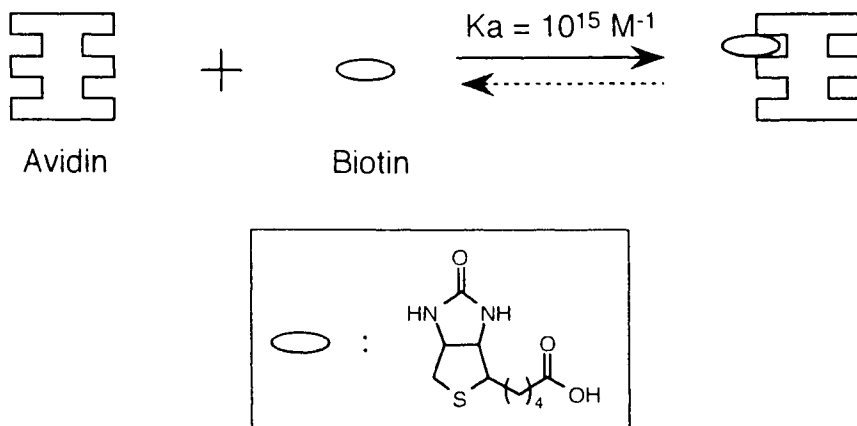
Figure 1. Complexation of avidin and biotin.

has recently been shown that the strong binding arises from the formation of multiple interactions between biotin heteroatoms and the binding site residues of avidin. According to the crystallographic study of avidin, the interactions include (1) a hydrogen-bond network between a biotin ureido group and amino acid residues in avidin, (2) an interaction between biotin sulfur atom and a hydroxyl group of threonine in avidin, and (3) a hydrogen bond between carboxylate in a biotin side chain and protein backbone.[7] Among these, the first interaction plays a predominant role in biotin binding. In addition, the contribution of hydrophobic and van der Waals interactions between biotin and aromatic residues in the binding pocket of avidin have been also suggested.[8]

As discussed briefly, avidin is a tetrameric protein having a 222 molecular symmetry, and each subunit is organized in an eight-stranded antiparallel orthogonal β-barrel. In the binding pocket, several polar residues are available including asparagine, tyrosine, serine, and threonine which participate in the network of the hydrogen bond with a biotin ureido group. These amino acid residues are deeply buried inside the barrel and, in the presence of biotin, water accessibility is severely limited. The aromatic amino acid residues such as phenylalanine and tryptophan, are also suggested to interact with the bicyclic ring of biotin to stabilize the avidin–biotin complex. It should be noted that the complementary hydrogen bond between the biotin ureido group and polar residues, in avidin is responsible for the strong binding of biotin. The importance of complementarity is clearly shown by the effects of chemical modification of the ureido ring of biotin on the binding constant. For example, the binding constant of diaminobiotin (1) and 2'-iminobiotin (2) are reported to be reduced to $10^6$–$10^9$ $M^{-1}$ as compared with the value of $10^{15}$ $M^{-1}$ for the original form of biotin, while the binding of desthiobiotin (3) is rather strong (i.e., $10^{13}$ $M^{-1}$) (Figure 2).[9] In this connection, the molecular recognition
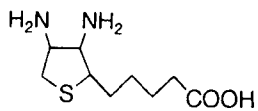
Diaminobiotin   (1)
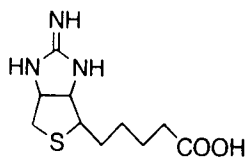


2-Iminobiotin   (2)
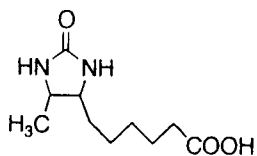


Desthiobiotin   (3)

*Figure 2.* Structure of biotin analogues.



● :biotin binding site
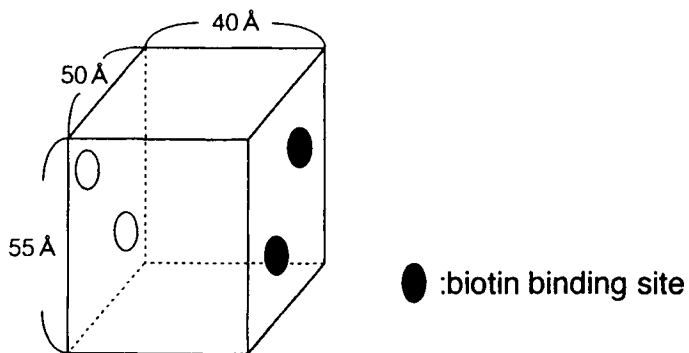
*Figure 3.* Molecular shape and size of avidin.

and the supramolecular systems have been studied extensively based on the formation of complementary, multiple hydrogen bonds using synthetic small molecules.[10]

The avidin molecule (tetramer) is a cube-like shape, the size being approximately $55 \times 50 \times 40$ Å. The binding sites to biotin are arranged in two pairs on opposed faces of the avidin molecule. The two binding sites on the same faces ($50 \times 55$ Å) are separated $20-25$ Å from each other, according to X-ray crystallography[7] and electron microscope studies of bis-biotin-linked avidin polymers[11] (Figure 3). The shape and size together with the favorable arrangement of the binding sites of avidin make its use promising as a building block for the construction of supramolecular protein architectures, in which avidin may be compared to "molecular Lego".

## 3. BIOSENSOR APPLICATIONS OF AVIDIN–BIOTIN COMPLEXATION

### 3.1. Use of Avidin–Biotin Systems for Enzyme Immobilization

Biosensors are fabricated by immobilizing enzymes or other functional proteins on the surface of electrodes, semiconductors, optrodes, etc.[12] The chemical events on the electrode surface induced by the proteins (i.e., molecular recognition, catalytic reaction, etc.) can be transferred into output signals such as electric current and potential, mass changes, or photons. Figure 4 illustrates a typical structure and reactions involved in a glucose sensor which is fabricated by immobilizing glucose oxidase (GOx) on the surface of a metal electrode. Thus, the technique of protein immobilization is of crucial importance for the development of high-performance biosensors.

Many different types of techniques for protein immobilization have been developed using, in most cases, enzyme sensors. Early studies of enzyme biosensors often employed thick polymer membranes (thickness: $0.01-1$ mm) in which enzymes are physically entrapped or chemically anchored. The electrode surface was covered with the enzyme-immobilized polymer membranes to prepare electrochemical enzyme sensors. Although these biosensors functioned appropriately to
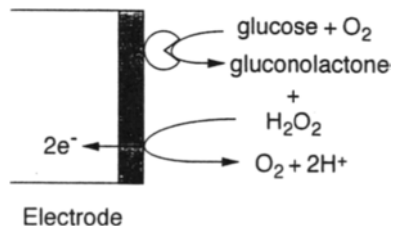
*Figure 4.* Chemical reactions involved in electrochemical glucose sensor.

determine the specific substrates, they sometimes suffered from such drawbacks as insufficient reusability arising from poor adhesion of the membrane to the electrode surface and slow response due to the suppressed diffusion of analytes in the thick polymer membrane. In order to overcome these problems, much attention has been devoted to the molecular-level modification of electrode surfaces with enzymes or other proteins by techniques including simple adsorption, covalent bonding and monolayer deposition.[13] One of the advantages of the molecular-level modification techniques is that rapid-response sensors can be prepared due to the thinner enzyme layer (thickness: 10–100 nm) than the conventional types of thick polymer membranes.

In 1989, to the best of our knowledge, the first report appeared on the use of an avidin–biotin system for the immobilization of enzymes in the preparation of biosensors. Walt et al. have immobilized biotin-modified enzymes (urease, esterase, and penicillinase) on the surface of biotin-modified optical fiber using avidin as a binder (Figure 5a).[14] They have demonstrated the general use of this procedure in immobilizing several types of enzymes. At nearly the same time, Gunaratna and Wilson used an enzyme column in which choline esterase and choline oxidase were immobilized through avidin–biotin complexation for the determination of acetyl-



(a)

(b)

⊒⊒ :Avidin     ⊕— :Biotin     ◁ :Enzyme
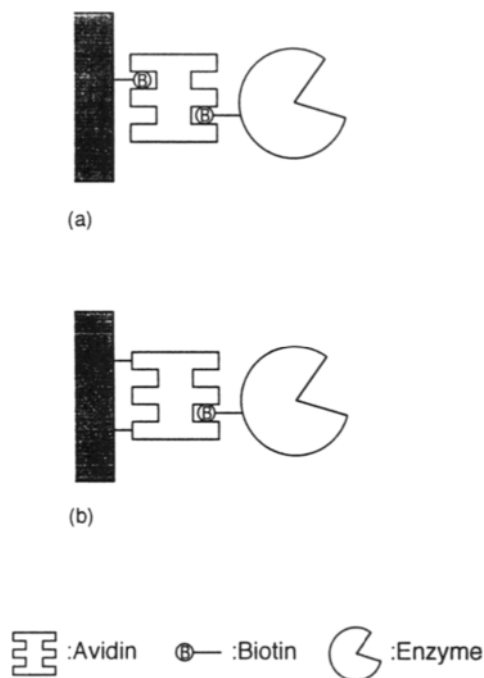
**Figure 5.**  Immobilization of enzyme on electrode surface through avidin.

choline.[15] They attached avidin covalently to the support, followed by coupling it with biotin-labeled enzymes (Figure 5b).

As schematically depicted in Figure 5, two different routes are available for immobilizing biotin-labeled enzymes on the support through avidin–biotin complexation. The first procedure employs the biotin-modified surface on which biotin-labeled enzymes are immobilized through avidin as binder protein. For this procedure, the covalent linkage of biotin onto the surface of a carbon electrode[16] and the preparation of biotin-labeled lipid bilayer on electrode[17] have been studied. An alternative way involves the direct modification of an electrode surface with avidin. If avidin could be immobilized directly without loss of the binding activity to biotin, biotin-labeled enzymes could be loaded more easily on the electrode surface.

## 3.2. Avidin–Biotin Monolayer and Multilayer on LB Film Surface

Avidin is known to be adsorbed strongly on the hydrophobic surfaces through hydrophobic interactions.[18] Therefore, we tried to immobilize avidin by simple adsorption on the surface of Langmuir-Blodgett (LB) monolayer film composed of stearic acid.[19] The surface of a metal electrode was first coated with the LB monolayer and the resulting hydrophobic electrode was immersed in an avidin solution to form an avidin layer. Then, the avidin-modified electrode was treated with biotin-labeled GOx to cover the electrode surface with the monolayer of biotin-labeled GOx (Figure 6a). Alternatively, to immobilize much amount of enzyme on the electrode, the LB film-coated electrode was immersed in a diluted solution of the multiple complex of avidin and biotin-labeled GOx (Figure 6b). One can expect the former procedure to afford a monomolecular layer of enzyme on the electrode surface, while the giant aggregates of proteins composed of avidin and enzyme molecules are adsorbed randomly in the latter procedure. From the viewpoint of enzyme sensors, the latter sensors would show higher response than the former sensors because the total activity of the enzyme (or total amount of enzyme) directly determines the rate of the catalytic reaction. This is clearly shown in Figure 7. The amperometric response of the enzyme sensors arises from the oxidation current of $H_2O_2$ produced enzymatically in the presence of glucose (Eq. 1). These

$$\text{glucose} + O_2 \rightarrow \text{gluconolactone} + H_2O_2 \tag{1}$$
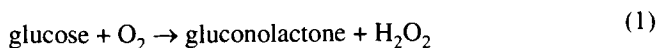
results show that GOx is still active even in the multiple complex with avidin. A colorimetric estimation of the catalytic activity of GOx at both electrodes revealed the rate of $H_2O_2$ generation to be $0.8 \times 10^{-11}$ and $3.0 \times 10^{-11}$ mol cm$^{-2}$ s$^{-1}$ of $H_2O_2$ generation rate for the monolayer and multilayer GOx sensors, respectively. The use of native GOx in place of biotin-labeled GOx in the preparation of glucose sensor resulted in negligibly small response to glucose, confirming that GOx is immobilized through avidin–biotin complexation.
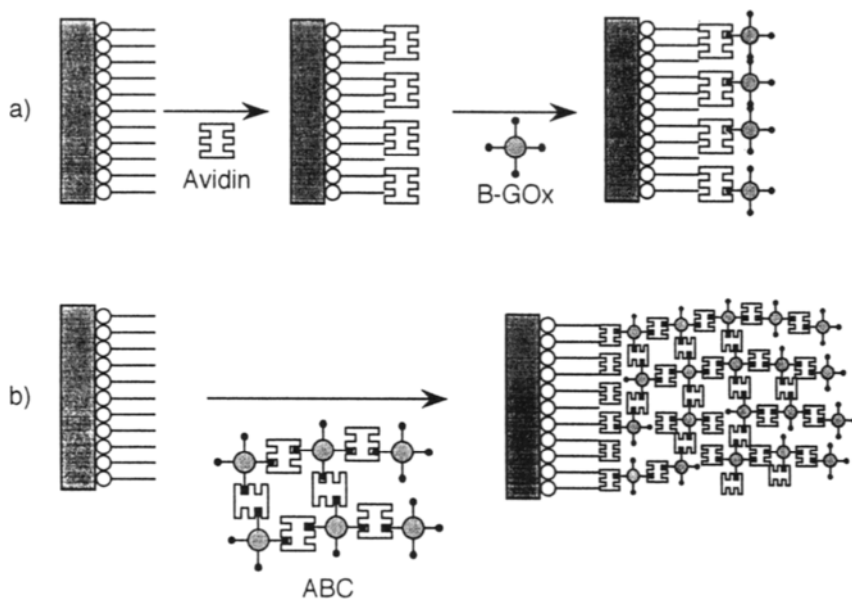
**Figure 6.** Immobilization of enzyme on LB film-coated electrode.

The LB film can be endowed with a variety of functions by being modified with functional molecules. We assembled a GOx monolayer on the surface of redox-active LB film composed of ferrocene-bearing amphiphile, according to the similar procedure as shown in Figure 6.[19] The glucose sensor thus prepared showed an
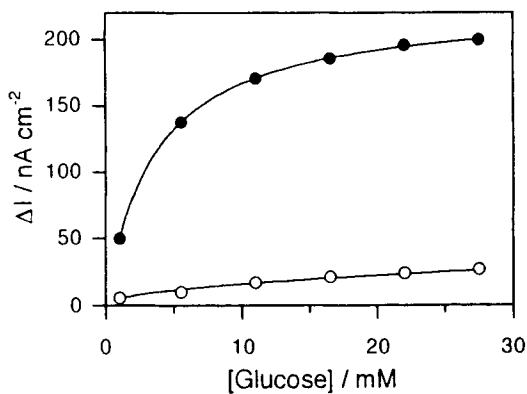


**Figure 7.** Amperometric response of glucose sensors prepared using LB film-coated electrodes. (●) multilayer GOx; (○) monolayer GOx sensors.
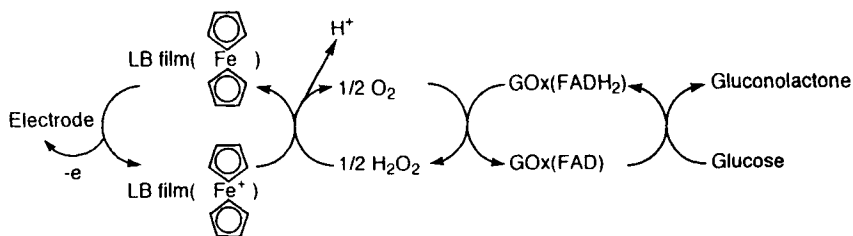
**Figure 8.** Electron relay of glucose sensors mediated by ferrocene LB film.

amperometric response to glucose at +0.5 V vs. Ag/AgCl, which is an inadequate potential for the electrochemical oxidation of $H_2O_2$ on the electrode used (indium tin oxide electrode). Indeed, the glucose sensor based on the stearic acid LB film did not give any current response to glucose at this electrode potential. The electron relay was considered to be accelerated in the LB film/GOx assembly on the electrode as illustrated in Figure 8.

## 3.3. Electrodeposition of Avidin Film

It has been known that adsorption kinetics and/or thermodynamics of proteins depend on the electric or electrochemical properties of solid supports on which the proteins are adsorbed.[20] This has led us to elucidate the effects of electrode potential on the adsorption behavior of avidin on the electrode surface. For this purpose, the electrode potential of a Pt electrode was varied systematically in the range of −0.5–+2.0 V in an avidin solution (pH 7.4). Although the data was somewhat scattered, a general trend was observed that the adsorption of avidin is suppressed by the application of a positive potential (+1.0–+2.0 V).[21] This may be originating from the fact that avidin is a basic protein and has net positive charges in the solution of neutral pH. In the potential range tested, no significant acceleration in the adsorption was induced.

In the course of the experiments, on the other hand, unexpected effects of alternating potential was observed; the adsorption of avidin was accelerated more than 10 times under the influence of alternating potential of triangular wave form from −0.5 to +2.1 V (200 V s$^{-1}$).[21,22] The loading of avidin was monitored by a quartz-crystal microbalance (QCM). The QCM technique has been widely used to monitor surface phenomena which are accompanied by a change in mass, including selective adsorption and reaction,[23] electrodeposition,[24] molecular recognition on solid surface,[25] etc. We employed the QCM with a 9 MHz AT-cut quartz crystal to examine the loading of avidin onto the surface of a platinum (Pt) electrode coated on the quartz crystal. Figure 9 shows the frequency changes ($\Delta F$) caused by the deposition of avidin. The decrease in the frequency means that avidin molecules are adsorbed onto the surface of Pt electrode, increasing the mass loading on the
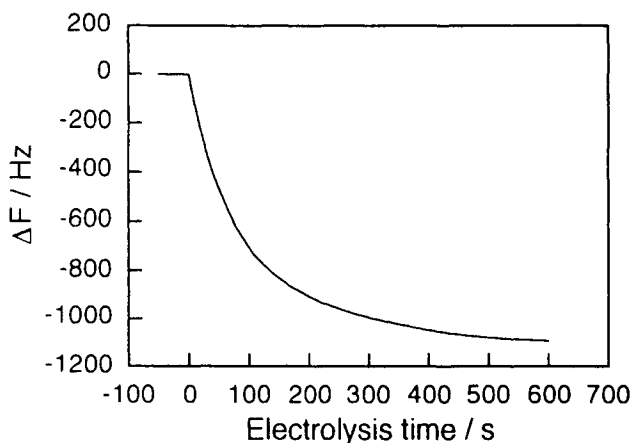
**Figure 9.** Electrodeposition of avidin as monitored by QCM.

quartz crystal. The Sauerbrey equation (Eq.2) is routinely used to calculate the mass change ($\Delta M$/g cm$^{-2}$) from the frequency change ($\Delta F$)

$$\Delta F = 2F_0^2 \Delta M / A(\rho\mu)^{1/2} \tag{2}$$

where the frequency shift $\Delta F$ is a function of the initial frequency $F_0$, the mass loading $\Delta M$, the active area of the electrode $A$, the density $\rho$ (2.645 g cm$^{-3}$), and the shear modulus $\mu$ (2.947 × 10$^{11}$ g cm$^{-3}$s$^{-2}$) of the quartz.[26] For the 9 MHz AT-cut device, 1 ng of mass loading induces −0.91 Hz of frequency change. The data in Figure 9 show clearly that the multilayer of avidin was deposited by the application of alternating potential, because ca. 1000 Hz of the frequency change was induced by 10-min treatment. The QCM data demonstrate also that the loading of avidin (or thickness of the avidin layer) can be regulated by changing the adsorption time. A disadvantage of this technique to prepare an avidin layer is that the orientation of avidin molecules in the surface layer cannot be controlled at all. The electrodeposited avidin film retained its binding activity to biotin and enzyme sensors were prepared successfully using biotin-labeled enzymes.

### 3.4. Enzyme Multilayers: Layer-by-Layer Deposition of Avidin and Enzymes

It may be possible to build up a two- or three-dimensional architecture composed of proteins using avidin and biotin-labeled enzymes as building blocks. If we use enzymes tagged with more than two biotin residues, an enzyme multilayer illustrated in Figure 10 would be constructed because avidin contains four biotin-binding sites per molecule. Fortunately, the biotin-binding sites are located in two pairs on the opposed faces of the avidin molecule. Thus, the use of biotin-labeled enzyme
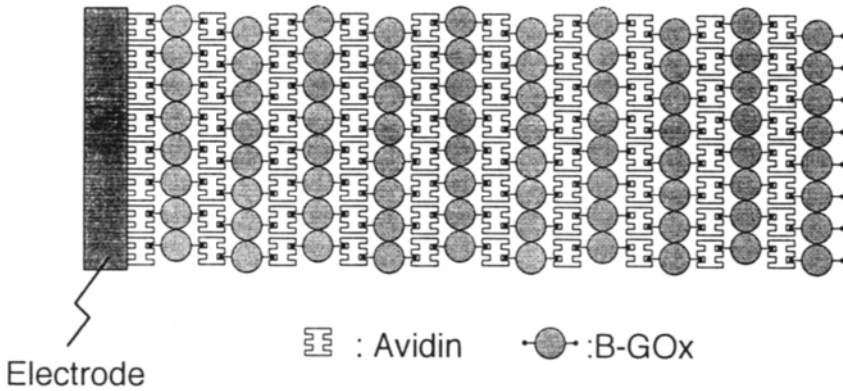
**Figure 10.** Three dimensional protein multilayer based on avidin–biotin complexation.

whose diameter is 5 nm, for example, should result in the formation of a multiple protein layer composed of approximately 10 nm double layers of avidin plus enzyme. In other words, the thickness of the multilayer can be regulated strictly by changing the number of depositions.

As a first step toward the construction of three-dimensional protein architectures, formation of an avidin monolayer and an avidin plus enzyme double layer was studied.[27] The adsorption behavior of avidin and biotin-labeled enzymes onto a Pt electrode was monitored by means of QCM. Figure 11 illustrates the frequency changes induced by the adsorption of the avidin first layer and the next layer of
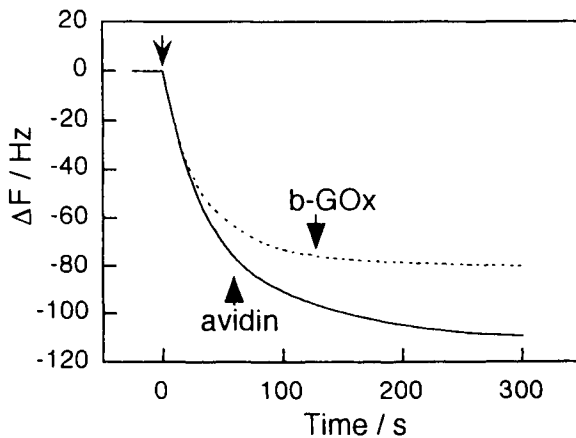


**Figure 11.** Frequency changes in QCM induced by the adsorption of avidin and biotin-labeled GOx.

biotin-labeled GOx. The loading of avidin onto the Pt surface by a simple adsorption is estimated from Eq. 2 to be ca. 400 ng cm$^{-2}$ in equilibrium. Assuming that avidin is a cube-like molecule with dimensions of $55 \times 50 \times 40$ Å, three different orientations of the avidin molecule on the Pt surface can be considered as extreme cases, as schematically shown in Figure 12. If the Pt surface is covered with a
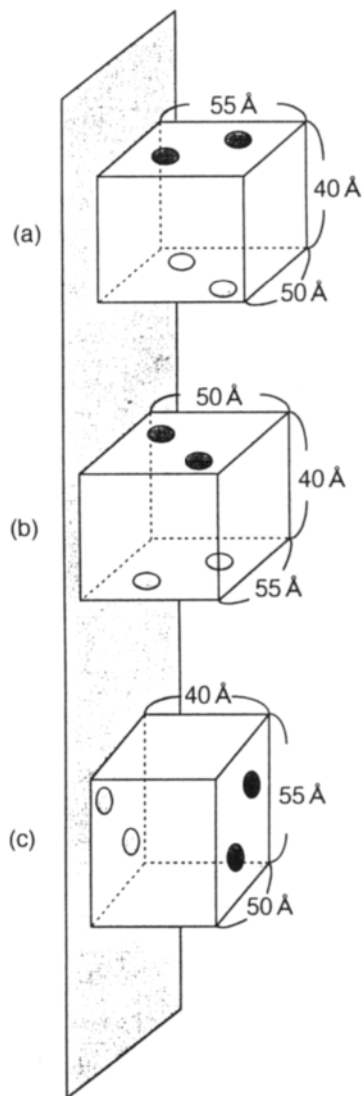


*Figure 12.* Three different orientation modes of avidin on the solid surface.

monomolecular layer of avidin which is adsorbed in type (a) orientation, the loading of avidin should be in a maximum value among the three possible orientations and ca. 510 ng cm$^{-2}$ calculating from the molecular mass of 68,000 Da. On the other hand, the type (c) orientation would result in a loading of avidin of ca. 340 ng cm$^{-2}$, which is a minimum value among the three orientations. In practice, it is reasonable to assume that the surface layer of avidin on the Pt electrode contains all three orientations simultaneously, and a large portion of avidin molecules are probably tilting more or less from the extreme orientations. The data in Figure 11 suggest avidin loading between the two extreme values, further suggesting the formation of a monomolecular layer in random orientation. This seems quite reasonable because the driving force of the binding of avidin onto the Pt surface is a combination of hydrophobic, van der Waals, and electrostatic interactions and no site-specific interaction which determines the orientation of avidin exclusively is involved. The binding of avidin is practically irreversible; no appreciable desorption is observed upon exposing the avidin monolayer-modified QCM to buffer solution or to pure water.

It is interesting to verify whether the avidin monolayer is still active to bind biotin or not. To check this, the avidin monolayer-modified QCM was immersed in a diluted solution of biotin-labeled GOx (10 μg mL$^{-1}$) and the frequency was measured (Figure 11). The frequency change of –80 – –90 Hz (i.e., 360–400 ng cm$^{-2}$) was induced, showing that the avidin monolayer is active to bind biotin-labeled GOx through an avidin–biotin complexation on the QCM electrode. This view is further supported by the fact that no frequency change was induced by native GOx bearing no biotin label. These results suggest that the avidin molecules circumvent the surface-induced denaturation (conformational change) and deactivation, which are often the case for proteins at an interface. This may relate to the robust nature of avidin molecule against heat, acid and base, detergent, etc. Taking the size (60 × 52 × 77 Å) and molecular mass (186,000 Da) of GOx into account, the QCM data suggest the formation of submonomolecular layer (surface coverage: 50–60%) of GOx on the surface of avidin monolayer. This value of the surface coverage may be an underestimation because the frequency change in QCM is often attenuated by an intervention of elastic layer between the quartz crystal and adsorbent.[28] The effects of mass loading of GOx was probably canceled in part by the first layer of avidin due to the elastic nature of the protein in water. Nevertheless, the formation of a submonomolecular layer of GOx is plausible in view of the fact that the avidin molecules are randomly orientated in the underlying layer and, as a result, some portion of biotin-binding sites in avidin cannot be available to anchor the biotin-labeled GOx.

In any event, ambiguity still remains in the surface coverage of GOx. The protein double layer thus prepared is schematically shown in Figure 13. The catalytic activity of GOx in the double layer was elucidated electrochemically by measuring an amperometric response originating from the oxidation current of H$_2$O$_2$ produced enzymatically in the presence of glucose (Eq. 1), and was found to be still active.
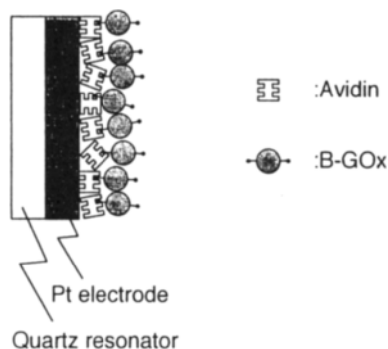
**Figure 13.** A possible assembly of avidin and biotin-labeled GOx on the surface of QCM electrode.

Thus, we have succeeded in the construction of monomolecular layer of active avidin and avidin plus GOx double layer.

These results strongly stimulated us to prepare protein multilayers by layer-by-layer deposition of avidin and enzymes. On the uppermost surface of the double-layer-modified electrode, free biotinyl residues are still available to further deposit the avidin second layer because the GOx used is tagged with several biotin residues per molecule. In order to ascertain the formation of a multilayer structure of avidin and enzyme, we immobilized fluorescein-5-isothiocyanate (FITC)-conjugated avidin and biotin-labeled GOx alternately on a quartz slide.[29] Prior to the formation of a protein multilayer, the quartz slide was first modified with dichlorodimethyl-silane to make the surface hydrophobic. The silylated quartz slide was immersed in FITC–avidin and biotin-labeled GOx solutions alternately and repeatedly, which treatment provides both sides of the slide with the protein multilayer. An increase in absorbance at 459 nm, originating from the FITC moiety of FITC–avidin, was monitored after each deposition of FITC–avidin and enzyme (Figure 14). The absorbance increased in proportion to the number of layers deposited (deposition number), suggesting the formation of a multilayer structure on the quartz slide. This result indicates that FITC–avidin is immobilized in each layer as a roughly monomolecular layer considering the molecular dimension of avidin and molar extinction coefficient of $176,000 \text{ M}^{-1} \text{ cm}^{-1}$ for the FITC–avidin at 495 nm. The multilayer-modified slide exhibited a slight increase in absorbance around 380 nm ascribable to a cofactor flavin adenine dinucleotide (FAD) in the biotin-labeled GOx, though the absorbance was too small to be treated quantitatively.

For further characterization of the protein multilayer, two electrochemical techniques were employed independently. The first technique involves amperometric measurements of the GOx multilayer-modified electrode in the presence of glucose. Figure 15 plots the output current ($\Delta I$) of the electrode to 1 mM glucose as a function of the deposition number.[29] The response current depends linearly on the number
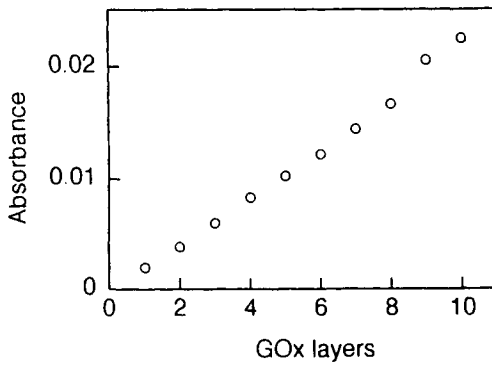
**Figure 14.** A formation of protein multilayers as monitored by UV absorbance.

of GOx layers. On the contrary, when native GOx bearing no biotin residue was used in place of biotin-labeled GOx, $\Delta I$ was negligibly small and did not increase, even after several treatments with avidin and GOx. These results are clear indications that a constant amount of GOx is immobilized in each layer through avidin–biotin complexation because the size of output current of the enzyme-modified electrode should depend linearly on the total catalytic activity of the enzyme.

Another technique used is a cyclic voltammetry (CV) in the presence of electron mediator.[30] In the GOx-catalyzed oxidation reaction of glucose, cofactor FAD, which is contained at the active center of GOx, oxidizes glucose to gluconolactone and resultant $FADH_2$ is converted back to the active FAD form by $O_2$. In the conventional type of enzyme sensors, the $H_2O_2$ generated from $O_2$ is oxidized at the electrode surface.
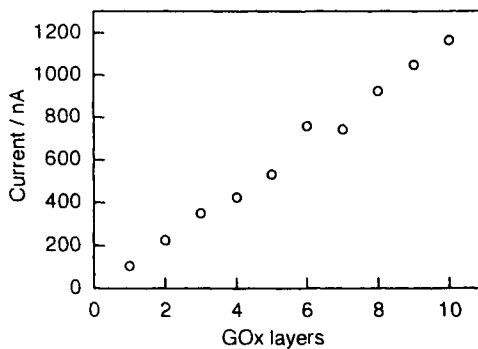


**Figure 15.** A linear dependence of the output current of glucose sensors on the number of GOx layers. Sample; 1 mM glucose.
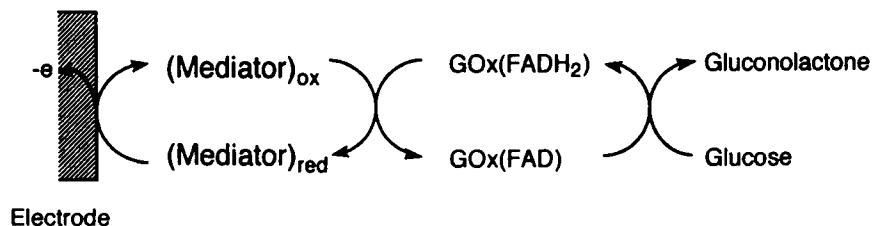
**Figure 16.** Chemical reactions involved in the mediator-type glucose sensors.

It has recently been reported that GOx-catalyzed reaction can be mediated by synthetic redox compounds including hydroquinone, ferrocyanide, ferrocene, etc.[30] The mediation behavior of these compounds can be evaluated electrochemically by CV measurements, the reaction scheme being depicted in Figure 16. The role of these redox compounds in the enzyme-linked electrode reaction is to mediate electron relay from $FADH_2$ in GOx to electrode. For this reason, they are usually called "electron mediators". In this situation, the magnitude of oxidation current in CV of the electron mediator is a function of the concentration of glucose and mediator and the catalytic activity of enzyme (or, for enzyme-modified electrodes, the loading of enzyme on the electrode surface). Therefore, the CV measurements in the solution dissolving a constant concentration of mediator and glucose reveal the loading of GOx immobilized on the electrode. Thus, the oxidation current in CV was measured in the presence of ferrocenemethanol as mediator and plotted as a function of the deposition number of GOx layers (Figure 17).[31] The oxidation current depends linearly on the number of GOx layers, confirming that the present
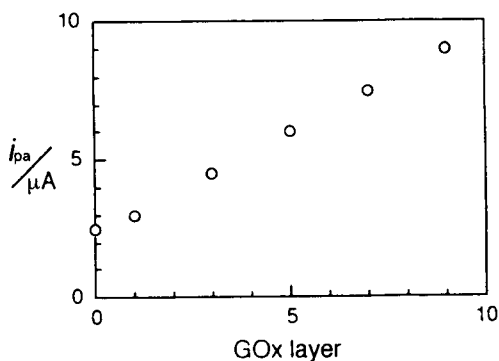


**Figure 17.** A linear dependence of oxidation current ($i_{pa}$) in CV on the number of GOx layers in the presence of glucose (30 mM) and ferrocenemethanol (0.5 mM).

procedure affords an enzyme multilayer which is composed of monolayers containing a constant amount of GOx.

From the viewpoint of biosensor use, the enzyme multilayers would provide many advantages as compared to the conventional type of enzyme membranes. The most important feature of the enzyme multilayers is referred to feasibility of precise regulation of output current by changing the number of depositions. It should be emphasized that the regulation of enzyme loading (or the thickness of enzyme layer) can be attained in molecular level or in nanometer level. The response time of the GOx multilayer-modified glucose sensors was fast (10–20 s) and virtually independent of the thickness of the GOx layer, implying that the avidin/GOx multilayers do not influence significantly the mass transfer of analyte and the reaction product of the enzymatic reaction. This is in striking contrast to the general trend that the response time of enzyme sensors becomes longer with increasing the thickness of the enzyme membrane due to slow diffusion of analytes and reaction products in the membrane.

Another merit of the enzyme multilayer is that two or more different kinds of enzymes can be assembled simultaneously in the multilayer. This enables us to prepare multienzyme biosensors easily. As a prototype of bienzyme biosensors, we prepared interferent-free glucose sensors by assembling ascorbate oxidase (AOx) together with GOx on the surface of Pt electrode (Figure 18).[32] Glucose sensors often suffer from interference arising from the direct oxidation of oxidizable substances such as ascorbic acid (vitamin C) and uric acid in biological fluids. A physiological level of ascorbate (ca. 0.1 mM) in blood usually disturbs the determination of glucose in blood.[33] For the elimination of ascorbate interference, the enzyme multilayers composed of 10 GOx layers and additional 10 AOx layers were
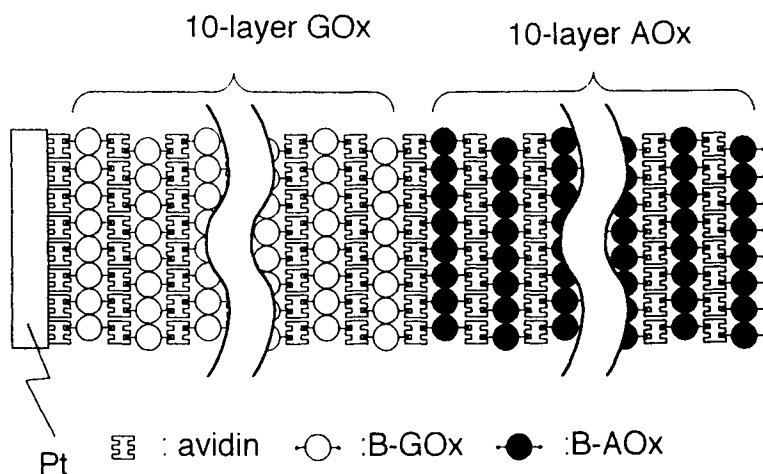


**Figure 18.** Bienzyme multilayers for interferent-free glucose sensors.
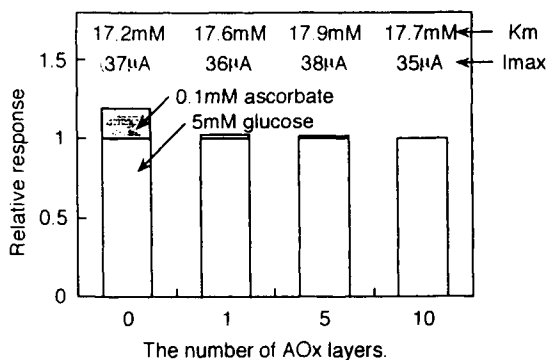
**Figure 19.** Relative response of GOx (10 layers)/AOx multilayer-modified sensors.

assembled by a stepwise deposition of avidin and biotin-labeled GOx and AOx. In this glucose sensor, one can expect that ascorbic acid is oxidized to an electrochemically inactive form of dehydroascorbic acid in the outer AOx layer, and the concentration of ascorbic acid at the Pt surface can be lowered considerably depending on the catalytic activity of the AOx.

Figure 19 summarizes relative response of GOx/AOx bienzyme glucose sensors to 5 mM glucose and 0.1 mM ascorbate. About 20% of interfering current was observed for the glucose sensor (10 GOx layers) in which no AOx layer is equipped. On the contrary, the deposition of AOx monolayer on the glucose sensor reduced the interference to a 2–3% level. The interference was further decreased by 5-layer AOx and eliminated completely when 10 AOx layers were assembled on the glucose sensor. These results support the reaction mechanism that ascorbate can be oxidized to dehydroascorbate in the outer AOx layer. The effect of the deposition of AOx layers on the kinetics of GOx-catalyzed reaction was also elucidated. The Michaelis–Menten constant ($K_m$) of the immobilized GOx and the maximum current of the sensors did not depend on the thickness of AOx layer, suggesting no influence of the AOx layers on the transport of glucose from sample solution into the GOx layer.

## 4. CONCLUSION

A supramolecular complexation between avidin and biotin-labeled enzyme results in the formation of enzyme multilayers composed of avidin and enzyme monolayers, in which each monolayer is connected through avidin–biotin complexation with each other. The thickness of the multilayers can be precisely controlled by regulating the deposition number (the thickness of each avidin plus enzyme double layer is approximately 10 nm). The enzyme multilayers are useful in preparing high

performance biosensors. The output current of the multilayer-modified biosensors can be modulated arbitrarily by regulating the multilayer thickness. The present technique for constructing enzyme multilayers makes it possible to prepare bienzyme biosensors. A deposition of GOx and AOx monolayers successively on the Pt electrode affords interferent-free glucose sensors.

# REFERENCES

1. Diederich, F. *Angew. Chem. Int. Ed. Engl.* **1988**, *27*, 362.
2. Rebek, J. Jr., *Acc. Chem. Res.* **1990**, *23*, 399.
3. Lehn, J.-M. *Angew. Chem. Int. Ed. Engl.* **1990**, *29*, 1304.
4. Ulman, A. *Chem. Rev.* **1996**, *96*, 1533.
5. Wilchek, M.; Bayer, E. A. *Anal. Biochem.* **1988**, 171, 1.
6. Guesdon, J.-L.; Ternynck, T.; Avramess, S. *J. Histchem. Cytochem.* **1979**, *27*, 1131.
7. Pugliese, L.; Coda, A.; Malcovati, M.; Bolognesi, M. *J. Mol. Biol.* **1995**, *23*, 698.
8. Chilkoti, A.; Stayton, P. S. *J. Am. Chem. Soc.* **1995**, *117*, 10622.
9. Hofmann, K.; Titus, G.; Montibeller, J. A.; Finn, F. M. *Biochemistry* **1982**, *21*, 978.
10. Chang, S.-K.; Engen, D. V.; Fan, F.; Hamilton, A. D. *J. Am. Chem. Soc.* **1991**, *113*, 7640.
11. Green, N. M.; Konieczny, L.; Toms, E. F.; Valentine, R. C. *Biochem. J.* **1971**, *125*, 781.
12. Alcock, S. J.; Karayannis, M.; Turner, A. P. F. *Biosens. Bioelectron.* **1991**, *6*, 647.
13. Ahluwalia, A.; Rossi, D. D.; Ristori, C.; Schirone, A.; Serra, G. *Biosens. Bioelectron.* **1991**, *7*, 207.
14. Luo, S.; Walt, D. R. *Anal. Chem.* **61**, *61*, 1069.
15. Gunaratna, P.; Wilson, G. S. *Anal. Chem.* **1990**, *62*, 402.
16. Achtnich, U. A.; Tiefenauer, L. X.; Andres, R. Y. *Biosens. Bioelectron.* **1992**, *7*, 279.
17. Snejdarkova, M.; Rehak, M.; Otto, M. *Anal. Chem.* **1993**, *65*, 665.
18. Ebersole, R. C.; Miller, J. A.; Moran, J. R.; Ward, M. D. *J. Am. Chem. Soc.* **1990**, *112*, 3239.
19. Lee, S.; Anzai, J.; Osa, T. *Sens. Actuators B* **1993**, *12*, 153.
20. Young, B. R.; Pitt, W. G.; Cooper, S. L. *J. Colloid Interface Sci.* **1988**, *125*, 246.
21. Hoshi, T.; Anzai, J.; Osa, T. *Anal. Chim. Acta* **1994**, *289*, 321.
22. Anzai, J.; Hoshi, T.; Osa, T. *Chem. Lett.* **1993**, 1231.
23. Ebersole, R. C.; Ward, M. D. *J. Am. Chem. Soc.* **1988**, *110*, 8623.
24. Hillman, A. R.; Loveday, D. C. *Langmuir* **1991**, *7*, 191.
25. Ebara, Y.; Okahata, Y. *J. Am. Chem. Soc.* **1994**, *116*, 11209.
26. Sauerbrey, G. *Z. Phys.* **1959**, *155*, 206.
27. He, P.-G.; Takahashi, T.; Anzai, J.; Suzuki, Y.; Osa, T. *Pharmazie* **1994**, *49*, 621.
28. Muramatsu, H.; Suda, M.; Ataka, T.; Seki, A.; Tamiya, E.; Karube, I. *Sens. Actuators A* **1990**, 21-23, 362.
29. Hoshi, T.; Anzai, J.; Osa, T. *Anal. Chem.* **1995**, *67*, 770.
30. Heller, A. *Acc. Chem. Res.* **1990**, *23*, 128.
31. Anzai, J.; Osa, T., unpublished data.
32. Anzai, J.; Takeshita, H.; Hoshi, T.; Osa, T. *Denki Kagaku* **1995**, *63*, 1141.
33. Jung, S.-K.; Wilson, G. S. *Anal. Chem.* **1996**, *68*, 591.

This Page Intentionally Left Blank

# ARTIFICIAL ION CHANNELS

## Yoshiaki Kobuke

# 1. INTRODUCTION

Biological energy-producing membrane generates a $H^+$ concentration gradient across the membrane. This is then transformed and stored as the chemical bond energy of ATP, which is distributed to various biological organs for supplying free energy to drive endergonic reactions. By consuming ATP thus produced, $Na^+-K^+$ ATPase accumulates $Na^+$ and $K^+$ ions outside and inside the cell, respectively. With such a concentration gradient, the opening of a path for ion transport in the membrane induces rapid ionic flux across the membrane. In this way, nerve axons transmit an induced local variation of membrane potential through voltage-dependent $Na^+$ and $K^+$ channels as the waveforms of voltage, i.e., the action potential. At the end of the synapse, $Ca^{2+}$ flows into the cell through $Ca^{2+}$ channels. $Ca^{2+}$ flow then triggers the release of nerve-transducing hormones into the narrow synaptic cleft. Upon hormonal reception by ligand-gated ion channels, an electrical signal is again generated in the next synapse (Figure 1). Such a signal transduction triggers the movement of skeletal muscle or coordinates contraction of the heart.[1,2]

The primary sequences of important channel peptides, such as the nicotinic acetylcholine receptors, and sodium, potassium, and calcium channels, have been determined by the innovative work of the late professor Numa and his group.[3-7] Thereafter, various structural models on the basis of empirical as well as molecular mechanics or molecular dynamics calculations were proposed[8-13] and tested by specific point mutation studies.[14-20]

There are two mechanisms for ion transport across biological membranes, i.e. carrier and channel (Figure 2). The carrier encapsulates metal ions into the ligating site and transfers across the membrane in the form of a carrier–metal ion complex and releases the ion into the other aqueous phase. The relatively large molecular entity of the carrier–ion complex limits the rate of diffusion through the membrane, which exists as a mixture of gel and liquid crystalline phases. Many antibiotics, known as ionophore families, transport ions by this mechanism and facilitate the leakage of metal ions, thus acting as a decoupling agent in an energy-producing membrane. The channel is, in principle, a pore in the membrane through which ions flow in a state more or less similar to that in the bulk aqueous phase. Therefore, a large ionic flux is easily obtainable and the mechanism is exactly what is adopted by nature in cases where large ionic fluxes of alkali and alkaline earth metal and chloride ions are required.

In spite of the overwhelming importance of the channel mechanism for the transport of alkali and alkaline earth metal ions in biological systems, only carrier transport has been studied extensively by chemists. Studies on ion channel mimics of simple structures have long been limited to antibiotic families of gramicidin, amphotericin B, and others. Several pioneers have reported successful preparation of non-peptide artificial channels. However, their claims have been based on kinetic characteristics observed for the release of metal ions through liposomal membrane and lacked the very critical proofs of channel formation.[21-26] Such a situation was
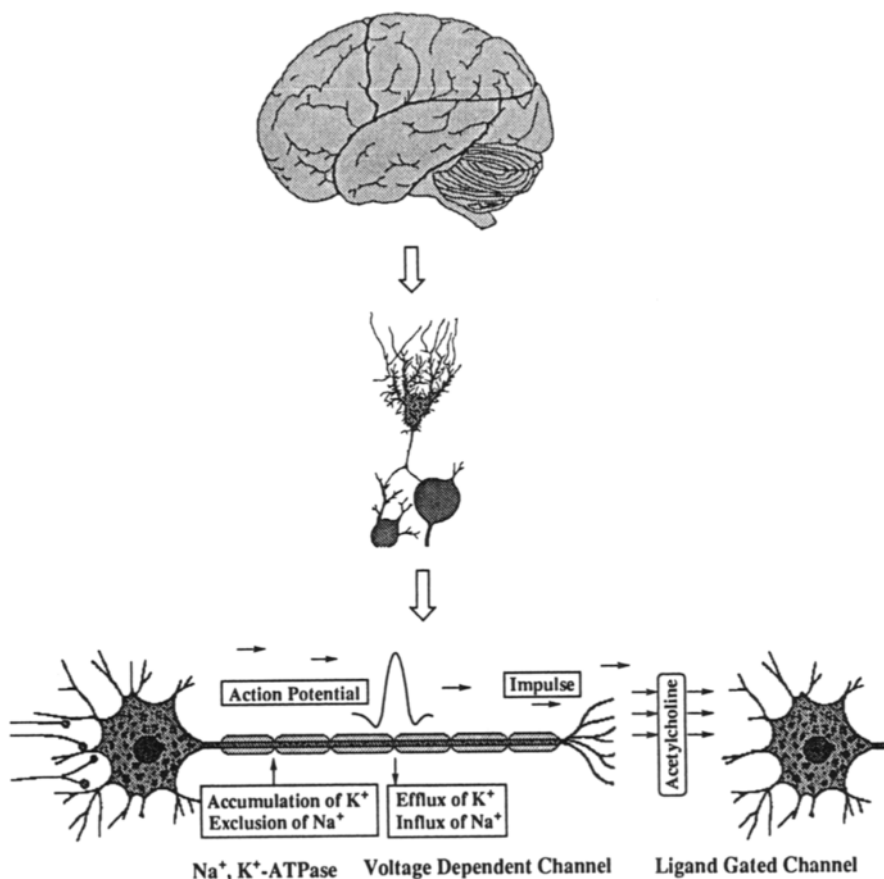
**Figure 1.** Mode of signal transduction of nerve system. Under concentration gradients, generated by $Na^+,K^+$-ATPase, opening of ion channel induces variation of the local membrane potential, which opens the adjacent voltage dependent ion channel. By this way the variation of the local membrane potential, called action potential, is conveyed along the axon. This electrical signal is once transformed into signal of chemical nature by ejecting nerve hormone, such as acethylcholin. Ligand gated channel in the synapse membrane accepts the hormone and restarts the signal transduction as an electrical wave form.

overcome in 1988 by the introduction of synthetic oligopeptides,[27–29] which have been incorporated into lipid bilayer membrane and characterized by the measurement of single channel currents.[30–34] All of the succeeding artificial oligopeptide channels were characterized by this method to obtain very basic, fundamental features of ion channels.[35–43] However, none of non-peptidic artificial compounds[44–48] even after 1988 has been tested by such a measurement of single
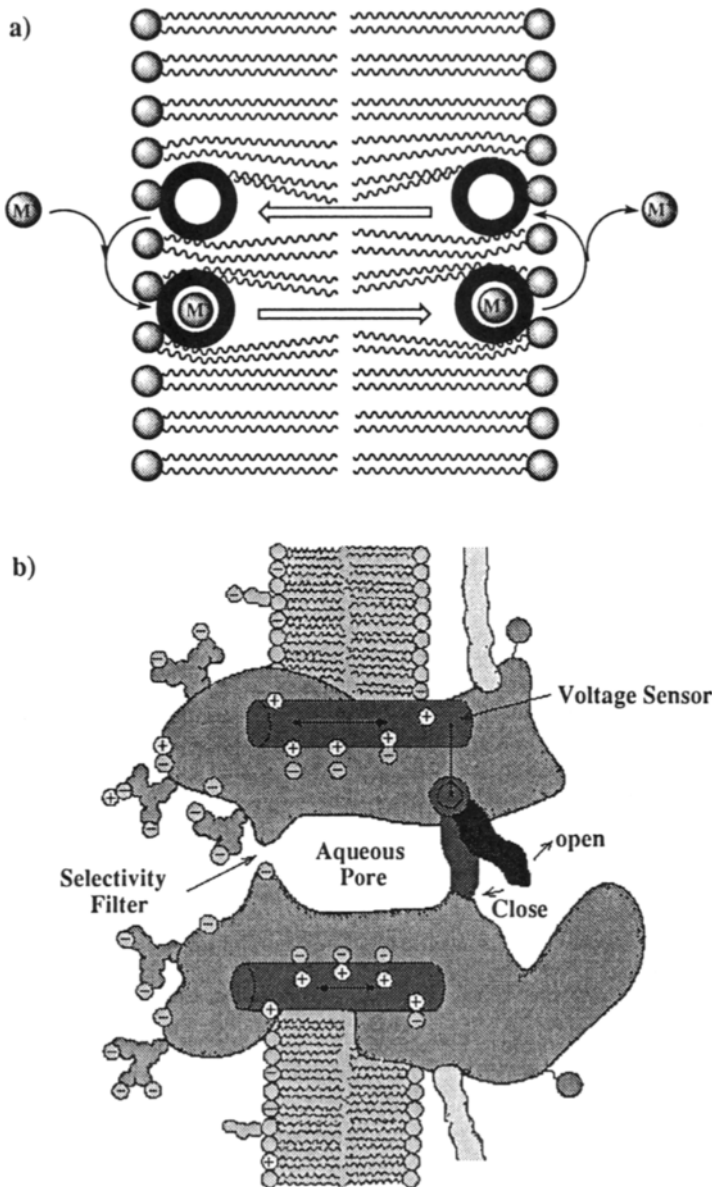
**Figure 2.** Carrier (**a**) and channel (**b**) mechanisms for facilitated ion transport across the membrane. Carrier encapsulates ion and moves across the membrane and releases the ion at the other end. It shuttles in the membrane as a carrier–metal complex. Channel is, in principle, an aqueous pore structured in the membrane. Ion can traverse through the membrane more or less freely in the pore with recognition at the selectivity filter when the gate is open. Here illustrated is a voltage sensitive gate as an example.[4]

channel current before the author reported the first successful demonstration of single-channel properties by using planar bilayer membrane.[49]

Studies on artificial ion channels are expected to provide important information on molecular mechanisms and to deepen our understanding of natural ion channels through the establishment of a detailed structure–function relationship. At the same time, the research will contribute to the fascinating area of nanoscale transducers, and may eventually lead to the development of so-called molecular ionics. Here, the author would like to describe the basic concept for the molecular design of various artificial ion channels and to compare their characteristics in the hope of stimulating a future explosion of this research field.[50–53] Special attention is focused on non-peptidic approaches. Helical bundle approaches[54–59] and studies on modified antibiotics[60–66] are beyond the scope of this review.

## 2. SUPRAMOLECULAR ION CHANNELS

### 2.1. Doubly Amphiphilic Lipid Ion Pairs

A molecular arrangement of the voltage-gated $Na^+$ channel proposed by Numa is illustrated in Figure 3.[4] Here the central ion-conducting pore is composed of four sets of amphiphilic α-helical segment 2, which is supplied from each repeating unit I–IV, and is surrounded by bundle arrays of all the remaining hydrophobic α-helices.

This generalized structure was mimicked by a very simplified artificial molecule 1. The hydrophilic core part 2 was substituted simply by an oligoether carboxylate anion. The carboxylate may act as the polar ionic head group outside the membrane and the ether part of the molecule may be located in the interior part of the membrane to make an ion-conducting pathway. The molecular lengths were adjusted to fit the lipid monolayer in an extended or a helical conformation, with $n$ being 2 or 3 in 1. The hydrophobic exterior was substituted by dioctadecyldimethylammonium cation, which was ion-paired with the carboxylate.

The planar lipid bilayer system employed for the measurement is illustrated in Figure 4 along with typical records of ionic currents on incorporating 1 into the bilayer membrane separating two chambers. Currents of constant pico ampere levels showed well-defined, frequent transitions in amplitude between the main current level and zero. Several current levels were observed at different runs. The appearance of each level appeared to be random and the overlap of currents with the same or different levels was observed, although less frequently. It should be noted, however, that each level, once apparent, remained stable and persisted for times over 1 h without change to different current levels. This was even so when the voltage was varied in the range ±150 mV. Current recordings were digitized and the histogram analysis of current amplitude and open–closed times was undertaken. Single-channel current amplitude was read from peak-to-peak values of the histogram, each peak representing the open and the closed level.
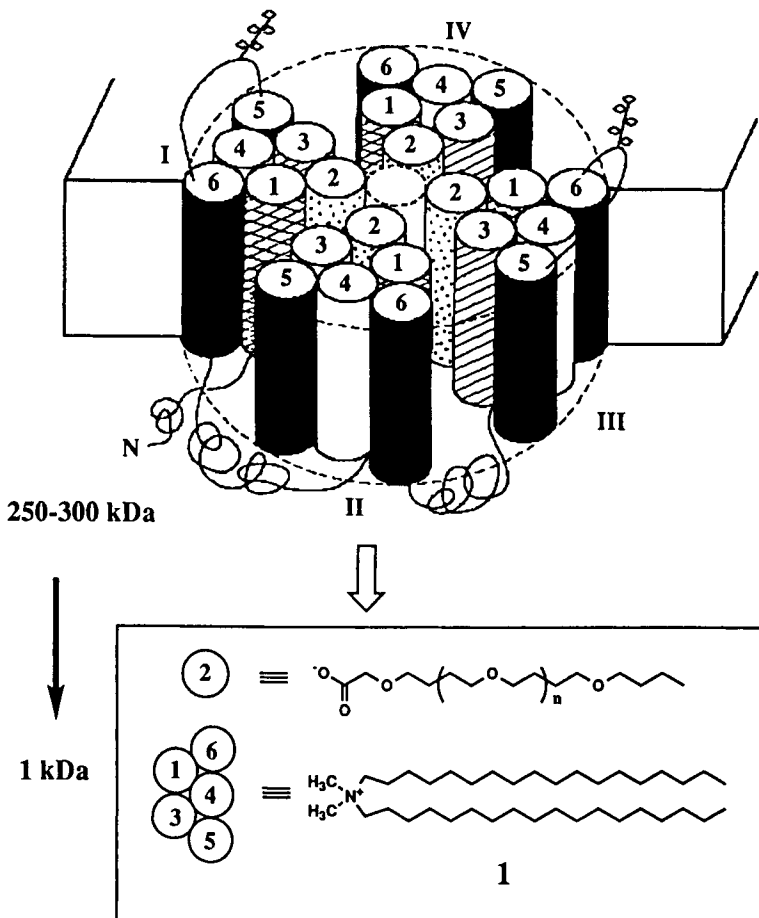
**Figure 3.** A supramolecular arrangement of α helices of voltage-gated Na⁺ channel proposed by Numa [Noda et al. (1984)]. Four helix bundles of segment **2** from each repeat unit constitute the wall of hydrophilic pore through which ions pass. All the other helices 1, 3–6, cover the pore and stabilize it in bilayer membranes. The ion pair **1** is a mimic from oligoether carboxylate and dioctadecyldimethylammonium representing hydrophilic helix **2** and all the other hydrophobic helices 1 and 3–6, respectively.

Currents were obtained under a series of voltages, ranging usually from +100 to −100 mV and a constant conductance was always obtained from the linear slope of the current–voltage plot: 97 pS in the example shown in Figure 4. In spite of the appearance of such a stable conductance level, the very next run usually gave a different conductance level. These observations are reconciled only by assuming

a)

Planar Lipid Membrane

Outer Chamber    Inner Cell

Lipid    Channel Molecule

b)

Records 101-104

Records 105-108

Records 109-112

Records 113-116

Records 117-120

5pA

0.2 s
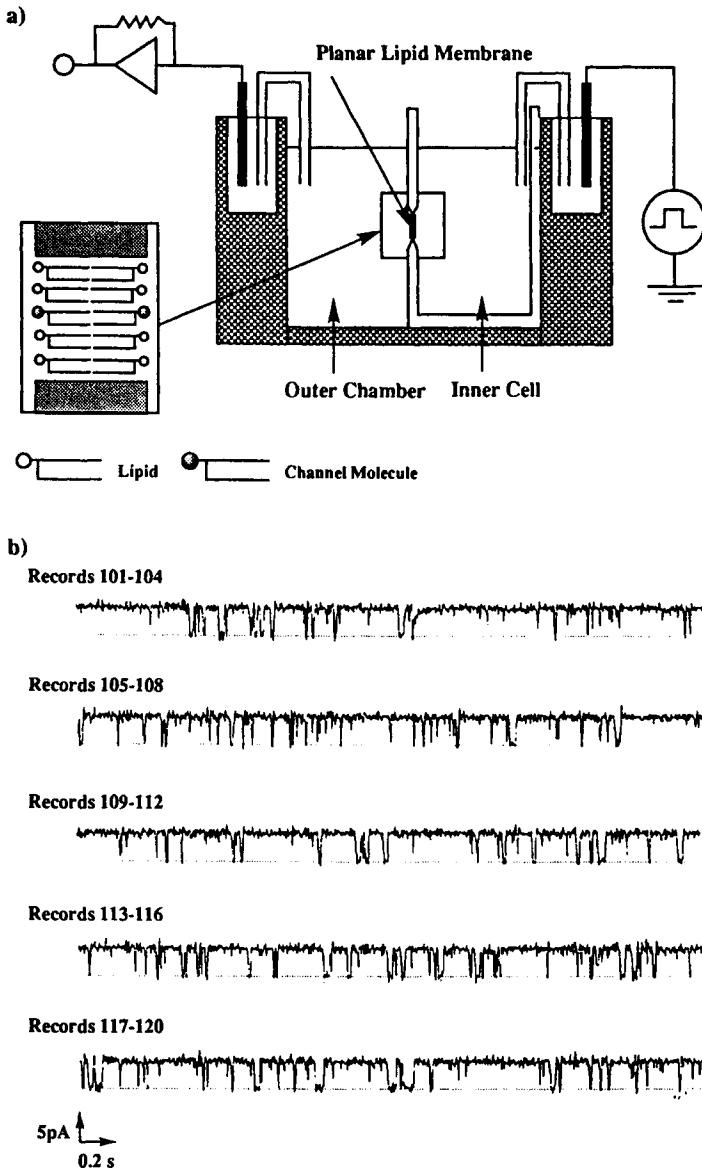
*Figure 4.* (a) Planar bilayer membrane system for single-channel currents measurement. Soybean lecithin in *n*-decane was applied to a hole separating two aqueous chambers. Chambers were filled with metal chloride salt at pH 7.2. The voltage was applied to the outer cell with respect to the inner. The currents across the bilayer were recorded on a PCM recorder through a patch-clamp amplifier and a lowpass filter. (b) Typical records of current observed at +50.0 mV (symmetrical 0.5 M solution). Currents increase upward from the zero level shown by the dotted line in each panel.

the existence of several stable conductance states. We observed one of them in any given trial and others for different runs. The existence of multiple conductance levels is not at all unusual but commonly observed for all known supramolecular ion channels made from oligopeptide bundles. The opening and closing processes seem to be random and to behave as a stochastic process. The histogram analysis of open and closed times for the conductance level of 97 pS gave fast gating kinetics with lifetimes of 1 to 10 ms order.

Next, the ion selectivity was examined, since the existence of molecular recognition between cation and anion, $K^+$ and $Na^+$, or others may be important criteria for differentiating the ion channel from a defect formed in the membrane. Under an asymmetrical salt concentration (0.5 M/0.1 M KCl), the current–voltage plot gave a reversal potential of $-23.5$ mV for the run shown in Figure 4. From the Goldmann–Hodgkin–Katz equation, the permeability ratio between $K^+$ and $Cl^-$ was calculated as approximately 5, indicating that the channel was selectively permeable to cations. On the other hand, the single channel conductance in 0.5 M NaCl was almost identical to that obtained at 0.5 M KCl, indicating no selectivity between $K^+$ and $Na^+$ cations.

From the characteristics observed—constant and stable current levels, transitions between zero and nonzero current levels with a stochastic process on millisecond-to-second time scale, multiple and heterogeneous conductance levels, and selectivity of cations over anion—it can safely be concluded that the ion pair 1 constitutes *single ion channels*. The similarity of the activity with those of natural ion channels is fantastic and seems far beyond the expectation if one considers the simplicity of the molecular structure.

The observation of single channel currents may suggest the successful self-organization of supramolecular channels. This process may require several steps: (1) incorporation of the amphiphilic carboxylate–ammonium ion pair into the bilayer lipid membrane; (2) molecular recognition of the relatively polar oligoether chain from the surrounding hydrophobic lipid components to induce domain formation of molecular level; and (3) interlayer connection of these hydrophilic domains existing in different lipid layers.

These elementary steps are based on molecular recognition via subtle differences in hydrophobicity–hydrophilicity between the channel-forming material and lipid components. Using ammonium with a single long alkyl chain instead of two to make ion pairs 1, only a transient disturbance of the zero current level was observed. Also, none of the components by themselves—oligoether–carboxylic acids or ammoniums having one or two long alkyl groups—could give rise to ionic channel currents. Therefore the alkyl chains in the ammonium complex contribute significantly to favor both the incorporation and the domain formation of the channel-forming material in the lipid phase.

The observation of open–closed transitions and of different conductance levels can be interpreted according to such a molecular aggregation mechanism. Pores

having different aggregation numbers may define different conductance levels. Open–closed transitions may be accounted for by three mechanisms:

1. Association–dissociation equilibrium of artificial amphiphiles in either lipid layer may produce ion-conducting and nonconducting states, which may correspond to open and closed states, respectively.
2. Encounter–separation model of half channels may give rise to the open–closed transition.
3. Conformational fluctuations within the transmembrane aggregate produce the open–closed transitions.

Either or all of these processes may account for the open–closed transitions. The hypothetical scheme of supramolecular organization and open–closed transitions is summarized in Figure 5.

Figure 6 shows the proposed subunit assembly structure of the nicotinic acetylcholine receptor channel.[11] The inner wall of the lower half part is surrounded by hydroxyl side chains from Ser and Thr, and by carboxylates or amides from Asp, Glu, and Gln at the mouth. Furthermore, a Lys residue seems to offer ion pairing with the carboxylate at the mouth. Considering the possibly similar stabilizing effect of ether and hydroxyl groups to cations, the proposed artificial supramolecular channel could be regarded as a good model of the acetylcholine receptor channel, which selects cations over anions, but does not discriminate between alkali metals.

While the ion pair combination **1** is found to be a successful example to afford artificial ion channels, it may not be difficult to find analogous solutions. Illustrated in Figure 7 is a small expanded scheme for constructing artificial supramolecular ion channels from synthetic amphiphilic pairs of hydrophilic and hydrophobic counterions (note that the combination **2a–2e** corresponds to **1**). All of these compounds gave stable single-channel currents when incorporated into a bilayer lipid membrane.

In the supramolecular structure **4**, the hydrophilic component is assumed to be assembled at the inner surface of the channel to make an inner wall. Then the carboxylate anions are assembled at the inner mouth of the channel and may concentrate cations at the mouth of the channel. This may contribute significantly to the cation selectivity, which was tentatively explained by a stabilized coordination of oligoether oxygen in the membrane. In order to know which is important in determining the cation selectivity, combinations **2d–2f** and **2d–2g** were tested since these may concentrate anions at the channel mouth and give the reverse selectivity, if the charge at the mouth is a determining factor. Observed at the channel mouth were cation selectivities, with $P_{K^+}/P_{Cl^-}$ being 5 and 16.8 for **2d–2f** and **2d–2g**, respectively. Therefore, the important factor determining the ion selectivity is certainly not charges at the channel mouth, but the unit existing in the membrane phase. Compared to a **2a–2e** combination, a pair **2b–2e** having a longer separation unit between ether oxygens showed significant differences in single-channel char-

Separated Unit

Separated
Small Assembly

Interconnected
Small Assembly

Association-
Dissociation

Association-
Dissociation

Dynamic
Equilibrium

Separated
Half Channel

Conformationally
Closed

**Closed**

Encounter Dependent

Conformational Fluctuation

**Open**

Open Full Channel

**Channel Forming Amphiphile**
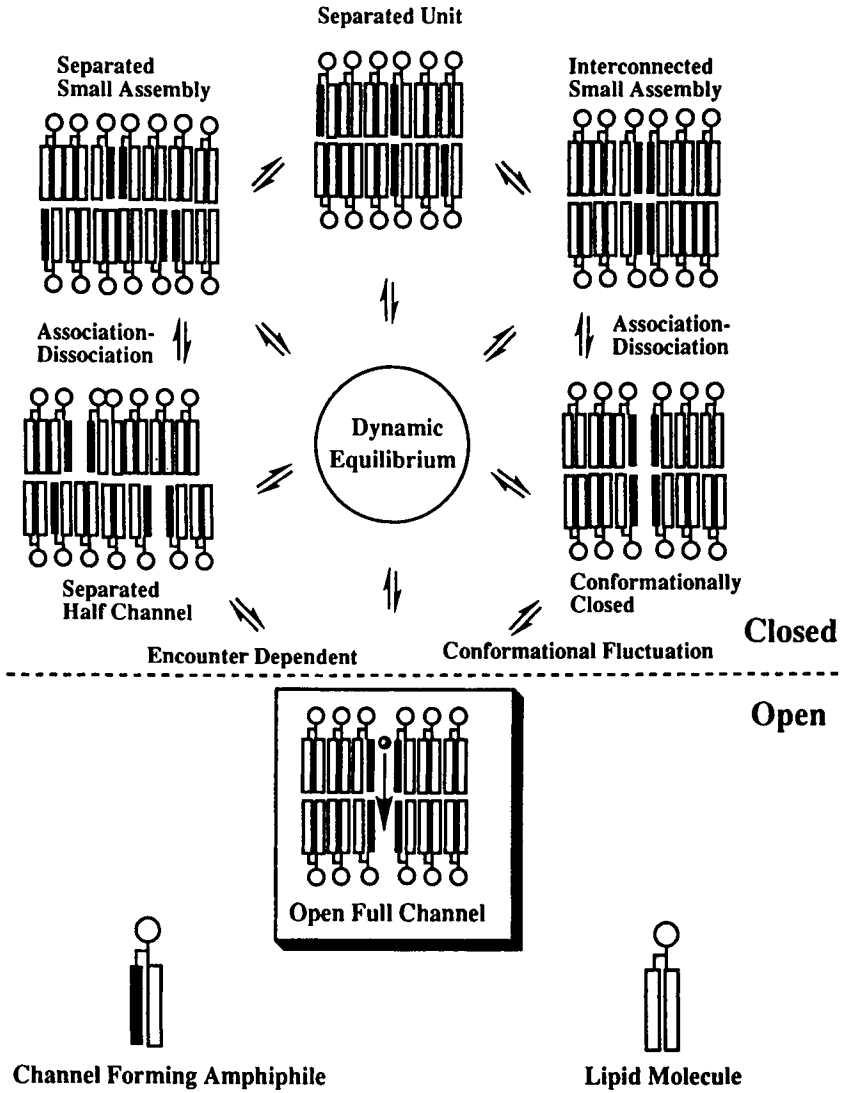
**Lipid Molecule**

*Figure 5.* Possible mechanisms of supramolecular organization of amphiphilic ion pair **1** to form the transmembrane channel and its open–closed transitions. The amphiphilic units are incorporated into bilayer lipid membrane and organized to the ion channel through aggregation and interconnection between two lipid layers. Ions can pass through the pore only when the aggregates are large enough, and interconnected between layers, and conformationally open.

OUT
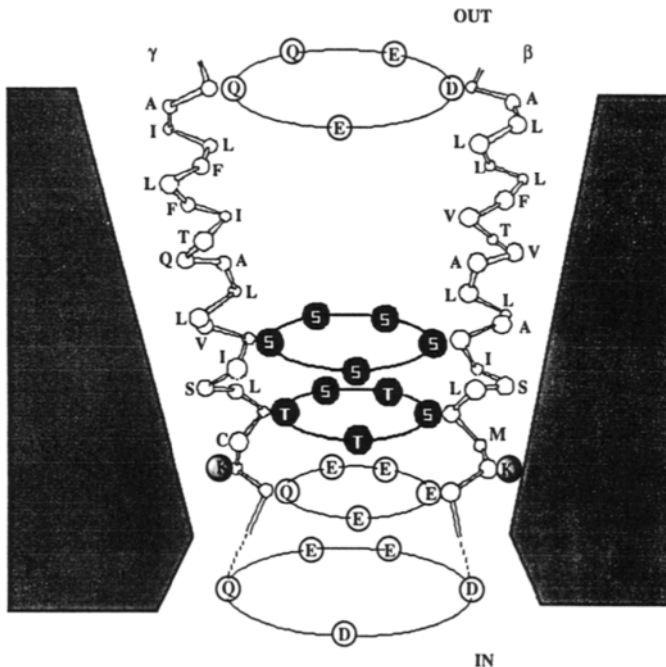


**Figure 6.** Proposed inner wall structure of the nicotinic acetylcholine receptor–channel composite from $\alpha_2\beta\gamma\delta$ subunit assembly.[11] The channel mouth is constructed from charged amino acids and their amides such as Asp, Glu, and Gln. A Lys is located at just the inner mouth. The lower half is covered by the amino acids having hydroxyl such as Ser and Thr, while the upper half is lined up with hydrophobic residues such as Leu, Val, Ala, Ile, and Phe.

acteristics. Small conductances near 8 pS were mostly observed; larger conductances in the order $10^1$–$10^2$ could not be observed. At the same time, two or three channels were incorporated frequently. Such behavior is compatible with expectations from a longer separation distance. The efficiency of metal ion fluxes may be decreased by a higher activation energy for the transfer of metal ions from one ether site to the next, but the increased hydrophobicity may favor the incorporation of the molecule into the membrane phase. The observed characteristics are in the range of expected structure–function relationship.

In view of the use of a similar repeating unit, tetramethylenecarboxyl, Seebach's approach should be included here.[67] He incorporated oligomers and polymers of 3-hydroxybutanoic acid (3-HB) into planar bilayers and observed single-channel currents. It is known that poly(3-HB) forms lamellar crystallites with thickness in the range of 40 to 60 Å when crystallized from dilute solutions. Therefore it is assumed that poly(3-HB) forms lamellar crystallites with a thickness of ca. 50 Å.
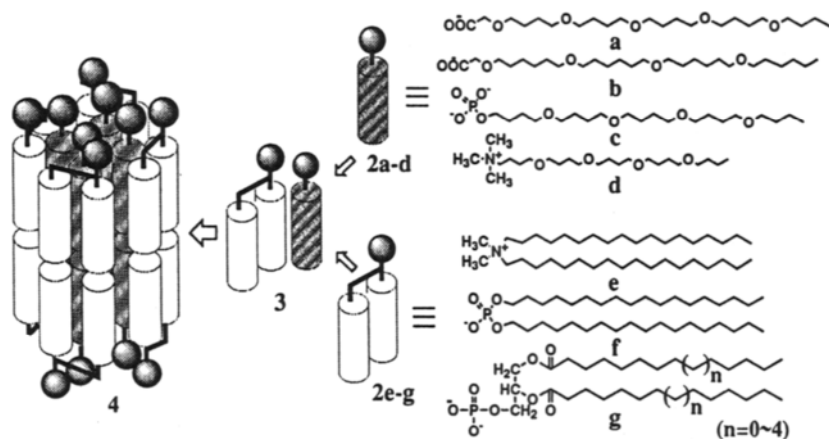
**Figure 7.** Schematic representation for the formation of supramolecular channel **4** from lipid units **2**. A relatively hydrophilic synthetic lipid component of oligoether structure **2a-d** is combined with appropriate counter ion having two hydrophobic alkyl chains **2e-g** to make doubly amphiphilic synthetic lipid **2**. Combinations **2c-2e** and **2d-2g** afforded voltage dependent channels as will be described later.

These hydrophobic crystallites fit properly into a planar bilayer by formation of H-bonds between the free end groups of the oligomers and the polar head groups of the phospholipids. In other words, a membrane contains islands of crystalline poly(3-HB) within the liquid crystalline phospholipid phase. A schematic representation is shown in Figure 8. Single-channel current fluctuations are assumed to



**3-Hydroxybutyrate oligomers**
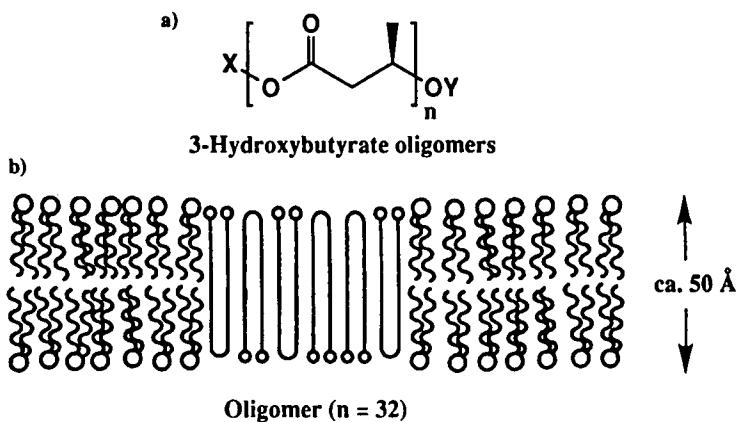


**Oligomer (n = 32)**

**Figure 8.** (a) Structure of oligomeric and poly(3-hydroxybutanoic acid). (b) Crystallite formation of oligo(3-HB) for the case $n = 32$ in planar phospholipid. The end group represents hydroxyl and carboxylic acid functionalities.[67]

be occurring at the interfacial regions between the phospholipids and the poly(3-HB) crystallites, and in a similar manner to the phenomena observed for phospholipid bilayers at their phase-transition temperature. Current–voltage measurement of stable currents may be a key for concluding the formation of channels of certain conductance levels.

## 2.2. Amphiphiles Containing an Oligo(oxyethylene) Unit

As a prototype of the polyene macrolide antibiotic, amphotericin B, Regen prepared a sterol–polyether conjugate, 5-androstene-3β,17β-bis[(oxycarbonyl)hexaethylene glycol] (5) (Figure 9).[68] Two flexible hydrophilic chains with a pendant hydroxyl head group was attached to a long and rigid hydrophobic steroidal unit in the hope that the molecule may exist as a "folded" conformation where one face of the steroid is covered by polyether and the other is not, bearing a facial amphiphile[69] structure. Monolayer aggregation experiments supported such a conformation. When 5 was incorporated into egg PC vesicles in the aqueous solution containing a shift reagent ($Dy^{3+}$) externally with $Na^+$(external)/$Li^+$(internal) gradient, a slow entry of $Na^+$ was detected directly by $^{23}Na$ NMR spectroscopy. Although the activity is low, the channel mechanism was suggested by the fact that the activity was similar both in gel-phase vesicles from dipalmitoyl phosphatidylcholine and in fluid-phase egg phosphatidylcholine. The kinetic order with respect to 5 was three to four, suggesting the aggregate channel structure.
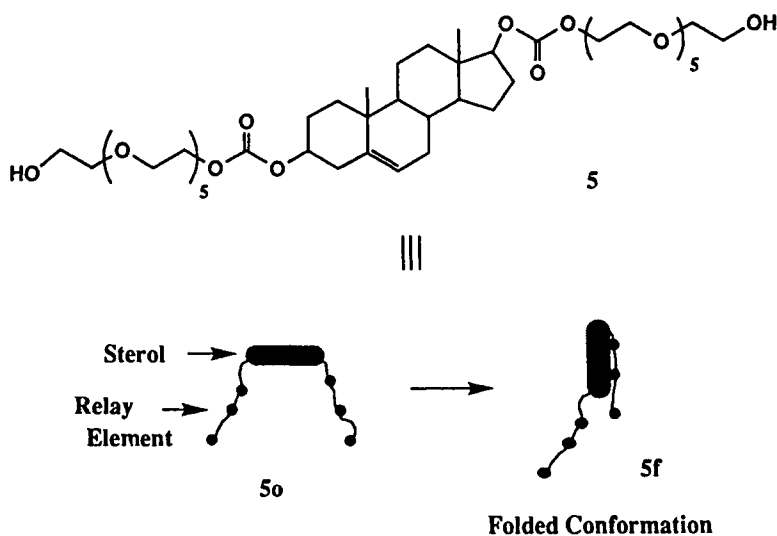


**Figure 9.** A sterol–polyether conjugate **5**, 5-androstene-3β,17β-bis[(oxycarbonyl)-hexaethylene glycol] could take a folded conformation **5f** and assemble upon insertion into lipid layers.[68]

Menger reports that $CH_3(CH_2)_{10}COO(CH_2CH_2O)_5CH_2Ph$ (**6**) fortuitously obtained but very specifically, conducts protons at extremely low concentrations and eventually faster than gramicidin.[70,71] The rate measurement relies on the decay of pH-sensitive fluorescent dye, pyranine, entrapped in vesicles by proton influx when proton potential was generated by adding HCl externally.[72] He explains the structure specificity by three sets of requirements: $S_1$, $S_2$, and $S_3$. The benzyl group anchors to the membrane surface through an ion–dipole attraction with quaternary nitrogen of the lipid head group,[73] the hydrophobic tail embeds the molecule in the membrane interior, and finally polyether moiety is thereby forced to span the leaflet and conduct ions. A minimum of two molecules of **6** are supposed to be aligned to permit passage protons across the membrane as shown in Figure 10. The channel mechanism was claimed because **6** was inert when it was used in a chloroform "liquid membrane".
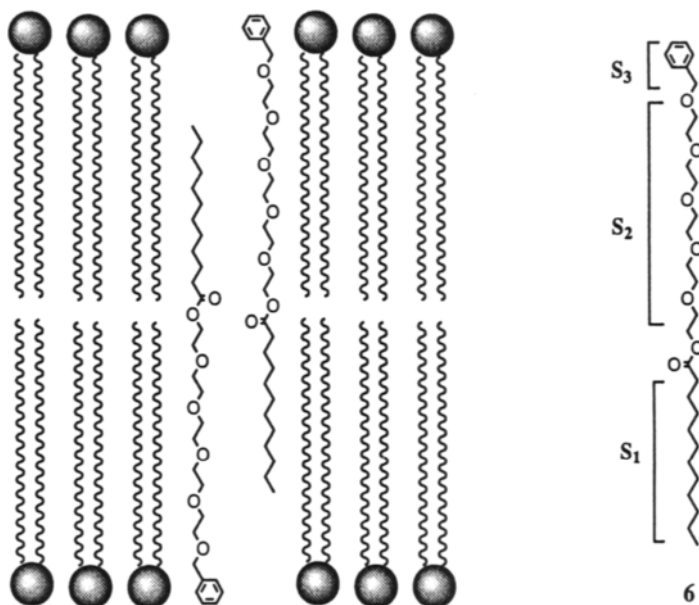


***Figure 10.*** The specific structure of flux-promoting compound **6**. $S_3$ anchors to the membrane surface through $N^+$-aromatic interaction and the hydrophobic $S_1$ locates in the interior membrane, thereby spanning the oxyethylene part $S_2$.[71]

## 2.3. Macroring D,L-Peptide Stacks

Recently, Ghadiri introduced a brilliant idea for the construction of a new class of artificial ion channels.[74–77] He employed an eight-residue 24-membered macro-

cyclic peptide with the sequence: cyclo[-(Trp-D-Leu)$_3$-Gln-D-Leu] 7. Alternating D- and L-amino acid sequence adopts a ring-shaped flat conformation. All backbone amide functionalities lie approximately perpendicular to the plane of the structure. Then the units stack in an antiparallel fashion with intermolecular hydrogen bonding to produce a contiguous β-sheet structure. In order to make the self-assembled molecule membrane-spanning, about eight to ten units are required to be stacked, assuming an average thickness of the membrane bilayer of 40–50 Å and intersubunit distance of about 4.7–5.0 Å. Here, the alternating D- and L-amino acid sequence extrudes all of the side chains in a plane extending outside the backbone structure. Such a structural arrangement may find an analogy with a gramicidin A channel. The nano structure assembly is illustrated in Figure 11. The hollow tubular structure is provided by a H-bond network to supply an internal medium of low dielectric constant. Its outside is covered with hydrophobic amino acid side chains.

The peptide subunit was easily incorporated into lipid bilayers of liposome, as confirmed by absorption and fluorescence spectroscopy. Formation of H-bonded transmembrane channel structure was confirmed by FT IR measurement, which suggests the formation of a tight H-bond network in phosphatidylcholine liposomes. Liposomes were first prepared to make the inside pH 6.5 and the outside pH 5.5. Then the addition of the peptide to such liposomal suspensions caused a rapid collapse of the pH gradient. The proton transport activity was comparable to that of antibiotics gramicidin A and amphotericin B.

Subsequently the ion channel activity was tested by single-channel current measurements using planar lipid bilayers. Single-channel conductances of ca. 55 in 500 mM NaCl and 65 pS in KCl were obtained. The weak ion selectivity was claimed to reflect a slightly larger mobility of K$^+$ compared to that of Na$^+$ ion in bulk solution. Therefore a large 7.5-Å pore structure in lipid bilayers is assumed to resemble the bulk aqueous solution.

A unique advantage of this strategy is that the internal diameter of the tubular ensemble can be adjusted by simply varying the ring size of the peptide subunit. Then a 10-residue, hydrophobic peptide subunit, cyclo[Gln-(D-Leu-Trp)$_4$-D-Leu], was prepared. Upon self-assembling it produces tubular ensembles having a uniform 10 Å internal diameter, which is large enough to pass glucose. The glucose transport rate was linearly dependent on the glucose concentration and did not obey Michaelis–Menten saturation kinetics, suggesting a simple transmembrane channel-mediated diffusion process. Furthermore, neither gramicidin A having an internal diameter of approximately 4.5 Å, nor cyclo[Gln-(D-Leu-Trp)$_3$-D-Leu], having an internal diameter of approximately 7.5 Å, displayed any glucose transport activity. Therefore the mechanism of size-selective, pore-mediated transport of glucose was strongly supported.
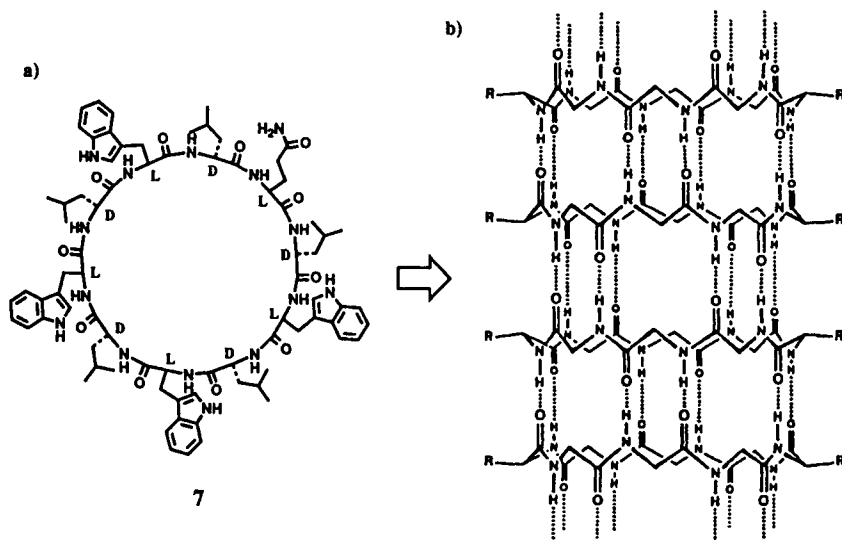
**Figure 11.** (a) The chemical structure of a 24-membered macrocyclic molecule composed of alternating D- and L-amino acids, cyclo[Gln-(D-Leu-Trp)4-D-Leu] 7. (b) A self-assembled tubular structure spanned across the bilayer lipid membrane. Flat ring-shaped units in the antiparallel configuration stack to form a tubular structure through extensive inter subunit hydrogen bonding and peptide side chain–lipid interactions.[75]

## 3. BIMOLECULAR CHANNELS FROM MACROCYCLE*

### 3.1. Resorcin[4]arene-Based[78]

Observation of several single-channel conductances in supramolecular channels is ascribed to reflect different aggregation numbers. Then, if a unimolecular macrocyclic compound defines the channel structure, it may afford only a single conductance level without any other heterogeneous levels. Such a candidate is macrocyclic resorcinol tetramer **8**, which develops a H-bond network between adjacent phenolic hydroxyl groups to give rise to a bowl-shaped rigid conformation. All the alkyl chains are known to be in an axial and *cis* configuration.[79] The small aromatic pore may differentiate alkali metal families, e.g., $K^+$ from $Na^+$. Eight phenolic hydroxyl groups are partly dissociated even at neutral pH to act as the head group and long alkyl chains are insertable into the molecule by the choice of the condensing agent of alkanals. Therefore, resorcinol was condensed with octadecanal under acidic conditions to afford amphiphilic cyclic tetramer **8** in a simple

one-batch reaction. The octanal was chosen so that the alkyl chain length may fit the lipid layer of soybean lecithin.

The expected channel shown in Figure 12 is of a bimolecular structure. The rigid channel mouth may prohibit the consecutive long alkyl chains from assembling themselves and to prevent lipid molecules from invading the area. The space thus provided may accommodate water molecules to make the domain sufficiently hydrophilic to pass ions. Such a domain would recognize its counterpart located in another lipid layer to make a tail-to-tail dimer of **8**, i.e. a symmetric transmembrane channel, as in the case of Gramicidin A dimer.[†]

A premixture of **8** and soybean lecithin gave stable single channel currents with well-defined transitions between open and closed states with the 0.1-1s time scale. The conductance level detected was $6.1 \pm 0.5$ pS at 0.5 M KCl solution. At various transmembrane voltages with different molar ratios of **8**-to-lipid in the range 1/200 ~ 1/3000, an identical conductance level was always observed. This observation is therefore compatible with the original idea that monomeric **8** itself defines a pore mouth with a specified diameter in the single lipid layer. It gave a cation/anion
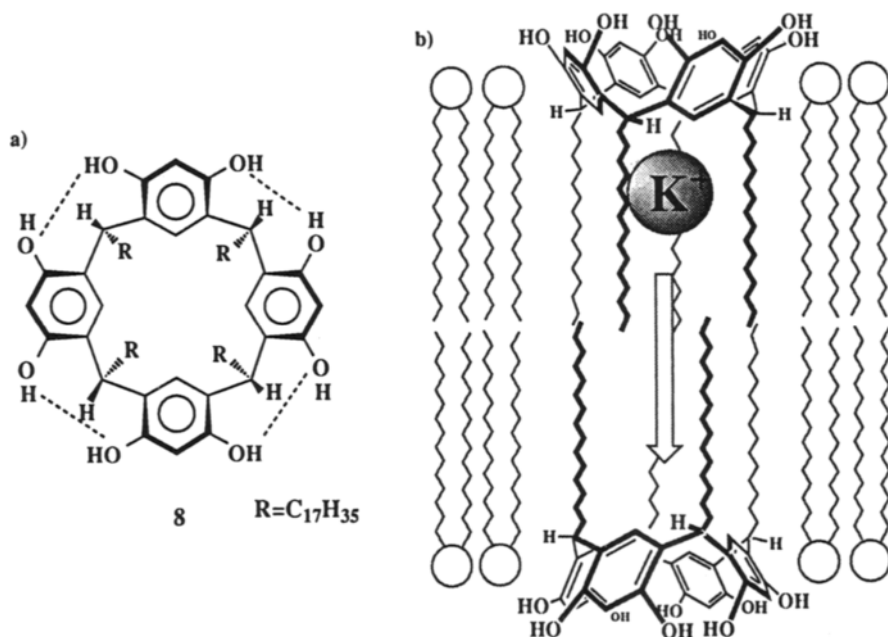


**Figure 12.** (a) Macrocyclic resorcinol tetramer **8** has a rigid bowl shaped conformation with the long alkyl tails in an all-axial and all-*cis* configuration. (b) Model of $K^+$ flow in a hypothetical bimolecular ion channel composed of tail–tail dimer of **8**. The ion passes through the inner pore of macrocyclic resorcinol unit which acts as a selectivity filter and then to the area formed by the loose assembly of long alkyls.[78]

permeability ratio ($P_{K^+}/P_{Cl^-}$) of 20. Furthermore, the channel discriminated $K^+$ over $Na^+$ with a permeability ratio ($P_{K^+}/P_{Na^+}$) of ca. 3. In contrast, $Rb^+$ blocked the $K^+$ current: the biionic solution containing $Rb^+$ [(50 mM KCl + 450 mM RbCl)/(450 mM KCl + 50 mM RbCl), or vice versa] provided little stable channel current in 20 independent experiments. Once the biionic solution switched to symmetric 500 mM KCl solutions, however, $K^+$ currents appeared immediately. The blocking behavior finally excludes the formation of aggregated channel from **8**. With such a significant selectivity, this channel is regarded as an *artificial bimolecular $K^+$ channel*.

Ion selectivity is determined primarily by the narrowest region of the channel pore, termed the "selectivity filter". The relation between the electric field strength of the selectivity filter and the dehydration energy of the permeating ion determines the extent of dehydration; the resulting ion with the corresponding hydration states is then discriminated by molecular sieving. The narrowest ion-conducting pore comprises four resorcinol rings and provides only a weak electric field which allows full dehydration of $K^+$ fully but fails to produce naked $Na^+$. The size of this selectivity filter resembles that of the pore of *p-tert*-butyl-calix[4]arenetetraamide, which permits $K^+$ (r = 1.33 Å) but not $Cs^+$ (r = 1.69 Å) to pass through, on the basis of molecular dynamics simulation.[80] The rigid macrocyclic cage seems to be just enough to pass $K^+$ and even blocked by $Rb^+$ (r = 1.47 Å). The negative π-cloud on the aromatic face, although weak in producing the electric field, should contribute to lower the potential barrier for passing $K^+$ through attractive cation–π interactions. A stabilizing interaction between $K^+$ and π-electrons on the face of aromatic rings has been proposed to interpret the selectivity of $K^+$ channels.[81–84] It is interesting to note also that the selectivity filter of $K^+$ channel has been suggested to comprise four tyrosine residues by recent point mutation studies.[85,86] Therefore, all of the information from natural $K^+$ channels seems to support the appropriateness of the molecular design of the $K^+$-selective artificial channel.

### 3.2. Cyclodextrin-Based

The very first trial for obtaining artificial channels was reported early in 1982 by Tabushi who synthesized A,B,D,F-tetra-6-*n*-butyrylaminohexylsulfenyl)-β-cyclodextrin, a β-cyclodextrin substituted at four primary hydroxyl sites out of seven by long alkyl thioethers having amide functionality for the ion-stabilizing site in the central membrane.[87] The ion channel activity is based on the finding that the $Co^{2+}$ transport followed second-order kinetics with respect to the concentration of substituted cyclodextrin in the membrane in a range of 0–55 μM, while $Cu^{2+}$ transport followed first-order kinetics with a lower activity. The second-order rate for $Co^{2+}$ matches the mechanism of putative transmembrane channel formation by encountering two components in lipid bilayers. The question is: why do $Co^{2+}$ and $Cu^{2+}$ ions show different behavior? Further, the transport rates have also been reported to be sensitive to the types of potential gradients applied across the

membrane. Unfortunately answers did not appear before Tabushi's early death in 1987. These answers may now be obtained because closely related compounds are being actively investigated as ion channels.

Once the concept of a bimolecular half-channel is established, many macrocyclic compounds can be utilized as a unit for constructing artificial ion channels. It may be useful for a basic structural unit, a channel mouth part, a receptor site, or many other functional units of channels depending on their own molecular design. Among various candidates, cyclodextrin may be interesting from several points of view. It provides in aqueous media a rigid hydrophobic inner space, where guest molecules are included. Regioselective reactions on primary and secondary hydroxyls have been scrutinized extensively and selective introductions of desired functional groups at the desirable positions are now even possible.

Therefore, the authors have synthesized heptakis(carboxymethyl)-substituted α-cyclodextrin which was combined with hydrophobic ammonium to afford **9** (Figure 13), whereby the number of carboxylate–ammonium ion pairs was regulated to six. This compound was incorporated into BLM and subjected to single-channel current measurements. The current–voltage plot gave a single straight line to afford a conductance level of 7.7 pS under several different experimental conditions. Then the modified cyclodextrin successfully controlled the ion channel structure and therefore the conductance.

Cyclodextrin-substituted molecular channel approaches have now been extended to include acyl substituents through a covalent bond formation. Stearoyl and methyl cholate-substituted cyclodextrins **10** and **11**, respectively, have been synthesized. It may be worthwhile commenting on the molecular design of methyl cholate-substituted α-cyclodextrin. All of the ether groupings are convergent at the inner side of the steroidal backbone of a bent structure to make the molecule amphiphilic. Once the cyclodextrin derivative is incorporated into the membrane phase, it may easily be expected that the ether parts are assembled inside the channel in the sea of hydrophobic lipid molecules and the hydrophobic steroidal skeletons cover its outside to stabilize the inner hydrophilic pore (Figure 13).

Two covalent channel models **10** and **11** also afforded single conductances of 7.5 and 10.2 pS, respectively. The larger conductance of **11** may be accounted for by the increased hydrophilicity of the pore wall. Interestingly, the bimolecular ion channels examined here afforded cation selectivities, $P_K/P_{Cl}$ for **8**, **9**, **10**, and **11** being 20, 29, 14, and 7, respectively. All the helical bundle channels hitherto reported also showed cation selectivities. Furthermore, macrocyclic channels containing long alkyl groups **8**, **9**, and **10** gave large cation selectivity ratios. In contrast, the cation selectivity of **11** having a hypothetical ether-networked inner wall decreased and approached the value obtained by oligoether channels **1** ($P_K/P_{Cl} =$ 5). The increase of hydrophobicity of the pore wall apparently seems to favor the cation selectivity. However, it may be too early to draw any conclusive reasons for these selectivity ratios at present. The pore nature by the combination of macrocyclic mouth and hydrophobic long alkyl tails may need further investigation. It may

a)

b)



$R =$
$-COCH_2COO^-$
$^+N(CH_3)_2(CH_2)_{17}CH_3$  **9**

$-CO(CH_2)_{16}CH_3$  **10**

**11**
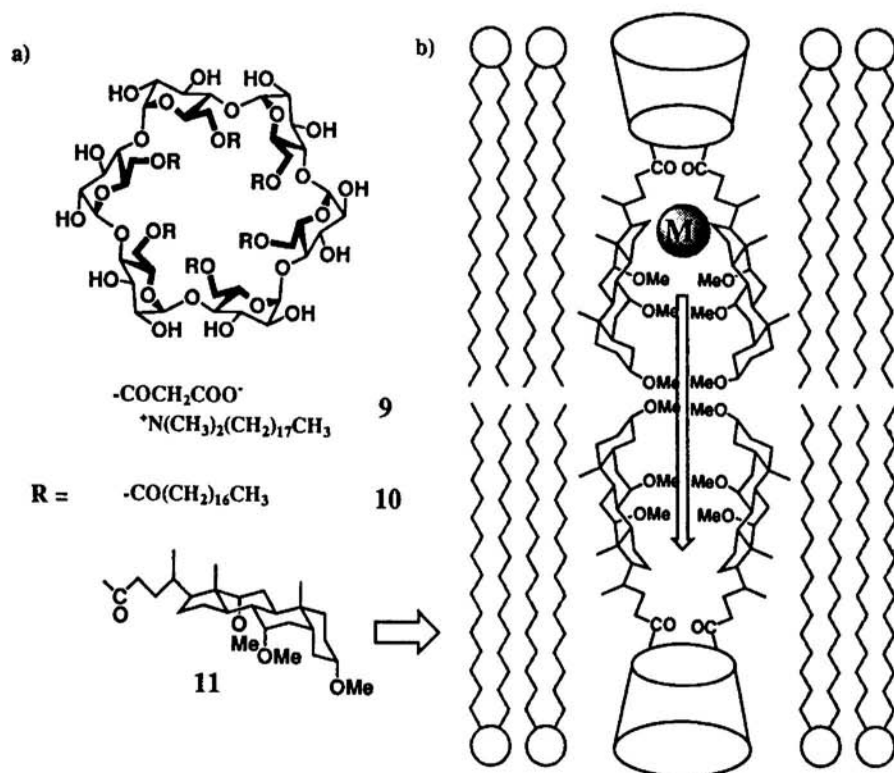
**Figure 13.** α-Cyclodextrin-based bimolecular ion channels. **(a)** Hexa(carboxymethyl)-substituted α-cyclodextrin combined with dioctadecyldimethylammonium cation to afford hexa ion pairs **9**, hexa(stearoyl)substituted α-cyclodextrin **10**, and hexa(trimethylcholyl)-substituted α-cyclodextrin **11**. **(b)** A hypothetical side view for the passage of metal ion through a hydrophilic channel wall comprised of ether network convergently extended from steroidal backbone.

also be a challenging target to synthesize any anion selective channel, which may really answer the true reason for these selectivities.

## 4. UNIMOLECULAR CHANNELS

Much interest for ion transport has its origin in the field of crown ether chemistry. Therefore, most model studies of ion channels have been more or less based on crown ether chemistries. Pioneering work has been undertaken by Fyles, who not only synthesized varieties of gigantic molecules starting from crown ethers,[88-91] but established a method of the rate assay for ion transport across lipid bilayer membranes, a pH stat technique.[92-95] Vesicles having different inside and outside

pHs were prepared. The addition of a proton carrier FCCP (1,3-dinitrilo-2-propanone (4-(trifluoromethoxy)phenyl)hydrazone) and the transporter has little effect on the slow rate of proton efflux due to the gradual collapse of the pH gradient. Upon addition of metal ion, a *trans*-membrane cation gradient is established and starts to collapse rapidly via cation/proton countertransport to maintain the electroneutrality in the vesicle, if the transporter is active. The proton efflux can then be determined by the addition of a base to maintain the external pH. Efflux rate eventually slows to the background rate, whereupon addition of Triton X100 provokes complete vesicle lysis and releases any entrapped buffer. Then the rate constant for the metal ion influx can be estimated from the first-order rate analysis.

According to this method, Fyles analyzed the transport rate of alkali metal cations for a series of 21 synthetic transporters (Figure 14). The whole molecules were designed to elucidate the structure–function relationship. They are composed of three parts: core, wall, and head units. The core units were derived from tartaric acids so that the wall units may be fixed to provide structural control by incorporating both the polar and nonpolar functionality (Y and Z in Figure 14). The head groups (X) are attached to provide an overall amphiphilic nature.

Transport activity was controlled by structural variables; the most active materials had hydrophilic head groups, a balance of hydrophilic and lipophilic groups in the wall units, and overall length compatible with the bilayer thickness. The relative activities of the most active synthetic transporters were comparable to valinomycin but a factor of 2–20-fold less active than gramicidin. Some of the synthetic transporters showed an interesting cation selectivity among alkali metals. Selectivity patterns relative to $Na^+$ are illustrated in Figure 15. The most active transporter $(G8TrgP)_4Tet$ was strongly $Na^+$-selective, while the isomeric $(G8TrgP)_4mTet$, the second active one, was strongly $K^+$-selective with the $Na^+/K^+$ selectivity ratios being 3.3 and 0.19, respectively.

The "peak" metal ion selectivity observed in some cases followed the Eisenman III/IV selectivity sequence typical of many crown ether cation complexes.[96] However, the $Na^+$-selective patterns of $(G8TrgP)_4Tet$, $(A8_2P)_4Tet$, $(A8TrgP)_4Tet$, and possibly $(A8TrgP)_6Hex$ were not related to any Eisenman selectivity sequences, indicating that equilibrium ion binding cannot be the rate-limiting process. In some cases, transport of one cation was inhibited by the addition of another cation. Since the carrier mechanism is known to give rise to an enhancement rather than inhibition of the transport rate, the observation of significant inhibition may indicate the channel mechanism. These data along with zero-th order transport kinetics have been proposed as criteria to recognize the channel-like transporter. According to these criteria, transporters were classified into channel and carrier types, which were marked by circle and square, respectively in Figure 15. Probable carriers were found among the derivatives of the Di core unit, while channel-like transporters were derivatives of the Tet and Hex core units. The wall units $8_2$, 8Trg, and $5_2$ seem to be suitable for either mode of action, but a balance of lipophilic character is essential for active materials. The case of the isomers Tet and mTet is particularly

Head

Wall

Core

= R

(G8TrgP)₆Hex

184

Core units

Wall units

mDi   Di   mTet   Tet   Hex

(A8₂P)₄Tet ○

(G8₂P)₂Di □

(G8₂P)₄Tet ○   (G8₂P)₆Hex

(P8₂P)₄Tet

8₂
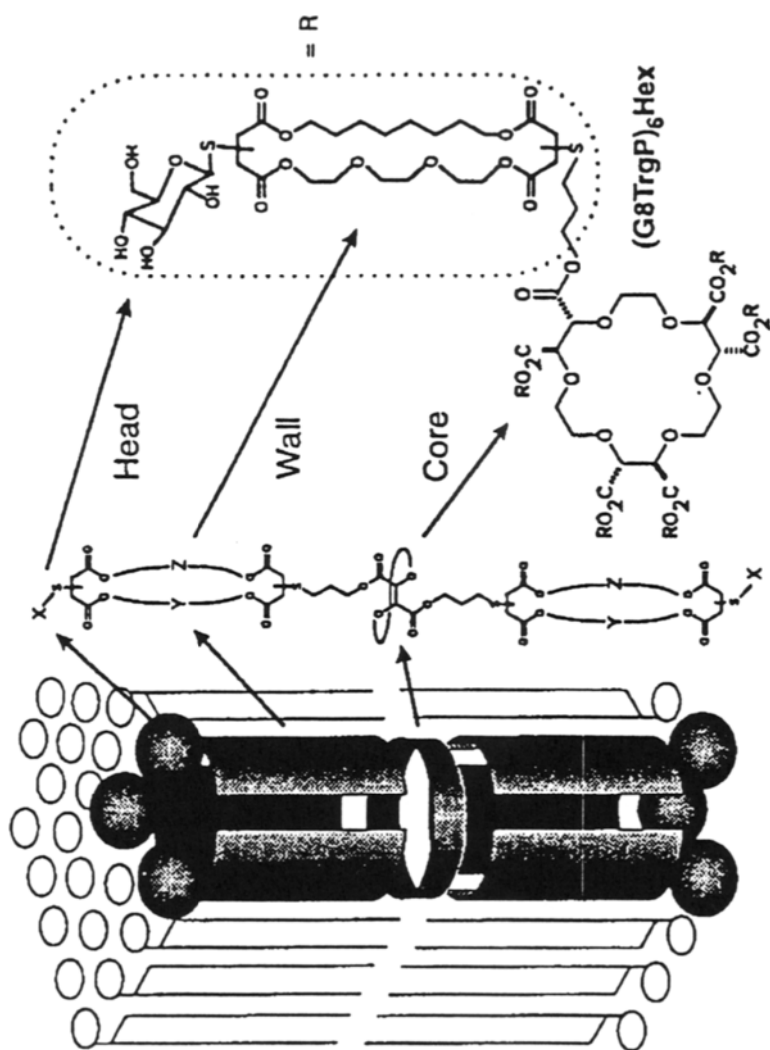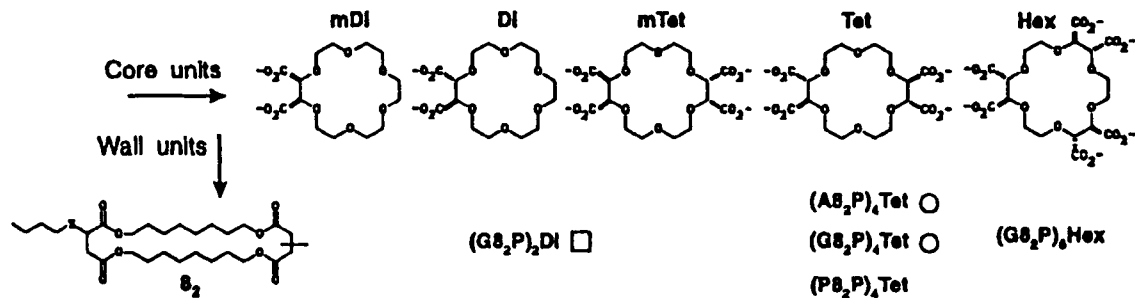
**Figure 14.** A general view of the designed transporter, which is composed of three units.[91] The "core" unit lying near the bilayer mid-plane with "wall" units radiating from it. The core unit provides a rigid framework to direct the wall units to the face of the bilayer. The wall units are stiff to provide structural control, and incorporate both the polar and nonpolar functionality (Y, Z) required for a channel. The structure is completed with hydrophilic "head" groups (X) to provide overall amphiphilic character and to assist in the transmembrane orientation of the molecule.

(G8TrgP)₂mDl (G8TrgP)₂Dl (G8TrgP)₄mTet ☐

(A8TrgP)₄Tet ○    (A8TrgP)₄Hex
(G8TrgP)₄Tet ○    (G8TrgP)₄Hex ○
(P8TrgP)₄Tet      (P8TrgP)₄Hex

(G5₂P)₂Dl ☐       (G5₂P)₄Tet ○

(G12₂P)₂Dl        (G12₂P)₄Tet

(GTrg₂P)₂Dl       (GTrg₂P)₄Tet    (GTrg₂P)₄Hex

Head groups ⟶   G   A   P
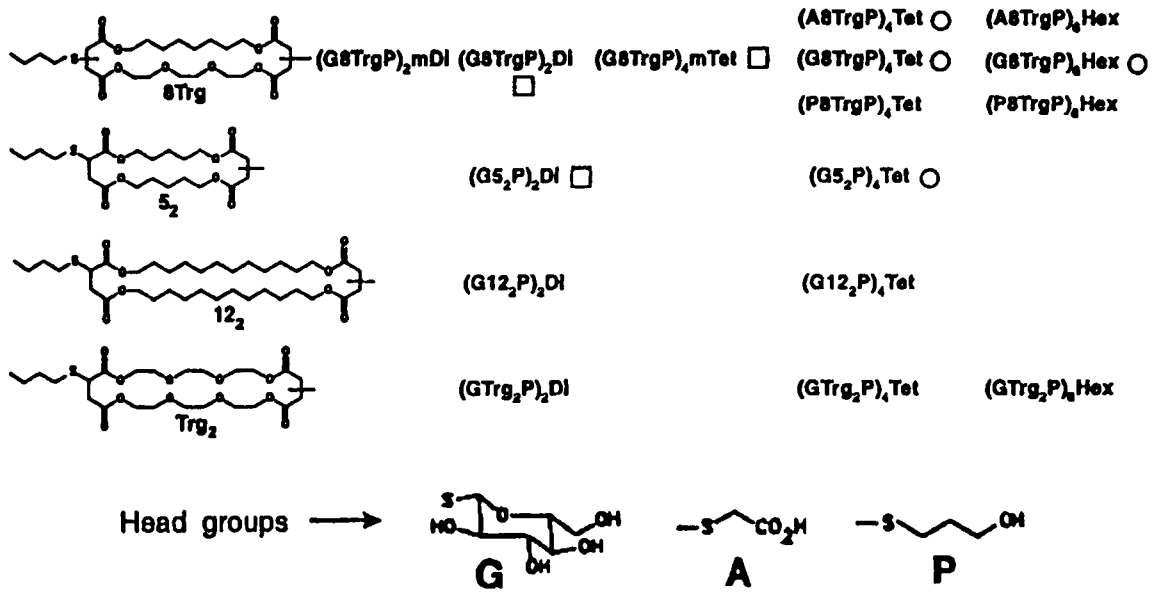
**Figure 14.**  (Continued)
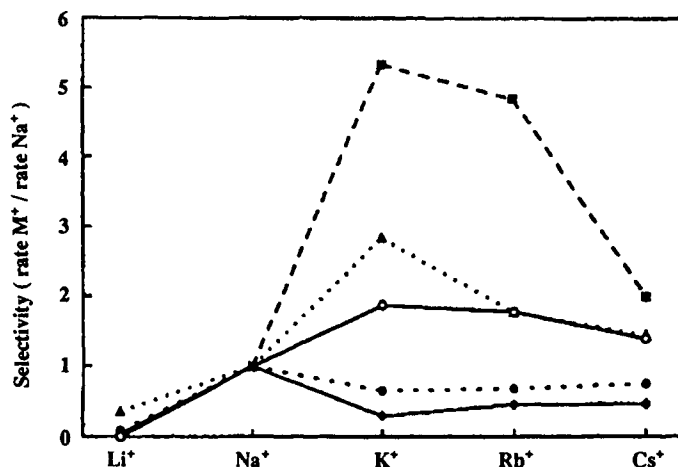
**Figure 15.** Selectivity of transport rate of alkali metal cations relative to Na⁺ by active transporters: (G8TrgP)4mTet (■), (G8TrgP)6Hex(△), (G82P)2Di (○), (A82P)4Tet (●), (G8Trg)4Tet (♦).[91]

instructive. The marked conformational preference for an *anti* relationship between the carboxylate groups, if translated to the transporter molecule as a whole, would give columnar structures similar to those depicted in Figure 15 for Tet derivatives, but would give Y-shaped structures for derivatives of mTet. The marked differences between the isomeric transporters (G8TrgP)$_4$Tet and (G8TrgP)$_4$mTet must be related to the basic conformational differences, implying a very strong structural control.

Nolte introduced stacked arrays of benzo-18-crown-6 by using rigid helices of isocyanide polymer (R–N=C<)$n$. Since the polymer has four repeating units per helical turn,[97-99] four crown ether rings run parallel to the polymer helix axis (Figure 16). The compound **12** was incorporated into dihexadecyl phosphate 4-(2-pyridylazo)resorcinol monosodium salt (DHP) vesicles and the permeability of $Co^{2+}$ ion was monitored by the absorption change of entrapped PAR at ~400 nm or the increase in absorption of the $Co^{2+}$–PAR complex at 510 nm. Channel compound **12** was found to have a pronounced effect on the ion permeability of the DHP vesicle bilayer. The Arrhenius activation energy ($E_a$ = 24 kJ mol$^{-1}$) was comparable to that found for ion channel antibiotics Gramicidin A ($E_a$ = 20.5–22.5 kJ mol$^{-1}$),[100] which is significantly lower than those for a carrier transport mechanism ($E_a$ = 90–120 kJ mol$^{-1}$).[101] The electroneutrality in the vesicles seems to be maintained by a countertransport of protons, as monitored by the shift in $\lambda_{max}$ value of entrapped, uncomplexed PAR.

Gokel prepared a series of novel bis- and tris(macrocyclic) compounds, which have been designed as models for cation-conducting channels that function in
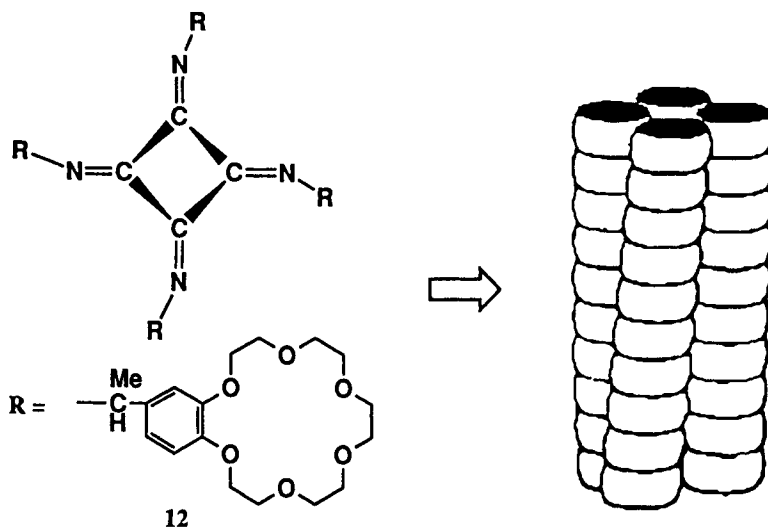
**Figure 16.** Isocyanide polymer $(R-N=C<)_n$ containing benzo-18-crown-6 sidechains **12**. Rigid helices with four repeating units per helical turn arrange the crown ether rings on top of each other and four channel structures are formed.[99]

phospholipid bilayer vesicle membranes.[102–105] His basic design has a central cation relay unit which was connected by several spacer units to two distal crown ethers, which may anchor as head groups to the whole molecule in an extended conformation and function as a cation entry point. Therefore molecules of the general structure "sidearm-crown-spacer-crown-spacer-crown-sidearm" **13** equipped with or without (for control) the above requisites have been prepared to assess the structure–activity relationship (Figure 17).

The ionophores have been incorporated into the vesicle membranes and cation flux was assessed either by monitoring the fluorescence of pyranine dye encapsulated within vesicles for estimating the proton transport rate or by analyzing the line shape of $^{23}Na$ nucleus by NMR spectroscopy to evaluate the flux rate of $Na^+$.[106–110] The flux data of ionophores were expressed by percent activity relative to the rate with gramicidin as 39, 28, 28, 25, and 14 for **13g**, **13a**, **13h**, **13e**, and **13f**, respectively. Others showed significantly less or no activity. It may be remarkable that synthetic ionophores showed cation conduction of as much as 40% of the activity of gramicidin. All of five active ionophores have a general structure— diazacrown-$C_{12}$ spacer-central unit-$C_{12}$ spacer-diazacrown—that can span the membrane. The central macroring enhances the flux a little bit compared to an open-chain analogue (cf. **13a**, **13e**, with **13f**), but the ionophore does not require a tunnel-like conformation in order to function. Introduction of hydrophilic spaces (**13b**, **13c**, and **13d**) cancel the activity. The distal crowns are important as anchors once protonated, since the deletion of one of the N-atoms (cf. **13h** with **13i**) loses
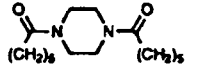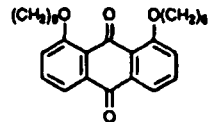
the activity. Steroidal units as spacers seem to "close" the channel or at least dramatically impede the cation transport. It is suggested that two or more molecules are assembled in the membrane phase.

Voyer employed a rigid peptide helix for the columnar stacking of benzo-type crown ethers.[111,112] Therefore, six 21-crown-7 units were introduced in **14** via attachment to L-phenylalanine into a 21 amino acid peptide composed of 15 L-leucines and six L-phenylalanine, whose incorporation position was chosen at 2, 3, 8, 13, 16, and 20 of the sequence (Figure 18). Since these amino acids have a high tendency to form the $\alpha$-helix conformation, the crown ethers are expected to be all located on the same side of the helix and form a transmembrane channel for ions. Circular dichroism studies of **14** and similarly designed tubular hexacrown peptides[111] in trifluoroethanol demonstrated that these peptides adopt a stable $\alpha$-helix conformation, which suggests that the ligand side chains are positioned on the same side of the helix. The ion transport ability was monitored through a pH stat technique.[112] Upon addition of a transporter to the outer aqueous solution of unilamellar vesicle containing $H^+$ carrier under a $Cs^+$ concentration gradient as well as a pH gradient, a rapid release of $H^+$ has been observed. No $H^+$ release was observed before the addition of the transporter and the rapid increase on the addition of the transporter results from the neutralization of $Cs^+$ influx by the efflux of $H^+$ to maintain the electroneutrality of the vesicle inside. The release rate of protons was rapid and comparable to gramicidin A, although the monomeric crown ether and the heptapeptide, too short to span the membrane, behaved as typical carriers by slowly and constantly transporting $Cs^+$ at a similar rate. The transport rates of $Li^+$, $Na^+$, $K^+$, and $Rb^+$ were similar to that of $Cs^+$.

Fuhrhop tackled artificial ion channels in his own unique way and introduced a modified monensin **15** by the attachment of monopyromellitic ester at the hydroxyl terminus to prohibit the formation of cyclic conformation, which is well known to be an active form for complexing with alkali metal ions, and to induce a stretched conformation.[113,114] When this amphiphile was co-sonicated with an $\alpha,\omega$-bifunctional amphiphile, a bola-amphiphile **16a**, which forms extremely thin (20 Å) monolayered vesicle membrane, no lithium ion was entrapped in the resulting vesicles (Figure 19). Without the addition or with a small incorporation of **15**, bola-amphiphile vesicles entrapped lithium ion within the inner aqueous volume. When dipalmitoylphosphatidyl–choline bilayer membrane vesicles were employed, no leakage of lithium occurred. Therefore, the lithium ion must be released across the thin monolayer membrane of bola-amphiphile probably through an ion channel assembly. Then the channel forming unit **15** was co-sonicated with an uncharged membrane component **16b**. Lithium permeable membranes were obtained only at relatively high concentrations of **15** in the neutral membrane. Under such a condition, the pore from the negatively charged channel forming unit **16b** was sealed by the use of positively charged bola-amphiphiles **17**. The channel blocking experiment is critical for proving the ion channel. Unfortunately in this
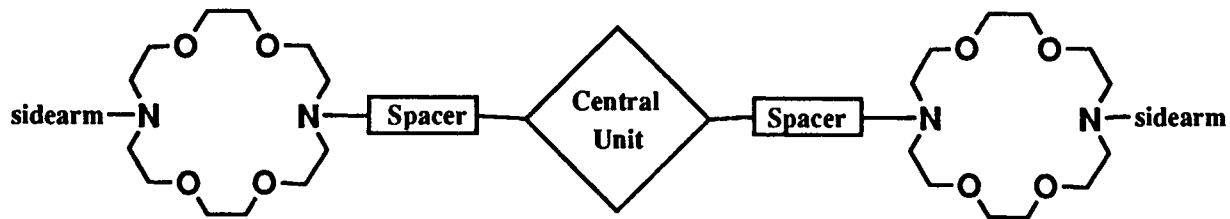
**13**

| no. | sidearms | spacers | central unit | distal crowns |
|---|---|---|---|---|
| 13 a | $C_{12}H_{25}$ | $C_{12}H_{24}$ | <N18N> | <N18N> |
| b | $C_{12}H_{25}$ | EOEOEOE | <N18N> | <N18N> |
| c | $C_{12}H_{25}$ | (piperazine diacyl structure) | <N18N> | <N18N> |
| d | $C_{12}H_{25}$ | (anthraquinone dialkoxy structure) | <N18N> | <N18N> |
| e | $C_{12}H_{25}$ | $C_{12}H_{24}$ | <N15N> | <N18N> |
| f | $C_{12}H_{25}$ | $C_{12}H_{24}$ | OEOEOEO | <N18N> |
| g | $C_6H_5CH_2$ | $C_{12}H_{24}$ | <N18N> | <N18N> |
| h | H | $C_{12}H_{24}$ | <N18N> | <N18N> |
| i | – | $C_{12}H_{24}$ | <N18N> | <N18> |
| j | $CH_2CH_2O$-3-cholestanyl | $C_{12}H_{24}$ | <N18N> | <N18N> |
| k | $CH_2COO$-3-cholestanyl | $C_{12}H_{24}$ | <N18N> | <N18N> |
| l | $C_{12}H_{25}$ | | <N18N> | |
| m | $C_6H_5CH_2$ | | <N18N> | |
| n | $C_{12}H_{25}$ | $C_{12}H_{24}$ (1) | <N18N> | <N18N> (1) |

**13a**
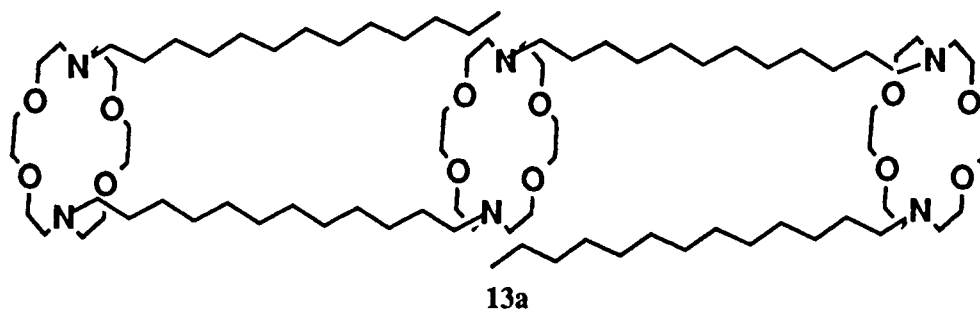
***Figure 17.*** Synthetic model compounds having generalized structure **13** to assess the bilayer cation flux.[105] <N18N>: Diaza-18-crown-6, OE: Oxyethylene, <N18>: Monoaza-18-crown-6.
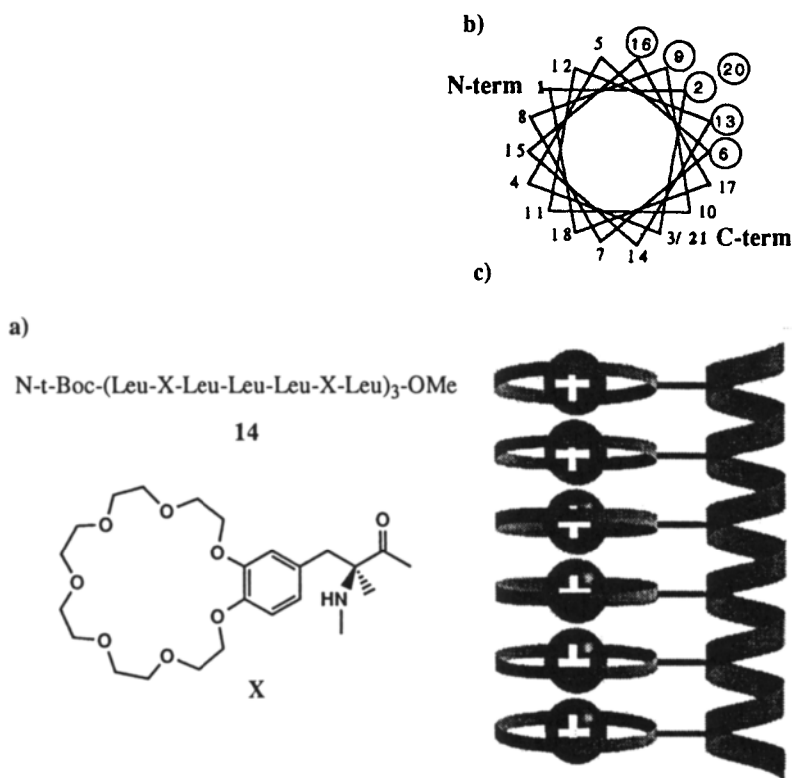
**Figure 18.** (a) Transmembrane channel molecule **14** with 21 amino acid peptide composed of 15 L-leucines and 6 21-crown-7-L-phenylalanine. (b) Axial projection of the helix. (c) Side view of the channel structure.[112]

case, however, the rate process of leakage itself has not been traced in the whole experiment.

"Bouquet" molecules, grafting poly(oxyethylene) or polymethylene chains bearing charged endgroups onto a cyclodextrin- or 18-crown-6 core were Lehn's approach to artificial ion channels.[115–118] Alkali metal ions in the aqueous solution inside and outside the liposomes were differentiated by adding a shift reagent ($Dy^{3+}$) to the external aqueous solution and two resonance signals—shifted (external) and unshifted (internal)—were directly observed under the opposing gradients of $Na^+$ and $Li^+$ ion concentrations across the membrane. This system allowed determinations of both influx of $Na^+$ ions into liposomes and efflux of $Li^+$ ions by monitoring $^{23}Na$ and $^7Li$ nuclei simultaneously. Observed were almost identical values, which established the mechanism of $Na^+$–$Li^+$ one-for-one antiport transport.

A carrier mechanism was excluded for these molecules when ion-transport activity was undiminished in membranes in the gel state. The transport rates
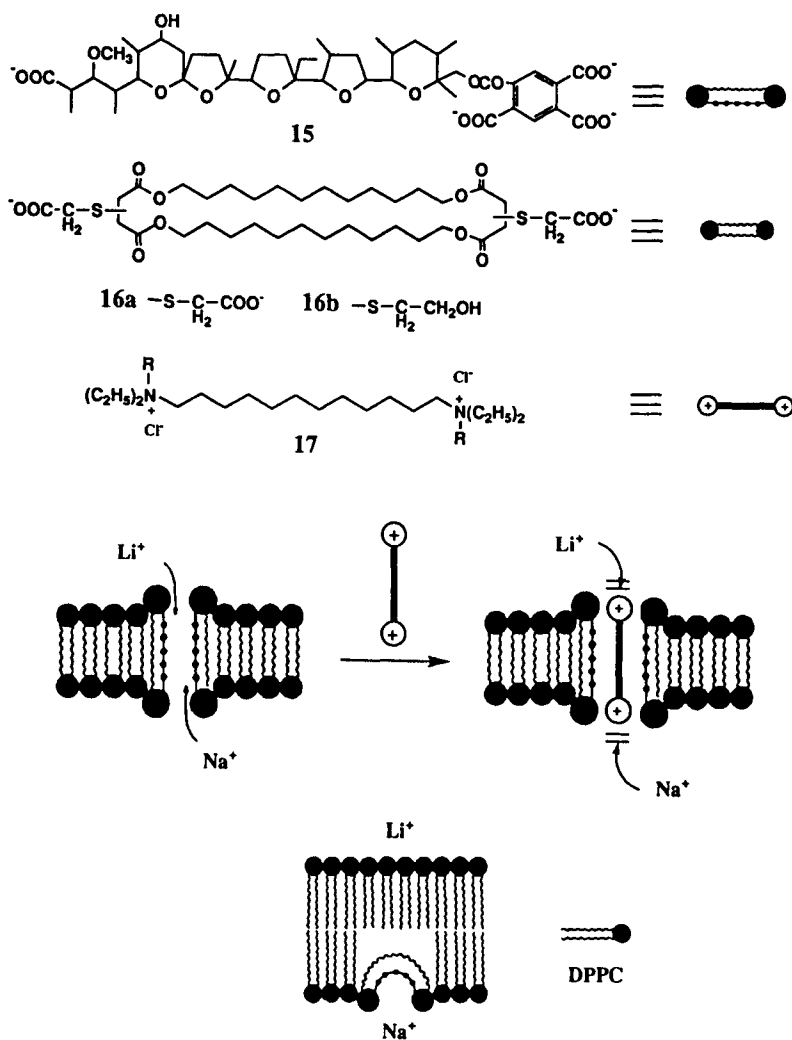
***Figure 19.*** (A) Monensin modified channel forming unit **15**, negatively charged α,ω-bifunctional amphiphile **16a** and neutral one **16b**, capable of forming monolayered membrane and positively charged bolaamphiphiles **17** as a sealing agent of the channel. (B) Model of channel formation by **15** in the monolayered membrane composed of **16** and the proposed blocking mode by **17**.[113]

themselves were rather low and structural variations of cyclodextrin **18** and crown ether **19** showed only a slight difference. Furthermore, bouquet molecules with simple polymethylene chains (b) transport about as efficiently as those with poly(oxyethylene) chains (a) (Figure 20). These rather unexpected results and a

18a  ◄───  polyoxyethylene  ───►  19a

18b  ◄───  polymethylene  ───►  19b
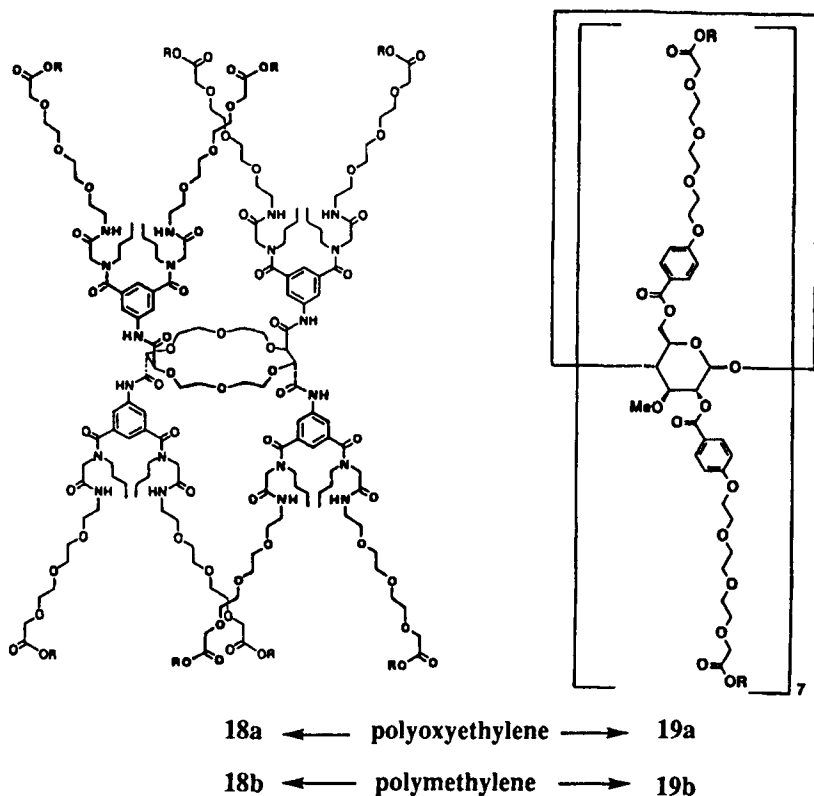
*Figure 20.* Bouquet molecules having a macrocyclic 18-crown-6-ether annulus **18** and a cyclodextrin annulus **19**. Figure shows poly(oxyethylene) side chains (**a**). Analogous compounds with polymethylene side chains (**b**) were also prepared.[118]

possibility that highly hydrated $Li^+$ ion is difficult to be transferred and determines the overall rate of transport will be explained soon.

## 5. GATING

Since ion channels can afford large ionic fluxes across the membrane, they should have been equipped with their own gating systems. Otherwise the concentration gradient will vanish immediately to result in death of the cell. More significantly, gating is a sophisticated tool to control the ionic flux and hence the biological functions. Voltage gating is a key mechanism to convey the electrical signals along the nerve axon. The variation of local membrane potential generated by the channel action itself becomes its own sensory device to allow the firing of an electrical signal. Ligand gating, another mechanism, is the way that an electrical or ionic

signal transduction system is once subjected to the chemical (hormonal) control, through which the biological functions are modulated in a variety of chemical modes. Mechanoreceptors are another important class of quick and direct sensory devices. Along with additional artificial gating systems, the mimic of gating is a fascinating target for obtaining a molecular ionics device.

## 5.1. Voltage-Dependent Channels[119]

In a series of double amphiphilic lipid ion pairs, the authors combined a phosphate ester of oligo(butylene glycol) **2b** with hydrophobic dioctadecyl-di-methylammonium cation **2e** to make an ion pair **20** (Figure 21). The difference from the carboxylate–ammonium ion pair **1** is clear so that the phosphate group is dissociated into the form having ca. 1.5 anionic charges at pH 7.2. Therefore, the ion pair formed with equimolar ammonium compound does not neutralize the charge and leaves extra anionic charges in the membrane phase.

When this amphiphile was incorporated into planar bilayer membrane, interesting current behavior was observed: the open–closed probabilities varied with the applied voltage. A typical record of the channel current is shown in Figure 22. At 50 mV, the channel is almost closed with only occasional opening. At 70 to 85 mV, the open frequency increases and its duration becomes significantly longer. At 100
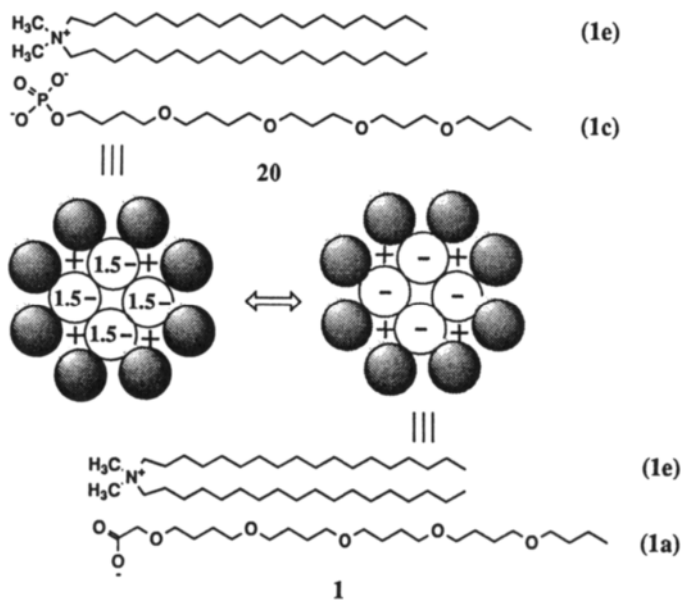


**Figure 21.** Ion pair **20** prepared from oligoether phosphate **1c** with hydrophobic ammonium **1e** (Figure 7). Supramolecular assemblage in the membrane phase may incorporate excess anionic charges at the pH range employed.

**50.0 mV**



**70.2 mV**



**85.0 mV**



**100.0 mV**



**10 pA**

**256 ms**
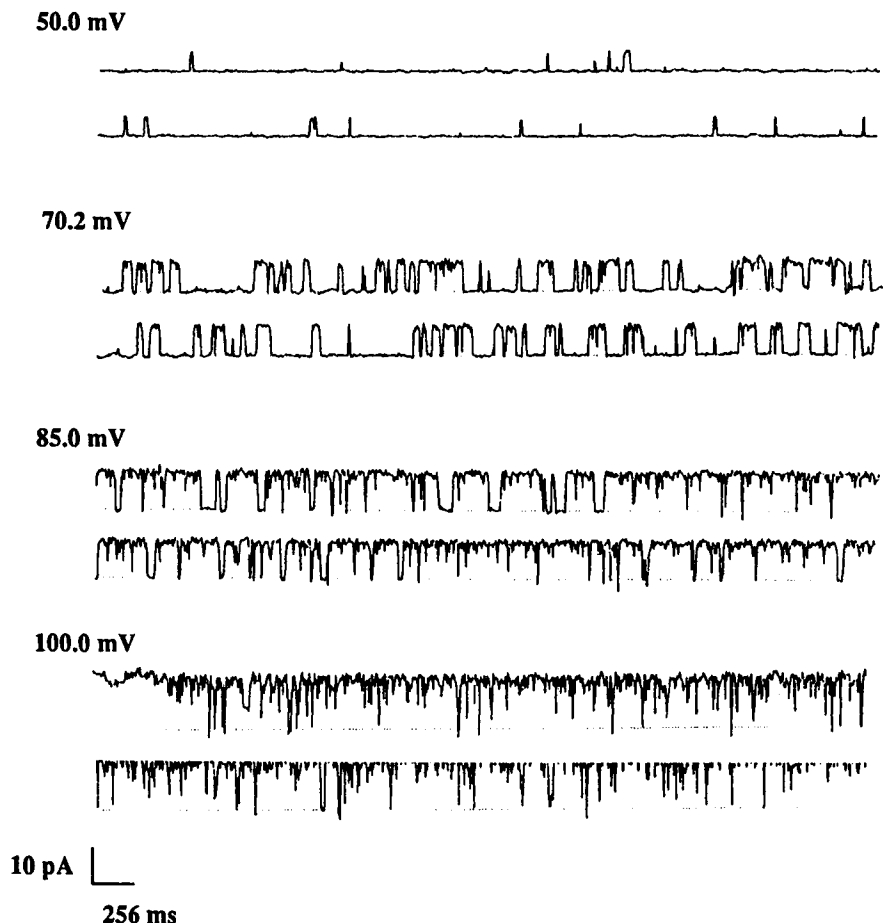
***Figure 22.*** Typical records of ionic currents at several voltages under symmetric 0.5 M KCl bath solutions at pH 7.2.[119] Currents increase upward from the zero level, shown by the dotted line in each panel.

mV, the channel resides almost completely in the open state with only transient closings. The histogram analysis of this record shows a clear voltage dependence of both the open and closed times, shifting to the open state at higher voltages (which will be defined as a positive voltage dependence). Throughout the range of applied voltage, the conductance was approximately constant at 126 pS for this run. Therefore, this artificial channel mimics the way that natural ion channels control the total current, i.e. by both the probability of being open as well as the amplitude of the current.

Several sets of ionic currents were recorded at various voltages using the same molecule under the same experimental conditions. As is usual for supramolecular

channels, various conductance levels were observed, although that level remained constant during the voltage series. In Figure 23, open probabilities are plotted as a function of applied voltage for several runs. Here, interestingly, positive, negative, and zero (not shown) voltage dependencies were clearly observable. The occurrence of either of these three dependencies was apparently random and independent of the conductance levels. Furthermore, the midpoint voltage, which is defined by the voltage at which the channels are 50% open, seems to be independent of both the magnitude of the conductance and the polarity of the voltage dependence.

It should be noted that such a voltage dependence has never been observed when an electrically neutral ion pair **1** was employed. The net negative charges of the ion pair are therefore responsible for the voltage dependence of **20**. A similar voltage dependence was observed when oligoether ammonium **2d** (see Figure 7) was combined with monoalkylphosphate **2g**, but not with dialkylphosphate **2f**. Here again the unbalanced electrical charge for the inverse set of the head groups seems to be the origin of the voltage dependence.

Based on the supramolecular ion channel model of **1**, the combined observations suggest a mechanism for the voltage dependence as schematically shown in Figure 24: Amphiphilic molecules are assembled to construct a half-channel in each
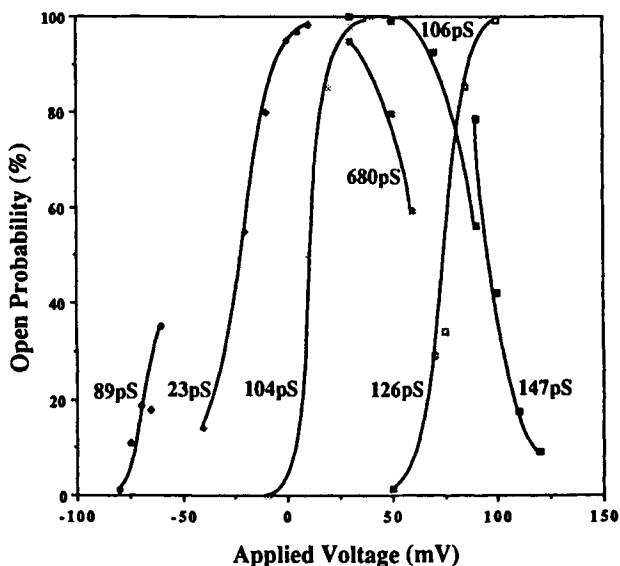


***Figure 23.*** Plot of open probabilities against applied voltages. The numbers in the figure are the respective single channel conductances obtained from the linear current–voltage dependence for each run. The currents shown in Figure 22 had conductance of 126 pS and gave a positive voltage dependence, shifting to open the state at higher voltages.[119]
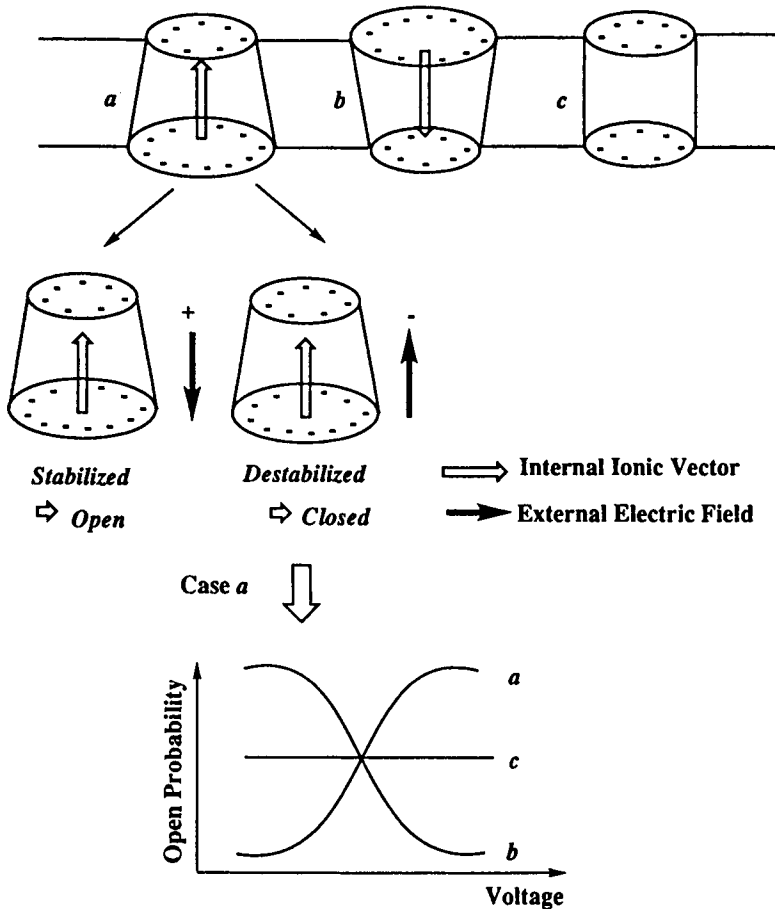
**Figure 24.** A plausible mechanism for the formation of voltage-dependent ion channels. Trapezoidal cylinders symbolize the transmembrane ion channel composed of assembles of uneven (cases *a* and *b*) or even (case *c*) aggregation number of the net negative ion pair 2, which is symbolized by -, at both surfaces of the membrane.[119]

membrane layer. This process occurring in one of the membrane layers should be independent of the one occurring in the other layer. When two supramolecular half-channels thus formed are interconnected, the assembly numbers in two layers are generally different from each other unless strong interactions are operating and the resulting trans-membrane channel may possess a net dipole vector across the membrane. When the case *a* channel is stabilized by e.g. a positive external voltage and destabilized by a negative one, a positive voltage dependence may result. The case *b* channel having the opposite dipole vector should then give a negative voltage dependence. Since no asymmetry exists across the membrane and we are observing

a single molecule of ion channel formed in the membrane in each run, the formation of case *a* and *b* channels must be of statistically equal probability and we observe positive and negative voltage dependencies in an equal frequency. When the assembly numbers in both layers happens to be identical (case *c*), no voltage dependence should be observed. These were our exact observations in the above experiment.

Although these explanations still await further experimental proof, it was clearly demonstrated that the simple incorporation of charges induced a voltage control which exactly mimicked the way of current control in the biological system. It may be interesting to discuss the way of flux control in a more general viewpoint. Here the flux control was accomplished by the variation of open–closed times, while keeping the conductance constant. There may be allowed an alternative mechanism, i.e., a variation of resistance or conductance, which seems simpler and is adopted for electronic devices in our artificial world. In the chemical devices such as employed in the biological system, however, modulation of conductance may need structural variation of the ion channel, e.g. cross section, length, or nature of the pore wall of ion channel, which may not be easily compared to the conformational movement. The exact controlling factor of such movement could not be clearly demonstrated at present, and further investigation will elucidate the molecular mechanism. Voltage gating is also reported for helix bundle ion channels,[42,43,54] as well as for modified gramicidin A's.[66] Gating events in natural ion channels are identified in molecular level and demonstrated visually in recent reports.[120,121]

## 5.2. Photochemical Gate[122]

In view of the easy handling and a high signal-to-noise ratio, light may be an interesting energy source for controlling the ionic flux. Therefore, even apart from mimicking biological systems, photosensitive gating may be an interesting target for implanting in artificial channels. Based on the doubly amphiphilic lipid ion pairs in Section 2.1, azo functionality as a photoresponsive unit to undergo structural transformation on light irradiation was introduced into a hydrophobic ammonium to cover the central pore of the supramolecular assembly of the oligoether unit. Therefore, a hydrophobic ammonium cation containing azo functionality in one of the two long alkyl chains was combined with glycolate ester of oligo(butylene 1,4-glycol) to afford the ion pair **21** (see Figure 26).

When *trans*-**21** was incorporated into planar lipid bilayers, characteristic single channel currents, i.e., a single stable current level with open–close transitions, were observed. The histogram analysis clearly indicates the presence of only one current level. Similar channel currents were obtained at several different membrane voltages and their current–voltage plot gave an ohmic relationship to give one conductance. Several runs by using the same compound gave different conductances, as is normal for any supramolecular ion channels. Histogram analysis of conductances is shown in Figure 25. Several conductances ranging from 2 pS to 12 pS were

**Total Observation = 9095 s**
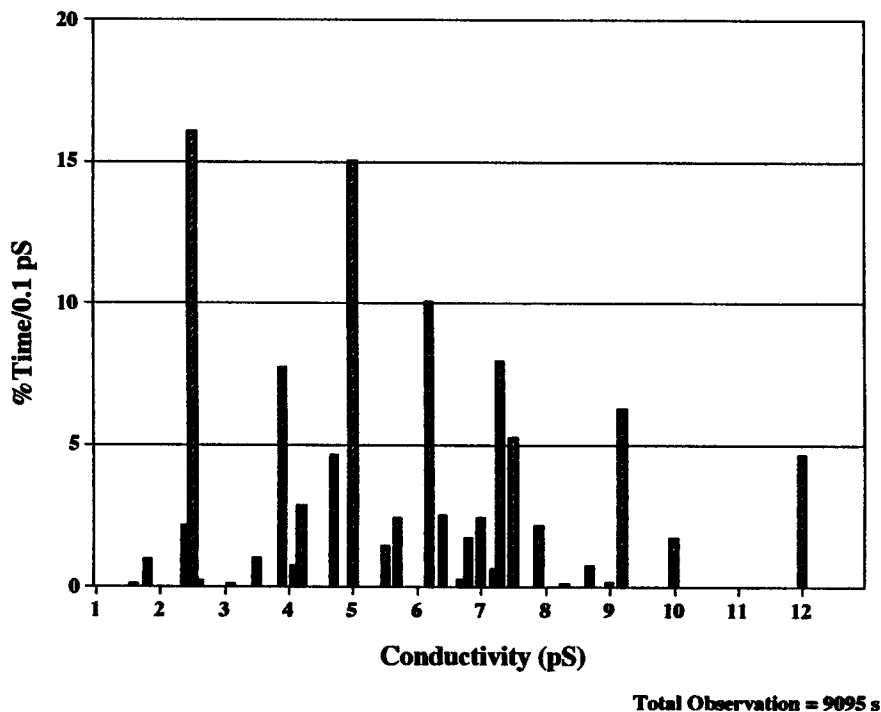
*Figure 25.* Histogram analysis of conductances obtained for total 9095 s observations by the combination of *trans*-azo-ammonium and oligoether carboxylate ion pair **21**.

recorded. Among these several channels, 2.5 and 5 pS channels show a relatively high frequency of total observations for 9000 s.

The permeability selectivity ratio for $P_{K^+}/P_{Cl^-}$ ion was estimated to be 5 for the channel of 5 pS. The selectivity again favors cation and the ratio resembles the value obtained by supramolecular oligoether channels. Open and closed transitions were relatively slow and the time distributions were 300 ms and 400 ms, respectively. Therefore, the ion pair, *trans*-**21**, can be concluded to show typical characteristics of the single-ion channel in all respects.

*trans*-**21** was then irradiated by the light at 367 nm and the azo functionality was confirmed to be isomerized to the *cis*. This ion pair was subjected to the single-channel current measurements under dark with repeated incorporation into bilayer lipid membranes. No stable channel currents were detected, although unstable drift of the base line was frequently observed showing probable leaky currents across the bilayer membrane. All of the measurements were performed within 2 hours in order to avoid the *cis*- to -*trans* isomerization. When *cis*-**21** was isomerized back to the *trans* by irradiating light at 450 nm or by standing a longer time, again single-channel currents regenerated.

These observations suggest that the *trans*-azo ammonium can stabilize the supramolecular channel structure, which is formed by assembling relatively hydrophilic oligoether units based on the molecular recognition in the membrane phase. Compared to the extended molecular form of the *trans*-azo compound, which is appropriate for covering the hydrophilic component from the outside, the *cis* compound with a bulky structure cannot stabilize the structure and hence prohibits the assembly formation because it requires a large void structure in the membrane. Therefore, only leaky currents are observable (Figure 26).

The present observation shows a contrast to the previously known photochemical control of currents or other physical constants by using membrane, where *cis*- and *trans*-azo compounds have been claimed as a photo-switch.[123-127] In these experiments, the incorporation ratio of the azo compound to lipid has been relatively high, being, e.g., ranging from 10% to even 100%, i.e. pure azo membrane and *cis*-azo compounds usually exhibited larger conductance or capacitance, suggesting that the observation is based on leak currents or increased disorders in the membrane. In the present case, however, we are observing single-channel currents, which certainly exceed the leak current by one or two orders of magnitude (azo). Then the
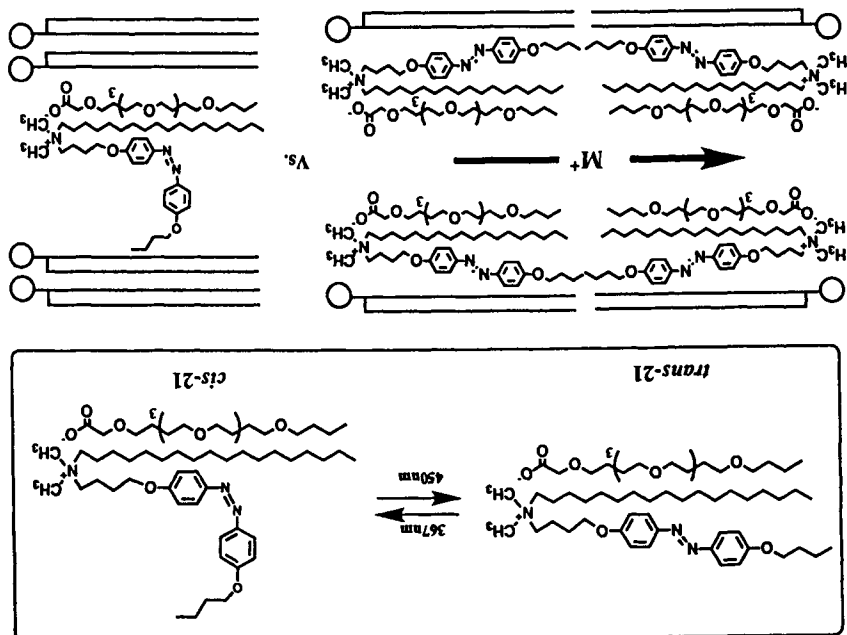


*Figure 26.* Scheme for the control of ionic fluxes by light irradiation. *trans*-Azo ammonium, covering the hydrophilic oligoether parts from the outside, can stabilize the supramolecular ion channel structure, while *cis* cannot because of its bent structure. Therefore, *trans*-azo generates ion channel currents, while for *cis* only small leak currents across the membrane.

on–off signal ratio is expected to be superior than in the case of observing disordered leak events.

# 6. TOWARDS NANO MATERIALS

One of the interesting fields of ion-channel studies may be an application for molecular ionics devices that are small and fast, store information with high density, and transfer informations through transporting ions with reliable switching between on and off states. Nanometer-sized structures and molecular materials may be formed by polymeric material, supramolecular self-organization, or Langmuir–Blodgett (LB) multilayers.

As an extension of Ghadiri's study, a 12-residue cyclic peptide, cyclo[(Gln-D-Ala-Glu-D-Ala)$_3$], afforded self-assembled nanotube materials having a uniform 13-Å tailored pore diameter. Specifically sized tubular nanostructures with channel structures can expect various applications.[128,129]

Nolte prepared phthalocyanines (Pc) having benzo-18-crown-6 **22**.[130,131] Bis(decyloxy)substituted phthalocyanine appears liquid crystalline in a *meso*-phase transition at 148°C. The structure of the crystalline phase determined by small angle X-ray scattering measurements is shown in Figure 27. The Pc cores are stacked along c-axis in an eclipsed position with inter-Pc distance of 3.4 Å, very close to the van der Waals contact, with a tilt angle of 38°. Crown ether rings are superimposed along the c-axis with a separating distance of 4.3 Å; in other words, in an ion channel arrangement. Also in the *meso* phase, the ion channel structure with a longer separation distance exists.

Another spectacular property of this compound is a strong tendency to produce linear self-assembled aggregates of up to $10^4$ molecules as a gel in chloroform solution. The molecules are most likely stacked in an eclipsed conformation as in the crystalline phase. Therefore the self-assembled molecules can be regarded as molecular cables, containing a central electron wire and closely connected four ion channels by phthalocyanine and crown ether parts, respectively, and a surrounding insulating hydrocarbon mantle (c). The ion- as well as electron-conducting properties are interesting.

A cumulative success of artificial ion-channel functions by simple molecules may disclose a wide gate for the design of ion channels and possible applications to ionics devices. Incorporation of these channels into bilayer lipid membrane systems may trigger the developments towards ionics devices. The conventional BLM system, however, is not very stable, one major drawback for the practical applications, and some stabilization methods, such as impregnating the material in microporous polycarbonate or polyester filters, are required.[127,132–137] On the other hand, the conventional LB technique prohibits rapid photochemical reactions of incorporated chromophores and many efforts to overcome the problems have been made.[138–141]

M = H₂ is shown as $M = H_2$

**22**

(a)          (b)

(c)

Isolating mantle ◄—

Ion Channel ◄—

Electron wire ◄—
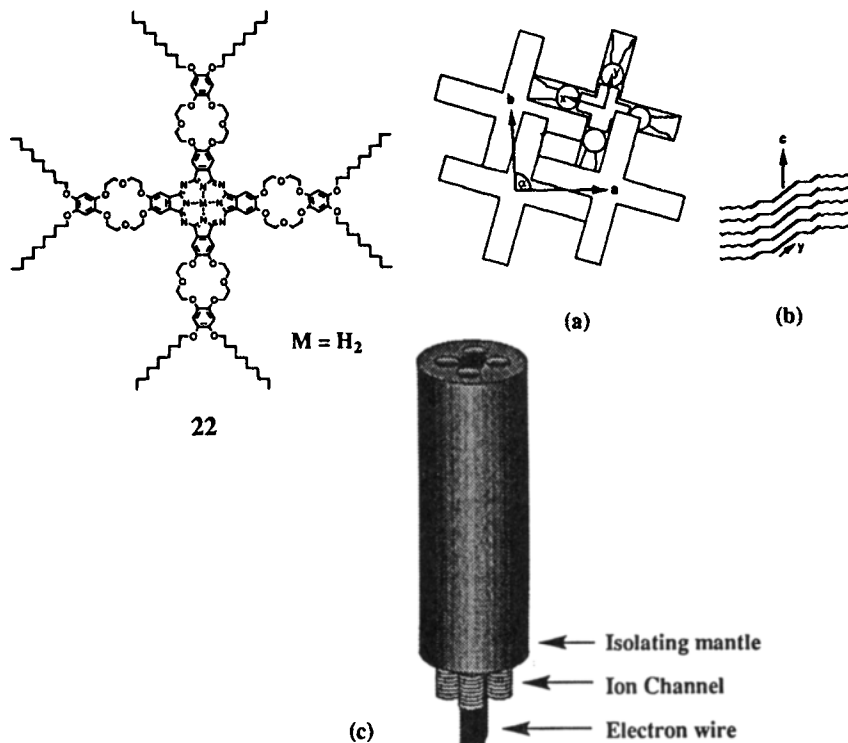
***Figure 27.*** Tetrakis[4′,5′-bis(decoxy)benzo-18-crown-6]phthalocyanine **22**.[131] Proposed structure of the crystalline phase (**a**) view along the normal on the Pc xy-plane and (**b**) view along the molecular x-axis. (**c**) Multiwired molecular cable self-assembled in chloroform solution.

## 7. ESTIMATION METHODS

Before concluding this review, it is appropriate to comment on estimation methods of artificial ion channels. As described in each experimental method, both planar and liposomal membranes could be used for detecting the ion transport via the channel mechanism. For estimating the ion transport rate across the liposomal membrane, a variety of methodologies have been employed. These may be summarized as follows:

1. *pH stat.* Driven by the influx of metal ions, protons are ejected to outside the liposome and the base is titrated to maintain the pH. The rate can be estimated from the amount of the base added.

2. *Chromophoric change.* UV/vis- or fluorescent-active and water-soluble chromophores such as pyranine and carboxyfluorescein are encapsulated in

the liposome. Chromophoric changes on metal complexation can be employed for the rate analysis. Since alkali metals are generally inert to the chromophoric change, proton countertransport is detected except in the case that $Ca^{2+}$ is detected directly by specific chromophores such as Fura 2.[142] Otherwise, transition metals with strong chromophoric interaction are employed.

3.  *NMR technique.* NMR-active metal ions entrapped in the liposome can be differentiated from those outside by the addition of shift reagents such as Dy(III) or Gd(III) to the external phase. Then metal concentrations inside and outside the liposome can be determined directly. This is attractive for $^7Li^+$, $^{23}Na^+$, and $^{39}K^+$ ions because of high sensitivities and natural abundances. The direct determination of the metal ion concentrations are attractive but limited only for slow kinetics. When the rate becomes faster, line shape analysis or magnetization-inversion transfer techniques are employed. The latter method has been successfully applied to gramicidin channels,[143–144] but not to artificial ion channels.

The rates obtained by these methods vary in a wide range. These values may represent true transport rates independent of the evaluation methods. Different experimental conditions sometimes hamper the strict comparisons of data. These points must be overcome for further development of this field.

Discrimination of the channel mechanism from the carrier is very critical and a variety of criteria are proposed from research groups. The following criteria have been employed:

1.  *Comparison of rates in the gel and liquid state of the membrane.* In the case of channel mechanism, ions can pass through a structured pathway which is more or less similar to the bulk aqueous phase, while carriers encapsulate ions and transfer in the membrane. Therefore, the former is insensitive to gel–liquid phase transition of the membrane, while the gel state inhibits the carrier transport.

2.  *Satisfaction of kinetic order.* Carriers follow Michaelis–Menten-type saturation kinetics or first-order kinetics. Ion channels follow the type of respective structure—unimolecular transmembrane channels and bimolecular half-channels follow first- and second-order kinetics, respectively. The kinetic order of supramolecular channels depends on the assembly number. However, this principle can be applied only when the association constants are small. If the association becomes strong, the kinetic order decreases down to zero. Then the validity becomes dubious in view of the absolute criterion of the mechanism. Decreased activation energy compared to the carrier transport mechanism and competitive inhibition by added other cations stand as criteria.

3. *Observation of single-channel current.* This may provide the most convincing evidence when full characterization of basic properties is provided. Observation of unstable, leak currents must be eliminated. Blocking agents provide a certain basis for assuming the presence of a channel pore in the membrane. Although the only observation of single-channel currents is not enough to prove the channel mechanism, it is indispensable for characterizing basic features of ion channels. Liposomal measurements are important for analyzing total efficiency of the ionic flow across the bilayer membrane, but certainly lack in information on data accumulated for natural and antibiotic ion channels as well as helical bundles through single-channel measurements and better be combined with the this method.

# 8. CONCLUDING REMARKS

Extensive work on natural ion channels has been undertaken in order to elucidate detailed mechanisms, and key amino acid sequences in core parts have been identified in many cases now, especially through point mutation experiments. However, it is still not known with certainty in most cases (1) what functional groups serve as cation relays, (2) how large ionic fluxes with large discrimination factors are possible, (3) what are molecular recognition sites comprised of, (4) what conformational motions determine the time scale of on–off fluctuation, (5) what molecular movements on receiving a gating signal open and close the gate, and (6) how the transmembrane segments self-assemble or aggregate to form the ion-transducing pathway. Artificial channel-forming systems, being of simple structure and amenable to structural modification, are expected to shed light on these points and also to afford applications of biomimetic materials.

Along these lines, supramolecular, bimolecular, as well as unimolecular approaches successfully mimicked the function of natural ion channels by using completely artificial and very simple molecules. Ion fluxes satisfied several criteria that these molecules form ion channels embedded in the bilayer lipid membrane. Non-peptidic artificial ion channels as well as helical bundles are now in our hands and it is likely that many more will soon emerge. The biological importance of these molecules may attract interest from many diverse branches of science—neurobiology, clinical medicine, biophysics, membrane technology, materials science, and others.

The studies presented here along with helical bundle approaches provide a vehicle for exploring in detail the structure–function relationships of ion channels through the synthesis of artificial molecules with simple and controllable structural features. The control of electric fields at the ion-selective filter may elucidate the molecular mechanism of $K^+/Na^+$ and $Na^+/Ca^{2+}$ selectivities. Variation of the critical pore size by synthetic elaboration may give direct clues on the magnitude of conductance and discrimination of metal ions. Further studies on voltage depend-

ence, rectification, specific channel blockers, and anion-selective channels coupled with electron transport are considered to be immediate targets for research. A fascinating challenge also includes the control of gating by sensory receptors coupled to completely artificial channels. These possibilities are expected to expand the interesting areas of bioorganic, bioinorganic, as well as supramolecular chemistries and lead to the development of an intelligent multisensing device of nanometer scale as a possible application to real hardware in the future.

## ACKNOWLEDGMENTS

## NOTES

*Tanaka et al., 1993.
†Wallace, 1987.

## REFERENCES

1. Hille, B. *Ionic Channels of Excitable Membranes*, 2nd ed.; Sinauer: Sunderland, MA, 1992.
2. *Thermodynamics of Membrane Receptors and Channels*; Jackson, M. B., Ed.; Jackson: CRC, FL, 1993.
3. Noda, M.; Takahashi, H.; Tanabe, T.; Toyosato, M.; Kikyotani, S.; Furutani, Y.; Hirose, T.; Takashima, H.; Inayama, S.; Miyata, T.; Numa, S. *Nature (London)* **1983**, *302*, 528.
4. Noda, M.; Shimizu, S.; Tanabe, T.; Takai, T.; Kayano, T.; Ikeda, T.; Takahashi, H.; Nakayama, H.; Kanaoka, Y.; Minamino, N.; Kangawa, K.; Matsuo, H.; Raftery, M. A.; Hirose, T.; Notake, M.; Inayama, S.; Hayashida, H.; Miyata, T.; Numa, S. *Nature (London)* **1984**, *312*, 121.
5. Noda, M.; Ikeda, T.; Kayano, T.; Suzuki, H.; Takeshima, H.; Kurasaki, M.; Takahashi, H.; Numa, S. *Nature (London)* **1986**, *320*, 188.
6. Tanabe, T.; Takeshima, M.; Mikami, A.; Flockerzi, V.; Takahashi, H.; Kangawa, K.; Kojima, M.; Matsuo, H.; Hirose, T.; Numa, S. *Nature (London)* **1987**, *328*, 313.
7. Kayano, T.; Noda, M.; Flockerzi, V.; Takahashi, H.; Numa, S. *FEBS Lett.* **1988**, *228*,187.
8. Kosower, E. M. *FEBS Lett.* **1985**, *183*, 234.
9. Greenblatt, R. E.; Blatt, Y.; Montal, M. *FEBS Lett.* **1985**, *193*, 125.
10. Guy, H. R.; Conti, F. *Trends Neurosci.* **1990**, *13*, 201.
11. Revah, F.; Galzi, J. L.; Giraudat, J.; Haumont, P. Y.; Lederer, F.; Changeux; J. P. *Proc. Natl. Acad. Sci. USA* **1990**, *87*, 4675.
12. Eisenman, G.; Alvarez, O. *J. Membr. Biol.* **1991**, *119*, 109.
13. Durell, S. R.; Guy, H. R. *Biophys. J.* **1992**, *62*, 238.
14. Heinemann, S. H.; Terlau, H.; Stühmer, W.; Imoto, K.; Numa, S. *Nature (London)* **1992**, *356*, 441.
15. Yang, J.; Ellinor, P. T.; Sather, W. A.; Zhang, J. F.; Tsien, R. W. *Nature (London)* **1993**, *366*, 158.
16. Lopez, G. A.; Jan, Y. N.; Yan, L. Y. *Nature (London)* **1994**, *367*, 179.

17. Lü, Q.; Miller, C. *Science* **1995**, *268*, 304.
18. Fairman, W. A.; Vandenberg, R. J.; Arriza, J. L.; Kavanaugh, M. P.; Amara, S. G. *Nature (London)* **1995**, *375*, 599.
19. Labarca, C.; Nowak, M. W.; Zhang, H.; Tang, L.; Deshpande, P.; Lester, H. A. *Nature (London)* **1995**, *376*, 514.
20. Moss, S. J.; Gorrie, G. H.; Amato, A.; Smart, T. G. *Nature (London)* **1995**, *377*, 344.
21. Tabushi, I.; Kuroda, Y.; Yokota, K. *Tetrahedron Lett.* **1982**, *23*, 4601.
22. van Beijnen, A. J. M.; Nolte, R. J. M.; Zwikker, J. W.; Drenth, W. *Recl. Trav. Chim. Pays-Bas* **1982**, *101*, 409.
23. Neevel, J. G.; Nolte, R. J. M. *Tetrahedron Lett.* **1984**, *25*, 2263.
24. Kragten, U. F.; Roks, M. F. M.; Nolte, R. J. M. *J. Chem. Soc., Chem. Commun.* **1985**, 1275.
25. Fuhrhop, J. H.; Liman, U. *J. Amer. Chem. Soc.* **1984**, *106*, 4643.
26. Fuhrhop, J. H.; Liman, U.; David, H. H. *Angew. Chem., Int. Ed. Engl.* **1985**, *24*, 339.
27. Lear, J. D.; Wasserman, Z. R.; DeGrado, W. F. *Science* **1988**, *240*, 1177.
28. Oiki, S.; Danho, W.; Montal, M. *Proc. Natl. Acad. Sci. USA* **1988**, *85*, 2393.
29. Oiki; S.; Danho, W.; Madison, V.; Montal, M. *Proc. Natl. Acad. Sci. USA* **1988**, *85*, 8703.
30. Mueller, P.; Rudin, D. O. *Nature (London)* **1962**, *194*, 979.
31. Mueller, P.; Rudin, D. O.; Tien, H. T.; Wescott, W. C. *Circulation* **1962**, *26*, 1167.
32. Montal, M.; Mueller, P. *Proc. Natl. Acad. Sci. USA* **1972**, *69*, 3561.
33. *Single-Channel Recording*; Sakmann, B.; Neher, E., Ed.; Plenum Press: NY, 1983.
34. Montal, M.; Anholt, R.; Labarca, P. *Ion Channel Reconstitution*; Miller, C., Ed.; Plenum: New York, 1986.
35. DeGrado, W. F.; Wasserman, Z. R.; Lear, J. D. *Science* **1989**, *243*, 622.
36. Tosteson, M. T.; Auld, D. S.; Tosteson, D. C. *Proc. Natl. Acad. Sci. USA* **1989**, *86*, 707.
37. DeGrado, W. F.; Lear, J. D. *Biopolymers* **1990**, *29*, 205.
38. Montal, M.; Montal, M. S.; Tomich, J. M. *Proc. Natl. Acad. Sci. USA* **1990**, *87*, 6929.
39. Anzai, K.; Hamasuna, M.; Kadono, H.; Lee, S.; Aoyagi, H.; Kirino, Y. *Biochim. Biophys. Acta* **1991**, *1064*, 256.
40. Grove, A.; Tomich, J. M.; Montal, M. *Proc. Natl. Acad. Sci. USA* **1991**, *88*, 6418.
41. Åkerfeldt, K. S.; Kim, R. M.; Camac, D.; Groves, J. T.; Lear, J. D.; DeGrado, W. F. *J. Am. Chem. Soc.* **1992**, *114*, 9656.
42. Chung, L. A.; Lear, J. D.; DeGrado, W. F. *Biochem.* **1992**, *31*, 6608.
43. Åkerfeldt, K. S.; Kim, R. M.; Camac, D.; Groves, J. T.; Lear, J. D.; DeGrado, W. F. *J. Am. Chem. Soc.* **1992**, *114*, 9656.
44. Carmichael, V. E.; Dutton, P. J.; Fyles, T. M.; James, T. D.; Swan, J. A.; Zojaji, M. *J. Am. Chem. Soc.* **1989**, *111*, 767.
45. Fyles, T. M.; James, T. D.; Kaye, K. *Can. J. Chem.* **1989**, *68*, 976.
46. Fyles, T. M.; Kaye, K.; James, T. D.; Smiley, D. W. M. *Tetrahedron Lett.* **1990**, *31*, 1233.
47. Nakano, A.; Xie, Q.; Mallen, J. V.; Echegoyen, L.; Gokel, G. W. *J. Am. Chem. Soc.* **1990**, *112*, 1287.
48. Menger, F. M.; Davis, D. S., Persichetti, R. A., Lee, J. J. *J. Am. Chem. Soc.* **1990**, *112*, 2451.
49. Kobuke, Y.; Ueda, K.; Sokabe, M. *J. Am. Chem. Soc.* **1992**, *114*, 7618.
50. Kobuke, Y. *Mol. Electr. Biocomputing* **1993**, *7*, 33.
51. Kobuke, Y. *J. Oil Chem. Japan* **1994**, *43*, 830.
52. Kobuke, Y. *J. Synth. Org. Chem., Japan* **1995**, *53*, 451.
53. Kobuke, Y.; Tanaka, Y.; Sokabe, M. *Towards Molecular Biophysics of Ion Channels*; Sokabe, M., Ed.; Elsevier: Amsterdam, in press.
54. Åkerfeldt, K. S.; Lear, J. D.; Wasserman, Z. R.; Chung, L. A.; DeGrado, W. F. *Acc. Chem. Res.* **1993**, *26*, 191.
55. Reddy, G. L.; Iwamoto, T.; Tomich, J. M.; Montal, M. *J. Biol. Chem.* **1993**, *268*, 14608.
56. Grove, A.; Mutter, M.; Rivier, J. E.; Montal, M. *J. Am. Chem. Soc.* **1993**, *115*, 5919.

57. Reddy, G. L.; Iwamoto, T.; Tomich, J. M.; Montal, M. *J. Biol. Chem.* **1993**, *268*, 14609.
58. Montal, M. O.; Buhler, L. K.; Iwamoto, T.; Tomich, J. M.; Montal, M. *J. Biol. Chem.* **1993**, *268*, 14601.
59. Montal, M. O.; Iwamoto, T.; Tomich, J. M.; Montal, M. *FEBS Lett.* **1993**, *320*, 261.
60. Anderson, O. S.; Koeppe II, R. E. *Physiol. Rev.* **1992**, *72*, S89.
61. Killian, J. A. *Biochim. Biophys. Acta* **1992**, *1113*, 391.
62. Busath, D. D. *Annu. Rev. Physiol.* **1993**, *55*, 473.
63. Oiki, S.; Koeppe II, R. E.; Anderson, O. S. *Biophys. J.* **1994**, *66*, 1823.
64. Jaikaran, D. C.; Woolley, G. A. *J. Phys. Chem.* **1995**, *99*, 13352.
65. Wooley, G. A.; Jaikaran, A. S. I.; Zhang, Z.; Peng, S. *J. Am. Chem. Soc.* **1995**, *117*, 4448.
66. Oiki, S.; Koeppe II, R. E.; Anderson, O. S. *Proc. Natl. Acad. Sci. USA.* **1995**, *92*, 2121.
67. Seebach, D.; Brunner, A.; Bürger, H. M.; Reusch, R. N.; Bramble, L. L. *Helv. Chim. Acta* **1996**, *79*, 507.
68. Stadler, E.; Dedek, P.; Yamashita, K.; Regen, S. L. *J. Am. Chem. Soc.* **1994**, *116*, 6677.
69. Cheng, Y.; Ho, D. M.; Gottlieb, C. R.; Kahne, D. *J. Am. Chem. Soc.* **1992**, *114*, 7319.
70. Menger, F. M.; Davis, D. S., Persichetti, R. A., Lee, J. J. *J. Am. Chem. Soc.* **1990**, *112*, 2451.
71. Menger, F. M.; Aikens, P. *Angew. Chem. Int. Ed. Engl.* **1992**, *31*, 898.
72. Kano, K.; Fendler, J. H. *Biochim. Biophys. Acta* **1978**, *509*, 289.
73. Gillberg, G. *Acta Chem. Scand.* **1966**, *20*, 2019.
74. Ghadiri, M. R.; Granja, J. R.; Milligan, R. A.; McRee, D. E.; Khazanovich, N. *Nature (London)* **1993**, *366*, 324.
75. Ghadiri, M. R.; Granja, J. R.; Buehler, L. K. *Nature (London)* **1994**, *369*, 301.
76. Granja, J. R.; Ghadiri, M. R. *J. Am. Chem. Soc.* **1994**, *116*, 10785.
77. Engels, M.; Bashford, D.; Ghadiri, M. R. *J. Am. Chem. Soc.* **1995**, *117*, 9151.
78. Tanaka, Y.; Kobuke, Y.; Sokabe, M. *Angew. Chem. Int. Ed. Eng.* **1995**, *34*, 693.
79. Aoyama, Y.; Tanaka, Y.; Sugahara, S. *J. Am. Chem. Soc.* **1989**, *111*, 5397.
80. Guilbaud, P.; Varnek, A.; Wipff, G. *J. Am. Chem. Soc.* **1993**, *115*, 8298.
81. Heginbotham, L.; MacKinnon, R. *Neuron* **1992**, *8*, 483.
82. Miller, C. *Science* **1993**, *261*, 1692.
83. Kumpf, R. A.; Dougherty, D. A. *Science* **1993**, *261*, 1708.
84. Dougherty, D. A. *Science* **1996**, *271*, 163.
85. Durell, S. R.; Guy, H. R. *Biophys. J.* **1992**, *62*, 238.
86. Bogusz, S.; Boxer, A.; Dusath, D. D. *Protein Eng.* **1992**, *5*, 285.
87. Tabushi, I.; Kuroda, Y.; Yokota, K. *Tetrahedron Lett.* **1982**, *23*, 4601.
88. Carmichael, V. E.; Dutton, P. J.; Fyles, T. M.; James, T. D.; Swan, J. A.; Zojaji, M. *J. Am. Chem. Soc.* **1989**, *111*, 767.
89. Fyles, T. M.; James, T. D.; Kaye, K. *Can. J. Chem.* **1989**, *68*, 976.
90. Fyles, T. M.; Kaye, K.; James, T. D.; Smiley, D. W. M. *Tetrahedron Lett.* **1990**, *31*, 1233.
91. Fyles, T. M.; James, T. D.; Kaye, K. C. *J. Am. Chem. Soc.* **1993**, *115*, 12315.
92. Cybulska, B.; Ziminski, T.; Borowski, E.; Gary-Bobo, C. M. *Mol. Pharm.* **1983**, *24*, 270.
93. Thomas, C.; Sauterey, C.; Castaing, M.; Gary-Bobo, C. M.; Lehn, J. M.; Plumere, P. *Biochem. Biophys. Res. Comm.* **1983**, *116*, 981.
94. Herve, M.; Cybulska B.; Gary-Bobo, C. M.; *Eur. J. Biochem.* **1985**, *12*, 1212.
95. Cybulska, B.; Herve, M.; Borowski, E.; Gary-Bobo, C. M. *Molecular Pharm.* **1986**, *29*, 293.
96. Eisenman, G. *Ion Selective Electrodes*; Durst, R. A., Ed.; NBS: Special Pub. 314. NBS: Washington, Chapter 1, 1969.
97. van Beijnen, A. J. M.; Nolte, R. J. M.; Zwikker, J. W.; Drenth, W. *Recl. Trav. Chim. Pays-Bas* **1982**, *101*, 409.
98. Neevel, J. G.; Nolte, R. J. M. *Tetrahedron Lett.* **1984**, *25*, 2263.
99. Kragten, U. F.; Roks, M. F. M; Nolte, R. J. M. *J. Chem. Soc., Chem. Commun.* **1985**, 1275.
100. Hladky, S. B.; Jaydon, D. A. *Biochim. Biophys. Acta* **1972**, *274*, 294.

101. Donis, J.; Grandjean, J.; Grosjean, A.; Laszlo, P. *Biochim. Biophys. Acta* **1981**, *102*, 690 and references cited therein.
102. Nakano, A.; Xie, Q.; Mallen, J. V.; Echegoyen, L.; Gokel, G. W. *J. Am. Chem. Soc.* **1990**, *112*, 1287.
103. Muñoz, S.; Mallén, J. V.; Nakano, A.; Chen, Z.; Echegoyen, L.; Gay, I.; Gokel, G. W. *J. Chem. Soc., Chem. Commun.* **1992**, 520.
104. Muñoz, S.; Mallen, J.; Nakano, A.; Chen, Z.; Gay, I.; Echegoyen, L.; Gokel, G. W. *J. Am. Chem. Soc.* **1993**, *115*, 1705.
105. Murillo, O.; Watanabe, S.; Nakano, A.; Gokel, G. W. *J. Am. Chem. Soc.* **1995**, *117*, 7665.
106. Riddell, F. G.; Hayer; M. K. *Biochim. Biophys. Acta* **1985**, *817*, 313.
107. Buster, D. C.; Hinton, J. F.; Millett, F. S.; Shungu, D. C. *Biophys. J.* **1988**, *53*, 145.
108. Riddell, F. G.; Arumugam, S.; Brophy, P. J.; Cox, B. G.; Payne, M. C. H.; Southon, T. E. *J. Am. Chem. Soc.* **1988**, *110*, 734.
109. Riddell, F. G.; Arumugam, S. *Biochim. Biophys. Acta* **1989**, *984*, 6.
110. Riddell, F. G.; Tompsett, S. J. *Biochim. Biophys. Acta* **1990**, *1024*, 193.
111. Voyer, N. *J. Am. Chem. Soc.* **1991**, *113*, 1818.
112. Voyer, N.; Robitaille, M. *J. Am. Chem. Soc.* **1995**, *117*, 6599.
113. Fuhrhop, J. H.; Liman, U. *J. Amer. Chem. Soc.* **1984**, *106*, 4643.
114. Fuhrhop, J. H.; Liman, U.; David, H. H. *Angew. Chem. Int. Ed. Engl.* **1985**, *24*, 339.
115. Jullien, L.; Lehn, J. M. *Tetrahedron Lett.* **1988**, *29*, 3803.
116. Jullien, L.; Lehn, J. M. *J. Inclusion Phenom. Mol. Recognit. Chem.* **1992**, *12*, 55.
117. Canceill, J.; Jullien, L.; Lacombe, L.; Lehn, J. M. *Helv. Chim. Acta* **1992**, *75*, 791.
118. Pregel, M. J.; Jullien, L.; Lehn, J. M. *Angew. Chem. Int. Ed. Engl.* **1992**, *31*, 1637.
119. Kobuke, Y.; Ueda, K.; Sokabe, M. *Chem. Lett.* **1995**, 435.
120. Unwin, N. *Nature (London)* **1995**, *373*, 37.
121. Mannuzzu, L. M.; Moronne, M. M.; Isacoff, E. Y. *Science* **1996**, *271*, 213.
122. Kobuke, Y. Proc. Internat. Congr. Membr. Processes, 1996, 672.
123. Tachibana, H.; Nakamura, T.; Matsumoto, M.; Komizu, H.; Manda, E.; Niino, H.; Yabe, A.; Kawabata, Y. *J. Am. Chem. Soc.* **1989**, *111*, 3080.
124. Tachibana, H.; Azumi, R.; Nakamura, T.; Matsumoto, M.; Kawabata, Y. *Chem. Lett.* **1992**, 173.
125. Yamaguchi, H.; Nakanishi, H. *Biochim. Biophys. Acta* **1993**, *1148*, 179.
126. Nakanishi H.; Yamaguchi, H. *Bioelectrochem. Bioenerg.* **1993**, *32*, 27.
127. Nakanishi, H. *Prog. Surf. Sci.* **1995**, *49*, 197.
128. Khazanovich, N.; Granja, J. R.; McRee, D. E.; Milligan, R. A.; Ghadiri, M. R. *J. Am. Chem. Soc.* **1994**, *116*, 6011.
129. Hartgerink, J. D.; Granja, J. R.; Milligan, R. A.; Ghadiri, M. R. *J. Am. Chem. Soc.* **1996**, *118*, 43.
130. Sielcken, O. E.; van de Kuil, L.A.; Drenth, W.; Schoonman, J.; Nolte, R. J. M. *J. Am. Chem. Soc.* **1990**, *112*, 3086.
131. van Nostrum, C. F.; Picken, S. J.; Schouten, A-J.; Nolte, R. J. M. *J. Am. Chem. Soc.* **1995**, *117*, 9957.
132. Tien, H. T. *Bilayer Lipid Membranes (BLM): Theory and Practice*, Marcel Dekker: New York, 1974.
133. Ottova-Leitmannova, A.; Tien, H. T. *Molecular Electronics and Bioelectronics*; Birge, R., Ed.; Adv. Chem. Series No. 240, ACS: Washington, DC, 1994.
134. Kobatake, Y.; Irimajiri, A.; Matsumoto, N. *Biophys. J.* **1970**, *10*, 728.
135. Kamo, N.; Miyake, M.; Kurihara, K.; Kobatake, Y. *Biochim. Biophys. Acta* **1974**, *367*, 1.
136. Thompson, M.; Lennox, R. B.; McClelland, R. A. *Anal. Chem.* **1982**, *54*, 76.
137. Sackmann, E. *Science* **1996**, *271*, 43.
138. Yabe, A.; Kawabata, Y.; Niino, H.; Tanaka, M.; Ouchi, A.; Takahashi, H.; Tamura, S.; Takagi, W.; Nakahara, H.; Fukuda, K. *Chem. Lett.* **1988**, 1.

139. Yabe, A.; Kawabata, Y.; Niino, H.; Matsumoto, M.; Ouchi, A.; Takahashi, H.; Tamura, S.; Takagi, W.; Nakahara, H.; Fukuda, K. *Thin Solid Films* **1988**, *160*, 33.
140. Nishiyama, K.; Fujihira, M. *Chem. Lett.* **1988**, 1257.
141. Nishiyama, K.; Kurihara, M. Fujihira, M. *Thin Solid Films* **1989**, *179*, 477.
142. Grynkiewicz, G.; Poenie, M.; Tsien, R.Y. *J. Biol. Chem.* **1985**, *260*, 3440.
143. García-Calvo, M.; Valdivieso, F.; Mayor, F. Jr.; Vázquez, J. *Neurosci. Lett.* **1992**, *136*, 102.
144. Hinton, J. F.; Kewkirk, D.; Fletcher, T. G.; Shungu, D. C. *J. Mag. Reson. Ser. B* **1994**, *105*, 11.

# CHEMICAL SENSING BASED ON MEMBRANES WITH SUPRAMOLECULAR FUNCTIONS OF BIOMIMETIC AND BIOLOGICAL ORIGIN

Kazunori Odashima, Philippe Bühlmann,

Masao Sugawara, Koji Tohda, Kenji Koga, and

Yoshio Umezawa

# 1. INTRODUCTION: MOLECULAR RECOGNITION AT MEMBRANE SURFACES

Molecular recognition based on the formation of host–guest complexes is a fundamental chemical process controlling a number of significant biological reactions. In many cases, 1:1 inclusion complexes are formed between macromolecular hosts such as enzymes, antibodies, carriers, channels, or receptors and their specific guests such as substrates, antigens, metal ions, drugs, hormones, or neurotransmitters. The highly organized structures of these host–guest complexes lead to the high efficiencies and selectivities of the biological reactions mediated by these hosts.[1,2] Host–guest complexation in biological systems occurs not only in homogeneous solutions but also at membranes, leading to various supramolecular functions as schematically depicted in Figure 1.

Efforts to mimic molecular recognition processes in biological systems by the use of artificial organic hosts with much simpler structures have been extensively studied in these several decades as "host–guest chemistry".[3] This field, together with some other related fields, has recently begun evolving into "supramolecular chemistry",[4–10] which involves every aspect of sophisticated functions based on molecular assemblies. Its applications cover not only control of organic reactions and development of new materials but also the analytical fields concerning separation and sensing of target chemical substances.

Of the biological functions depicted in Figure 1, transduction of electrochemical signals as well as active transport of chemical substances across membranes is interesting as a principle for chemical sensing. In this chapter, our recent efforts toward the development of new types of sensing membranes based on the supramolecular functions of biomimetic and biological systems will be described. The major chemical principles exploited for these sensing membranes are (1) guest-induced changes in membrane potential, (2) guest-induced changes in membrane permeability, and (3) active transport of guests. In addition to these principles, guest-induced optical changes, i.e., changes in UV absorption, second harmonic generation (SHG), and surface plasmon resonance (SPR) have also been examined. The observation of optical SHG helps to understand the surface phenomena related to guest-induced changes in membrane potential.

**Host-Guest Recognition in *Homogeneous Solutions***



(a) Separation

(b) Transformation

(c) Translocation

(d) Transduction

**Host-Guest Recognition at *Membrane Surfaces***



(a) Separation    (b) Transformation    (c) Translocation    (d) Transduction
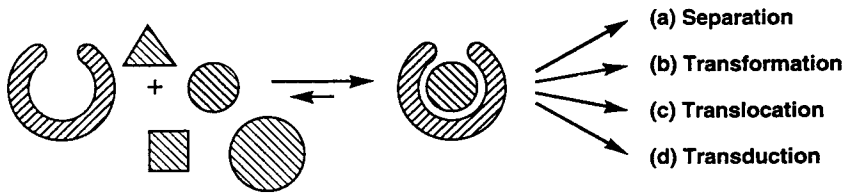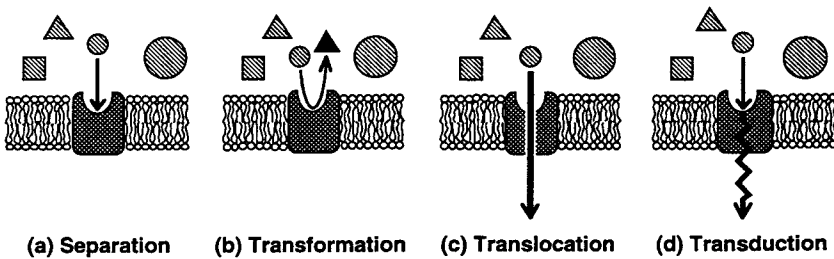
**Figure 1.** Schematic representations of significant biological functions displayed by host–guest complexation in homogeneous solutions or at membrane surfaces. (a) Separation (e.g., antibody–antigen complex formation). (b) Transformation (e.g., enzymatic reaction). (c) Translocation (e.g., carrier- or channel-mediated transport). (d) Transduction (e.g., receptor-mediated transmembrane signaling).

# 2. CHEMICAL SENSING BASED ON SUPRAMOLECULAR FUNCTIONS OF BIOMIMETIC SYSTEMS

## 2.1. Chemical Sensing by Biomimetic Systems

Recent advances in the chemistry of molecular recognition to mimic bioreceptor functions by synthetic host molecules have stimulated a number of research groups to develop novel types of sensing membranes containing synthetic hosts as sensory elements. Of the sensing principles described above, guest-induced *potential* changes, and more recently *optical* changes, have been most widely exploited for chemical sensing by biomimetic systems, as evidenced by extensive application of ion-selective electrodes (ISEs)[11–16] as well as optodes[16] in clinical, process, or environmental analyses. In particular, many successful applications of acyclic ligands, crown ethers, and more recently calixarene derivatives for sensing of alkali or alkaline earth metal cations have been made with liquid-membrane-type ISEs.[12,13,15,16] In these types of systems, hydrophobic derivatives of appropriate host molecules are dissolved in a liquid membrane supported by a polymer matrix
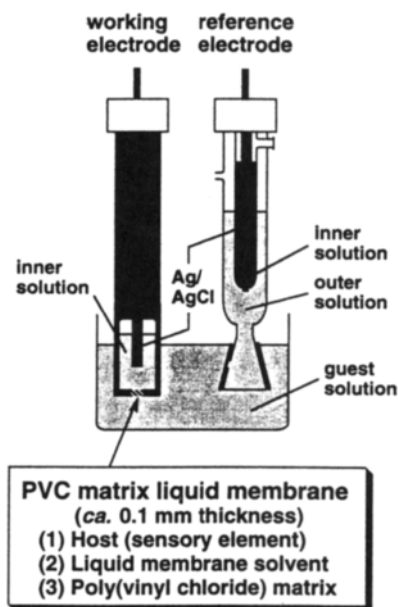
**Figure 2.** Experimental system for the measurement of membrane potential by a PVC matrix liquid-membrane-type electrode (reprinted with permission from *Yakugaku Zasshi* **1995**, *115*, 432. Copyright 1995 The Pharmaceutical Society of Japan).

(solvent polymeric membrane) (Figure 2). The polymer most frequently used for this purpose is polyvinyl chloride (PVC). A guest-induced, selective change in membrane potential, i.e., a potentiometric response, occurs as a result of host–guest complexation at the membrane surface, leading to an increase or decrease in the extent of charge separation across the organic/aqueous interface in response to the concentration of the guest (analyte) in the aqueous sample solution (Figure 3).[17-20]

In contrast to the potentiometric sensing of inorganic cations, there is still only a limited number of selective membranes for inorganic anions or organic guests because of the difficulties in developing hosts that are capable of discriminating the structural differences of these guests in the membrane/aqueous phase boundary. To establish the basic principles for potentiometric discrimination of these kinds of guests, studies aiming at the recognition of both polar and nonpolar structures of guests at membrane surfaces are necessary. From this viewpoint, we have developed some new types of PVC matrix liquid membranes that are capable of potentiometrically discriminating organic guests according to the differences in their polar or nonpolar structures.[14] Potentiometric discrimination of inorganic anions such as chloride, sulfate, or anionic metal–cyano complexes was also examined. In these membranes, the supramolecular functionalities of macrocyclic polyamines and related compounds,[21-25] nucleobase derivatives, and other hydrogen-bonding re-

## (a)



## (b)
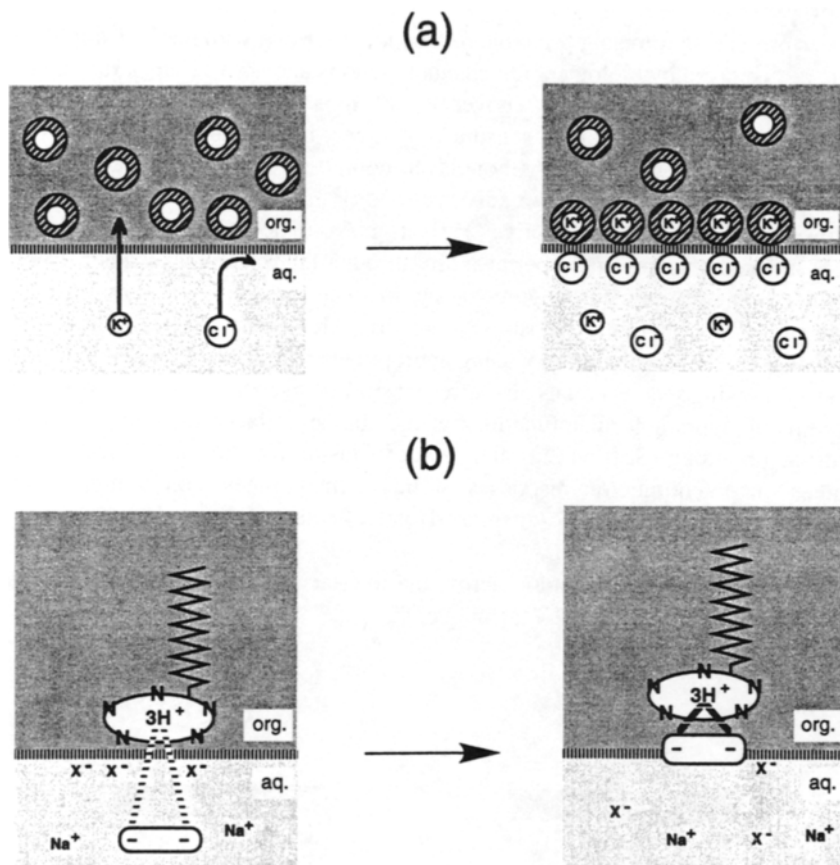


**Figure 3.** Schematic representations of models based on charge separation for membrane potential changes induced by host–guest complexation at liquid membrane surfaces. (a) Membrane potential change induced by a cationic guest. (b) Membrane potential change induced by an anionic guest (reproduced with permission of Elsevier Science Ltd. from *Comprehensive Supramolecular Chemistry*, **1996**, Vol. 2, p. 176).

ceptors,[25-29] as well as hosts with inclusion cavities (derivatives of calix[6]arene, cyclodextrin, and cyclophane),[30,31] were exploited to obtain guest-selective changes in membrane potential.

In contrast to chemical sensing based on membrane potential changes, there are still only a limited number of investigations on chemical sensing based on guest-induced changes in *membrane permeability*, or based on *active transport* of target guests. An increase or decrease in membrane permeability as a result of selective host–guest complexation leads to rapid flux of a large amount of ions. Active transport across a membrane can be used to concentrate target guests. Both of these

modes provide a promising principle for chemical sensing with marked amplifica-
tion, as displayed by biological ion channel proteins and active transport systems.

Aiming at the development of a novel class of signal-amplifying sensors that may
be designated as "ion channel sensors",[32-38] guest-induced permeability control
was studied for oriented multi- or monolayers composed of natural or synthetic host
molecules (valinomycin,[32,33] macrocyclic polyamine,[33,34] cyclodextrin,[34,35]
calixarene,[36] nucleobase derivative[37]). Host–guest complexation by these mole-
cules induced changes in the permeability through intermolecular voids between
the membrane components (Figure 4a) and in some cases through intramolecular
channels of the membrane hosts (Figure 4b). Membrane permeabilities were
evaluated by cyclic voltammetry using appropriate electroactive markers.

The following sections focus on our recent studies on chemical sensing based on
biomimetic supramolecular functions at membrane surfaces involving multiple
hydrogen bonding (Section 2.2) and cavity inclusion (Section 2.3). Mechanistic
studies on potentiometric responses of liquid membranes, employing surface
specific techniques, i.e., FTIR (attenuated total reflection mode) and optical second
harmonic generation (SHG),[39-43] will also be described (Section 2.4). Direct
observation of charge separation across the interface of membrane and aqueous
solution was made by the SHG technique.

## (a)                                          (b)
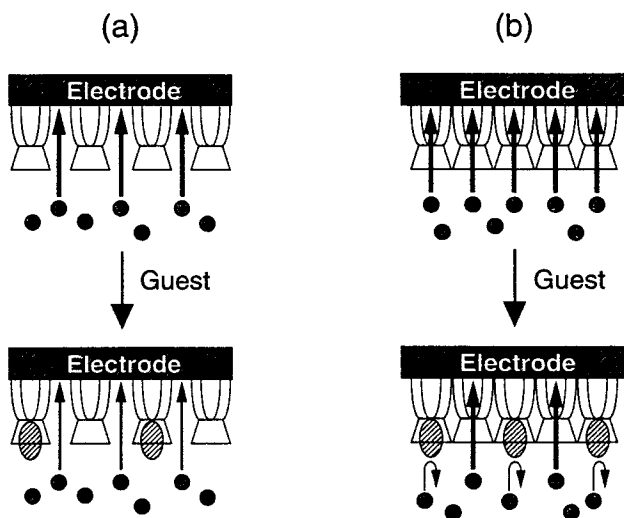


*Figure 4.* Schematic representations of possible modes of controlling permeability
through an oriented membrane by host–guest complexation. (a) Control of permeabil-
ity through intermolecular voids. (b) Control of permeability through intramolecular
channels (reprinted with permission from *Anal. Chem.* **1993**, *65*, 928. Copyright 1993
American Chemical Society).

## 2.2. Chemical Sensing Based on Multiple Hydrogen Bonding

### *Sensing Based on Interactions with Polar Moieties of Guests*

Host–guest complexation at membrane surfaces based on the recognition of polar moieties of guests is an important principle for chemical sensing of inorganic and organic guests. For organic guests, such a mode of potentiometric discrimination has been first demonstrated by a series of studies on anion-selective electrodes using long alkyl chain derivatives of macrocyclic polyamines as the sensory elements.[21-23,44] The macrocyclic polyamines, in their multiply-protonated polycationic forms, displayed potentiometric discrimination of adenine nucleotides[21,23] or dicarboxylate isomers[22,23] according to the amount or proximity of negative charges of these guests. By the comparison of the potentiometric response behaviors of hosts **1–4**, the most important factor for effective potentiometric discrimination of multiply-charged guests was found to be concentrated positive charges on the host due to multiprotonation within a restricted cyclic system.[44] It was also possible to potentiometrically discriminate with related hosts (**5, 6**) anionic metal–cyano complexes with planar and octahedral structures.[24]

Discrimination of multiply-charged organic guests such as adenine nucleotides and dicarboxylate isomers was also achieved for guest-induced changes in the permeability through intermolecular voids in Langmuir–Blodgett-type oriented membranes, as evaluated by cyclic voltammetry using $[Fe(CN)_6]^{4-}$ or other electroactive markers.[34,38] As the membrane components, long alkyl chain derivatives of macrocyclic polyamines (**1, 2**) which can discriminate multiply-charged guests by electrostatic interactions, were used.

Concerning the recognition of polar moieties of guests, multiple hydrogen bonding such as complementary base pairing is another important and more sophisticated principle because it involves directed, multipoint interactions. The first potentiometric discrimination based on complementary hydrogen bonding has been achieved by PVC matrix liquid membranes containing a host with ditopic receptor function (**7**)[26] or a mixture of hosts for electrostatic binding and complementary base pairing (**2** or **6** + **8**;[25,27] **9** + **10a, 10b, 11a** or **12**[28]), which were shown to be capable of potentiometrically discriminating nucleotides bearing guanine and



1: X = H₂     2: X = H₂     3     4
5: X = O      6: X = O

R = -(CH₂)₁₅CH₃

7

8 (R = Si[CH(CH₃)₂]₃)

9

10a,b    11a,b

12

a:  R =  —CH₂CH(CH₂)₈CH₃
                   |
              (CH₂)₆CH₃

b:  R = –(CH₂)₁₇CH₃

R =
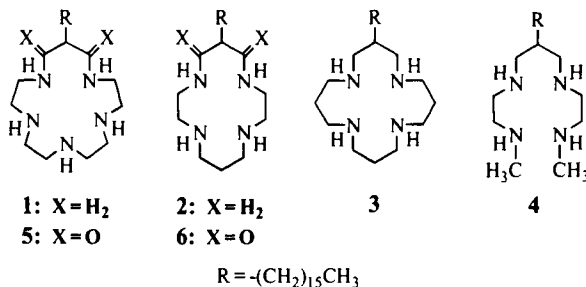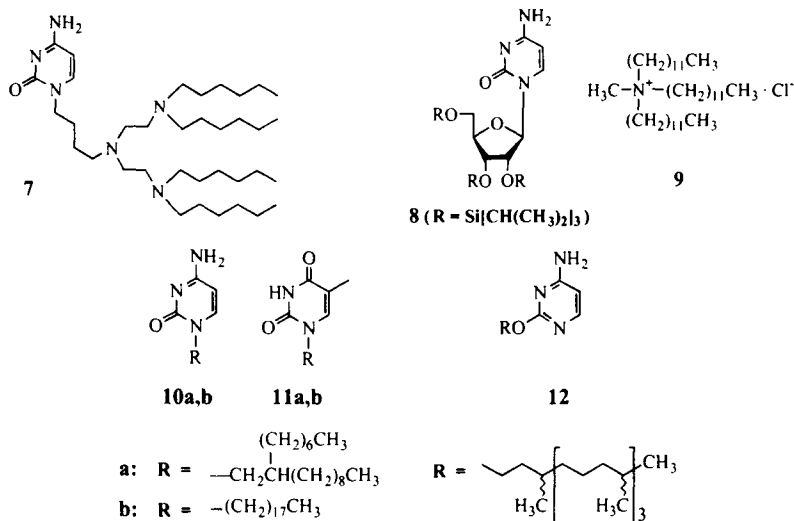
adenine bases. More recently, complementary hydrogen bonding by bis-thiourea derivatives[29] was shown to be effective for potentiometric discrimination of sulfate or chloride, as will be described in the next section.

## Potentiometric Sensing of Inorganic Anions

*Synthetic Anion Receptors.*    The development of synthetic hosts for anions has been based mainly on charged or coordination systems such as protonated polyamines and related hosts, transition metal complexes, or organometallic compounds.[45] Following the first report in 1968 on cryptand-type diamines,[46] protonated polyamine-type hosts for inorganic and organic anions were extensively studied as anion receptors by Lehn[6,47] and Kimura.[48,49] Other types of cationic hosts such as poly(quaternary ammonium) or polyguanidinium compounds and transition metal complexes were also reported. Some of these hosts were used for liquid membrane electrodes, mainly as sensory elements for inorganic anions. Examples include vitamin $B_{12}$ derivatives, metalloporphyrins, bis(quaternary ammonium) or diphosphonium salts, and metallopolyamines.[15,50] With regard to organic anions, macrocyclic polyamines are examples of sensory elements for ISEs that are capable of discriminating structural differences of polyanionic organic guests.[14,15] However, only very few examples of sensor applications of neutral hosts that bind anions primarily by hydrogen bonding, which have recently drawn much attention in host–guest chemistry,[51] have so far been reported. The particular need for sensing of inorganic phosphate has led us to search for such receptor molecules for phosphate.

**13:** X = O, R = -(CH$_2$)$_3$CH$_3$
**14:** X = S, R = -(CH$_2$)$_3$CH$_3$
**15:** X = S, R = -C$_6$H$_5$
**16:** X = S, R = 1-naphthyl

**17:** X = S, Y = NH, R = -(CH$_2$)$_3$CH$_3$
**18:** X = S, Y = NH, R = -C$_6$H$_5$
**21:** X = Y = O, R = -CH$_2$C$_6$H$_5$

**19:** X = O
**20:** X = S
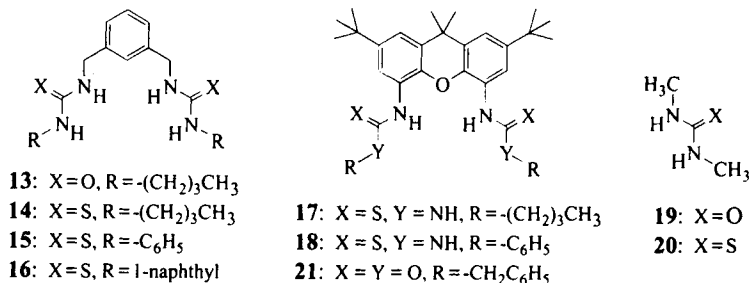
**Table 1.** Association Constants ($K_{11}$, M$^{-1}$, in DMSO–$d_6$) of Receptors **13–18** with Various Anions[29,61–63]

| Anion[a] | Host **13** | Host **14** | Host **15** | Host **16** | Host **17** | Host **18** |
|---|---|---|---|---|---|---|
| H$_2$PO$_4^-$ | 110 | 820 | 4600 | 1000 | 55000 | 195000 |
| CH$_3$CO$_2^-$ | 47 | 470 | 2300 | 350 | 38000 | |
| Cl$^-$ | 4 | 9 | 10 | 5 | 840 | 1000 |
| HSO$_4^-$ | 1 | 2 | | | | |
| NO$_3^-$ | <1 | <1 | | | | |
| ClO$_4^-$ | NC[b] | NC[b] | | | | |

*Notes:* [a]Countercation: C$_4$H$_9$)$_4$N$^+$.
[b]NC = negligible complexation.

## Bis-urea and Bis-thiourea Derivatives as Neutral Receptors for Anions.

Recently, several neutral receptors based on a Lewis acid and/or hydrogen bond donor groups that bind inorganic and organic phosphates have been developed.[52–60] Particularly, the reports on receptors with two urea groups that bind dicarboxylates, disulfonates, and diphosphonates,[58–60] and on a receptor with two thiourea groups that complexes a dicarboxylate,[59] suggested the possibility of developing strong receptors for phosphate by appropriate preorganization of more than one urea or thiourea group.

On the basis of this concept, bis-urea (**13**) and bis-thioureas (**14–18**) were synthesized and their binding with dihydrogenphosphate (H$_2$PO$_4^-$) and various other anions in dimethyl sulfoxide (DMSO) was investigated by $^1$H NMR spectroscopy.[29,61] Stability constants, $K_{11}$, for the 1:1 complexes are given in Table 1, together with those for the 1:1 complexes with $N$,$N'$-dimethylurea (**19**) and $N$,$N'$-dimethylthiourea (**20**).[29,61–63]

Receptors with two urea or thiourea groups clearly bind H$_2$PO$_4^-$ more strongly than receptors with one of those groups only, as can be seen from the increases in the $K_{11}$ value from **19** (28 M$^{-1}$) to **13** (110 M$^{-1}$) or from **20** (120 M$^{-1}$) to **14** (820 M$^{-1}$). Considerable downfield shifts induced in the $^1$H NMR chemical shifts of the

X = O, S
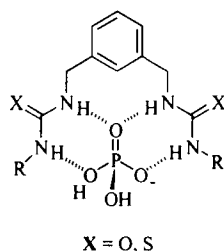
**Figure 5.** Suggested structure of 1:1 complex between dihydrogenphosphate ($H_2PO_4^-$) and bis-urea (X = O) and bis-thiourea (X = S) receptors.

NH hydrogens of **13–20** upon $H_2PO_4^-$ binding, as well as the extremely weak binding of $H_2PO_4^-$ by $N,N$-dimethylurea and $N,N,N'$-trimethylthiourea (3 and 5 $M^{-1}$, respectively), show that the NH hydrogens are involved in the $H_2PO_4^-$ binding. The structure of the $H_2PO_4^-$ complexes of these bis-urea and bis-thiourea receptors is suggested to involve four hydrogen bonds (Figure 5), and thus strongly resembles that suggested for the complex of $H_2PO_4^-$ and a bisguanidine.[64]

The considerable increases in binding strengths of the thiourea compounds (**14, 20**) compared to the corresponding urea compounds (**13** and **19**, respectively) can be explained by the $pK_a$ of the hydrogen bond donating groups, which is roughly 6 units[65] larger for thioureas than for ureas ($pK_a[(H_2N)_2CS] = 21.0$; $pK_a[(H_2N)_2CO] = 26.9$; in DMSO at 25 °C),[64] making the former much stronger hydrogen bond donors.[59] Similarly, the replacement of butyl by phenyl substituents leads to much stronger complex stabilities ($K_{11}$: **15 > 14**; **18 > 17**), the electron-withdrawing effect of the phenyl groups further enhancing the acidity of the hydrogen bond donor ($pK_a[(PhNH)_2CS] = 13.5$).[65] Similar effects have also been observed for complexes between aryl thioureas and a zwitterionic ammonioalkane-sulfonate[66] and for complexes between calix[6]arene receptors and halide ions.[67] The naphthyl group is less beneficial for complexation ($K_{11}$: **16 < 15**). CPK models indicate that, due to steric hindrance, coplanarity of the naphthyl rings and the thiourea groups in the $H_2PO_4^-$ complex is not possible, decreasing the conjugation between the thiourea groups and their aromatic substituents and reducing the hydrogen bond strength.

A very large stabilizing effect is obtained by replacing the $m$-xylene by a xanthene spacer ($K_{11}$: **17, 18 > 14, 15**), which has previously been also used by Rebek and co-workers for carboxylate receptors.[58] While other explanations for the success of this spacer for linking the two thiourea groups have been discussed,[61] it seems that the rigidity of this spacer is the primary reason for the high stabilities of the $H_2PO_4^-$ complexes of **17** and **18**. The importance of formation of four hydrogen bonds is however emphasized by the weakness of the $H_2PO_4^-$ complex of bis-ure-thane **21**, where only two NH's are available as hydrogen donors and in addition

the two carbonyl groups of the receptor are not efficient hydrogen bond acceptors. To the best of our knowledge, there are no published neutral receptors that form $H_2PO_4^-$ complexes stronger than those of bisthioureas **17** and **18**.

Both bis-urea and bis-thiourea hosts bind $H_2PO_4^-$ preferentially, $CH_3CO_2^-$ being the only other anion bound substantially (Table 1). The complexation strength seems to reflect not only the hydrogen-bonding complementarity of $H_2PO_4^-$ and each host but also the hydrogen bond acceptor strength of each anionic guest. The latter is appropriately reflected by the free energies of hydration of $X^-$ [$\Delta G_{n-1,n}^0$ for the hydration equilibria $X^- \cdot (H_2O)_{n-1} + H_2O \rightleftharpoons X^- \cdot (H_2O)_n$] in the gas phase.[68,69] Comparison of the free energies of hydration $\Delta G_{0,1}^0$ (in kcal/mol) in the gas phase for $CH_3CO_2^-$, $Cl^-$, $H_2PO_4^-$, $NO_3^-$, $HSO_4^-$ and $ClO_4^-$ (9.4, 8.2, 7.6, 7.1, 5.9, and 4.8, respectively)[70,71] and $K_{11}$ ($M^{-1}$) for the 1:1 complexation of host **14** with these anions (470, 9, 820, <1, 2, and no binding observed) shows that the weak binding of $NO_3^-$, $HSO_4^-$, and $ClO_4^-$ reflects their relatively low hydrogen bond acceptor strength. The weak binding of $Cl^-$ to the receptors **13** and **14**, on the other hand, may be explained by a solvation effect resulting from strong ion–dipole interactions between $Cl^-$ and DMSO.[72]

*Ion-Selective Electrodes based on Bis-Thiourea Receptors.* Bis-thiourea derivatives **14**, **15**, and **17**, which have a good membrane solubility, sufficient lipophilicity to prevent leaching into the aqueous sample solution, and a low tendency for self-aggregation in nonpolar solvents, were incorporated into PVC matrix liquid membranes for ISEs.[62,63] While membrane electrodes based on the dibutyl derivative **14** gave a phosphate response almost identical to that of a conventional anion-exchanger electrode, a membrane electrode based on the phenyl-substituted bis-thiourea **15** exhibited a slightly improved phosphate response, which seems to be the result of improved complexation of phosphate in the sensor membrane.

Figure 6a shows the measured potential (potentiometric response) as a function of the guest concentration (logarithm) for various anions at pH 6.8 for the membrane with receptor **15** [*o*-nitrophenyl octyl ether (*o*-NPOE) as the membrane solvent]. Anion exchanger **9** was also added in the membrane to provide lipophilic cationic sites, which are necessary for stable, countercation-independent responses of neutral carrier-based anion selective electrodes.[42,43,50] Figure 6b shows the response of a reference membrane containing only **9**. The potentiometric selectivity of the former membrane was of the order $NO_3^- > SO_4^{2-} > Cl^- > H_2PO_4^- > CH_3CO_2^-$ (Figure 6a). This order differs significantly from that of the classical anion exchanger-based membrane (Figure 6b), the selectivity of which is governed by the hydrophobicity of the anion (Hofmeister series: $ClO_4^- > SCN^- > I^- >$ salicylate$^- > NO_3^- > Br^- > Cl^-$ $> HCO_3^- > CH_3CO_2^- > SO_4^{2-} > HPO_4^{2-}$). As compared to the Hofmeister-type selectivity of Figure 6b, enhanced responses to $SO_4^{2-}$, $Cl^-$, and phosphate ($H_2PO_4^-$ or $HPO_4^{2-}$) are observed for the electrode based on **15**.

# (a)



# (b)
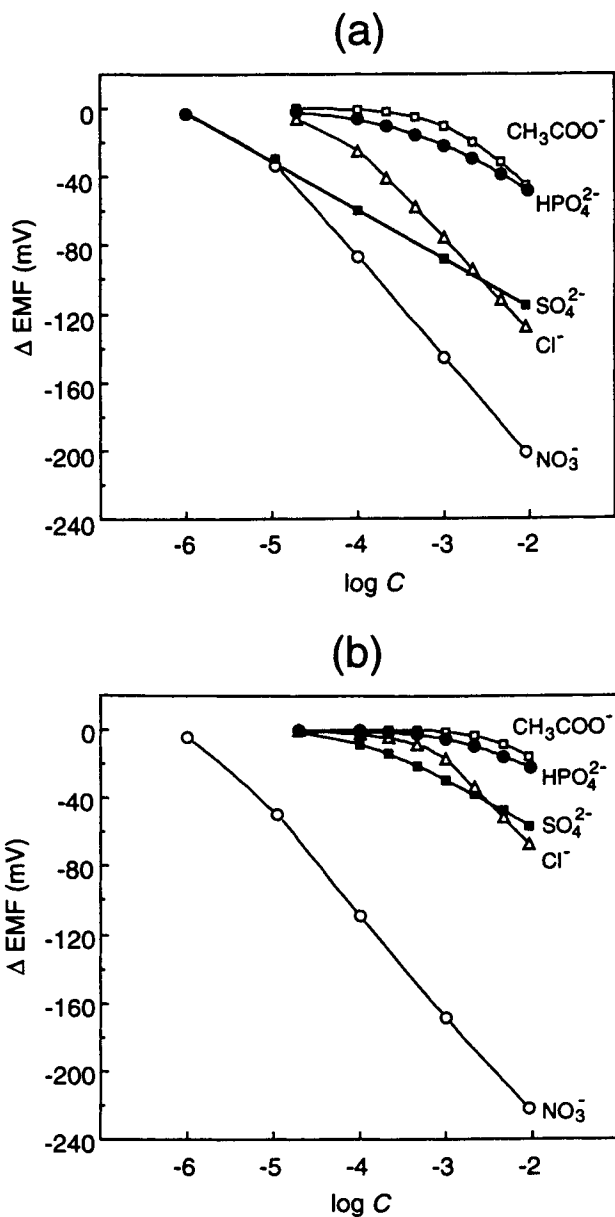


*Figure 6.*   Potentiometric responses to anions by o-NPOE/PVC (2:1 wt/wt) membranes
containing (a) 1 wt% receptor **15** and 55 mol% of cationic site **9** (relative to the
receptor), and (b) 6 wt% of cationic site **9** (without receptor). Measured at pH 6.8 (0.1
M HEPES-NaOH buffer).

The potentiometric response of receptor **15** for $H_2PO_4^-$ is not sufficient for a phosphate-selective electrode, but the strong response and high selectivity of this electrode for the dianion $SO_4^{2-}$ is striking.[62] The response down to $10^{-6}$ M is a very big improvement as compared to the response of the anion exchanger ISE, for which the linear range of the $SO_4^{2-}$ response extends only down to $10^{-3}$ M. The linear range of response of the former ISE from $1.0 \times 10^{-6}$ to $1.0 \times 10^{-2}$ M with a slope of $-28.1 \pm 1.8$ mV decade$^{-1}$ shows that the present electrode responds to $SO_4^{2-}$ and not to $HSO_4^-$. The electrode based on **15** is the first neutral host-based electrode with an appreciable selectivity for sulfate.

The need for chloride determination in clinical analysis and environmental monitoring has inspired the development of a number of receptors for this ion. ISEs based on organometallics (trialkyltin compounds,[73] organomercury derivatives[74]) as well as metal complexes [magnesium(III) and indium(III) porphyrins[75,76]] have so far been reported. Electrodes based on neutral receptor **17**, which binds anions only by formation of hydrogen bonds, have been found to give ISEs with a good selectivity for Cl$^-$.[63] As can be seen from Figure 7, receptor **17** does not appreciably increase the potentiometric response to $H_2PO_4^-$ but gives a large enhancement of the Cl$^-$ response. In contrast to electrodes based on receptor **15**, $SO_4^{2-}$ is fairly well discriminated. Because of this good Cl$^-$ selectivity, an electrode based on **17** was used to measure the chloride concentration in control serum samples obtained from
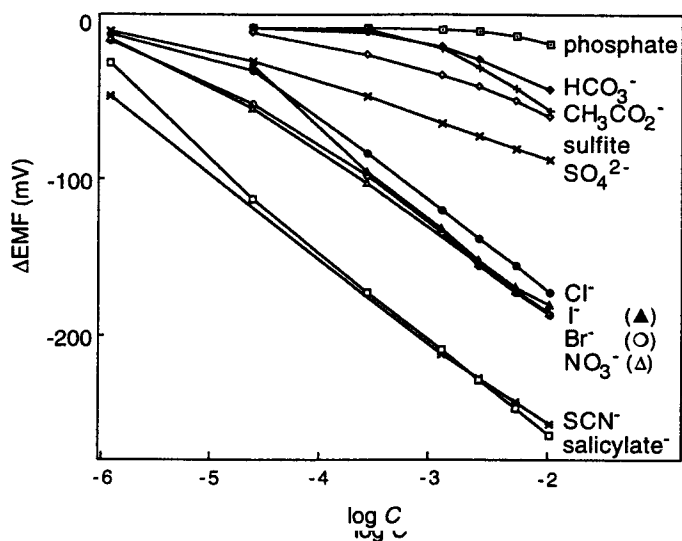


***Figure 7.*** Potentiometric responses to anions by an o-NPOE/PVC (2:1 wt/wt) membrane containing 1 wt% receptor **17** and 50 mol% cationic site **9** (relative to the receptor). Measured at pH 7.0 (0.1 M HEPES-NaOH buffer). Phosphate: $H_2PO_4^-$ or $HPO_4^{2-}$; sulfite: $HSO_3^-$ or $SO_3^{2-}$ (reprinted with permission from *Anal. Chem.* **1997**, *69*, 1042. Copyright 1997 American Chemical Society).

horse blood ($[Cl^-] = 102.3$ mM]. The concentration of $Cl^-$ determined with the ISE based on receptor **17** was 102.1 mM while use of a conventional anion exchanger electrode gave a much too high chloride concentration (114.2 mM on average). Reasons for the much better selectivity of **17** for $Cl^-$ vs $SO_4^{2-}$ than in case of receptor **15** are probably related to how easily all the nitrogen-bound hydrogens of these receptors can converge on the relatively small $Cl^-$ anion to form a 2:1 host–guest complex bound by eight hydrogen bonds.

The above receptors are to the best of our knowledge the first examples for the use of hydrogen bonds between an unambiguously neutral receptor and inorganic anions for potentiometric sensing. However, with regard to complexation, hydrogen bonds have been recently used for the design of several synthetic receptors for anions. Formation of hydrogen bonds between amides and $Cl^-$ for example was shown to significantly increase the stability of complexes in which $Cl^-$ is electrostatically bound to cobalticinium or ruthenium(II)bipyridyl moieties.[77] Reinhoudt and co-workers have reported that neutral thiourea-derivatized *p-tert*-butylcalix[4]arenes[78] and *p-tert*-butylcalix[6]arenes[67] bind halide anions exclusively through hydrogen bonding. It seems that hydrogen bond donor groups may become just as commonly used in anion sensing as ether oxygen and amide functional groups are presently used for cation sensing.

### Potentiometric Sensing of Nucleotides

The biological significance of recognizing nucleobases in double-stranded DNA and RNA by complementary base pairing has stimulated a number of research groups to develop synthetic receptors capable of complementary hydrogen bonding.[51] The recognition of nucleobases by hydrogen bonding is characteristic in that it requires a correct array of both hydrogen bond donors and acceptors, whereas only hydrogen bond acceptor or donor sites have been used for the recognition of inorganic guests as discussed above. So far, only very few synthetic receptors with both hydrogen bond acceptor and donor sites have been used in potentiometry, even though a large number of them have been described in supramolecular chemistry.

The earliest potentiometric sensors for nucleotides were the liquid membrane ISEs based on macrocyclic polyamines (**1, 2**),[21,23] which upon multiple protonation displayed potentiometric responses to adenine nucleotides primarily due to electrostatic interactions with the phosphate groups of these analytes. These ISEs are capable of discriminating $ATP^{4-}$, $ADP^{3-}$, and $AMP^{2-}$ according to the amount of negative charge, but discrimination of differences in the nucleobase unit was achieved only recently by electrodes based on nucleobase derivatives. Electrodes based either on the cytosine-pendant triamine **7**[26] or, in the presence of either macrocyclic polyamine **2** or **6**, the neutral cytidine derivative **8**[25,27] were able to discriminate potentiometrically among guanine and adenine nucleotides. To the best of our knowledge, these electrodes were the first examples of ISEs capable of discriminating differences in the base unit and of ISEs with sensory elements with

hydrogen bond acceptor and donor sites that interact simultaneously with the analyte ion.

Electrodes based on the cytosine-pendant triamine **7** responded to guanosine 5'-monophosphate (5'-GMP) and guanosine 5'-triphosphate (5'-GTP), while adenosine 5'-monophosphate (5'-AMP) and adenosine 5'-triphosphate (5'-ATP) did not yield any response.[26] This good selectivity was explained by ditopic recognition based on complementary base pairing and moderately strong electro-static interactions between the guanine nucleotides and the protonated cytosine-pendant triamine **7**, in analogy with the interactions in the complex formed in dimethyl sulfoxide.[79] However, the slopes of the EMF responses of this electrode were smaller than expected from the charge of the guanine nucleotides, reducing the sensor sensitivity. Also the response slope of electrodes containing the lipophilic cytidine derivative **8** and either macrocyclic polyamine **2** or **6**,[25,27] the selectivity of which was explained by ditopic recognition involving a ternary complex formed by neutral host **8**, analyte nucleotide, and one of the macrocyclic tetraamines, could not be easily interpreted. In these systems, the potentiometric response mechanism could be complicated by multiple protonation equilibria involving the polyamine hosts.

In order to obtain a better understanding of the factors determining the poten-tiometric selectivities, simpler systems of PVC matrix liquid membranes containing either only sterically crowded, cationic site (**9**) and/or neutral nucleobase deriva-tives (**10a, 11a, 12**) were investigated.[28] 5'-Monophosphates of guanosine and adenosine, which are both expected to form Watson–Crick analogous base pairs with **10a** and **11a**, respectively, were used as analyte ions. ISE membranes contain-ing only the neutral cytosine derivatives (**8, 10b**) and no added cationic site give no appreciable potentiometric response to nucleotides[25,26] because ionic sites that are confined to the membrane phase and have a charge sign opposite to that of the analyte ions are necessary for obtaining stable, counterion-independent responses with ISEs based on neutral receptors.[42,43]

Electrodes based on **9** but no nucleobase derivative [3.0 wt% **9**; bis(2-ethylhexyl) phthalate ("dioctyl phthalate", DOP) as the membrane solvent] showed similar potentiometric responses to 5'-GMP and 5'-AMP (Figure 8a), which is not surpris-ing because cation **9** cannot interact specifically with the base pairing site of nucleotides. The EMF slope ($-29$ mV decade$^{-1}$; 0.1 M HEPES–NaOH buffer solution, pH 6.8) was much greater than in case of the electrode based on the macrocyclic pentaamine **1** ($-15$ mV decade$^{-1}$)[21,23] and corresponds to the slope as expected for a dianion according to the Nernstian equation. Extraction experiments confirmed that at this pH it is indeed the dianion that enters the organic phase.

Electrodes based on neutral cytosine derivative **10a** (1.3 wt%) and **9** (150 mol% relative to **10a**) gave EMF slopes of $-29$ mV decade$^{-1}$ for both 5'-GMP and 5'-AMP (Figure 8b), suggesting that these electrodes respond in a Nernstian manner to nucleotides in their divalent form, just as in the case of the anion exchanger electrode. The potentiometric response was selective for 5'-GMP over 5'-AMP with
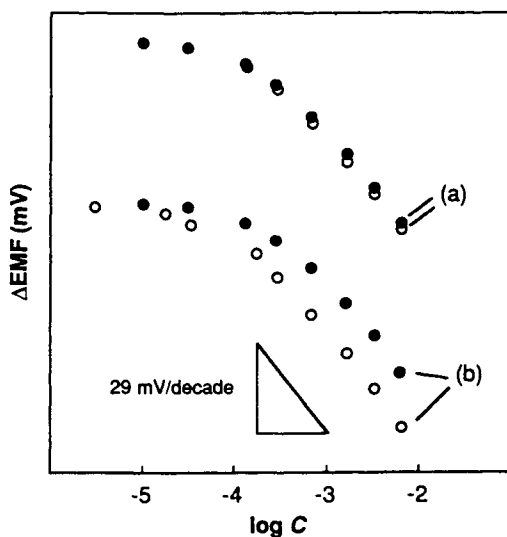
**Figure 8.** Potentiometric responses to 5'-GMP (o) and 5'-AMP (●) by PVC matrix liquid membranes (DOP/PVC = 2:1 wt/wt) containing (a) lipophilic cation 9 (3.1 wt%) and (b) lipophilic cation 9 (3.1 wt%) plus neutral cytosine derivative 10a (1.3 wt%) (150 mol% 9 relative to 10a). Measured at pH 6.8 (0.1 M HEPES–NaOH buffer) (adapted with permission from *Anal. Chim. Acta* **1997**, *341*, 134. Copyright 1997 Elsevier Science Ltd.).

the potentiometric selectivity coefficient ($K^{pot}_{5'-GMP, 5'-AMP}$) of 0.42, which corresponds to an EMF difference of 12 mV and hence to a free energy difference, $\Delta G^0$, of 2.0 kJ mol$^{-1}$ (as obtained from $\Delta G^0 = zF\Delta\Phi$; z being the charge of the analytes and $\Delta\Phi$ the difference in the EMF). Considering the formation of three hydrogen bonds with the guest 5'-GMP but only two hydrogen bonds with 5'-AMP, respectively, the $\Delta G^0$ of 2.0 kJ mol$^{-1}$ is much smaller than the value of ca. 5.0 ± 1.0 kJ mol$^{-1}$ as expected for a typical free energy of hydrogen bond formation in CDCl$_3$.[51,80,81] This suggests that the experimentally observed potentiometric selectivity is not determined by the stabilities of the 1:1 complexes alone, but that other factors diminish that selectivity (*vide infra*). On the other hand, electrode with receptor **11a**, which can form only two hydrogen bonds to the guest, showed no significant discrimination between 5'-GMP and 5'-AMP.

For the alkoxy receptor **12**, which can also form 1:1 complexes with guanine nucleotides, the influence of the cationic site/receptor ratio on the EMF selectivity was determined (Table 2). Electrodes based on **12** and 210 mol% **9** gave similar, Nernstian responses to both 5'-GMP and 5'-AMP, as expected for an excess of cationic sites.[50] Due to the high concentration of cation **9**, the concentration of uncomplexed nucleotides in these membrane is high and a selectivity typical for a

***Table 2.*** Response Slope and Selectivities of ISEs Based on Receptor **12** and Cationic Site **9**[28]

| Site/Receptor Ratio (mol %) | Slope (mV/decade)[a] | | Selectivity[b] $K^{pot}_{5'-GMP, 5'-AMP}$ |
|---|---|---|---|
| | 5'-GMP | 5'-AMP | |
| 50 | −31.7 | −29.5 | 0.83 |
| 80 | −31.0 | −29.2 | 0.71 |
| 150 | −30.8 | −28.7 | 0.45 |
| 210 | −30.9 | −29.6 | 0.71 |

*Notes:* [a]For linear regression between $10^{-3.5}$ and $10^{-2.2}$ M of 5'-GMP or 5'-AMP.

     [b]Calculated according to the separate solution method, using ΔEMF values obtained at $10^{-2.2}$ M of 5'-GMP or 5'-AMP.

classical anion exchanger results. Electrodes based on ionophore **12** and 150 mol% **9** show a selective response for 5'-GMP over 5'-AMP, the selectivity being the same as that of electrodes based on ionophore **10a** and the same amount of **9**, confirming selective binding of receptor and nucleotides. However, a decrease in the amount of **9** to 80 and 50 mol% decreases the selectivity. The maximum in potentiometric selectivity in the presence of 150 mol% **9** would not be expected if 5'-GMP and 5'-AMP would both form only 1:1 complexes with the receptor. Formation of 1:1 and 1:2 host–guest complexes for 5'-GMP and 5'-AMP, respectively, in analogy to similar complexes as observed in chloroform and dimethyl sulfoxide, is one example of stoichiometries that might explain the observed selectivities but higher stoichiometries cannot be excluded.

Possible measures that are expected to improve the potentiometric selectivity are (1) use of hosts that form stronger complexes, (2) modification of the host to avoid ionophore self-association, and (3) an improved choice of the membrane solvent to avoid strong solvation of the hosts in the membrane. Evidence for the importance of (2) and (3) has been obtained from $^{13}$C NMR spectra of **12**.[28] While the properties of 1:1 host–guest complexes are very often of primary interest in supramolecular chemistry, the above results show that use of receptors for sensing purposes must be based on a receptor design that goes beyond this viewpoint.

## Optical Sensing of Nucleotides

To increase the selectivity of the above guanine nucleotide receptors **10a** and **12**, two receptors **22** and **23** that can form five instead of three hydrogen bonds to guanosine derivatives (Figure 9) were synthesized.[37] The UV-vis spectra of **22** and **23** in a mixture of CHCl$_3$ and DMSO (4:1, v/v) did not change significantly upon complexation with the lipophilic deoxyguanosine derivative **24**, but the fluorescence emission of both receptors is quenched by this guest.[82] The lipophilic deoxyadenosine derivative **25**, on the other hand, did not influence the fluorescence spectrum. The stability constant ($K_{11}$) of the 1:1 complex of receptor **22** and guest

X = O, S
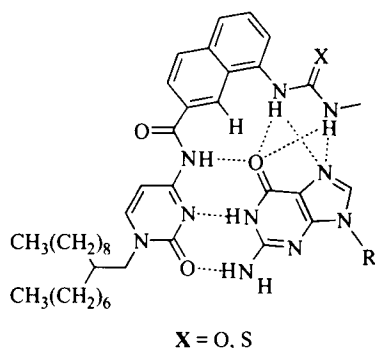
**Figure 9.** Possible structure of the 1:1 complexes of receptor **22** (X = O) or **23** (X = S) and 5'-GMP.

**24** was $1.7 \times 10^2$ $M^{-1}$, as determined by fluorescence spectroscopy and $^1H$ NMR spectroscopy. A similar effect was also observed for receptor **23**, but this receptor was unfortunately found to decompose under irradiation.

The fluorescence response of an optical sensor based on a PVC matrix liquid membrane containing receptor **22** and ionic sites [bis(2-ethylhexyl) sebacate



22: X = O
23: X = S
R = -(CH₂)₈CH₃
R' = -(CH₂)₆CH₃

24          25

R = Si[CH(CH₃)₂]₃

o-NPOE

DOP

DOS

5'-GMP²⁻ (n = 1)          5'-AMP²⁻ (n = 1)
5'-GDP³⁻ (n = 2)          5'-ADP³⁻ (n = 2)
5'-GTP⁴⁻ (n = 3)          5'-ATP⁴⁻ (n = 3)
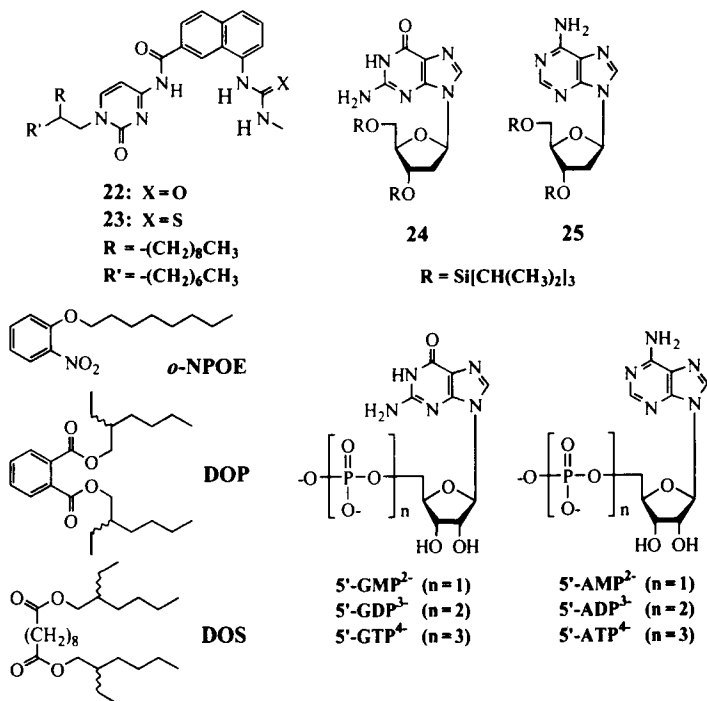
("dioctyl sebacate", DOS) as the membrane solvent] was examined by using 5'-triphosphates of guanosine and adenosine (5'-GTP and 5'-ATP, respectively) as analytes. The response mechanism of this optode is based on ion exchange: nucleotides enter the membrane where they form complexes with the receptor while, in exchange, chloride ions leave the membrane, thus maintaining electroneutrality in the bulk phases. Whereas the selectivity of this sensor is smaller than that observed for the fluorescence quenching in homogeneous solution, this optode still has a high selectivity for 5'-GTP over 5'-ATP (Figure 10).

An optical transduction has also been found for a receptor derived from 2-amino-4(3*H*)pyrimidone that forms three hydrogen bonds to creatinine (Figure 11).[83,84] In this case, the changes in the UV spectrum of the receptor are based on a shift in the tautomerization equilibrium of the receptor due to stabilization of one of its tautomers in the creatinine complex. Using this receptor, extraction of creatinine from aqueous solutions into an organic solvent could be significantly enhanced and directly observed spectroscopically.[83] Recently, a similar approach based on a more highly preorganized receptor forming four hydrogen bonds has allowed to decrease the detectable concentration of creatinine.[85,86]
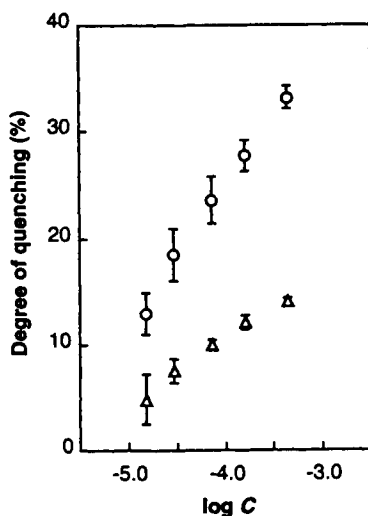


**Figure 10.** Fluorescence responses of a PVC–matrix liquid membrane based on receptor **22** as a function of concentration of 5'-GTP (○) and 5'-ATP (△) in a buffer solution (10 mM Tris/HCl, pH 7.4). Membrane composition: DOS/PVC = 2:1 wt/wt, 3.3 wt% **22** + **9** (400 mol% relative to **22**). Excitation at 375 nm, detection at 470 nm.
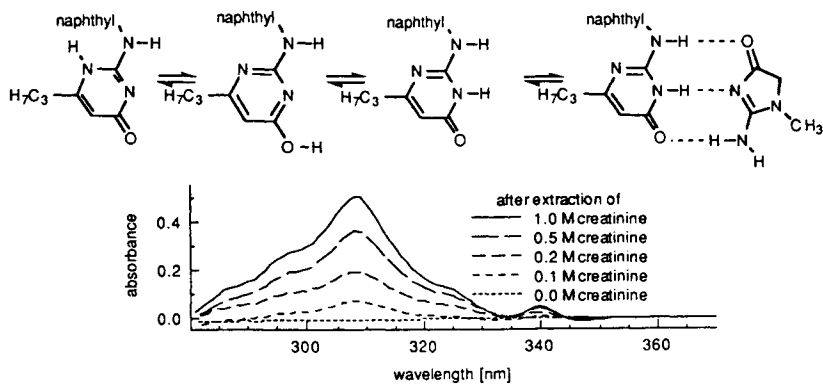
*Figure 11.* (a) Stabilization of one tautomer of the receptor by complexation with creatinine. (b) Increase of the UV absorption of a creatinine receptor upon extraction of creatinine from an aqueous solution into a 1 mM CH$_2$Cl$_2$ solution of the receptor (reprinted from *Tetrahedron* **1993**, *49*, 596. Copyright 1993, with permission from Elsevier Science Ltd.).

## Channel Mimetic Sensing Membranes for Guanosine 5'-Monophosphate

Kunitake and co-workers[87] have reported that monolayers of amphiphiles with diaminotriazine and orotate head groups, formed at the air/water interface, effectively bind thymidine and adenine, respectively. This study suggested that multiple hydrogen-bonding interactions by oriented monolayers containing receptors such as **10b**, **11b**, or **22** could be used for nucleotide recognition based on guest-induced changes in the permeability through intermolecular voids in such monolayers.[37] The guest-induced permeability changes can be evaluated on the basis of the ease of access of electroactive markers to the electrode surface, which can be measured by cyclic voltammetry, as reported previously by Umezawa and co-workers.[32–36] For the monoalkylated receptors **10b** and **11b**, mixed membranes with 1-octadecanol were prepared because the membrane stabilities increased by addition of the latter, as indicated by the increased collapse pressures in surface pressure–molecular area ($\pi$–$A$) isotherms. The permeabilities were evaluated with the membranes transferred onto glassy carbon electrodes by the Langmuir–Blodgett method. On the other hand, since mixing with 1-octadecanol did not improve the membrane stability in the case of the dialkylated receptor **22**, the membrane permeability in that case was evaluated in situ by horizontal touch cyclic voltammetry.

Figure 12 shows the voltammetric responses toward 5'-GMP and 5'-AMP for the oriented membranes with receptors **10b**, **11b**, or **22**. The membrane based on receptor **10b** with complementarity for the guanine base was selective for 5'-GMP (Figure 12a). The factor expressing the selectivity for 5'-GMP over 5'-AMP,

$K_{5'GMP,5'-AMP}$, as defined by the ratio of the response factor ($R_{sample}$, see Figure 12 caption) for 1.00-mM solutions of each analyte, was determined to be 2.38. The voltammetric selectivity for 5'-AMP for the membrane based on receptor **11b**, which can form only two hydrogen bonds to the adenine base (Figure 12b), was smaller ($K_{5'-AMP,5'-GMP} = 1.89$), as expected. The best voltammetric discrimination of nucleotides was however attained with the membrane based on receptor **22** ($K_{K5'-GMP,5-AMP} = 3.85$; Figure 12c), which may form a total of five hydrogen bonds to 5'-GMP (see Figure 9). Although the extent of discrimination is not sufficiently high at present for analytical use, these are the first examples of channel mimetic sensing membranes based on recognition of guests with hydrogen bonding.
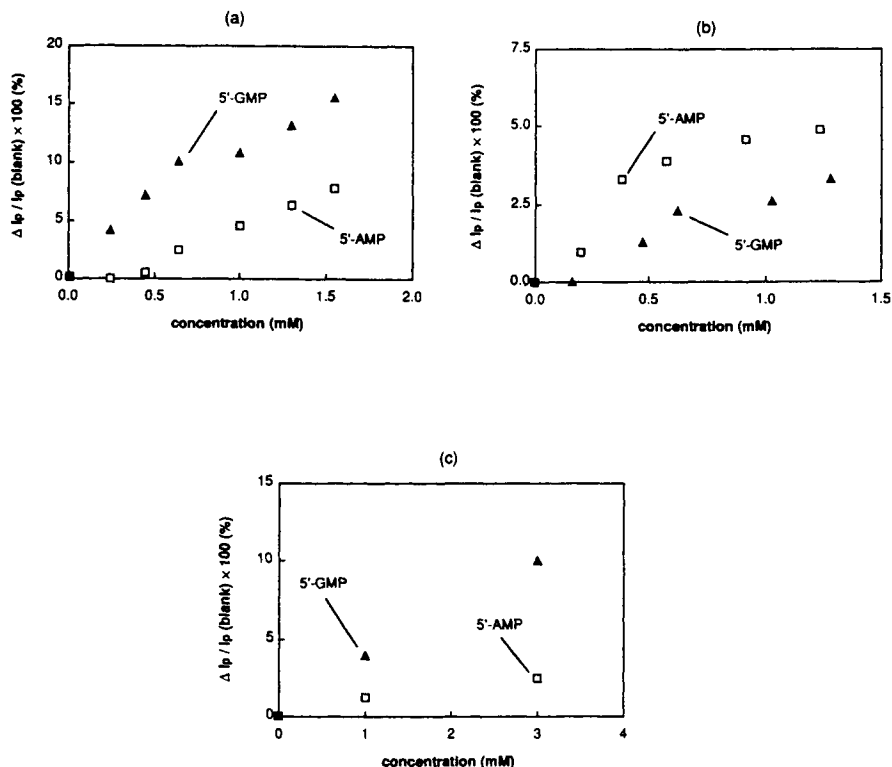


***Figure 12.*** Concentration dependence of the responses to 5'-GMP and 5'-AMP of the oriented membranes based on (**a**) cytosine derivative **10b**, (**b**) thymine derivative **11b**, and (**c**) cytosine derivative **22**. The response factor, $R$(sample), is expressed by the decrease in the oxidation peak current ($I_E$) upon analyte addition [$R$(sample) = [$I_p$(blank) - $I_p$(sample)]/$I_p$(blank)]. Measured at 20 °C with a 0.1 M phosphate buffer solution (pH 6.0, 20 °C) containing 1.00 mM [Fe(CN)$_6$]$^{4-}$.

## 2.3.  Chemical Sensing Based on Cavity Inclusion

### Sensing Based on Interactions with Nonpolar Moieties of Guests

Considering the ubiquitous existence of nonpolar moieties in the structures of organic guests, discrimination according to differences in *nonpolar* structures will be equally important as discrimination according to differences in polar structures. In homogeneous solutions, the former mode of discrimination can be achieved by inclusion into well-defined hydrophobic cavities of hosts such as cyclodextrins and cyclophanes, particularly in aqueous systems. However, in organic membrane systems there exists a difficulty in achieving inclusion-based discrimination of nonpolar structures because of competitive inclusion of guests and membrane components. Due to such an intrinsic difficulty, discrimination involving nonpolar moieties of organic guests in membrane systems has so far been achieved mainly on the basis of simple hydrophobicity or chirality of guests.[12,13,16] Recently, discrimination according to differences in steric structures of nonpolar moieties, based on guest-induced changes in membrane potential or permeability, have been achieved by hosts with inclusion cavities capable of facing an aqueous solution.

### Calix[6]arene Derivatives

*Guest-Induced Changes in Membrane Potential.*   Calixarenes have attracted increasing attention as a class of versatile hosts with well-defined cavities.[88-94] In chemical sensing of alkali metal ions, the calixarene structure contributes as a rigid support for the ester or ether substituents, which afford convergent binding sites for metal ions. A number of investigations on potentiometric discrimination of alkali metal ions have been carried out, particularly with calix[4]arene tetraesters (e.g., **26, 27**) and calix[6]arene hexaesters (e.g., **28, 29**), which have been shown to display selectivities for sodium and cesium ions, respectively.[94-97] More recently, much improved $Na^+/K^+$ selectivity was achieved for calix[4]arene derivatives by optimization of the alkyl groups on the upper rim (**30**)[98] as well as proper choice of the liquid membrane solvent.[99] Furthermore, most sophisticated molecular



**26:** $R^1 = -CH_2CH_3$
    $R^2 = -H$ or $-C(CH_3)_3$
**27:** $R^1 = -(CH_2)_9CH_3$
    $R^2 = -C(CH_3)_3$
**30:** $R^1 = -CH_2CH_3$
    $R^2 = -C(CH_3)_2CH_2C(CH_3)_3$

**28:** $R^1 = -CH_2CH_3$
    $R^2 = -H$ or $-C(CH_3)_3$
**29:** $R^1 = -(CH_2)_9CH_3$
    $R^2 = -H$

**31:**  $R = -C(CH_3)_3$
    $X = -OCH_2CH_3$

32

33

34

35

Na⁺ · ⁻B

R =

$-C$
CF₃
OCH₃
CF₃

HFPB

NH₃⁺

36

37

$\nearrow$NH₃⁺

HO
HO

X R
NH₂⁺

38: X = R = H (dopamine)
39: X = OH, R = H (noradrenaline)
40: X = OH, R = CH₃ (adrenaline)
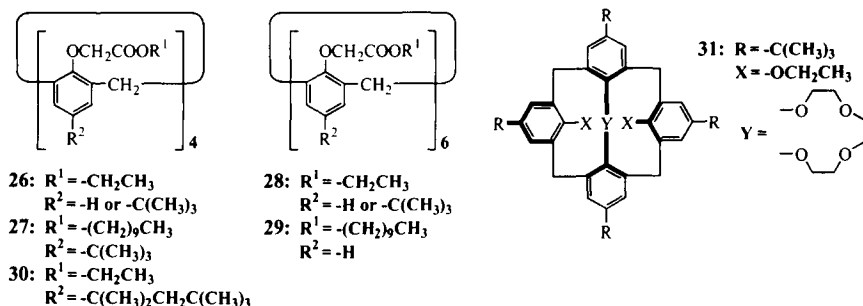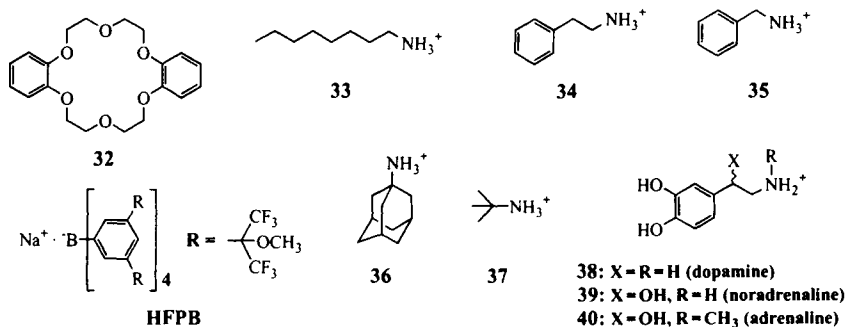
design based on crowned calix[4]arene (31) has led to a $Na^+/K^+$ selectivity ($>10^5$),[100] which is by far greater than that of any of the previously reported ones.

For complexation and discrimination of organic amine guests, calix[6]arene hexaesters, such as 28 and 29, are a suitable type of hosts, first because the calix[6]arene cavity is sufficiently large to accommodate organic guests and second because their hexagonally arranged ester carbonyl groups afford excellent binding sites for protonated primary amines, as in the case of 18-crown-6 derivatives (e.g., host 32). Potentiometric discrimination of protonated primary amines according to the steric structures of their nonpolar moieties can be expected when the host–guest complexation occurs with a geometry involving *inclusion* into the calix[6]arene cavity (Figure 13a, geometry A).

The potentiometric response behavior of lipophilic calix[6]arene hexaester 29 was investigated with a PVC matrix liquid membrane system, using DOS as membrane solvent.[30] Responses and selectivities of host 29 for protonated amine guests were compared with those of dibenzo-18-crown-6 (32) at pH 7.0. Figure 14a and Figure 14b show potentiometric responses obtained by hosts 29 and 32, respectively, for simple primary amines having different nonpolar moieties (33–37). As shown in Figure 14b, the 18-crown-6 derivative 32 showed a selectivity according to the lipophilicity of each guest (magnitude of response: **33 > > 36 > 34 ≥ 35 > > 37**). In contrast, the calix[6]arene hexaester 29 displayed quite a different selectivity, the magnitude of response being in the order **33 ≥ 34 > > 35 > > 36 > 37** (Figure 14a). Potentiometric responses for catecholamines (38–40), which are an important group of neurotransmitters as well as adrenal medulla hormones, were also examined. Of these guests, by far the strongest response was observed for dopamine (38), particularly by calix[6]arene hexaester 29. Potentiometric selectivity coefficients $(K_{i,j}^{pot})$,[101] which indicate relative magnitudes of potentiometric responses, are listed in Table 3 for simple amines and catecholamines.

Potentiometric responses to cationic guests by neutral hosts can be interpreted on the basis of charge separation across the membrane interface with cationic host–guest complexes at the membrane side and hydrophilic counteranions at the aqueous side (Figure 3a).[17–20] The amount of the cationic complexes at the membrane side of the interface is determined by the lipophilicity of the guest, the stability

## (a)                                          (b)



A                    B
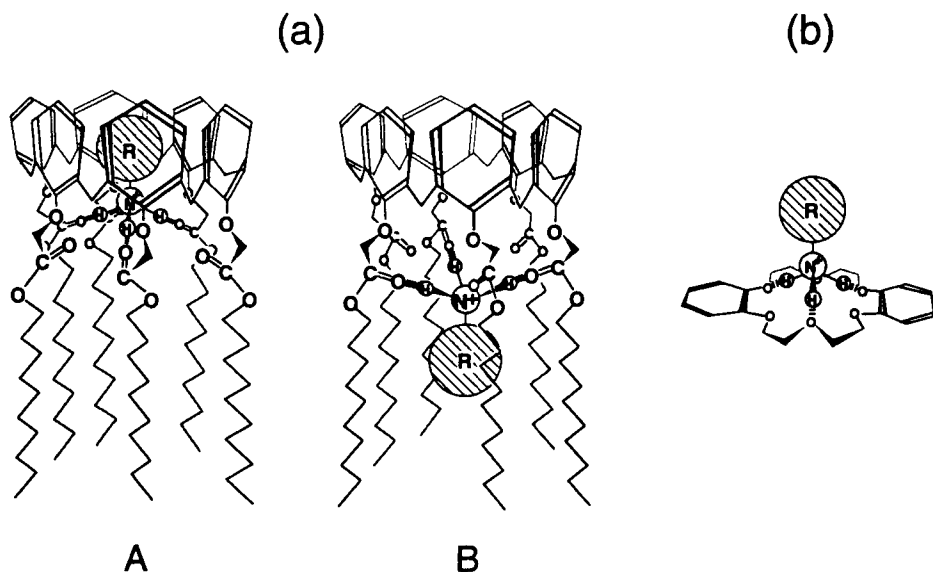
**Figure 13.** Schematic representations of the geometries of host–guest complexes. (a) Two possible geometries of the host–guest complex between calix[6]arene hexaester (**29**) and a protonated primary amine guest. (b) Plausible geometry of the host–guest complex between dibenzo-18-crown-6 (**32**) and a protonated primary amine guest (reprinted with permission from *Anal. Chem.* **1993**, *65*, 1077. Copyright 1993 American Chemical Society).

### (a)                                          (b)
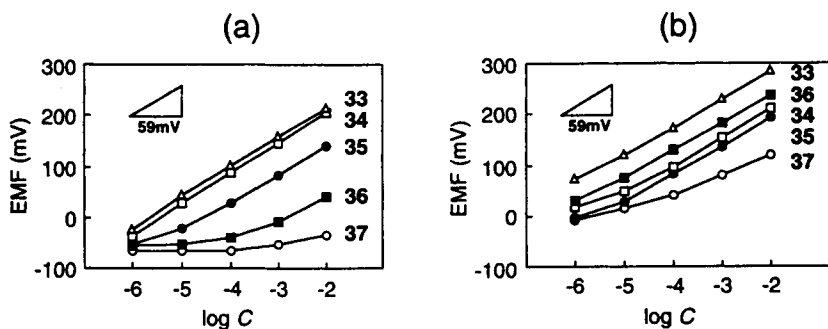


**Figure 14.** Potentiometric responses to simple amine guests (**33–37**) by PVC matrix liquid membranes. (a) Membrane based on calix[6]arene hexaester (**29** ($R^2$ = H)/DOS/PVC = 5:68:27 wt%). (b) Membrane based on dibenzo-18-crown-6 (**32**/DOS/PVC = 2:66:32 wt%). Measured in 0.1 M Tris-HCl buffer (pH 7.0) at room temperature (ca. 20 °C) (reproduced with permission of American Chemical Society from *Anal. Chem.* **1993**, *65*, 1079).

**Table 3.** Potentiometric Selectivity Coefficients for PVC Matrix Liquid Membranes Based on Calix[6]arene Hexaester or Dibenzo-18-crown-6[a]

| Guest | $C_{10}$-Cal[6][a] (pH 7.0)[e] | $C_{10}$-Cal[6][a] (pH 5.0)[f] | $C_2$-Cal[6][b] (pH 5.0)[f] | $C_2$-Cal[6][c] (pH 5.0)[f] | DB18C6[d] (pH 7.0)[e] |
|---|---|---|---|---|---|
| 33 | 2.60 | 22.9 | 22.3 | | 20.0 |
| 34 | 1 | 1 | 1 | 1 | 1 |
| 35 | 0.29 | 0.14 | 0.13 | 0.20 | 4.77 |
| 36 | <0.01 | 0.034 | 0.031 | <0.01 | 20.0 |
| 37 | <0.01 | <0.01 | <0.01 | <0.01 | 0.35 |
| 38 | 1 | 1 | 1 | 1 | 1 |
| 39 | 0.20 | 0.11 | 0.088 | 0.12 | 0.94 |
| 40 | 0.27 | 0.08 | 0.092 | 0.10 | 0.88 |
| $K^+$ | | 4.59 | 6.09 | 7.02 | |
| $Na^+$ | | 0.025 | 0.034 | 0.063 | |

*Notes:* [a] Host **29** ($R^2$ = H)/DOS/PVC = 5:68:27 wt%.[30]

[b] Host **28** ($R^2$ = H)/DOS/PVC = 4:66:30 wt%.[102]

[c] Host **28** ($R^2$ = H)/DOS/PVC/HFPB = 4:65:30:0.5 wt%. The molar ratio of host **28** and HFPB was 1 to 0.1.[102] HFPB: sodium tetrakis[3,5-bis(1,1,1,3,3,3-hexafluoro-2-methoxy-2-propyl)phenyl]borate.

[d] Host **32**/DOS/PVC = 2:66:32 wt%.[30]

[e] Measured in 0.1 M Tris-HCl buffer.

[f] Measured in 0.1 M $CH_3CO_2Li$–$CH_3COOH$ buffer.

of the complex, and the concentration of host and ionic sites in the membrane. In the case of dibenzo-18-crown-6 (**32**), strong tripodal hydrogen bonds as depicted in Figure 13b are available for all of protonated primary amine guests because the formation of host–guest complexes occurs only through the $NH_3^+$ group without any interaction with the nonpolar moiety of the guest. Then, the differences in the lipophilicity of each guest, leading to the differences in the organic/aqueous partition of the guest and hence the extent of complexation at the membrane side of the interface, reflects to the potentiometric selectivities. In the case of calix[6]arene hexaester **29**, however, if the host–guest complex formed is of the inclusion type (geometry A in Figure 13a), the extent of complexation at the membrane side of the interface will be determined by steric fit between the nonpolar moiety of the guest and the inclusion cavity of the host; the difference in the steric structure of the nonpolar moiety of the guest leads to a considerable difference in the stability of the complex, depending on the availability of tripodal hydrogen bonds (Figure 13a, geometry A).

This view is consistent with the fact that host **29** displays potentiometric selectivities for guests **33**, **34**, and **38**. For these guests, the formation of strong tripodal hydrogen bonds will not be interfered because there is no substituent around the $NH_3^+$ group. Complexation with geometry A is supported by the ^{1}H NMR results,

which indicate the formation of *inclusion* complexes between calix[6]arene **29** and the guests that induced the strongest potentiometric responses (**33, 34**). The guests with a tertiary alkyl structure at the α-position (**36, 37**), as well as with a phenyl group attached directly to the α-carbon (**35**), are sterically hindered from forming tripodal hydrogen bonds and hence will be unfavorable for complexation with geometry A.

Thus, the characteristic potentiometric selectivity of calix[6]arene hexaester **29** for primary amine guests can be reasonably interpreted on the basis of the structural factors relevant to the nonpolar moieties of guests. Such a mode of discrimination can also be achieved by a calix[6]arene hexaester with short alkyl chains [**28** ($R^2 =$ H)]. In addition, the selectivity was found to be essentially the same in the presence or absence of lipophilic anionic site HFPB added in the membrane (Table 3).[102] Potentiometric discrimination of protonated amines[103] by host **28** ($R^2 =$ H, Bu$^t$) as well as of aldehydes (as the protonated hydrazones generated in situ) by hosts **26** ($R^2 =$ Bu$^t$) and **28** ($R^2 =$ H)[104,105] was also reported. Recently, quantitative estimation of "optical selectivities" for alkali metal ions or protonated amines were made with liquid membranes containing chromogenic derivatives of calixarenes.[106-109]

*Guest-Induced Changes in Membrane Permeability.* Calixarene derivatives are also used for sensing systems other than ISEs or optodes. Recently, a systematic investigation on the control of membrane permeability by use of oriented monolayers composed of calixarene esters was carried out.[36] The hosts used were short alkyl chain esters of calix[6]arene [**28** ($R^2 =$ Bu$^t$)] and calix[4]arene [**26** ($R^2 =$ Bu$^t$), **30**; both cone conformers]. The permeabilities through the intermolecular voids of these monolayers were evaluated by cyclic voltammetry, as described earlier for oriented membranes of nucleobase derivatives. Cationic, anionic, and neutral electroactive compounds were used as the permeability markers. The voltammetric measurements were carried out either for a monolayer
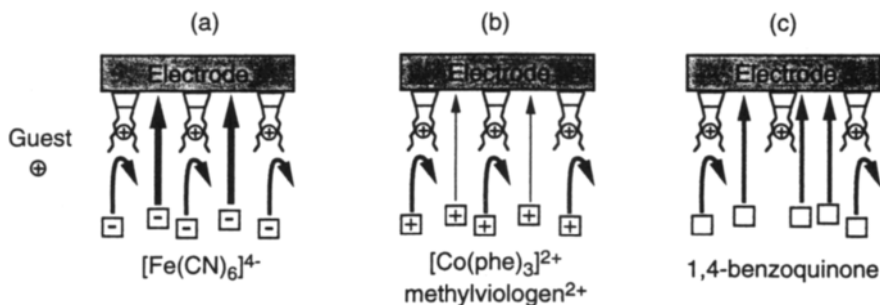


**Figure 15.** Possible mechanism of guest-induced permeability changes for electroactive markers by oriented membranes of the calix[6]arene hexaester **28** ($R^2 =$ Bu$^t$) in the cases that (a) anionic, (b) cationic, and (c) neutral markers are used.[36]

formed at the air/water interface under an applied surface pressure, or for a monolayer transferred on an electrode by the Langmuir–Blodgett method. Alkali metal cations induced an increase in the permeability for an anionic marker ion such as $[Fe(CN)_6]^{4-}$ and a decrease in the permeability for cationic marker ions such as $[Co(phen)_3]^{2+}$ (phen = 1,10-phenanthroline) and methylviologen$^{2+}$ [(1,1'-dimethyl-4,4'-bipyridinium)$^{2+}$]. These permeability changes can be ascribed to an attractive or repulsive electrostatic interaction between the marker ions and the calixarene hosts in the membrane bearing positive charges by complexation with alkali metal ions Figure 15a,b). A cationic guest-induced increase in the membrane permeability was also observed in the case of using a neutral marker (1,4-benzoquinone), possibly because of an increase in the intermolecular voids (or microscopic defects) due to conformational contraction upon host–guest complexation (Figure 15c). A selectivity was observed for the calix[6]arene monolayer with the magnitude of response $Cs^+ > Rb^+ > K^+ > Na^+$, $Li^+$ (Table 4), which is consistent with the selectivities in solvent extraction or transport[110,111] and in potentiometry.[98,99,112,113]

**Table 4.** *Selectivities of Guest-Induced Permeability Change for Oriented Monolayer of Calix[6]arene Hexaester **28** ($R^2$ = Bu$^t$)[36] a*

| | Relative Area of Cyclic Voltammogram (%)[b] | | | |
|---|---|---|---|---|
| *Guest* | $[Co(phen)_3]^{2+\ c}$ | $[Fe(CN)_6]^{4-\ d}$ | $MV^{2+}$ | *p-Quinone*[d] |
| none | 86.7 ± 0.5 | 84.7 ± 2.0 | 97.3 ± 0.9 | 85.1 ± 0.6 |
| Li$^+$ | 81.5 ± 0.2 | 86.2 ± 1.8 | 97.3 ± 0.6 | 85.1 ± 1.1 |
| | (−5.2) | (+1.5) | (0) | (0) |
| Na$^+$ | 81.5 ± 0.2 | 86.7 ± 1.5 | 97.2 ± 0.5 | 85.6 ± 0.9 |
| | (−5.2) | (+2.0) | (−0.1) | (+0.5) |
| K$^+$ | 75.5 ± 0.3 | 87.5 ± 1.8 | 95.3 ± 0.8 | 87.2 ± 0.6 |
| | (−11.2) | (+2.8) | (−2.0) | (+2.1) |
| Rb$^+$ | 73.2 ± 0.1 | 87.8 ± 1.0 | 91.9 ± 0.7 | 89.6 ± 0.9 |
| | (−13.5) | (+3.1) | (−5.4) | (+4.5) |
| Cs$^+$ | 69.7 ± 0.2 | 89.1 ± 1.5 | 86.4 ± 0.7 | 91.8 ± 0.9 |
| | (−17.0) | (+4.4) | (−10.9) | (+6.7) |

*Notes:* [a]Guest-induced permeability changes at 20 °C and pH 6.0 (0.1 M Tris-HCl buffer) were estimated on the basis of cyclic voltammogram area.

[b]Calculated as the percentage of the voltammogram peak area relative to that measured in the absence of the calix[6]arene monolayer. Guest-induced increase (+) or decrease (−) are shown in the parentheses.

[c]Measured by horizontal touch cyclic voltammetry with an HOPG electrode at an applied surface pressure of 10 mN m$^{-1}$. The marker was added as [Co(1,10-phenanthroline)$_3$](ClO$_4$)$_2$ (1.00 × 10$^{-4}$ M).

[d]Measured by conventional cyclic voltammetry. A monolayer of **28** ($R^2$ = Bu$^t$), prepared on water and compressed at 25 mN m$^{-1}$, was transferred on a glassy carbon electrode by the Langmuir–Blodgett method. The markers were added as Na$_4$[Fe(CN)$_6$], methylviologen dichloride, or p-quinone (1,4-benzoquinone) (1.00 × 10$^{-3}$ M concentration in all cases).

## Cyclodextrin Derivatives

*Guest-induced Changes in Membrane Potential.* Cyclodextrins,[114–118] which have even more rigid cavities than ordinary calix[n]arenes ($n \geq 6$) or macrocyclophanes, comprise another class of suitable hosts for discrimination of nonpolar moieties of organic guests at membrane surfaces. The use of natural and modified cyclodextrins for analytical purposes has focused increasing attention.[119–121] With regard to host–guest recognition at membrane surfaces, the following major types of hydrophobic derivatives of cyclodextrins have been reported so far:[121]

1.  Derivatives alkylated at the primary face (C-6 side).
2.  Derivatives alkylated at the secondary face (C-2 and C-3 side).
3.  Derivatives alkylated at both primary and secondary faces.

Potentiometric sensing based on type 3 derivatives of $\alpha$-, $\beta$-, and $\gamma$-cyclodextrins has been reported.[122–125] We have been interested in the type 1 cyclodextrin derivatives developed by Tagaki,[126] e.g., host **41**. This type of cyclodextrin derivative is characteristic in that the primary hydroxyl groups at the C-6 positions are exhaustively substituted with long alkyl chains. At the surface of an organic membrane, this structural feature allows the secondary hydroxyl side (wider open end of the cavity) to face the aqueous solution to accommodate a guest molecule. The interfacial receptor functions of these cyclodextrin hosts have been confirmed mainly by $\pi$-A isotherm studies.[127,128]

Potentiometric response behaviors of host **41** toward primary amine guests (**34–36, 38, 42–51**) were investigated with a PVC matrix liquid membrane system.[31] Of various liquid membrane solvents examined, by far the best potentiometric responses were obtained with FNDPE (**52**). Figure 16a and Figure 16b show potential vs. concentration curves for amine guests (**34–36, 38, 42**) by the membrane without a host and the membrane containing host **41**, respectively. The membrane containing host **41** displayed much stronger responses and, in addition, a different selectivity (magnitude of response: **34 > 36 > 35 > 42 > 38**; Figure 16b) as compared to the membrane without a host (magnitude of response: **36 > 34, 35** $\geq$ **42 > 38**; Figure 16a). The magnitudes of the responses to methoxybenzylamines **43–51** were also increased by host **41**. Particularly for dimethoxybenzylamines, the FNDPE membrane containing host **41** displayed, again, a selectivity (**47 > 49 > 46 > 48**), which was quite different from that of the membrane without a host (**46 > 47** $\geq$ **48 > 49**). These results seem to indicate the effect of inclusion of guests in the cyclodextrin cavity at the surface of the liquid membrane.

*Guest-induced Changes in Membrane Permeability.* As mentioned earlier, guest-induced changes in membrane permeability may be effected by oriented membranes through the intermolecular voids between or the intramolecular channels within the membrane molecules (see Figure 4a and Figure 4b, respectively).

**41:** X = S, Y = -COCH₃
R = -(CH₂)₁₅CH₃

**34**

**35**

**36**

**38** (dopamine)

**42**

**43:** 2-OCH₃
**44:** 3-OCH₃
**45:** 4-OCH₃

**46:** 2,3-(OCH₃)₂
**47:** 3,5-(OCH₃)₂
**48:** 3,4-(OCH₃)₂
**49:** 2,4-(OCH₃)₂

**50:** 2,4,6-(OCH₃)₃
**51:** 3,4,5-(OCH₃)₃

**52** (FNDPE)

**(a)**

**(b)**
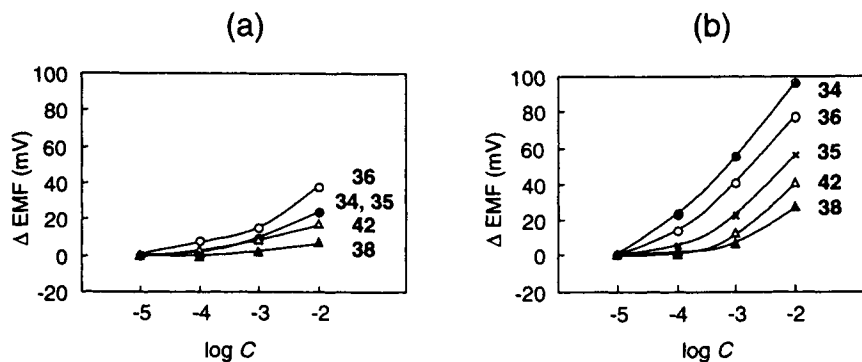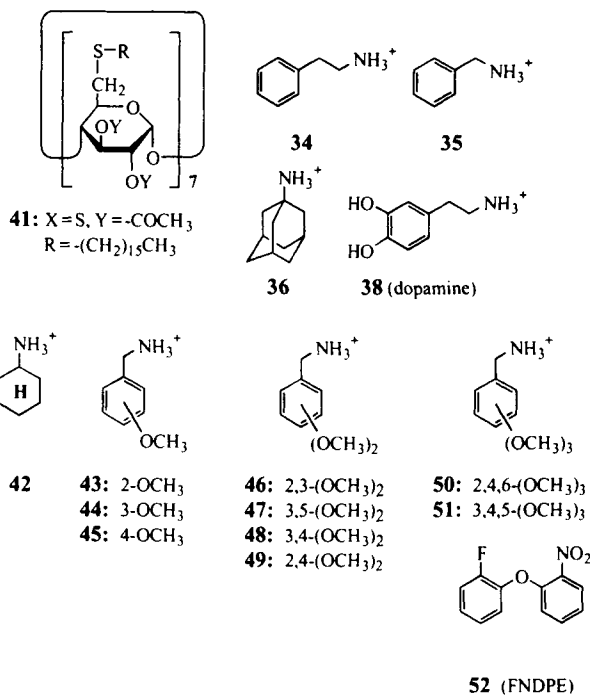


*Figure 16.* Potentiometric responses to amine guests (**34–36, 38, 42**) by PVC matrix liquid membranes. (**a**) Membrane containing no particular sensory element (FNDPE/PVC = 81:19 wt%). (**b**) Membrane containing β-cyclodextrin derivative (**41**/FNDPE/PVC = 2:80:18 wt%). Measured in 0.01 M AcONa-AcOH buffer (pH 5.0) at room temperature (ca. 20 °C) (reproduced by permission of Springer-Verlag from *Mikrochim. Acta* **1994**, *113*, 228).

**1**          **2**

$R^1$ = -$(CH_2)_{15}CH_3$

**53:** X = NH, Y = H
R = -$(CH_2)_{11}CH_3$
**41:** X = S, Y = -$COCH_3$
R = -$(CH_2)_{11}CH_3$

5'-ATP$^{4-}$  (n = 3)
5'-ADP$^{3-}$  (n = 2)
5'-AMP$^{2-}$  (n = 1)

**54 (cis)**
**55 (trans)**

**56 (ortho)**
**57 (meta)**
**58 (para)**

**59**      **60**      **61**

**adenosine**      **cytidine**
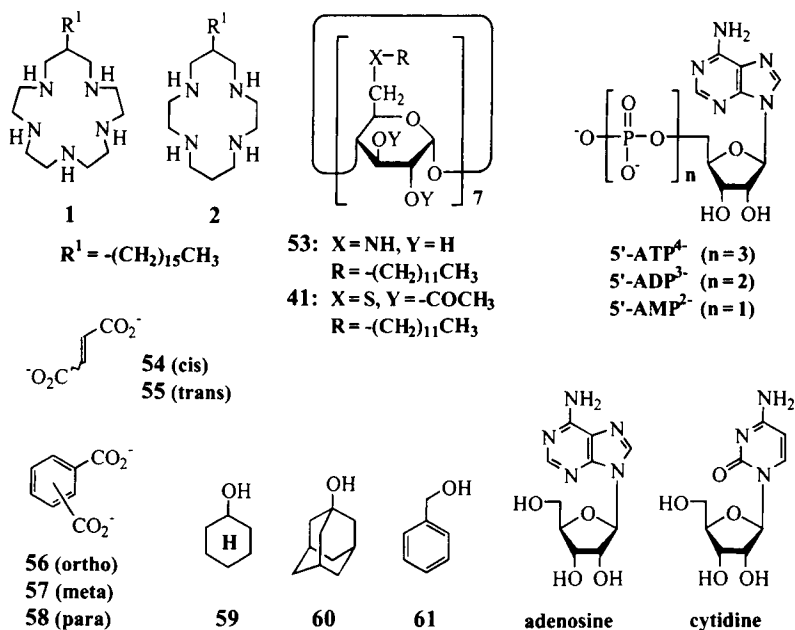
***Table 5.*** Selectivities of Guest-Induced Permeability Changes for Oriented Multilayers Containing Polyamine Hosts[34,38] [a]

| Guest Anion | Membrane 1 | Membrane 2 | Membrane 53 |
|---|---|---|---|
| 5'-ATP$^{4-}$ | 1.00 (1.00)[b] | 1.00 | 1.00 (1.00)[b] |
| 5'-ADP$^{3-}$ | 0.78 | 0.87 | 0.44 |
| 5'-AMP$^{2-}$ | 0.19 | 0.38 | 0.15 |
| 54 (cis) | 1.00 (0.69)[b] | 1.00 | 1.00 (0.31)[b] |
| 55 (trans) | 0.03 | 0.06 | 0.41 |
| 56 (ortho) | 1.00 (0.44)[b] | 1.00 | 0.55 (0.77)[b] |
| 57 (meta) | 0.37 | 0.89 | 1.00 |
| 58 (para) | 0.02 | 0.10 | 0.83 |

*Notes:* [a]Selectivity factors for guest-induced permeability changes at ca. 20 °C and pH 6.0 (0.01 M CH$_3$CO$_2$Na–CH$_3$COOH buffer containing 0.05 M K$_2$SO$_4$) were estimated on the basis of cyclic voltammogram area, using 1.5 × 10$^{-3}$ M [Fe(CN)$_6$]$^{4-}$ as the electroactive marker. The oriented membranes (4–6 layers) were prepared on glassy carbon electrodes by the Langmuir–Blodgett method (horizontal lifting method).
[b]The values in the parentheses are the cross selectivity factors for the primary guests of each group.

Both of these modes have been achieved by oriented membranes of long alkyl chain derivatives of cyclodextrin.[34,35]

*Control of Permeability through Intermolecular Voids.* Guest-induced changes in membrane permeability were examined for an oriented multilayer composed of polyamino-β-cyclodextrin **53** and, for comparison, of macrocyclic polyamines (**1**, **2**).[34] The membranes were deposited directly onto glassy carbon electrodes by the horizontal lifting Langmuir–Blodgett method. The polyamine host **53**, as well as the neutral host **41**, are two of the type 1 derivatives of cyclodextrin developed by Tagaki.[126] However, host **53** contrasts **41** in that the former acquires polycationic property by multiple protonation, which is a prerequisite not only for complexation with anionic guests but also for control of permeability for marker ions, as in the case of the macrocyclic polyamine hosts **1** and **2** (Section 2.2). Guest-induced permeability changes were evaluated by cyclic voltammetry using $[Fe(CN)_6]^{4-}$ as the permeability marker. Complexation of the multiprotonated, polycationic hosts in the membrane with anionic guests decreases the membrane positive charge, leading to a decrease in the permeability for the anionic marker ions through the intermolecular voids between the cyclodextrin molecules (see Figure 4a). This leads to a decrease in the access of these markers to the electrode surface and hence to a decrease in the voltammogram area. The selectivity factors for guest-induced decrease in permeability were determined at pH 6.0 (Table 5), at which the polyamine hosts are sufficiently protonated while the guests occur sufficiently in their anionic forms.

For the adenine nucleotides ($ATP^{4-}$, $ADP^{3-}$, $AMP^{2-}$) and the *cis/trans* isomers of dicarboxylates (**54**, **55**), membrane **53** containing polyamino-β-cyclodextrin **53** showed selectivities similar to those of membranes **1** and **2** containing macrocyclic polyamines **1** and **2**, respectively. For the adenine nucleotides, both types of membranes showed a greater response to the guests with a greater negative charge (selectivity factor: $ATP^{4-} > ADP^{3-} > AMP^{2-}$). On the other hand, for the dicarboxylate isomers, a greater response was observed for the guests having a shorter distance between the two anionic groups [selectivity factor: **54** (*cis*) > **55** (*trans*)]. The selectivities displayed for these guests seem to be controlled by electrostatic interactions between the protonated polyamine hosts and the anionic guests.

However, for the positional isomers of phthalate (**56–58**), the response selectivity was different for the two types of membranes. Whereas membranes **1** and **2** showed responses in the order of **56** (*ortho*) > **57** (*meta*) > **58** (*para*), membrane **53** interestingly showed a different response order, i.e., **57** (*meta*) > **58** (*para*) > **56** (*ortho*), a selectivity which is quite different from that expected on the basis of simple electrostatic effects. Such a difference in the selectivity is possibly due to host–guest complexation involving not only electrostatic interactions but also inclusion into the β-cyclodextrin cavity, which is capable of recognizing differences in the steric structures of the guests.

Guest-induced changes in permeability through intermolecular voids between membrane molecules has also been applied by other groups for chemical sensing of various analytes. Sensing of $Ca^{2+}$ [129] or urea[130] by electrodes coated with polypeptides, sensing of quinacrine[131] or $Mg^{2+}$ [132] by electrodes coated with DNA, and sensing of $H^+$ by electrodes coated with organized alkanethiol monolayer[133] have been reported.

*Control of Permeability through Intramolecular Channels.*     Control of membrane permeability is effected in a most sophisticated and efficient manner in ligand-gated ion channels having discrete molecular entities with well-defined channel structures.[134-136] Cyclodextrin derivatives of type **41** and **53** are interesting because their basic structure should allow them to function not only as receptor sites but also as *intramolecular channels*. If intramolecular channel function is effected by this type of cyclodextrin derivatives, a more sophisticated control of membrane permeability will be possible by blocking the cyclodextrin cavity (channel entrance) with a guest molecule (see Figure 4b). Experimental evidence supporting such a mode of permeability control was obtained by horizontal-touch cyclic voltammetry for a condensed monolayer of host **41** formed at the air/water interface.[35] Horizontal-touch cyclic voltammetry[137-139] applied for a condensed monolayer with no intermolecular voids (in a statistical sense) allows evaluation of intramolecular channel function when an appropriately sized marker that can pass
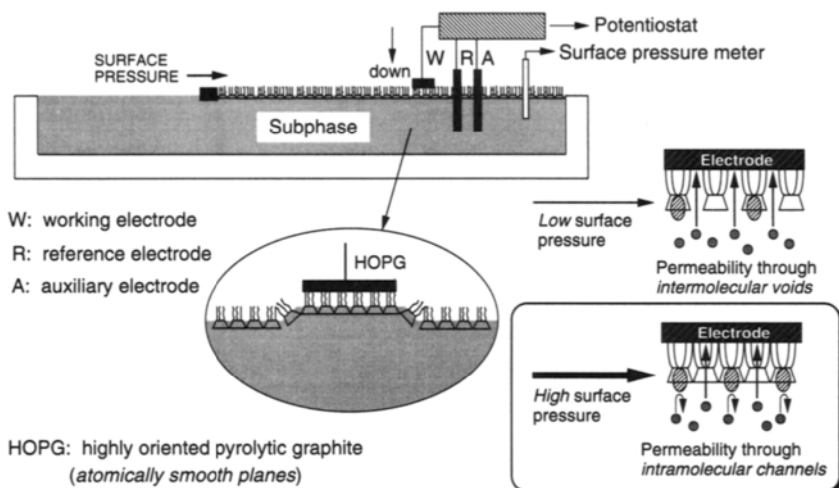


***Figure 17.*** Experimental system for the measurement of surface pressure–molecular area (π–A) isotherms and the horizontal touch cyclic voltammetry,[35] and schematic representations for the control of permeabilities through oriented monolayers formed at low and high applied surface pressures.

the channel entrance is used (Figure 17). This aspect contrasts that of the membrane composed of host **53** described above; in the latter membrane, the electroactive marker ion used ($[Fe(CN)_6]^{4-}$) cannot pass through the β-cyclodextrin cavity due to steric reasons.

A controlled surface pressure of 50 mN m$^{-1}$ was applied for the formation of a condensed monolayer of **41**, in which the molecular area is limited to ca. 210 Å$^2$ molecule$^{-1}$ if complete integrity of the monolayer is assumed. Since this molecular area corresponds to the basal area of β-cyclodextrin, the area of intermolecular voids that could cause membrane leakage are expected to be minimized. The permeability of this condensed membrane both in the presence and absence of a guest in the subphase solution was measured with the electroactive markers that may pass [1,4-benzoquinone (*p*-quinone)] or cannot pass [[$Co(phen)_3]^{2+}$, [$Mo(CN)_8]^{4-}$] through the β-cyclodextrin cavity. Highly oriented pyrolytic graphite (HOPG) was used as a working electrode because the surface of freshly cleaved HOPG contains a fair extent of atomically smooth planes.[140] As guests to block the channel and control the membrane permeability, uncharged organic molecules (e.g., **59**) have been chosen to avoid complications by electrostatic effects on the guest-induced permeability change, as described above for the membrane composed of polyamino-β-cyclodextrin **53**.

Figure 18 shows the cyclic voltammograms obtained with 1,4-benzoquinone as permeability marker. The presence of the cyclodextrin monolayer caused some decrease in the area of the reduction peak (upper half of curve A vs. B; ca. 31% decrease). In addition, the reduction peak remained within the investigated potential window though the peak shifted to a more negative potential. This contrasts with a much more pronounced decrease with almost complete suppression of voltammogram peak when [$Co(phen)_3]^{2+}$ or [$Mo(CN)_8]^{4-}$ was used as a marker (ca. 85 and 70% decrease, respectively; figure not shown). These results clearly indicate much easier access of 1,4-benzoquinone to the electrode surface, which can be interpreted by the permeability of 1,4-benzoquinone (ca. 6.3 Å shorter width) through the intramolecular channel of the β-cyclodextrin derivative **41** (ca. 7.5 Å diameter). The bulkier markers [$Co(phen)_3]^{2+}$ and [$Mo(CN)_8]^{4-}$ (ca. 13 and 9 Å minimum diameters, respectively) cannot pass through the β-cyclodextrin cavity due to steric reason.

Addition of guest **59** to the subphase solution caused a further decrease in the voltammogram area (curve B vs. C in Figure 18). Furthermore, the extent of decrease became greater by increasing the concentration of **59** in the subphase (curve C → D → E). These observations can be most reasonably explained by a channel-blocking effect of the guest, leading to inhibition of the permeation of 1,4-benzoquinone through the β-cyclodextrin cavity (Figure 19a). In the case of using [$Co(phen)_3]^{2+}$ or [$Mo(CN)_8]^{4-}$ as a marker, the addition of guest **59** did not further decrease the voltammogram area, indicating that channel blocking does not affect the permeability for the bulkier markers (Figure 19b). The effect of the surface pressure on the cyclic voltammogram area was consistent with the capability of

200 µA

+0.6                +0.2            -0.2              -0.5

E / V vs. Ag/AgCl
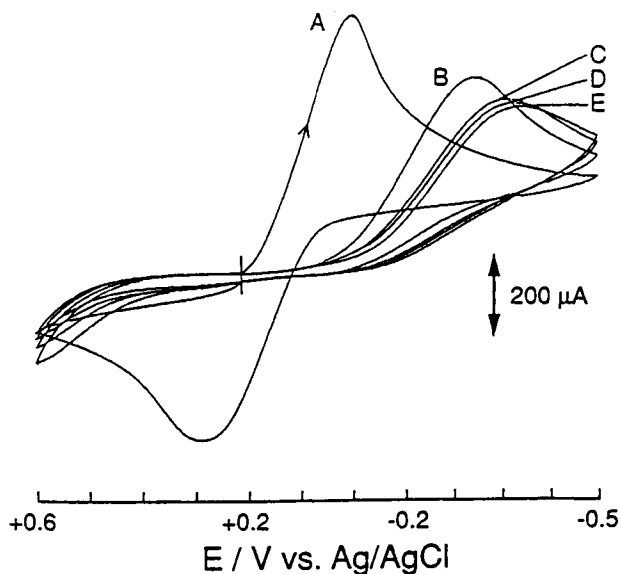
*Figure 18.* Cyclic voltammograms of 1,4-benzoquinone (*p*-quinone) as permeability marker. Curve **A**: in the absence of a cyclodextrin monolayer on a buffer solution containing no guest (p.1 M CH$_3$CO$_2$Na–CH$_3$COOH, pH 6.0). Curve **B**: in the presence of the condensed monolayer of β-cyclodextrin derivative **41** on a buffer solution containing no guest. Curve **C–E**: in the presence of the condensed monolayer of **41** on a buffer solution containing guest **59** at concentrations of 5.0 × 10$^{-3}$, 1.0 × 10$^{-2}$, and 2.0 × 10$^{-2}$ M, respectively (reprinted with permission from *Anal. Chem.* **1993**, *65*, 930. Copyright 1993 American Chemical Society).

1,4-benzoquinone and incapability of the other two bulky markers to sterically pass through the β-cyclodextrin cavity.

The selectivity of voltammetric responses were examined for several uncharged guests (**59–61**, adenosine, cytidine) using 1,4-benzoquinone as a permeability marker. The magnitudes of decrease in the voltammogram area for each guest are shown in Table 6. The magnitude of voltammetric response can be considered as **60** >> **59** > adenosine > cytidine **61**. This can be regarded as a channel mimetic selectivity, which is based on the differences in the ability of these guests to decrease the membrane permeability by blocking the intramolecular channel of the cyclodextrin molecule. To the best of our knowledge, this is the first example of controlling permeability through intramolecular channels by host–guest complexation with *organic* guests. A similar mode of permeability control is found in the efficient action mechanisms of neurotoxins such as tetrodotoxin and saxitoxin in the inhibition of biological ion channels.

(a)                                                    (b)

1,4-benzoquinone                        $[Co(phen)_3]^{2+}$

$[Mo(CN)_8]^{4-}$
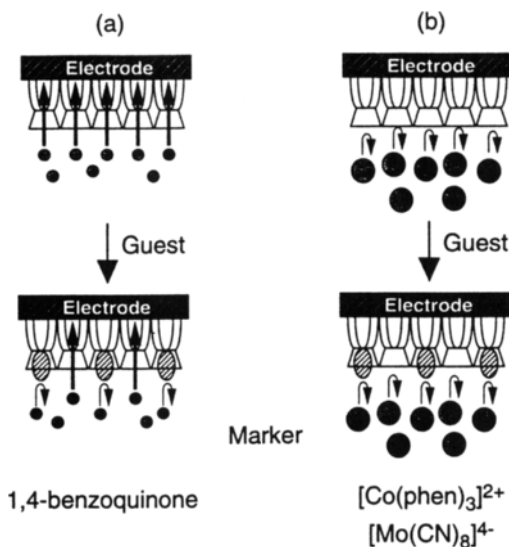
**Figure 19.** Schematic representations of the permeation behaviors of electroactive markers through the condensed monolayer of β-cyclodextrin derivative **41** in the presence and absence of the guest. (a) Permeable markers. (b) Nonpermeable markers.[38]

**Table 6.** Selectivity of Guest-Induced Permeability Decrease for a Channel Mimetic Sensing Membrane Composed of a Condensed Monolayer of β-Cyclodextrin Derivative (**41**)[35] [a]

| Guest | Concentration of Guest (M) | Relative Area of Cyclic Voltammogram (%)[b] | Guest-Induced Decrease (%) |
|---|---|---|---|
| without guest | — | 69.2 | — |
| **59** | $1.0 \times 10^{-2}$ M | $62.5 \pm 1.5$ | 6.7[c] |
| adenosine | $1.0 \times 10^{-2}$ M | $63.7 \pm 1.2$ | 5.5 |
| cytidine | $1.0 \times 10^{-2}$ M | $64.6 \pm 0.3$ | 4.6 |
| **61** | $1.0 \times 10^{-2}$ M | $65.3 \pm 0.7$ | 3.9 |
| **60** | $3.0 \times 10^{-4}$ M | $64.5 \pm 1.3$ | 4.7[c] |

*Notes:* [a] Measured at 17 °C by horizontal touch cyclic voltammetry with an HOPG electrode at an applied surface pressure of 50 mN m$^{-1}$. 1,4-Benzoquinone (*p*-quinone, $1.00 \times 10^{-3}$ M) was used as electroactive marker. Solution pH = 6.0 (0.1 M CH$_3$CO$_2$Na–CH$_3$COOH).

[b] Calculated as a percentage of the voltammogram peak area relative to that measured in the absence of the cyclodextrin monolayer (bare electrode).

[c] Guest-induced decrease in the relative area of cyclic voltammogram was negligible at $3.0 \times 10^{-4}$ M concentration of guest **59**.

The design and synthesis of artificial channel mimics have been a subject of increasing interest.[141-144] In addition to peptidal and nonpeptidal multicomponent aggregates, a number of approaches to unimolecular channels based on macrocycles with pendant channel units have been reported. With regard to the latter approach, observation of single-channel currents has been achieved by transmembrane channels with suitable channel units appended on cyclic peptide,[145-148] porphyrin,[149] or crown ether,[150] and also by a half-channel with long alkyl chains appended on calix[4]resorcarene.[151] A sophisticated strategy for properly connecting two gramicidin A units (half-channel) to construct a transmembrane hybrid channel molecule has also been reported.[152,153] Control of membrane permeability by host–guest complexation with organic guests will be an important target for chemical sensing and further for control of biomembrane functions.

## Cyclophanes

Cyclophanes consist of a class of artificial hosts featured with well-defined hydrophobic cavities constructed by aromatic rings incorporated in their macrocyclic structures, and also with high design versatility because they are totally synthetic.[154-158] The first direct evidence of the formation of an *inclusion* complex with an organic guest was obtained for tetraazacyclophane **62**, the cavity of which is constructed with diphenylmethane units bridged by tetramethylene chains.[159,160] This type of cyclophanes (e.g., **62–65**) were shown to be able to discriminate organic guests in aqueous solutions by recognition of both steric structure and charge.[14,161,162]

Recently, efforts have been made for application of this type of cyclophane cavity for recognition and discrimination of nonpolar structures of organic guests at membrane surfaces.[163] Various types of long alkyl chain derivatives (**66, 68, 70, 72**) were synthesized, and their abilities for guest-induced changes in membrane potential were compared with those of acyclic reference compounds (**67, 69, 71, 73**). However, the results were disappointing in that the guest-induced changes displayed by these cyclophanes were very small or, even if moderate, similar to or smaller than those induced by acyclic reference compounds. Since these results implied the importance of distinct hydrophilic groups located in close proximity of the inclusion cavity, cyclophane **74** was designed and synthesized. This cyclophane is featured by distinct hydrophilic groups ($-NH_3^+$) attached to one side and hydrophobic groups (long alkyl chains) attached to the other side of the benzene rings. Potentiometric behaviors of **74** were compared with those of reference compounds **75–77** by PVC matrix liquid membrane electrodes using DOS as a membrane solvent. Aromatic anion **78** was used as a guest.

The stepwise protonation property of the tetraaminocyclophane **74** leads to a pH-dependent amount of positive charge which affects the membrane potential. Figure 20a shows potential vs. pH curves in the presence and absence of anionic guest **78**. In the absence of the guest, the membrane potential increased with
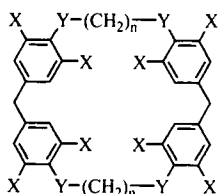
62: X = H, Y = NH$_2$$^+$·Cl$^-$ (CP44·4HCl)
63: X = H, Y = N$^+$(CH$_3$)$_2$·Cl$^-$ (QCP44)
64: X = CO$^-$·K$^+$, Y = O
65: X = CH$_2$SCH$_2$CO$^-$·K$^+$, Y = O

66, 68          67, 69

66, 67: R = -COCH$_2$N[(CH$_2$)$_9$CH$_3$]$_2$
68, 69: R = -CH$_2$CH[(CH$_2$)$_{11}$CH$_3$]$_2$

70, 72          71, 73

70, 71: R = -CO(CH$_2$)$_{16}$CH$_3$
R$^2$ = -H
72, 73: R$^1$ = R$^2$ = -CH$_2$—⟨⟩
O-(CH$_2$)$_{17}$CH$_3$

74, 76, 77          75          78

74, 75: X = CH$_2$NH$_3$$^+$·Cl$^-$, R = CH$_2$O(CH$_2$)$_{11}$CH$_3$
76: X = CH$_2$NH$_3$$^+$·Cl$^-$, R = CH$_3$
77: X = CN, R = CH$_2$O(CH$_2$)$_{11}$CH$_3$
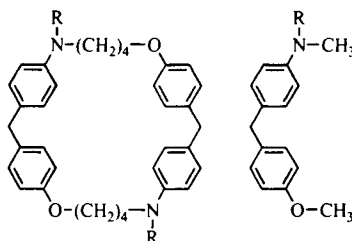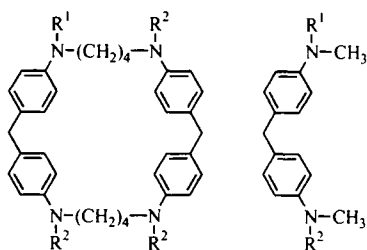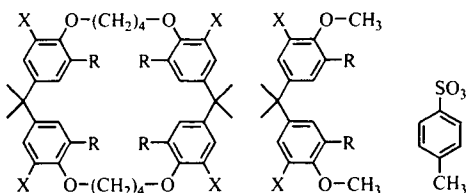
decreasing pH. Upon addition of the guest, the potential–pH curve deviated to the negative direction from that in the absence of the guest below ca. pH 8.5, a similar pH profile for anionic guests as with the membranes containing macrocyclic polyamines.[21–23] Although such anionic potentiometric responses were observed for all compounds capable of bearing positive charges by multiple protonation (74–76), the magnitude was greatest for cyclophane 74. Figure 20b shows potential vs concentration curves at pH 5.0 for anionic guest 78. Here again, concentration-dependent decreases in membrane potential (anionic potentiometric responses) were observed for the positively charged compounds 74–76, the magnitude of response being greatest for cyclophane 74. These results clearly indicate that the fundamental structural requirements for guest-induced membrane potential changes with this type of host are (1) a cyclophane ring capable of inclusion of guest (74 vs. 75), (2) distinct hydrophilic group(s) located in close proximity to the inclusion cavity (74 vs. 77), and (3) long alkyl chains (74 vs. 76).

Because of totally synthetic nature, cyclophanes are one of the most important class of hosts which will contribute to understanding of the detailed aspects of
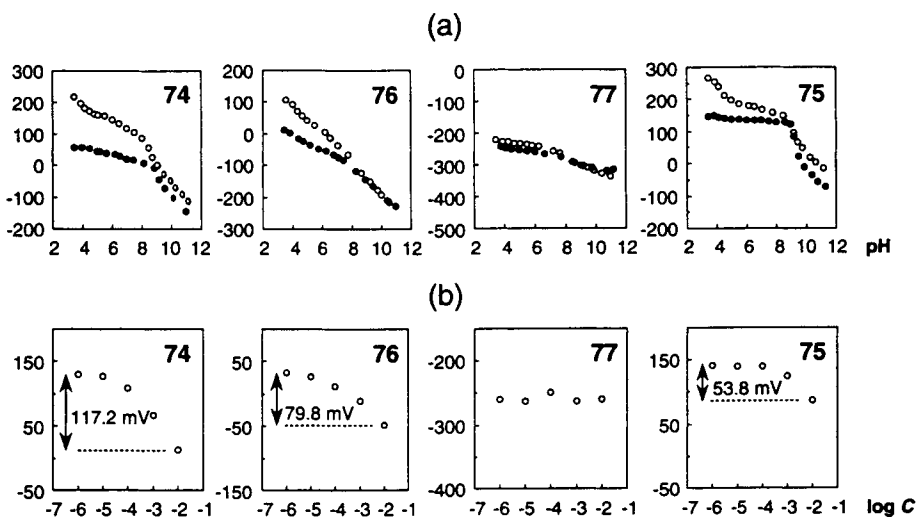
**Figure 20.** Potentiometric responses to anionic guest **78** by PVC matrix liquid membranes containing cyclophanes (**74, 76, 77**) or acyclic reference compound (**75**). (a) Membrane potential as a function of pH in the presence (●) or absence (○) of 1.00 × 10$^{-2}$ M guest. (b) Membrane potential as a function of guest concentration at pH 5.0 (0.01 M AcONa-AcOH buffer) and room temperature (ca. 20 °C). Membrane composition: DOS (95 mg) and PVC (44 mg) containing 6.2 × 10$^{-3}$ mmol host.

molecular recognition concerning organic guests not only in aqueous solutions but also at membrane surfaces.

## 2.4. Molecular Mechanism of Potentiometric Sensing at the Surface of Ion-Selective Liquid Membranes

The potential across the liquid membrane of ion-selective electrodes (ISEs) can be described as the sum of the diffusion potential across the membrane bulk and of the boundary potentials at the interfaces of the membrane to the inner filling and to the sample solutions.[50,164] Because changes of the diffusion potential in the membrane bulk take place only very slowly, the quick response of ISEs is due mainly to changes in the boundary potential at the sample solution interface.[165–167] It would thus be interesting to observe the processes occurring at the surface of ISEs at the molecular level. For this purpose we have used surface specific techniques, i.e., attenuated total reflection infrared spectrometry (ATR-IR) and optical second harmonic generation (SHG), and photoswitchable molecular probes, i.e., azobis(crown ether)s capable of effecting photoinduced changes in EMF (electromotive force).

### Attenuated Total Reflection Infrared Spectrometry

Pungor and co-workers[165-167] were the first to observe the processes occurring at the surface of ISE liquid membranes by using ATR-IR. Upon contact of membranes containing crown ether ionophore **79** with aqueous KCl, the formation of $K^+$ complexes on the membrane side of the phase boundary was observed. The complexes were easily removed by rinsing with water. In contrast, when $K^+SCN^-$ (lipophilic counteranion) was used in place of $K^+Cl^-$, a large number of complexes were observed deep in the membranes and were no longer easily removable by rinsing. Because the transport of complexes into the membranes was much slower than the EMF response, it was concluded that the EMF was determined essentially at the membrane surface rather than in the membrane bulk.

Recently, an ATR-IR study was carried out with ISE membranes containing ionophores **80–83** with the aim to quantitatively assess permselectivity by determining the stoichiometric ratio of primary cation ($M^+$) and counteranion ($X^-$) on the membrane side of the phase boundary.[39] Cation permselectivity was shown not to be violated as long as the counteranions were sufficiently hydrophilic ($X = SO_4^{2-}$, $NO_3^-$). In these cases, only IR bands of $M^+$ complexes but no signal for $X^-$ could be observed. The concentration of the complex cations in membranes decreased substantially within fractions of micrometers from the interface. When either lipophilic anionic site **84** [potassium tetrakis($p$-chlorophenyl)borate, KT$p$ClPB] was added or carboxylated PVC was used as membrane matrix, the concentration of complexes deeper in the membranes increased, showing that a greater amount of $M^+$ ions enter the membranes due to exchange with the initial countercations of the tetraphenylborate or the carboxylate groups.

However, when the membranes were exposed to aqueous solutions of an intermediate to high concentration of primary cation thiocyanate ($M^+SCN^-$), IR bands of the $M^+$ complex as well as the $X^-$ could be observed. At very high analyte concentrations, no preferential permeation for either $M^+$ or $SCN^-$ occurred and the slope of the electrode response was considerably decreased as compared to a Nernstian response. Cation permselectivity for $M^+SCN^-$ was observed only for the **84**-incorporated membranes at low analyte concentrations.

All spectroscopic evidence on the composition of a relatively thin layer at the membrane surface was thus found to be in agreement with the interpretation of permselectivity as being due to the exclusion of counteranions from the membrane phase. However, the depth accessible to ATR-IR is of the order of 0.1~1.0 μm and is thus too large for the observation of phenomena in the region in closest proximity to the membrane/aqueous interface in which charge separation is assumed to take place. Optical second harmonic generation (SHG), which has an even more pronounced surface sensitivity than ATR-IR, was recently shown to be very suitable for the investigation of the interface between ISE membranes and sample solutions.[40,41,168]

## Optical Second Harmonic Generation

Optical second harmonic generation (SHG), which stems from the conversion of two photons of frequency $\omega$ to a single photon of frequency $2\omega$, is an inherently surface-sensitive technique.[169] Whereas no optical second harmonic wave is generated in the centrosymmetric bulk of a liquid, molecules participating in the asymmetry of the interface between two liquids (noncentrosymmetric environment) contribute to SHG. Since the square root of SHG signal intensity, $\sqrt{I_{(2\omega)}}$, is proportional to the number $N$ (per unit area), the molecular orientation $\langle T \rangle$ and the second order nonlinear polarizability $\alpha^{(2)}$ of the SHG active species at the interface of the two liquids, the SHG technique provides a valuable tool to investigate the surface of liquid membrane ISEs.

*SHG Induced by Ionophore–Metal Ion Complexation at the Membrane Surface.* The dependence of $\sqrt{I_{(2\omega)}}$ on the concentration of primary cation chlorides ($M^+Cl^-$) in aqueous sample solutions, obtained for PVC matrix liquid membranes based on crown ether ionophores **80**, **83**, **85**, and **86** (membranes **80**, **83**, **85**, and **86**, respectively), is shown in Figure 21a–d. The SHG intensity for membrane **83** increased steeply at low $Li^+$ ion concentrations but leveled off at higher concentrations (Figure 21a). Because the SHG signal was negligible both in the absence of $Li^+$ ions in the aqueous solution and of ionophore **83** in the membrane (figure not shown), the generation of the SHG signals can be ascribed to the formation of oriented $Li^+$ complexes of ionophore **83** at the membrane surface, facing across the interface the hydrophilic counteranions, $Cl^-$, in the adjacent aqueous phase. Assuming negligible changes in the molecular orientation, the saturation of the SHG signal

79

80

81 (valinomycin)

**82**   **83**   **84 (KT*p*ClPB)**

**85**   **86**
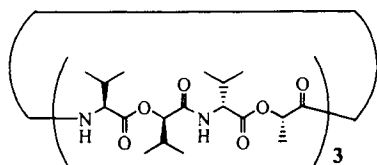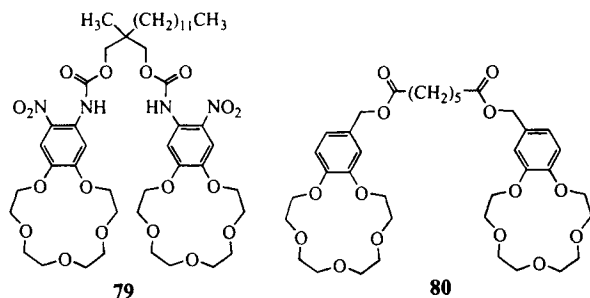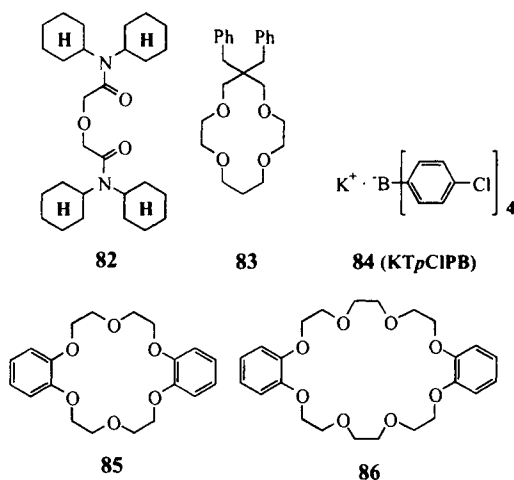
at high Li$^+$ ion concentrations indicates that the number of SHG active species located at the membrane interface becomes constant beyond a certain Li$^+$ ion concentration. Similar SHG responses were observed for membranes **80, 85**, and **86**.

Treatment of the above SHG curves for membranes **80, 83, 85**, and **86** by a Langmuir–isotherm type analysis indicates Langmuir-type "saturation" occurring at the membrane surface at high cation concentrations, which may be interpreted in terms of a tightly packed monolayer of the SHG active cation complexes at the membrane surface. However, the SHG active layer may actually have a thickness of several monolayers if the electrical field aligns the complexes with respect to the interface.

*Correlation between the SHG and EMF Responses.* As shown in Figure 22a, the SHG response of membrane **80** to aqueous KSCN was found to be substantially different from that to KCl. Upon increasing the KSCN concentration, the SHG signal initially increased but reached a maximum at 0.2 M and then decreased. An effect of the counteranion was also observed for the EMF response of the same membrane (Figure 22b), the decrease in the potentiometric response starting approximately at the same KSCN concentration as that for the SHG response. These results demonstrate that the anionic effect, caused by coextraction of K$^+$ and SCN$^-$ ions into the membrane bulk, is accompanied by a decrease in the number of oriented K$^+$ complexes at the interface.

To prevent such anionic effects, so-called anionic sites are conventionally used as additives for ISE membranes. In fact, upon addition of **84**, the SHG response of membrane **80** to KSCN was improved (data not shown). This result suggests that the lipophilic anion assists the surface orientation of the **80**-K$^+$ complexes by inhibiting the uptake of SCN$^-$ from the adjacent aqueous solution.
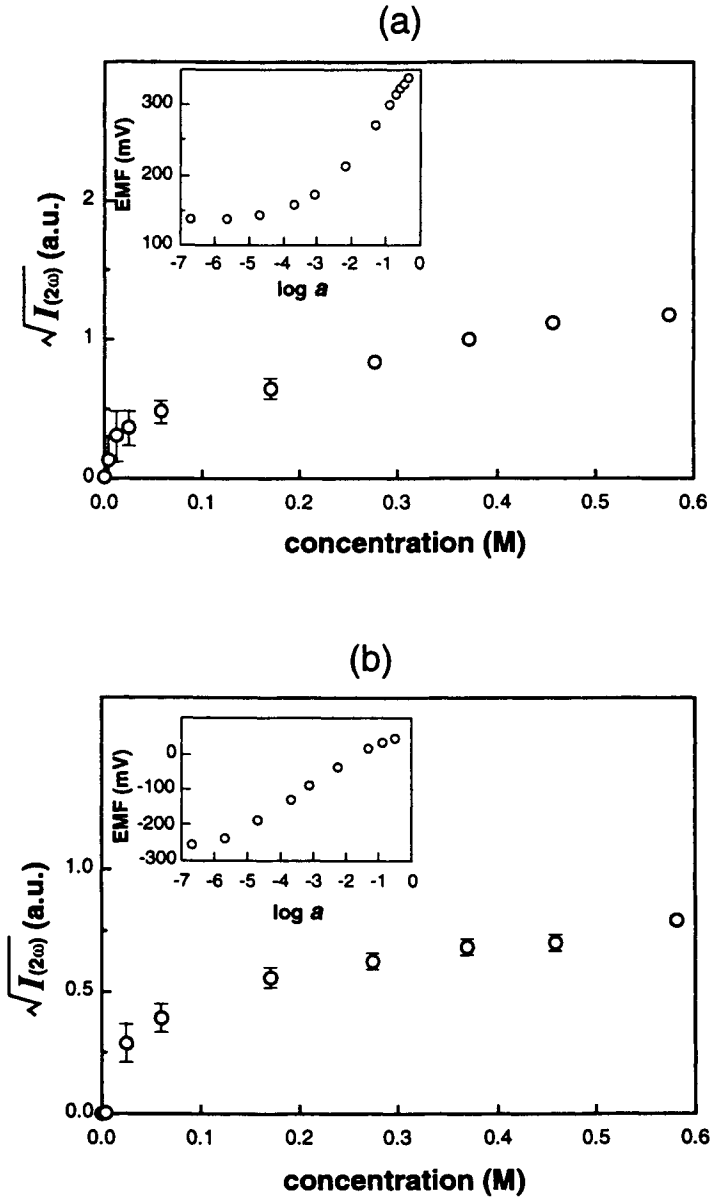
**Figure 21.** Dependence of the square root of the SHG intensity ($\sqrt{I_{(2\omega)}}$) on primary ion concentrations for (a) membrane **83** (Li$^+$ ion), (b) membrane **80** (K$^+$ ion), (c) membrane **85** (K$^+$ ion), and (d) membrane **86** (Na$^+$ ion). The corresponding observed membrane potentials are also shown (*inset*). (continued)

## (c)



## (d)
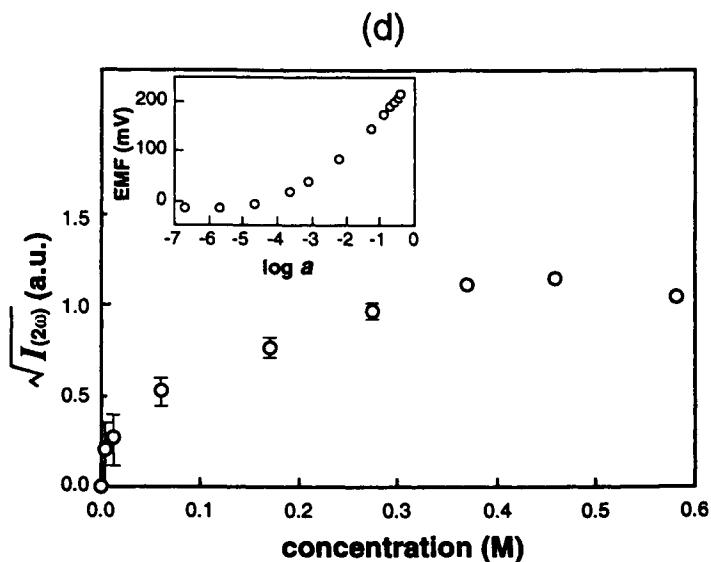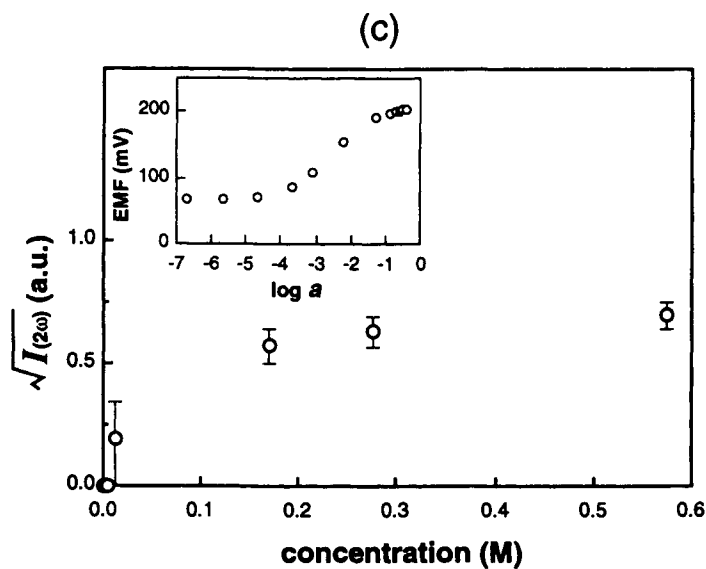


*Figure 21.* (continued) Membrane compositions: **83**/DOS/PVC = 0.2:64.2:35.6; **80**/DOS/PVC = 1.4:63.4:35.2; **85**/DOS/PVC = 0.6:63.9:35.5; **86**/DOS/PVC = 0.9:63.7:35.4. The ionophore concentration in the membrane was $1.0 \times 10^{-2}$ M in all cases (reprinted with permission from *Anal. Chem.* **1995,** *67,* 575. Copyright 1995 American Chemical Society).

## (a)



## (b)
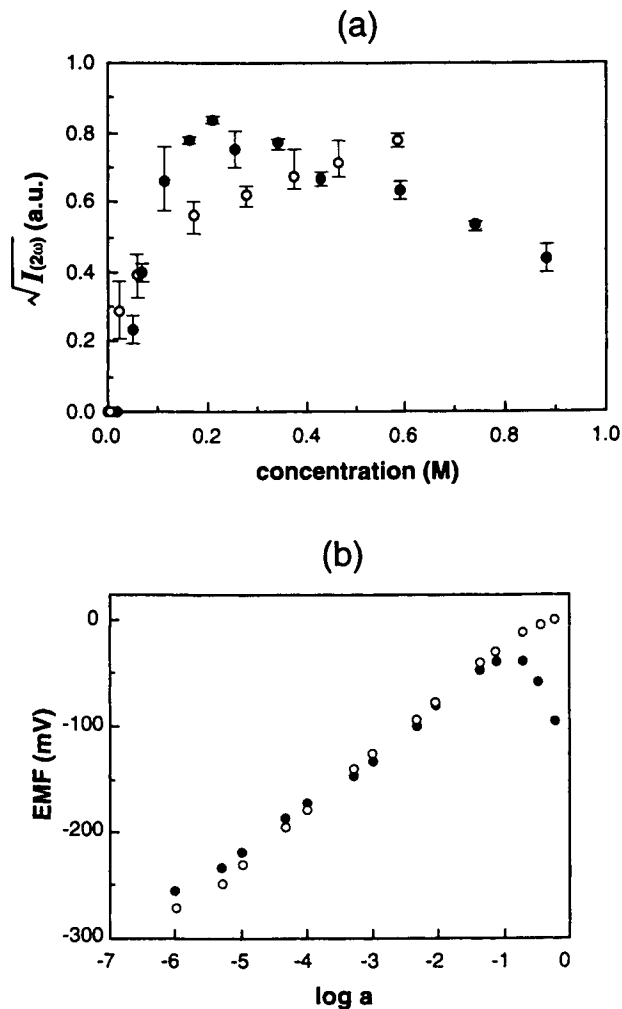


*Figure 22.* (a) Square root of the SHG intensity ($\sqrt{I_{(2\omega)}}$) and (b) observed membrane potential as a function of the concentration of $K^+$ ion in the adjacent aqueous solution containing KCl (o) and KSCN (●), respectively. The composition of the PVC matrix liquid membrane containing ionophore **80** is the same as in Figure 21b (reprinted with permission from *Anal. Chem.* **1995**, *67*, 574. Copyright 1995 American Chemical Society).

Similar but even more pronounced anionic effects were observed with liquid membranes based on ionophore **80** and exhaustively purified organic solvents (nitrobenzene or 1,2-dichloroethane) but no polymer matrix.[168] The use of such membranes allows to minimize the concentration of ionic impurities that could take the role of anionic sites. For a membrane with ionophore **80**, the SHG response

toward K$^+$ ion (KCl) was found to be negligibly small and no lasting EMF response could be observed. On the other hand, when the lipophilic anion **84** was added to the membrane, EMF and SHG responses to KCl were regained, showing the necessity of such ionic sites for ISEs based on neutral carriers.

The parallel changes in membrane potentials and SHG signals indicate that the observed membrane potential changes are primarily governed by the SHG active oriented species at the membrane surface. However, another important property of the SHG response of membranes **80, 83, 85**, and **86** is that saturation occurs at very high primary cation concentrations (0.5–1.0 M), where Nernstian potentiometric responses are still observed (Figure 21a–d). Although such high concentrations are of little significance for practical ISE measurements, the above observation shows an interesting aspect on the mechanism of potentiometric response; the generation of the membrane potential at such very high primary cation concentrations is governed not only by the SHG active cation complexes at the membrane surface but also by complexes located behind the SHG active layer, which are SHG inactive due to a lack of molecular orientation.

It is at present still difficult to correlate the absolute intensity of the SHG with the number of cationic complexes at the membrane surface. Therefore, a quantitative discussion, showing how the permselective uptake of primary cations forming SHG active complexes into the membrane side of the phase boundary corresponds to the increase in the membrane potential, is not possible yet. Lipophilic derivatives of photoswitchable azobis(benzo-15-crown-5) were recently shown as a molecular probe to determine photoinduced changes in the amount of the primary cation uptake into the membrane phase boundary in relation to the photoinduced EMF changes under otherwise identical conditions.

### Studies by Photoswitchable Azobis(benzo-15-crown-5) Derivatives as a Molecular Probe

*Design of Lipophilic Azobis(15-crown-5) Derivatives.* When the PVC matrix liquid membrane containing an azobenzene-bearing crown ether (e.g., **87**) in contact with the primary cation solution (KCl) is exposed to UV or visible light, photoinduced changes in membrane potential (EMF) are observed.[170–172] These changes are based on the difference in complexation ability between the *cis* and *trans* isomers of the azobenzene ionophore, which can be interconverted photochemically. If the photoequilibrium concentrations of the *cis* and *trans* forms of the photoswitchable ionophores and the stability constants for their complexes with primary ions can be estimated, the photoinduced changes in EMF can be correlated quantitatively to the amount of primary ion uptake or release into or out of the membrane phase boundary. Photoswitchable ionophores may thus serve as a molecular probe to quantitatively determine the change in the concentration of complex cations at the membrane surface, which corresponds to the membrane potential changes.
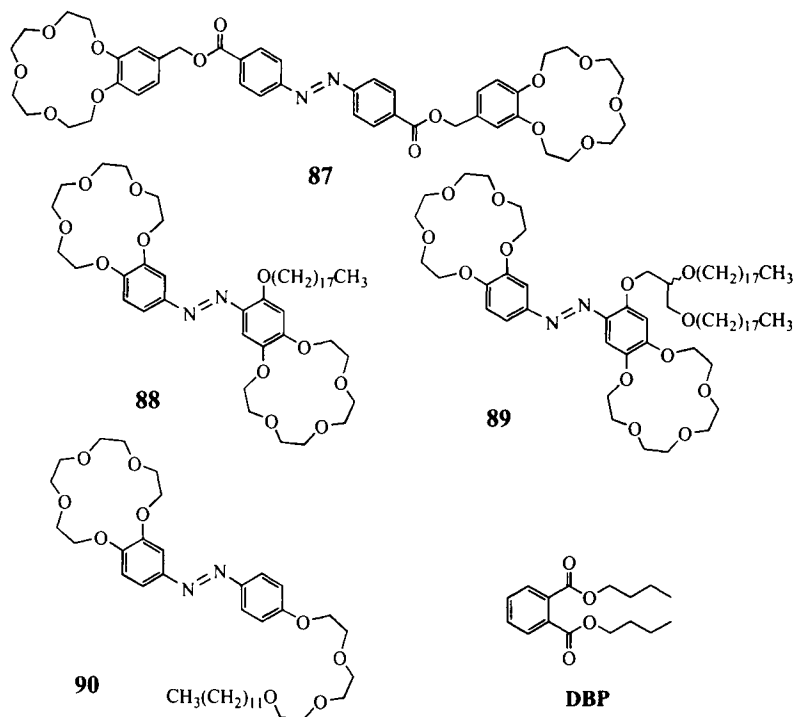
For this purpose, the photoswitchable bis(crown ether)s **88** and **89** as well as the reference compound **90** have been synthesized.[173] Compounds **88** and **89** are highly lipophilic derivatives of azobis(benzo-15-crown-5). The parent azobis crown ether was originally developed by Shinkai[174–176] and its photoresponsive changes in complexation, extraction, and transport properties thoroughly examined. Compared to **87**, more distinct structural difference between the *cis* and *trans* isomers can be expected for **88** and **89** because in the latter compounds the 15-crown-5 rings are directly attached to the azobenzene group. The photoequilibrium concentrations of the *cis* and *trans* forms and the photoinduced changes in the complexation constants for alkali metal ions are summarized in Table 7.

*Photoinduced Changes in Phase Boundary Potentials.* The photoinduced membrane potentials were measured by using PVC matrix liquid membranes in contact with a polypyrrole-coated Pt electrode [dibutyl phthalate (DBP) as the membrane solvent]. The polypyrrole layer allows to obtain a stable and sample-independent potential drop between Pt and the PVC membrane. The phase boundary potential at the interface of a membrane containing ionophore and an aqueous RbCl or KCl solution could be reversibly altered by UV and visible light irradiation, as shown for ionophore **89** in Figure 23a,b. The values of the photoinduced potential

***Table 7.*** Photostationary *cis/trans* Percentages and Extractabilities of Alkali Metal Picrates with Ionophores **88**, **89**, and **90** under Visible and UV Light Irradiation[173]

| Ionophore | Irradiation | Percentage[a] | *Extracted Picrate / %[b]* | | | |
|---|---|---|---|---|---|---|
| | | | $Na^+$ | $K^+$ | $Rb^+$ | $Cs^+$ |
| **88** | visible | 0:100 | 21.8 | 32.2 | 24.2 | 18.4 |
| | UV | 42:58 | 19.4 | 28.6 | 33.6 | 22.3 |
| **89** | visible | 0:100 | 34.4 | 36.7 | 12.3 | 13.1 |
| | UV | 39:61 | 33.1 | 29.2 | 22.0 | 21.5 |
| **90** | visible | 0:100 | 37.5 | 42.3 | 31.2 | 14.2 |
| | UV | 50:50 | 35.4 | 31.3 | 25.0 | 8.2 |

*Notes:* [a]Measured in PVC matrix liquid membranes (dibutyl phthalate/PVC = 2:1; [ionophore] = 1 mM; membrane thickness 50 μm).

[b]Measured in two-phase systems. Organic phase (dibutyl phthalate): [ionophore] = $1.00 \times 10^{-3}$ M; aqueous phase: [picric acid] = $5.00 \times 10^{-5}$ M, [metal hydroxide] = $1.00 \times 10^{-3}$ M, [metal chloride] = $5.00 \times 10^{-1}$ M.

changes, i.e., $\Delta E = E_{UV} - E_{Vis}$, for membranes based on ionophores **88–90** are summarized in Table 8. Importantly, the direction of the photoinduced potential changes depend on the photoinduced changes in the corresponding cation extractability (see Table 7). This result indicates that the photoinduced changes in the phase boundary potential arise from changes in the amount of cations that enter or leave the membrane phase at the interface between the membrane and aqueous sample solution.

To quantitatively correlate the photoinduced changes in the phase boundary potential to the number of complexed cations entered in a permselective manner into the membrane surface, the photoinduced potential changes were analyzed on the basis of a space-charge model proposed by Buck.[18,177] Theoretical treatment of this model including the complexation equilibrium at the membrane and aqueous sides of the interface was made[173] as an extension of the theory proposed by others,[178–181] assuming Gouy–Chapman-type double-diffuse layers as a space-charge region that enables charge separation across the membrane/aqueous solution interface. Based on this model, the phase boundary potential between the membrane and aqueous bulk can be approximately expressed as a function of the surface-charge density, which in turn can be expressed as a function of the surface concentrations of the complex cations, defined as the concentrations at the outer Helmholtz plane at the membrane side of the interface. The total surface concentrations, corresponding to the sum of those of the complexes of the *cis* and *trans* isomers, can be estimated from the photoequilibrium *cis/trans* ratio and complexation stability constants for each isomer described in Table 7.

For the membrane containing 1 mM of ionophore, the UV-induced increase in the phase boundary potential thus calculated (+8.2 mV) is close to that of the

## (a)



## (b)
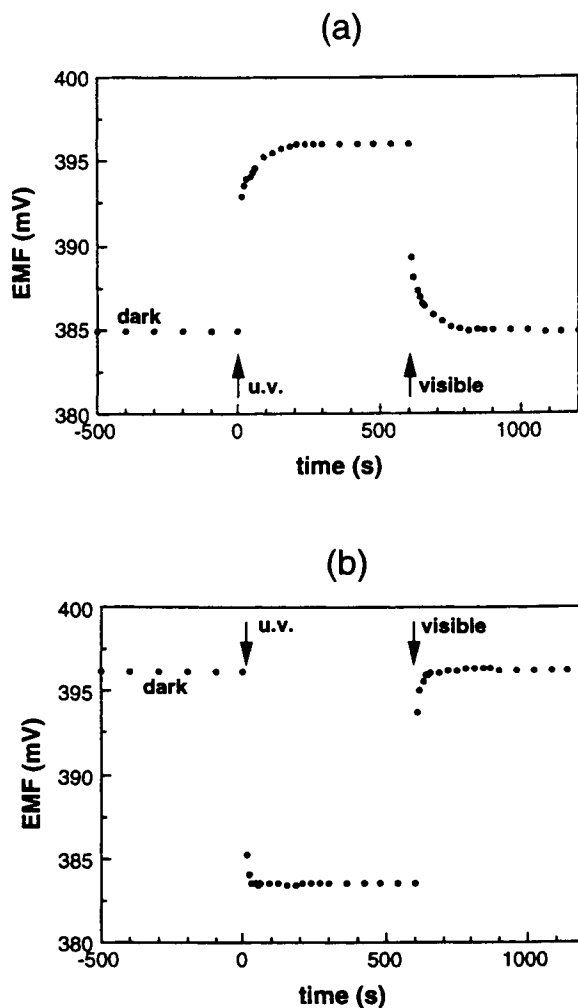


*Figure 23.* Photoresponse of the EMF induced by UV and visible light irradiation for membrane **89** in contact with (**a**) 0.1 M aqueous RbCl and (**b**) 0.1 M aqueous KCl. Membrane composition: DBP/PVC = 2:1 wt/wt containing 1 mM of **89**.

observed value (+7.5 mV). The comparison of the observed and calculated potential changes is shown in Table 8. It can be seen that the calculated potential changes of membranes with 1 mM of ionophores **88–90** in contact with 0.1 and 0.01 M aqueous KCl or RbCl were in good agreement with the corresponding observed values. This quantitative agreement indicates that the phase boundary potential is determined by the amount of the primary cations permeated across the membrane interface.

***Table 8.*** Photoinduced Potential Changes, ΔE (mV), for Membranes Based on Ionophores **88–90** [173] a

| | RbCl | | | KCl | | |
|---|---|---|---|---|---|---|
| *Ionophore* | *0.1 M* | *0.01 M* | *Calc*[b] | *0.1 M* | *0.01 M* | *Calc*[b] |
| **88** | −17.1 | −17.2 | −20.0 | +7.5 | +7.2 | +8.5 |
| **89** | −12.6 | −12.5 | −12.4 | +11.0 | +10.8 | +11.2 |
| **90** | −7.9 | −8.2 | −7.7 | −7.4 | −6.5 | −5.7 |

*Notes:* a$\Delta E = E_{UV} - E_{Vis}$. Membrane composition: DBP/PVC = 2:1 wt/wt with 1.0 mM ionophore.

bThe potential changes were calculated by treatment based on a space charge mode.

*Photoinduced Changes in the EMF Response Slope.*    In the case that the EMF response slope is smaller than the theoretical value according to the Nernst equation (sub-Nernstian slope), UV irradiation induced changes in not only phase boundary potentials but also EMF response slopes (Figure 24). When a membrane containing 1 mM of ionophore **89** was exposed to visible light, a linear response to $Rb^+$ ion with a nearly Nernstian slope was observed. Upon UV light irradiation, a parallel shift in the linear response was observed with an increase in the EMF (Figure 24a). However, reduction of ionophore **89** to 0.1 or 0.01 mM concentration resulted in sub-Nernstian slopes under both UV and visible light irradiation. In these cases, the EMF slope under visible light was smaller than that under UV light (Figure 24b,c), reflecting the smaller uptake of $Rb^+$ ions into the membrane side of the interface with the *trans* isomer, which has a weaker binding affinity for $Rb^+$ ion than the *cis* isomer.

For the membrane containing 0.1 mM of ionophore, the quantitative relationship between the EMF response slope and the amount of primary cation uptake into the membrane side of the interface was confirmed by comparing the observed photoinduced changes in the EMF slope and the calculated values based on the surface-charge density as described above. In this case, the slope of the EMF response to $Rb^+$ ion under visible light irradiation was sub-Nernstian (38.5 mV decade$^{-1}$). On the other hand, the corresponding surface-charge density is estimated to be $2.5 \times 10^{-8}$ C cm$^{-2}$. Upon UV light irradiation, 24.6% augmentation in the surface-charge density was estimated by the increase in the concentration of the *cis* isomer. The resulting calculated slope increases to 43.2 mV decade$^{-1}$ which is close to the observed slope upon UV light irradiation (44.1 mV decade$^{-1}$). The improvement of the EMF response slope by adding anionic site **84** to the membrane could also be quantitatively explained by the same theoretical treatment based on a surface-charge model.

The agreement between the calculated and observed response slopes indicates that the primary factor determining the EMF slope is the surface-charge density which is governed by the ionophore concentration in the membrane. As a result,

# (a)

# (b)

# (c)
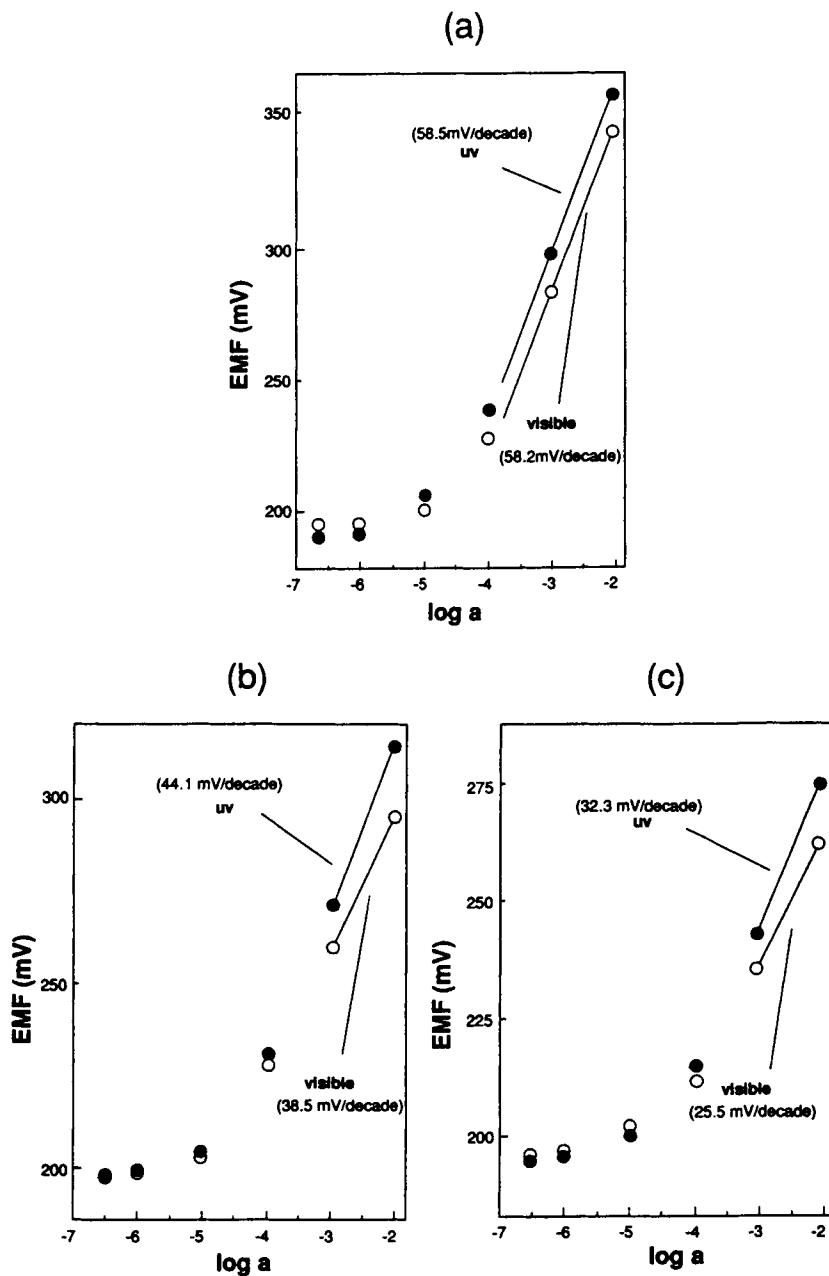
*Figure 24.* Potentiometric responses toward RbCl of membrane **89** with various concentrations of ionophore **89** under UV and visible light irradiation. Membrane composition: DBP/PVC = 2:1 wt/wt containing (**a**) 1 mM, (**b**) 0.1 mM, and (**c**) 0.01 mM of **89**, respectively.

sufficient primary cation uptake due to sufficient concentration of ionophore (1 mM in the present case) leads to Nernstian responses, whereas insufficient primary cation uptake due to low ionophore concentrations leads to sub-Nernstian responses.

# 3. CHEMICAL SENSING BASED ON THE SUPRAMOLECULAR FUNCTIONS OF BIOLOGICAL SYSTEMS

## 3.1. Chemical Sensing Based on Glutamate Receptor (GluR) Ion Channels

Glutamate receptor (GluR) ion channels are known to play a key role in transmembrane signaling at postsynaptic membranes in mammalian brain.[182,183] The specific binding of the principal neurotransmitter L-glutamate (L-Glu) to these receptor ion channels triggers the opening of the channels through which a large number of ions are allowed to permeate following their electrochemical gradients. Such transmembrane signaling displayed by GluRs provides an important principle for designing highly sensitive and selective sensing membranes.[184] Also, evaluation of chemical selectivity of GluRs towards different excitatory amino acids is important for studies of the mechanisms underlying the biological signal transduction process,[183] design and synthesis of excitatory amino acids[185] and structure–function relationships.[186]

An ion channel sensor for L-Glu has been fabricated by incorporating GluR ion channel proteins, isolated from the synaptic membrane of rat brain, into reconstituted planar bilayer lipid membranes.[187–189] A purified preparation of the receptor ion channel proteins was incorporated into planar bilayer lipid membranes (BLMs) formed by two different methods, i.e., the monolayer folding method (Takagi–Montal Method)[188] and the tip–dip method,[187] and the channel currents triggered by L-Glu were measured. The experimental setup for the former method is shown in Figure 25. In this system, the concentration of L-Glu can be determined on the basis of the integrated transmembrane cation current, which corresponds to the total number of ions passed through the open channel during the period of L-Glu binding. Hence, this integrated current is an amplified "physiologically relevant" measure, including both agonist concentration and agonist potency to activate the GluR ion channels. Two types of ion channel sensors, i.e., multichannel and single-channel sensors, have been fabricated in which the number of GluRs incorporated into the BLMs is purposely different.

The relationship between the concentration of L-Glu and the response as an integrated channel current for the multichannel-type sensor (most likely containing ≥10 GluR ion channel proteins) is shown in Figure 26a. A sharp concentration dependence was observed up to ca. $1.5 \times 10^{-7}$ M of L-Glu. The detection limit of this sensing system is lower than the lowest concentration tested, i.e., $3.0 \times 10^{-8}$ M.
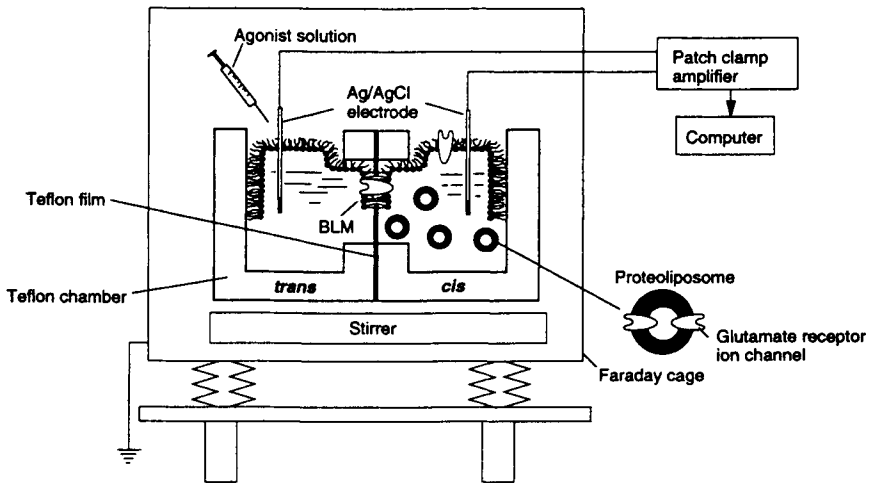
**Figure 25.** Experimental setup for the formation of bilayer lipid membranes and current measurements.[188]

A high sensitivity to L-Glu with a detection limit lower than $3.0 \times 10^{-7}$ M was also observed for the single-channel-type sensors containing only one and two active GluR ion channel proteins (Figure 26b). Recently, the detection limit was successfully lowered down to $1.0 \times 10^{-10}$ M with a multichannel sensor containing ~37 GluRs.[190] The high sensitivity of the present sensing systems is evidently based on the intense signal amplification function of the GluRs; the amplification factor was estimated to be ca. $2.1 \times 10^5$ ions/channel on the basis of the average number of ions which pass through the channel during a single open channel period (average 7.6 ms).[187]

The GluR ion channels are grouped into three subtypes, i.e., N-methyl-D-aspartic acid (NMDA) receptors, α-amino-3-hydroxy-5-methylisoxazole-propionic acid (AMPA) receptors, and kainic acid receptors.[191–193] The potency of agonists and antagonists to induce or block the channel activity of GluRs has been described in terms of the binding affinity obtained by radioligand techniques[185] and by the dose–response curve technique with voltage-clamped whole cells.[194–196] Besides the binding assay approach, the kinetic parameters of GluR channels, such as the decay time of the agonist-induced currents and the life time of the agonist-gated current obtained by single-channel patch-clamp techniques, have been reported; more potent agonists exhibited longer decay time of multichannel currents[197] and longer open time of single-channel currents.[198]

A new approach for evaluating chemical selectivity of GluRs, in which the integrated channel currents, corresponding to the total amount of ions passed through the multiple open channels, are used as an amplified "physiologically

(a)                                    (b)
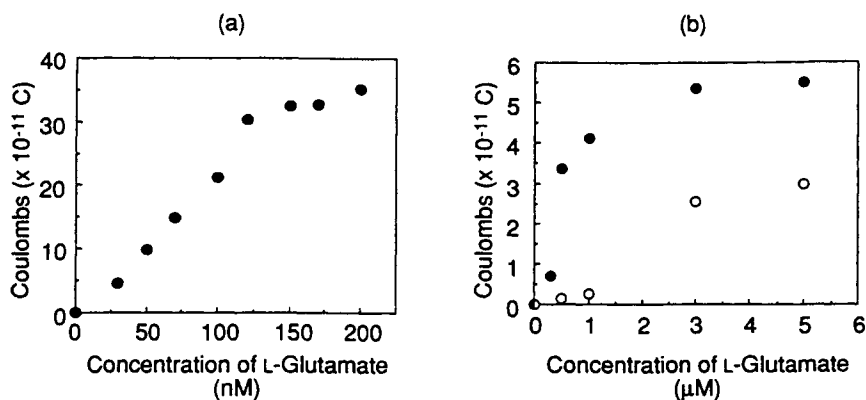


**Figure 26.** Relationship between the concentration of L-Glu and the integrated channel current. (a) Multichannel BLM. (b) Single-channel BLMs constructed with different preparations of BLMs, which most likely contain one (○) and two (●) GluR ion channel protein(s) (reproduced by permission of American Chemical Society from *Anal. Chem.* **1991**, *63*, 2792, 2793).

relevant" measure of agonist potency to activate each of the GluR subtypes. Chemical selectivity for activating each of the GluR subtypes was evaluated by utilizing integrated channel currents.[190] For fabricating a multichannel sensor, GluR ion channels from rat synaptic plasma membranes were incorporated into planar BLMs formed by the folding method. The experimental setup is the same as shown in Figure 25. Using three typical agonists, NMDA, L-Glu, and the 2*S*,3*R*,4*S* isomer of 2-(carboxycyclopropyl)glycine (L-CCG-IV, **91**),[199] the chemical selectivity of these three agonists toward the NMDA receptor subtype was evaluated on the basis of integrated channel currents of a multichannel type sensor.

One of the unavoidable factors encountered in evaluating the potency of different agonists to activate GluRs was that the magnitude of the integrated channel currents arising from different BLMs cannot meaningfully be compared to one another due to the difference in the number of incorporated proteins and their subtypes. As exemplified in Figure 27, the multichannel responses obtained with two BLMs (BLMs (a) and (b)) gave rise to markedly different magnitudes of integrated currents in response to an identical concentration of L-Glu. Considering the multichannel currents to be comprised of the sum of the single-channel currents generated by several GluR channels, the larger response obtained with BLM (b) shows that the BLM contained a larger number of GluRs (~37) than the BLM (a) (~4 GluRs). Furthermore, as shown in Figure 28, the kind (or ratio) of receptor subtypes incorporated into BLMs was found to be different for each membrane preparation, as indicated by the identification of the GluRs in the BLMs by using the antagonists 6,7-dinitroquinoxaline-2,3(1*H*,4*H*)-dione (DNQX) and (+)-5-methyl-10,11-dihydro-5*H*-dibenzo[*a,d*]cyclohepten-5,10-imine maleate (MK-

## (a)



## (b)
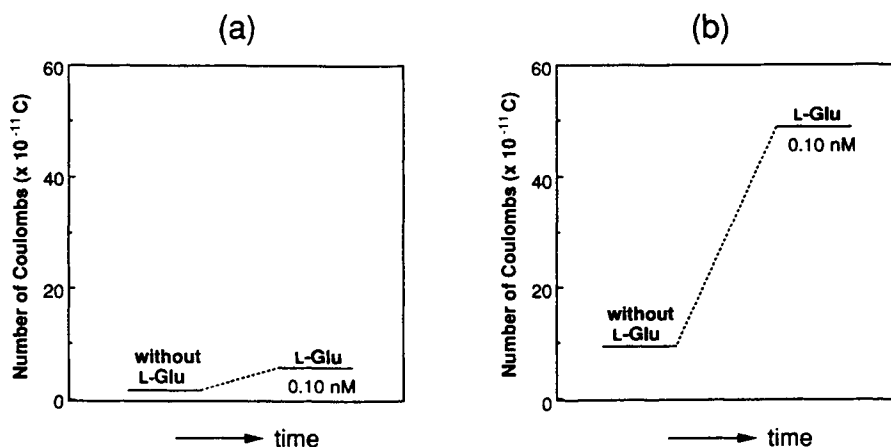


**Figure 27.** Comparison of the L-Glu-induced integrated channel currents between two different preparations of GluR-incorporated BLMs upon injecting the identical concentration of L-Glu (0.10 nM). Applied potential: +50 mV. Conditions: 9.8 mM HEPES-NaOH (pH 7.6) containing 0.52 M NaCl, 0.19 mM $CaCl_2$, 4.8 mM glycine, 24 µg $mL^{-1}$ of concanavalin A, 8.1 mM sucrose and 0.40 M formamide in both *cis* and *trans* side solutions. Proteoliposomes were injected only to the *cis* side and agonist solution was added to the *trans* side. Applied potential: +50 mV. The L-Glu solution was injected to the *trans* side.[190]

801), which are specific for non-NMDA and NMDA subtypes, respectively. Consequently, the multichannel responses induced by agonists can only be compared within single BLM preparation, in which the number of receptors can be regarded as constant and the kind of GluR species does not vary.

Taking the above facts into consideration, BLMs designed to contain exclusively NMDA subtype of GluRs were used to evaluate the chemical selectivity of NMDA subtype receptor for NMDA, L-Glu, and L-**91**. This was achieved by measuring channel currents through NMDA subtype receptor channels in the presence of DNQX, which is a specific antagonist of non-NMDA subtype receptors. While DNQX blocks the channel activity of non-NMDA subtype channels in the BLM, only NMDA subtype receptors remain unblocked, which can then be selectively activated by agonists of interest. The relative potency of two agonists, (1) NMDA and L-Glu and (2) L-Glu and L-**91**, toward NMDA subtype receptors was determined, as shown in Figure 29a and Figure 29b, respectively by using identical concentrations of two agonists in series. From the relative magnitude of the integrated channel currents for the two agonists, the relative potency toward NMDA subtype receptors was determined as being (1) L-Glu > NMDA and (2) L-**91** > L-Glu. Based on these results, the order of selectivity of the three agonists for the

## (a)



## (b)



## (c)
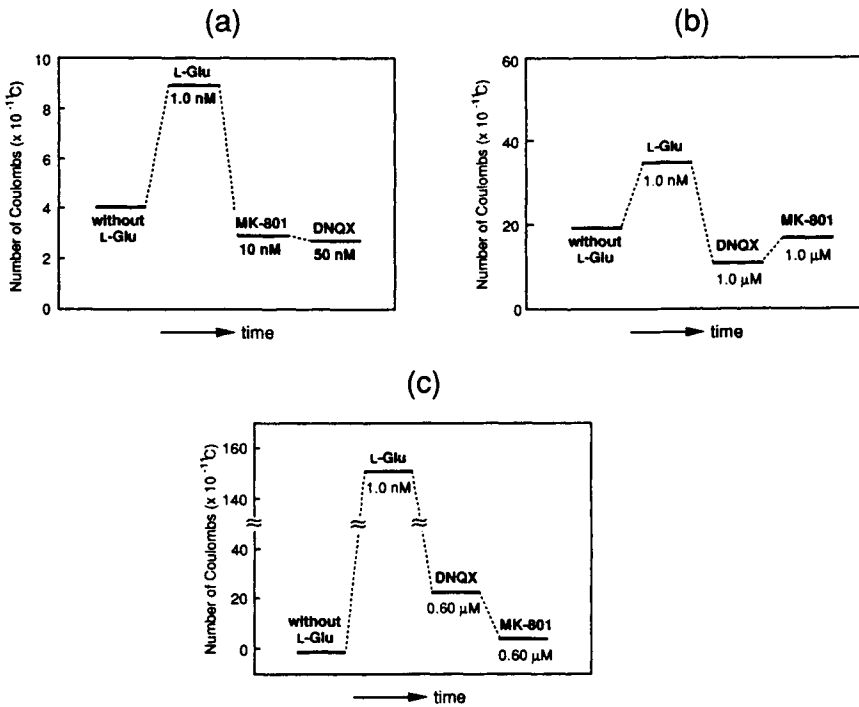


*Figure 28.* Changes in the integrated channel currents for multichannel BLM upon addition of L-Glu, MK-801, and DNQX in series. Solution condition: (a) the same as in Figure 27, (b) 20 mM citric acid, 42 mM Tris, 0.15 M NaCl, 5.0 mM glycine, 0.20 mM $CaCl_2$, and 25 mg mL$^{-1}$ of concanavalin A, pH 7.6, and (c) the same as in Figure 27. Applied potential: (a) +30 mV, (b) –30 mV, and (c) +30 mV. The L-Glu solution was injected to the *trans* side. The antagonist was injected to both sides.[190]

NMDA receptor subtype is found to be L-**91** > L-Glu > NMDA. This selectivity is consistent with that of the binding affinity of these agonists to NMDA subtype receptors.[199] However, the selectivity based on the integrated channel current covered a much narrower range than that based on the binding affinity; while the relative binding affinity of the three agonists was NMDA:L-Glu:L-**91** = 0.022:1.0:17,[199] the selectivity based on the integrated current was found to be NMDA:L-Glu:L-**91** = 0.47:1.0:2.9. This suggests that the present selectivity, reflecting not only the binding ability of each agonist to the NMDA subtype receptor but also the signal transduction efficiency, provides a measure of agonist potency that is physiologically more relevant than the binding affinity.

The present approach can be applied not only to AMPA and kainate subtype receptors of GluRs but also to other receptor ion channels.

## (a)



## (b)
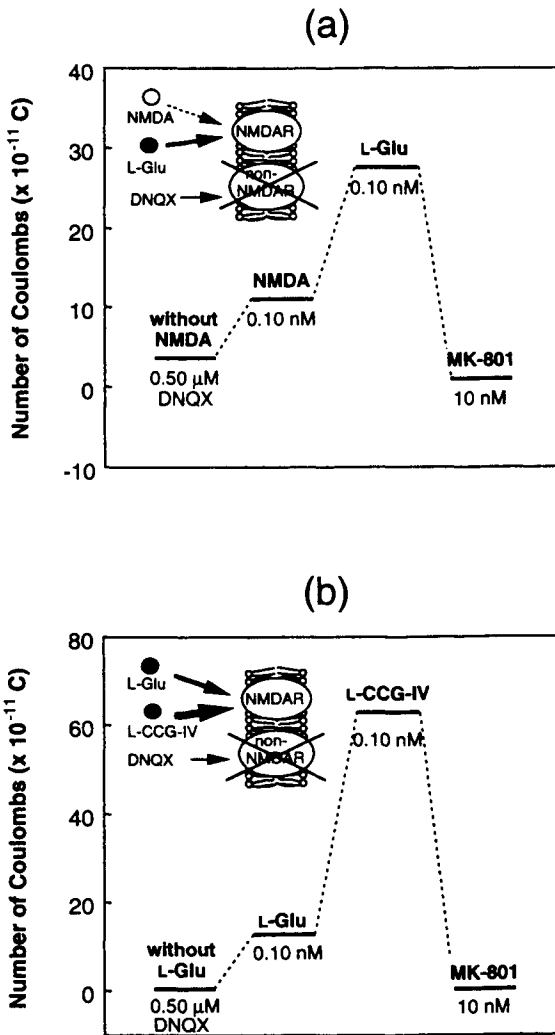


**Figure 29.** Typical examples of changes in the integrated channel currents upon successive addition of (a) NMDA, L-Glu, and MK-801, and (b) L-Glu, L-CCG-IV (L-**91**), and MK-801. Applied potential: (a) +50 mV and (b) +30 mV. Solution condition was the same as in Figure 26 (multichannel BLM), except for the presence of 0.50 μM DNQX in both *cis* and *trans* sides. The agonist was injected to the *trans* side. The antagonist was injected to both sides.[190]

## 3.2. Chemical Sensing Based on Active Transport of Target Compounds

The active transport of target compounds is interesting as a new mode of mass transfer for designing separation and sensing systems with signal amplification.[200–202] Since the first uphill (active) transport membrane sensor was proposed in 1986,[203] this method has already been demonstrated for several liquid membrane systems[204–206] by exploiting synthetic molecules, such as methyltrioctylammonium chloride (92; $Cd^{2+}$),[203,204] dicyclohexyl-18-crown-6 (93; $K^+$),[206] and dibenzoyl-methane (94; $Cu^{2+}$),[206] and biomolecules such as $Na^+$/D-glucose cotransporter[207] and $Na^+$,$K^+$-ATPase.[208]

### *Na⁺/D-Glucose Cotransporter-Based Sensing Membrane*

The $Na^+$/D-glucose cotransporter protein is known to display active transport of D-glucose across cell membranes by using an electrochemical $Na^+$ gradient as the driving force. The energy conversion proceeds in a coupled transport (symport) with a coupling stoichiometry of $Na^+$:D-glucose = 1:1 or 2:1.[1] Considering the efficiency and specificity of glucose transport displayed by the $Na^+$/D-glucose cotransporter, a purified preparation of the cotransporter from the small intestine of guinea pigs was embedded into a planar BLM for constructing a highly sensitive BLM sensing system for D-glucose.[207] The principle of the D-glucose sensor based



| | | | R¹ | R² | R³ | R⁴ |
|---|---|---|---|---|---|---|
| dopamine (38) | | | H | H | H | OH |
| (*R*)-noradrenaline [(*R*)-39] | | | H | H | OH | OH |
| (*R*)-phenylephrine [(*R*)-96] | | | CH₃ | H | OH | H |
| (*R*)-adrenaline [(*R*)-40] | | | CH₃ | H | OH | OH |
| L-DOPA (L-97) | | | H | CO₂H | H | OH |
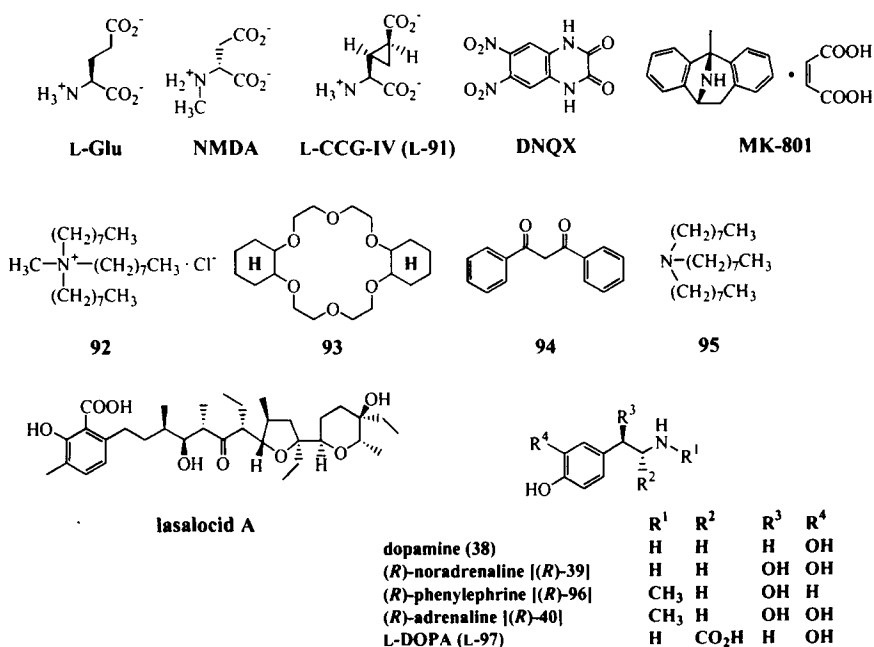
on a $Na^+$/D-glucose cotransporter is shown in Figure 30. The driving force for D-glucose to be pumped is provided as an electrochemical $Na^+$ gradient created by applying a potential across the BLM facing to the solutions containing $Na^+$ ions at a given concentration. The electrochemical $Na^+$ gradient in the present system is maintained by the applied potential, while in biological membranes the $Na^+$ gradient is infinitely maintained by $Na^+$,$K^+$-ATPase, which pumps $Na^+$ out of the cell. The $Na^+$/D-glucose cotransporter in the BLM is specifically activated by $Na^+$ ions, and the energy conversion proceeds in a coupled transport. The $Na^+$ ions cotransported across the BLM are measured as a $Na^+$ current, which is a measure of the concentration of D-glucose in the sample solution.

The incorporation of purified $Na^+$/D-glucose cotransporter into the BLM formed by the monolayer folding method was achieved either by fusion of its proteoliposomes or by folding the lipid layer containing the proteoliposomes. The experimental setup for measuring the currents is the same as in Figure 25. The concentration dependence of the observed currents is shown in Figure 31. A $Na^+$



$$\Delta\tilde{\mu} = \tilde{\mu}_{Na^+}^{trans} - \tilde{\mu}_{Na^+}^{cis} = RT \ln \frac{a_{Na^+}^{trans}}{a_{Na^+}^{cis}} + F \cdot \Delta E$$
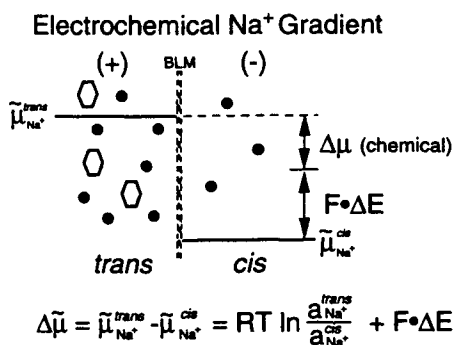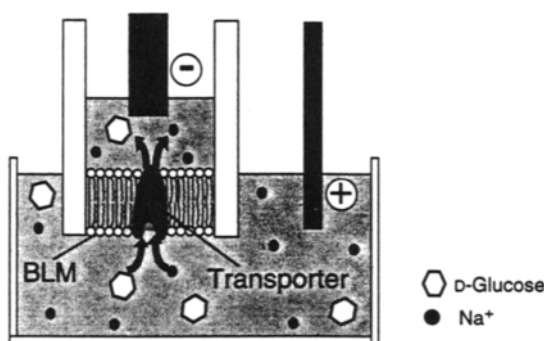
Figure 30. Principle of the D-glucose sensor based on the $Na^+$/D-glucose cotransporter-embedded BLM (reprinted with permission from Anal. Chem. 1993, 65, 364. Copyright 1993 American Chemical Society).
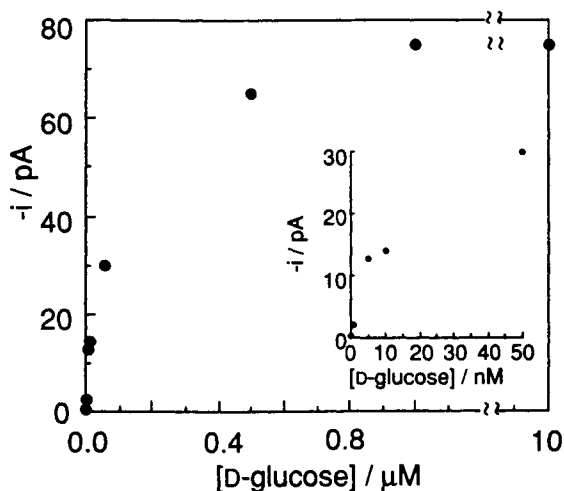
**Figure 31.** A plot of the observed current against the concentration of D-glucose for the Na⁺/D-glucose cotransporter-based BLM sensor. The static potential of –50 mV was applied to the system in the presence of 10 mM Na⁺ in the sample solution (reprinted with permission from *Anal. Chem.* **1993**, *65*, 366. Copyright 1993 American Chemical Society).

current coupled with the D-glucose transport was observed even at $10^{-9}$ M of D-glucose, followed by a steep rise in the response up to $5 \times 10^{-8}$ M. At higher concentrations of D-glucose, the current increased more gradually and virtually leveled off above $10^{-6}$ M. Compared to the conventional glucose sensors based on glucose oxidase, which typically show a detection limit of 1 µM to several hundred µM, the detection limit of $10^{-9}$ M attained by the present sensing system should be regarded as extremely low. Among several related monosaccharides tested, i.e., L-glucose, D-fructose, D-mannose, and D-galactose, only D-galactose ($10^{-6}$ M), which is known to competitively bind to the Na⁺/D-glucose cotransporter protein, induced a response. The observed amperometric selectivity is consistent with the binding and transport selectivities displayed by this transporter protein in biomembranes.[209,210]

The approach described here can be applied to other cotransporters and antiporters for the development of highly sensitive and selective sensing membranes for substrates (analytes) such as sugars other than D-glucose and amino acids.

### Na⁺,K⁺-ATPase-Based Sensing Membrane

The Na⁺,K⁺-ATPase is known to actively pump Na⁺ out and K⁺ into a cell against their concentration gradients. The active transport of these ions is tightly coupled to hydrolysis of adenosine 5′-triphosphate (5′-ATP). For every molecule of 5′-ATP

hydrolyzed, three $Na^+$ ions are pumped out and two $K^+$ ions are pumped in, so that one net positive charge ($Na^+$) is translocated.

A sensor for 5'-ATP was fabricated with a purified preparation of $Na^+,K^+$-ATPase embedded into a BLM.[208] The experimental setup used for these experiments is the same as that shown in Figure 25, except that a vibration-reed electrometer (input impedance $>10^{15}$ $\Omega$) was used for measuring membrane potentials. The typical time course of generation of membrane potential responding to 5'-ATP is shown in Figure 32. Upon adding 5'-ATP, the membrane potential shifted toward a negative value and reached a steady potential. The 5'-ATP-induced membrane potential almost completely disappeared when the specific inhibitor ouabain was injected. This confirms that the observed membrane potential originated from the pumping action of $Na^+,K^+$-ATPase in the BLM. This potentiometric sensor enabled us to detect 5'-ATP over a range from $1.0 \times 10^{-6}$ to $1.0 \times 10^{-3}$ M with a detection limit (S/N $\geq$ 3) of $6.3 \times 10^{-6}$ M. The selectivity against several nucleotides as well as acetyl phosphate was found to be in the order of 5'-ATP > 5'-UTP, 5'-GTP > acetyl phosphate, 5'-CTP >> 5'-ADP, which is parallel to that for the rate of hydrolysis by ATPase in biomembranes.[211,212]

To date, there are only a few reports that describe the use of BLMs in obtaining membrane potentials as analytical signals. To the best of our knowledge, the first potentiometric BLM sensor was developed by our group[213] by exploiting the natural
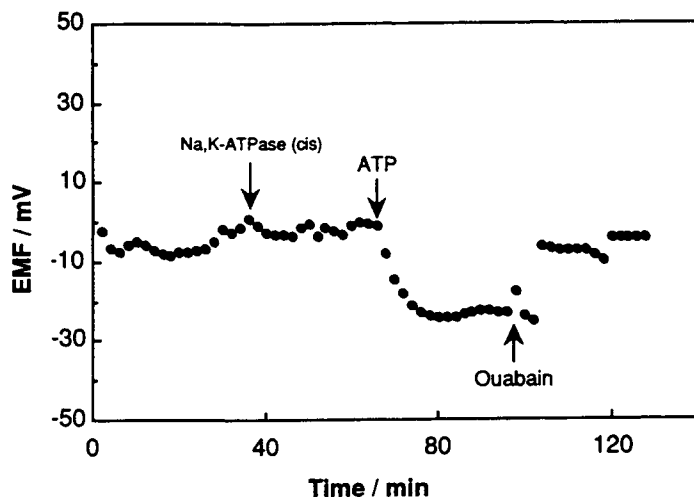


*Figure 32.* Time course of generation of 5'-ATP-induced membrane potential and disappearance of the membrane potential by adding a specific inhibitor ouabain for a single preparation of $Na^+,K^+$-ATPase-based BLM. 5'-ATP was injected into the *cis* side solution (final concentration: 10 mM) and ouabain (DMSO solution) into the *trans* side solution (final concentration: 1 mM) (reprinted with permission from *Anal. Chim. Acta* **1993**, *281*, 583. Copyright 1993 Elsevier Science Ltd.).

ionophore valinomycin incorporated into BLMs obtained with the folding method. This shows the potentiality of bioreceptors for designing potentiometric BLM sensors.

### Lasalocid-A-Based Uphill Transport Membrane

Lasalocid A is one of the naturally occurring ionophoric antibiotics capable of transporting metal cations,[214,215] metal complexes,[215,216] and organic cations such as (protonated) biogenic amines[217–221] across bilayer and liquid membranes. The crystal structure of the 1:1 complex of dissociated lasalocid and protonated amine shows that the lasalocid anion binds the ammonium cation via three N–H····O hydrogen bonds.[222] An uphill transport liquid membrane for the neurotransmitter dopamine (**38**) using lasalocid A was designed and fabricated; complete transfer (100%) of dopamine from the feed to receiving solution was achieved by this membrane.[223]

An uphill transport membrane system for dopamine in which lasalocid ($pK_a$ = 3.7) was dissolved in $o$-dichlorobenzene is shown in Figure 33. The driving force for transporting dopamine against its concentration gradient is provided by a concentration gradient of $H^+$ in a counter transport mode. At the feed solution interface, an electroneutral complex between protonated dopamine cation and dissociated lasalocid anion is formed and diffuses to the receiving solution interface, where the protonated dopamine is released into the acidic receiving solution. The protonated lasalocid diffuses back to the feed solution interface. Thus, energy conversion proceeds in a 1:1 counter transport.

An important feature of the present system is concentration of dopamine based on the feed/receiving volume effect. According to a theoretical model,[206] enhancement of the concentrations of analytes can be achieved most efficiently by a
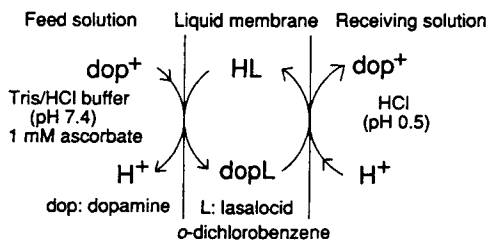


**Figure 33.** Principle of proton-driven uphill transport for dopamine under a counter-transport mode. The concentration of the carrier lasalocid A in $o$-dichlorobenzene was 0.1 M. The feed phase (100 mL) was 10 mM Tris-HCl buffer solution (pH 7.4) containing 1 mM ascorbic acid. The receiving phase (0.5–2.0 mL) was a hydrochloric acid solution (pH 0.5–3.0). The initial dopamine concentration in the feed solution was in the range from $1.00 \times 10^{-5}$ to $1.00 \times 10^{-3}$ M (reprinted with permission from *Anal. Sci.* **1996**, *12*, 333. Copyright 1996 The Japan Society for Analytical Chemistry).

countertransport mode as used in the present system. The uphill transport of
dopamine was carried out with two kinds of transport cells, i.e., a thin layer cell
and a nylon capsule system (Figure 34). The former utilizes a small inner space
between two liquid membranes as a receiving compartment and the latter a small
inner space of a nylon capsule prepared by interfacial polymerization. Concentra-
tions of dopamine transported into the receiving solution were determined in the
receiving compartment by cyclic voltammetry or HPLC after sampling a small
volume of the receiving solution.

Table 9 gives the concentrating factors for dopamine as a function of the volume
of the receiving solutions. It can be seen that the smaller the volume of the receiving
solution, the larger the concentrating factor for dopamine. The concentrating factor
obtained with the thin-layer-type cell was nearly equal to the ratio of the volumes
for the feed to receiving solutions, in accordance with theoretical expectation.[206]
Although no complete transfer of dopamine was attained even after transport for
16 h with the nylon-capsule-type cell, concentrating factors up to $2.8 \times 10^2$ were
obtained with a nylon capsule having a 20-µL-volume receiving solution. The
transport selectivity for the five amines tested was found to be: dopamine (38) >>
(R)-(–)-noradrenaline [(R)-(–)-39] > (R)-(–)-phenylephrine [(R)-(–)-96] (RS)-ad-
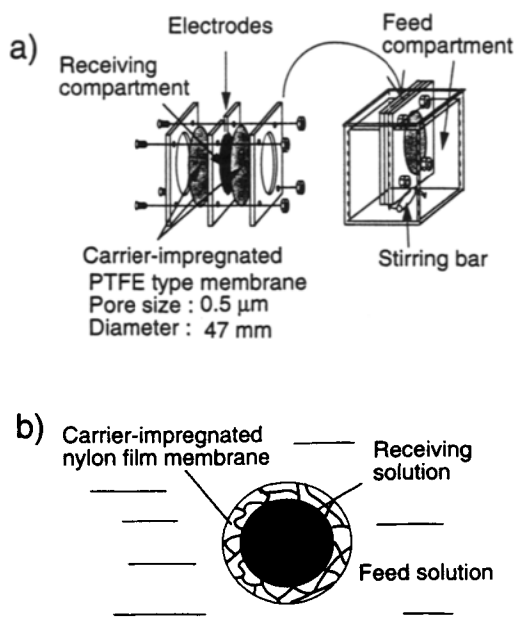


**Figure 34.** Structures for (a) thin-layer-type and (b) nylon capsule-type transport cells
(reprinted with permission from *Anal. Sci.* **1996**, *12*, 332. Copyright 1996 The Japan
Society for Analytical Chemistry).

***Table 9.*** Concentrating Factors for Dopamine (**38**) with the Uphill Transport System[223]

| Volume of Feed Solutions[a,b] (mL) | Volume of Receiving Solutions[c] (μL) | Concentration of **38** in Receiving Solutions (M) | Concentrating Factor[h] |
|---|---|---|---|
| $1.00 \times 10^2$ | $2.00 \times 10^{3\,d}$ | $4.90 \times 10^{-4\,f}$ | $4.90 \times 10$ |
| $1.00 \times 10^2$ | $1.00 \times 10^{3\,d}$ | $9.60 \times 10^{-4\,f}$ | $9.60 \times 10$ |
| $1.00 \times 10^2$ | $5.00 \times 10^{2\,d}$ | $1.96 \times 10^{-3\,f}$ | $1.96 \times 10^2$ |
| $1.0 \times 10$ | $2.0 \times 10^{\,e}$ | $2.8 \times 10^{-3\,g}$ | $2.8 \times 10^2$ |

*Notes:* [a]10 mM Tris-HCl buffer solution (pH 7.4) containing 1 mM ascorbate.

[b]The initial concentration of **38** prior to starting transport was $1.00 \times 10^{-5}$ M.

[c]pH 0.5 with hydrochloric acid.

[d]Transport with a thin layer cell.

[e]Transport with a nylon capsule.

[f]The equilibrium concentration was determined by HPLC.

[g]Determined by HPLC after transport time of 16 h.

[h]Defined as the equilibrium concentration of **38** in the receiving solution relative to the initial concentration in the feed solution prior to starting transport.

renaline [(*RS*)-**40**] > L-DOPA (*L*-**97**). The selectivity obtained here is in accordance with the results of Kinsel et al.[217,218] who observed that the rate of lasalocid A-mediated facilitated transport across a bilayer membrane decreases in the order of **38** > (*R*)-(−)-**96** > (*RS*)-**40**. No increase in the L-**97** concentration by the present uphill transport system was observed, probably because L-**97** existed mainly in the zwitterionic form at the experimental pH[224] and was not capable of forming an electroneutral complex with lasalocid A.

## Double-Carrier Membrane

The inherent function of $Na^+,K^+$-ATPase in biological membranes is the generation of a $Na^+$ gradient across the cell membrane and its maintenance using the energy of the hydrolysis of 5′-ATP, providing a constant driving force for $Na^+$-driven active transport systems. The energy conversion proceeds by countertransport or symport (secondary active transport). Accumulation of the cotransported $Na^+$ ions, which leads to a drop of the concentration gradient of $Na^+$ ions, is restored by $Na^+,K^+$-ATPase that pumps $Na^+$ out again. This function of $Na^+,K^+$-ATPase maintains high efficiency of secondary active transport.

A double-carrier membrane system that mimics, in principle, the function of $Na^+,K^+$-ATPase in biological membranes was developed, although chemical compounds involved are completely different (Figure 35).[225] The double-carrier system utilizes dicylohexyl-18-crown-6 (**93**) and trioctylamine (**95**) for enhanced transport of $K^+$ ions from the feed to the receiving solution using picrate ion (pic⁻) as the pumping ion. The carrier **93** is for uphill transport of $K^+$ using a concentration
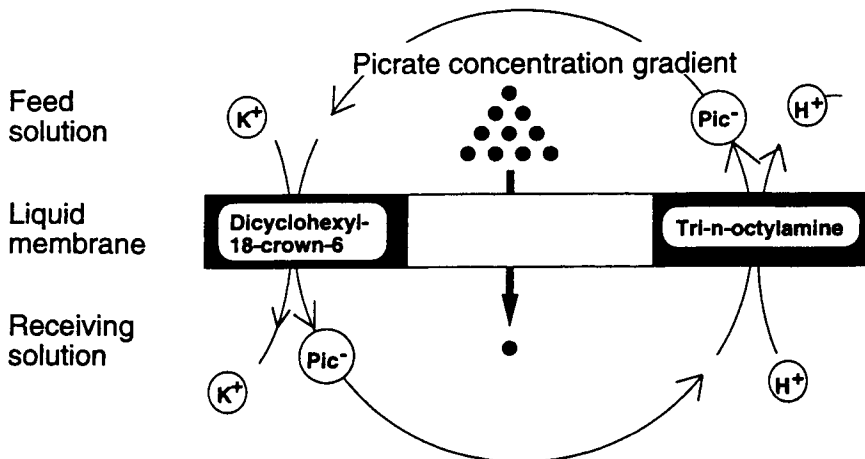
**Figure 35.** A double carrier membrane system for enhanced uphill transport of K⁺ ions.[225]

gradient of pic⁻ ions. The other carrier **95** is used to pump the cotransported pic⁻ from the receiving solution back to the feed solution using H⁺ as the pumping ion. The time course of uphill transport of K⁺ ions with the double-carrier system is shown in Figure 36. For comparison, uphill transport of K⁺ by a conventional symport system is also shown. The concentration of K⁺ ions in the receiving solution after transport of 23 h in the double-carrier system is 9 times larger than
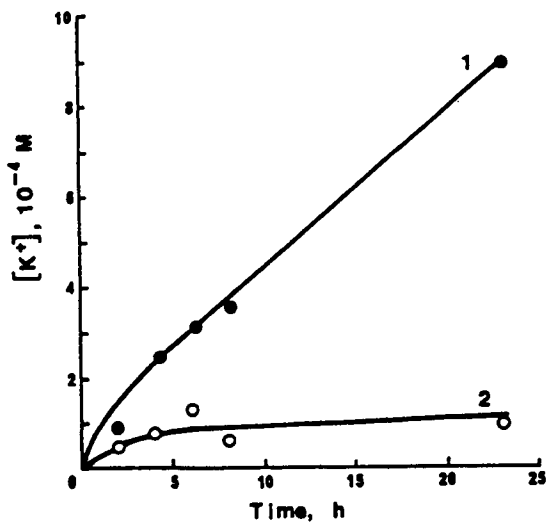


**Figure 36.** Uphill transport of K⁺ ions as a function of time with (1) double carrier membrane system and (2) a symport system (reprinted with permission from *Anal. Chem.* **1988**, *60*, 2302. Copyright 1993 American Chemical Society).

that in the simple symport system. This demonstrates that the double-carrier approach is useful for enhancing the efficiency of uphill transport. The double-carrier approach is totally different from the enzymatic process of $Na^+,K^+$-ATPase in biological membranes; the present system utilizes only gradient pumping, while $Na^+,K^+$-ATPase is a reaction pumping system. However, the role of the second carrier **95** is, in principle, the same as that of the ATPase in the sense that the concentration gradient of pumping ions is restored by action of the second carrier.

### 3.3. Chemical Sensing Based on Calmodulin/Peptide Interaction

Calmodulin (CaM; 148 amino acid residues, 16.7 kDa) is the ubiquitous $Ca^{2+}$ binding protein which serves as a multifunctional $Ca^{2+}$ sensor in a variety of cellular processes.[1] CaM has four $Ca^{2+}$ binding sites within two helix-loop-helix (EF-hand) motifs, organized in two structurally similar globular domains.[226] One of the EF-hands has high-affinity sites with binding constants for $Ca^{2+}$ of $10^7 M^{-1}$ and the other has low-affinity sites with binding constants of $10^6 M^{-1}$.[227] After the selective recognition of $Ca^{2+}$ by CaM, in many cases, they interact with target enzymes and proteins, while the $Ca^{2+}$-free forms do not bind the targets. Conformational transitions of CaM induced by $Ca^{2+}$ enable binding with the target proteins and lead to their activation and regulation. Mimicking the molecular mechanisms of such a fine tuning of protein conformation is important not only for understanding the cellular processes of $Ca^{2+}$-mediated signal transmission but also for the development of ion-selective sensors that enable evaluation of chemical selectivity of the $Ca^{2+}$-dependent on/off switch for cellular processes.

A sensing system for $Ca^{2+}$ was developed by using CaM as primary receptor and a synthetic peptide M13 as target protein.[228] The peptide M13 consists of 26 residues of amino acids comprising a CaM binding domain of myosin light-chain kinase (MLCK). In Figure 37 is shown the principle of the present sensing system. The target peptide M13 is immobilized in the dextran matrix attached to the surface of a gold film. The immobilization of M13 is achieved by coupling the activated carboxylic groups of the dextran matrix with primary amines of the target peptide. Sample solutions containing CaM and $Ca^{2+}$ are allowed to flow over the surface of the target protein (M13)-immobilized dextran matrix. The CaM-$Ca^{2+}$-target protein interaction and resulting formation of a ternary complex $Ca^{2+}$-CaM-target protein on/in dextran matrix is detected by means of surface plasmon resonance (SPR). By doing so, a $Ca^{2+}$ ion sensing system that matches a physiological signal transduction is designed.

The $Ca^{2+}$-induced change in SPR signals was defined as a difference of the two SPR signals; one is measured after injection of $Ca^{2+}$ ions and the other is successively measured after injection of a running buffer containing EGTA. The dependence of the SPR signals on the concentration of free $Ca^{2+}$ is shown in Figure 38. The SPR signal was found to increase with the concentration of $Ca^{2+}$, due to the formation of the $Ca^{2+}$-CaM-M13 ternary complex on/in the dextran matrix. $Ca^{2+}$-
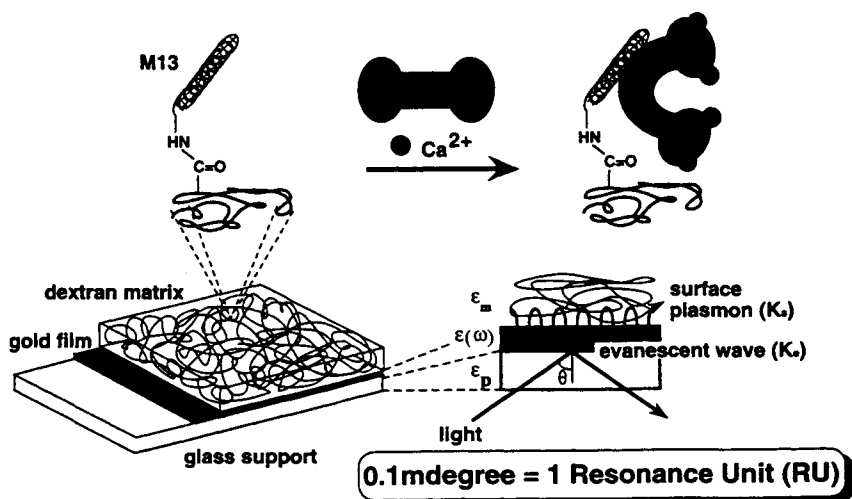
**Figure 37.** Principle of an optical $Ca^{2+}$ ion sensor based on a calmodulin (CaM)-mediated $Ca^{2+}$ signaling pathway and surface plasmon resonance.[228]

dependent SPR signals were obtained in the concentration range of $Ca^{2+}$ from 3.2 $\times 10^{-8}$ to $1.1 \times 10^{-5}$ M, which matches the concentration of $Ca^{2+}$ under physiological conditions. The detection limit for free $Ca^{2+}$ of the present sensing system is 1.6 $\times 10^{-8}$ M (S/N = 3). On the other hand, no changes in the SPR signal were induced by $Mg^{2+}$, $K^+$, and $Li^+$ at concentrations as high as $1.0 \times 10^{-1}$ M. The CaM is known to bind not only $Ca^{2+}$ but also $Mg^{2+}$ ions, the essential difference being that $Mg^{2+}$ is incapable of inducing a conformational change of CaM that is required for the successive activation of the target molecules. Thus, the present sensing system shows "all or none" type discrimination of $Ca^{2+}$ from $Mg^{2+}$ based on a fine tuning of CaM conformation. Among the alkaline earth metal ions examined, only $Sr^{2+}$ at $5.1 \times 10^{-4}$ M gave a response that indicates formation of a $Sr^{2+}$-CaM-M13 ternary complex, showing the potency of $Sr^{2+}$ ions to switch on the CaM-mediated biological processes.

The present sensing system utilized a $Ca^{2+}$ signaling pathway by CaM and its target peptide M13 for detecting $Ca^{2+}$. The unique feature of this approach is the use of a target protein to which a $Ca^{2+}$–CaM complex is bound reversibly. The ternary complex thus formed has a mass much larger than the immobilized M13 or $Ca^{2+}$ ions in solution, enabling sensitive detection of small ions or molecules like $Ca^{2+}$ by the SPR method. This approach can be applied to other receptor signaling pathways, such as hormonal activation of enzymes for evaluating the chemical selectivity of the biological process based on a physiologically matched measure rather than the so-called binding assay. The development of highly sensitive and
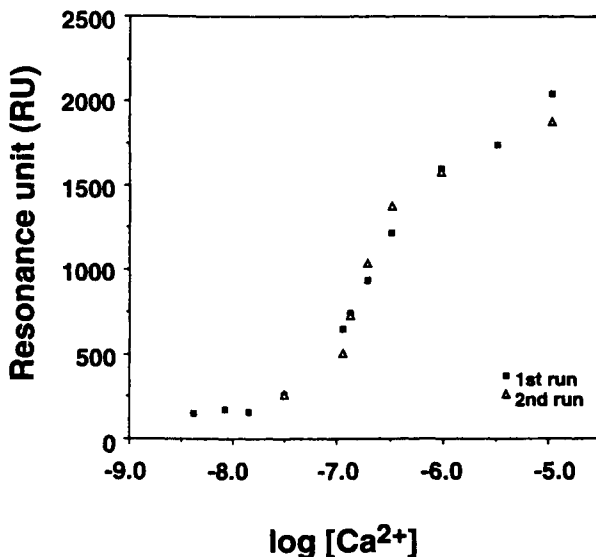
**Figure 38.** The SPR signal intensities as a function of concentration of free $Ca^{2+}$ ions in 150 mM NaCl containing 0.5 mM EGTA and 10 mM HEPES buffer (pH 7.5).[228]

selective sensing systems that will enable detecting bioactive small molecules by the SPR method is thus promising.

## 4. CONCLUDING REMARKS

The advance of host–guest chemistry and its recent evolution to supramolecular chemistry has made significant contributions to the development of new analytical reagents and systems. In fact, it was only several years after the first report of crown ethers by Pedersen[229,230] that analytical use of these compounds began in areas such as solvent extraction, chromatography, and potentiometric sensing with liquid-membrane-type ISEs.[231,232] In this chapter, our recent efforts in the development of new types of sensing membranes that are based on supramolecular functions of biomimetic and biological receptors at membranes have been described.

With regard to biomimetic approaches, this chapter has focused on multiple hydrogen bonding and cavity inclusion for discrimination of polar or nonpolar moieties of guests. For analysis and separation involving homogeneous solutions or bulk-to-bulk extraction, these modes of discrimination have been extensively utilized. However, their use for chemical sensing involving molecular recognition at membrane surfaces has been quite limited. Detailed studies of biomimetic systems, including the specific observation of the membrane boundary region, have

shown that the three chemical principles described in this chapter, i.e. (1) guest-induced changes in membrane potential, (2) guest-induced changes in membrane permeability, and (3) active transport of guests, can be major principles of chemical sensing at membrane surfaces.

With regard to biological approaches, the development of analytical systems based on biological functions is now fairly established by utilizing enzymes, antibodies, receptors, organs, or whole cells in such bioanalytical methods as affinity chromatography, bioassays, and biosensors. Compared to these general approaches, those described in this chapter are featured by the use of recognition modes other than simple binding functions of biomolecules; more sophisticated functions such as transmembrane signaling, coupled active transport, and ternary complex formation have been exploited for sensing of target substances in an amplified or magnified manner.

High versatility of biomimetic systems and sophisticated functions of biological systems should be regarded as complementary for sensing of target chemical substances, and various new sensing systems are expected to be developed by taking advantage of either of these systems. Furthermore, development of hybrid systems by combination of biomimetic and biological systems would also be an interesting future prospect.

# REFERENCES

1. Alberts, B.; Bray, D.; Lewis, J.; Raff, M.; Roberts, K.; Watson, J. D. *Molecular Biology of the Cell*, 3rd ed.; Garland Publishing: New York, 1994.
2. Branden, C.; Tooze, J. *Introduction to Protein Structure*; Garland Publishing: New York, 1991.
3. Cram, D. J.; Cram, J. M. *Science* **1974**, *183*, 803–809.
4. Pedersen, C. J. *Angew. Chem. Int. Ed. Engl.* **1988**, *27*, 1021–1027.
5. Cram, D. J. *Angew. Chem. Int. Ed. Engl.* **1988**, *27*, 1009–1020.
6. Lehn, J.-M. *Angew. Chem. Int. Ed. Engl.* **1988**, *27*, 89–112.
7. Vögtle, F. *Supramolecular Chemistry, an Introduction*; John Wiley & Sons: Chichester, UK, 1991.
8. *Host–Guest Molecular Interactions: from Chemistry to Biology*; Chadwick, D. J., Widdows, K., Eds.; Ciba Foundation Symposium 158; John Wiley & Sons: Chichester, UK, 1991.
9. *Advances in Supramolecular Chemistry*; Gokel, G. W., Ed.; JAI Press: Greenwich, CT, 1990, 1992, 1993, Vols. 1–3.
10. *Comprehensive Supramolecular Chemistry*; Atwood, J. L., Davies, J. E. D., MacNicol, D. D., Vögtle, F., Eds.; Elsevier Science: Oxford, UK, 1996, Vols. 1–11.
11. *CRC Handbook of Ion-Selective Electrodes: Selectivity Coefficients*; Umezawa, Y., Ed.; CRC Press: Boca Raton, FL, 1990.
12. Ammann, D.; Morf, W. E.; Anker, P.; Meier, P. C.; Pretsch, E.; Simon, W. *Ion-Selective Electrode Rev.* **1983**, *5*, 3–92.
13. Kimura, K.; Shono, T. In *Crown Ethers and Analogous Compounds*; Hiraoka, M., Ed.; Studies in Organic Chemistry 45; Elsevier Science: Amsterdam, 1992, Chapter 4, pp. 198–264.
14. Odashima, K.; Koga, K. In *Molecular Recognition: Receptors for Molecular Guests*; Vögtle, F., Ed.; Comprehensive Supramolecular Chemistry 2; Elsevier Science: Oxford, UK, 1996, Chapter 5, pp. 143–194.
15. Brzózka, Z. In *Supramolecular Technology*; Reinhoudt, D. N., Ed.; Comprehensive Supramolecular Chemistry 10; Elsevier Science: Oxford, UK, 1996, Chapter 8, pp. 187–212.

16. Lockhart, J. C. In *Molecular Recognition: Receptors for Cationic Guests*; Gokel, G. W., Ed.; Comprehensive Supramolecular Chemistry 1; Elsevier Science: Oxford, UK, 1996, Chapter 16, pp. 605–634.

17. Eisenman, G. In *Ion-Selective Electrodes*; Durst, R. A., Ed.; Special Publication 314; National Bureau of Standards: Washington, DC, 1969, Chapter 1, pp. 1–56.

18. Buck, R. P. In *Ion-Selective Electrodes in Analytical Chemistry*; Freiser, H., Ed.; Plenum Press: New York, 1978, Chapter 1, pp. 1–141.

19. Morf, W. E. *The Principles of Ion-Selective Electrodes and of Membrane Transport*; Elsevier Scientific Publishing: Amsterdam, 1981.

20. Lindner, E.; Tóth, K.; Pungor, E. *Dynamic Characteristics of Ion-Selective Electrodes*; CRC Press: Boca Raton, FL, 1988.

21. Umezawa, Y.; Kataoka, M.; Takami, W.; Kimura, E.; Koike, T.; Nada, H. *Anal. Chem.* **1988**, *60*, 2392–2396.

22. Kataoka, M.; Naganawa, R.; Odashima, K.; Umezawa, Y.; Kimura, E.; Koike, T. *Anal. Lett.* **1989**, *22*, 1089–1105.

23. Naganawa, R.; Kataoka, M.; Odashima, K.; Umezawa, Y.; Kimura, E.; Koike, T. *Bunseki Kagaku* **1990**, *39*, 671–676.

24. Naganawa, R.; Radecka, H.; Kataoka, M.; Tohda, K.; Odashima, K.; Umezawa, Y.; Kimura, E.; Koike, T. *Electroanalysis* **1993**, *5*, 731–738.

25. Odashima, K.; Naganawa, R.; Radecka, H.; Kataoka, M.; Kimura, E.; Koike, T.; Tohda, K.; Tange, M.; Furuta, H.; Sessler, J. L.; Yagi, K.; Umezawa, Y. *Supramol. Chem.* **1994**, *4*, 101–113.

26. Tohda, K.; Tange, M.; Odashima, K.; Umezawa, Y.; Furuta, H.; Sessler, J. L. *Anal. Chem.* **1992**, *64*, 960–964.

27. Tohda, K.; Naganawa, R.; Lin, X. M.; Tange, M.; Umezawa, K.; Odashima, K.; Umezawa, Y.; Furuta, H.; Sessler, J. L. *Sensors and Actuators B* **1993**, *14*, 669–672.

28. Amemiya, S.; Bühlmann, P.; Tohda, K.; Umezawa, Y. *Anal. Chim. Acta* **1997**, *341*, 129–139.

29. Nishizawa, S.; Bühlmann, P.; Iwao, M.; Umezawa, Y. *Tetrahedron Lett.* **1995**, *36*, 6483–6486.

30. Odashima, K.; Yagi, K.; Tohda, K.; Umezawa, Y. *Anal. Chem.* **1993**, *65*, 1074–1083.

31. Odashima, K.; Hashimoto, H.; Umezawa, Y. *Mikrochim. Acta* **1994**, *113*, 223–238.

32. Sugawara, M.; Kojima, K.; Sazawa, H.; Umezawa, Y. *Anal. Chem.* **1987**, *59*, 2842–2846.

33. Sugawara, M.; Kataoka, M.; Odashima, K.; Umezawa, Y. *Thin Solid Films* **1989**, *180*, 129–133.

34. Nagase, S.; Kataoka, M.; Naganawa, R.; Komatsu, R.; Odashima, K.; Umezawa, Y. *Anal. Chem.* **1990**, *62*, 1252–1259.

35. Odashima, K.; Kotato, M.; Sugawara, M.; Umezawa, Y. *Anal. Chem.* **1993**, *65*, 927–936.

36. Yagi, K.; Khoo, S. B.; Sugawara, M.; Sakaki, T.; Shinkai, S.; Odashima, K.; Umezawa, Y. *J. Electroanal. Chem.* **1996**, *401*, 65–79.

37. Tohda, K.; Amemiya, S.; Nagahora, S.; Tanaka, S.; Ohki, T.; Bühlmann, P.; Umezawa, Y. *Isr. J. Chem.*, in press.

38. Odashima, K.; Sugawara, M.; Umezawa, Y. In *Interfacial Design and Chemical Sensing*; Mallouk, T. E., Harrison, D. J., Eds.; ACS Symposium Series 561; American Chemical Society: Washington, D. C., 1994, Chapter 11, pp. 123–134.

39. Umezawa, K.; Lin, X.; Nishizawa, S.; Sugawara, M.; Umezawa, Y. *Anal. Chim. Acta* **1993**, *282*, 247–257.

40. Yoshiyagawa, S.; Tohda, K.; Umezawa, Y.; Hashimoto, S.; Kawasaki, M. *Anal. Sci.* **1993**, *9*, 715–718.

41. Tohda, K.; Umezawa, Y.; Yoshiyagawa, S.; Hashimoto, S.; Kawasaki, M. *Anal. Chem.* **1995**, *67*, 570–577.

42. Bühlmann, P.; Yajima, S.; Tohda, K.; Umezawa, K.; Nishizawa, S.; Umezawa, Y. *Electroanalysis* **1995**, *7*, 811–816.

43. Bühlmann, P.; Yajima, S.; Tohda, K.; Umezawa, Y. *Electrochim. Acta* **1995**, *40*, 3021–3027.

44. Naganawa, R.; Odashima, K.; Umezawa, Y.; Kimura, E.; Koike, T. Unpublished results.

45. Seel, C.; de Mendoza, J. In *Molecular Recognition: Receptors for Molecular Guests*; Vögtle, F., Ed.; Comprehensive Supramolecular Chemistry 2; Elsevier Science: Oxford, UK, 1996, Chapter 5, pp. 143–194.

46. Park, C. H.; Simmons, H. E. *J. Am. Chem. Soc.* **1968**, *90*, 2431–2432.

47. Potvin, P. G.; Lehn, J. M. In *Synthesis of Macrocycles. The Design of Selective Complexing Agents*; Izatt, R. M., Christensen, J. J., Eds.; Progress in Macrocyclic Chemistry 3; John Wiley & Sons: New York, 1987, Chapter 4, pp. 167–239.

48. Kimura, E. In *Crown Ethers and Analogous Compounds*; Hiraoka, M., Ed.; Studies in Organic Chemistry 45; Elsevier: Amsterdam, 1992, Chapter 8, pp. 381–478.

49. Kimura, E. *Tetrahedron* **1992**, *48*, 6175–6217.

50. Bakker, E.; Bühlmann, P.; Pretsch, E., submitted for publication.

51. Hamilton, A. D. In *Advances in Supramolecular Chemistry*; Gokel, G. W., Ed.; JAI Press: Greenwich, CT, 1990, Vol. 1, pp. 1–64.

52. Glazier, S. A.; Arnold, M. A. *Anal. Chem.* **1991**, *63*, 754–759.

53. Carey, C. M.; Riggan, W. B. *Anal. Chem.* **1994**, *66*, 3587–3591.

54. Raposo, C.; Almaraz, M.; Martin, M.; Weinrich, V.; Mussons, L.; Alcazar, V.; Caballero, C.; Moran, J. R. *Chem. Lett.* **1995**, 759–760.

55. Raposo, C.; Pérez, N.; Almaraz, M.; Mussons, L.; Caballero, C.; Moran, J. R. *Tetrahedron Lett.* **1995**, *36*, 3255–3258.

56. Rudkevich, D. M.; Verboom, W.; Brzóka, Z.; Palys, M. J.; Stauthamer, W. P. R. V.; van Hummel, G. J.; Franken, S. M.; Harkema, S.; Engbersen, J. F. J.; Reinhoudt, D. N. *J. Am. Chem. Soc.* **1994**, *116*, 4341–4351.

57. Rudkevich, D. M.; Verboom, W.; Reinhoudt, D. N. *J. Org. Chem.* **1994**, *59*, 3683–3686.

58. Hamann, B. C.; Branda, N. R.; Rebek, J., Jr. *Tetrahedron Lett.* **1993**, *34*, 6837–6840.

59. Fan, E.; Van Arman, S. A.; Kincaid, S.; Hamilton, A. D. *J. Am. Chem. Soc.* **1993**, *115*, 369–370.

60. Kelly, T. R.; Kim, M. H. *J. Am. Chem. Soc.* **1994**, *116*, 7072–7080.

61. Bühlmann, P.; Nishizawa, S.; Xiao, K. P.; Umezawa, Y. *Tetrahedron* **1997**, *53*, 1647–1654.

62. Nishizawa, S.; Bühlmann, P.; Xiao, K. P.; Umezawa, Y. Submitted for publication.

63. Xiao, K. P.; Bühlmann, P.; Nishizawa, S.; Amemiya, S.; Umezawa, Y. *Anal. Chem.* **1997**, *69*, 1038–1044.

64. Dixon, R. P.; Geib, S. J.; Hamilton, A. D. *J. Am. Chem. Soc.* **1992**, *114*, 365–366.

65. Bordwell, F. G.; Algrim, D. J.; Harrelson, J. A., Jr. *J. Am. Chem. Soc.* **1988**, *110*, 5903–5904.

66. Wilcox, C. S.; Kim, E.-I.; Romano, D.; Kuo, L. H.; Burt, A. L.; Curran, D. P. *Tetrahedron* **1995**, *51*, 621–634.

67. Scheerder, J.; Engbersen, J. F. J.; Casnati, A.; Ungaro, R.; Reinhoudt, D. N. *J. Org. Chem.* **1995**, *60*, 6448–6454.

68. Blades, A.; Ho, Y.; Kebarle, P. *J. Phys. Chem.* **1996**, *100*, 2443–2446.

69. Blades, A. T.; Ho, Y.; Kebarle, P. *J. Am. Chem. Soc.* **1996**, *118*, 196–201.

70. Blades, A. T.; Klassen, J. S.; Kebarle, P. *J. Am. Chem. Soc.* **1995**, *117*, 10563–10571.

71. Arshadi, M.; Yamdagni, R.; Kebarle, P. *J. Phys. Chem.* **1970**, *74*, 1475–1482.

72. Taft, R. W.; Bordwell, F. G. *Acc. Chem. Res.* **1988**, *21*, 463–469.

73. Fluri, K.; Koudelka, J.; Simon, W. *Helv. Chim. Acta* **1992**, *75*, 1012–1022.

74. Rothmaier, M.; Schaller, U.; Morf, W. E.; Pretsch, E. *Anal. Chim. Acta* **1996**, *327*, 17–28.

75. Brown, D. V.; Chaniotakis, N. A.; Lee, I. H.; Ma, S. C.; Park, S. B.; Meyerhoff, M. E.; Nick, R. J.; Groves, J. T. *Electroanalysis* **1989**, *1*, 477–484.

76. Park, S. B.; Matuszewski, W.; Meyerhoff, M. E.; Liu, Y. H.; Kadish, K. M. *Electroanalysis* **1991**, *3*, 909–916.

77. Beer, P. D.; Szemes, F. *J. Chem. Soc., Chem. Commun.* **1995**, 2245–2247.

78. Scheerder, J.; Fochi, M.; Engbersen, J. F. J.; Reinhoudt, D. N. *J. Org. Chem.* **1994**, *59*, 7815–7820.

79. Furuta, H.; Magda, D.; Sessler, J. L. *J. Am. Chem. Soc.* **1991**, *113*, 978–985.

80. Fersht, A. *Enzyme Structure and Mechanism*, 2nd ed.; Freeman: New York, 1985.

81. Schneider, H.-J. *Chem. Rev.* **1994**, *94*, 227–234.
82. Amemiya, S.; Bühlmann, P.; Umezawa, Y. *Chem. Comm.* In press.
83. Bühlmann, P.; Badertscher, M.; Simon, W. *Tetrahedron* **1993**, *49*, 595–598.
84. Bühlmann, P.; Simon, W. *Tetrahedron* **1993**, *49*, 7627–7636.
85. Bell, T. W.; Hou, Z.; Luo, Y.; Drew, M. G. B.; Chapoteau, E.; Czech, B. P.; Kumar, A. *Science* **1995**, *269*, 671–674.
86. Beckles, D. L.; Maioriello, J.; Santora, V. J.; Bell, T. W.; Chapoteau, E.; Czech, B. P.; Kumar, A. *Tetrahedron* **1995**, *51*, 363–376.
87. Taguchi, K.; Ariga, K.; Kunitake, T. *Chem. Lett.* **1995**, 701–702, and references therein.
88. Gutsche, C. D. *Calixarenes*; Monographs in Supramolecular Chemistry 1; The Royal Society of Chemistry: Cambridge, UK, 1989.
89. *Calixarenes: A Versatile Class of Macrocyclic Compounds*; Vicens, J., Böhmer, V., Eds.; Topics in Inclusion Science 3; Kluwer Academic Publishers: Dordrecht, The Netherlands, 1991.
90. Shinkai, S. *Tetrahedron* **1993**, *49*, 8933–8968.
91. Shinkai, S. In *Advances in Supramolecular Chemistry*; Gokel, G. W., Ed.; JAI Press: Greenwich, CT, 1993, Vol. 3, pp. 97–130.
92. Böhmer, V. *Angew. Chem. Int. Ed. Engl.* **1995**, *34*, 713–745.
93. McKervey, M. A.; Schwing-Weill, M.-J.; Arnaud-Neu, F. In *Molecular Recognition: Receptors for Cationic Guests*; Gokel, G. W., Ed.; Comprehensive Supramolecular Chemistry 1; Elsevier Science: Oxford, UK, 1996, Chapter 15, pp. 537–603.
94. Pochini, A.; Ungaro, R. In *Molecular Recognition: Receptors for Molecular Guests*; Vögtle, F., Ed.; Comprehensive Supramolecular Chemistry 2; Elsevier Science: Oxford, UK, 1996, Chapter 4, pp. 103–142.
95. Diamond, D. J. *Inclusion Phenom.* **1994**, *19*, 149–166.
96. O'Connor, K. M.; Arrigan, D. W. M.; Svehla, G. *Electroanalysis* **1995**, *7*, 205–215.
97. Diamond, D.; McKervey, M. A. *Chem. Soc. Rev.* **1996**, *25*, 15–24.
98. Sakaki, T.; Harada, T.; Deng, G.; Kawabata, H.; Kawahara, Y.; Shinkai, S. *J. Inclusion Phenom. Mol. Recognit. Chem.* **1992**, *14*, 285–302.
99. Sakaki, T.; Harada, T.; Kawahara, Y.; Shinkai, S. *J. Inclusion Phenom. Mol. Recognit. Chem.* **1994**, *17*, 377–392.
100. Yamamoto, H.; Shinkai, S. *Chem. Lett.* **1994**, 1115–1118.
101. Umezawa, K.; Umezawa, Y. In *CRC Handbook of Ion-Selective Electrodes: Selectivity Coefficients*; Umezawa, Y., Ed.; CRC Press: Boca Raton, FL, 1990, pp. 3–9.
102. Yagi, K.; Tohda, K.; Odashima, K.; Umezawa, Y. Unpublished results.
103. Chan, W. H.; Shiu, K. K.; Gu, X. H. *Analyst* **1993**, *118*, 863–867.
104. Chan, W. H.; Cai, P. X.; Gu, X. H. *Analyst* **1994**, *119*, 1853–1857.
105. Chan, W. H.; Yuan, R. *Analyst* **1995**, *120*, 1055–1058.
106. Tóth, K.; Lan, B. T. T.; Jeney, J.; Horváth, M.; Bitter, I.; Grun, A.; Agai, B.; Toke, L. *Talanta* **1994**, *41*, 1041–9.
107. Chan, W. H.; Lee, A. W. M.; Wang, K. *Analyst* **1994**, *119*, 2809–2812.
108. Chan, W. H.; Lee, A. W. M.; Lee, C. M.; Yau, K. W.; Wang, K. *Analyst* **1995**, *120*, 1963–1967.
109. Chan, W. H.; Lee, A. W. M.; Kwong, D. W. J.; Tam, W. L.; Wang, K. *Analyst* **1996**, *121*, 531–534.
110. Arnaud-Neu, F.; Collins, E. M.; Deasy, M.; Ferguson, G.; Harris, S. J.; Kaitner, B.; Lough, A. J.; McKervey, M. A.; Marques, E.; Ruhl, B. L.; Schwing-Weill, M. J.; Seward, E. M. *J. Am. Chem. Soc.* **1989**, *111*, 8681–8691.
111. Chang, S.-K.; Cho, I. *J. Chem. Soc., Perkin Trans. 1* **1986**, 211–214.
112. Cadogan, A. M.; Diamond, D.; Smyth, M. R.; Deasy, M.; McKervey, M. A.; Harris, S. J. *Analyst* **1989**, *114*, 1551–1554.
113. Cadogan, A.; Diamond, D.; Smyth, M. R.; Svehla, G.; McKervey, M. A.; Seward, E. M.; Harris, S. J. *Analyst* **1990**, *115*, 1207–1210.
114. Cramer, F. *Einschlußverbindungen*; Springer-Verlag: Berlin, 1954.

115. Bender, M. L.; Komiyama, M. *Cyclodextrin Chemistry. Reactivity and Structure*; Concepts in Organic Chemistry 6; Springer-Verlag: Berlin, 1978.

116. Szejtli, J. *Cyclodextrins and Their Inclusion Complexes*; Akadémiai Kiadó: Budapest, 1982.

117. Szejtli, J. *Cyclodextrin Technology*; Topics in Inclusion Science 1; Kluwer Academic Publishers: Dordrecht, The Netherlands, 1988.

118. *Cyclodextrins*; Szejtli, F., Osa, T., Eds.; Comprehensive Supramolecular Chemistry 3; Elsevier Science: Oxford, UK, 1996.

119. Snopek, J.; Smolková-Keulemansová, E.; Cserháti, T.; Gahm, K. H.; Stalcup, A. In *Cyclodextrins*; Szejtli, F., Osa, T., Eds.; Comprehensive Supramolecular Chemistry 3; Elsevier Science: Oxford, UK, 1996, Chapter 18, pp. 515–571.

120. Hinze, W. L.; Dai, F.; Frankewich, R. P.; Thimmaiah, K. N.; Szejtli, J. In *Cyclodextrins*; Szejtli, F., Osa, T., Eds.; Comprehensive Supramolecular Chemistry 3; Elsevier Science: Oxford, UK, 1996, Chapter 20, pp. 587–602.

121. Jicsinszky, L.; Fenyvesi, É.; Hashimoto, H.; Ueno, A. In *Cyclodextrins*; Szejtli, F., Osa, T., Eds.; Comprehensive Supramolecular Chemistry 3; Elsevier Science: Oxford, UK, 1996, Chapter 4, pp. 57–188.

122. Bates, P. S.; Kataky, R.; Parker, D. *J. Chem. Soc., Chem. Commun.* **1992**, 153–155.

123. Kataky, R.; Bates, P. S.; Parker, D. *Analyst* **1992**, *117*, 1313–1317.

124. Bates, P. S.; Kataky, R.; Parker, D. *J. Chem. Soc., Chem. Commun.* **1993**, 691–693.

125. Bates, P. S.; Kataky, R.; Parker, D. *Analyst* **1994**, *119*, 181–186.

126. Tagaki, W. *J. Jpn. Oil Chem. Soc. (Yukagaku.)* **1988**, *37*, 394–401.

127. Kawabata, Y.; Matsumoto, M.; Nakamura, T.; Tanaka, M.; Manda, E.; Takahashi, H.; Tamura, S.; Tagaki, W.; Nakahara, H.; Fukuda, K. *Thin Solid Films* **1988**, *159*, 353–358.

128. Taneva, S.; Ariga, K.; Okahata, Y.; Tagaki, W. *Langmuir* **1989**, *5*, 111–113.

129. Maeda, M.; Tsuzaki, Y.; Nakano, K.; Takagi, M. *J. Chem. Soc., Chem. Commun.* **1990**, 1529–1531.

130. Maeda, M.; Fujita, Y.; Nakano, K.; Takagi, M. *J. Chem. Soc., Chem. Commun.* **1991**, 1724–1725.

131. Maeda, M.; Mitsuhashi, Y.; Nakano, K.; Takagi, M. *Anal. Sci.* **1992**, *8*, 83–84.

132. Maeda, M.; Nakano, K.; Uchida, S.; Takagi, M. *Chem. Lett.* **1994**, 1805–1808.

133. Nakashima, N.; Taguchi, T.; Takada, Y.; Fujio, K.; Kunitake, M.; Manabe, O. *J. Chem. Soc., Chem. Commun.* **1991**, 232–233.

134. *Ion Channel Reconstitution*; Miller, C., Ed.; Plenum Press: New York, 1986.

135. Stein, W. D. *Channels, Carriers, and Pumps: An Introduction to Membrane Transport*; Academic Press: San Diego, CA, 1990.

136. Hille, B. *Ionic Channels of Excitable Membranes*; 2nd edn.; Sinauer Associates: Sunderland, MA, 1992.

137. Fujihira, M.; Araki, T. *Chem. Lett.* **1986**, 921–922.

138. Zhang, X.; Bard, A. J. *J. Am. Chem. Soc.* **1989**, *111*, 8098–8105.

139. Miller, C. J.; Bard, A. *J. Anal. Chem.* **1991**, *63*, 1707–1714.

140. Chang, H.; Bard, A. J. *Langmuir* **1991**, *7*, 1143–1153.

141. Gokel, G. W.; Murillo, O. *Acc. Chem. Res.* **1996**, *29*, 425–432.

142. Fyles, T. M.; van Straaten-Nijenhuis, W. F. In *Supramolecular Technology*; Reinhoudt, D. N., Ed.; Comprehensive Supramolecular Chemistry 10; Elsevier Science: Oxford, UK, 1996, Chapter 3, pp. 53–77.

143. Åkerfeldt, K. S.; Kienker, P. K.; Lear, J. D.; DeGrado, W. F. In *Supramolecular Technology*; Reinhoudt, D. N., Ed.; Comprehensive Supramolecular Chemistry 10; Elsevier Science: Oxford, UK, 1996, Chapter 22, pp. 659–686.

144. Lee, D. H.; Ghadiri, M. R. In *Templating, Self-assembly, and Self-organization*; Sauvage, J.-P., Hosseini, M. W., Eds.; Comprehensive Supramolecular Chemistry 9; Elsevier Science: Oxford, UK, 1996, Chapter 12, pp. 451–481.

145. Montal, M.; Montal, M. S.; Tomich, J. M. *Proc. Natl. Acad. Sci. USA* **1990**, *87*, 6929–6933.

146. Grove, A.; Tomich, J. M.; Montal, M. *Proc. Natl. Acad. Sci. USA* **1991**, *88*, 6418–6422.

147. Reddy, G. L.; Iwamoto, T.; Tomich, J. M.; Montal, M. *J. Biol. Chem.* **1993**, *268*, 14608–14615.

148. Grove, A.; Mutter, M.; Rivier, J. E.; Montal, M. *J. Am. Chem. Soc.* **1993**, *115*, 5919–5924.

149. Åkerfeldt, K. S.; Kim, R. M.; Camac, D.; Groves, J. T.; Lear, J. D.; DeGrado, W. F. *J. Am. Chem. Soc.* **1992**, *114*, 9656–9657.

150. Fyles, T. M.; Heberle, D.; van Straaten-Nijenhuis, W. F.; Zhou, X. *Supramol. Chem.* **1995**, *6*, 71–77.

151. Tanaka, Y.; Kobuke, Y.; Sokabe, M. *Angew. Chem. Int. Ed. Engl.* **1995**, *34*, 693–694.

152. Stankovic, C. J.; Heinemann, S. H.; Delfino, J. M.; Sigworth, F. J.; Schreiber, S. L. *Science* **1989**, *244*, 813–817.

153. Stankovic, C. J.; Heinemann, S. H.; Schreiber, S. L. *J. Am. Chem. Soc.* **1990**, *112*, 3702–3704.

154. *Cyclophanes*; Vögtle, F., Ed.; Topics in Current Chemistry 113, 115; Springer-Verlag: Berlin, 1983, Vols. 1, 2.

155. *Cyclophanes*; Keehn, P. M., Rosenfeld, S. M., Eds.; Organic Chemistry 45; Academic Press: New York, 1983, Vols. 1, 2.

156. Diederich, F. *Cyclophanes*; Monographs in Supramolecular Chemistry 2; The Royal Society of Chemistry: Cambridge, UK, 1991.

157. Vögtle, F. *Cyclophanes: Synthesis, Structures, and Reactions*; John Wiley & Sons: New York, 1993.

158. *Molecular Recognition: Receptors for Molecular Guests*; Vögtle, F., Ed.; Comprehensive Supramolecular Chemistry 2; Elsevier Science: Oxford, UK, 1996.

159. Odashima, K.; Itai, A.; Iitaka, Y.; Koga, K. *J. Am. Chem. Soc.* **1980**, *102*, 2504–2505.

160. Odashima, K.; Itai, A.; Iitaka, Y.; Koga, K. *J. Org. Chem.* **1985**, *50*, 4478–4484.

161. Odashima, K.; Soga, T.; Koga, K. *Tetrahedron Lett.* **1981**, *22*, 5311–5314.

162. Odashima, K.; Koga, K. In *Cyclophanes*; Keehn, P. M., Rosenfeld, S. M., Eds.; Organic Chemistry 45; Academic Press: New York, 1983, Vol. 2, Chapter 11, pp. 629–678.

163. Odashima, K.; Kobayashi, Y.; Koga, K. Unpublished results.

164. Bakker, E.; Nägele, M.; Schaller, U.; Pretsch, E. *Electroanalysis* **1995**, *7*, 817–822.

165. Kellner, R.; Götzinger, G.; Pungor, E.; Tóth, K.; Polos, L. *Fresenius' Z. Anal. Chem.* **1984**, *319*, 839–840.

166. Kellner, R.; Zippel, E.; Pungor, E.; Tóth, K.; Lindner, E. *Fresenius' Z. Anal. Chem.* **1987**, *328*, 464–468.

167. Tóth, K.; Lindner, E.; Pungor, E.; Zippel, E.; Kellner, R. *Fresenius' Z. Anal. Chem.* **1988**, *331*, 448–453.

168. Yajima, S.; Bühlmann, P.; Tohda, K.; Umezawa, Y. *Anal. Chem.* **1997**, *69*, 1919–1924.

169. Higgins, D.; Corn, R. M. *J. Phys. Chem.* **1993**, *97*, 489–493 and references cited therein.

170. Anzai, J.; Sasaki, H.; Ueno, A.; Osa, T. *J. Chem. Soc., Perkin Trans. 2* **1985**, 903–907.

171. Anzai, J.; Ueno, A.; Osa, T. *J. Chem. Soc., Perkin Trans. 2* **1987**, 67–71.

172. Anzai, J.; Hasebe, Y.; Ueno, A.; Osa, T. *J. Polym. Sci., Part A, Polym. Chem.* **1988**, *26*, 1519–1529.

173. Tohda, K.; Yoshiyagawa, S.; Kataoka, M.; Odashima, K.; Umezawa, Y. *Anal. Chem.* In press. Odashima, K.; Tohda, K.; Yoshiyagawa, S.; Yamashita, S.; Kataoka, M.; Umezawa, Y. Submitted for publication.

174. Shinkai, S.; Nakaji, T.; Ogawa, T.; Shigematsu, K.; Manabe, O. *J. Am. Chem. Soc.* **1981**, *103*, 111–115.

175. Shinkai, S.; Shigematsu, K.; Kusano, Y.; Manabe, O. *J. Chem. Soc., Perkin Trans. 1* **1981**, 3279–3283.

176. Shinkai, S.; Ogawa, T.; Kusano, Y.; Manabe, O.; Kikukawa, K.; Goto, T.; Matsuda, T. *J. Am. Chem. Soc.* **1982**, *104*, 1960–1967.

177. Buck, R. P. *Anal. Chem.* **1976**, *48*, 23R–39R.

178. Gavach, C.; Seta, P.; D'Epenoux, B. *J. Electroanal. Chem.* **1977**, *83*, 225–235.

179. Reid, J. D.; Melroy, O. R.; Buck, R. P. *J. Electroanal. Chem.* **1983**, *147*, 71–82.

180. Gros, M.; Gromb, S.; Gavach, C. *J. Electroanal. Chem.* **1978**, *89*, 29–36.

181. Morf, W. E.; Simon, W. *Helv. Chim. Acta* **1986**, *69*, 1120–1131.
182. *The NMDA Receptor*; Collingridge, G. L., Watkins, J. C., Eds.; Oxford University Press: Oxford, UK, 1994.
183. McBain, C. J.; Mayer, M. L. *Physiol. Rev.* **1994**, *74*, 723–760.
184. Sugawara, M.; Sugao, N.; Umezawa, Y.; Adachi, Y.; Taniguchi, K.; Minami, H.; Uto, M.; Odashima, K.; Michaelis, E. K.; Kuwana, T. In *Proceedings of the Fifth International Symposium on Redox Mechanism and Interfacial Properties of Molecules of Biological Importance 1993*; Schultz, A. F., Taniguchi, I., Eds.; The Electrochemical Society, Proc. Vol. 93-11; The Electrochemical society: Pennington, UK, 1993, pp. 268–279.
185. *Excitatory Amino Acid Receptors. Design of Agonists and Antagonists*; Krogsgaard-Larsen, P., Hansen, J. J., Eds.; Ellis Horwood: Chichester, UK, 1992.
186. *Single-Channel Recording*; Sakmann, B., Neher, E., Eds.; Plenum Press: New York, 1985.
187. Uto, M.; Michaelis, E. K.; Hu, I. F.; Umezawa, Y.; Kuwana, T. *Anal. Sci.* **1990**, *6*, 221–225.
188. Minami, H.; Sugawara, M.; Odashima, K.; Umezawa, Y.; Uto, M.; Michaelis, E. K.; Kuwana, T. *Anal. Chem.* **1991**, *63*, 2787–2795.
189. Minami, H.; Uto, M.; Sugawara, M.; Odashima, K.; Umezawa, Y.; Michaelis, E. K.; Kuwana, T. *Anal. Sci.* **1991**, *7 (Supplement)*, 1675–1676.
190. Sugawara, M.; Hirano, A.; Rehák, M.; Nakanishi, J.; Kawai, K.; Sato, H.; Umezawa, Y. *Biosensors & Bioelectronics*, in press.
191. Watkins, J. C. E., R. H. *Ann. Rev. Pharmacol. Toxicol.* **1981**, *21*, 165–204.
192. Monaghan, D. T. B., R. J.; Cotman, C. W. *Ann. Rev. Pharmacol. Toxicol.* **1989**, *29*, 365–402.
193. Watkins, J. C.; Krogsgaard-Larsen, P.; Honoré, T. *Trends in Pharmacol. Sci.* **1990**, *11*, 25–33.
194. Patneau, D. K.; Mayer, M. L. *J. Neuroscience* **1990**, *10*, 2385–2399.
195. Nakanishi, S. *Science* **1992**, *258*, 597–603.
196. Kutsuwada, T.; Kashiwabuchi, N.; Mori, H.; Sakimura, K.; Kushiya, E.; Araki, K.; Meguro, H.; Masaki, H.; Kumanishi, T.; Arakawa, M.; Mishina, M. *Nature* **1992**, *358*, 36–41.
197. Lester, R. A. J.; Jahr, C. E. *J. Neuroscience* **1992**, *12*, 635–643.
198. Gration, K. A. F.; Lambert, J. J.; Ramsey, R. L.; Rand, R. P.; Usherwood, P. N. R. *Brain Research* **1981**, *230*, 400–405.
199. Kawai, M.; Horikawa, Y.; Ishihara, T.; Shimamoto, K.; Ohfune, Y. *Eur. J. Pharm.* **1992**, *211*, 195–202.
200. Odashima, K.; Sugawara, M.; Umezawa, Y. *Trends Anal. Chem.* **1991**, *10*, 207–215.
201. Umezawa, Y.; Uto, M.; Abe, H.; Takami, W.; Sugawara, M.; Kataoka, M.; Yasuda, Y.; Kimura, E. In *Bioelectroanalysis, 1*; Akadémiai Kiadó: Budapest, 1986, pp. 407–420.
202. Umezawa, Y.; Sugawara, M.; Kataoka, M.; Odashima, K. In *Ion-Selective Electrodes*; Pungor, E., Ed.; Akadémiai Kiadó Pergamon Press: Budapest, Oxford, 1989, Chapter 5, pp. 211–234.
203. Uto, M.; Yoshida, H.; Sugawara, M.; Umezawa, Y. *Anal. Chem.* **1986**, *58*, 1798–1803.
204. Uto, M.; Sugawara, M.; Umezawa, Y. *Nippon Kagaku Kaishi* **1987**, 489–494.
205. Sugawara, M.; Khoo, S. B.; Yoshiyagawa, S.; Yagi, K.; Sato, H.; Namba, M.; Wakabayashi, M.; Minami, H.; Sazawa, H.; Odashima, K.; Umezawa, Y. *Anal. Sci.* **1994**, *10*, 343–347.
206. Sugawara, M.; Yoshida, H.; Henmi, A.; Umezawa, Y. *Anal. Sci.* **1991**, *7*, 141–147.
207. Sugao, N.; Sugawara, M.; Uto, M.; Minami, H.; Umezawa, Y. *Anal. Chem.* **1993**, *65*, 363–369.
208. Adachi, Y.; Sugawara, M.; Taniguchi, K.; Umezawa, Y. *Anal. Chim. Acta* **1993**, *281*, 577–584.
209. Umbach, J. A.; Coady, M. J.; Witght, E. M. *Biophys. J.* **1990**, *57*, 1217–1224.
210. Ikeda, T. S.; Hwang, S. S.; Coady, M.; Hirayama, B. A.; Hediger, M. A.; Wright, E. M. *J. Memb. Biol.* **1989**, *110*, 87–95.
211. Beaugé, L.; Berberián, G. *Biochim. Biophys. Acta* **1984**, *772*, 411–414.
212. Campos, M.; Berberián, G.; Beaugé, L. *Biochim. Biophys. Acta* **1988**, *938*, 7–16.
213. Minami, H.; Sato, N.; Sugawara, M.; Umezawa, Y. *Anal. Sci.* **1991**, *7*, 853–862.
214. Grandjean, J.; Laszlo, P. *J. Am. Chem. Soc.* **1986**, *108*, 3483–3487.

215. Chia, P. S. K.; Lindoy, L. F.; Walker, G. W.; Everett, G. W. *J. Am. Chem. Soc.* **1991**, *113*, 2533–2537 and references therein.
216. Poonia, N. S.; Bajaj, A. V. *Chem. Rev.* **1979**, *79*, 389–445.
217. Kinsel, J. F.; Melnik, E. I.; Lindenbaum, S.; Sternson, L. A.; Ovchinnikov, Y. A. *Biochim. Biophys. Acta* **1982**, *684*, 233–240.
218. Kinsel, J. F.; Melnik, E. I.; Sternson, L. A.; Lindenbaum, S.; Ovchinnikov, Y. A. *Biochim. Biophys. Acta* **1982**, *692*, 377–383.
219. Kinsel, J. F.; Melnik, E. I.; Lindenbaum, S.; Sternson, L. A.; Ovchinnikov, Y. A. *Int. J. Pharm.* **1982**, *12*, 97–106.
220. Mollenhauer, H. H.; Morré, D. J.; Rowe, L. D. *Biochim. Biophys. Acta* **1990**, *1031*, 225–246.
221. Antonenko, Y. N.; Yaguzhinsky, L. S. *Biochim. Biophys. Acta* **1988**, *938*, 125–130.
222. Westrey, J. W.; Evans, R. H., Jr.; Blount, J. F. *J. Am. Chem. Soc.* **1977**, *99*, 6057–6061.
223. Sugawara, M.; Okude, K.; Tohda, K.; Umezawa, Y. *Anal. Sci.* **1996**, *12*, 331–335.
224. Dawson, R. M. C.; Elliott, D. C.; Elliott, W. H.; Jones, K. M. *Data for Biochemical Research*, 3rd ed.; Clarendon Press: Oxford, UK, 1986.
225. Sugawara, M.; Omoto, M.; Yoshida, H.; Umezawa, Y. *Anal. Chem.* **1988**, *60*, 2301–2303.
226. Babu, Y. S.; Sack, J. S.; Greenhough, T. J.; Bugg, C. E.; Means, A. R.; Cook, W. *Nature* **1985**, *315*, 37–40.
227. Haiech, J.; Klee, C. B.; Demaille, J. G. *Biochemistry* **1981**, *20*, 3890–3897.
228. Ozawa, T.; Kakuta, M.; Sugawara, M.; Umezawa, Y.; Ikura, M. *Anal. Chem.* In press.
229. Pedersen, C. J. *J. Am. Chem. Soc.* **1967**, *89*, 2495–2496.
230. Pedersen, C. J. *J. Am. Chem. Soc.* **1967**, *89*, 7017–7036.
231. Kolthoff, I. M. *Anal. Chem.* **1979**, *51*, 1R–22R.
232. Yoshio, M.; Noguchi, H. *Anal. Lett.* **1982**, *15*(A15), 1197–1276.

This Page Intentionally Left Blank

# SUPRAMOLECULAR ANION
# RECEPTORS

K. Travis Holman, Jerry L. Atwood, and

Jonathan W. Steed

# 1.  INTRODUCTION

From the onset of this jurisdiction known as *Supramolecular Chemistry*, parallels have been drawn between the molecular recognition events of supramolecular chemical systems and the those found in nature.[1] So often is this the case that the mimicry of Nature's chemical tasks may now in fact be considered a dominant theme of the field.

It is apparent that in the chemistry of natural processes anion recognition plays a central role. This is evidenced by the fact that the substrates of a large majority of characterized enzymes are anionic in nature.[2] Several X-ray crystal structure determinations[3-7] have demonstrated that biochemical anion discrimination is typically a result of complex arrays of hydrogen-bonding interactions, together with a fit process based upon anion size. For example, the 2.5 Å resolution structure of *Yersina* protein tyrosine phosphatase binding tungstate[3] shows the anion embedded within a network of 12 hydrogen bonds ranging in length from 2.7 to 3.4 Å. Notably, four of these hydrogen bonds originate from guanidinium moieties of the arginine residues within the enzyme, highlighting the importance of this functionality in anion recognition. Appropriately, the guanidinium moiety has been the center of focus for the development of a number of supramolecular anion receptors (*vide infra*).

The structures of the sulfate-binding protein (SBP) of *Salmonella typhimurium*, and the related phosphate-binding protein (PBP) have also been determined.[4,5] In the SBP the anion is deeply sequestered, away from solvent, counterions, and salt bridges and is stabilized solely by seven hydrogen bonds between 2.67 and 2.84 Å in length. Similarly, the $HPO_4^{2-}$ guest within the PBP is bound some 8 Å below the protein surface and is held in place by a total of 12 hydrogen bonds, between 2.63 and 2.92 Å. The crucial difference between the two proteins that accounts for the high selectivity of the PBP for $H_2PO_4^-$ and $HPO_4^-$ over $SO_4^{2-}$ is the presence of a carboxylate side chain in the PBP, capable of acting as a hydrogen bond acceptor. Hence, substrate recognition depends primarily on the state of protonation of the guest anion.[6,7] A Cambridge Crystallographic Database study has highlighted the subtle structural differences associated with the biological recognition of phosphate vs. sulfate.[8]

Despite the prominence of anion recognition chemistry in biological systems, the design of supramolecular anion receptors was slow to develop with respect to the analogous chemistry of cations,[9] and this discrepancy may readily be traced to a number of inherent difficulties in anion binding:[10-12]

1.  First, anions are somewhat large and therefore generally require receptors of considerably greater size than cations. For example, one of the smallest anions, $F^-$, is comparable in ionic radius to $K^+$ (1.36 Å vs. 1.33 Å).[10]

2.  Even the most common anions occur in a diverse range of shapes, charges, and sizes, making it often necessary to incorporate a third dimension into the recognition design, e.g. spherical (halides), tetrahedral ($PO_4^{3-}$, $SO_4^{2-}$), planar ($NO_3^-$), linear ($SCN^-$, $N_3^-$), as well as more complicated examples as in the case of biologically important oligophosphate anions.[11]

3.  In comparison to cations of similar size, anions have high free energies of solvation and hence anion hosts are required to compete more effectively with the surrounding medium (e.g. $\Delta G_{F^-}$ 434.3 kJ $mol^{-1}$, $\Delta G_{K^+}$ 337.2 kJ $mol^{-1}$).[13]

4.  The pH dependence of many anions may cause problems in designing an appropriate host. For example, a receptor based upon polyammonium moieties may not be sufficiently protonated in the pH region where the anion is present in the desired form (*vide infra*).

These problems have been addressed in a wide variety of imaginative and novel ways and progress in anion complexation has been rapid in recent years[10–12,14–17] to the extent that it has now been described by Lehn as a "full member of the field of supramolecular chemistry."[10b] It is important to note that the search for anion-selective receptors has not been limited to the mimicry of Mother Nature's approach. Indeed, a great number of the hosts developed are far from being biocompatible as the tools of the chemist are not limited to the building blocks of natural systems. This aspect of anion recognition chemistry lies at the heart of supramolecular chemistry, the interface between chemistry and biology.[1]

Nonnatural anion receptor systems are nonetheless of great interest because of numerous potential abiotic applications such as anion sensing, anion transport, environmental cleanup, and supramolecular catalysis. In this chapter we highlight the development of this aspect of supramolecular chemistry, describing the different approaches to the problems of anion binding and emphasizing those hosts exhibiting a high degree of anion affinity or *selectivity*. In particular the results of X-ray crystallographic studies will be examined as well as aspects of solution binding related to discrimination between anionic guests based upon structure and shape, as distinct from charge density considerations.

## 2. PROTONATED POLYAMINE-BASED HOSTS

### 2.1. Acyclic and Monocyclic Hosts

By far the most common type of anion-binding host is based upon numerous substituted forms of the ammonium ion. Protonated alkyl ammonium receptors have the advantages of positive charge (for anion binding via electrostatic attrac-

tion), polar N–H bonds (capable of forming hydrogen-bonding interactions and an extensive degree of synthetic versatility (enabling them to be incorporated into a wide range of multidentate host frameworks of the desired solubility and geometry). Furthermore, polyammonium-based anion hosts are derived, conceptually at least, from analogous cation-binding polyamine ligands and hence a change in pH is often sufficient to form an anion-binding host from a known amine ligand. To take a very simple example, ethylenediamine (en) forms numerous Lewis acid–base complexes with a variety of metal ions.[18] Similarly, the ethylenediammonium cation (en-2H$^+$) forms simple salts with anions such as citrate.[19] In contrast to the stabilization of metal complexes by the chelating en ligand, however, the interaction of en-2H$^+$ with anions is not chelating in nature in as much as the central C–C bond adopts a *trans* configuration with the two -NH$_3^+$ moieties binding to different anions. This bridging mode of interaction is attributed to the need for the two positively charged centers to move as far away from one another as possible, thus minimizing unfavorable cation–cation interactions.

A similar situation is found in the structure of putrescine diphosphate[20] (a model system for amine–nucleic acid interactions) which divides into layers of H$_2$PO$_4^-$ anions bridged by protonated putrescine (1,4-diamino-$n$-butane) cations. In a real biological system (yeast phenylalanine transfer RNA) phosphate residues are found to be enveloped by the polyamine spermine [NH$_2$(CH$_2$)$_3$NH(CH$_2$)$_4$NH(CH$_2$)$_3$NH$_2$] which again adopts a linear, nonchelating conformation.[21]

This evidence points towards a markedly decreased tendency of acyclic polyammonium hosts to form chelate complexes with anions as a consequence of the need to separate the cationic nitrogen centers. This tendency is also important in the case of cyclic structures in which the cationic nitrogen centers cannot move as far away from one another. For example, potentiometric titration results demonstrate that hexaprotonated hexacyclen (**1**, the nitrogen analogue of 18-crown-6) is a strong diprotic acid, existing predominantly as the tetraprotonated form (**1-4H$^+$**) in aqueous solution, suggesting that the enforced proximity of six cationic centers is highly energetically unfavorable. Solution complexation experiments indicate that while **1-4H$^+$** exhibits a greater affinity for NO$_3^-$ over Cl$^-$, Br$^-$, I$^-$, and ClO$_4^-$, it paradoxically forms stronger hydrogen bonds to Cl$^-$. The X-ray crystal structure of [**1-4H$^+$**][NO$_3$]$_2$Cl$_2$·2H$_2$O demonstrates the binding of chloride ions above and below the host ring plane, N(H)···Cl$^-$ = 3.07–3.28 Å, while nitrate ions are indirectly



**1**
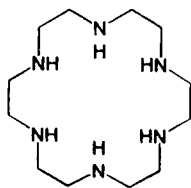
bound via enclathrated water molecules.[22] In spite of the high acidity of the hexaprotonated form (1-6H$^+$), crystallization of the hydrochloride salt of hexacyclen from concentrated nitric acid yields [1-6H$^+$] [NO$_3$]$_4$Cl$_2$. In this case the nitrate ions are directly hydrogen bonded to the hexacyclen ring in a unidentate fashion, N(H)$\cdots$ONO$_2^-$ = 2.77–2.88 Å.[23] In contrast, molecular mechanics calculations (MM2) suggest a bidentate mode of coordination for the binding of carbonate by 1-3H$^+$,[24] indicating that the nature of protonated hexacyclen–anion interactions is both complex and highly variable. In no case is anion inclusion *within* the macrocycle observed, consistent with the relatively large size of the anions studied, and as a result little size selectivity is observed, with complex enthalpic and solvent effects dominating complexation behavior. Related work on 1 and similar *penta*cycloamine macrocycles shows that these materials also act as efficient, selective binding agents for *syn*-type polycarboxylate anions such as those found in the tricarboxylate cycle. This selectivity is attributed to geometrical factors enabling a macrocyclic/chelating effect to enhance binding.[25] An analogous material containing amide functionalities has been shown to bind azide in the solid state with the guest anion bridging unsymmetrically across pairs of host cations in the crystal structure, N$\cdots$N = 2.76–3.07 Å. $^1$H NMR measurements of this complex indicate that only weak binding is observed in solution, consistent with the nonincluded position of the guest anion.[26]

In contrast, Lehn and co-workers have synthesized a variety of larger polyammonium-based macrocycles incorporating greater separations between the nitrogen centers (2–4). These species were all found to exhibit p$K_a$ values around or above 7 and, as a consequence, displayed strong anion-binding behavior at neutral pH. While no X-ray crystallographic results are available, solution studies indicate a number of structural preferences, interpreted in terms of inclusion of anionic guests within the macrocyclic ring. For example, larger anions such as squarate and fumarate form stronger complexes (log $K_s$ = 2.9–3.6) with the larger macrocycle 3-8H$^+$ than with 2-6H$^+$. Similarly very high stability constants (log $K_s$ = 6.0 and 8.9) are observed for Co(CN)$_6^{3-}$ and Fe(CN)$_6^{4-}$ with the fourfold symmetric macrocycle 3-8H$^+$. It should be noted, however, that electrostatic effects also play a major



2                                3                                4

**5**                           **6**                          **7**
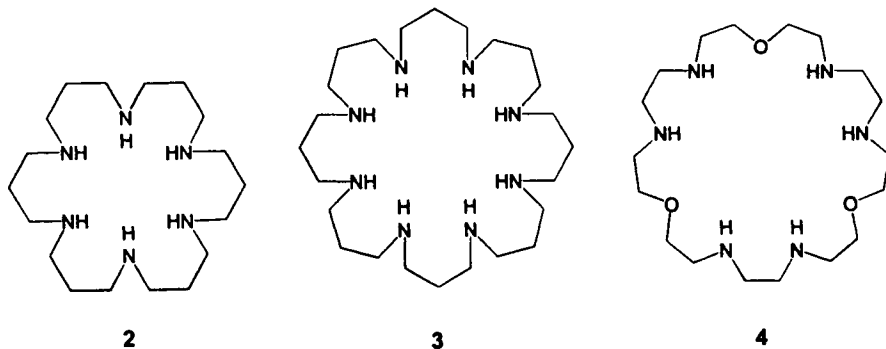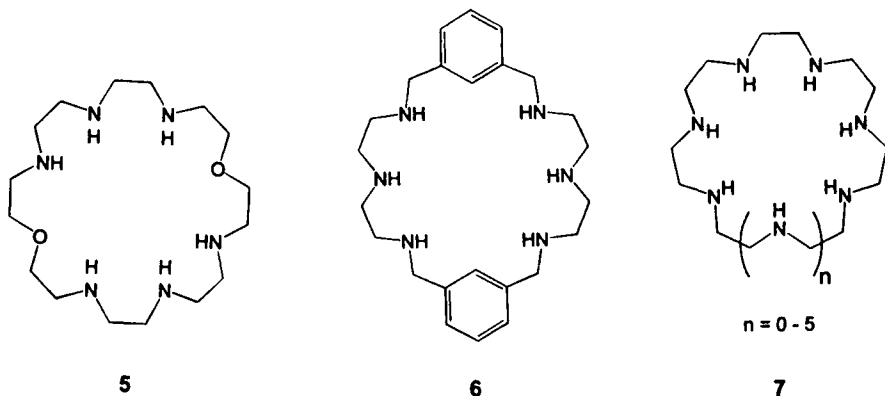
role in both the strength and selectivity of anion binding, consistent with the fact that there is always more than one anion associated with the macrocyclic host.[27]

Protonated forms of the large-ring macrocycle $[24]N_6O_2$ (**5**) and related compounds have been shown to be active as synthetic phosphorylation catalysts in ATP synthesis.[28] It is likely that in this case the substrate enters the macrocyclic cavity to some extent, or is enveloped by it. Evidence for this possibility comes from the crystal structure of the chloride salt of **5**-6H$^+$ (Figure 1) in which a chloride ion is enveloped within a cleft formed by the boat-shaped conformation of the macrocycle.[29a] The crystal structure of the nitrate salt of **5**-4H$^+$ has also recently been determined and the host again adopts a boat-like conformation as it interacts with the anion.[29b] The hydrochloride salt of the smaller $[22]N_6$ binds two chloride anions above and below the host plane in a similar way to **1**. Molecular dynamics simulations indicate that the pocket-like conformation for **5**-6H$^+$ is maintained in solution, although $^{35}Cl$ NMR experiments demonstrate that halide ions are in rapid exchange between the complexed and solvated state.[29]

The versatility of host **5** and related forms has recently been highlighted by Martell et al. who have shown **5**-4H$^+$ to effectively complex malonate in aqueous solution[30] and have shown that a similar benzo-substituted derivative (**6**) displays remarkable affinity for oligophosphates.[31] Furthermore, **5**-4H$^+$ and its protonated $[36]aneN_8O_4$ relative have recently been shown to efficiently catalyze α-proton exchange in malonate ions (rate enhancements of $1.4 \times 10^3$ and $1.8 \times 10^5$, respectively) at neutral pH.[32]

Consistent with the theme of increasing macrocycle size in order to induce strong complexation by inclusion of anionic guests within the macrocyclic ring, Bianchi et al. have carried out a great deal of work with protonated $[3 \cdot k]aneN_k$ (**7**, $k = 7-12$) type hosts. These materials, related to hexacyclen **1**, consist of macrocyclic rings of up to 36 atoms.[33-36] As with **1**, measurements of acidity constants indicate that, starting from the fully protonated macrocycles, the first three protons are readily lost (e.g. for $k = 12$, log $K_a = 1.0$, 2.3, and 2.65 for the first three protons), again as a consequence of the accumulation of positive charge density on sites in close

**Figure 1.** Two views of the 5-6H$^+$ macrocycle showing only the centrally located Cl$^-$ anion (sphere of arbitrary radius).[29]

proximity to one another. In spite of this, the partially protonated forms of these hosts form a number of interesting "supercomplexes" with coordination complex anions such as $[Co(CN)_6]^{3-}$, $[Fe(CN)_6]^{4-}$, and $[PtCl_4]^{2-}$. X-ray crystallographic studies demonstrate that in the majority of cases the anions bridge between the macrocycles and little anion selectivity is observed, indicating that binding occurs primarily by coulombic attraction.[33] However, in the case of the $[PdCl_4]^{2-}$ complex of the fully protonated $H_{10}[30]aneN_{10}^{10+}$ host, $[(PdCl_4)(H_{10}[30]aneN_{10})][PdCl_4]_2Cl_4$ **8**, one of the $[PdCl_4]^{2-}$ anions is included within the macrocyclic cavity. The macrocyclic receptor adopts an "S" shaped conformation in order to wrap around the guest anion and maximize N–H···Cl hydrogen bonding interactions (Figure 2). Solution measurements indicate that $[PdCl_4]^{2-}$ is bound by macrocycles with $k = 9$ and greater, with $[30]aneN_{10}$ exhibiting a cavity size most complementary to the dimensions of the complex anion. The included anion is found to exchange only slowly with other complex anions in solution and the binding is exothermic with $\Delta H^\circ = -16.3(4)$ kJ mol$^{-1}$ per $[PdCl_4]^{2-}$ unit.[34] Binding of $[PtCl_6]^{2-}$ has also been
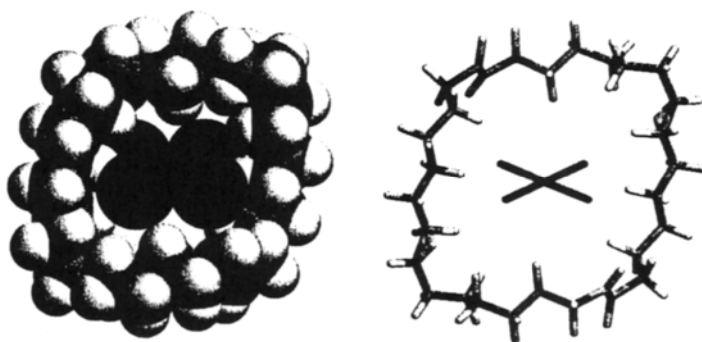


**Figure 2.** Spacefilling and stick representation of the $[(PdCl_4)(H_{10}[30]aneN_{10})]^{8+}$ cation in **8**.[34]

reported for hosts based upon crystalline thiamine in which the metal complex anions are sandwiched between hydrogen-bonded pairs of host molecules.[37]

Recently, Czarnik et al. have reported the use of the acyclic protonated amine host **9** as a chemosensor of pyrophosphate. Typical fluorescence sensing methods rely on the ability of a complexed anion to quench the fluorophore. The fluorescence intensity of host **9**, however, is actually *increased* upon complexation of anions and its 2200-fold selectivity of pyrophosphate over phosphate allows for real-time assay of pyrophosphate hydrolysis by inorganic pyrophosphatase.[38]

More complex, polyamine-based macrocycles capable of complexation of anions within the macrocyclic ring have been recently synthesized. Work by Sessler et al. upon the "expanded porphyrin" sapphyrin **10a** has shown that this molecule, in its diprotonated form, is capable of complexation of fluoride. The X-ray crystal structure of the mixed fluoride–$PF_6^-$ salt of **10a-2H$^+$** (Figure 3) demonstrates the inclusion of the fluoride ion within a regular array of five N–H···F hydrogen bonds with N(H)···F$^-$ distances in the range 2.70–2.79 Å. The deviation of the fluorine atom from the plane defined by the five nitrogen atoms is only 0.03 Å, indicating a high degree of size complementarity between the sapphyrin ring and the small fluoride anion.[39a] In contrast, the analogous dichloride salt exhibits binding of chloride ions above and below the plane of the macrocycle[39b] with relatively long N(H)···Cl$^-$ contacts in the range 3.12–3.41 Å, confirming the fact that the chloride is too large to fit snugly within the macrocyclic ring. Consistent with the structural results, the stability constant $K_s$ of the F$^- \subset$ **10a-2H$^+$** complex is of the order of $10^8$ M$^{-1}$, with a selectivity factor over Cl$^-$ and Br$^-$ in excess of 1000. The same group has very recently exploited the anion binding propensity of these sapphyrins for the design of self-assembling dimers. The carboxylate-derivatized sapphyrins **10b,c**



9



**a** : R$^1$ = R$^2$ = R$^3$ = CH$_3$
**b** : R$^1$ = CH$_3$; R$^2$ = H; R$^3$ = CH$_2$CO$_2$H
**c** : R$^1$ = CH$_2$CO$_2$H; R$^2$ = R$^3$ = CH$_3$

10

R = (CH₂)₃CO₂H
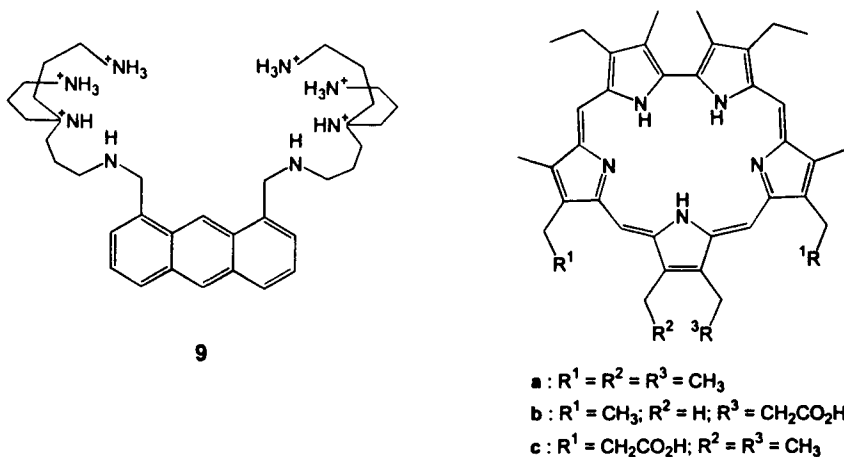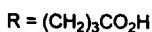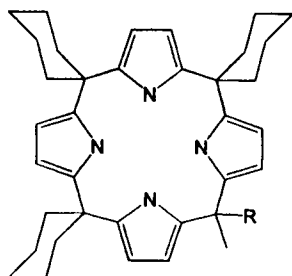
**11**
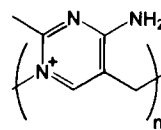


n = 4, 6

**12a,b**

and calix[4]pyrole **11** are preprogramed to complex one another and assemble as homo- and heterodimers in the gas phase, in solution, and in the solid state.[40] For a more detailed discussion of anion binding by expanded porphyrins the interested reader is referred to the excellent chapter by Sessler in this volume.

Finally, another series of novel monocyclic polyamine derivatives, 4-$n$-pyrimidinium crown-$n$ cations ($n = 4$, **12a**; $n = 6$ **12b**) has been reported in connection with the complexation of anions such as Cl⁻ and $NO_3^-$, as well as $[HgI_4]^{2-}$. In the case of both the chloride and nitrate salts of **12a** the macrocycle adopts a pincher-like conformation, with the anion held between two opposing pyridinium rings (Figure 4). Interestingly, the guest anions do not hydrogen bond to the N–H protons, but are in close contact with the protons of the pyridinium ring. The C(H)···Cl⁻ distances range from 3.70–3.79 Å, while in the analogous nitrate salt the C(H)···$ONO_2^-$ contacts are ca. 3.2–3.3 Å.[41]
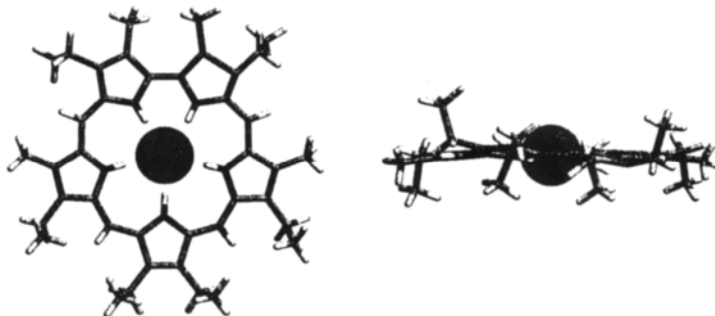


***Figure 3.*** Two views of the molecular structure of the sapphyrin dication **10a**-2H⁺ complex with F⁻.[39a]
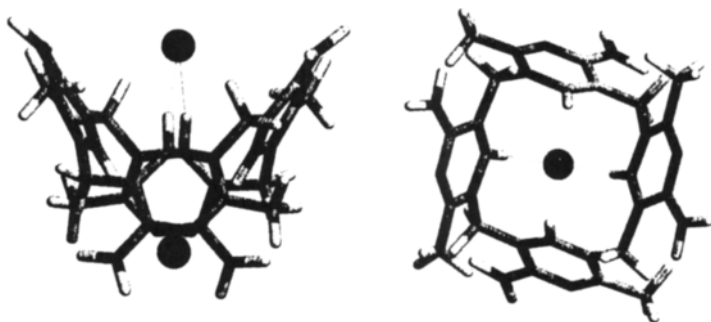
**Figure 4.** Side and top views of the [16-pyridinium crown-4]$^{4+}$ cation showing the C–H···Cl$^-$ interactions with two guest chloride anions.[41]

## 2.2. Polycyclic Hosts

The first report of designed anion hosts, the bicyclic *katapinands* (**13a–d**), was published as early as 1968,[42] nearly in parallel with the discovery of crown ethers. The original solution $^1$H NMR work of Simmons and Park suggested that the *in,in-*forms of **13c** and **13d** complex halide ions *within* the macrocyclic cavity. This was confirmed in 1975[43] by the X-ray crystal structure determination of the chloride salt of the diprotonated nonacosane *in,in-***13c**. The structure reveals that one chloride ion is centrally located within the macrocyclic cavity with N(H)···Cl$^-$ hydrogen-bonded distances of 3.10(1) Å, suggesting a reasonable degree of size complementarily between chloride and host. The concept of size-based selectivity in these systems is bourn out by solution work upon similar katapinands. In the case of the smaller macrocycles *in,in-***13a** and *in,in-***13b** (estimated distance between the faces of NH protons: 1.6 and 2.8 Å, respectively) no solution binding of Cl$^-$, Br$^-$, or I$^-$ is noted. The larger *in,in-***13d** (diameter 4.5 Å, cf. 3.6 Å for *in,in-***13c**), however, exhibits a strong affinity for all three anions and little selectivity is observed.[42] Extension of these katapinand complexes by addition of rigid aromatic spacer



(n = 7 - 10)
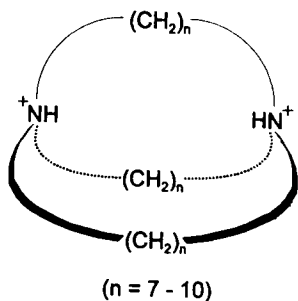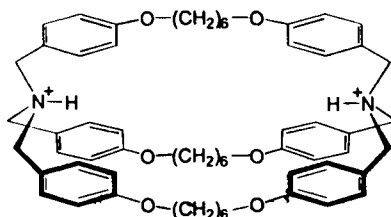
**13a-d**                                              **14**
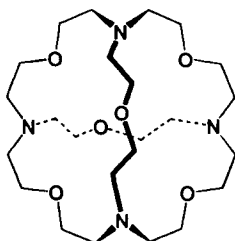
**15**
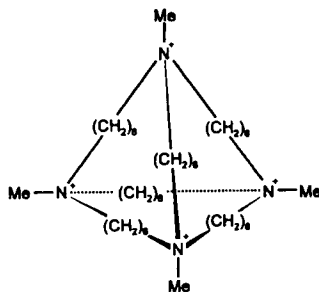


**16**

groups gives **14** which, in its diprotonated form, can include one or even two bromide or iodide ions within its large, macrocyclic cavity.[44]

The macrotricyclic cryptand **15**, in its tetraprotonated form, has also been shown to be an excellent host for spherical anions such as halides. Also, unlike many of the smaller polyammonium type hosts there is no problem associated with complete protonation of all of the nitrogen atoms since all four are widely separated. Stability constant measurements demonstrate that **15**-4H$^+$ is strongly selective for Cl$^-$ with log $K_s$ > 4 in aqueous solution, as opposed to the bromide complex with log $K_s$ < 1 (1.75 in methanol/water mixture).[45] It is notable that this value for chloride complexation is more than 3 orders of magnitude greater than that for the chloride selective katapinand **13c**. It is suggested that this selectivity arises from the presence of a closed and rigid cavity, preorganized[46] for anion binding. The chloride cryptate Cl$^-$ ⊂ **15**-4H$^+$ has been characterized by X-ray crystallography[47] (Figure 5). All four nitrogen atoms adopt the *in* conformation with N(H)···Cl$^-$ hydrogen bonding distances of 3.09(2) Å (av), similar to those observed for the chloride katapinand complex. This compares with average O···Cl$^-$ separations of 3.25(3) Å while in the analogous ammonium cation complex of the unprotonated macrotricycle the average NH$_4$···N and NH$_4$···O distances are almost identical, 3. 13(1) and 3.11(2) Å.[47]

In almost all of the examples mentioned so far, hydrogen bonding has played a central role in stabilizing the host–guest interaction. Work by Schmidtchen, however, has demonstrated the inclusion of iodide by the macrotricyclic receptor **16** solely by a combination of electrostatic and space-filling type interactions (Figure 6). The absence of N–H···I$^-$ bonds is exemplified by the long N···I$^-$ contacts of 4.54(2) Å (av).[48] It is noteworthy that the host provides a nearly ideal tetrahedral coordination environment about the iodide anion, and the aqueous solution binding constants are still relatively high, although generally less than those obtained for complexes of **12**-4H$^+$. Interestingly, association constants for halide ion complexes of **13** are significantly increased in methanol solution, presumably as a consequence of diminished anion–solvent interactions.[49]

**O** O
**●** N
**○** C
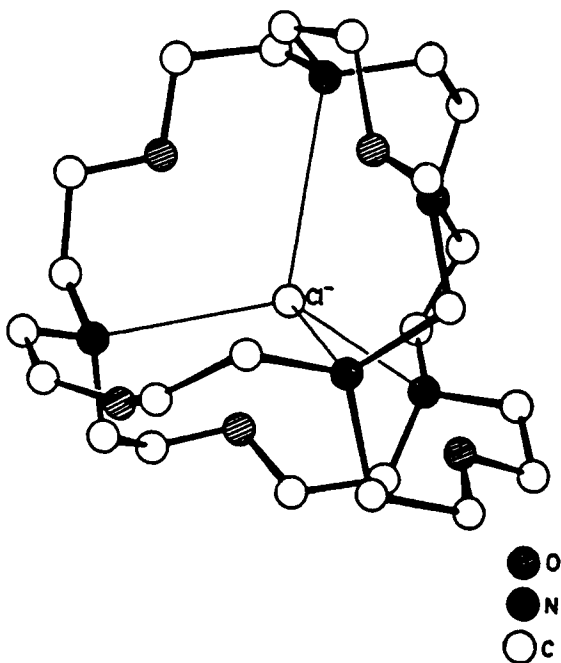
***Figure 5.*** X-ray crystal structure of the macrotricyclic cryptate [Cl⁻ ⊂ **15-4H⁺**].[47]

In the previous section it was noted that hexacyclen **1** does not possess a macrocyclic cavity of sufficient size to encapsulate anionic guests such as Cl⁻ and NO$_3^-$. In contrast, the octaaza macrobicyclic analogue of hexacyclen (**17**) forms the fluoride cryptate [F⁻ ⊂ **17-6H⁺**] (Figure 7).[50] Consistent with the observed high
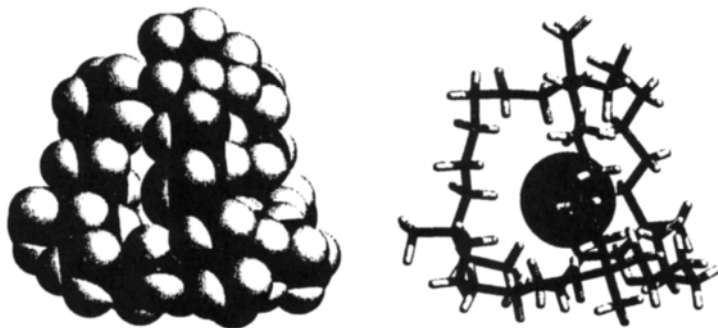


***Figure 6.*** X-ray crystal structure of the iodide cryptate of the macrotricyclic quaternary ammonium receptor **16**.[48]
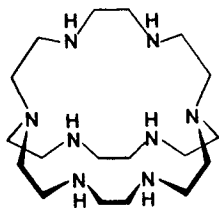
**17**
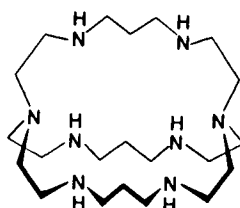


**18**

acidity of the hexacyclen hexacation, the cryptand **17** carries only six of a possible eight protons, with N(H)···F⁻ hydrogen-bonded distances between 2.76 and 2.86 Å. This contrasts to the 3.3 Å N···F⁻ distances to the nonprotonated, bridgehead nitrogen atoms, although the macrocycle does retain the characteristic *in,in*- conformation. While the fluoride anion is situated within the center of the macrocycle in a quasi trigonal prismatic coordination environment, the mode of interaction is not dissimilar to that observed for the chloride complex of hexacyclen,[22] with the fluoride anion situated above the plane of each of the 18-membered rings.

Recently, in an elegant study by Smith and coworkers, the magnitude of fluoride binding by **17**-6H⁺ ($10^{-11.2}$) and its other protonated forms has been determined by potentiometry.[50b] This host, in particular, exhibits an astounding $10^{7.6}$ fluoride/chloride selectivity. These results are in excellent agreement with a similar study by Lehn and coworkers who compare the fluoride/chloride selectivity of protonated **17** with that of the less discriminating **18**.[50c]

A majority of the host systems mentioned so far have been shown to encapsulate halide guests as a consequence of the symmetrical nature of their binding pockets, which readily adapt to the spherical symmetry of the halide ion. A study of the bis-tren macrobicyclic ligand **19**-6H⁺, however, has revealed that, in addition to accommodating halide anions, it is also able to encapsulate azide, $N_3^-$, within its cylindrical cavity.[51] Solution stability constant measurements indicate that the host
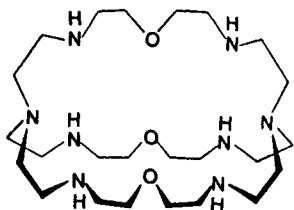


**19**
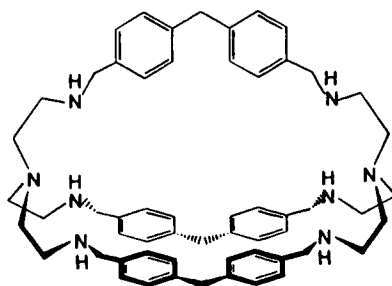


**20**
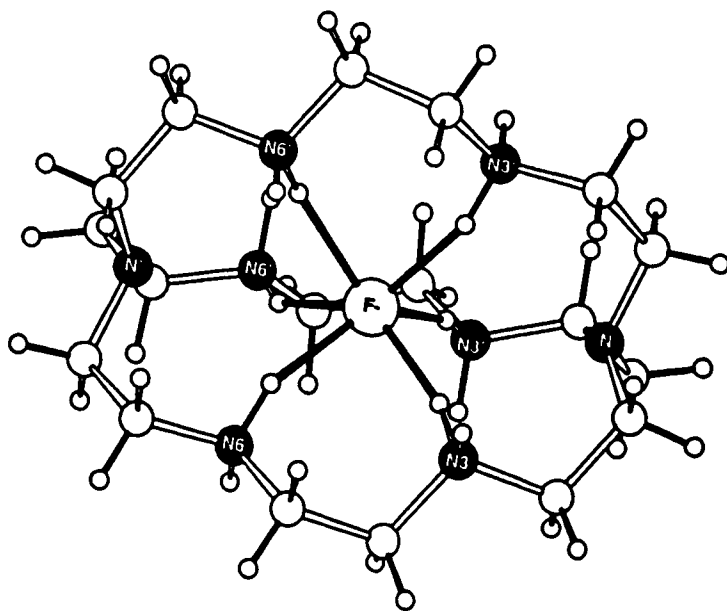
***Figure 7.*** X-ray crystal structure of the fluoride cryptate [F⁻ ⊂ **17**-6H⁺].[50a,b]

is indeed somewhat selective for the azide anion with log $K_s$ = 4.30. Interestingly, the fluoride cryptate is also stable (log $K_s$ = 4.10) in comparison to the chloride, bromide, and iodide complexes (log $K_s$ = 3.0, 2.6, and 2.15, respectively).[51b] Large stability constants (log $K_s$ up to 10.30 in the case of $P_2O_7^{4-}$) are also observed for a number of polyanions, especially the polyphosphates including ATP, ADP, etc.[51b] These results are rationalized in terms of a large electrostatic component to the binding, thus the host is selective for anions of high charge density such as F⁻ and multiply charged ions. The high preference for $N_3^-$ binding in comparison to halides other than F⁻ and other monovalent anions such as nitrate (factor of ca. 100) must however, represent evidence for the operation of some *structural* selectivity.

The X-ray crystal structures of the F⁻, Cl⁻, and Br⁻ cryptates of **19**-6H⁺ demonstrate the inclusion of one of the halide anions in an unsymmetrical fashion.[51b] In the case of the small fluoride ion complex a tetrahedral coordination environment is observed for the guest anion with a mean N(H)··· F⁻ hydrogen-bonding distance of 2.72(8) Å. The Cl⁻ and Br⁻ cryptates exhibit octahedrally coordinated halide ions situated more centrally within the host framework with N(H)···X⁻ distances in the ranges 3.19–3.39 Å (X = Cl⁻) and 3.33–3.47 Å (X = Br⁻). It is noteworthy that the hydrogen-bonded distances for the anion within the cryptand host are *longer* by up to ca 0.15 Å than those for the other anions in the lattice, suggesting a particularly
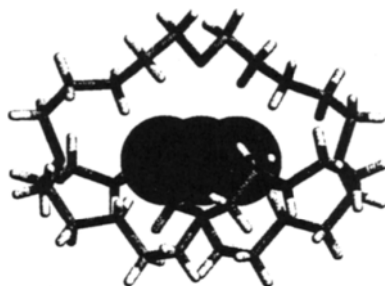
**Figure 8.** Azide inclusion within the cylindrical bis-tren macrobicycle **19**-6H$^+$.[51]

poor size match with the host cavity. This contrasts with the symmetrical inclusion of azide (Figure 8) with N(H)$\cdots$N$_3^-$ contacts that fall in the range of 2.91–3.02 Å.

The binding of larger, linear anions by bis-tren type macrocycles has been extended by cyclophane receptors like **20**-6H$^+$. Solution measurements at pH 5.5 indicate that this host exhibits an impressive degree of structural selectivity within a series of linear $\alpha,\omega$-dicarboxylate anions $O_2C(CH_2)_nCO_2^-$, with adipate ($n = 4$) being bound much more strongly than either shorter or longer homologues. Also notable is the extremely strong binding of the terphthalate dianion ($p$-$^-O_2CC_6H_4CO_2^-$, tph) arising from both electrostatic and hydrophobic interactions, as well as a high degree of structural complimentarity. The X-ray crystal structure of [tph $\subset$ **15**-6H$^+$] (Figure 9) demonstrates the inclusion of one of the three tph anions within the macrocyclic cavity, with N(H)$\cdots$O contacts in the range 2.77–2.96 Å.[52]

As with the related inclusion compounds of protonated **19** there is also a significant structural change in the macrocycle itself upon complexation in comparison to the structure of the nonprotonated host. The distance between the two
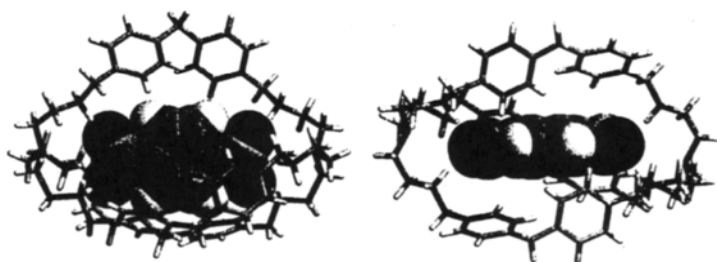


**Figure 9.** X-ray crystal structure of the terphthalate dianion cryptate [tph $\subset$ **20**-6H$^+$].[52]
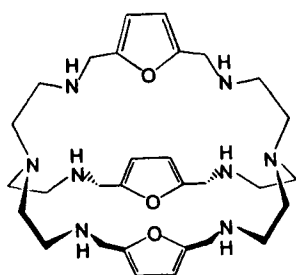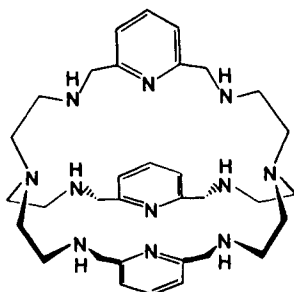
**21**                                      **22**

bridgehead nitrogen atoms is decreased by ca. 1.8 Å in order to maximize interactions with the guest anion. The hydrogen-bonding coordination sphere of both host and guest is completed by a number of water molecules and it is noteworthy that one of the nonincluded tph anions interacts with the host only via one of these water molecules.[52]

Recently, two related bis-tren type macrocycles, **21** and **22** have been shown to complex $ClO_4^-$ and $SiF_6^{2-}$ anions in the solid state, highlighting the potential of these types of hosts for inorganic anion complexation.[53]

## 3. THE GUANIDINIUM MOIETY

The guanidinium ion $[C(NH_2)_3]^+$ and its many derivatives have been widely studied in the context of anion binding. In particular, guanidinium moieties are ubiquitous in biochemical systems since the arginine residues of enzymes play a major role in the binding of anionic substrates and in maintaining protein tertiary structure (*vide supra*). Most importantly, the guanidinium moiety exhibits a particularly high $pK_a$ (13.5 for the parent ion); thus it remains protonated over a wide pH range and retains its positive charge and hydrogen bond donor properties.[10]

The X-ray crystal structure determination of a number of simple guanidinium salts[54] (e.g., methylguanidinium dihydrogenphosphate)[55] clearly demonstrates the existence of bidentate ionic hydrogen bonds as shown in Figure 10, with N(H)···O contacts in the region of 2.9 Å.[55]

Early work upon the guanidinium group by Lehn and coworkers resulted in the synthesis of a number of guanidinium-containing macrocycles with two or three of these separated by various spacer groups.[56] No crystallographic results were reported for these compounds and pH-metric titration results with $PO_4^{3-}$ demonstrated only weak binding in aqueous solution (log $K_s$ 1.7–2.4) with little macrocyclic effect being observed. The weakness of the anion binding was ascribed to the delocalized nature of the positive charge on the guanidinium fragment, resulting in fewer regions of high positive charge density in comparison with ammonium-containing macrocycles.[10] In general, observed anion selectivities are attributable
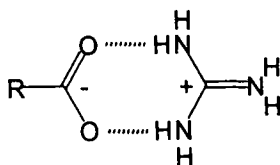
***Figure 10.*** Bidentate hydrogen bonding between multidentate anions and the guanidinium moiety.

simply to electrostatic interactions, although selectivity between monovalent anions reveals that those such as the carboxylates which are capable of engaging in bidentate hydrogen-bonding interactions are bound more strongly than halides.[56]

In spite of these relatively unencouraging results, the biological role of the guanidinium group has prompted a significant amount of work in the design and synthesis of hosts capable of catalyzing biological reactions or transporting phosphate and polyphosphate anions.[57] In particular, an elegant study of the bis(acylguanidinium) host **23** in relatively noncompetitive solvent media has shown it to accelerate the rate of phosphodiester cleavage by factors of up to 700,[57b] with a bis(bidentate) binding resulting in association constants in the region of $5 \times 10^4$ $M^{-1}$.[57a,b]

In an attempt to achieve anion binding in a protic medium Schmidtchen et al. have developed a number of acyclic, bifunctional hosts such as **24**. Molecular modeling studies suggest that **24a** adopts an extended conformation and shows no significant affinity for monoanions such as iodide or acetate. $^1$H NMR titration results in deuterated methanol solution with a wide variety of dicarboxylate anions, however, indicate that this host possesses a significant affinity and selectivity for malonate ($K_s = 16,500\ M^{-1}$) over both longer and shorter chain analogues, suggesting a significant degree of size compatibility with that substrate. Binding is not



**23**



**a** = SiPh$_2$$^t$Bu

**b** = H

**24**
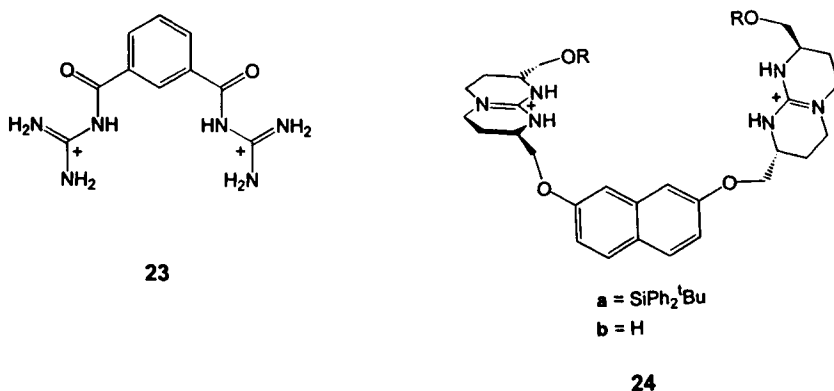
dominated by simple geometrical considerations however. A similarly large association constant ($14,500$ $M^{-1}$) is found for nitro-isophthalate. This is compared to the unnitrated analogue which exhibits a much smaller association constant ($6060$ $M^{-1}$), suggesting an influence of effects such as $\pi$-stacking and charge transfer.[58] The same host also displays a marked affinity for phosphates in methanol with an association constant of $38,000$ with $5'$-$AMP^{2-}$. For solvent comparison, host **24b** also complexes $5'$-$AMP^{2-}$ in methanol ($K_s = 9330$), but the association is considerably weaker in aqueous solution ($K_s = 204$).[57c] Related work with bis(guanidinium)-, bis(urea)-, and bis(thiourea)-based hosts incorporating the $p$-xylyl spacer units has demonstrated binding constants of up to $50,000$ $M^{-1}$ in the relatively competitive solvent DMSO, although addition of water results in a dramatic decrease in association.[59]

Unfortunately, given the complexity of host–guest systems involving **24**, no crystallographic results are available. The simpler hosts, **25**, have been structurally characterized, however, as their acetate and nitrate salts, respectively.[57d,e] In the case of **25a** the results of the X-ray structure determination clearly indicate bidentate hydrogen bonding of the guanidinium NH functionalities to the acetate anion [N(H)$\cdots$O $2.850(5)$ Å]. Additional stabilization comes from interactions with the pendant hydroxyl functionalities with hydrogen-bonded O(H)$\cdots$O contacts of $2.733(5)$ Å.[57d] Complex **25b** contains two chiral centers and, in optically resolved form, is capable of enantiodifferentiation of racemic mixtures of chiral carboxylic acids such as $N$-acetyl-D,L-alanine as determined by $^1$H NMR in acetonitrile solution. The X-ray crystal structure of the nitrate salt of **25b** demonstrates the chiral nature of the molecular cleft[57e] with the nitrate ion fitting only poorly within the large cavity. Similar chiral recognition has also been reported in related species by Lehn et al.[6]

Finally, bidentate bis(guanidinium) hosts like **26** reported by Anslyn et al. have recently been shown to bind phenyl phosphate anions in a bis(bidentate) fashion. Hydrogen-bonding N(H)$\cdots$O distances are in the range $2.658(7)$–$2.868(6)$ Å, while solution studies in $15\%$ $H_2O$/DMSO give binding constants of ca. $500$ $M^{-1}$ with dibenzyl phosphate.[61]
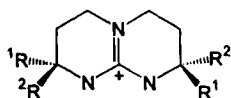


a: $R^1 = R^2 = CH_2CH_2CH_2OH$
b: $R^1 = SiPh_2{}^tBu$; $R^2 = H$

**25**
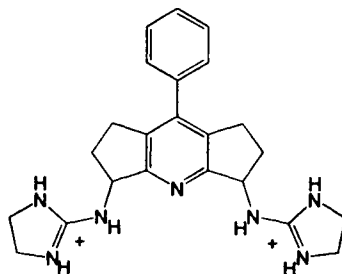
**26**

# 4. NEUTRAL ANION HOSTS

In the case of cationic host molecules, the binding of a target anion usually must occur in the presence of other counterions and hence association constants often represent more a measure of the effectiveness with which the target anion is bound *relative* to the others in the system. Neutral receptor molecules do not suffer from this drawback and also have the potential for greater anion selectivity since they do not rely upon nondirectional electrostatic forces to achieve anion coordination.[12]

## 4.1. Organic Hosts

A very simple modification of the parent amine of the macrotricyclic cation **16** by formation of its borane adduct is sufficient to produce the neutral zwitterionic host **27**.[62] Complex **27** has been characterized by X-ray crystallography (in the absence of guest anion) and adopts a related conformation to that observed for the iodide complex of **16**, although the cavity is significantly distorted from tetrahedral symmetry and hence is markedly smaller (N···N distances for **16** 7.10–7.52 Å, cf. **27** 6.92–8.10 Å).[48] Molecular modeling calculations indicate that **27** is capable of forming 1:1 inclusion complexes with small anions such as $Br^-$ and $CN^-$ (calculated $\Delta H_a = -16$ and $-26$ kcal $mol^{-1}$, respectively) although $^1H$ NMR titrations indicate weak binding of $Br^-$ with a dissociation constant of $K_{diss} = 80 \times 10^{-3}$ M.

In addition to the possibility of such ion–dipole type interactions found for **27**, it is possible to design neutral receptors with either hydrogen bond donor/acceptor and/or Lewis acid character. Work by Reinhoudt et al. have shown that extremely simple hosts such as **28**[63] containing both hydrogen-bond donor and acceptor functionalities may act as remarkably effective anion hosts, mimicking the extensive array of hydrogen-bonding interactions found in natural anion-binding proteins.

Ligand **28** and a number of related compounds were all found to be selective for $H_2PO_4^-$ over $HSO_4^-$ and $Cl^-$ with binding constants up to 14,200 $M^{-1}$ (R = naphthyl). This affinity is attributed to the high electrophilicity of the sulfonamide NH group
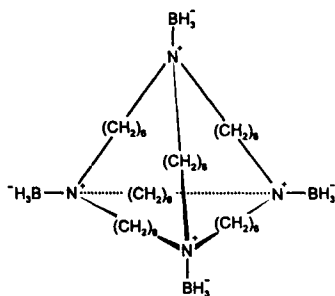


**27**
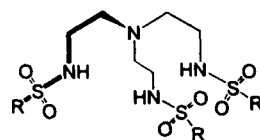
**28**

and preorganization of the binding sites by $\pi$-stacking interactions involving the naphthyl groups.[63] Extension of this work to a range of calix[4]arenesulfonamides **29** resulted in binding constants of up to 103,400 $M^{-1}$ and significant selectivity for $HSO_4^-$ over chloride and nitrate.[64]

From a topological standpoint, the urea functionality is closely related to the guanidinium moiety in that it is similarly predisposed to form bidentate hydrogen bonds to an appropriately functionalized substrate. Appropriately, there has been a recent surge in the design of *neutral* urea- and thiourea-based supramolecular anion receptors.[59,65–69] The increased acidity of the NH protons of thiourea with respect to urea ($pK_a = 21.0$ and 26.9, respectively) suggests that utilization of the former should always lead to stronger binding. This is typically the case, as seen for thioureas **30** and **31** which each show an ~10-fold increase in binding of acetate relative to their urea analogues.[52,69] The urea/thiourea-derivatized calixarenes **32**, however, do not follow this trend and **32a** binds chloride and bromide more effectively. In this instance the increased hydrogen-donating ability of the thiourea functionality may be inhibiting anion complexation by increasing the competing intra- or intermolecular associations among host molecules.[67] Exchange of urea for thiourea may also, in some cases. alter the anion selectivity of a particular host.[70]

Recently, Kelly and Kim have compared the relative binding affinities of urea and bisurea **33** and **34** with carboxylate and its isosteres.[68] They find that both hosts preferentially associate with functionalities according to the following ranking: $ArOPO_3^{2-} \geq ArPO_3^{2-} > ArCO_2^- \geq ArP(OH)O_2^- \geq ArOP(OH)O_2^- > ArSO_3^- > ArSO_3^-$ $\delta$-lactone > $ArNO_2$.

Other neutral hosts have also been prepared based upon the hydrogen-bond donating ability of appropriately arranged amide groups,[71–74] highly fluorinated macrocycles,[75] or even $^{\delta+}S{=}O^{\delta-}$ and $^{\delta+}P{=}O^{\delta-}$ dipoles.[76]



$R^1$ = $CH_2CH_2OCH_3$
$R^2$ = $CH_2CH_2NHC(O)CH_3$

**29**
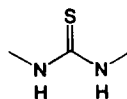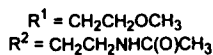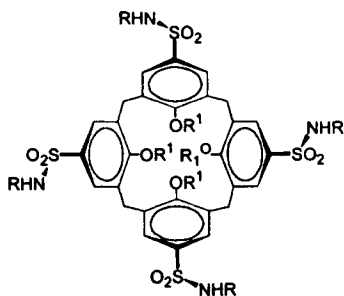
**30**
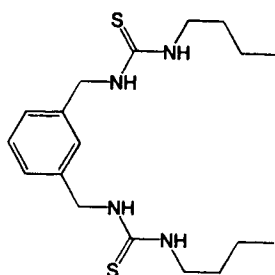
**31**
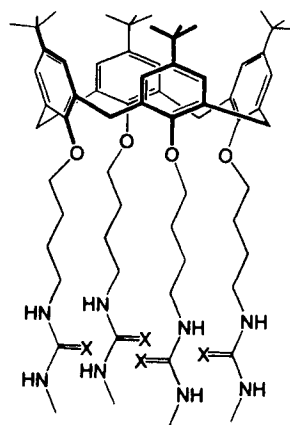
a: X = O
b: X = S

**32**
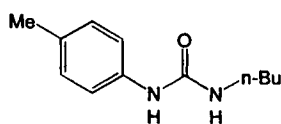
**33**
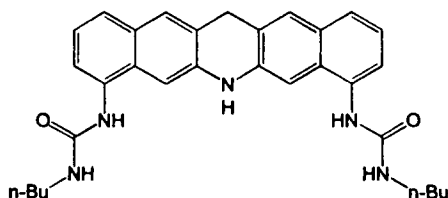
**34**

## 4.2. Inorganic Hosts

Macrocycles such as the calixarenes have become increasingly topical in recent years as a basic framework for the design of various biomimetic host systems.[77,78] In addition to compounds such as **29**, a number of inorganic calixarene-based systems have also been reported in which a Lewis acid metal center is coupled with the hydrophobic nature of the calixarene cavity. The uranyl calixarene complex **35** has been found to be selective for $H_2PO_4^-$, although binding constants are only in the region of 400 $M^{-1}$.[79] It is suggested that anion binding occurs via coordination of the phosphate anion to the oxophilic uranium center and is stabilized by additional hydrogen-bonding interactions to the amide functionalities. In such a case the anion is likely to be significantly removed from the calixarene cavity. Indeed a similar host strategy involving uranyl salene complexes containing pendant benzo-15-crown-5 moieties results in the simultaneous complexation of $K^+$ and $H_2PO_4^-$ with association constants in the region of 1000 $M^{-1}$.[80] Further studies
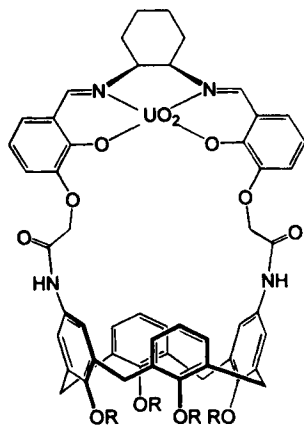
R = n-Pr, CH₂C(O)OEt

**35**
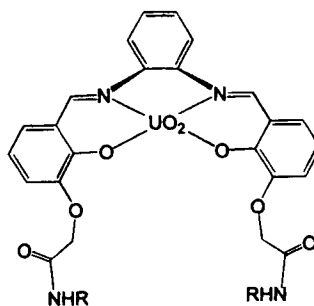


R = 4-MeC₆H₄

**36**

involving X-ray crystallography, multinuclear NMR, cyclic voltammetry, and conductometry upon a wide range of similar hosts such as **36** indicate that the anionic guests do indeed coordinate to the uranium center with $H_2PO_4 \cdots U$ distances in the region of 2.28(2) Å, while additional stabilization is gained by amide$\cdots$phosphate and phosphate$\cdots$acetoxy hydrogen-bonding interactions [N(H)$\cdots$O and O(H)$\cdots$O distances of 2.79(2) and 2.84(2) Å, respectively; Figure 11]. In addition, in the case of **36**, a second phosphate anion is also bound in the solid state via hydrogen-bonding interactions. It is likely that this guest is more weakly held in solution. This multiple recognition, in which the phosphate guest anion acts both as a hydrogen bond donor and acceptor as well as a ligand for the uranium center is reflected in the high value for $K_s$ (measured by conductometry and NMR) which is in excess of $10^5$ in acetonitrile solution and drops to $1.5 \times 10^3$ in DMSO, presumably as a consequence of greater anion solvation.[81]
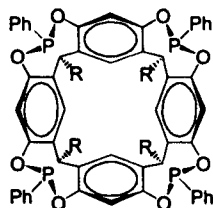


R = CH₂CH₂Ph

**37**
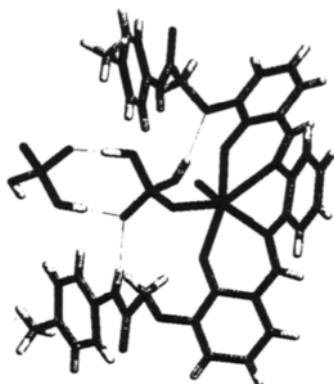
**Figure 11.** Binding of two $H_2PO_4^-$ anions by the uranyl salene host **36**.[81]

An interesting example of halide anion recognition based solely upon size considerations has recently been reported by Puddephatt et al. Reaction of the phosphonito calix[4]arene derivative **37** with silver or copper salts gives the respective tetranuclear metal halide-bridged complexes [**37** $M_4(\mu\text{-Cl})_4(\mu_n\text{-Cl})]^-$ (M = Cu, $n = 3$; M = Ag, $n = 4$) in which a guest chloride engages in a multidentate face-bridging interaction with the square plane containing the metal centers. In the case of the copper complex (Figure 12a) the X-ray crystal structure reveals a triply bridging coordination mode with bound Cu-$(\mu_3\text{-Cl})$ distances ranging from 2.467(5) to 2.548(6) Å. The copper atom that is left out of the $\mu_3$-bridging coordination is in an approximately trigonal planar geometry 2.98 Å away from the $\mu_3$-chloride.[82]
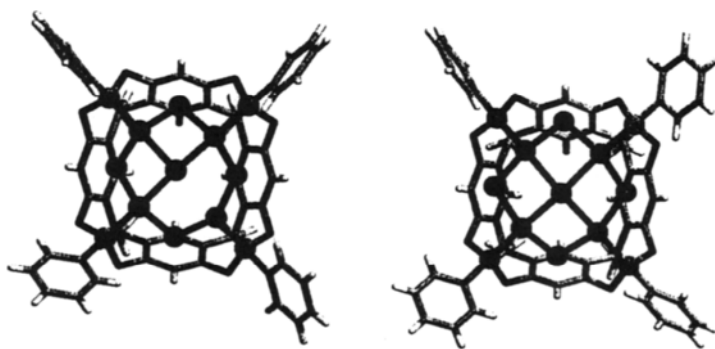


**Figure 12.** (a) X-ray crystal structure of the Cu derivative of the phosphonito calixarene **37**.[82] (b) The Ag complex.[83]

In the case of the silver complex, the presence of the larger metal ion results in a much more symmetrical quadruply bridging coordination mode with Ag-($\mu_4$-Cl) distances 2.69(1)–2.76(1) Å (Figure 12b).[83] Fascinatingly, the $\mu_3$-chloride ligand in the copper complex may be selectively replaced by iodide to give a compound related to that observed in the Ag case, with a symmetrically bridging iodide guest anion [Cu-($\mu_4$-I) = 2.75–2.85 Å].[84] In each case the guest anion is not within the plane of the metal centers but resides below them, within the center of the host cavity, with a unique trigonal or square pyramidal coordination. It is clear that both coordination number and geometry are significantly more malleable in the case of anions than cations.

# 5.  LEWIS ACID HOSTS

Even before the discovery of the katapinands (*vide supra*), work upon bidentate Lewis acid hosts suggested the possibility of chelation of anionic species by acyclic-boron-containing ligands such as $BF_2CH_2CH_2BF_2$. In many ways multidentate Lewis acid hosts may be regarded as the "anticrown",[12] anion-binding equivalent of the crown ethers. Cyclic as well as acyclic compounds of B, Sn, Si, and Hg have been extensively studied. Much of the following chemistry has been reviewed by Katz in 1991[14] and the interested reader is referred to this comprehensive summary as the primary source for further reading. In this section important structural results will be summarized along with the more recent work.

## 5.1.  Hosts Containing Boron and Silicon

One of the simplest neutral anion hosts so far examined is the so-called hydride sponge[85] (1,8-napthalenediylbis(dimethylborane), **38**, cf. proton sponge[86]) which contains two strongly Lewis acidic–$BMe_2$ functionalities preorganized in such a fashion to be able to chelate an anionic or Lewis basic guest. Compound **38** readily and irreversibly abstracts a single hydride anion from a range of hydride sources and the resulting complex is stable even in the presence of moderately strong acids such as acetic acid and $HNEt_3Cl$, although it is slowly decomposed by trityl cation. The X-ray crystal structure of **38-H⁻** shows the chelation of the hydride anion by the two -$BMe_2$ moieties, with refined B–H bond distances of 1.20(5) and 1.49(5) Å. It is unclear whether the hydride ligand is genuinely situated asymmetrically between the boron atoms since related hydride systems[87] exhibit symmetrical bridging modes. Compound **38** also forms stable anion complexes with F⁻ and OH⁻ but not with Cl⁻, presumably as a consequence of the larger ionic radius of the chloride ion, resulting in a poor fit between the two boron binding sites, as well as the weaker Lewis acidic nature of **38**.

In contrast, the more strongly Lewis acidic -$BCl_2$ analogue of **38**[88] is capable of binding chloride. The crystal structure of this material reveals that the guest chloride lies out of the plane of the naphthalene ring, again consistent with the larger size
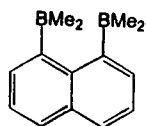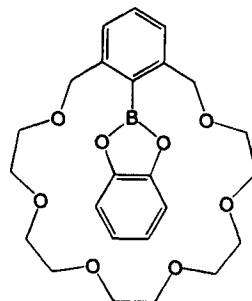
of the chloride anion. The chloride is asymmetrically situated between the two boron atoms with B···Cl distances of 1.66–1.94 Å (two disordered orientations) and B–Cl–B angles of 102° and 110°.

Related work upon mixed borane–silyl compounds of type **39** also results in anion binding, as evidenced by the X-ray crystal structure of the fluoride complex **39-F⁻** in which the silicon expands its coordination number to five, albeit with one long bond to fluorine, 2.714(7) Å, and shorter bonds to the four carbon atoms of 1.87 Å (av).[89] The B···F distance is much shorter at 1.475(6) Å and it is clear that the relatively low Lewis acidity of tetravalent silicon results in only a weak interaction, thought to kinetically, but not thermodynamically, stabilize the complex relative to the unhindered dimethylnapthylborane.[14,89] Larger Lewis basic guests may also be accommodated by the use of longer rigid spacer units as in 1,8-anthracenediethynylbis(catechol boronate).[84]

Simultaneous complexation of anions and cations, in a similar way to that reported for 15-crown-5 uranyl salene complexes,[80] has been observed in the 21-membered ring boronate crown ether **40**. Ligand **40** is capable of dissolving stoichiometric amounts of KF in dichloromethane at room temperature to give the KF adduct shown at Figure 13.[91] The fluoride ion is bound to the boron atom out of the plane of the crown ether, which contains the K⁺ ion. Ligand **40** fails to dissolve either KCl or KBr as a consequence of the weaker nature of the B–X bonds. KI and KSCN are dissolved by **40** but without complexation of the boron atom. The stabilization of the K⁺ ion by the crown ether moiety is apparently sufficient in these cases.[91]

A theoretical (AMI molecular orbital) treatment of boron analogues of the katapinand series as well as macrotricyclic compounds related to **16** has also recently appeared. As with the ammonium-based host molecules the macrotricyclic hosts containing four boron atoms exhibited a greater degree of anion specificity as a consequence of the rigidity of their binding sites. In all cases, size selective complexation of halide anions was observed with accompanying decreases in B···B distances and partial $sp^2 \rightarrow sp^3$ rehybridization.[92]
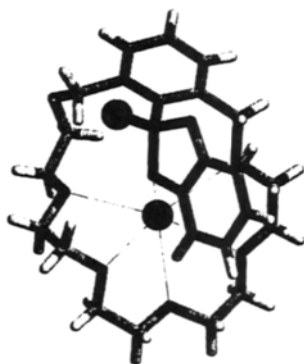
**Figure 13.** A view of one unit of the chain structure created with the solid state complexation of KF by **40**.[91]

## 5.2. Hosts Containing Mercury

A large number of mercuric host compounds have been reported based upon the *o*-phenylenedimercurial moiety **41**.[93] Interaction of **41a** with halide ions results in the formation of complexes soluble in nonpolar media under conditions in which the free hosts are insoluble, while monomercurials disproportionate. Solution $^{199}$Hg NMR measurements indicate that 1:1 complexes with chloride are favored in solution, while the 2:1 host guest complex crystallizes (Figure 14).[93a] Primary bonds to the mercury centers adopt the usual linear arrangement, Hg-Cl 2.93 Å, while the guest anion as well as secondary Hg···Cl interactions form longer bonds 3.17 Å.[93a] This chemistry has been extended to give macrocyclic *o*-phenylenedimercurial-based host compounds by reaction of polymeric mercuric oxo species with various α,ω-dicarboxylic acids.[93b] Tractable products were only obtained from perfluoroglutaric acid, which gave the tetradentate macrocycle **42** in ca 80% yield.



X = Cl, Br, I, CF₃CO₂

**41a-d**

**42**

**43**

**44**



= $C_2B_{10}H_{10}$ (*o*-carborane)
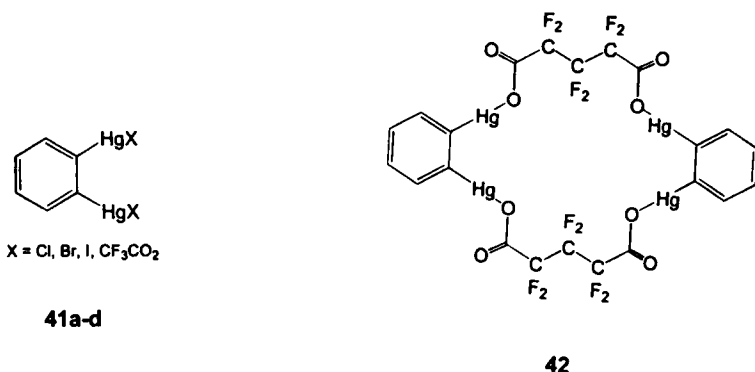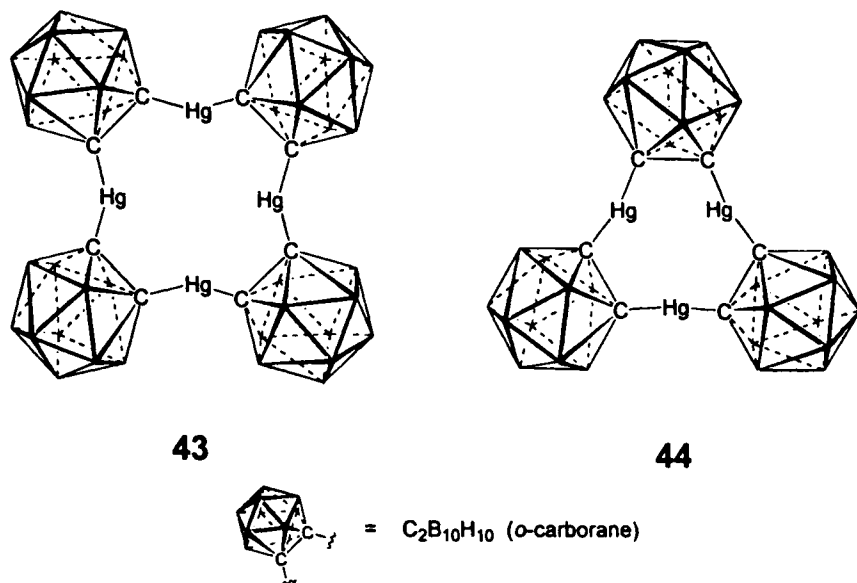
An X-ray crystal structure determination of the bis(thf) adduct of this macrocycle revealed an approximately planar ring of dimensions ca. 12 × 7 Å with the thf guests each chelated by two Hg atoms. No structural results relating to the anion-binding properties of these macrocycles have yet been reported.[93b]

More recent work has yielded another class of carborane-based mercury-containing macrocycles **43** and **44** related to crown ethers such as 12-crown-4 and 9-crown-3.[94] "Anticrown" **43** associates with one or two moles of lithium halide, depending on conditions. The X-ray crystal structure of the chloride salt is shown in Figure 15.
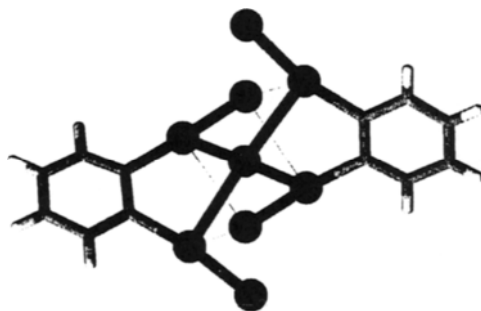


**Figure 14.** X-ray crystal structure of the chloride complex of the *o*-phenylenedimercurial host **41a**.[93a]

**Figure 15.** X-ray crystal structure of the mercuric carborand chloride complex **43**-Cl⁻.[94]

The guest chloride anion interacts equally with all four electrophilic Hg centers with long Hg···Cl bonds of 2.944(2) Å. The anion is situated almost in the plane of the four mercury atoms which deviate from linear coordination with a C–Hg–C angle of 162.0(3)°, suggesting a distortion of the Hg centers towards the guest anion. In the analogous bromide complex the larger ionic radius of the bromide ion results in its being displaced some 0.96 Å (av) out of the plane containing the Hg atoms. The average Hg–Br contact is 3.063(5) Å. A related 1:2 structure is formed between **43** and iodide with iodide ions 1.96 Å above and below the plane of the mercury atoms.

The X-ray crystal structures of the related, though less complex, "anticrown" mercury-containing macrocycles **45** and **46** have also recently been reported.[95,96] Complex **45** may form either 1:1 complexes with Br⁻ or I⁻ or a 3:2 complex with Cl⁻. In the case of the bromo derivative, crystallographic results reveal an infinite chain of alternating Br⁻ and **45** with each halide bridging between six Hg atoms, Hg···Br 3.07–3.39 Å. It is postulated that the related 3:2 chloride complex exhibits a similar, though finite layered structure. The related pentameric species **46** forms



**45**



**46**

(n = 6, 8, 10, 12)
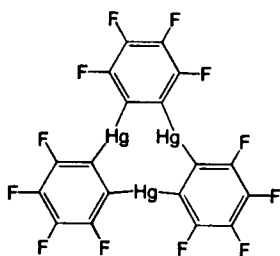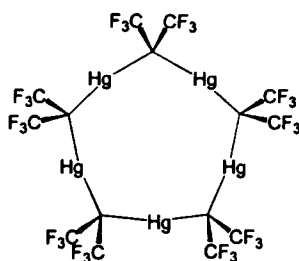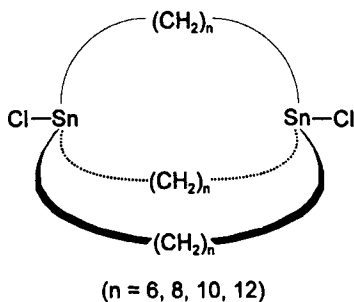
**47a-d**

1:2 complexes with Cl⁻ and Br⁻ with halide ions residing above and below the plane containing the Hg ions, Hg···Cl 3.09–3.39 Å.

## 5.3. Hosts Containing Tin

Work by Newcomb et al. has resulted in the synthesis of a number of macrocyclic and macrobicyclic host molecules somewhat related to the katapinands (*vide supra*) containing two Lewis acidic chloro-substituted tin centers separated by macrocyclic



a                    b
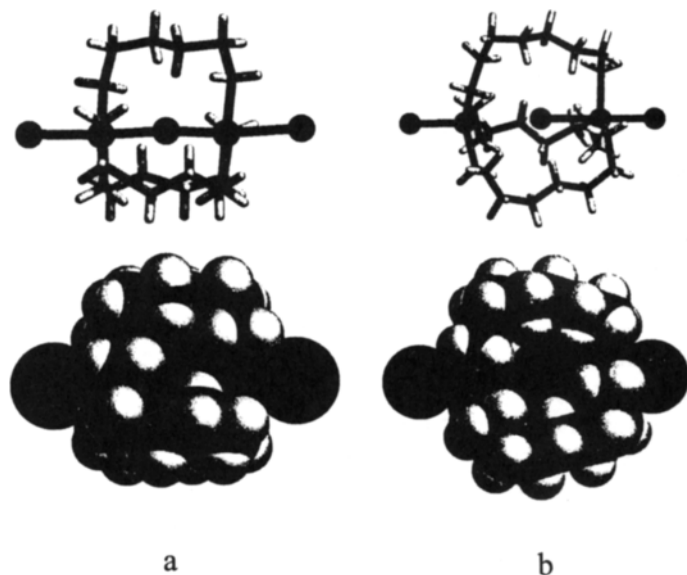
**Figure 16.** X-ray crystal structures (a) of the fluoride complex of the tin containing macrobicycle **47a** and (b) the chloride complex of **47b**.[98b]

cavities of varying dimensions. In the case of the monocyclic compounds, solution $^{119}$Sn NMR measurements indicate that the halide affinity is relatively weak ($K_s$ up to ca. 1000 M$^{-1}$), presumably as a consequence of the relatively flexible nature of the ligands.[97] In contrast, the macrobicyclic analogues **47** in which the conformation at tin and the size of the macrocyclic cavity are more rigidly enforced, demonstrate a marked anion affinity and selectivity.[98] In particular, complexes **47b** and **47c** bind chloride markedly more strongly than either the smaller or longer chain analogues, while **47a** is selective for fluoride.

The binding of halide ions within the cavity of these macrocycles has been confirmed for **47a**-F$^-$ and **47b**-Cl$^-$ by X-ray crystal structure determinations (Figure 16).[98b] In the case of **47a**, the fluoride anion adopts an approximately symmetrically bridging mode with relatively short Sn–F distances of 2.12(4) and 2.28(4) Å. In comparison the chloride ion is situated asymmetrically in the larger macrocycle **47b**, apparently frozen between dissociation from one Sn center and binding to the other; Sn···Cl distances are 2.610(5) and 3.388(5) Å. Sn···Cl distances to the exterior chloride ligands are 2.745(5) Å, for the trigonal bipyramidal metal center; 2.415(5) Å, for the tetrahedrally coordinated tin; and 2.373(3) Å in the free host. Solution $^{119}$Sn NMR measurements indicate that a rapid equilibrium exists in solution with the chloride ion hopping between the two metal centers even at −100 °C.[98]

# 6. ORGANOMETALLIC HOSTS

Extensive work by Beer et al.[99] has resulted in the synthesis of a range of anion-binding hosts containing cationic electrochemically active tris(bipyridyl)ruthenium(II),[100] cobalticinium,[101] and/or ferrocenyl[101d,101i,102] moieties coupled with additional recognition sites such as crown ethers,[101f] porphyrins,[101i] calixarenes,[100,101e,101g] and, particularly, amide functionalities.[100,101b–101i] A number of these materials are capable of either spectral or electrochemical recognition of inorganic phosphate, biologically relevant polyphosphate anions, carboxylates, halides, or hydrogen sulfate. These types of materials are of great interest since they are among the few which display the ability to *sense* anionic components of a solution. In most cases anion recognition is guided by electrostatic attraction to the transition metal ion and hydrogen-bonding interactions with an amide functionality as well as hydrophobic and topological considerations. Unfortunately, relatively few X-ray crystal structure determinations have appeared, and little is known about the exact nature of the synergy between these diverse interactions. The X-ray crystal structure of calixarene **48** and its acyclic analogue **49**, however, clearly demonstrate the role of the amide functionalities concerning the interaction of the host complexes with H$_2$PO$_4^-$ and chloride, respectively. The crystal structure of the cobaltocenium complex **50** has also appeared but shows no remarkable association with the PF$_6^-$ anions in the solid state (Figure 17). A brief review of these excellent studies by Beer et al. has recently appeared.[99] Also, related work using resolved, chiral
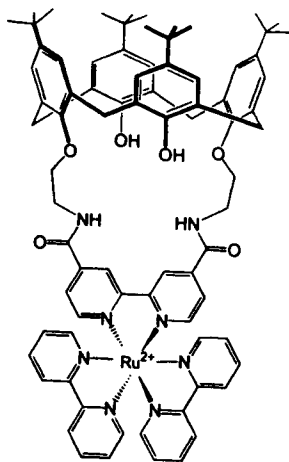
**48**
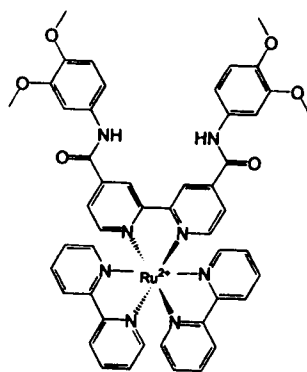
**49**

cobaltocenium complexes has resulted in a series of receptors capable of responding to the chirality of guests such as camphor-10-sulfonate.[103]

Recently, our own group has taken a different approach to the use of calixarenes and related macrocycles as anion hosts. Direct attachment of cationic transition metal fragments to the outside arene faces of the calixarene bowl transforms the ostensibly electron-rich cavity into one which is amenable for the inclusion of anionic species.

Typically, the cumulative electron-withdrawing effect of metallating *more* than half of the arenes of the macrocycle is required in order to observe anion inclusion.[104] Thus, we have focused on tetrametallated derivatives of calix[4]arene and di- or trimetalated derivatives of the related *ortho*-cyclophane, cyclotriveratrylene (CTV). The X-ray crystal structure of the $BF_4^-$ salt of the water soluble "bear trap" **51** demonstrates the suitability of the narrow calix[4]arene cavity for small tetra-
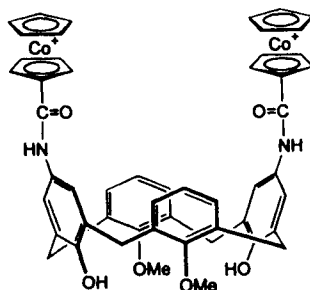


**50**

**Figure 17.** X-ray crystal structure of cobaltocenium host **50**.

hedral anions (Figure 18a). Strong electrostatic attractions exist between the fluorine atoms of the anion and the ring carbon atoms with F···C contacts as short as 2.85 Å.[105] For comparison, $BF_4$···C distances are almost exclusively longer than 3.0 Å in noncavity systems. The tetrafluoroborate anion may be displaced by treatment with [$NBu_4$]I to give the analogous iodide salt (Figure 18b) which exhibits I···C contacts of ca. 3.7 Å, consistent with the large ionic radius of iodide. Interestingly, the iodide anion is situated some 0.11 Å lower in the cavity than the boron atom in the $BF_4^-$ salt, consistent with the larger size of the tetrafluoroborate anion.[105] Formation of such organometallic hosts is extremely general[106,107] and a number of crystallographic results involving **51**,[105] the iridium metallated host **52**,[106] or the metallated p-t-butylcalix[5]arene[108] derivative **53** highlight the anion inclusion capabilities of these molecules.

$^1$H NMR titration data in aqueous solution involving the triflate salt of **51** with a variety of anions is often complex and must be modeled in terms of a number of
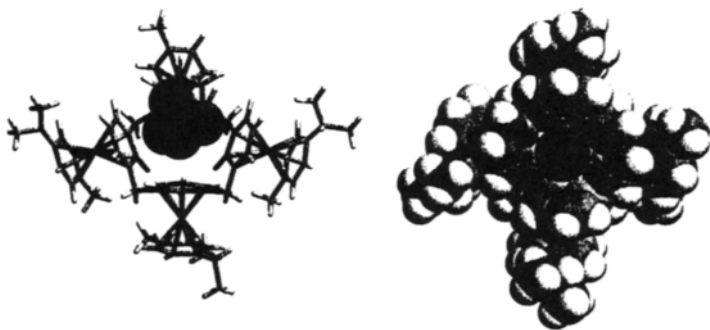


**Figure 18.** X-ray crystal structure of the organometallic "bear trap" host (**a**) with included $BF_4^-$ anion[105] and (**b**) included iodide.[106]
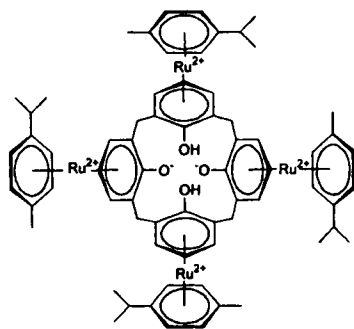
**51**

binding processes, suggesting that anion association occurs at the exterior of the cavity as well as within. This is not surprising considering that, in the solid state of these types of sandwich compounds, anions are typically found to be located on either side of the metal center. Thus, it would be reasonable to observe binding sites exterior to the cavity due to the close proximity of multiple metal centers. Host **51** displays a somewhat size selective association with chloride over other halides.[106]

In analogous fashion, the ruthenium- or iridium-based bimetallic and trimetallic CTV complexes such as **54–57** also make excellent anion hosts. The CTV cavity, however, is wider and more shallow and hence, the $BF_4^-$ anion is too small to be effectively bound. This is evidenced by the crystal structures of the $BF_4^-$ salts of **56** and the iridium analogue **57** in which the anion within the cavity is either extremely disordered or is situated to one side of the cavity. We have found that host **54** exhibits a pronounced selectivity for $TcO_4^-$ in nonaqueous solutions, presumably as a consequence of the wide cavity in conjunction with the larger anion size.[104,109] Indeed, the X-ray crystal structure of the mixed $ReO_4^-/CF_3SO_3^-$ salt shows the
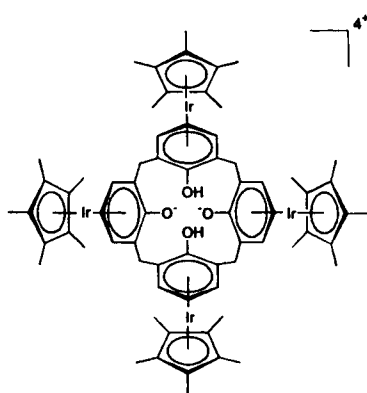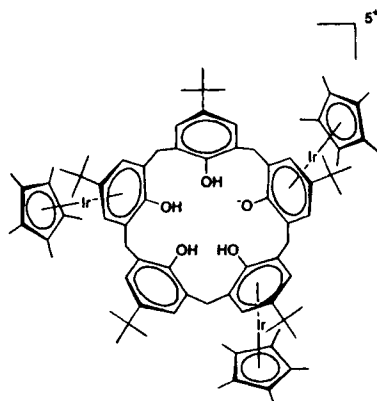
**52**                                    **53**
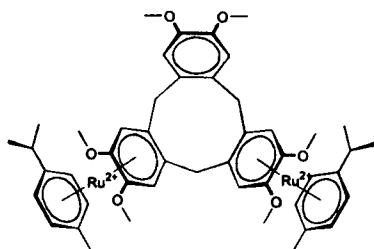
**54**
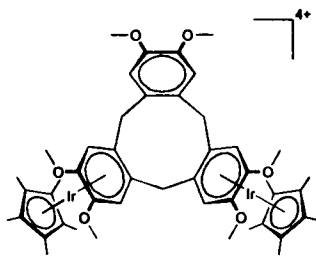


**55**
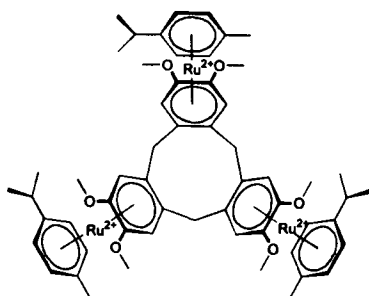


**56**
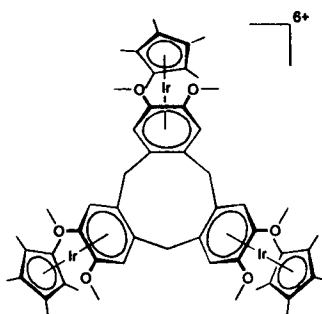


**57**

TcO$_4^-$ analogue to be almost perfectly situated with its three oxygen atoms down into the cavity and more or less in line with the pseudo threefold axis (Figure 19).

We have shown that host **54** can be employed to extract TcO$_4^-$ from aqueous solutions at relatively low concentrations. When a NO$_2$Me solution of **54** [CF$_3$SO$_3$]$_4$ (3.25 mM) is vortexed with a equal volume saline solution of Na[TcO$_4$] (3.25 mM) spiked with radiotracer $^{99m}$TcO$_4^-$, 84(1)% of the radioactivity is transferred into the organic phase. Up to 88(2)% of the TcO$_4^-$ can be extracted if the host concentration is increased to 10 mM. Remarkably, the extraction can also be performed in the
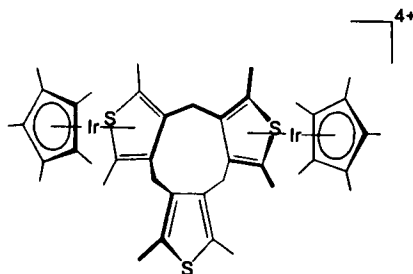


**58**
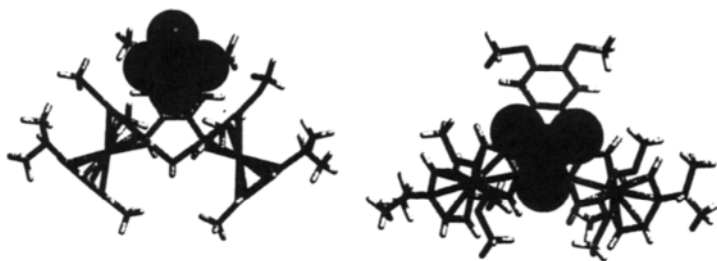
**Figure 19.** Perrhenate inclusion within the cavity of **54**.[109a] (a) top view; (b) side view.

presence of large excesses of chloride, sulfate, or nitrate with almost no loss in extraction efficiency.

In an effort to examine the "cavity effect" in these systems we have recently compared the anion binding ability of host **54** with that of the related dimetallated tricyclic macrocycle **58** which does not adopt the bowl conformation.[110] The crystal structure of **58** shows its twisted conformation (Figure 20). $^1$H NMR titration experiments were used to measure the affinity of host **54** for bromide in NO$_2$Me-$d_3$. Again, as with **50**, the chemical shift changes indicate complicated binding equilibrium in solution and these were best modeled in terms of three binding sites—one within the cavity, and two exterior to it, in association with the metal centers. Association constants of up to 1100 were determined. The $^1$H NMR spectrum of host **58** shows very little change upon addition of bromide under the same conditions.

Much work by Lehn et al. has been dedicated to the self-assembly of helical coordination complexes. Recently, ligand **59** has been shown to self-assemble with five iron(II) ions to form an intricate circular double helicate of 10$^+$ charge which surrounds and encapsulates a chloride ion.[111] This chloride ion seemingly cannot be exchanged for larger ions as the inner core of the helicate ($r_{core}$ = 1.75 Å) is nearly of perfect size for this anion ($r_{Cl^-}$ = 1.81 Å).
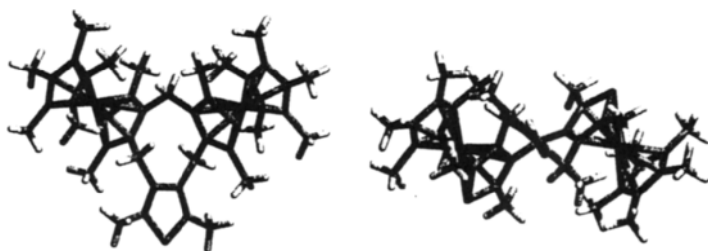


**Figure 20.** X-ray crystal structure of host **58** which lacks a molecular cavity.
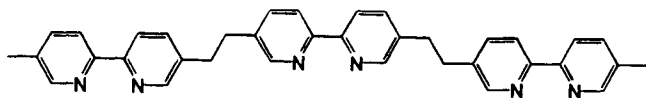
**59**

# 7. TRANSITION METAL COORDINATION HOSTS

An obvious possibility in the design of supramolecular anion receptors is the incorporation of a metal center in with which the anion may form a coordinate bond. Some examples of this type (e.g. **36**) have already been mentioned. This section discusses a number of other metal complexes capable of "multipoint" molecular recognition based upon binding anionic ligands to a metal center along with the incorporation of other stabilizing interactions.

## 7.1. Zinc Complexes

Reaction of $Zn(ClO_4)_2 \cdot 6H_2O$ with acridine-pendant cyclen affords the Zn(II) host molecule **60**.[112] The combination of π-stacking interactions with the acridine functionality, hydrogen bonding with the NH protons of the cyclen ring, and coordinative interaction with the metal center enables **60** to recognize and bind thymidine and its analogues from a mixture of nucleosides in aqueous solution at physiological pH. Selectivity for thymidine analogues is dependent on the fact that these substrates possess an imide functionality enabling them to bind to the Zn(II) center. Stability constant measurements in aqueous buffer suggest a high affinity of both **60** and its acridine-free analogue for thymidine-related nucleosides with log $K_s$ values in the range 5.7–7.2. The X-ray crystal structure of the complex formed between **60** and deprotonated methylthymine (Figure 21) demonstrates the remarkable multipoint recognition of this and related anions. In addition to Zn(II)-$N_{thymine}$ coordination, two of the three cyclen NH groups form hydrogen bonds to the carbonyl functionalities either directly [N(H)···O = 2.881(5) Å], or via a water molecule. π-Stacking interactions between the thymine and the acridine fragments
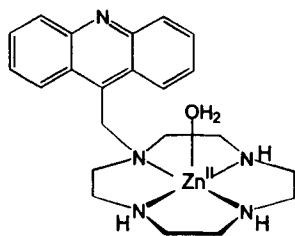


**60**
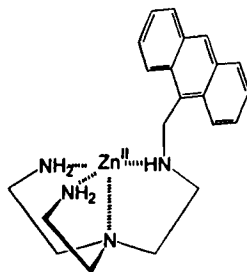


**61**
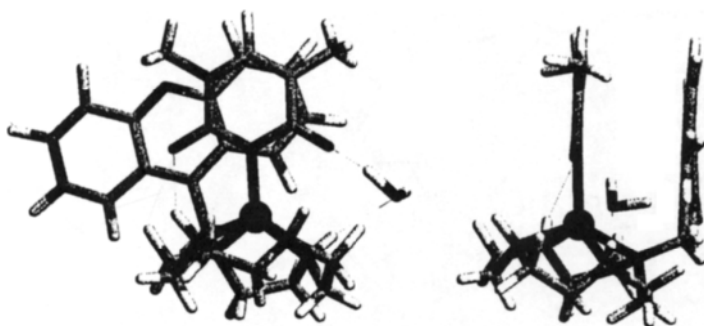
**Figure 21.** X-ray crystal structure of the Zn(II) cyclen complex **60** with the methylthymine anion[112] showing a view (**a**) perpendicular to and (**b**) parallel with the plane of the acridine moiety.

also play an important role in the recognition and enhance the binding ability of **60** with respect to its acridine-free analogue. Stacking separations (C···C) are in the range of 3.28–3.42 Å.[112]

A related receptor based upon a chiral, resolved Zn(II) porphyrin complex has been shown to differentiate between enantiomers of a range of substituted amino acids with selectivity of up to 96% for L-benzyloxycarbonylvalinate. The combination of metal coordination and hydrogen-bonding interactions are again responsible for the observed selectivity.[113]

Ultimately, one of the goals in the development of supramolecular anion receptors is to make use of their ability in the form of anion-sensing devices. In this regard, the Zn(II) containing host **61** is able to signal the binding of carboxylates with electron-donating or electron-accepting properties (e.g. 4-$N$,$N$-dimethylaminobenzoate, DMAB) by quenching the fluorescence intensity of the anthracenyl group. Notably, no quenching is observed with nitrate or thiocycanate and these anions do not interfere with the quenching activity of DMAB.[114]

## 7.2. Copper Complexes

Reaction of copper perchlorate with a silver complex of the 30-membered macrocyclic Schiff's base ligand **62** (L) gives the di-copper host $Cu_2L(ClO_4)_4 \cdot 3H_2O$. In the presence of anions such as $N_3^-$ and $OH^-$ the perchlorate anions are replaced by both terminal and bridging azide or hydroxide to give a five-coordinate square pyramidal di-copper complex. The X-ray crystal structure of the azide derivative has been determined and shows that longer bonds are formed to the singly bridging azide anion (2.25 Å) than to the terminal ligands (1.94 Å). The anion bridges between the two metal centers to give a Cu···Cu distance of 6.02 Å (Figure 22).[115]
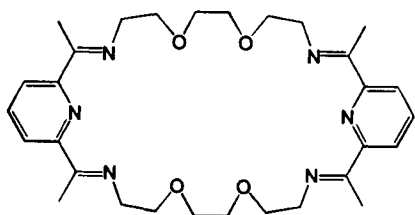
**62**
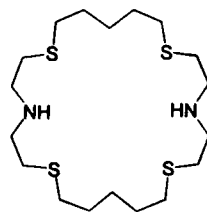


**63**
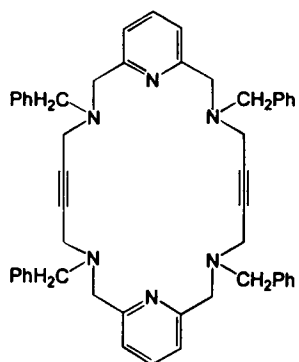


**64**



***Figure 22.*** X-ray crystal structure of the di-copper complex of **62** with azide anion.[115]

A related di-copper complex of the 24-membered macrocycle **63** binds four azide ions to give a neutral species containing two bridging and two terminal anions,[116] while the di-copper species of another 24-membered cryptand has also been shown to bind the imidazolate anion in a singly bridging fashion, $Cu-N_{imid} = 1.946$ Å.[117] Also, work by Martell et al. has shown that a wide range of related complexes may be formed in solution with various anions including inorganic phosphates, often with remarkably high stability constants.[118]

Recently, a cyanide-recognition electrode based upon a copper(II) complex of ligand **64** embedded in a plasticized PVC membrane has been described. The electrode response is fast, reversible, and very selective for cyanide with working concentration ranges of $10^{-2}$ to $10^{-2}$ M (pH = 10).[119]

## 7.3. Oxovanadium Hosts

A final class of anion host is based upon the reaction of various vanadate salts with alkyl phosphates in the presence of halides. Formation of a wide variety of oxovanadium cage-like cluster species has been observed, many of which incorporate anions or both anions and cations within large, spherical cavities. Reaction of $tBuPO_3H$ with $[PPh_4][VO_2Cl_2]$ gives the chloride inclusion species $[(V^VO)_5(V^{IV}O)(tBuPO_3)_8Cl]$ **65**. The X-ray crystal structure of this material (Figure 23) reveals the fact that the single halide anion is encapsulated within the cage-like oxovanadium system, and indeed may well act as a template for cluster formation.[120]

A related reaction results in the formation of the bis(ammonium chloride) inclusion species $[2NH_4^+, 2Cl^- \subset V_{14}O_{22}(OH)_4(H_2O)_2(C_6H_5PO_3)_8]^{6-}$ in which a
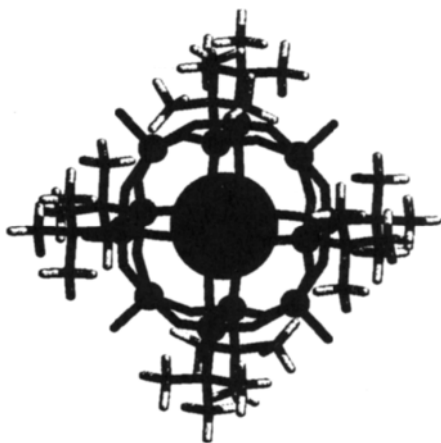


***Figure 23.*** X-ray crystal structure of the chloride inclusion complex **65**.[120]

nanometer wide cavity contains a square planar array of two ammonium cations and two chloride anions. The ammonium cation is located at the center of a near-planar coronand fragment analogous to a hypothetical 16-crown-8 macrocycle with $NH_4\cdots O$ distances of 2.99–3.66 Å. The chloride anions are situated between 3.32 and 3.63 Å to the vanadium centers.[121]

## 8. CONCLUDING REMARKS

For reasons such as high anion solvation energy, coordinative saturation, and large size it is clear that anion binding occurs much less readily than in related cation systems. Host–anion interactions are, to a large extent, dominated by nondirectional electrostatic forces, with small chelate and macrocyclic effects as well as considerations based upon host geometry, size, and degree of preorganization playing a distinctly secondary role.

For anions, it is tempting to try and attribute a preferential coordination geometry analogous to that so well established for various metal cations. In many cases simple anions such as the halides exist in approximately tetrahedral or octahedral environments, but it is clear from the diversity of examples reviewed herein that anion coordination geometry is highly flexible and may be adjusted to fit the properties of the various host systems.

It is clear that, in spite of dramatic recent advances and the enormous variety of anion hosts synthesized to date, the problem of achieving strong, selective complexation still remains for a large majority of anionic guests and will doubtless be the subject of a great deal of rich and innovative chemistry in the future.

## ACKNOWLEDGMENTS

## REFERENCES

1. Lehn, J.-M. *Supramolecular Chemistry*; VCH Publishers: Weinheim, 1995.
2. (a) Lange III, L. G.; Riordan, J. F.; Vallèe, B. L. *Biochem.* **1974**, *13*, 4361; (b) Schmidtchen, F. P. *Nachr. Chem. Tech. Lab.* **1988**, *36*, 8.
3. Stuckey, J. A.; Schubert, H. L.; Fauman, E. B.; Zhang, Z.-Y.; Dixon, J. E.; Saper, M. A. *Nature* **1994**, *370*, 571.
4. Pflugrath, J. W.; Quiocho, F. A. *Nature* **1985**, *314*, 257.
5. Pflugrath, J. W.; Quiocho, F. A. *J. Mol. Biol.* **1988**, *200*, 163.
6. He, J. J.; Quiocho, F. A. *Science* **1991**, *251*, 1497.
7. Luecke, H.; Quiocho, F. A. *Nature* **1990**, *347*, 402.
8. Kanyo, Z. F.; Christianson, D. W. *J. Biol. Chem.* **1991**, *266*, 4264.
9. (a) Hiraoka, M. *Crown Compounds. Their Characteristics and Applications*; Kodansha: Tokyo, 1978; (b) Gokel, G. *Crown Ethers and Cryptands*; RSC Publishers: Cambridge, 1991; (c) *Cation Binding by Macrocycles*; Inoue, Y.; Gokel, G. W., Eds., Marcel Dekker: New York, 1990.

10. (a) Dietrich, B. In *Inclusion Compounds*; Atwood, J. L.; Davies, J. E. D.; MacNicol, D. D., Eds.; Oxford University Press: Oxford, 1984, Vol. 2, Ch. 10, pp. 373–405; (b) Dietrich, B. *Pure Appl. Chem.* **1993**, *7*, 1457.

11. (a) Hosseini, M. W.; Lehn, J.-M. *Helv. Chim. Acta* **1987**, *70*, 1312; Sessler, J. L.; Furuta, H.; Král, V. *Supramol. Chem.* **1993**, *1*, 209.

12. Kaufmann, D.; Otten, A. *Angew. Chem. Int. Ed. Engl.* **1994**, *33*, 1832.

13. Goldman, S.; Bates, R. G. *J. Am. Chem. Soc.* **1972**, *94*, 1476.

14. Katz, H. E. In *Inclusion Compounds*; Atwood, J. L.; Davies, J. E. D.; MacNicol, D. D., Eds.; Oxford University Press: Oxford, 1991, Vol. 4, Ch. 9, pp. 391–405.

15. Izatt, R. M.; Pawlak, K.; Bradshaw, J. S.; Bruening, R. L. *Chem. Rev.* **1991**, *91*, 1721.

16. Vögtle, F.; Sieger, H.; Müller, W. M. *Topp. Curr. Chem.* **1981**, *98*, 107.

17. Pierre, J.-L.; Baret, P. *Bull. Soc. Chim. Fr.* **1983**, 367.

18. House, D. A. In *Comprehensive Coordination Chemistry*; Wilkinson, G.; Gillard, R. D.; McCleverty, J. A., Eds.; Pergamon Press: Oxford, 1987, Vol. 2, Ch. 13, pp. 30–34.

19. Gavrushenko, N.; Carrell, H. L.; Stallings, W. C.; Glusker, J. P. *Acta Crystallogr., Sect. B* **1977**, *33*, 3936.

20. Woo, N. H.; Seeman, N. C.; Rich, A. *Biopolymers* **1979**, *18*, 539.

21. Quigley, G. J.; Teeter, M. M.; Rich, A. *Proc. Natl. Acad. Sci. USA* **1978**, *75*, 64.

22. Cullinane, J.; Gelb, R. I.; Margulis, T. N.; Zompa, L. J. *J. Am. Chem. Soc.* **1982**, *104*, 3048.

23. Margulis, T. N.; Zompa, L. J. *Acta Crystallogr., Sect. B* **1981**, *37*, 1428.

24. Santos, M. A.; Drew, M. G. B. *J. Chem. Soc., Faraday Trans.* **1991**, *87*, 1321.

25. (a) Kimura, E.; Sakonaka, A.; Yatsunami, T.; Kodama, M. *J. Am. Chem. Soc.* **1981**, *103*, 3041. (b) Kimura, E.; Sakonata, A.; Kodama, M. *J. Am. Chem. Soc.* **1982**, *104*, 4984.

26. Kimura, E.; Anan, H.; Koike, T.; Shiro, M. *J. Org Chem.* **1989**, *54*, 3998.

27. Dietrich, B.; Hosseini, M. W.; Lehn, J. -M.; Sessions, R. B. *J. Am. Chem. Soc.* **1981**, *103*, 1282.

28. (a) Hosseini, M. W.; Lehn, J. -M. *J. Chem. Soc., Chem. Commun.* **1988**, 397. (b) Hosseini, M. W.; Lehn, J. -M. *Helv. Chim. Acta* **1987**, *70*, 1312. (c) Fenniri, H.; Lehn, J -M. *Chem. Soc., Chem. Commun.* **1993**, 1819.

29. (a) Boudon, S.; Decian, A.; Fischer, J.; Hosseini, M. W.; Lehn, J. -M.; Wipff, G. *Coord. Chem.* **1991**, *23*, 113. (b) Papoyan, G.; Gu, K. J.; Wiorkiewiczkuczera, J.; Kuczera, K.; Bowman-James, K. *J. Am. Chem. Soc.* **1996**, *118*, 1354.

30. Motekaitis, R. J.; Martell, A. E. *Inorg. Chem.* **1992**, *31*, 5534.

31. Nation, D. A.; Reibenspies, J.; Martell, A. E. *Inorg Chem.* **1996**, *35*, 4597.

32. Fenniri, H.; Lehn, J.-M.; Marquis-Rigault, A. *Angew. Chem. Int. Ed. Engl.* **1996**, *35*, 337.

33. Bianchi, A.; Micheloni, M.; Paoletti, P. *Pure Appl. Chem.* **1988**, *60*, 525.

34. (a) Bencini, A.; Bianchi, A.; Micheloni, M.; Paoletti, P.; Dapporto, P.; Paoli, P; Garcia-España, E. *J. Incl. Phenom.* **1992**, *12*, 291. (b) Bencini, A.; Bianchi, A.; Dapporto, P.; Garcia-España, E.; Micheloni, M.; Paoletti, P.; Paoli, P. *J. Chem. Soc., Chem. Commun.* **1990**, 753.

35. Bencini, A.; Bianchi, A.; Dapporto, P.; Garcia-España, E.; Micheloni, M.; Ramirez, J. A.; Paoletti, P.; Paoli, P. *Inorg. Chem.* **1992**, *31*, 1902.

36. (a) Bianchi, A.; Garcia-España, E.; Mangani, S.; Micheloni, M.; Orioli, P.; Paoletti, P. *J. Chem. Soc., Chem. Commun.* **1987**, 729. (b) Bencini, A.; Bianchi, A.; Garcia-España, E.; Giusti, M.; Mangani, S.; Micheloni, M.; Orioli, P.; Paoletti, P. *Inorg Chem.* **1987**, *26*, 3902.

37. Aoki, K.; Tokuno, T.; Takagi, K.; Hirose, Y.; Suh, I. -H.; Adeyemo, A. O.; Williams, G. N. *Inorg. Chim. Acta* **1993**, *210*, 17.

38. Vance, D. H.; Czarnik, A. E. *J. Am. Chem. Soc.* **1994**, *116*, 9397.

39. (a) Sessler, J. L.; Cyr, M. J.; Lynch, V.; McGhee, E.; Ibers, J. A. *J. Am. Chem. Soc.* **1990**, *112*, 2810. (b) Shionoya, M.; Furuta, H.; Lynch, V.; Harriman, A.; Sessler, J. L. *J. Am. Chem. Soc.* **1992**, *114*, 5714.

40. Sessler, J. L.; Andrievsky, A.; Gale, P. A.; Lynch, V. *Angew. Chem. Int. Ed. Engl.* **1996**, *35*, 2782.

41. Cramer, R. E.; Fermin, V.; Kuwabara, E.; Kirkup, R.; Selman, M.; Akoi, K.; Adeyemo, A.; Yamazaki, H. *J. Am. Chem. Soc.* **1991**, *113*, 7033.
42. Park, C. H.; Simmons, H. E. *J. Am. Chem. Soc.* **1968**, *90*, 2431.
43. Bell, R. A.; Christoph, G. G.; Fronczek, F. R.; Marsh, R. E. *Science* **1975**, *190*, 151.
44. (a) Wester, N.; Vogtle, F. *Chem. Ber.* **1980**, *113*, 1487. (b) Rossa, L.; Vogtle, F. *Liebig's Ann. Chem.* **1981**, 459.
45. Graf, E.; Lehn, J. -M. *J. Am. Chem. Soc.* **1976**, *98*, 6403.
46. (a) Cram, D. J.; Trueblood, K. N. *Top. Curr. Chem.* **1981**, *98*, 43. (b) Cram, D. J. *Angew. Chem. Int. Ed. Engl.* **1986**, *25*, 1039.
47. Metz, B.; Rosalky, J. M.; Weiss, R. *J. Chem. Soc., Chem. Commun.* **1976**, 533.
48. Schmidtchen, F. P.; Müller, G. *J. Chem. Soc., Chem. Commun.* **1984**, 1115.
49. (a)Schmidtchen, F. P. *Chem. Ber.* **1981**, *114*, 597.
50. (a) Dietrich, B.; Lehn, J. -M.; Guilhem, J.; Pascard, C. *Tetrahedron Lett.* **1989**, *30*, 4125. (b) Reilly, S.; Khalsa, G. R. K.; Ford, D. K.; Brainard, J. R.; Hay, B. P.; Smith, P. H. *Inorg. Chem.* **1995**, *34*, 569. (c) Dietrich, B.; Dilworth, B.; Lehn, J.-M.; Cesario, M.; Guilhem, J.; Pascard, C. *Helv. Chim. Acta* **1996**, *79*, 569.
51. (a) Lehn, J. -M.; Sonveaux, E,; Willard, A. K. *J. Am. Chem. Soc.* **1978**, *100*, 4914. (b) Dietrich, B.; Guihem, J.; Lehn, J. -M.; Pascard, C.; Sonveaux, E. *Helv. Chim. Acta* **1984**, *67*, 91.
52. Lehn, J. -M.; Méric, R.; Vigneron, J. -P.; Bkouche-Waksman, I.; Pascard, C. *J. Chem. Soc., Chem. Commun.*, **1991**, 62.
53. Morgan, G.; McKee, V.; Nelson, J. *J. Chem. Soc., Chem. Commun.* **1995**, 1649.
54. (a) Adams, J. M.; Small, R. W. H. *Acta. Crystallogr., Sect B* **1974**, *30*, 2191. (b) Adams, J. M.; Pritchard, R. G. *Acta Crystallogr., Sect B* **1976**, *32*, 2438. (c) Adams, J. M.; Small, R. W. H. *Acta Crystallogr., Sect. B* **1976**, *32*, 832.
55. Cotton, F. A.; Day, V. W.; Hazen, E. E. Jr.; Larsen, S. *J. Am. Chem. Soc.* **1973**, 95, 4834.
56. Dietrich, B.; Fyles, D. L.; Fyles, T. M.; Lehn, J. -M. *Helv. Chim. Acta* **1979**, *62*, 2763.
57. (a) Dixon, R. P.; Geib, S. J.; Hamilton, A. D. *J. Am. Chem. Soc.* **1992**, *114*, 365. (b) Jubian, V.; Dixon, R. P.; Hamilton, A. D. *J. Am. Chem. Soc.* **1992**, *114*, 1120. (c) Schießl, P.; Schmidtchen, F. P. *J. Org. Chem.* **1994**, *59*, 509. (d) Müller, G.; Riede, J.; Schmidtchen, F. P. *Angew. Chem. Int. Ed. Engl.* **1988**, *27*, 1516. (e) Gleich, A.; Schmidtchen, F. P.; Mikulcik, P.; Müller, G. *J. Chem. Soc., Chem. Commun.* **1990**, 55.
58. Schießl, P.; Schmidtchen, F. P. *Tetrahedron Lett.* **1993**, *34*, 2449.
59. Fan, E.; Van Arman, S. A.; Kincaid, S.; Hamilton, A. D. *J Am. Chem. Soc.* **1993**, *115*, 369.
60. Echavarren, A.; Galan, A.; Lehn, J. -M.; de Mendoza, J. *J. Am. Chem. Soc.* **1989**, *111*, 4994.
61. Kneeland, D. M.; Ariga, K.; Lynch, V. M.; Huang, C. -Y.; Anslyn, E. V. *J. Am. Chem. Soc.* **1993**, *115*, 10042.
62. Worm, K.; Schmidtchen, F. P.; Schier, A.; Schafer, A.; Hesse, M. *Angew. Chem. Int. Ed. Engl.* **1994**, *33*, 327.
63. Valiyaveettil, S.; Engbersen, J. J. F.; Verboom, W.; Reinhoudt, D. N. *Angew. Chem. Int. Ed. Engl.* **1993**, *32*, 900.
64. Morzherin, Y.; Rudkevich, D. M.; Verboom, W.; Reinhoudt, D. N. *J. Org Chem.* **1993**, *33*, 7602.
65. Smith, P. J.; Reddington, M. V.; Wilcox, C. S. *Tetrahedron Lett.* **1992**, *33*, 6085.
66. Hamann, B. C.; Branda, N. R.; Rebek, J. Jr., *Tetrahedron Lett.* **1993**, *34*, 6837.
67. Scheerder, J.; Fochi, M.; Engberson, J. F. J.; Reinhoudt, D. N. *J. Org Chem.* **1994**, *59*, 7815.
68. Kelly, T. R.; Kim, M. H. *J. Am. Chem. Soc.* **1994**, *116*, 7072.
69. Nishizawa, S.; Buhlmann, P.; Iwao, M.; Umezawa, Y. *Tetrahedron Lett.* **1995**, *36*, 6483.
70. Scheerder, J.; Engberson, J. F. J.; Casnati, A.; Ungaro, R.; Reinhoudt, D. N. *J. Org. Chem.* **1995**, *60*, 6448.
71. Pascal, R. A.; Spergel, J.; Engen, D. V. *Tetrahedron Lett.* **1986**, *27*, 4099.
72. Heyer, D.; Lehn, J.-M. *Tetrahedron Lett.* **1986**, *27*, 5869.

73. Raposo, C.; Pérez, N.; Almaraz, M.; Mussons, L.; Caballero, C.; Móran, J. R. *Tetrahedron Lett.* **1995**, *36*, 3255.
74. Davis, A. P.; Gilmer, J. F.; Perry, J. J. *Angew. Chem. Int. Ed. Engl.* **1996**, *35*, 1312.
75. Farnham, W. B.; Roe, D. C.; Dixon, D. A.; Calbrese, J. C.; Harlow, R. L. *J. Am. Chem. Soc.* **1990**, *112*, 7707.
76. Savage, P. B.; Holmgren, S. K.; Gellman, S. H. *J. Am. Chem. Soc.* **1994**, *116*, 4069.
77. Gutsche, C. D. *Calixarenes*; Stoddart, J. F., Ed.; Royal Society of Chemistry Publishers: Cambridge, 1989.
78. *Calixarenes: A Versatile Class of Macrocyclic Compounds*; Vincens, J.; Bohmer, V.; Eds.; Kluwer Publishers: Dordrecht, 1991.
79. Rudkevich, D. M.; Verboom, W.; Reinhoudt, D. N. *J. Org. Chem.* **1994**, *59*, 3683.
80. Rudkevich, D. M.; Brzozka, Z.; Palys, M.; Visser, H. C.; Verboom, W.; Reinhoudt, D. N. *Angew. Chem. Int. Ed. Engl.* **1994**, *33*, 467.
81. Rudkevich, D. M.; Verboom, W.; Brzozka, Z.; Palys, M. J.; Stauthamer, W. P. R. V.; van Hummel, G. J.; Franken, S. M.; Harkema, S.; Engbersen, J. F. J.; Reinhoudt, D. N. *J. Am. Chem. Soc.* **1994**, *116*, 4341.
82. Xu, W.; Rourke, J.P.; Vittal, J. J.; Puddephatt, R. J. *J. Chem. Soc., Chem. Commun.* **1993**, 145.
83. Xu, W.; Vittal, J. J.; Puddephatt, R.J. *J. Am. Chem. Soc.* **1993**, *115*, 6456.
84. We thank Prof. R. J. Puddephatt for permission to quote these results prior to publication.
85. Katz, H. E. *J. Org. Chem.* **1985**, *50*, 5027.
86. Alder, R. W.; Bowman, P. S.; Steel, W. R. S.; Winterman, D. R. *Chem. Soc., Chem. Commun.* **1968**, 723.
87. Saturnino, D. J.; Yamauchi, M.; Clayton, W. R.; Nelson, R. W.; Shore, S. G. *J. Am. Chem. Soc.* **1975**, *97*, 6063.
88. Katz, H. E. *Organometallics* **1987**, *6*, 1134.
89. Katz, H. E. *J. Am. Chem. Soc.* **1986**, *108*, 7640.
90. Katz, H. E. *J. Org Chem.* **1989**, *54*, 2179.
91. (a) Reetz, M. T.; Niemeyer, C. M.; Harms, K. *Angew Chem.* **1991**, *103*, 1515. (b) *idem, Angew. Chem. Int Ed. Engl.* **1991**, *30*, 1472.
92. Jacobson, S.; Pizer, R. *J. Am. Chem. Soc.* **1993**, *115*, 11216.
93. (a) Beauchamp, A. L.; Oliver, M. J.; Wuest, J. D.; Zacharie, B. *J. Am. Chem. Soc.* **1986**, *108*, 73. (b) Wuest, J. D.; Zacharie, B. *J. Am. Chem. Soc.* **1987**, *109*, 4714.
94. (a) Yang, X.; Knobler, C. B.; Zheng, Z.; Hawthorne, M. F. *J. Am. Chem. Soc.* **1994**, *116*, 7142. (b) Hawthorne, M. F.; Yang, X.; Zheng, Z. *Pure Appl. Chem.* **1994**, *66*, 245.
95. Shur, V. B.; Tikhonova, A. I.; Yanovsky, A. I.; Struchkov, Yu. T.; Petrovskii, P. V.; Panov, S. Yu., Furin, G. G., Vol'pin, M. E. *J. Organomet. Chem.* **1991**, *418*, C29.
96. Shur, V. B.; Tikhonova, I. A.; Dolgushin, F. M.; Yanovsky, A. I.; Struchkov, Yu. T.; Volkonsky, A. Yu.; Solodova, E. V.; Panov, S. Yu.; Petrovskii, P. V.; Vol'pin, M. E. *J. Organomet. Chem.* **1993**, *443*, C19.
97. Newcomb, M.; Madonik, A. M.; Blanda, M. T.; Judice, J. K. *Organometallics* **1987**, *6*, 145.
98. (a) Newcomb, M.; Horner, J. H.; Blanda, M. T. *J. Am. Chem. Soc.* **1987**, *109*, 7878. (b) Newcomb, M.; Horner, J. H.; Blanda, M. T.; Squattrito, P. J. *J. Am. Chem. Soc.* **1989**, *111*, 6294.
99. Beer, P. D. *Chem. Commun.* **1996**, 689.
100. Beer, P. D.; Chen, Z.; Goulden, A. J.; Grieve, A.; Hesek, D.; Szemes, F.; Wear, T. *J. Chem. Soc., Chem. Commun.* **1994**, 1269.
101. (a) Beer, P. D.; Keefe, A. D. *J. Organomet. Chem.* **1989**, *375*, C40. (b) Beer, P. D.; Hesek, D.; Hodacova, J.; Stokes, S. E. *J. Chem. Soc., Chem. Commun.* **1992**, 270. (c) Beer, P. D.; Hazelwood, C.; Hesek, D.; Hodacova, J.; Stokes, S. E. *J. Chem. Soc., Dalton Trans.* **1993**, 1327. (d) Beer, P. D.; Chen, Z.; Goulden, A. J.; Graydon, A.; Stokes, S. E.; Wear, T. *J. Chem. Soc., Chem. Commun.* **1993**, 1834. (e) Beer, P. D.; Drew, M. G. B.; Hazelwood, C.; Hesek, D.; Hodacova, J.; Stokes, S. E. *J. Chem. Soc., Chem. Commun.* **1993**, 229. (f) Beer, P. D.; Graydon, A. R. *J. Organomet. Chem.*

**1994**, *466*, 241. (g) Beer, P. D.; Hesek, D.; Kingston, J. E.; Smith, D. K.; Stokes, S. E.; Drew, M. G. B. *Organometallics* **1995**, *14*, 3288. (h) Beer, P. D.; Drew, M. G. B.; Graydon, A. R.; Smith, D. K.; Stokes, S. E. *J. Chem. Soc., Dalton Trans.* **1995**, 403. (i) Beer, P. D.; Drew, M. G. B.; Hesek, D.; Jagessar, R. *J. Chem. Soc., Chem. Commun.* **1995**, 1187.

102. Beer, P. D.; Chen, Z.; Drew, M. G. B.; Kingston, J.; Ogden, M.; Spencer, P. *J. Chem. Soc.. Chem. Commun.* **1993**, 1046.

103. Uno, M.; Komatsuzaki, N.; Shirai, K.; Takahashi, S. *J. Organomet. Chem.* **1993**, *462*, 343.

104. Atwood, J. L.; Holman, K. T.; Steed, J. W. *Chem Commun.* **1996**, 1401.

105. (a) Steed, J. W.; Juneja, R. K.; Atwood, J. L. *Angew. Chem.* **1994**, *106*, 2571. (b) *idem, Angew. Chem. Int. Ed. Engl.* **1994**, *33*, 2456.

106. Staffilani, M.; Hancock, K. S. B.; Steed, J. W.; Holman, K. T.; Atwood, J. L.; Juneja, R. K.; Burkhalter, R. S. *J. Am. Chem. Soc.* **1997**, *119*, accepted for publication.

107. Steed, J. W.; Juneja, R. K.; Burkhalter, R. S.; Atwood, J. L. *J. Chem. Soc., Chem. Commun.* **1994**, 2205.

108. Steed, J. W.; Johnson, C. P.; Juneja, R. K.; Burkhalter, R. S.; Atwood, J. L. *Supramol. Chem.* **1996**, *6*, 235.

109. (a) Holman, K. T.; Halihan, M. M.; Steed, J. W.; Jurisson, S. S.; Atwood, J. L. *J. Am. Chem. Soc.* **1995**, *117*, 7848. (b). Holman, K. T.; Halihan, M. M.; Jurisson, S. S.; Atwood, J. L.; Burkhalter, R. S.; Mitchell, A. R.; Steed, J. W. *J. Am. Chem. Soc.* **1996**, *118*, 9567.

110. Staffilani, M.; Steed, J. W.; Holman, K. T.; Atwood, J. L.; Elsegood, M. R. J. unpublished results.

111. (a) Hasenknopf, B.; Lehn, J.-M.; Kneisel, B. O.; Baum, G.; Fenske, D. *Angew. Chem.* **1996**, *108*, 1987. (b) *idem.,Angew. Chem., Int. Ed. Engl.* **1996**, *35*, 1838.

112. Shionoya, M.; Ikeda, T.; Kimura, E.; Shiro, M. *J. Am. Chem. Soc.* **1994**, *116*, 3848.

113. Konishi, K.; Yahara, K.; Toshishige, H.; Aida, T.; Inoue, S. *J. Am. Chem. Soc.* **1994**, *116*, 1337.

114. (a) De Santis, G.; Fabbrizzi, L.; Licchelli, M.; Poggi, A.; Taglietti, A. *Angew. Chem.* **1996**, *108*, 224. (b) *idem., Angew. Chem. Int. Ed. Engl.* **1996**, *35*, 202.

115. Drew, M. G. B.; McCann, M.; Nelson, S. M. *J Chem. Soc., Chem. Commun.* **1979**, 481.

116. Agnus, Y.; Louis, R.; Weiss, R. *J. Am. Chem. Soc.* **1979**, *101*, 3381.

117. Coughlin, P. K.; Dewan, J. C.; Lippard, S. J.; Watanabe, E.; Lehn, J. -M. *J. Am. Chem. Soc.* **1979**, *101*, 265.

118. Motekaitis, R. J.; Martell, A. E. *Inorg. Chem.* **1992**, *31*, 5534.

119. (a) Ahlers, B.; Cammann, K.; Warzeska, S.; Kramer, R. *Angew. Chem.* **1996**, *108*, 2270. (b) *idem., Angew. Chem. Int. Ed. Engl.* **1996**, *35*, 2141.

120. Salta, J.; Chen, Q.; Chang, Y. -D.; Zubieta, J. *Angew. Chem.* **1994**, *106*, 781. (b) *idem, Angew. Chem. Int. Ed. Engl.* **1994**, *33*, 757.

121. (a) Müller, A.; Hovemeier, K.; Rohlfing, R. *Angew. Chem.* **1992**, *104*, 1214. (b) *idem, Angew. Chem. Int. Ed. Engl.* **1992**, *31*, 1192.

# INDEX

# Advances in Supramolecular Chemistry

Edited by **George W. Gokel**,
*Department of Molecular Biology and
Pharmacology, Washington University
School of Medicine, St. Louis*

**CONTENTS:** Introduction to the Series: An Editor's Foreword, *Albert Padwa.* Preface, *George W. Gokel.* Hydrogen Binding in Biological and Artificial Molecular Recognition, *Andrew D. Hamilton.* Synthetic Ditopic Receptors, *Ian O. Sutherland.* Molecular Recognition by Macrocycles Having a Three-Dimensionally Extended Hydrophobic Cavity, *Yukito Murakami, Jun-ichi Kikuchi and Teruhisa Ohno.* Pre-Organization and Molecular Recognition in the Formation and Reactions of Binuclear Metal Complexes, *Arthur E. Martell.*

**REVIEW:** "This is a strong second volume for what promises to be an important series in the field of supramolecular chemistry. The quality of the graphics is somewhat inconsistent among the chapters, reflecting direct reproduction of the authors' variable originals However, this does not detract from an excellent compilation of studies from five laboratories with very diverse approaches to supramolecular chemistry."

> — *Journal of Inclusion Phenomena and
> Molecular Recognition in Chemistry*

**CONTENTS:** Preface, *George W. Gokel.* Cyclodextrin Complexation of Amphiphilic Compounds, *Angel Kaifer.* Monolayer Lipid Membranes (MLMs) from Bola-amphilhiles, *Jurgen-Hinrich Fuhrhopa and Reinhard Bach.* Accumulation of Unit-Binding Sites: Hydrogen Bonding Fixation in Multi-Functional Polar Organic Molecules, *Yasuhiro Aoyama.* Thermal Fluctuations of Membranes, *M.D. Mitov, J. F. Faucon, P. Meleard, P. Bothorel, Paul Pascal.* Molecular Recognition in the Solid State, *Fumio Toda.* Photoactivation of Metal Complexes on Porous Vycor Glass, *Harry D. Gafney.* Index.

JAI PRESS

# JAI PRESS

**REVIEWS:** "The third book in this timely series continues the tradition of excellence started with the first two volumes. The book comprises six chapters written by internationally recognized scientists and covers widely different areas in which the common theme is supramolecualar chemistry. All chapters are up to date reviews (Latest reference 1992 and many in the 1990) on specific aspects of supramolecular chemistry and are intended not only for supramolecular chemists but for a wide range of scientists working in related fields."

— *Journal of American Chemical Society*